SCHOLARLY PUBLICATIONS

A CURRENT AWARENESS BULLETIN
OF RESEARCH OUTPUT

@DTU

(34th Edition)

OCTOBER 2015

BY: CENTRAL LIBRARY

DELHI TECHNOLOGICAL UNIVERSITY
(FORMERLY *DELHI COLLEGE OF ENGINEERING)*
GOVT. OF N.C.T. OF DELHI
SHAHBAD DAULATPUR, MAIN BAWANA ROAD
DELHI 110042

PREFACE

This is the **Thirty Fourth** Issue of Current Awareness Bulletin started by Delhi Technological University, Central Library. The aim of the bulletin is to compile, preserve and disseminate information published by the faculty, students and alumni for mutual benefits. The bulletin also aims to propagate the intellectual contribution of Delhi Technological University (DTU) as a whole to the academia.

The bulletin contains information resources available in the internet in the form of articles, reports, presentations published in international journals, websites, etc. by the faculty and students of DTU. The publications of faculty and student which are not covered in this bulletin may be because of the reason that the full text either was not accessible or could not be searched by the search engine used by the library for this purpose.

The learned faculty and students are requested to provide their uncovered publications to the library either through email or in CD, etc to make the bulletin more comprehensive.

This issue contains the information published during **October 2015**. The arrangement of the contents is alphabetical. The full text of the article which is either subscribed by the university or available in the web is provided in this bulletin.

Central Library

CONTENTS

1. An Investigation into the Factors Affecting the Adoption Intention of eLearning in India, ***3.Anoushka Sharma***, ***3.Kapil Sharma***, ***3.Shashank Kashyap*** and ***3.Vipul Maheshwari***, DSM, DTU

2. Analysis of Small Signal Behaviour of Transparent Gate Recessed Channel (TGRC) MOSFET for High Frequency/RF Applications, ***3.Ajay Kumar***, ***3.Neha Gupta*** and **3.Rishu Chaujar**, Engineering Physics, DTU

3. Biodiesel A Promising Renewable Alternative Fuel, Manish Jain and ***3.Shashank Mohan***, Mechanical Engineering, DTU

4. Biodiesel Conversionionof high FFA Neem oil by blending it with low FFA Sesame oil, ***3.Amit Pal***, ***3.Raj Kumar Singh*** and ***3.Shashank Mohan***, Mechanical Engineering, DTU

5. Buffer Overflow Exploit Prevention, ***3.Kushal Ahuja*** and ***3.Vinod Kumar***, Computer Science, DTU

6. !-cycle Compatible Splitting Signed Graphs S(S) and !(S), ***3.Rashmi Jain***, ***3.Sangita Kansal*** and Mukti Acharya, Applied Mathematics, DTU

7. Comparative Performance of R438A and R32/R125/R600A Mixture for Replacing HCFC22 used in Air-Conditioners, Suneel Kumar Kalla, J. A. Usmani and ***3.B. B. Arora***, , Mechanical Engineering, DTU

8. Detection of Enterobacter sakazakii from Commercial Children Dry Milk, Mohammed Mosa Jaffaar, Mohammed K. Shebli, Abdul Khaliq Abbas Mussa, Bayan Hassan Hadi, ***3.Allaa M. Aenab*** and ***3.S.K.Singh***, Environmental Engineering, DTU

9. DNA Steganography: Literature Survey on its Viability as a Novel Cryptosystem, ***3.Aditi Bhateja*** and Kanika Mittal, Computer science, DTU

10. Economic assessment of use of pond ash in Pavements, ***3.Raju Sarkar*** and A.R. Dawson, Civil Engineering, DTU

11. Effect of Condenser Fouling on Performance of Vapor Compression Refrigeration System Naveen Solanki, ***3.Akhilesh Arora*** and S. C. Kaushik, Mechanical Engineering, DTU

12. Energy and Exergy Analyses of a new Solar Assisted Cogeneration Cycle for Simultaneous Production of Power and Double Effect Cooling, Surendra Kumar Agrawal and ***3.Rajesh Kumar***, Mechanical Engineering, DTU

13. ENERGY AND EXERGY ANALYSIS OF A DOUBLE EFFECT PARALLEL FLOW LIBR/H2O ABSORPTION REFRIGERATION SYSTEM, ***3.Akhilesh Arora***, Manoj Dixit and S.C. Kaushik, Mechanical Engineering, DTU

14. Evaluation of Protocols to Support IP Mobility in Aeronautical Communications, ***3.Kapil Sharma***, DTU

15. Exergetic Analysis of Combined Power and Ejector Refrigeration Cycle using Solar Energy as Heat Source, ***3.Rajesh Kumar***, Mechanical Engineering, DTU

16. Exergetic analysis of Solar Operated Power and Cooling Cycle, ***3.Rajesh Kumar***, Mechanical Engineering, DTU

17. Exergy Destruction Analysis of Double-effect LiBr-H2O Absorption Refrigeration System, ***3.Rajesh Kumar*** and ***3.Ravindra Kannojiya***, Mechanical Engineering, DTU

18. Exergy Destruction Analysis of Single-effect LiBr-H2O Absorption Refrigeration System, ***3.Rajesh Kumar*** and ***3.Ravindra Kannojiya***, Mechanical Engineering, DTU

19. Is CSR a win-win situation? A study of Listed Companies of India, ***3.Seema Singh***, ***8.Anngad Singh*** and ***8.Yatin Arora***, DTU

20. Literature review of multi-aspect research works carried out on the concept and implementation of GSCM, ***7.1.Sheetal Soda***, Anish Sachdeva and Rajiv Kumar Garg, Production Engineering, DTU

21. Modeling and Analysis of Current and Weld Speed on Weld Hardness of Steel-Cu Weldments by RSM Approach, Ramakant Rana, Surabhi Lata, Alok Shankaran, Vinay Sharma, Amit Saraswat and ***3.Roop Lal***, Mechanical Engineering, DTU

22. Modelling of critical factors for responsiveness in supply chain, ***3.Rajesh Kumar Singh***, Mechanical Engineering, DTU

23. Optimization of process parameters on Over-Cut in drilling of Al- B4C MMC, Ravinder Kumar, Ramakant Rana, Surabhi Lata, Rahul kumar Sonkar, Abhinav Kumar, Shekhar Pawar and ***3.Roop Lal***, Mechanical Engineering, DTU

24. Performance Analysis of Turbo Codes under Different Parameters in AWGN Environment, ***7.Mudita Chandra*** and ***3.Sanjay Kumar Soni***, Electronics & Communication Engineering, DTU

25. Affinity of Smectite and Divalent Metal Ions (Mg2+, Ca2+, Cu2+) with L-leucine: An Experimental and Theoretical Approach Relevant to Astrobiology, Pramod Pandey, Chandra Kala Pant, Kavita Gururani, Priyanka Arora, Neetu Pandey, Preeti Bhatt, Yogesh Sharma, Jagmohan Singh Negi and ***3.Mohan Singh Mehta***, Applied Physics, DTU

26. An integrated framework of interpretive structural modeling and graph theory matrix approach to fix the agility index of an automobile manufacturing organization, ***3.Pravin Kumar***, ***3.Rajesh K. Singh*** and ***3.Rakesh Kumar***, Mechanical Engineering, DTU

27. Prediction of Change Prone Classes using Threshold Methodology ***3.Ruchika Malhotra*** and ***3.Ankita Bansal***, Software Engineering, DTU

28. Regression Analysis for the Adsorption Kinetics of Methylene Blue onto Activated Carbon, ***3.Abhinav Jain*** and ***3.Abhishek Pandey***, Environmental Engineering, DTU

29. Sliding wear behavior of aluminum alloy coating prepared by two-wire electric arc spray process, ***3.Dalip Kumar***, Qasim Murtaza and ***3.R. C. Singh***, DTU

30. Solar Thermal Technologies for Power Generation in India, ***3.Rajesh Kumar***, Mechanical Engineering, DTU

31. Stress induced enhanced polarization in multilayer BiFeO3/ BaTiO3 structure with improved energy storage properties, Savita Sharma, Monika Tomar, Ashok Kumar, and ***3.Nitin K. Puri***, and Vinay Gupta, Applied Physics, DTU

32. Study of Automobile Exhaust Emissions, ***8.Kshitij Aggarwal*** and ***8.Mridul Garg***, DTU

33. TCAD Analysis of Frequency Dependent Intrinsic and Extrinsic Parameters of GEWE-SiNW MOSFET, ***3.Neha Gupta***, ***3.Ajay Kumar*** and ***3.Rishu Chaujar***, Engineering Physics, DTU

34. Thermodynamic Analysis of Double-effect LiBr- H2O Absorption Refrigeration System, ***3.Rajesh Kumar***, Mechanical Engineering, DTU

35. Thermodynamic Analysis of Power and Ejector Cooling Cycle, ***3.Rajesh Kumar***, Mechanical Engineering, DTU

36. Treatment of Heavy Metals Contaminated industrial waste water by functionalized Polymers, ***6.Tarundeep Gill***, ***3.S.K. Singh*** and ***3.P. Albino Kumar***, Environmental Engineering, DTU

37. Two Layer Soil Modelling & Optimal Designing of Grounding System of High Voltage Gas Insulated Substation (GIS) & Air Insulted Substation (AIS), Using Matlab GUI, ***7.Rajesh kumar***, Kamal Bansal, Devender K. Saini and Ips Poul, Electrical Engineering DTU

38. Vertical Handoff decision based on MADM for etwork selection in 4G Heterogeneous Wireless Networks, ***3.Kapil Sharma***, DTU

1. Vice Chancellor	***1.1. Ex Vice Chancellor***
2. Pro Vice Chancellor	***2.1. Ex Pro Vice Chancellor***
3. Faculty	***3.1. Ex Faculty***
4. Teaching-cum-Research Fellow	
5. Alumni	
6. Research Scholar	***6.1. Ex Research Scholar***
7. PG Scholar	***7.1. Ex PG Scholar***
8. Undergraduate Student	***8.1. Ex Undergraduate Student***

Advances in Computer Science and Information Technology (ACSIT)
Print ISSN: 2393-9907; Online ISSN: 2393-9915; Volume 2, Number 6; April-June, 2015 pp. 559-563
© Krishi Sanskriti Publications
http://www.krishisanskriti.org/acsit.html

An Investigation into the Factors Affecting the Adoption Intention of eLearning in India

Anoushka Sharma[1], Kapil Sharma[2], Shashank Kashyap[3] and Vipul Maheshwari[4]

[1,2,3,4]*Delhi School of Management, Delhi Technological University*

Abstract—*The aim of this paper is to understand the factors affecting the adoption intention of eLearning as a means of learning amongst individuals (specifically learners and teachers). eLearning is a scalable, efficient, cost effective and fast form of learning but its acceptance levels are still low. The study endeavors to come forward with factors and outcomes, which when analyzed, will help examine the reasons for the low acceptance rate of the eLearning education model in India. The Paper will help all the stakeholders in the field of eLearning to develop a fair understanding of low acceptance of eLearning.*

1. INTRODUCTION

With evolution of information technologies like virtual classes and digital libraries, there has been the creation of a new teaching and learning environment which is flexible and independent of time and space. Thousands of online courses are available that not only provide online instructional material but online discussions and collaborative eLearning experience as well. eLearning can be thought of as a learning experience delivered with the help of Information and Communication Technologies (ICTs) that makes information or knowledge available to learners without any limitation of time or space [22, 24].

When researching the adoption intention of new technologies and models based out of them amongst individuals, Technology Acceptance Model is a widely accepted technology model. It is an established fact that factors such as user's perceived ease of use and perceived usefulness are crucial in such researches. [9, 19, 23, 27, 28]. Over the years, the TAM model has found widespread support, appreciation and inclusion in such major studies and researches [7, 14, 15, 19, 20]

In the following sections, existing literature and TAM's factors are discussed. A research design based on TAM has been used to predict user's acceptance behavior. Finally, the outcomes are analyzed and presented.

2. REVIEW OF LITERATURE

A proper review of existing literature is essential and of high importance to have a proper bird's eye view of the views and studies of the academics and researchers of the present times.

eLearning or Blended Learning can be perceived as the amalgation of all the existent modes and means of web-based technology to accomplish an educational objective and consequently attaining enhancement in the knowledge levels. [10, 14, 22, 24]. Learning provides ''intellectual growth that leads to scientific reasoning, abstract thought, and formal operations'' [16, 33].

Major advantages of eLearning include control over the content offering and pace of learning, ease of distribution, ease in updating material, standardized course material, lifelong learning, interactive session, cost effectiveness and accountability. [3, 22, 29, 32, 33]. eLearning is emerging as the paradigm of modern education by becoming an essential part of teaching and learning process and implementation of systems across borders of time and space [8, 21, 26]. With the shift from product based economy to knowledge based economy, the organizations are looking for knowledge workers who can be trained on an anytime, anywhere basis [3, 17].

Learner Satisfaction (or Acceptance) is a vital factor that has a far and wide mention in all studies based on eLearning. [12, 13, 14, 22, 25, 26, 29, 33]. The benefits of eLearning will not be maximized unless the learners are ready to accept and use the system [21]. Additionally, a peek into what leads to learner dissatisfaction and dropout from online courses and a thereby mild adoption intention rate is also essential. [2, 5, 11, 13, 14, 18, 20, 30].

The quality and reliability of the eLearning system is an important factor for increasing the acceptance of eLearning [31]. It is also essential that the system should be developed in such a way that it has minimal technical problems and is able to support different platforms and application.

This paper aims to look for the possible factors for the low adoption intention of eLearning services in India. Though there is wide literature in general, there is almost no existing literature that focuses on the eLearning adoption intention in India. Using the TAM Model as the research model, this paper will try and identify the major factors and their correlation for the low acceptance rate of eLearning in India.

3. RESEARCH METHODOLOGY

The purpose of the study is to understand and investigate into the factors affecting the adoption of eLearning in India.

The impact of various factors was studied using an exploratory-descriptive approach. An Online Questionnaire was designed for the same based on the demographic and TAM model factors.

The objectives for the paper have been defined as follows (1) O1: To determine the effect of Perceived Usefulness on Attitude Towards the eLearning services in India. (2) O2: To determine the effect of Perceived Ease of Use on Attitude Towards the eLearning services in India. (3) O3: To determine the effect of Attitude Towards the eLearning services on Behavioral Intention of users in India.

The study is based upon the analysis of primary data collected through floatation of an Online Questionnaire based on the TAM Model Factors (Perceived Usefulness, Perceived Ease of Use and Attitude Towards eLearning). The questionnaire is a prominent tool for primary data collection which consists of a set of questions used for collecting information and data from individuals. [4]

The Questionnaire made use of the Likert Scale, which is a very common format used for surveys in which the respondents rank the quality of their responses either from high to low or from low to high [1]. A 5-point Likert scale was chosen for better understanding of the responses of individuals by attaching the labels to each point in the scale and the mid-point of the scale was set as the neutral response point. The Likert Scale used was as follows:

(1- Strongly Agree, 2- Agree, 3- Neutral, 4- Disagree, 5- Strongly Disagree)

The research model used for this study is Technology Acceptance Model (TAM) . This model helps in predicting the intention to use and acceptance of Information System and Information Technology by individuals. This Model consists of three important factors for understanding the behavioral intention of users. They are:

(1) Perceived Usefulness, which decides the degree to which an individual believes that his or her job or life performance can be enriched by using a particular Information System or Information Technology;

(2) Perceived Ease of Use, which decides the degree to which an individual believes that by using a particular Information System or Information Technology would be very convenient to use; and

(3) Attitude Towards using, decides the degree to which an individual will adapt the system or not depending on his positive or negative attitude towards Perceived Usefulness and Perceived Ease of Use factors by using a particular Information System or Information Technology. [6]

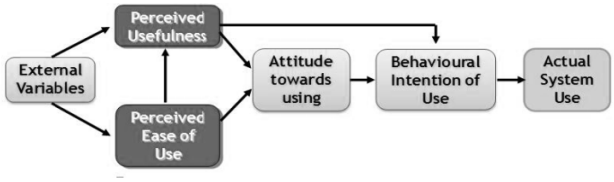


Fig. 1: TAM Model

4. DATA REPORTING AND ANALYSIS

In the surveyed 212 respondents, about 56.13% of respondents were male (119 in number) and 43.87% were female (93 in number. Out of the said respondents, 126 were Students (59.43%), 10 were Research Scholars/ Teaching Assistants (4.72%), 29 were Teachers/Professors (13.68%)and 47 were other direct and indirect stakeholders in the eLearning Model (22.17%).Out of the 212 respondents, about 90% (190/212) use Internet services on a daily basis (161 used it every few hours and 29 use it once in a day).

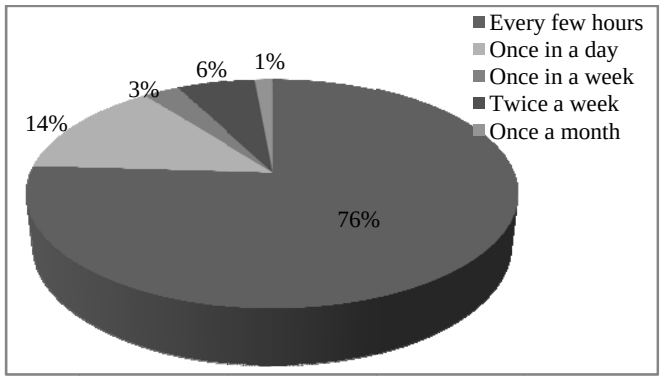


Fig. 2: Internet Usage Statistics

Out of the respondents that use Internet Services daily, along with Social Media and Surfing, there is a wide inclination towards eLearning as well (83% use Internet for eLearning as well)

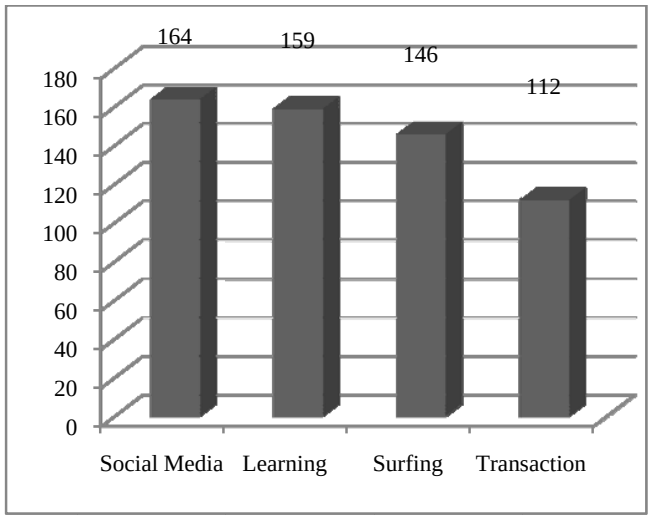


Fig. 3: Purpose of Internet Use Statistics

Out of the total 174 respondents who use the Internet services on a daily basis, a significant three-fourths (76%) agree to the Perceived Usefulness of the e-Learning services in India. A staggering 83% agree to the Perceived Ease of Use of the eLearning services and around 72% agree having a positive attitude towards the eLearning services in India

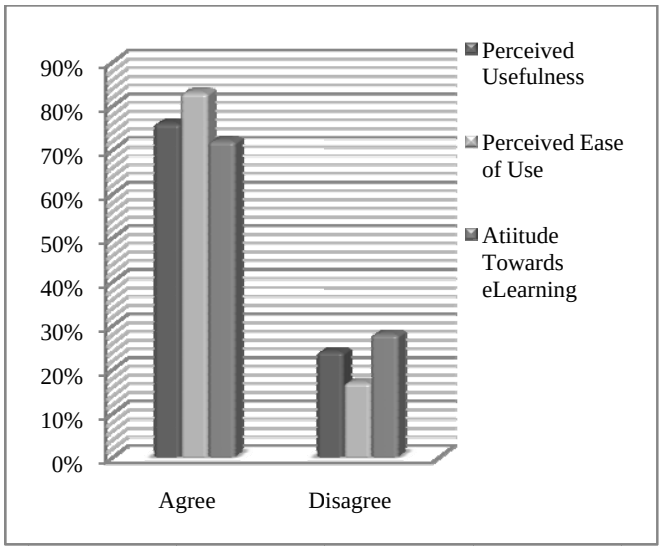


Fig. 4: TAM Factor Statistics

Regression was carried out using the software. The Regression statistics are as follows:

Table 1: Regression Statistics

Multiple R	**0.810179437**
R Square	0.65639072
Adjusted R Square	0.642849468
Standard Error	0.445171928
Observations	212

Table 2: Table for t-Statistics and P- Value

Factors	**t stat**	**P-value**
eLearning provides easy subscription to a Certification Course of a renowned University.	2.1003	0.0369
eLearning is more relevant to a particular specialization course.	0.3696	0.7120
eLearning allows repeated access to video lectures for better understanding of the concept.	8.4138	7.0514
eCertificates from renowned universities can help in career enrichment.	1.8631	0.0638
eLearning saves time.	1.8441	0.0666
eLearning is cost effective.	3.6072	0.0003
eLearning provides easy access to the study material.	1.8119	0.0714
eLearning offers study material that is reliable and more valid in present times.	5.0240	1.1106

Responses were analyzed by applying regression model and calculating the P-value for each factor. In regression models, we adopted the attitude towards eLearning as a dependent variable and tried to find out whether independent variables (Perceived Usefulness and Perceived Ease of Use) are linearly related to it or not. Table 1 and Table 2 provides the details of the test.

This analysis consists of the data of 212 respondents. In a linear regression model, adjusted coefficient of determination is 64.28 %, so the model's fit is good. P-value of each factor gives the insight of relation of factors with the dependent variable. Thus, there is enough evidence to infer that the variables (eLearning provides easy subscription to a Certification Course of a renowned University, eLearning is cost effective) are linearly related to attitude towards eLearning. We have found weak evidences to infer eLearning. There is not enough evidence to conclude that the variables (eLearning is more relevant to a particular specialization course, eLearning allows repeated access to video lectures for better understanding of the concept, eLearning offers study material that is reliable and more valid in present times) are linearly related to attitude towards eLearning. that the variable (eCertificates from renowned universities can help in career enrichment, eLearning saves time, eLearning provides easy access to the study material) are linearly related to attitude towards eLearning.

5. FINDINGS

The findings of the study can be summarized as follows:

There is sufficient evidence at the 5% significance level to infer that each of the following variables is linearly related to attitude towards eLearning:

1. eLearning provides easy subscription to a Certification Course of a renowned University.
2. eLearning is cost effective.

There is weak evidence to infer that following variables is linearly related to attitude towards eLearning

1. eCertificates from renowned universities can help in career enrichment.
2. eLearning saves time.
3. eLearning provides easy access to the study material.

There is not enough evidence to conclude that each of the following variables is linearly related to attitude towards eLearning

1. eLearning is more relevant to a particular specialization course.
2. eLearning allows repeated access to video lectures for better understanding of the concept.
3. eLearning offers study material that is reliable and more valid in present times.

The findings, with respect to the objectives of the paper are as follows:

(1) There is a positive relationship between the Perceived Usefulness and Attitude Towards the eLearning services in India. With a significant three-fourths (76%) agreeing to the Perceived Usefulness of the eLearning services in India, the factor becomes an important consideration to analyze the adoption intention. (3) O3: To determine the effect of Attitude Towards the eLearning services on Behavioral Intention of users in India.

(2) There is a positive relationship between the Perceived Ease of Use and Attitude Towards the eLearning services in India. With a staggering greater than four-fifths (83%), agreeing to the Perceived Ease of Use of the eLearning services in India, the factor becomes a vital component.

(3) There is a positive relationship between the Attitude Towards the eLearning services in India and Behavioral Intention of users in India. Around 72% agree to this factor being prominent and important.

6. CONCLUSION

Internet has become one of the most important means to provide educational and learning resources for teachers and learners alike for the purpose of sharing and obtaining information. The findings of our study reveal that factors like Subscription to Certification Course of a renowned university and cost of effectiveness of eLearning courses are prominent factors in the adoption intention of eLearning services in India. Factors like easy access to the study material, time saving and eCertificates from the renowned universities can help in career enrichment and this consequentially affects the adoption intention of eLearning Services. Factors like reliable study material, repeated access to video lectures and relevance to a particular specialization course does not affect the adoption intention of eLearning.

7. FUTURE SCOPE

The study conducted to investigate the factors affecting the adoption intention of the eLearning services in India was based on the widely accepted TAM Model. Further studies can base their research on factors other than those that form a part of the TAM Model. Additionally, the average age group of the survey respondents was 20-25 Years. Future studies can focus on different age groups.

REFERENCES

[1] Albaum, G. (1997). The Likert scale revisited. Journal-Market research society, 39, 331-348.

[2] Berge, Z. L., & Huang, Y. P. (2004). 13: 5 A Model for Sustainable Student Retention: A Holistic Perspective on the Student Dropout Problem with Special Attention to e-Learning.

[3] C.-S. Ong, J.-Y.Lai, Y.-S. Wang, Factors affecting engineers' acceptance of asynchronous e-learning systems in high-tech companies, Information & Management 41(6), 2004, pp. 795–804

[4] CDC (2008). Data collection methods for programme evaluation: questionnaires, Department of health and human services, Centers for Disease Control and Prevention. Available from http://www.cdc.gov/HealthyYouth/evaluation/pdf/brief14.pdf

[5] Chang, Y. J., Chen, C. H., Huang, W. T., & Huang, W. S. (2011, July).Investigating students' perceived satisfaction, behavioral intention, and effectiveness of English learning using augmented reality. In Multimedia and Expo (ICME), 2011 IEEE International Conference on (pp. 1-6). IEEE.

[6] Chen, S. C., Li, S. H., & Li, C. Y. (2011). Recent related research in technology acceptance model: A literature review. Australian Journal of Business and Management Research, 1(9), 124-127.

[7] Chuttur, M. (2009). Overview of the technology acceptance model: Origins, developments and future directions.

[8] D. Zhang, J.L. Zhao, L. Zhou, J. Nunamaker, Can e-learning replace traditional classroom learning—evidence and implication of the evolving e-learning technology, Communications of the ACM 47(5), 2004, pp. 75–79.

[9] Davis, F. D., Bagozzi, R. P., &Warshaw, P. R. (1989). User acceptance of computer technology: A comparison of two theoretical models. Management Science, 35(8), 982–1003.

[10] Driscoll, M. (2002). Blended learning: Let's get beyond the hype. E-learning,1(4). accessed from https://www-07.ibm.com/services/pdf/blended_learning.pdf on 3rd April, 2015.

[11] Levy, Y. (2007).Comparing dropouts and persistence in e-learning courses.Computers& education, 48(2), 185-204.

[12] Liaw, S. S. (2008). Investigating students' perceived satisfaction, behavioral intention, and effectiveness of e-learning: A case study of the Blackboard system. Computers & Education, 51(2), 864-873.

[13] Liaw, S. S., & Huang, H. M. (2007).Developing a Collaborative e-learning System Based on Users' Perceptions. Lecture Notes in Computer Science, 4402, 751–759.

[14] Liu, S. H., Liao, H. L., &Peng, C. J. (2005).Applying the technology acceptance model and flow theory to online e-learning users' acceptance behavior. E-learning, 4(H6), H8.

[15] Liu, S., Liao, H. & Pratt, J. (2009).Impact of media richness and flow on e-learning technology acceptance. Computers & Education, 52(3), 599-607. http://dx.doi.org/10.1016/j.compedu.2008.11.002

[16] M. O'Loughlin, Rethinking science education: beyond Piagetian constructivism toward a sociocultural model of teaching and learning, Journal of Research in Science Teaching 29(8), 1992, pp. 791–820

[17] Ong, C. S., Lai, J. Y., & Wang, Y. S. (2004).Factors affecting engineers' acceptance of asynchronous e-learning systems in high-tech companies.Information& management, 41(6), 795-804.

[18] Park, J. H., & Choi, H. J. (2009).Factors Influencing Adult Learners' Decision to Drop Out or Persist in Online Learning. Educational Technology & Society,12(4), 207-217.

[19] Park, N. (2009). User acceptance of e-learning in higher education: An application of Technology Acceptance Model. Paper presented at the Annual meeting of the International Communication Association, New York

[20] Park, S. Y. (2009). An Analysis of the Technology Acceptance Model in Understanding University Students' Behavioral Intention to Use e-Learning.Educational technology & society, 12(3), 150-162.

[21] Pituch, K. A., & Lee, Y.-K. (2006). The influence of system characteristics on e-learning use. Computers & Education, 47, 222–244.
[22] Ruiz, J. G., Mintzer, M. J., & Leipzig, R. M. (2006).The impact of e-learning in medical education. Academic medicine, 81(3), 207-212.
[23] Schepers, J., &Wetzels, M. (2007). A meta-analysis of the technology acceptance model: Investigating subjective norm and moderation effects.Information& Management, 44(1), 90-103
[24] Sun, P. C., Tsai, R. J., Finger, G., Chen, Y. Y., &Yeh, D. (2008). What drives a successful e-Learning? An empirical investigation of the critical factors influencing learner satisfaction. Computers & education, 50(4), 1183-1202.
[25] Tselios, N. K., Daskalakis, S., &Papadopoulou, M. (2011). Assessing the Acceptance of a Blended Learning University Course. Educational Technology & Society, 14(2), 224-235.
[26] Van Raaij, E. M., &Schepers, J. J. (2008).The acceptance and use of a virtual learning environment in China. Computers & Education, 50(3), 838-852.
[27] Venkatesh, V., & Davis, F. D. (1996). A model of the antecedents of perceived ease of use: Development and test. Decision Sciences, 27, 451–481.
[28] Venkatesh, V., Morris, M. G., Davis, G. B., & Davis, F. D. (2003). User acceptance of information technology: Toward a unified view. MIS quarterly, 425-478.
[29] Wentling, T., Waight, C., Gallaher, J., La Fleur, J., Wang, C., &Kanfer, A. (2005). E-Learning: A Review of Literature (2000).
[30] Willging, P. A., & Johnson, S. D. (2009).Factors that Influence Students' Decision to Dropout of Online Courses. Journal of Asynchronous Learning Networks, 13(3), 115-127.
[31] Yiong, B. L. C., Sam, H. K., &Wah, T. K. (2008). Acceptance of e-learning among distance learners: A Malaysian perspective. In Proceedings: Ascilite Conference.
[32] Zhang, D., Zhou, L., Briggs, R. O., &Nunamaker, J. F. (2006). Instructional video in e-learning: Assessing the impact of interactive video on learning effectiveness. Information & management, 43(1), 15-27.
[33] Zhang, S., Zhao, J., & Tan, W. (2008).Extending TAM for online learning systems: An intrinsic motivation perspective. Tsinghua Science & Technology,13(3), 312-317.

ResearchGate

See discussions, stats, and author profiles for this publication at: http://www.researchgate.net/publication/275957974

Analysis of Small Signal Behaviour of Transparent Gate Recessed Channel (TGRC) MOSFET for High Frequency/RF Applications

CONFERENCE PAPER · JUNE 2015

DOI: 10.13140/RG.2.1.2819.0566

READS

22

3 AUTHORS:



Ajay Kumar

Delhi Technological University

16 PUBLICATIONS **3** CITATIONS

SEE PROFILE



Neha Gupta

Delhi Technological University

10 PUBLICATIONS **5** CITATIONS

SEE PROFILE



Rishu Chaujar

Delhi Technological University

73 PUBLICATIONS **108** CITATIONS

SEE PROFILE

Available from: Ajay Kumar

Retrieved on: 06 October 2015

Analysis of Small Signal Behaviour of Transparent Gate Recessed Channel (TGRC) MOSFET for High Frequency/RF Applications

Ajay Kumar[1], Neha Gupta[2] and Rishu Chaujar[3]

Microelectronics Research Lab, Department of Engineering Physics,
Delhi Technological University, Bawana Road, Delhi-110042, India
ajaydtu@gmail.com[1]
nehagupta_dtu@yahoo.com[2]
rishu.phy@dce.edu[3]

ABSTRACT

In this paper, small signal behavior have been investigated for Transparent Gate Recessed Channel (TGRC) MOSFET in terms of Y-parameters and Z-parameters, the results are compared with Conventional Recessed Channel (CRC) MOSFET at THz frequency range, using ATLAS device simulator. Small-signal Y-parameters and Z-parameters are commonly employed for those networks which are operating at RF and microwave frequencies, where admittances are more easily computed in compared to voltages and currents. Since, at high frequency it is very difficult to estimate current and voltages.

Keywords: CRC-MOSFET, cut-off frequency, ITO, RF, TGRC-MOSFET, Y-parameter, Z-parameter.

.

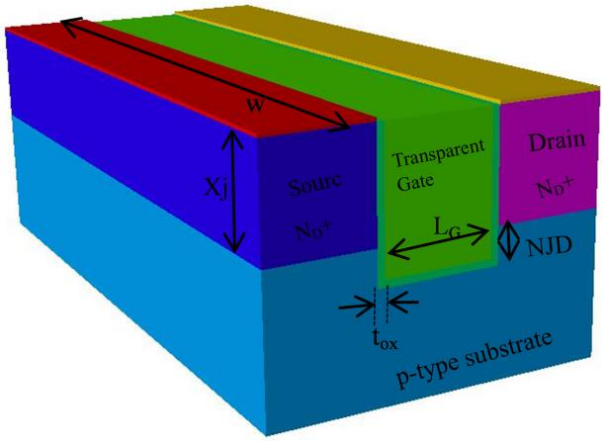
1. INTRODUCTION

In the era of sub –100 nm dimensions, continuing scaling of conventional MOSFETs is done to advance opportunities for further high speed and low power applications. Highly scaled MOSFETs achieved cut-off frequencies in several THz range making CMOS technology appropriate for RF application and wireless communications [1-4]. In the conventional MOSFET, as the channel length reduces, the gate control over the channel gets reduced due to the increased source/drain capacitances [5]. However, with scaling down the device dimensions, the so-called SCEs arises such as mobility degradation, hot carrier effects, drain induced barrier lowering, parasitic capacitances etc. making the scaled devices inapt for RF/ wireless applications [6].

In TGRC-MOSFET, the metal gate is replaced by a transparent conducting oxide [7-8] called indium tin oxide (ITO). ITO is a solid solution of indium oxide (In_2O_3) and tin oxide (SnO_2). It is transparent and colourless in thin layers. Moreover, due to the increased demand for high-speed electronics products, the accurate modeling of the small signal behaviour at high frequencies (HF) is necessary in microwave circuits and systems [9].

All simulations have been performed using ATLAS and DEVEDIT 3D device simulator [10]. For the simulations authors adopted physical models accounting for the electric field-dependent and concentration-dependent carrier mobilities, Shockley–Read–Hall recombination/generation with doping dependent carrier lifetime, inversion layer Lombardi CVT mobility model, wherein concentration-dependent mobility, high field saturation model are all included [10]. To incorporate all non-local effects, we have adopted the hydrodynamic energy transport model and are more accurate than drift-diffusion method.

2. DEVICE STRUCTURE AND METHODOLOGY



1 (a)

Fig.1(a) Schematic structure of TGRC-MOSFET.

Fig. 1(a-b) shows the simulated 3D device structure of TGRC-MOSFET and 2-D meshed structure of TGRC-MOSFET respectively. All simulations have been performed using ATLAS and DEVEDIT 3D device simulator. The Source/Drain region is highly doped with n-type impurity of 1×10^{19} cm^{-3}. While substrate is doped with a p-type impurity of 1×10^{17} cm^{-3} and t_{ox} thick oxide layer of 2.0 nm is embodied in it as shown in Fig.1.In order to fairly analyze the device performances, both the devices are optimized to have the same threshold voltage, i.e., 0.4V. In this simulation all the junctions of the structure are assumed as abrupt and the biasing

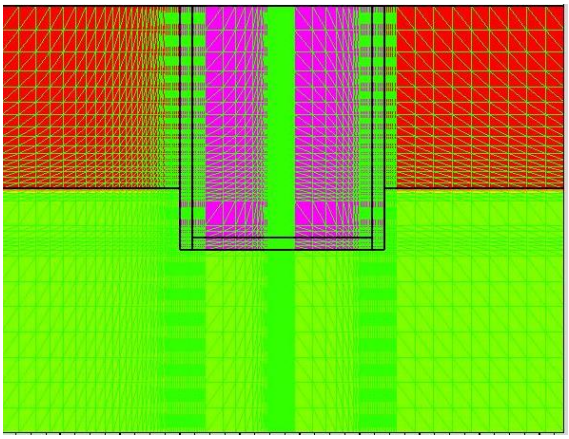


Fig.1(b) 2-D Meshed structure of TGRC-MOSFET.

conditions are considered at room temperature (T=300K) and the doping profiles are uniform. Further, two numerical techniques Gummel and Newton have been considered to obtain the solutions [10]. Negative Junction Depth (NJD) is taken 10 nm. Gate bias (V_{gs}) is applied 0.7 V and drain bias (V_{ds}) is applied 0.5V. Gate workfunction of TRC-MOSFET (Φ_{ITO}) is 4.7 eV and 4.4 for CRC-MOSFET.

3. RESULTS AND DISCUSSIONS

Fig. 2 (a-d) compares the real components of Y-parameters and Z-parameters of CRC-MOSFET with TGRC-MOSFET. Without any additional appropriate parameters, the Y-parameters and Z-parameters characteristics are well reproduced up to the cutoff frequency. Correct calculation of Y-parameters and Z-parameters promises the applicability for RF and very fast switching [11]. Z_{11} is higher (lower Y_{22}) at low frequency and decreases gradually as frequency is

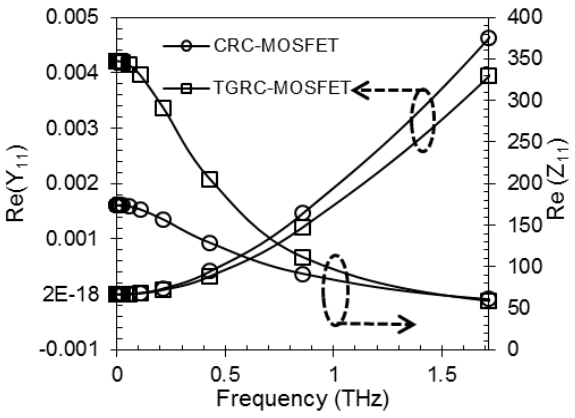


Fig. 2(a): Y-parameters Re (Y_{11}) and Z-parameters Re(Z_{11}) at V_{gs}=0.7 V and V_{ds}=0.5 V.

increases while Z_{22} is higher (lower Y_{11}) at low frequency and deceases gradually w.r.t. frequency in TGRC-MOSFET as compared to CRC-MOSFET i.e. input impedance is high and output impedance is less as shown in Fig. 2(a) and 2(d) respectively. If the input impedance of the device is high, it means the device is useful for RF application of MOSFETs [5]. Z_{12} and Z_{21} (open circuit transfer impedance) parameters are also high in TGRC-MOSFET and reduce gradually when frequency is increases as shown in Fig. 2(b) and 2(c) respectively. Similarly Y_{12} and Y_{21} (short circuit transfer admittance) are enhanced in TGRC-MOSFET which leads to high input impedance as evident from Fig. 2(b) and 2(c) respectively.

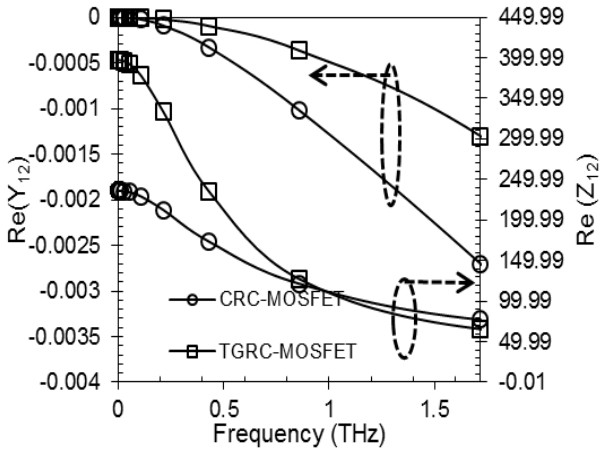


Fig. 2(b): Y-parameters Re (Y_{12}) and Z-parameters Re(Z_{12}) at V_{gs}=0.7 V and V_{ds}=0.5 V.

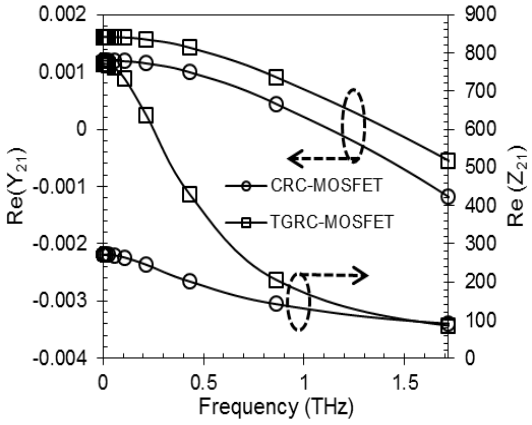


Fig. 2(c): Y-parameters Re(Y_{21}) and Z-parameters Re(Z_{21}) at V_{gs}=0.7 V and V_{ds}=0.5 V.

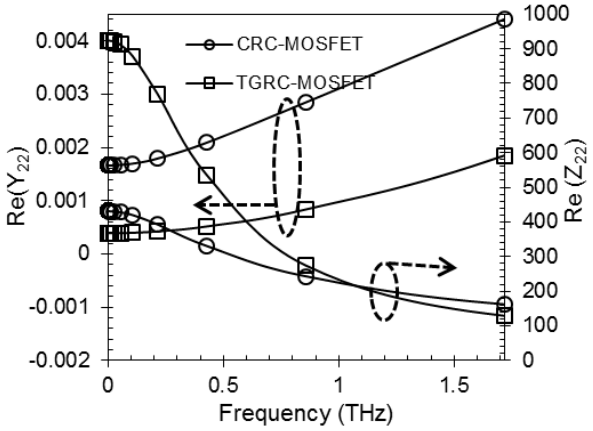


Fig. 2(d): Y-parameters Re(Y_{22}) and Z-parameters Re(Z_{22}) at V_{gs}=0.7 V and V_{ds}=0.5 V.

CONCLUSION

In this paper, small signal behavior has been investigated for Transparent Gate Recessed Channel (TGRC) MOSFET in terms of Y-parameters and Z-parameters. All the results have been compared with conventional one. All Y-parameters (Y_{11}, Y_{12}, Y_{21}, Y_{22}) and Z-parameters (Z_{11}, Z_{12}, Z_{21}, Z_{22}) shows the improved performance when a transparent conducting oxide incorporate in place of metal oxide. Here a transparent conducting oxide known as ITO is used. All simulations have been performed using ATLAS and DEVEDIT 3D device simulator. . Scaling of MOSFETs achieved cut-off frequencies in several THz range making CMOS technology suitable for RF application and wireless communications.

REFERENCES

[1] M. Saito, M. Ono, R. Fujimoto, H. Tanimoto, H. Nobuyuki, T. Yoshitomi. "0.15-m RF CMOS technology compatible with logic CMOS for low-voltage operation". IEEE Trans Electron. Vol.45, pp.737–42, 1998.

[2] L.E. Larson. "Silicon technology tradeoffs for radio-frequency/mixed-signal system-on-a-chip". IEEE Trans Electron.Vol.50, pp.683–99, 2003.

[3] V. Kilchytska, A. Neve, L. Vancaillie, D. Levacq, S. Adriaensen, H.V. Meer, K.D. Meyer, C. Raynaud, M. Dehan, J.P. Raskin, D. Flandre. "Influence of device engineering on the analog and RF performances of SOI MOSFETs". IEEE Trans Electron. Vol.50, pp.577–88, 2003.

[4] J.Y. Yang, K. Benaissa, D. Crenshaw, B. Williams, S. Sridhar, J. Ai, G. Boselli, S. Zhao, S.P. Tang, N. Mahalingam, S. Ashburn, P. Madhani, T. Blythe, H. Shichijo, "0.1 pm RFCMOS on high resistivity. Substrate for system on chip (SOC) applications". IEDM Technol, pp.667–70, 2002.

[5] R. Murali, J.D. Meindle, "Modeling the effect of source/drain junction depth on bulk-MOSFET scaling", Solid-State Electronics. Vol.51, pp.569-574, 2004.

[6] Q. (Brian) Chen. "Compact Modeling of Multi-Gate MOSFETs for RF Designs", IEEE International Wireless Symposium. 2013.

[7] V. Kylchytska, A. Neve, L. Vancaillie, D. Levacq, S. Adriaensen, H. Van Meer, K. DeMeyer, C. Raynaud, M. Dehan, J. P. Ruskin, and D. Flandre. "Influence of Device Engineering on the Analog and RF Performances of SOI MOSFETs". IEEE Trans Electron Device. 50, 577-588.

[8] J. Y. Yang et al. "0.1 pm RFCMOS on high resistivity. Substrate for system on chip (SOC) applications" IEDM Technol Dig 2002:667–70, 2003.

[9] C.H. Doan, S. Emami, A.M. Niknejad, R.W. Brodersen, "Millimeter-wave CMOS design", IEEE J Solid-State Circuits, vol. 40, pp. 144–5, 2005.

[10] ATLAS Device Simulator, SILVACO International 2011.

[11] S. Cho, K. R. Kim, B. G. Park, I. M. Kang, "RF Performance and Small-Signal Parameter Extraction of Junctionless Silicon Nanowire MOSFETs" IEEE Transactions on Electron Devices, vol. 58, no. 5, pp. 1388-1396, May 2011.

Journal of Basic and Applied Engineering Research
Print ISSN: 2350-0077; Online ISSN: 2350-0255; Volume 1, Number 4; October, 2014 pp. 71-74
© Krishi Sanskriti Publications
http://www.krishisanskriti.org/jbaer.html

Biodiesel A Promising Renewable Alternative Fuel

Manish Jain[1], Shashank Mohan[2]

[1]*Department of Mechanical Engineering, RJIT, BSF Academy, Takenpur, Gwalior, India*
[2] *Department of Mechanical Engineering, Delhi Technological University, Bawana Road, Delhi 110042, India*

Abstract: **Demand of engine fuels is increasing tremendously, due to steep rise in the transportation activities. Fossil fuels are being used conventionally but their use results in high global warming, acid rain, ozone depletion and many other problems related to climatic changes and diseases. It is therefore required to find out the alternative fuels in to substitute fossil fuels, which shall be eco-friendly and also reduces import of fossil fuels.**

In this research paper we found that in order to meet the growing energy needs as a consequence of spiraling demand and diminishing supply, in today's world renewable energy and biomass sources mostly biofuels are receiving more attention. The demand for energy has been phenomenon due to the rapid development of certain growing economies, especially in developing countries. It can be concluded that biodiesel can be used as a promising renewable alternative fuel.

Keywords: **Alternative fuel, Biodiesel, Diesel engine, Pollution, Environments**

1. INTRODUCTION

In various western countries, edible vegetable oils have been used as an alternative fuel, in India; it will be very costlier affair to use edible oils as an alternative fuels in place of diesel. Mass production of Non-edible oils can be suitably planned in India, because of availability of large area of waste lands.

Energy is one of the most significant inputs for growth of all sectors including agricultural, industrial service and transport sectors. Energy has been at the centre stage of national & global economic development for several decades. The demand for energy, around the world is increasing exponentially, specifically the demand for petroleum-based energy. Petroleum derived fuels, actually, exceeds the demand of any other fuels or energy resources. The future energy availability is a serious global concern. Another, major global concern is environmental degradation or climate change such as global warming. Global warming is related with the greenhouse gases which are mostly emitted from the combustion of petroleum fuels. In order to control the emissions of greenhouse gases, Kyoto Protocol targets to reduce the greenhouse gas emission by a collective average of 5% below 1990 level of respective countries. The Intergovernmental Panel on Climate Change (IPCC) concludes in the Climate Change 2007 that, because of global warming effect the global surface temperatures are likely to increase by 1.1°C to 6.4°C between 1990 and 2100 [1].

2. INDIAN ENERGY SCENARIO

India had experienced robust growth for the past few years, and after an impressive 9.6 per cent gross domestic product (GDP) growth in 2006-07 the Indian economy is headed towards 8.7 per cent growth in the current fiscal [3]. The energy needs of India are also rising to cope up the growth rate Of the 156.1 million tonnes of crude oil that India consumed in 2007-08, it produced only 34.12 million tonnes [4]. Indian economy is mainly agriculture based and modern agriculture system is heavily dependent upon internal combustion engines for running farm machinery, irrigation pump sets, and other equipments. Indian growth is mainly based on energy, produced by "oil-burning" in IC engines. It is very difficult to find clear blue sky in Indian metropolis. Petroleum fuels are major contributor to ecological imbalance in India. As Indian economy is heavily based upon IC engines, it is not possible in any case to discard them and some other, easily available renewable fuels in India. These renewable fuels must be sought to lease new life to existing engines in order to curb the twin problems of fuel scarcity and air pollution. Various national emission standards have been set by the Government of India through which the fleets are facing greater pressures to switch to cleaner alternative fuels. The alternative fuels are desirable from the fact that they are the only fuels used with recent engine developments, which can meet the stringent EURO-IV emission norms, which are expected to be enforced in India from 2010. India being richer in flora and fauna can look forward to use fuels from bio origin as the suitable alternatives. The prominent bio fuels from Indian perspective are ethanol and biodiesel. India, the world's second most populous nation, has seen its population exploding from 300 million in 1947 to around 1.2 billion today. This rapidly growing population has placed a strain not only on India's infrastructure, but also on its environment. According to the World Health Organization, New Delhi is one of the top ten most polluted cities in the world. Two primary sources of air pollution in India are vehicular emissions and untreated industrial smoke. The number of

vehicles has registered a sharp increase more so, during the last decade. In Delhi alone, the vehicle number has crossed about 4.6 million. Today, the vehicular pollution contributes roughly 64 % of total air pollution in Delhi, followed closely by Mumbai at 52% and somewhat controlled figure of 30% for Kolkata. About 50% of the total petroleum products consumed in the country go into the transport sector mainly in the form of high-speed diesel and gasoline [5]. India's per capita energy use and carbon emissions, while lower than the world average, result in a substantial percentage of world energy use and carbon emissions, due to the country's large population and heavy reliance on fossil fuels. Increased use of renewable energy is one means of reducing carbon emissions.

3. ENERGY DEMAND AND SUPPLY

Energy Security is driven by the demand and supply behaviour. India ranks sixth in the world in terms of energy demand accounting for 3.64% of world commercial energy demand in 2007. Although India ranks fifth in total energy consumption in the world (404.4 MTOE (million tones of oil equivalent), this is only 17.12% of the energy consumed by the largest consumer, i.e. USA (2361.4 MTOE). In per capita terms, its consumption is only about 20% of the global average. Rapid Industrialization and Globalization have pushed the demand of energy to new heights. In the year 2011, India will have a total population of about 1.3 billion people of which 68% will be living in rural areas. Since diesel constitutes 37 % of total petroleum consumption mainly for transportation and other purposes, its demand is integrally related to economic growth and is seen as a growth inducing factor. Stress of the over-burdening population will augment the strain in terms of the volume of fuel required, but the picture of proven oil reserves distribution doesn't reflect the pleasant sight at all. The share with respect to the energy distribution of the remaining oil reserves across the world is shown in Figure 1.

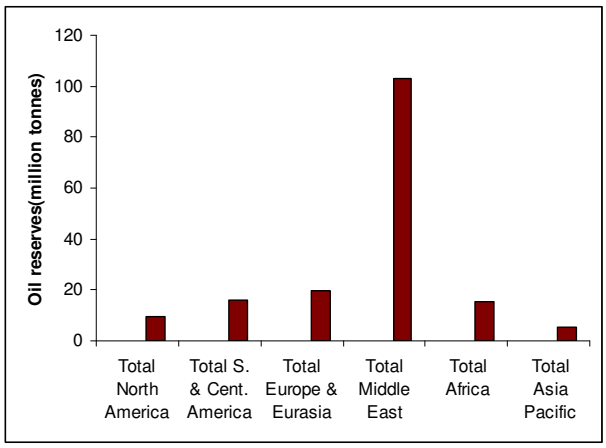


Figure 1: World Oil Reserves, 2008 [6]

As the prices of diesel are escalating and it creates more pollution, its alternative is required which shall be renewable, non-toxic and non-polluting. It is found that biodiesel is one of the most appropriate alternatives to diesel. The biodiesel is renewable, safe, non-toxic and non-polluting. Biodiesel is mainly fatty acid methyl ester and it is derived from triglycerides by transesterification. There are various processes of biodiesel production among which high level of conversion of triglycerides is obtained by transesterification using alkali as catalyst in short duration.

4. ALTERNATE FUELS

To solve dual problems of fossil fuel depletion and environmental degradation, the renewable fuels with lower environmental impact are necessary. Nowadays, many new fuels have been used and biomass derived fuels are among them. Some of the well known biomass derived fuels are ethanol for gasoline engines and bio-diesel for compression ignition engines. Biodiesel is a renewable and environmental friendly alternative fuel for diesel engine which is produced from variety of vegetable oils and animal fats by the trans-esterification process. Transesterification is a chemical reaction in which vegetable oils and animal fats are reacted with alcohol in the presence of a catalyst. The products of reaction are fatty acid alkyl ester and glycerine, and the fatty acid alkyl ester is known as biodiesel. Bio-diesel is an oxygenated fuel containing 10% to 11% oxygen by weight. Also it is a sulphur-free fuel.

These lead biodiesel to more complete combustion and less harmful exhaust emissions. However, biodiesel fuel has higher viscosity, density, pour point, flash point and cetane number than diesel fuel. Also the energy content or net calorific value of biodiesel is about 12% lower than that of diesel fuel on a mass basis. Using biodiesel can help in reducing the world's dependence on fossil fuels and also has significant environmental benefits. Using biodiesel instead of the conventional diesel fuel reduces exhaust emissions such as the overall life circle carbon dioxide (CO_2), particulate matter (PM), carbon monoxide (CO), sulphur oxides (SO_x), volatile organic compounds VOCs), and unburned hydrocarbons (UBHC). However, most of the biodiesels give 10% to 15% higher oxides of nitrogen (NO_x) when fuelling with 100% biodiesel [7]. Depending on the abundantly availability of feedstock in local region, the different feedstocks are tried for the biodiesel production.

In the United States, the primary sources for biodiesel production is soy bean oil, while EU nations prefer to utilize rapeseed oil, and in South East Asia regions, palm oil, coconut oil and Jatropha oil are used for biodiesel productions. Growing the production of biodiesel in many countries around the world has been accompanied by the development of standards to ensure high fuel quality. The biodiesel standards are ASTM D6751 in the United States and EN 14214 in EU

Nations. The properties of biodiesel are mainly determined by the structure of fatty acids alkyl esters which constitutes it, particularly, the combustion characteristics such as ignition quality, and the fuel properties such as density, viscosity, pour point and oxidation stability of biodiesel are mostly affected by the structure of fatty acids alkyl esters [8].

5. BIODIESEL ALTERNATIVE

Biodiesel is defined as the monoalkyl esters of fatty acids derived from vegetable oils or animal fats. It is known as Methyl ester chemically. Biodiesel can be produced when vegetable oil is chemically reacted with an alcohol in presence of catalyst such as Sodium Hydroxide or Potassium Hydroxide. Biodiesel can be produced from Methanol or Ethanol. When biodiesel is made from ethanol, it is called Ethyl Ester and when made from Methanol, it is called Methyl Esters. Due to large price differences, biodiesel is usually made from Methanol. The properties of biodiesel depend on the type of transesterification and the vegetable oil used.

Biodiesel is an organic, non-toxic and biodegradable fuel made from everyday renewable resources, like vegetable oils or animal fats. It can power your car's engine and help the environment at the same time. It doesn't contain any petroleum, so forget about escalating gas prices. Biodiesel cuts down on CO2 emissions; in fact, it's the only alternative fuel to have fully completed the health effects testing requirements of the US Clean Air Act. Biodiesel can be purchased at a growing number of fuelling stations around the world but you can also make it in your own backyard. Even if you don't like chemistry, you can brew your own. The vegetable oils cannot be used directly because of its high viscosity and it can be used after transesterification of oils to esters. [1]

Table 1: summary of proposed BIS (Bureau of Indian Standards) standards for biodiesel [9]

Standard / specification	Unit	Proposed BIS	Standard / specification	Unit	Proposed BIS
Density @ 15°C	g/cm^3	0.87 – 0.90	Methanol	%mass	<=0.02
Viscosity @ 40°C	mm^2/s	3.5 - 5.0	Ester content	%mass	>=96.5
Flash point	°C	>=100	Diglyceride	%mass	<=0.2
Sulphur, max.	%mass	0.035	Triglyceride	%mass	<=0.2
CCR,100%distilation residual	%mass	0.05	Free glycerol	%mass	<=0.02
Sulphated ash,max,	%mass	0.02	Total glycerol	%mass	<=0.25
Water.max	mg/kg	500	Iodine no		<=115
Total contamination, max.	mg/kg	20	Phosphorus	ppm	<=10
Cetane no	-	>=51	Distillation, T 95%	°C	<=360

Table 2: Properties of biodiesel from different oils

Vegetable oil methyl esters	Kinematic viscosity mm^2/s	Cetane no.	LHV MJ/kg	Cloud point (°C)	Pour point (°C)	Flash point °C	Density (kg/l)
Peanut	4.9	54	33.6	5	–	176	0.883
Soya bean	4.5	45	33.5	1	-7	178	0.885
Babassu	3.6	63	31.8	4	–	127	0.875
Palm	5.7	62	33.5	13	–	164	0.880
Sunflower	4.6	49	33.5	1	–	183	0.860
Tallow	–	–	–	12	9	96	–
Diesel	3.06	50	43.8	–	-16	76	0.855
20% Bid-d blend	3.2	51	43.2	–	-16		

Non-hydrogenated or partially hydrogenated oils will be the most common type of oils used in restaurants. Some will use completely hydrogenated oil that is solid at room temperature and should be avoided. Non-hydrogenated oil will have better cold flow properties, but will not store as well without adding stabilizers. Partially hydrogenated oil has a higher "cloud point" but will not oxidize as fast. The difference between non-hydrogenated and partially hydrogenated oil is small and both are treated the same when making biodiesel. Hydrogenation results in the conversion of liquid vegetable oils to solid or semi-solid fats. Complete hydrogenation converts unsaturated fatty acids to saturated ones. Changing the degree of saturation of the fat changes some important physical properties such as the melting point, which is why liquid oils become semi-solid. Since partially hydrogenated vegetable oils are cheaper than animal source fats and are available in a wide range of consistencies, and have other desirable characteristics (e.g., increased oxidative stability). Table 1 gives the summary of proposed BIS (Bureau of Indian Standards) standards for biodiesel.

Most restaurants tend to use partially hydrogenated oil due to cost and longer life of Non-hydrogenated or partially hydrogenated oils will be the most common type of oils used in restaurants. Some will use completely hydrogenated oil that is solid at room temperature and should be avoided. Non-hydrogenated oil will have better cold flow properties, but will not store as well without adding stabilizers. Partially hydrogenated oil has a higher "cloud point" but will not oxidize as fast. The difference between non-hydrogenated and partially hydrogenated oil is small and both are treated the same when making biodiesel. Hydrogenation results in the conversion of liquid vegetable oils to solid or semi-solid fats. Complete hydrogenation converts unsaturated fatty acids to saturated ones.

Changing the degree of saturation of the fat changes some important physical properties such as the melting point, which is why liquid oils become semi-solid. Since partially hydrogenated vegetable oils are cheaper than animal source fats and are available in a wide range of consistencies, and have other desirable characteristics (e.g., increased oxidative stability. Most restaurants tend to use partially hydrogenated oil due to cost and longer life of oil.Table 2 gives the Properties of biodiesel from different oils.

6. CONCLUSIONS

In this work it is observed that the fuel properties of biodiesel need to be monitored when different feedstocks are used. If the fuel properties of biodiesel are compared to petroleum diesel fuel, it can be seen that biodiesel has higher viscosity, density, pour point, flash point and cetane number, near-zero aromatic compound, and no sulphur link make it more suitable than petro-diesel. Keeping the large wasteland available in India a concrete planning is needed to use the vegetable oil biodiesel as a supplement/ substitute for the petro-diesel.

REFERENCES

[1] S.R. Kalbande, S N Pawar & S B Jadhav, " Production of Karanja biodiesel & its utilization in diesel engine generator set for power generation" Karnataka J. Agric. Sci. 20 (3): 680-683 / 2007.

[2] LC Meher, SN Naik & LM Das,"Methanolysis of Pongamia Pinnata (karanja) oil for production of biodiesel" Journal of Scientific and Industrial Research, Vol.63, Nov 2004, pp913-918

[3] Bringi, N. V., (1987). Non-traditional oilseeds and oils in India. Oxford & IBH Publishing Co. Pvt. Ltd, New Delhi

[4] National Oilseeds & vegetable oils development board (NOVOD BOARD), Ministry of Agriculture, Government of India, 2008.

[5] Srivastava A & Prasad R, "Triglycerides based diesel fuels" Renewable & Sustainable Energy Reviews, 4:111-133, 2000

[6] Bobade SN & Khyade VB, " Detail Study on the properties of Pongamia Pinnata (Karanja) for the production of biofuel" Research Journal of Chemical Sciences Vol.2 (7), 16-20, July,2012

[7] D.H. Qi,L.M. Geng, H. Chen,Y.ZH. Bian, J. Liu, X.CH. Ren. "Combustion and performance evaluation of a diesel engine fuelled with biodiesel produced from soybean crude oil." Renewable Energy 34 (2009), 2706–2713

[8] Avinash Kumar Agawal. "Biofuels (alcohols and biodiesel) applications as fuels for internal combustion engines." Progress in Energy and Combustion Science 33 (2007), 233–271.

[9] D. N. Tewari, Report of the committee on development of BIO-FUEL, New Delhi, 2003 (43 - 109)

[10] B. K. Barnwal, M.P. Sharma, Prospects of biodiesel production from vegetable oils in India, Renewable and Sustainable Energy Reviews, 9 (2005) 363–378.

[11] Suresh D. Mane and N. Nagesha, "Renewable Energy Technologies for Carriage Repair Shops: A Case Study of Two Workshops" The International Journal of Engineering And Science, Vol. 1(2) (2012), 324-331

Journal of Scientific and Innovative Research 2015; 4(3): 127-130
Available online at: www.jsirjournal.com



Research Article

ISSN 2320-4818
JSIR 2015; 4(3): 127-130
© 2015, All rights reserved
Received: 29-04-2015
Accepted: 16-07-2015

Amit Pal
Department of Mechanical Engineering, Delhi Technological University, Bawana Road, Delhi 110042, India.

Raj Kumar Singh
Department of Mechanical Engineering, Delhi Technological University, Bawana Road, Delhi 110042, India.

Shashank Mohan
Department of Mechanical Engineering, Delhi Technological University, Bawana Road, Delhi 110042, India.

Correspondence:
Amit Pal
Department of Mechanical Engineering, Delhi Technological University, Bawana Road, Delhi 110042, India.

Biodiesel Conversionionof high FFA Neem oil by blending it with low FFA Sesame oil

Amit Pal, Raj Kumar Singh, Shashank Mohan

Abstract

Biodiesel is a clean, renewable fuel and may be considered as a potential option to supplement fossil-based fuels. It is deduced from a variety of edible and non-edible vegetable oils, animal fats, waste cooking oil and animal fat, etc. Non-edible vegetable oils are second generation feedstocks and a better alternative to edible feed crops for biodiesel production.This paper deals with production of Biodiesel from the oils of Sesame (*Sesamum indicum* L.) and Neem (*Azadirachta indica*) which are available in India and other parts of the world. Neem oil is non edible oil having very high free fatty acid (FFA) content. It requires pre-treatment neutralization step before undergoing the alkali catalyzed transesterification process, very high alcohol to oil molar ratio and comparatively larger reaction time needed to obtain sustainable yield of biodiesel. Sesame oil is an edible oil mainly used in pharmaceuticals due to its medicinal properties and has low FFA content. These two oils, one having very high FFA content and other having low FFA content are mixed in suitable proportions and this mixture is transesterified without the pre-treatment process at a molar ratio of 6:1. A significant conversion yield is achieved by mixing the feedstocks before transesterification reaction.

Keywords: Neem oil, Sesame oil, Free Fatty Acid, Transesterification

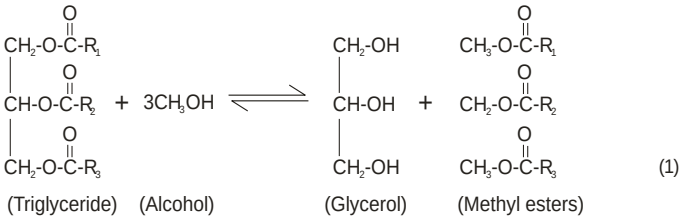
Introduction

The scarcity of world petroleum reserves, their uneven distribution, growing emissions of combustion-generated pollutants, uncertainties in its supply, rising prices and dramatic increase in an energy demand due to rapid industrialization may lead to severe energy crisis in near future[1]. A major part of the energy demand (about 88.6%) is fulfilled by fossil fuels, in which crude oil accounts for 33.7% [2]. With consumption rates of 4 billion tonnes a year, the oil deposits will be exhausted by 2052[3]. Biodiesel is the mixture of mono alkyl esters of long chain fatty acids, suitable for use in compression ignition engines[4]. The plant oils usually contain free fatty acids, phospholipids, sterols, water, odorants and other impurities. Due to these the oil cannot be used as fuel directly. To overcome these problems the oil requires slight chemical modification through transesterification, pyrolysis and emulsification[5]. Unlike fossil fuel, biodiesel contains a significant amount of oxygen in its molecular structure which helps in speeding up the combustion of fuel in compression ignition engines, resulting decrement in the emission of carbon monoxide (CO), soot etc[6]. Presently, more than 95% of biodiesel production feedstocks comes from edible oils since they are mainly produced in many regions. The properties of biodiesel produced from these oils are much suitable to be used as a diesel fuel substitute[6-7]. However the use of edible vegetable oils may jeopardize food supplies and biodiversities. Thus, non-edible oils are considered potential substitutes of edible food crops for biodiesel production[8]. A two-step transesterification process and longer time are required for transesterification of nonedible oils containing high FFA content.

Transesterification reaction is shown in Eq. (1). The catalysts used in transesterification reaction are mainly of three types: alkalis, acids and enzymes[9-11]. Due to faster transesterification reaction, less corrosive action of an alkaline catalyst to industrial equipment and requirement of low methanol to oil molar ratio, most commercial transesterification reactions are carried with alkali catalyst[12-13]. However, alkali catalysts have limitation for high FFA containing oils leading to soap formation, higher consumption of the catalyst and reduction in biodiesel yield[14]. The typical soap formation (saponification) reaction with alkali catalyst NaOH is shown in Eq. (2). Moreover, the alkali catalysts are highly hygroscopic and absorbs water from air during storage. Water is also formed during the

saponification reaction. Water retards the transesterification reaction through the hydrolysis reaction. It can hydrolyze the triglycerides to diglycerides and forms more FFA[14-15]. The typical hydrolysis reaction is shown in Eq. (3). Acid catalyst directly converts free fatty acid present in raw vegetable oils into biodiesel avoiding undesirable saponification reaction as shown in Eq. (4).

Non edible oil (containing high fatty acids more than 2.5%) is first neutralized in the presence of an acid and then undergoes alkali catalyzed transesterification reaction. Even after pre-treatment or neutralization of free fatty acids, the yield of biodiesel produced from high FFA oils is comparatively much less than that for biodiesel produced from oils with low FFA content. Figure 1 shows the flowchart of a commonly used alkali catalyzed transesterification process.

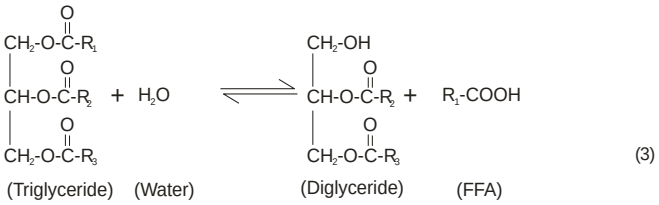


(1)

$$R_1COOH + NaOH \rightarrow R_1COONa + H_2O$$

(FFA) (Sodium hydroxide) (Soap) (Water)

(2)



(3)

$$R_1 - COOH + ROH \xrightarrow{H^+} R_1COONa + H_2O$$

(FFA) (Alcohol) (Soap) (Water)

(4)

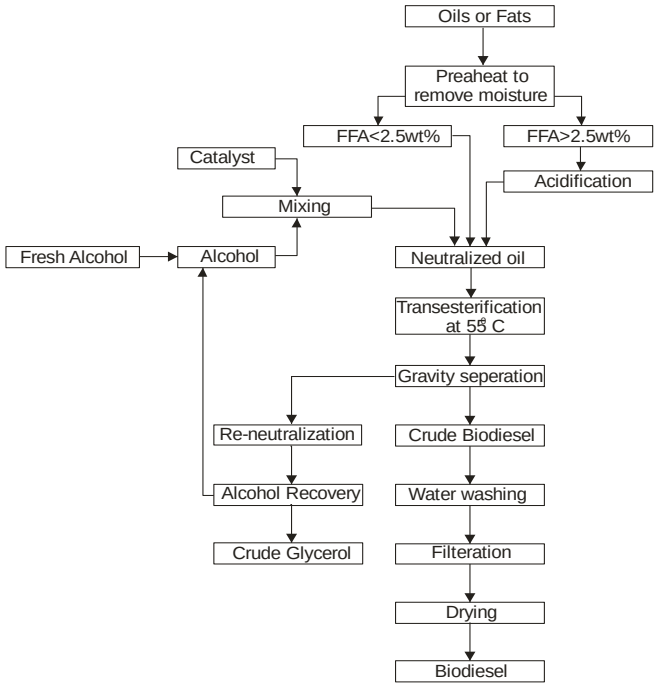


Figure 1: Process flow chart of alkali catalyzed biodiesel production

Material and Methods

Neem (*Azadirachta indica*) is a medium sized evergreen tree from the *Meliaceae* family. Neem trees are usually grown in several Asian countries and thrive well in areas with sub-arid to sub-humid conditions and with an annual rainfall of 400-1200 mm. Oil is extracted mainly from seeds. Neem seeds contain 20-30 wt. % oil, and its kernel contains 40-50% brown oil[8]. Neem oil is having very high FFA content. Neem seeds are available in huge quantity, which are mainly used for medicinal purposes and a large part of it remain untapped which can be utilised for biodiesel production.

Sesame is an oilseed herbacaceous crop of the Pedliaceace family, which is widely cultivated in many parts of the world, primarily in tropical and sub-tropical parts of the world and has recently been adapted to semi arid regions [15-16]. Sesame seeds contains 57-63 wt. % oil [17]. Neem oil and Sesame oil are extracted by mechanical pressing. The fruits are collected in a drum, and the kernels are separated to obtain the seeds. The crude oil is filtered to remove impurities and obtain pure oil. The various properties of Neem oil and sesame oil were analysed by the methods described by the association of Official Analytical Chemists [18]. These properties are given in Table 1. The densities of two oils are similar and their mixture can be formed by simple mechanical stirring for 2-3 minutes.

The FFA value of oil is calculated similarly to the basis of acid-base-titration neutralization reaction except that the base is titrated against oil, instead of an acid against the base. The FFA content of neem oil and sesame oil were found to be 15.4 and 0.28 respectively. Sesame oil contains sesamin and sesaminollignans in its nonglycerol fraction, which are known to play an important role in the oxidative stability [16].

Experimental work

Experiments were carried out for molar ratio of 6:1 for 1%, 1.5% & 2% catalyst KOH by weight of oil. Each catalyst is used with 3 mixtures of Neem and sesame oil taken in ratios of 30:70, 50:50 and 70:30. The three oil mixture are heated upto 120-130 °C and kept at this temperature for about 5-7 minutes to remove moisture present in oil to avoid soap formation and allowed to cool upto 65°C. 22 gm methanol and KOH (1%, 1.5% and 2% weight of oil) are mixed and stirred until entire Potassium hydroxide dissolves in methanol. This liquid mixture is then mixed with oil in a beaker placed on a hot plate of mechanical stirrer and the temperature of sample is maintained around 550C during the reaction time period of 30 min, 45min, 60 min and 75 min. A magnetic capsule is dipped in the mixture and rotated with the help of mechanical stirrer. After completing the process of mechanical stirring, the sample is poured into a separation flask for 2-3 hour for the separation. Methyl esters were separated from glycerol by means of gravity separation and finally water washed to remove soap and residual catalyst to obtain pure biodiesel. The properties of biodiesel so obtained for different mixture ratios along with properties of diesel are given in table 1.

Table 1: Properties of Raw oil, Biodiesel and Diesel

Property	Neem oil	Seasme oil	Acceptable limit for diesel engine	Diesel	Biodiesel N:S(30:70)	Biodiesel N:S(50:50)	Biodiesel N:S(70:30)
Fuel standard	ASTM D 6751	ASTM D 6751	-	ASTM D 975	ASTM D 6751	ASTM D 6751	ASTM D 6751
Density at 15°C(kg/m^3)	961	923	860-900	830	889	894	898
Viscosity at 40°C x10^{-6} (m^2/s)	22.75	39.97	2.5-6	2.86	4.56	4.64	4.78
Calorific value (MJ/kg)	35.90	40.20	-	42	38.20	37.98	37.85
Sulphur content (ppm)	88	75	Max 350	350	86	82	76
Flash Point (°C)	259	230	Min 100	51	208	204	202

Results

Figure 2 shows biodiesel yield from neem oil, sesame oil and their mixtures in different proportions at 2%, 1.5 % and 1 % catalyst concentration. The yield of biodiesel from these samples were calculated at reaction time periods of 30 min, 45min, 60 min and 75 min at 6:1 alcohol to oil molar ratio.

2% Catalyst

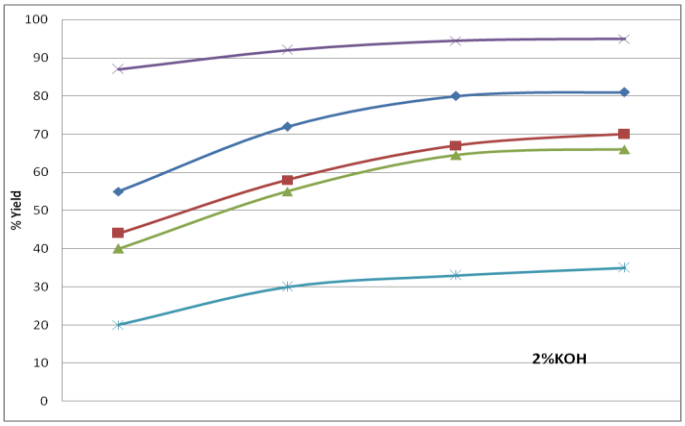
Variation of % yield achieves a linear trend with increase in reaction time and almost maximum yields were obtained at 75 minutes of reaction time for all blends. Biodiesel yield for pure sesame oil (95%) was approximately 63% higher than that for pure neem oil, 30.5 % than that for 70:30 mixture of Neem and Sesame oil, 26.3% than that for 50:50 mixture of Neem and Sesame oil and 14.7% than that for 30:70 mixture of Neem and Sesame oil.

1.5 %Catalyst

Variation of % yield achieves a linear trend with increase in reaction time and almost maximum yields were obtained at 75 minutes of reaction time for all blends. Biodiesel yield for pure sesame oil (97%) was approximately 74.2% higher than that for pure neem oil, 36 % than that for 70:30 mixture of Neem and Sesame oil, 33% than that for 50:50 mixture of Neem and Sesame oil and 23.1% than that for 30:70 mixture of Neem and Sesame oil.

1% Catalyst

Variation of % yield achieves a linear trend with increase in reaction time and almost maximum yields were obtained at 75 minutes of reaction time for all the blends. Biodiesel yield for pure sesame oil (99%) was approximately 52.5% higher than that for pure neem oil, 30.5 % than that for 70:30 mixture of Neem and Sesame oil, 44.4% than that for 50:50 mixture of Neem and Sesame oil and 30.3% than that for 30:70 mixture of Neem and Sesame oil.



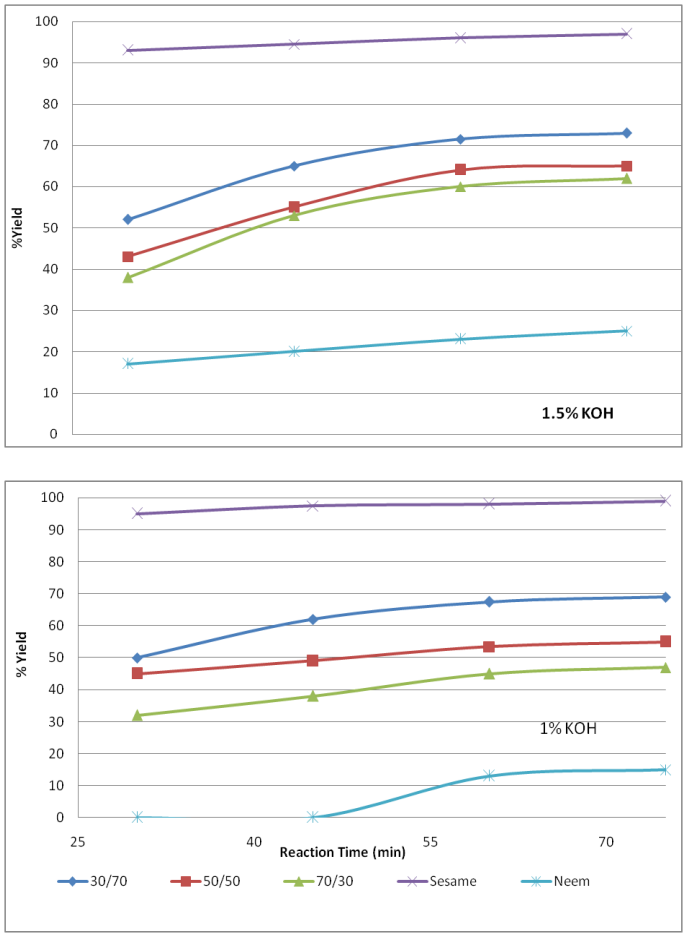


Figure 2: % yield of Biodiesel Production

Discussion

Neem oil and the 3 oil mixtures have high FFA content and the yield of biodiesel produced from the blends increases with increase in catalyst concentration. However Sesame oil has very low FFA content its biodiesel obtained is maximum (upto 99%) for 1 % catalyst and the yield progressively decreases with increase in catalyst concentration. A maximum of 81 % yield is obtained with 30:70 Neem and Sesame oil mixture in single step transesterification reaction with 2% catalyst concentration as shown in figure 3. This is well above 50.78% yield obtained for pure neem oil in two step transesterification rection carried by Mazloom Shah[19]. A statistical model predicted the highest conversion yield of sesame oil to biodiesel as 99.71% and actual yield was 98.36% in an experiment conducted by Eriola Betiku[20].

Conclusion

Mixing of two oils, one with low FFA content (Sesame) and one with high FFA content (Neem) results in a mixture of moderate FFA content. Appreciable yields of biodiesel is obtained from the mixture in one step transesterification reaction. Approximately 81 % biodiesel was obtained with 30:70 ratio of Neem and Sesame oil at 75 minute reaction time with 2 % catalyst concentration at 6:1 alcohol to oil molar ratio. Thus, high FFA non edible oils can be easily converted into biodiesel with a Low FFA oil. This method may prove to be economic and environmental friendly, requiring lower reaction time and low catalyst concentration and simultaneously eliminating the need for pre-treatment process.

Acknowledgment

Authors are thankful to the Delhi Technological University and Goverment of Delhi for financing the lab infrastructure and materials.

Conflict of interest

There is no conflict of interest involved in this work.

References

1. Sensoz S., Angin D., Yorgun S.. Influence of particle size on the pyrolysis of rapeseed (Brassica napus L.): fuel properties of bio-oil. Biomass Bioenerg. 2000; 19:271–279.

2. https://www.academia.edu/6747863/production_and_comparison_of_fuel_properties_engine_performance_and_emission_characteristics_of_biodiesel_from_various_nonedible_vegetable_oils_A_review. Accessed on 20thMarch2015 (4:30 PM).

3. CIA World Factbook. <https://www.cia.gov/library/publications/the-world-factbook/geos/af.html> (2013). Accessed on 21thMarch2015 (11 AM).

4. Bijalwan A., Bio-diesel Revolution. Science Reporter. January 2006; 14–17.

5. Murugesan A., Umarani C., Chinnusamy T.R., Krishnan M., Subramanian R., Neduzchezhain N.. Production and analysis of bio-diesel from non-edible oils—A review. Renew Sust Energ Rev. 2009; 13:825-834.

6. Lee S.B., Lee J.D., Hong I.K.. Ultrasonic energy effect on vegetable oil based biodiesel synthetic process. J Ind Eng Chem. 2011; 17:138-143.

7. Gui M.M., Lee K.T., Bhatia S.. Feasibility of edible oil vs. non-edible oil vs. waste edible oil as biodiesel feedstock. Energy.2008; 33:1646–53.

8. Ashraful A.M., Masjuki H.H., Kalam M.A., Rizwanul Fattah I.M., Imtenan S., Shahir S.A., Mobarak H.M.. Production and comparison of fuel properties, engine performance, and emission characterstics of biodiesel from various non-vegetable oils: A review. Energ Convers Manage. 2014; 80:202-228.

9. Canakci M., Van Gerpen J.. Biodiesel production via acid catalysis. Trans Am Soc Agric Eng. 1999; 42:1203–10.

10. Nelson L., Foglia T., Marmer W.. Lipase-catalyzed production of biodiesel. J Am Oil Chem Soc. 1996; 73:1191–5.

11. Shimada Y., Watanabe Y., Samukawa T., Sugihara A., Noda H., Fukuda H.. Conversion of vegetable oil to biodiesel using immobilized Candida Antarctica lipase. J Am Oil Chem Soc. 1999; 76:789–93.

12. Agarwal A.K.. Biofuels (alcohols and biodiesel) applications as fuels for internal combustion engines. Prog Energ Combust. 2007; 33:233–271.

13. Soriano Jr N.U., Venditti R., Argyropoulos D.S.. Biodiesel synthesis via homogeneous Lewis acid-catalyzed transesterification. Fuel. 2009; 88:560–5.

14. Abebe K.E., Yohannes K., Rolando Z.. Heterogeneous catalysis for biodiesel production from Jatropha curcas oil (JCO). Energy. 2011; 36: 2693-2700.

15. Elleuch M., Besbes S., Roiseux O., Blecker C. Attia H.. Quality characterstics of sesame seeds and by products. Food Chem. 2007; 103:641-650.

16. Wu H.N.. The contents of lignans in commercial sesame oils of Taiwan and their changes during heating. Food Chem. 2007; 104:34-344.

17. Tunde-Akintunde T.Y., Akintunde B.O.. Some physical properties of sesame seed. Biosystems Eng. 2004; 88(1):127-129.

18. Aransiola E., Betiku E., Layokun S., Solomon B.. Production of biodiesel by transesterification of refined soybean oil. Int J Biol Chem Sci. 2010; 4(2):391-399.

19. Shah M., Tariq M., Ali S., Guo Q.X.. Transesterification of jojoba oil, sunflower oil, neem oil, rocket seed oil and linseed oil by tin catalysts. Biomass Bioenerg. 2014; 70:225-229.

20. Betiku E., Adepoju T.F.. Methanolysis optimization of sesame (Sesamum indicum) oil to biodiesel and fuel quality characterization. Int. J. Energy Environ Eng. 2013; 4:10.1186/2251-6832-4-9.

EUROPEAN JOURNAL OF PURE AND APPLIED MATHEMATICS
Vol. 8, No. 4, 2015, 469-477
ISSN 1307-5543 – www.ejpam.com

$\mathscr{C}$-cycle Compatible Splitting Signed Graphs $\mathfrak{S}(S)$ and $\Gamma(S)$

Rashmi Jain [1,*], Sangita Kansal[1], Mukti Acharya[2]

[1] *Department of Applied Mathematics, Delhi Technological University, Delhi, India*
[2] *Department of Mathematics, Kalasalingam University, KrishnanKoil, India*

Abstract. A *signed graph* (or, in short, *sigraph*) $S = (S^u, \sigma)$ consists of an underlying graph $S^u := G = (V, E)$ and a function $\sigma : E(S^u) \longrightarrow \{+, -\}$, called the signature of S. A *marking* of S is a function $\mu : V(S) \longrightarrow \{+, -\}$. The *canonical marking* of a signed graph S, denoted μ_σ, is given as

$$\mu_\sigma(v) := \prod_{vw \in E(S)} \sigma(vw).$$

The *splitting signed graph* $\mathfrak{S}(S)$ of a signed graph S is formed as follows:

- Take a copy of S and for each vertex v of S, take a new vertex v'. Join v' to all vertices $u \in N(v)$ by negative edge, if $\mu_\sigma(u) = \mu_\sigma(v) = -$ in S and by positive edge otherwise.

The *splitting signed graph* $\Gamma(S)$ of a signed graph S is formed as follows:

- Take a copy of S and for each vertex v of S, take a new vertex v'. Join v' to all vertices $u \in N(v)$ and assign $\sigma(uv)$ as its sign. Here, $N(v)$ is the set of all adjacent vertices to v.

A signed graph is called *canonically consistent (or $\mathscr{C}$-consistent)* if its every cycle contains even number of negative vertices with respect to its canonical marking. A marked signed graph S is called *cycle-compatible* if for every cycle Z in S, the product of signs of its vertices equals the product of signs of its edges. A signed graph S is *$\mathscr{C}$-cycle compatible* if for every cycle Z in S,

$$\prod_{e \in E(Z)} \sigma(e) = \prod_{v \in V(Z)} \mu_\sigma(v).$$

In this paper, we establish a structural characterization of signed graph S for which $\mathfrak{S}(S)$ and $\Gamma(S)$ are isomorphic and $\mathscr{C}$-cycle compatible.

2010 Mathematics Subject Classifications: 05C22; 05C75

Key Words and Phrases: canonical marking, splitting signed graph, $\mathscr{C}$-consistent, $\mathscr{C}$-cycle compatible, $\mathscr{C}$-sign compatible

*Corresponding author.

Email addresses: rashmi2011f@gmail.com (R. Jain), sangita_kansal15@dce.ac.in (S. Kansal), mukti1948@gmail.com (M. Acharya)

 © 2015 EJPAM All rights reserved.

1. Introduction

A *graph* is an ordered pair $G = (V, E)$, where $V = V(G)$ is a set of *vertices or points* of G and $E = E(G)$ is a collection of pairs of vertices of G, called *edges or lines* of G. For graph theoretical terminology, we refer to [2]. All graphs considered in the paper are finite, simple and connected.

A *signed graph* is an ordered pair $S = (S^u, \sigma)$, where $S^u := G = (V, E)$ is a graph called the underlying graph of S and $\sigma : E(S^u) \longrightarrow \{+, -\}$ is a function, called the *signature* of S. In other terms, we say that the edges are *signed* by σ. In a pictorial representation of a signed graph S, its positive edges are shown as bold line segments ('Jorden curves' drawn on the plane) and negative lines as broken line segments as shown in Figure 1. $E^+(S) = \{e \in E(S^u) : \sigma(e) = +\}$ and $E^-(S) = \{e \in E(S^u) : \sigma(e) = -\}$. The elements of $E^+(S)$ ($E^-(S)$) are called *positive* (*negative*) *edges* of S and the set $E(S) = E^+(S) \cup E^-(S)$ is called the edge set of S.

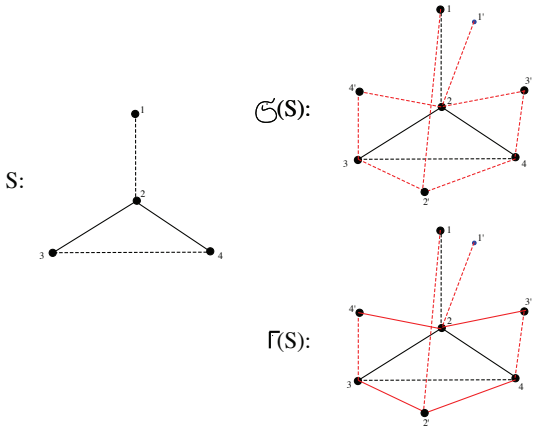


Figure 1: A signed graph S and its splitting signed graphs $\mathfrak{G}(S)$ and $\Gamma(S)$

A signed graph in which all the edges are positive, is called *all-positive signed graph* (*all-negative signed graph* is defined similarly). A signed graph is said to be *homogeneous* if it is either all-positive or all-negative and *heterogeneous* otherwise. By $d(v)$, we denote degree of $v \in V(S)$, $d(v) = d^+(v) + d^-(v)$, here $d^+(v)$ ($d^-(v)$) denotes the positive (negative) degree of v.

A *marking* of S is a function $\mu : V(S) \longrightarrow \{+, -\}$. Sampathkumar in [4] introduced the idea of marking derived from the signs of edges incident to vertices, given as

$$\mu_\sigma(v) := \prod_{vw \in E(S)} \sigma(vw).$$

This marking is called canonical marking. Clearly, $\mu_\sigma(v) = +$ if $d^-(v)$ is even and $\mu_\sigma(v) = -$ if $d^-(v)$ is odd. Thus, in canonical marking of a signed graph, we assign + sign to a vertex if its negative degree is even and - sign if its negative degree is odd. In this paper, a vertex v of $d^-(v) =$ even (odd) is called *positive* (*negative*) *vertex*.

Signed graphs S_1 and S_2 are called *isomorphic*, written as $S_1 \cong S_2$, if there is a graph isomorphism $f : S_1^u \to S_2^u$ that preserves edge signs.

A cycle in a signed graph is said to be *positive (negative) cycle* if the product of the signs of its edges is positive (negative), i.e., its an even (odd) number of edges are negative. A signed graph is said to be *balanced* if every cycle in it is positive (*see* [3]).

A cycle in a marked signed graph is said to be *consistent* if its an even number of vertices are negative and a marked signed graph is called consistent if its all cycles are consistent (*see* [6]). Similarly, a cycle in a signed graph is said to be *canonically consistent (or $\mathscr{C}$-consistent)* if for every cycle in S, the product of signs of its vertices with respect to canonical marking, is positive, i.e., its an even number of vertices are negative and a signed graph is called $\mathscr{C}$-consistent if its all cycles are $\mathscr{C}$-consistent.

A marked signed graph S is called *cycle-compatible* if for every cycle Z in S, the product of signs of its vertices equals the product of signs of its edges. A signed graph S is called *canonically cycle* (or *$\mathscr{C}$-cycle*) *compatible* if for every cycle Z in S,

$$\prod_{e\in E(Z)} \sigma(e) = \prod_{v\in V(Z)} \mu_\sigma(v).$$

A signed graph $S = (S^u, \sigma)$ is said to be *sign-compatible* [6] if it has a vertex marking μ such that every edge $e = uv$ has $\sigma(e) = -$ if and only if $\mu(u) = \mu(v) = -$. If the canonical marking μ_σ has this property, then S is said to be *canonically sign-compatible (or $\mathscr{C}$-sign-compatible)*.

2. Splitting Signed Graphs

Sampathkumar and Walikar introduced the concept of *splitting graph* of a graph in [5]. The splitting graph of a graph G, denoted here $\mathfrak{S}(G)$, is formed as follows:

Take a copy of G and for each vertex v of G, take a new vertex v'. Join v' to all adjacent vertices of v.

There are two notions of *splitting signed graphs* of a signed graph $S = (S^u, \sigma)$ in the literature, viz., $\mathfrak{S}(S)$ and $\Gamma(S)$, both of which have $\mathfrak{S}(S^u)$ as their underlying graph; only the rule to assign signs to the edges of $\mathfrak{S}(S^u)$ differ. An edge uv' in $\mathfrak{S}(S)$ is negative whenever u and v are negative vertices of S and an edge uv' in $\Gamma(S)$ is negative whenever uv is a negative edge of S as reported in [1] and [7] respectively.

A signed graph S is called a $\mathfrak{S}$-splitting (Γ-splitting) signed graph if there exists a signed graph T such that S is isomorphic to $\mathfrak{S}(T)$ ($\Gamma(T)$).

Theorem 1 (Acharya *et al.*[1]). *Following statements hold:*

(i) If $v \in V(S)$ is a positive vertex then $v, v' \in V(\mathfrak{S}(S))$ are positive.

(ii) If $v \in V(S)$ is a negative vertex having an even (odd) number of negative vertices in its neighbourhood then $v \in V(\mathfrak{S}(S))$ is negative (positive) vertex and v' is of opposite sign to v.

Here v' is the vertex as defined above.

Theorem 2 (Acharya *et al.* [1]). *$\mathcal{G}(S)$ is balanced if and only if the following conditions hold in S:*

(i) S is balanced and;

(ii) S does not contain a homogeneous path P_3 of marking +, -, - and the marking of a heterogeneous path P_3 is +, -, - only.

Lemma 1 (Sinha *et al.* [7]). *The following statements hold in $\Gamma(S)$:*

(i) If $v \in V(S)$ is any vertex then $v \in V(\Gamma(S))$ is positive.

(ii) If $v \in V(S)$ is a negative vertex then $v' \in V(\Gamma(S))$ is negative.

Theorem 3 (Sinha *et al.* [7]). *The splitting signed graph $\Gamma(S)$ of a signed graph S is balanced if and only if S is balanced.*

Figure 1 illustrates a signed graph S and its splitting signed graphs $\mathcal{G}(S)$ and $\Gamma(S)$.

3. Main Results

Theorem 4. *For a signed graph S, $\mathcal{G}(S) \cong \Gamma(S)$ if and only if S is any one of the following:*

(i) All-positive or;

(ii) All-negative in which degree of each vertex is odd or;

(iii) Heterogeneous in which end vertices of every negative (positive) edge are (are not) negative.

Proof. Necessity: Let, for a signed graph S, $\mathcal{G}(S) \cong \Gamma(S)$. Since S is a subsignedgraph of $\mathcal{G}(S)$ and $\Gamma(S)$, we concentrate our attention only on the sign of edge uv' in $\mathcal{G}(S)$ and $\Gamma(S)$. By the definition of $\mathcal{G}(S)$, $uv' \in E^-(\mathcal{G}(S))$ if and only if $u, v \in V(S)$ are negative and by the definition of $\Gamma(S)$, $uv' \in E^-(\Gamma(S))$ if and only if $uv \in E^-(S)$. Therefore, we have following three possible cases:

Case I: If $\mathcal{G}(S) \cong \Gamma(S)$ and both $\mathcal{G}(S)$ and $\Gamma(S)$ are all-positive then no edge of S will be negative. Hence, **(i)** follows.

Case II: If $\mathcal{G}(S) \cong \Gamma(S)$ and both are all-negative then every edge and every vertex of S will be negative. Hence, **(ii)** follows.

Case III: If $\mathcal{G}(S) \cong \Gamma(S)$ and both are heterogeneous then S will be heterogeneous and edge uv' in both $\mathcal{G}(S)$ and $\Gamma(S)$ must be of the same sign. This implies that end vertices of every negative (positive) edge of S are (are not) negative. Hence, **(iii)** follows.

Thus, the necessity follows.

Sufficiency: Suppose S is any one of the following:

(i) All-positive or;

(ii) All-negative in which degree of each vertex is odd or;

(iii) Heterogeneous in which end vertices of every negative (positive) edge are (are not) negative.

then by the definitions $\mathcal{S}$ - and Γ- splitting signed graphs, we obtain following results:

Case I: If S is all-positive then $\mathcal{S}(S)$ and $\Gamma(S)$ will be all-positive and $\mathcal{S}(S) \cong \Gamma(S)$.

Case II: If S is all-negative in which degree of each vertex is odd then $\mathcal{S}(S)$ and $\Gamma(S)$ will be all-negative and $\mathcal{S}(S) \cong \Gamma(S)$.

Case III: If S is heterogeneous in which end vertices of every negative (positive) edge are (are not) negative then $\mathcal{S}(S)$ and $\Gamma(S)$ will be heterogeneous as S be a subsignedgraph of $\mathcal{S}(S)$ and $\Gamma(S)$ and edge uv' in both $\mathcal{S}(S)$ and $\Gamma(S)$ will be of the same sign. Hence, $\mathcal{S}(S) \cong \Gamma(S)$.

This completes the proof. □

Corollary 1. *For a signed graph S, $\mathcal{S}(S) \cong \Gamma(S)$ if and only if S is $\mathscr{C}$-sign compatible.*

Theorem 5. *$\mathcal{S}(S)$ is $\mathscr{C}$-cycle compatible if and only if the following conditions hold in S:*

(i) if Z is a positive (negative) cycle then an even (odd) number of negative vertices of cycle Z contain even numbers of negative vertices in their neighbourhoods and;

(ii) for a path $P_3 = (u, v, w)$, any one condition holds:

- *it is homogeneous of marking +, +, +;*
- *it is heterogeneous of marking +, -, +;*
- *it is homogeneous (heterogeneous) of marking -, +, + or -, -, + and $N(u)$ contains an odd (even) number of negative vertices;*
- *it is homogeneous (heterogeneous) of marking -, +, - and vertices u, w are (are not) of same parity (i.e., $N(u)$ and $N(w)$ contain even number of negative vertices or odd number of negative vertices);*
- *it is homogeneous (heterogeneous) of marking -, -, - and vertices u, w are not (are) of the same parity.*

Proof. Necessity: Let $\mathcal{S}(S)$ be $\mathscr{C}$-cycle compatible. Therefore, every cycle in $\mathcal{S}(S)$ is either positive and $\mathscr{C}$-consistent or negative and $\mathscr{C}$-inconsistent. By Theorem 1, every positive vertex of S is positive in $\mathcal{S}(S)$ and every negative vertex of S having an even (odd) number of negative vertices in its neighbourhood is negative (positive) in $\mathcal{S}(S)$. Since S is subsignedgraph of $\mathcal{S}(S)$, if Z is a positive (negative) cycle of S then Z must be $\mathscr{C}$-consistent ($\mathscr{C}$-inconsistent) in $\mathcal{S}(S)$, i.e., an even (odd) number of negative vertices of cycle Z must contain an even numbers of negative vertices in their neighbourhoods. Thus, **(i)** follows.

By the definition of $\mathcal{S}(S)$, a path $P_3 = (u, v, w)$ of S induces a cycle $C_4 = (u, v, w, v')$ in $\mathcal{S}(S)$. The marking of path $P_3 = (u, v, w)$ may be one of the following:

1. +, +, + 2. +, -, + 3. -, +, + 4. -, -, + 5. -, +, - 6. -, -, -

Hence, the following cases arise:

- if marking of path $P_3 = (u, v, w)$ is +, +, + then by Theorem 1, vertices u, v, w, v' have signs +, +, +, + respectively in $\mathfrak{S}(S)$. Thus, path P_3 induces a $\mathscr{C}$-consistent cycle C_4 in $\mathfrak{S}(S)$. By Theorem 2, this cycle C_4 is positive (negative) if and only if P_3 is homogeneous (heterogeneous). Since $\mathfrak{S}(S)$ is $\mathscr{C}$-cycle compatible, P_3 will be homogeneous.

- if marking of path $P_3 = (u, v, w)$ is +, -, + then by Theorem 1, vertices u, v, w, v' have signs +, -, +, + or +, +, +, - respectively in $\mathfrak{S}(S)$. Thus, path P_3 induces a $\mathscr{C}$-inconsistent cycle C_4 in $\mathfrak{S}(S)$. By Theorem 2, this cycle C_4 is positive (negative) if and only if P_3 is homogeneous (heterogeneous). Since $\mathfrak{S}(S)$ is $\mathscr{C}$-cycle compatible, P_3 will be heterogeneous.

- if marking of path $P_3 = (u, v, w)$ is -, +, + and $N(u)$ contains an odd (even) number of negative vertices then by Theorem 1, vertices u, v, w, v' have signs +, +, +, + (-, +, +, +) respectively in $\mathfrak{S}(S)$. Thus, path P_3 induces a $\mathscr{C}$-consistent ($\mathscr{C}$-inconsistent) cycle C_4 in $\mathfrak{S}(S)$. By Theorem 2, this cycle C_4 is positive (negative) if and only if P_3 is homogeneous (heterogeneous). Since $\mathfrak{S}(S)$ is $\mathscr{C}$-cycle compatible, for homogeneous (heterogeneous) P_3, $N(u)$ must contain an odd (even) number of negative vertices.

  Similarly, if marking of path $P_3 = (u, v, w)$ is -, -, + and $N(u)$ contains an even (odd) number of negative vertices then by Theorem 1, vertices u, v, w, v' have signs -, -, +, + or -, +, +, - (+, -, +, + or +, +, +, -) respectively in $\mathfrak{S}(S)$. Thus, path P_3 induces a $\mathscr{C}$-consistent ($\mathscr{C}$-inconsistent) cycle C_4 in $\mathfrak{S}(S)$. By Theorem 2, this cycle C_4 is positive (negative) if and only if P_3 is heterogeneous (homogeneous). Since $\mathfrak{S}(S)$ is $\mathscr{C}$-cycle compatible, for heterogeneous (homogeneous) P_3, $N(u)$ will contain an even (odd) number of negative vertices.

- if marking of path $P_3 = (u, v, w)$ is -, +, - and vertices u and w are (are not) of the same parity, i.e., $N(u)$ and $N(w)$ contain even number of negative vertices or odd number of negative vertices, then by Theorem 1, vertices u, v, w, v' have signs -, +, -, + or +, +, +, + (-, +, +, + or +, +, -, +) respectively in $\mathfrak{S}(S)$. Thus, path P_3 induces a $\mathscr{C}$-consistent ($\mathscr{C}$-inconsistent) cycle C_4 in $\mathfrak{S}(S)$. By Theorem 2, this cycle C_4 is positive (negative) if and only if P_3 is homogeneous (heterogeneous). Since $\mathfrak{S}(S)$ is $\mathscr{C}$-cycle compatible, for homogeneous (heterogeneous) P_3, vertices u and w will (will not) be of the same parity;

- if marking of path $P_3 = (u, v, w)$ is -, -, - and vertices u and w are (are not) of the same parity, i.e., $N(u)$ and $N(w)$ contain even number of negative vertices or odd number of negative vertices, then by Theorem 1, vertices u, v, w, v' have signs -, -, -, +; -, +, -, - or +, -, +, +; +, +, +, - (-, -, +, +; -, +, +, - or +, -, -, +; +, +, -, -) respectively in $\mathfrak{S}(S)$. Thus, path P_3 induces a $\mathscr{C}$-inconsistent ($\mathscr{C}$-consistent) cycle C_4 in $\mathfrak{S}(S)$. By Theorem 2, this cycle C_4 is positive (negative) if and only if P_3 is homogeneous (heterogeneous). Since $\mathfrak{S}(S)$ is $\mathscr{C}$-cycle compatible, for homogeneous (heterogeneous) P_3, vertices u and w will not (will) be of the same parity.

Thus, the necessity follows.

Sufficiency: A cycle in $\mathfrak{S}(S)$ is induced due to a cycle or a path P_3 or their combinations in S. If conditions hold then it can be easily seen that every cycle in $\mathfrak{S}(S)$ is positive and $\mathscr{C}$-consistent or negative and $\mathscr{C}$-inconsistent, i.e, $\mathfrak{S}(S)$ is $\mathscr{C}$-cycle compatible. This completes the proof. □

Signed graph S shown in Figure 2 does not satisfy conditions **(i)** and **(ii)** of Theorem 5, $\mathfrak{S}(S)$ is $\mathscr{C}$-cycle incompatible.

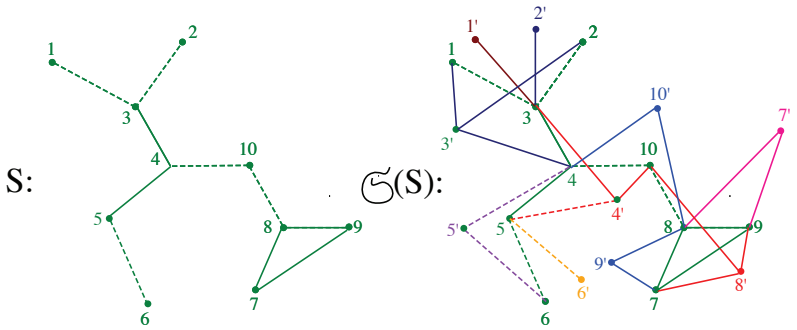


Figure 2: A signed graph S and its $\mathscr{C}$-cycle incompatible $\mathfrak{S}(S)$

Signed graph S shown in Figure 3 satisfies conditions **(i)** and **(ii)** of Theorem 5, $\mathfrak{S}(S)$ is $\mathscr{C}$-cycle compatible.

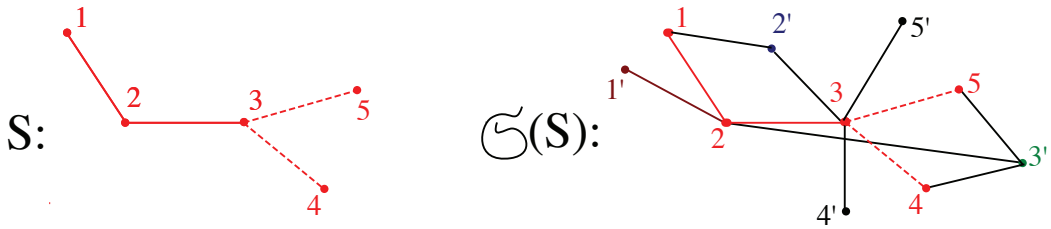


Figure 3: A signed graph S and its $\mathscr{C}$-cycle compatible $\mathfrak{S}(S)$

Theorem 6. *For a signed graph S, $\Gamma(S)$ is $\mathscr{C}$-cycle compatible if and only if the following conditions hold in S:*

(i) S is balanced;

(ii) each non-pendant vertex of S is positive.

Proof. Necessity: Let $\Gamma(S)$ be $\mathscr{C}$-cycle-compatible, i.e., every cycle in $\Gamma(S)$ is either positive and $\mathscr{C}$-consistent or negative and $\mathscr{C}$-inconsistent. By Lemma 1, every vertex of S is a positive vertex of $\Gamma(S)$. Hence, every cycle Z of $\Gamma(S)$ that is due to a cycle Z of S is $\mathscr{C}$-consistent. Since $\Gamma(S)$ is $\mathscr{C}$-cycle-compatible, this cycle Z of S must be positive. Therefore, S will be balanced. Thus, **(i)** follows.

By the definition of $\Gamma(S)$, a path $P_3 = (u, v, w)$ of S induces a positive cycle $C_4 = (u, v, w, v')$ in $\Gamma(S)$ and by Lemma 1, vertices u, v, w, v' have signs +, +, +, + or +, +, +, - in $\Gamma(S)$ if v is a positive (negative) vertex of S. Thus, this cycle C_4 is $\mathscr{C}$-consistent if $v \in V(S)$ is a positive vertex. Since $\Gamma(S)$ is $\mathscr{C}$-cycle compatible and cycle C_4 is positive, C_4 must be $\mathscr{C}$-consistent. Hence, every non-pendant vertex of S will be positive. Thus, the necessity follows.

Sufficiency: A cycle in $\Gamma(S)$ is induced due to a cycle or a path P_3 or their combinations in S. If conditions hold then it can be easily seen that every cycle in $\Gamma(S)$ is positive and $\mathscr{C}$-consistent, i.e, $\Gamma(S)$ is $\mathscr{C}$-cycle-compatible. This completes the proof. □

Signed graph S shown in Figure 4 satisfies conditions **(i)** and **(ii)** of Theorem 6, $\Gamma(S)$ is $\mathscr{C}$-cycle compatible.

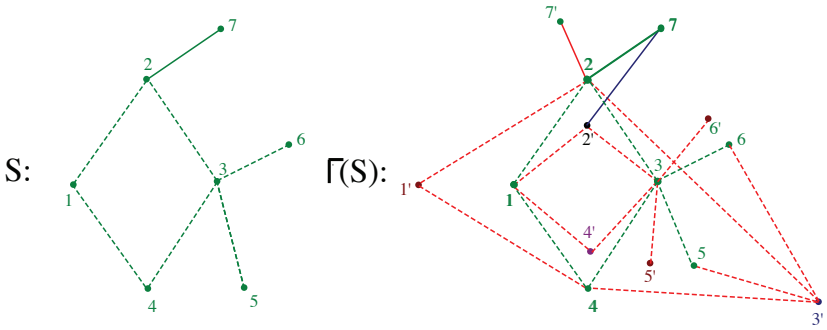


Figure 4: A signed graph S and its $\mathscr{C}$-cycle compatible $\Gamma(S)$

ACKNOWLEDGEMENTS The authors are thankful to Dr B. D. Acharya who always nurtured but could not witness the same. The corresponding author is thankful to the University Grants Commission (UGC), Govt. of India, for granting her research fellowship.

References

[1] M. Acharya, R. Jain, and S. Kansal. *Some results on the splitting signed graphs* $\mathfrak{S}(S)$, Journal of Combinatorics, Information and System Sciences, 39(1-2), 23-32. 2014.

[2] F. Harary. *Graph Theory*, Addison-Wesley Publishing Co., Reading, Massachusetts, 1969.

[3] F. Harary. *On the notion of balance of a signed graph*, Michigan Mathematical Journal, 2, 143-146. 1953.

[4] E. Sampathkumar. *Point-signed and line-signed graphs*, National Academy Science Letters, 7(3), 91-93. 1984.

[5] E. Sampathkumar and H.B. Walikar. *On the splitting graph of a graph*, Karnatak University Journal of Sciences, XXV-XXVI, 13-16. 1980-1981.

[6] D. Sinha. *New frontiers in the theory of signed graphs*, Ph.D. Thesis, University of Delhi, India, 2005.

[7] D. Sinha, P. Garg, and H. Saraswat. *On the splitting signed graphs*, Journal of Combinatorics, Information and System Sciences, 38(1-4), 103-111. 2013.

ResearchGate

See discussions, stats, and author profiles for this publication at: http://www.researchgate.net/publication/281464362

Comparative Performance of R438A and R32/R125/R600A Mixture for Replacing HCFC22 used in Air-Conditioners

ARTICLE · AUGUST 2015

READS
34

3 AUTHORS, INCLUDING:



Suneel Kalla
IMS Engineering College
1 PUBLICATION **0** CITATIONS
SEE PROFILE



B B Arora
Delhi Technological University
26 PUBLICATIONS **19** CITATIONS
SEE PROFILE

All in-text references underlined in blue are linked to publications on ResearchGate, letting you access and read them immediately.

Available from: B B Arora
Retrieved on: 04 November 2015

International Journal of Engineering Research & Technology (IJERT)
ISSN: 2278-0181
Vol. 4 Issue 08, August-2015

Comparative Performance of R438A and R32/R125/R600A Mixture for Replacing HCFC22 used in Air-Conditioners

Suneel Kumar Kalla
Research Scholar, Deptt. Of Mech. Engg.,
Jamia Millia Islamia
New Delhi, India

B. B. Arora
Deptt. Of Mech. Engg.,
Delhi Technological University
New Delhi, India

J. A. Usmani
Deptt. Of Mech. Engg.,
Jamia Millia Islamia
New Delhi, India

***Abstract*— In this study, the energy performance of R438A and M1 (R32/R125/R600A) mixture has been assessed theoretically in a residential air conditioner. The performance has been assessed for five different condensing temperatures, i.e. 35, 40, 45, 50 and 55 °C with an evaporator temperature of -10 °C. The volumetric cooling capacity, coefficient of performance, compressor power consumption and compressor discharge temperature were used as the parameters for comparing the performance of the residential air conditioner. Total equivalent warming impact of the air conditioner was assessed for a 15-year life time. The results indicated that volumetric cooling capacities of M1 and R22 are similar, so that R22 compressor can be used for M1 without modifications, but R438A has slightly lower volumetric cooling capacity. The coefficient of performance of R438A was found to be higher than that of M1 by at least 17 % with 26 % lower compressor power consumption at all condenser temperatures. The compressor discharge temperature of R438A was observed to be at least 10°C lower than that of M1. Total equivalent warming impact of R438Awas found to be lower than that of M1 by about 13% due to its higher energy efficiency. The results showed that R438A is a more energy efficient and environment-friendly alternative to R22 than M1 in residential air conditioners.**

Keywords*— *R32/R125/R600A Mixture; R438A; Residential air conditioner; Total equivalent warming impact

I. INTRODUCTION

Montreal Protocol was signed in 1987 and India ratified it in 1992. As per this protocol, developed countries like India have to phase out HCFCs completely by 2040 (Richard [1]).
As an alternative to R22 in air conditioning, R-407C is mainly used for retrofitting whereas R-410A is the next popular choice for new systems and use of HC-290 is growing in Europe as it requires minimal modifications (Devotta et al [2]). The major problem associated with R410A is its lower critical temperature, which restricts its usage in compression based systems working at higher condensing temperatures whereas for R407C, a change to POE lubricant is required and HC-290 is flammable.

Many researchers tested hydrocarbons (HCs) and their mixtures as alternatives to R22 in residential air conditioners due to their good thermodynamic and thermo-physical properties. In related work, Park et al [3] investigated experimentally the use of propylene, propane, seven mixtures composed of propylene, propane, HFC152a, and dimethylether in air-conditioners and heat pumps. In further work, R433A (30% propylene and 70% propane) was tested in air-conditioner (Park et al [4]). Zaghdoudi [5] simulated the performance of R134a, R290, R600, R404A, R407A, R407B, R407C, 407D, R410A, R410B, and R417A with the help of software Cycle_D and reported R290 to be the best candidate for R22. In another work, Cheng et al [6] assessed the performance of R32 and R290 in a small split household air conditioner with 5 mm finned tube heat exchanger and reported with COP of R32 and R290 were 26.8% and 20.4% higher than R22, 7.3% and 2.1% higher than R410A. Similarly, Al-Joudi & Al-Amir [7] tested R290, R407C and R410A in a split type air conditioner of 2 TR and reported that R290 is the better replacement for R22 when the air conditioning system works under high ambient temperature. Padalkar et al. [8] studied the performance of a split air conditioner with nominal cooling capacities up to 5.1 kW, using HC R290. It was found that with PFC (parallel flow condenser), HC-290 gave highest EER of 3.7 which was 37% higher than that of HCFC-22. However, HC refrigerants have their own drawbacks with respect to flammability.
Another option for replacing R22 in air conditioners is R407C. Devotta et al [9] in their experimental study on window air conditioner concluded that retrofitting with R-407C is an option to extend the life of old units, although the performance is slightly poorer. On the other hand, in a comprehensive review made with possible substitutes, it has been reported that use of R410A is not recommended because the plant will operate with a significant decrease of refrigeration power Sarbu [10].
Allgood & Lawson [11] reported that in existing refrigeration & air conditioning systems, the use of R438A (ASHRAE, 2009), which is a non-ozone depleting zeotropic blend of

(This work is licensed under a Creative Commons Attribution 4.0 International License.)

HFC-32, HFC-125, HFC-134a,HC-600 and 601a(8.5:45.0:44.2:1.7:0.6 wt%, respectively), resulted in similar cooling performance & energy efficiency, lower discharge temperature, similar evaporator & condenser pressure and no change of lubricant during retrofit. In related work, Elgendy et al [12] studied the performance of direct expansion water chiller working with

R438A. It has been reported that cooling capacity and COP of the system using R-438A are lower than R-22 by 11% and 12.5%, respectively. However, compressor discharge temperature using R-438A is slightly lower than R-22 which confirms that R-438A can be used as a retrofit refrigerant for R-22 to complete the remaining life time of the existing plants. Recently, Ramu et al [13] proposed the refrigerant mixture R32/R125/R600a (in the ratio of 0.4:0.4:0.2, by mass) to be used in air conditioners to replace R22 and reported that the new refrigerant mixture is an ozone-friendly alternative to phase out R22 in the existing refrigeration systems to extend its life without modifications. TEGWI of new refrigerant mixture was found to be higher than that of R22 by about 20%. Arora et al [14] performed the exergy analysis of vapour compression refrigeration system with R-22, R-407C and R-410A. Pardal et al [15] did a study of thermoeconomic analysis which can be incorporated into refrigeration or an air conditioning system. Kalla and Usmani [16] reported the comparative performance study of vapour compression refrigeration system with R134a/M09/R410a/R407c/R290/M50. Kalla and Usmani [17] also reviewed refrigeration cycles and systems.

To the authors' knowledge, there is no specific work reported on the energy performance comparison of R438A and R32/R125/R600a mixture (referred to as M1 in this paper) as an alternative to R22 in residential air conditioners. The main objective of this paper is to investigate which of these two refrigerant blends can be a potential alternative to R22.

II. CHARACTERISTICS OF R22, R438A AND M1

Refrigerant blend R438A composed of R32, R125, R134a, R600 and R601a (8.5:45.0:44.2:1.7:0.6 wt%, respectively) is considered as a viable alternative to R22. R438A is a zeotropic mixture with temperature glide of 6.19 °C and GWP of 2265 (Elgendy et al, 2014). The new refrigerant mixture M1 composed of R32/R125/R600a (in the ratio of 0.4:0.4:0.2, by mass) is also considered as candidate for R22 substitution. M1 is a zeotropic mixture with GWP of 1670 (Ramu et al, 2014). The properties of the refrigerants (such as vapour pressure, latent heat, density and specific heat) for wide range of temperatures (between 0 and 60 °C) are compared in Figs. 1–4. Fig. 1 depicts the variation of vapour pressure of R22, M1 and R438A against temperature. It is observed that R22 has approximately the same vapor pressure as R438A. However, M1 has 25% and 41% higher vapour pressures at lower temperatures and higher temperatures, respectively. Hence for M1, the compressors will operate relatively at higher pressures. The variation of latent heat of the three investigated refrigerants is shown in Fig. 2. At low temperatures (0-20ºC), the latent heat of M1 is found to be higher than that of R22

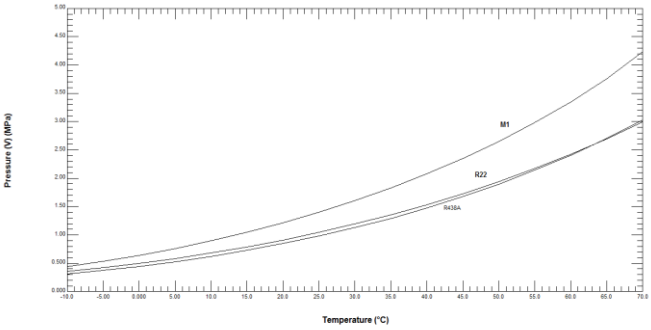


Fig.1. Variation of vapour pressure with temperature

which ensures more refrigeration effect in the evaporators. Similarly, at higher temperatures, the latent heat of M1 is found to be lower than that of R22 at higher temperatures between 40 and 60ºC. Hence, low heat rejection is expected with refrigerant mixture M1 in the condensers. However, R438A is having the latent heat lower than that of R22 throughout the temperature range considered. This will result in less refrigeration effect in the evaporator as well as low heat rejection in the condenser.

The liquid densities of R22, M1 and R438A are compared in Fig. 3.The liquid densities of M1 and R438A are found to be lower than that of R22 by about 45% and 2.6% respectively, across the considered range of temperatures between 0 and 60ºC. Due to the lower liquid density of M1 and R438A, the mass charge requirement would be reduced compared to that of R22. The lower liquid density values of the refrigerant mixtures have lower friction in the tubes of heat exchangers, which ensures better heat transfer coefficients compared to R22 in the condensers and evaporators.

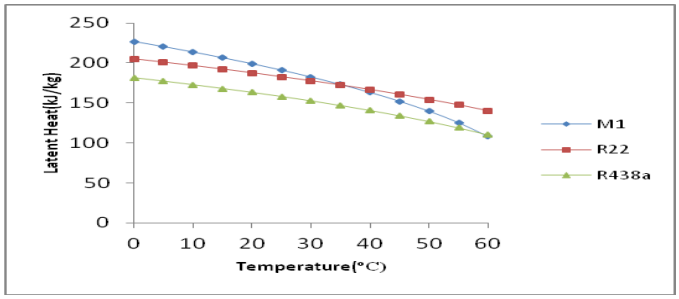


Fig.2. Variation of latent heat with temperature

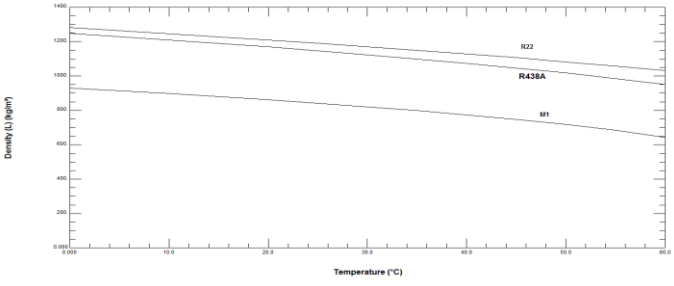


Fig. 3. Variation of liquid density with temperature.

(This work is licensed under a Creative Commons Attribution 4.0 International License.)

The variation of viscosity of R22, M1 and R438A against temperature is shown in Fig. 4.A low viscosity is desirable to achieve higher heat transfer coefficients. It is observed that liquid viscosity of M1 is found to be lower than that of R22 which yields better heat transfer coefficients in the condensers. Same is applicable for R438A for temperatures above 15ºC whereas for temperatures below 15ºC R438A and R22 have approximately the same viscosity. Properties such as critical temperature, critical pressure, boiling point, molecular weight, ODP and GWP of R22, M1 and R438A are compared in Table 1. M1 and R438A both have zero ODP. As compared to R22, GWP of M1 is lesser whereas GWP of R438A is higher. The critical temperatures of both M1 and R438A are lower than R22 whereas critical pressure of M1 was found to be approximately same as that of R22. Critical pressure of R438A is lower than that of R22.

I. THERMODYNAMIC ANALYSIS

Fig. 5(a) and (b) respectively show the schematic diagram and pressure enthalpy diagram of a vapour compression refrigeration cycle. In a residential air conditioner, throttle valve is replaced by a capillary tube. Process 3-4 represents compression, 4-1 condensation, 1-2 expansion and 2-3 evaporation. 3-4s is the isentropic compression. Refrigerant state at point 3 is saturated vapour, at point 4 it is superheated vapour, at point 1 it is saturated liquid and at point 2 it is two phase mixture. Theoretical assessment of the refrigerants is done from energy point of view using first law of thermodynamics. Environmental impact of refrigerants is also studied.

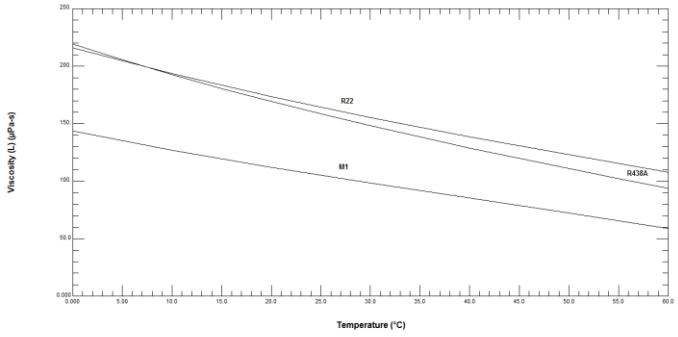


Fig. 4. Variation of liquid viscosity with temperature.

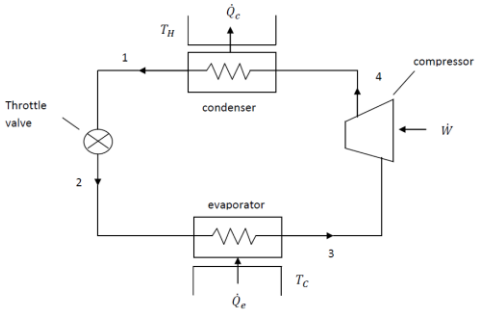


Fig.5(a). Vapour compression refrigeration cycle.

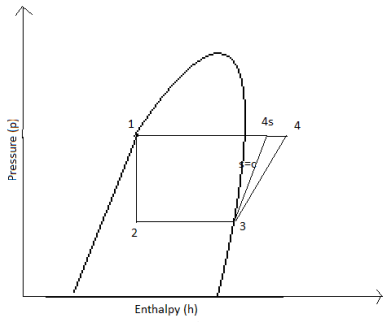


Fig.5(b). Pressure enthalpy diagram of Vapour compression refrigeration cycle.

The following assumptions have been made based on compressor displacement of $1 m^3/s$:

i Compressor isentropic efficiency is 0.7 (Genetron Properties v1.1[18])

ii Life of the air conditioner is 15 years, leakage is 25% per year,

iii Evaporator temperature -10ºC,

iv No pressure drop in condenser and evaporator,

v No superheating and subcooling,

vi Steady state processes in the system.

vii Charge required for R22 is 900g and for M1 and R438A it is 750g and 883g respectively, due to their lower liquid densities.

In this analysis, the thermodynamic properties of the refrigerants are taken from REFPROP version 8 [19] and simulation has been done with the help of Genetron Properties v1.1 and EES (Klein and Alvarado [20]) softwares.

II. TOTAL EQUIVALENT WARMING IMPACT

The method of calculating total equivalent warming impact(TEWI) is provided below (AIRAH [21]):

TEWI = GWP (**direct**; refrigerant leaks incl. EOL) + GWP (**indirect**; operation)

$$= (GWP \times m \times L_{annual} \times n) + GWP \times m \times (1 - \alpha_{recovery})) + (E_{annual} \times \beta \times n)$$

where:

GWP = Global Warming Potential of refrigerant, relative to CO_2 (GWP CO_2 = 1)

L_{annual} = Leakage rate p.a. (Units: kg)

n = System operating life (Units: years)

m = Refrigerant charge (Units: kg)

$\alpha_{recovery}$ = Recovery/recycling factor from 0 to 1

E_{annual} = Energy consumption per year (Units: kWh p.a.)

β = Indirect emission factor (Units: kg CO_2 per kWh)

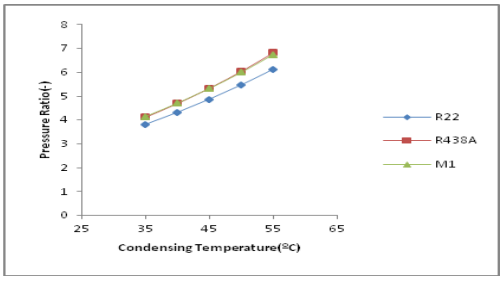


Fig. 6. Variation of pressure ratio with condensing temperature.

(This work is licensed under a Creative Commons Attribution 4.0 International License.)

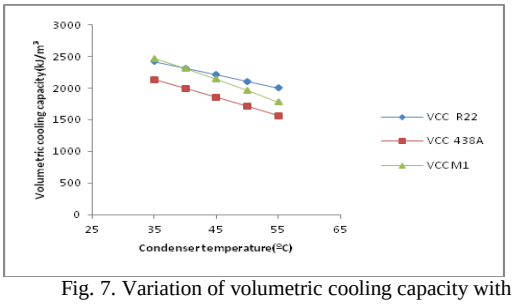


Fig. 7. Variation of volumetric cooling capacity with condensing temperature

In this work, the CO_2 emission factor is assumed to be 0.89 kg of CO2/kWh (IEA [22]).

III. RESULTS

Theoretical assessment of residential air conditioners has been done using R22, M1 and R438A at five different condensing temperatures (35, 40, 45, 50 and 55 °C) at an evaporator temperature of -10ºC and the results obtained are discussed in this section.

Variation of pressure ratio

The variations of pressure ratio against condenser temperature are compared in Fig. 6. The pressure ratios of M1 as well as R438A were observed to be higher than that of R22 by approximately 8.6%, 9.2%, and 10.1% at 35, 45 and 55 °C, respectively. Hence, volumetric efficiency will be lesser with M1 as well as with R438A.

Variation of volumetric cooling capacity (VCC)

The variation of VCC at different condensing temperatures is shown in Fig. 7. VCC of M1 was found to be closer to R22 for condensing temperatures up to 40ºC and deviations in VCC for 45 and 55 °C are found to be 3.3% and 11%, respectively. Hence, M1can be used as drop-in substitute without major modification in the existing R22 systems. As regards R438A, VCC is within 13-21% of R22 as the condensing temperature varies from 35 to 55ºC.

Variation of Coefficient of performance (COP)

The COPs of the three refrigerants are compared in Fig. 8. The COP of R438A is lower than that of R22 by about 6%, 9.5% and 14.2% at 35, 45 and 55 °C, respectively due to its lower

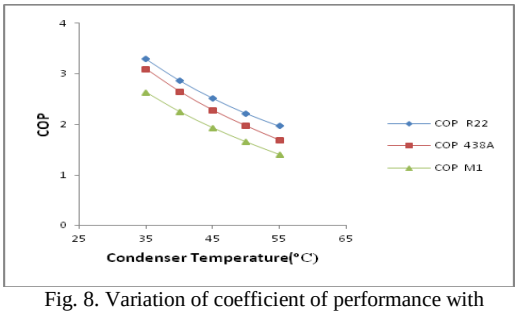


Fig. 8. Variation of coefficient of performance with condensing temperature

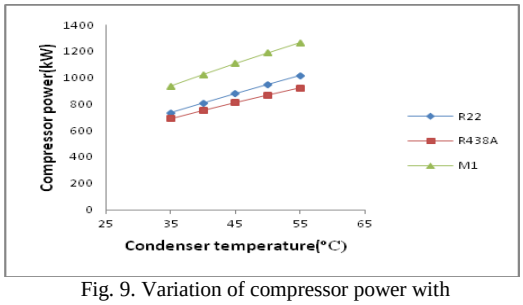


Fig. 9. Variation of compressor power with condensing temperature

evaporator capacity which offsets the advantage due to its lower compressor work consumption. The COP of M1 is much lower than that of R22 by about 20%, 23.4% and 28.9% at 35, 45 and 55 °C, respectively due to its lower evaporator capacity as well as higher compressor work.

Variation of compressor power consumption

Power consumptions of the three refrigerants are compared in Fig. 9. The power consumption of R438A was found to be lower than that of R22 by 5.7%, 7.4%, and 9.2% at 35, 45 and 55 °C condensing temperatures, respectively. On the other hand, the power consumption of M1 was found to be higher than that of R22 by 27.7%, 26.1%, and 24.5% at 35, 45 and 55 °C condensing temperatures, respectively.

Compressor discharge temperature

The comparison of compressor discharge temperature of the three refrigerants is shown in Fig. 10. The compressor discharge temperatures of R438A as well as M1 were found to be lower than that of R22 for a wide range of condenser temperatures due to their lower specific heat ratios. Due to the lower compressor discharge temperature, the life of the compressor will increase. The compressor discharge temperature of R438A was found to be lower than that of R22 by 18.2, 22.1 and 25.7 °C at 35, 45 and 55 °C condensing temperatures, respectively. However, the compressor discharge temperature of M1 was found to be lower than that of R22 by only 8.1, 10.1 and 11.9°C at 35, 45 and 55 °C condensing temperatures, respectively.

Total equivalent warming impact (TEWI)

The TEWI of the three refrigerants is calculated for 15 year life time of the air conditioner at 50 °C and −10 °C condensing and evaporator temperatures, respectively. The TEWIs of the

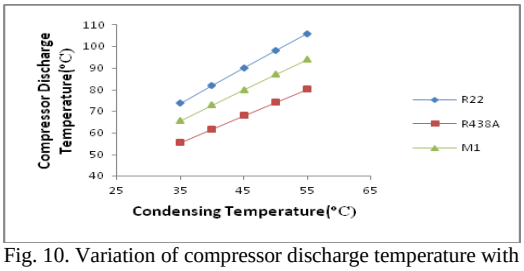


Fig. 10. Variation of compressor discharge temperature with condensing temperature

(This work is licensed under a Creative Commons Attribution 4.0 International License.)

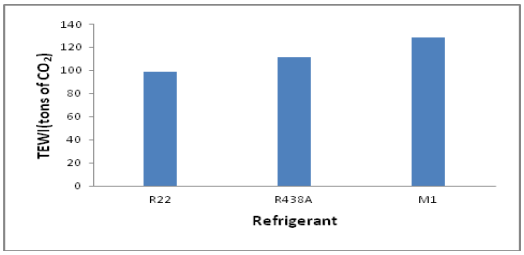


Fig. 11. Comparison of TEWI.

air conditioner working with R22, M1 and R438A are compared in Fig. 11. TEWI of R438A was found to be lower than that of M1 by about 13% due to its higher energy efficiency even though it is having higher GWP.

Oil management

R438A can be used to convert R22 systems without the need to change out the mineral oil (Allgood & Lawson, 2010). Similarly, in case of M1, R600a is taken as a viable additive to tackle the oil miscibility issue in the compressor.

IV. CONCLUSIONS

The energy performance assessment has been made for a residential air conditioner working with R22, M1 and R438A and the following conclusions were made.

- For R438A, cooling capacities are within 13-21% of R22 across the range of condenser temperature whereas for M1, cooling capacities are within 2-11% of R22.
- The COP of the residential air conditioner working with R438A was found to be lower than that of R22 by 6%, 9.5% and 14.2% at 35, 45 and 55 °C condensing temperatures, respectively. The COP of M1 is much lower than that of R22 by about 20%, 23.4% and 28.9% at 35, 45 and 55 °C, respectively.
- The power consumption of R438A was found to be lower than that of R22 by 5.7%, 7.4%, and 9.2% at 35, 45 and 55 °C condensing temperatures respectively. For M1, the power consumption was found to be higher than that of R22 by 27.7%, 26.1%, and 24.5% at 35, 45 and 55 °C condensing temperatures, respectively.
- The TEWI of R438A was found to be lower than that of M1 by about 13% due to its higher energy efficiency.
- The compressor discharge temperature of the air conditioner working with R438A is the lowest as compared to M1 as well as R22, which may increase the compressor life.
- In most systems, the existing mineral oil lubricant in the compressor can be used with both R438A and M1.

The results discussed in this paper confirmed that R438A is energy efficient and environment-friendly alternative to replace R22 systems as compared to M1.

REFERENCES

[1] L.P. Richard, “CFC phase out; have we met the challenge,” J.Fluor. Chem., vol. 114, pp. 237-250, 2002.
[2] S. Devotta, A.V. Waghmare, N.N. Sawant and B.M. Domkundwar, “Alternatives to HCFC-22 for air conditioners,” App. Therm. Eng., vol. 21, pp. 703-715, 2001.
[3] K. Park, T. Seo and D. Jung, “Performance of alternative refrigerants for residential air-conditioning applications,” App. Energy, vol. 84, pp. 985– 991, 2007.
[4] K. Park, Y. Shim and D. Jung, “Performance of R433A for replacing HCFC22 used in residential air-conditioners and heat pumps,” App. Energy, vol. 85, pp. 896–900, 2008.
[5] M.C. Zaghdoudi, S. Maalej, Y. Saad and M. Bouchaala, “A comparative study on the performance and environmental characteristics of alternatives to R22 in residential air conditioners for Tunisian market” J. Env. Sci. Eng., vol. 4, pp. 37-56, 2010.
[6] S. Cheng, S. Wang and Z. Liu, “Cycle performance of alternative refrigerants for domestic air-conditioning system based on a small finned tube heat exchanger,” App. Therm. Eng., vol. 64, pp. 83-92, 2014.
[7] K.A. Al-Joudi and Q.R.A. Al-Amir, “Performance evaluation of small scale air-conditioning system using R22 and alternative refrigerants,” J. Eng., vol. 20, pp. 62-77, 2014.
[8] A.S. Padalkar, K.V. Mali and S. Devotta, “Simulated and experimental performance of split packaged air conditioner using refrigerant HC-290 as a substitute for HCFC-22,” App. Therm. Eng., vol. 62, pp. 277-284, 2014.
[9] S. Devotta, A.S. Padalkar and N.K. Sane, “Performance assessment of HCFC-22 window air conditioner retrofitted with R-407C,” App. Therm. Eng., vol. 25, pp. 2937-2949, 2005.
[10] I. Sarbu, “A review on substitution strategy of non-ecological refrigerants from vapour compression-based refrigeration, air-conditioning and heat pump systems,” Int. J. Refrigeration, vol. 46, pp. 123-141, 2014.
[11] C.C. Allgood and C.C.Lawson, “Performance of R-438A in R22 refrigeration and air conditioning systems,” Int. Refrigeration and Air Conditioning Conference at Purdue, July 12-15,2010.
[12] E. Elgendy, M. Hassanain and M. Fatouh, “Assessment of R-438A as a retrofit refrigerant for R-22 in direct expansion water chiller,” Int. J. Refrigeration, 2014; doi:10.1016/j.ijrefrig.2014.07.017.
[13] N.S. Ramu, P.S. Kumar and M. Mohanraj, “Energy Performance Assessment of R32/R125/R600a Mixtures as Possible Alternatives to R22 in Compression Refrigeration Systems, Int. J. Mech. Mechatronics Eng., vol. 14, pp. 12-22, 2014.
[14] A. Arora, B.B. Arora, B.D. Pathak and H.L.Sachdev, ”Exergy analysis of Vapour Compression Refrigeration system with R-22, R-407C and R-410A,” Int. J.Exergy, vol. 4, pp. 441–454, 2007.
[15] R. Pardal, B.B. Arora and S Maji, “Study of Thermoeconomic Analysis,” Int. J. App. Eng. Res., vol. 7, pp. 1563-1567, 2012.
[16] S.K. Kalla and J.A.Usmani, “Comparative performance study of vapour compression refrigeration system with R134a/M09/R410a/R407c/R290/M50,” Indian J. Eng., vol. 5, pp.57-60, 2013.
[17] S. K. Kalla and J. A. Usmani,” Refrigeration cycles and systems: a review,” Int. J. Engg. Res. & Sci. & Tech., Vol. 3, pp.148-162, 2014.
[18] Y.M. Samuel, “Genetron Properties 1.1—Genetron Systems Modeling User Manual,” Version 1.1, Honeywell-Buffalo Research Laboratory, New York State, US, 2010.
[19] NIST Standard Reference Database 23. NIST Thermodynamic and Transport Properties of Refrigerants and Refrigerant Mixtures. National Institute of Standards and Technology, 2007, REFPROP Version 8.0.
[20] S.A. Klein and F. Alvarado, 2005. Engineering Equation Solver, Version 7.441. F-Chart software, Middleton, WI.
[21] AIRAH. Methods of calculating Total Equivalent Warming Impact (TEWI) 2012.Best practice guidelines available from http://www.iea.org/publications/freepublications/publication/name,32870, en.html, 2012. [accessed 14 Jan 2015].
[22] IEA. CO2 emissions from fuel combustion 2012 — highlights. Excel summary available from http://www.iea.org/publications/freepublications/publication/name,32870, en.html, 2012. [accessed 14 Jan 2015].

(This work is licensed under a Creative Commons Attribution 4.0 International License.)

Journal of Environmental Protection, 2015, 6, 1170-1175
Published Online October 2015 in SciRes. http://www.scirp.org/journal/jep
http://dx.doi.org/10.4236/jep.2015.610104

Detection of *Enterobacter sakazakii* from Commercial Children Dry Milk

Mohammed Mosa Jaffaar[1], Mohammed K. Shebli[1], Abdul Khaliq Abbas Mussa[2], Bayan Hassan Hadi[2], Allaa M. Aenab[3], S. K. Singh[3]

[1]Agricultural Research Directorate, Ministry of Science and Technology, Baghdad, Iraq
[2]Central Public Health Laboratory, Ministry of Health, Baghdad, Iraq
[3]Environmental Engineering Department, Delhi Technological University, Delhi, India
Email: Mohammedmosa1@yahoo.com, allaaaenab@gmail.com

Received 19 August 2015; accepted 25 October 2015; published 28 October 2015

Copyright © 2015 by authors and Scientific Research Publishing Inc.
This work is licensed under the Creative Commons Attribution International License (CC BY).
http://creativecommons.org/licenses/by/4.0/
Open Access

Abstract

This study included isolation and identification of *E. sakazakii* from 51 different samples of powdered infant formula milk involved (Dialak 1 & 2, Celia 1 & 2, Primalac, Biomil 1 & 2, Similac, Nictalia 1 & 2, MAMi, Novolac (AD), Novolac (AR), Novolac (Allernova), S-26 AR, Nursoy, S-26 PDF gold. The results showed that one batch from three of the batches identified of Novolac and Dialak were contaminated and all the types of other infants were non-contaminated. The strains code given as (E1, E2, E3, E4); the bacteria showed resistance to antibiotics used was cephalosporin batch; the third generation showed sensitive to antibiotics life results through inhibition processes such as (Cefotaxime, Sifutetan and Siftadizim), where the diameters of inhibition zone for Siftadizim (18 mm), Sifutetan (22 mm) & Cefotaxime (25 mm) confirmed the bacteria by API and Vitek Compact-2 (biomero).

Keywords

***Enterobacter sakazakii*, Infant Dry Milk, Antibiotic & Vitek Compact-2**

1. Introduction

Enterobacter sakazakii is a gram-negative bacteria, motile, non-spore forming, facultatively anaerobic, bacillus forming yellow pigmented colonies after 24 - 48 hours at 37˚C incubation on a non-selective medium rod that was formerly known as "yellow-pigmented *Enterobacter cloacae*" until 1980 [1]. This bacterium is an emerging opportunistic pathogen predominantly associated with bacterial meningitis in immune compromised neonates [2]. Other clinical presentations of infection include bacteremia and necrotizing enterocolitis [3]. It appears that

How to cite this paper: Jaffaar, M.M., Shebli, M.K., Mussa, A.K.A., Hadi, B.H., Aenab, A.M. and Singh, S.K. (2015) Detection of *Enterobacter sakazakii* from Commercial Children Dry Milk. *Journal of Environmental Protection*, **6**, 1170-1175.
http://dx.doi.org/10.4236/jep.2015.610104

the frequency of *E. sakazakii* infections is low. *Enterobacter sakazakii* has been associated with life-threatening infections in premature low-birth-weight infants. Contaminated infant milk formula (IMF) has been implicated in cases of *E. sakazakii* meningitis. Sensitive and quick methods to reveal low level of pollution sporadically present in IMF preparations would positively contribute towards risk reduction across the infant formula food chain. The bacterium has been cultured from an assortment of food matrices, including meat, grain, cheese, vegetables, spices, bread and herbs [4]. Though the normal habitat of *E. sakazakii* has yet to be specified, infant milk formula (IMF) has been epidemiologically linked to cases of neonatal meningitis. As an oral pathogen reason for systemic infection, *E. sakazakii* must be in possession the instrumentarium to interfere the epithelial cell obstacle in the bowel in order to access the blood circulation and diffusion. Availability of an *in vitro* cell culture model is essential to study the primary steps of entry of *E. sakazakii* into eukaryotic host cells and to identify possibility virulence factors involved in such procedures. We used gentamicin protection examinations and confocal imaging of fluorescently tagged *E. sakazakii* cells to presenting that this bacterium actively invades human epithelial Caco-2 cells. Both f-actin and microtubule structures are needs for infestation. Disruption of cellular tight intersection increased the primary assembly of *E. sakazakii* with Caco-2 cells and significantly enhanced the ability to pervade. Showed that *E. sakazakii* is able to penetrate rat brain endothelial cells and to survive inside macrophages. The locative evidence also implies that *E. sakazakii* has to be able to translocate through the intestinal barrier and establish a systemic infection with symptoms such as bacteremia and meningitis [5]. Invasive bacteria are able to manipulate the host cell cytoskeleton. Doing this either directly by active secretion of bacterium while actin microfilaments are frequently associated with the bacterial invasion process, microtubules can be also involved in breakthrough by microbial pathogens [6].

2. Objectives and Aim of the Study

Study aimed to detection and identification *Enterobacter sakazakii* from different type of infant dry milk by new methods and confirmatory API 20 E and Vitek compact-2.

3. Material and Methods

3.1. Milk Samples

Fifty one samples have been received from public health laboratory of the Central. Samples were collected over a period of nine months between February and December of 2014.

3.2. Isolation of *Enterobacter sakazakii*

Enrichment step dilution in peptone water and transfer (1 gm, 10 gm & 100 gm into (9 ml, 90 ml & 900 ml)) triple cat in EE broth (Enrichment Enterobacter broth) subsequent isolation of pure colonies on violet red bile glucose agar. Several isolated colonies were selected and streaked onto tryptone soy agar (TSA). Typical yellow-pigmented colonies are detected after an overnight incubation for 48 to 72 h at 25˚C.

3.3. The Identification

These presumptive colonies are identified biochemically [7]. This approach provides only a generic test for Enterobacteriaceae and lacks comparison of the effectiveness of antibiotics for the first and third generation cephalosporins within the group against bacteria the necessary capability to specifically identify *E. sakazakii.* Recently, a number of eclectic have become available to assist identification. One of these is the API 20 E biochemical test and vitek confirmatory system. Sakazakii were time and enriched for 6 h at 42˚C. summarizes the findings of these experiments. This method dependably revealed between 1 and 5 CFU *E. sakazakii* in 100 g with higher inocula producing a higher recovery of *E. sakazakii*. Tests were conducted according to the instructions and approach Food and Drug Administration [7]. The limit of detection was determined to be 10 CFU/ml (equivalent to 2.5×10^3 CFU in (250 ml)).Biochemical profiles are frequently used following primary isolation (**Figure 1**), but contradictions in identification may occur in different biochemical kits for the same strain [8].

3.4. Antibiotic Susceptibility Test

Antibiotic was done for each isolate by standard Kirby Bauer method [9]. Muller Hinton agar plates were used

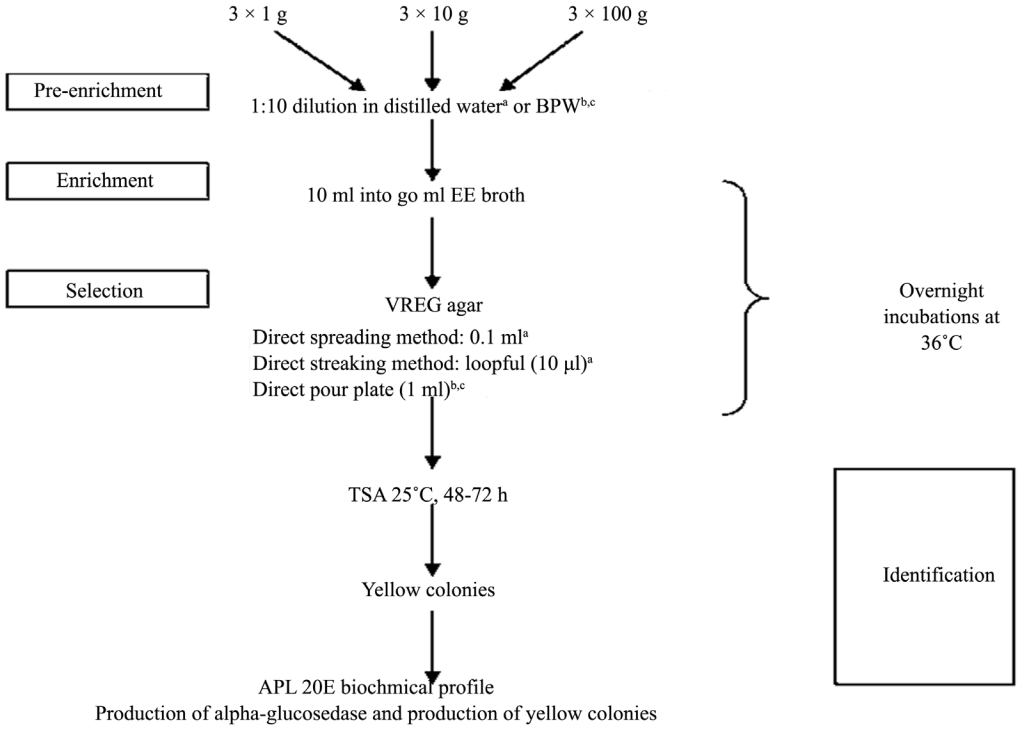


Figure 1. Quantitative *E. sakazakii* isolation procedure.

for bacterial culturing, disc of Cefotaxime, Sifutetan & Siftadizim. Were put over bacterial growth, plates were incubated for 18 hr at 37C, diameter of cleared zones were recorded for results.

3.5. Biochemical Test

Studies have demonstrated that 100% of *Enterobacter sakazakii* are positive for *α*-glucosidase while 100% of other Enterobacter species are negative for this enzyme [10]. On the basis of these observations, the chromogenic substrate 5-bromo-4-chloro-3-indolyl-*α*-D-glucopyranoside (X-*α*-glucoside) has been proposed to differentiate *Enterobacter sakazakii* from other members of the Enterobacteriaceae family [11]. The enzyme *α*-glucosidase hydrolyzes the X-*α* (**Tables 1-3**).

4. Results and Discussion

Enterobacter sakazakii was isolated from four (1.56%) out of the thirty-nine tested infant formula milk. Five strains were isolated and were identified by the FDA method 2002 and API 20 E and Vitek compact-2 (biomero) suggested that the inability to isolate *Enterobacter sakazakii* from powdered formula may have been due to its unequal allocation within the powdered formula or "its existence at such a low concentricity that it escaped disclosure by traditional methods as described by the Food and Agriculture Organization [5] [12]. This study proved that some international global milk powder contaminated with bacteria *Enterobacter sakazakii* and that the children of these bacteria have done a pathogencity represented by diarrhea and severe acute diarrhea. Bacteria were isolated from these four marks: Novolac (AD), Novolac (AR), Novolac (Allernova), Dialak and proven contamination by screening method that recommended by FDA 2002 where the isolation rate (1.56%). Isolates obtained from milk cans indicate resistance to these isolates heating during the manufacturing process and to the inefficiency of the manufacturing process [13]. The results of this study were in line with the results obtained by the researchers [14], as the isolated bacteria from baby milk powder and by (6.80%). The results of the study differed with the study [1]. The researchers have stressed the milk contamination with bacteria *Bacillus cereus* and the reason for their appearance is due to the production of toxins casuals and heat resistance. Tested isolates were resistant to antibiotics where used Cephalosporine group compared to the work of the antibiotic first generation and third. Study showed the first generation (Cephalothin, Safaberden, cefazolin, cephalexin and

Table 1. Biochemical test of *Enterobacter sakazakii* and different bacteria.

Citrate	Positive	Positive	Positive
Glucose	K/A Positive	A/A Positive	A/A Positive
Sucrose	Positive	Positive	Positive
Lactose	Positive	Positive	Positive
α-glucosidase	Positive	Negative	Negative
Urease	Positive	Negative	Negative

Table 2. The proportion of bacteria in milk samples.

Type of samples	Total of samples	Isolated	Percentage
Dialak 1, 2	51	1	1.49
Novolac AD	51	1	1.49
Novolac AR	51	1	1.49
Novolac Allernova	51	1	1.49

Table 3. Isolated bacteria from different types of children dry milk.

Type of Bacteria	Batch No.	Production time	Country of origin	Duplicates	Type of milk
	24 - 25	07.2013			
E. sakazakii	15 - 19	03.2013	Vietnam	3	Dialak 1, 2
	19 - 32	10.2013			
	19 - 27	11.2013			
	11 - 15	08.2013	USA	3	Celia 1, 2
	6 - 64	10.2013			
	15 - 20	04.2013			
	22 - 30	08.2013	Switzerland	3	Primalac
	12 - 45	12.2013			
	8500	10.2013			
	5500	07.2013	Belgium	3	Biomil 1, 2
	2000	04.2013			
	09 - 42	11.2013			
	03 - 26	07.2013	Ireland	3	Nursoy
	02 - 17	03.2013			
	41306	03.2013			
	41308	03.2013	Poland	3	Mami
	41900	11.2013			
	36420	03.2013			
	64222	06.2013	France	3	Nicalia 1, 2
	92391	09.2013			
	02 - 20	03.2013			
	06 - 44	07.2013	Ireland	3	Similac
	02 - 57	09.3013			
	20 - 57	02.2013			
E. sakazakii	16 - 32	07.2013	Germany	3	Novolaclernova
	05 - 46	10.2013			
	08 - 52	02.2013			
E. sakazakii	10 - 58	07.2013	Germany	3	Novolac AD
	03 - 36	10.2013			
	19 - 44	02.2013			
E. sakazakii	08 - 30	03.2013	Germany	3	Novolac AR
	16 - 16	07.2013			
	2A02	10.2012			
	2A27	03.2013	Ireland	3	S-26 AR
	2A34	10.2013			
	2L14	07.2012			
	2L22	03.2013	USA	3	S-26 LF
	2L28	11.2013			

Table 4. Sensitivity of test *Enterobacter sakazakii* for third generation measured in Millimeter (mm) zone of inhibition according to (NCCL).

Antibiotic	E1	E2	E3	E4
Cefotaxime	25	25	25	25
Sifutetan	22	22	22	22
Siftadizim	18	18	18	18

cephradine) did not have any result zone of inhibition. The third generation of the same batch of antibiotic which shows sensitive results through inhibition processes such as (cefotaxime (25 mm), Sifutetan (22 mm), Siftadizim (18 mm)), where the diameters of inhibition zone for Cefotaxime, Sifutetan and Siftadizim. The use of minimum inhibitory concentration Cephalosporine batch shows cefotaxime, Sifutetan and Siftadizim inhibition zone. The major cause is due to the group operates stop the work of the gyrase enzyme is present in prokaryotes and some eukaryotes work by competitive suppression of energy transduction of DNA gyrase by binding to the ATPase active site located on the GyrB subunit. Quinolones bind to these enzymes and prevent them from decatenation replicating DNA. Quinolone-resistant bacteria repeatedly harbor convert topoisomerases that resist quinolone binding 2009 Eukaryotic Cell, 11(8), 1759-1769. Gore J., Bryant Z., Stone M.D., Nollmann M., Cozzarelli N.R. 2006. Used in the study [5], this was identical to the present study in the case reported cephalosporins, such as cefepime, in collection with a second agent. Two studies in [15] and [2], supported the use of cefotaxime for childhood bacterial meningitis. In each of these studies, *Enterobacter sakazakii* meningitis was identified in at least 1 child, and the infection was treated successfully. In another study, [16] described *E. sakazakii* infection in 4 adults that occurred in 1995 and 1996 at the University of Massachusetts Medical Center. Of the 4 adults, 2 presented with pneumonia and 2 with bacteremia. The isolates were uniformly resistant to ampicillin, cefazolin, and extended-spectrum penicillins and were not uniformly susceptible to third-generation cephalosporins or to quinolones. This study proved that the four isolates were sensitive to the third generation cephalosporin group 9, **Table 4**.

References

[1] Forsythe, S. and Iversen, C. (2008) Isolation of *Enterobacter sakazakii* and Other Enterobacteriaceae from Powdered Infant Formula Milk and Related Products. *Food Microbiology*, **21**, 771-773.

[2] Lecour, H., Seara, A., Cordeiro, J. and Miranda, M. (1989) Treatment of Childhood Bacterial Meningitis. *Infection*, **17**, 343-346. http://dx.doi.org/10.1007/BF01650726

[3] Van Acker, J., DeSmet, F., Muyldermans, G., Bougatef, A., Naessens, A. and Lauwers, S. (2001) Outbreak of Necrotizing Enterocolitis Associated with *Enterobacter sakazakii* in Powdered Milk Formula. *Journal of Clinical Microbiology*, **39**, 293-297. http://dx.doi.org/10.1128/JCM.39.1.293-297.2001

[4] Kandhai, M., Reij, W., Gorris, L. and Guillaume, O. (2009) Occurrence of *Enterobacter sakazakii* in Food Production Environments and Households. *Lancet*, 363-369.

[5] Muytjens, H.L. and van der Ros-van de Repe, J. (1986) Comparative *in Vitro* Susceptibilities of Eight Enterobacter Species, with Special Reference to *Enterobacter sakazakii*. *Antimicrobial Agents and Chemotherapy*, **29**, 367-370. http://dx.doi.org/10.1128/AAC.29.2.367

[6] Hoekstra, R.M., Kuehnert, M. and McDonald, L.C. (2007) Invasive *Enterobacter sakazakii* Disease in Infants. *National Center for Infections Disease*, **5**, 885-895.

[7] FDA (2002) Isoilation and Enumeration of *Enterobacter sakazakii* from Dehydrated Infant Formula.

[8] Iversen, C., Druggan, P. and Forsythe, S.J. (2004) A Selective Differential Medium for *Enterobacter sakazakii*. *International Journal of Food Microbiology*, **96**, 133-139. http://dx.doi.org/10.1016/j.ijfoodmicro.2004.01.024

[9] (2002) Performance Standards for Antimicrobial Disk Susceptibility Testing. NCCLSS, Wayne.

[10] Muytjens, H. (1985) *Enterobacter sakazakii*: Identification and Clinical Significance. *Antonie van Leeuwenhoek*, **51**, 618. http://dx.doi.org/10.1007/BF00404602

[11] Iversen, C., Druggan, P. and Forsythe, S. (2004) A Selective Medium for *Enterobacter sakazakii*, a Preliminary Study. *International Journal of Food Microbiology*, **96**, 133-139. http://dx.doi.org/10.1016/j.ijfoodmicro.2004.01.024

[12] FAO (1994) Codex Alimenterius Code of Hygienic Practice for Foods for Infants and Children. CAC/RCP 21-1979.

Food and Agriculture Organization of the United Nations, Rome.

[13] Pagotto, F. (2009) Pathogenesis of Cronobacter Enterotoxin Production, Adherence and Invasion of the Blood-Brain Barrier, Burenu of Microbiol Hazards, Ireland.

[14] Joshua, B., Jeffery, L., Kornacki, B. and Larry, R. (2005) *Enterobacter sakazakii*: Acoliform of Increased Concern to Infant Heath. Center for Food Safety and Technology, Georgia.

[15] Naqvi, S.H., Maxwell, M.A. and Dunkle, L.M. (1985) Cefotaxime Therapy of Neonatal Gram-Negative Bacillary Meningitis. *The Pediatric Infectious Disease Journal*, **4**, 499-502. http://dx.doi.org/10.1097/00006454-198509000-00012

[16] Lai, K.K. (2001) *Enterobacter sakazakii* Infections among Neonates, Infants, Children, and Adults. Case Reports and a Review of the Literature. *Medicine*, **80**, 113-122. http://dx.doi.org/10.1097/00005792-200103000-00004

Journal of Computer Science and Engineering Research

ISSN No: 2349-3798

Journal of Computer Science and Engineering Research: 2015, 2 (1):8-14

DNA Steganography: Literature Survey on its Viability as a Novel Cryptosystem

Aditi Bhateja[1] and Kanika Mittal[2]

[1]Delhi Technological University, India
[2]Banasthali Vidyapeeth, Jaipur, India
Correspondence: aditibhateja89@gmail.com

(Received: 18/02/15) *(Accepted: 22/07/15)*

ABSTRACT

There is an extensive need for secure manner in which information can be sent to prevent intrusion. Researchers have lately focused upon some techniques of cyber security which are not in ordinary terms-conventional. Data-hiding techniques are gaining wide acceptance to protect sensitive information from adversary's attack. One such technique currently being explored by researchers is DNA Steganography. This paper aims at providing a holistic view on the current trends of DNA Steganography and providing details about viability of such techniques by studying their minute aspects relevant to information security.

Keywords: *DNA Steganography*; *Data Hiding*; *Intruders*; *Security*

INTRODUCTION

The word "steganography" is made of two words-"steganos" meaning "covered or protected" and "graphie" meaning "writing". Thus "steganography" means "covered (concealed) writing". Steganography marks its existence in the ancient Greek warring states where secret communication was their priority. Also, in today's era digital communication has become an integral part. A lot of applications are internet-based and so it is a necessary requirement to have secret communication. With the increase in the worldwide utilisation of internet and network technology, the threat to secret data from hackers and intruders is also increasing and so does the need to protect such data. The security of information passed over an open channel has become a fundamental issue of utmost importance and therefore, the confidentiality and data integrity are required to protect against unauthorized access and use of information. This has resulted in tremendous growth in the field of information hiding. Steganography is one such way to protect important information. Generally, steganography is confused with cryptography because they are similar in the manner in which they are used to protect secret data. Cryptography deals with protecting the message by making it unreadable for an unauthorized person whereas steganography focuses on embedding and hiding of the message, so that it doesn't draw the intruder's attention, with or without the garbling of data. Steganography requires a covert medium, for embedding data, which is not suspected by any attacker. Traditional media used for this purpose are paper, images and videos but their covertness has been lost due to better computing techniques available with the attackers. As a result security analysts are trying to find other covert medium which can hide the data more securely in present scenario. One such medium identified by them is Deoxyribonucleic acid (DNA). A steganographic technique employing DNA steganography uses the long sequence of DNA to hide and embed data with an aim that it doesn't reveal secret message which is hidden into that sequence. DNA sequence used to hide message can be extracted from the public databases of NCBI (National Centre for Biotechnology Information), EBI (European Bioinformatics Institute), etc. and is referred to as reference DNA sequence whereas the message to be embedded is known as secret message.

This paper is divided into six sections. Section 0 provides the overview of our research methodology which forms the basis on which we selected the research papers for study and accomplished our task of analysing the research papers. Section 0 provides the detailed description of DNA and its properties which makes it suitable for use in

DNA Steganographic techniques. Section 0 gives a brief introduction to DNA Steganography. Section 0 provides discussion on the techniques used to hide data in DNA. The last section concludes the paper by comparing some important techniques studied in section 0.

MATERIALS AND METHODS

Research Methodology

A lot of research has been done by researchers in the area of DNA steganography and they proved that DNA is an effective medium to store secret information as it has a very good data storage capacity as well as other characteristic properties which differentiates it from similar media of data storage. As a result, many articles and research papers were published which provides various research methodologies involved in hiding of secret message in DNA. Some journals which were referred are:

- IEEE
- Elsevier
- International Journal of Information and Computational Technology
- Springer Link Online Libraries
- American Journal of Engineering Research
- Journal of Global Research in Computer Science

Research papers searched on terms like “DNA Steganography”, “Data-hiding in DNA”, etc., were the major source of information. All the collected papers were read thoroughly and were reviewed as well as interpreted. These papers contained information about the procedures used to carry out the research, explanation on how to acquire the results of the research, experimental results which show how much the current method is more powerful than those discussed earlier. This survey was carried out to gather the knowledge of various methods given by well known researchers to hide the secret message in a DNA sequence. Exhaustive study was done on this topic before writing this paper.

Deoxyribonucleic Acid (DNA)

DNA is a polymer, having double helical structure discovered by two Nobel laureate Watson and Crick and therefore its structure is also called a Watson-Crick complementary structure where two polynucleotide chains are held together by weak thermodynamic forces which form a DNA molecule. The monomer units of DNA are called nucleotides which consists of nitrogenous bases, five carbon sugar and phosphate group. Nitrogenous bases are classified as Adenine (A), Thymine (T), Guanine (G) and Cytosine (C). Combination of these four bases is used to store complex information. Adenine and Guanine are called “Purines” whereas Thymine and Cytosine are called “Pyrimidines”. A DNA sequence comprises of these four nucleic acid bases of which ‘A’ and ‘T’ forms the complementary pair and ‘C’ and ‘G’ forms another complementary pair.

The term data storage refers to collection and retention of digital data, required for various computational works at some interval of time. It provides one of the vital functions of modern computer. As per researchers, biological cells store DNA, which in turn contains all the information needed to create life and to manufacture protein. These cells can further be programmed to store information. The information can also be digitally stored in a given nucleotide sequence by having a series of modifications into the DNA sequence by substitution, insertion or deletion of the nucleobases.

DNA STEGANOGRAPHY

A DNA sequence is a very complex code which may be over 3 billion characters long. A DNA sequence can store a vast amount of information. This property of DNA is exploited to hide secret message in a DNA sequence i.e. DNA sequence will act as information carrier and this is well known as DNA steganography.

In the recent years, much of the research work has been carried out in DNA based data-hiding techniques. Most of these techniques exploit the biological properties of DNA sequences. In order to use hiding techniques to hide/conceal the secret message in DNA sequence the representation format of nucleotides was transformed. In all the techniques discussed below, the researchers have transformed nucleotides into binary representation using binary coding rule. One such binary coding rule is as follows:

$$A = 00, C = 01, G = 10, T = 11$$

DNA steganography is very unique from traditional steganographic techniques in a sense that it is hard to break by adversaries because of the complex computations and covert nature of DNA. It also offers large storage density as

compared to the traditional storage devices. Making DNA as a medium to hide the data for secrecy is a novel method. Its advantages and a few disadvantages are listed below.

❖Advantages of DNA steganography

- Novel Covert medium.
- Large amount of data hiding space available.
- Publicly available database of DNA sequences.
- Flexible encoding scheme.
- Using suitable techniques of data compression large amount of data can be embedded in small DNA sequence whereas a similar technique using Image or other media as cover will embed lesser data.

❖Disadvantages of DNA steganography

- If data is stored in a digital DNA sequence its prone to computer based attacks
- DNA sequence if suspected by an attacker may somewhat make the data being transferred vulnerable to attacks as its cover will be lost
- Large amount of computations required for encoding procedures making it slower compared to traditional cryptographic methods.

DNA steganography can be classified on the basis of need and technique as shown in

Figure 1. On the basis of need techniques can be classified as dealing with either hiding capacity, compression of the message to be stored in DNA and on reversibility i.e. whether we can get back the original message sequence after extracting data from the DNA stream.

On similar lines classification can also be made on the basis of type of DNA used for hiding the information. On the basis of this, the information can be stored either in live DNA found in naturally occurring cells of organisms or in artificially created DNA strands or in simply the sequences of DNA available to us over the internet.

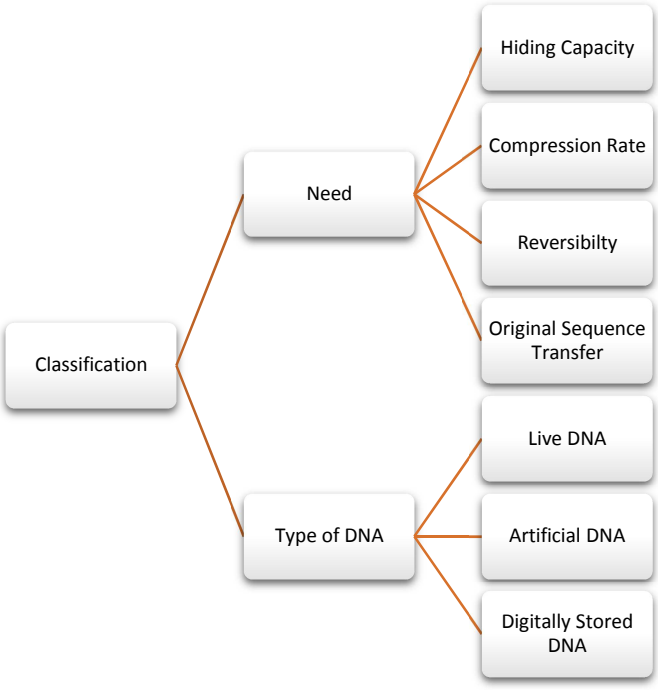


Figure 1: Classification of DNA steganography

Some Popular Techniques (Related Work)

S. No.	Technique	Proposed By	Year	Based On
1.	Hiding Data in DNA	Boris Shimanovsky *et al*. [1]	2003	Codon Redundancy
2.	Data hiding methods based upon DNA sequences	H.J. Shiu *et al*. [2]	2010	Binary coding rule and Hiding capacity of DNA
3.	Digital Steganalysis: Review on recent approaches	Indra Kanta Maitra *et al*. [3]	2011	Literature survey
4.	A new data hiding scheme based on DNA sequence	Cheng Guo *et al*. [4]	2012	Injective mapping between two secret bits and complementary rule
5.	A DNA-based data hiding technique with low modification rates	Ying Hsuan Huang *et al*. [5]	2012	Binary coding rule and histogram method
6.	A novel data hiding method based on deoxyribonucleic acid coding	Hongjun Liu *et al*. [6]	2013	Pseudo-random sequences and addition and subtraction operation on DNA sequence
7.	Steganography: A Review of Information Security Research and Development in Muslim World	Yunura Azura Yunus *et al*. [7]	2013	Literature survey
8.	DNA Based Cryptographic Techniques: A Review	Kritika Gupta and Shailendra Singh [8]	2013	Literature survey
9.	An information security based literature survey and classification framework of data storage in DNA	Shipra Jain *et al*. [9]	2013	Literature survey
10.	DNA based cryptography: A review	Ashish K. and A.K Verma [10]	2014	Literature survey
11.	A Watermarking Scheme for Coding DNA Sequences Using Codon Circular Code	S. H. Lee *et al*. [11]	2014	Coding DNA watermarking
12.	Coding DNA Sequence Watermarking	S. H. Lee *et al*. [12]	2014	DWT based watermarking for coding DNA sequence
13.	Modified technique of insertion methods for data hiding using DNA sequences	S. Manna [13]	2014	Random key generation, cumulative XOR operation of key value, selection of look up table index mapping.
14.	DNA sequence watermarking based on random circular angle	S. H. Lee [14]	2014	Random mapping table and Lipschitz regularity

- Shimanovsky *et al*. [1] put forward a technique known as codon redundancy. A codon is three bases long. There are 4 possible bases (A, C, G, T) and so there are 4^3 or 64 possible unique codes. But there are only 20 amino acids that are encoded shown in
-
- Table **1**. Thus, there is redundancy in mRNA to amino acid mapping.

Table 1: Amino Acid to Codon Mapping [1]

Amino Acid	Codons	Amino Acid	Codons
Ala	GCU, GCC, GCA,GCG	**Leu**	UUA, UUG, CUU, CUC, CUA, CUG
Arg	CGU, CGC, CGA, CGG, AGA, AGG	**Lys**	AAA, AAG
Asn	AAU, AAC	**Met**	AUG
Asp	GAU, GAC	**Phe**	UUU, UUC
Cys	UGU, UGC	**Pro**	CCU, CCC, CCA, CCG
Gln	CAA, CAG	**Ser**	UCU, UCC, UCA, UCG, AGU, AGC
Glu	GAA, GAG	**Thr**	ACU, ACC, ACA, ACG
Gly	GGU, GGC, GGA, GGG	**Trp**	UGG
His	CAU, CAC	**Tyr**	UAU, UAC
Ile	AUU, AUC, AUA	**Val**	GUU, GUC, GUA, GUG
START	AUG	**STOP**	UAA, UGA, UAG

They chose a DNA sequence long enough and converted it into binary sequence using the binary coding rule. They chose an mRNA sequence too and translated it into the corresponding amino acid sequence. Then they used Arithmetic Encoding to embed message into the mRNA sequence and a new mRNA sequence is obtained which represents the same amino acid sequence as the original mRNA but it contains our secret message in current form.

In 2010, Shiu *et al*. proposed three new schemes [2] which focuses on embedding of secret and important information in the DNA sequence. The proposed schemes include insertion method, complementary pair method and substitution method. All these schemes uses the reference DNA sequence, a secret message to be embedded, binary coding rule to convert DNA sequence into a binary sequence, and complementary rule.

1. Insertion Method: In this scheme the DNA sequence is converted into binary sequence using binary coding rule. This binary sequence is divided into segments of equal sizes. Now, each message bit is inserted at the end of each segment one after another. New binary sequence is converted back into DNA sequence using the inverse function of binary coding rule. This DNA sequence contains the secret message embedded into it. But this scheme undoubtedly increases redundancy and expands length of DNA thereby attracting the attention of intruders.

2. Substitution Method: In this method, the length of DNA sequence as well as secret message is calculated i.e. *s* and *m* respectively and randomly *m* numbers are selected into A from 1 to *s*. Here the complementary rule must satisfy that for each letter *x* of DNA sequence, *x*, *C*(*x*), *C*(*C*(*x*)), *C*(*C*(*C*(*x*))) are unequal, where *C*(*x*) is the complement of *x*. To transform sequence *S* into *S*' (DNA sequence containing message) following steps were followed:

For all integer i from 1 to *s*
If $i = A_j$ and $M_j = 1$, $1 \leq j \leq m$,
  set S_i to be $C(S_i)$;
Else if $i = A_j$ and $M_j = 0$, do not change S_i;
Else if *i* is not equal to any A_j,
  set S_i to be $C(C(S_i))$;

In this method the length of *S* is maintained by *S*'. For each change in the character of the reference DNA sequence one secret message bit is embedded. So, to a very long secret message, the reference DNA sequence will suffer from a high modification rate.

3. Complementary Pair Method: In this method a DNA sequence is chosen and the length of longest complementary pair existing in it is found. Two complementary string pairs having length one more than that existing in the sequence are randomly generated and padded with 'T' before as well as after. Thereafter, they are inserted one by one into *S* without overlapping. Also the message is divided into segments each containing even number of bits and using binary coding rule data is coded back into nucleotides. For each pair of complementary substring in converted sequence a message bit is inserted before Ta_jT where a_j represents the pair of longest complementary substrings. Sequence containing message *S*' is thus obtained. This scheme also changes the length of the DNA sequence significantly making it easy to draw attention of hacker.

- In 2012, Cheng Guo *et al*. proposed a new scheme which exploits the utilization of complementary rule proposed by Shiu *et al*. in [2] so as to enhance the embedding capacity and reduce the modification rate [4]. This method uses injective mapping between two secret bits and one complementary rule. Until now we have seen that to embed one message bit one character in reference DNA sequence is replaced. But in this scheme, two secret message bits are embedded by replacing only one character. Thus, the length of reference sequence doesn't expand and it also lowers the modification rate.
- In 2012, Chin-Chen Chang *et al*. proposed a reversible data hiding scheme [5] which was based on the binary coding rule proposed by Chang *et al*. and histogram method by Tseng *et al*. This scheme mainly focuses on maintaining the length of DNA sequence and decreasing the modification rate. This proposed scheme neither involves the use of compression technique and nor of an expansion technique. Experimental results have shown that modification rate of the proposed scheme is 17 times lower than that of Shiu *et al*.'s scheme. Also this scheme maintains the length of reference DNA sequence preventing it from attracting the attention of intruders.
- In 2013, in [6] another method of embedding message in DNA sequence was proposed. This technique makes use of embedding secret message into word document. Initially, a plaintext is encoded into a DNA sequence by using DNA coding. Next, this DNA sequence is encrypted by another equal-length DNA sequence generated by Chebyshev Maps and the result is attached to a primer DNA sequence. After circularly shifting the whole sequence for finite times, it is embedded into the word document by modifying the fore colour of the characters. Thus, each character in the word document can be embedded i.e. 6-bit DNA coding. The expression of Chebyshev maps used in this method is as follows:
-

$$Z_{i+1} = \cos\ (w\cos^{-1} Z_i), -1 \leq Z_i \leq 1$$

where *w* is the degree of the Chebyshev maps.

- In 2013, Yunura Azura Yunus *et al*. in [7] discussed an overview of steganography, its features, applications, history and how it differs from cryptography. This paper also highlighted a review of research and development of steganography in Muslim world from the year 2010 to 2013.

- In 2013, Kritika Gupta *et al*. proposed an encryption algorithm based on OTP (One Time Pad) using DNA sequence [8]. In this technique the plaintext is represented into its ASCII code. This ASCII code is then converted into binary code to obtain data in the form of 0's and 1's. Now, this binary sequence is converted into DNA sequence by using table for binary to nucleotide conversion. Next, a DNA sequence is selected as a key and grouped into blocks having 8 characters each. Then a table is created on the basis of positions of each character in DNA Sequence. Using this table and randomly selected DNA Sequence, the data gets converted into encrypted form.
- In 2014, in [10] A. K. Verma *et al*. surveyed and analyzed various trends in DNA cryptographic approaches and highlighted merits and demerits of each.
- In 2014, S. H. Lee *et al*. [11] presented a coding sequence watermarking on lifting based DWT domain. In the proposed scheme the codons are allocated to numerical codes using permutation table of histogram rank of amino acid and substitutes a sub-sequence of codons to a sequence having DWT coefficients which is optimum to a watermark bit among the set of DWT coefficients with same amino acids.
- In 2014, S. H. Lee *et al*. proposed a DNA watermarking method to preserve the privacy of data and to prevent illegal copy [12]. In this method, codons i.e. combination of three nucleotides, are allocated to random circular angles by using random mapping table and triplet codons are selected for embedding target with the help of Lipschitz regularity value of local modulus maxima of codon circular angles. The length and location of the triplet codon selected depends on the random mapping table for 64 codons including the start and stop codons. The table serves as the watermark key which is applied on any codon sequence regardless of the length of sequence. But, if the table is unknown then it is very difficult to detect the length and location of the codons for extracting watermarks.

CONCLUSION

The DNA Steganography has drawn the attention of various academicians and researchers to carry innovative as well as quality research work. The future of DNA Steganography looks very promising as DNA is a medium for ultra-compact information storage because the nucleotides 'A', 'C', 'G', and 'T' are capable enough to store the information. Also a DNA sequence has a large storage capacity to store large information within it. All the above discussed techniques work towards achieving the same goal i.e. data-hiding in DNA sequence so that only the receiver and sender can extract the message without drawing the attention of hackers. Thus, breaking DNA based Steganography represents a difficult biochemical problem making these techniques highly resistant to the attacks but these techniques vary from each other in their hiding capacities, modification rates.
We have provided a classification schema in Table 2 which differentiates some popular techniques of DNA steganography based on the parameters like hiding capacity of the technique in terms of bits per nucleotide, reversibility of the technique and whether the technique requires transfer of original reference sequence to the receiver of the message.

Table 3 provides comparison of Shiu's three schemes with that of Huang on the basis of modification rate and expansion of the same.

Table 2: Comparison of some popular techniques

Property	Shiu's scheme	Chang's scheme	Huang's Scheme	Hongjun's scheme	Cheng's scheme	Shimanovsky's scheme
Hiding Capacity(bpn)	Varied	0.78	Varied	Data not available	0.58	Data not available
Reversibility	Yes	Yes	Yes	Yes	Yes	No
Original Sequence transfer	Yes	Yes	No	No	Yes	No

Table 3: Comparison of modification rate and nucleotide expansion for Shiu *et al.*'s scheme and Huang's scheme

DNA Sequence	Shiu's Scheme						Huang's Scheme	
	Insertion Scheme		*Substitution Scheme*		*Complementary Pair*			
	Modification rate (%)	Nucleotide Expansion (%)	Modification rate (%)	Nucleotide Expansion (%)	Modification rate (%)	Nucleotide Expansion (%)	Modification rate (%)	Nucleotide Expansion (%)
AC153526	74.56	35.1	98.58	0	70.5	30	4.43	0
AC167221	74.37	31.5	98.96	0	70.5	29	4.17	0
AC168874	73.99	40.7	97.95	0	67.2	35	4.80	0
AC168897	72.47	32.6	96.27	0	65.5	30	4.07	0
AC168901	74.23	34.2	98.50	0	70.6	31	4.08	0
AC168907	74.54	20.1	99.01	0	70.8	15	4.20	0
AC168908	73.96	42.7	98.05	0	69.2	38	4.54	0

REFERENCES

[1] B. Shimanovsky, J. Feng, and M. Potkonjak, **2003**, Hiding data in DNA, Information Hiding, *Springer Berlin Heidelberg*, 373-386, 2003.
[2] H. J. Shiu, K. L. Ng, J. F. Fang, R. C. T. Lee, and C. H. Huang, **2010**, Data hiding methods based upon DNA sequences, *Information Sciences*, 180 (11), 2196-2208, 2010.
[3] I. K. Maitra, S. Nag, B. Datta, and S. K. Bandyopadhyay, **2011**, Digital Steganalysis: Review on recent approaches, *Journal of Global Research in Computer Science*, 2, 2011.
[4] C. Guo, C. C. Chang, and Z. H. Wang, **2012**, A new data hiding scheme based on DNA sequence, *International Journal of Innovative Computing, Information and Control*, 8 (1A), 139-149, 2012.
[5] Y. H. Huang, C. C. Chang, and C. Y. Wu, **2012**, A DNA-based data hiding technique with low modification rates, *Multimedia Tools and Applications*, 1-13, 2012.
[6] H. Liu, D. Lin, and A. Kadir, **2013**, A novel data hiding method based on deoxyribonucleic acid coding, *Computers & Electrical Engineering*, 39 (4), 1164-1173, 2013.
[7] Y. A. Yunus, S. A. Rahman, and J. Ibrahim, **2013**, Steganography: A Review of Information Security Research and Development in Muslim World, *American Journal of Engineering Research*, 2 (11), 121-128, 2013.
[8] K. Gupta and S. Singh, **2013**, DNA Based Cryptographic Techniques: A Review, *International Journal of Advanced Research in Computer Science and Software Engineering*, 3 (3), 2013.
[9] S. Jain, H. Chaudhary, and V. Bhatnagar, **2013**, An information security-based literature survey and classification framework of data storage in DNA, *International Journal of Networking and Virtual Organisations*, 13 (2), 176- 201, 2013.
[10] A. K. Kaundal and A. K. Verma, **2014**, DNA based cryptography: A review, *International Journal of Information & Computational Technology*, 4 (7), 693-698, 2014.
[11] S. H. Lee, E. J. Lee, W. J. Hwang, and K. R. Kwon**, 2014,** A Watermarking Scheme for Coding DNA Sequences Using Codon Circular Code, Bio-Inspired Models of Network, Information, and Computing Systems, *Springer*, 134, 208-219, 2014.
[12] S. H. Lee, W. J. Hwang, E. J. Lee, and K. R. Kwon, **2014**, Coding DNA Sequence Watermarking, Frontier and Innovation in Future Computing and Communications, *Springer*, 301, 21-27, 2014.
[13] S. Manna, S. Roy, P. Roy, and S. K. Bandyopadhyay, **2014**, Modified technique of insertion methods for data hiding using DNA sequences, in First International Conference on *Automation, Control, Energy and Systems (ACES)*, 2014.
[14] S. H. Lee, **2014**, DNA sequence watermarking based on random circular angle, *Digital Signal Processing, Elsevier*, 25, 173-189, 2014.



International Journal of Pavement Engineering

ISSN: 1029-8436 (Print) 1477-268X (Online) Journal homepage: http://www.tandfonline.com/loi/gpav20

Economic assessment of use of pond ash in pavements

Raju Sarkar & A.R. Dawson

To cite this article: Raju Sarkar & A.R. Dawson (2015): Economic assessment of use of pond ash in pavements, International Journal of Pavement Engineering, DOI: 10.1080/10298436.2015.1095915

To link to this article: http://dx.doi.org/10.1080/10298436.2015.1095915

Published online: 29 Oct 2015.

Submit your article to this journal

Article views: 37

View related articles

View Crossmark data

Full Terms & Conditions of access and use can be found at
http://www.tandfonline.com/action/journalInformation?journalCode=gpav20

Download by: [Delhi Technological University] **Date:** 04 November 2015, At: 03:33

INTERNATIONAL JOURNAL OF PAVEMENT ENGINEERING, 2015
http://dx.doi.org/10.1080/10298436.2015.1095915

Taylor & Francis
Taylor & Francis Group

Economic assessment of use of pond ash in pavements

Raju Sarkar[a] and A.R. Dawson[b]

[a]Department of Civil Engineering, Delhi Technological University, Delhi, India; [b]Nottingham Transportation Engineering Centre, University of Nottingham, Nottingham, UK

ABSTRACT

The paper introduces a new type of industrial waste-based subbase material which can replace conventional subbase material (CSM) in pavement construction. Utilisation of this industrial waste, namely pond coal ash produced from a thermal power plant in road construction will help to reduce the disposal problem of this waste and also will help to reduce the problem of scarcity of CSM. Lime and fibre were also added to the pond ash at various percentages to improve the suitability of this type of mix as subbase material. The optimum service life of pavement is studied with the help of numerical modelling and the cost benefit is also presented in the current study. The study reveals that stabilisation of the coal ash with 2% lime may produce an optimal material and, even though a greater thickness may be required to deliver the same pavement performance, direct cost savings of around 10% may be achieved in addition to less easily quantifiable environmental benefits. Design charts are provided to exploit the findings.

ARTICLE HISTORY
Received 7 July 2015
Accepted 23 July 2015

KEYWORDS
Pond ash; geotechnical characterisation; numerical analysis; economic assessment

Downloaded by [Delhi Technological University] at 03:33 04 November 2015

1. Introduction

One of the major challenges facing the manufacturing and processing industries is the disposal of residual waste products. Ash, resulting from the combustion of coal to produce electricity, is a readily available by-product – particularly in India, the focus of this paper. As this availability is becoming more appreciated, demand for economic pavement construction materials, that impose a low environmental impact, is rapidly growing. Therefore, ash is considered in this paper as an alternative subbase material. Though a powdered material, but, due to its pozzolanic properties and when stabilised with cement, it might be made to meet the requirements of cement bound subbase material. Alternatively, lime could be used instead of cement, to give comparable long-term strengths (Sherwood 1995) albeit less rapidly developed (Atkinson *et al.* 1999). Fibre reinforcement is another possible improvement strategy (Kumar and Singh 2008).

Thus, the aim of this paper is to provide means of reliably incorporating ash, as found in disposal ponds at Indian power stations, into viable layers of pavement construction. The paper draws on laboratory test data reported earlier, using this data to numerically compute likely *in situ* behaviour. The aim is ultimately achieved by the production of design charts to guide users to the appropriate material and thickness of pavement layer incorporating that material and by providing an illustrative cost comparison.

2. Pavement layer practice and materials used

In India, in practice, flexible pavements are considered to act as a three-layer structure – subgrade, unbound (so-called) and bound layer. The lowest part of the unbound layers, which is just above the subgrade layer, is commonly known as the subbase layer of the pavement. The higher 'unbound' layer usually comprises a water bound macadam (WBM) or a wet mix macadam that forms the pavement base layer. While no cementing agent is added, compaction and water combine to provide a material held together by physical interlock and suction. It lies just above the subbase layer. The bound layer is usually divided into two parts, viz. the dense bituminous macadam (DBM) that lies above WBM and the top layer, known as bituminous concrete (BC) or wearing course. The subgrade layer is made up of locally available soil. The subbase layer is typically formed of unbound granular materials viz. natural sand, moorum, gravel and or crushed stone based on a combination of availability, economic factors and previous experience. The commonly used materials for the WBM layer are crushed, graded aggregate and granular material, and premixed with water. Crushed stone is also used as coarse aggregate. A DBM is a binder course in which bitumen binds together with a mixture of coarse and fine aggregate. The top bituminous layer (BC) comes directly into contact with the vehicle tyres. It consists of a mixture of aggregates and sufficient bitumen so that it provides an impermeable barrier to water percolation (Chakroborty and Das 2003).

3. Environmental considerations when using conventional materials

The most common materials that are used in road construction are bitumen, aggregate, crushed rock, sand and gravel.

CONTACT Raju Sarkar rajusarkar@dce.ac.in

© 2015 Taylor & Francis

New bitumen is an oil product and, hence, its abstraction from the ground incurs similar issues as those associated with obtaining fossil fuels. However, it is a recyclable material; it can be used repeatedly by reheating it, allowing the asphalt that it binds to be softened, reworked and replaced. But the initial heating and subsequent reheating and recycling requires large amounts of heat energy and thus produces lots of harmful greenhouse gases which pollute the environment. Again in summer, temperature rises and thus bitumen becomes soft. Natural solar heating will also causes softening of the bitumen, resulting in asphalt bleeding, rutting and segregation, and hence leads to failure of the pavement. During winter, if temperature reduces, the bitumen becomes brittle and it can result in cracking, ravelling and unevenness.

The other materials used in pavement construction are the products of mining. While requiring relatively low energy to produce and lay, haul costs (i.e. fuel, labour and maintenance) are the single largest variables in determining the cost of material in road construction. To limit these costs, sand and gravel mines are often opened near to a specific road project and then abandoned once the project is completed (Blodgett 2004), leading to widespread despoliation and degraded air quality at the mining site and its vicinity. Aggregate and sand mines require water to wash some of its product and to control dust on site. To fulfil this demand, many use scarce ground water competing undesirably with the increasing demands of domestic water use.

4. Situation in India

At present, the National Highway network consists of about 71,772 km, comprising only 1.7% of the total length of roads in India, but carries over 40% of the total traffic across the length and breadth of the country (MORT&H 2011). To alleviate congestion and to provide for future development, the Government of India has recently launched an extensive road construction programme under which thousands of kilometres of roads are currently under construction or scheduled for construction in the future. Current methods to be used for the construction of the new roads are not as per international standards. As an example, India is still using very small amounts of recycled aggregate material for road construction. Instead, it mostly depends on conventional materials viz. aggregate, crushed rock, sand and gravel.

As reviewed above, such materials are associated with considerable problems. Thus, to counteract these problems, India needs to focus on recyclable aggregate material or must replace conventional subbase or base materials with alternative materials. These materials could be industrial and domestic waste products since these materials are cheaply available and their use in road construction provides an efficient solution to the associated problems of pollution and disposal of these wastes.

Thermal power is the chief source of energy and produces nearly 70% of total energy production in India. Over 100 million tons per year (Gulhati and Datta 1999) of coal ash is generated by these thermal power plants. Due to high ash content of coal along with a low-percentage utilisation of the fly ash, most of the fly ash is disposed of on land by creating an engineered ash pond to take care of environmental concerns. While many European countries and Japan use more than 50% of fly ashes in an environmentally acceptable manner, India has a modest record of only 5% utilisation (Subbarao *et al.* 2001). The disposal of the fly ash is a serious hazard to the environment and consumes millions of rupees and many hectares of precious land.

Pond ash is the fly ash, as well as the bottom ash, produced by a power plant when it is disposed of in an ash pond in the form of a slurry, typically at a ratio varying between 1 part ash and 6–10 parts of water. Pond ash is a non-crystalline pozzolanic and slightly cementitious material. On the basis of these properties, it might be converted into meaningful wealth as an alternative construction material in civil engineering works (Sarkar *et al.* 2012). Use of pond ash in pavement construction could allow it to be used in large quantities. Therefore, this paper addresses its potential, stabilised both with and without fibres.

5. Opportunities for replacing conventional materials by ash products

There are numerous successful case histories on the utilisation of fly ash either alone or mixed with other material. Typically, fly ash has been used for soil stabilisation in road pavements – Chu *et al.* (1995); as embankment material – Raymond (1961); as structural fill – DiGioia and Nuzzo (1972); for injection grouting – Joshi *et al.*(1981); and as a replacement to cement – Gopalan and Haque (1986). Maser *et al.* (1975) reported successful studies on fly ash–cement mixture for subsidence control. Fawconnier and Korsten (1982) reported that the use of pulverised fly ash filling had effectively stabilised mines, reducing the risk of pillar failure in areas of low safety factor. Galvin and Wagner (1982) observed improved strata control using fly ash fill. Palariski (1993) reported the use of fly ash, mill tailings, rock and binding agents to make consolidated backfill material to improve extraction percentage in coal mines.

Mixing of a predetermined amount of fibre to a soil gives a mesh-like configuration leading to a mechanical means for reinforcement of the matrix, if done at appropriate moisture content (Nataraj and McManis 1997). Tests were carried out on the soils in which fibres were oriented in particular directions by Bauer and Fatani (1991), and Shewbridge and Sitar (1989). Tests were also carried out by Hoover *et al.*(1982), Setty and Rao (1987), Gray and Maher (1989), Maher and Gray (1990), Maher and Ho (1994), Michalowski and Zhao (1996), Consoli *et al.* (1998), and Santoni and Webster (2001) with randomly oriented fibres in soils. There, however, have been very few studies that discussed about fibre-reinforced and stabilised pond ash. Experimental studies have been carried out on some Indian fly ashes mixed with randomly oriented fibres. Chakraborty and Dasgupta (1996) studied the strength characteristics of polymer fibre-reinforced fly ash through triaxial shear tests. Kaniraj and Havanagi (2001) carried out experiments on randomly oriented fibre-reinforced fly ash–soil mixtures.

Dawson and Bullen (1991) investigated the engineering properties and possible use of furnace bottom ash as a subbase material. Index and large-scale pavement facility testing of furnace bottom ash in the laboratory and outdoor were carried out in this and subsequent investigations. Lee and Fishman (1993) studied the resilient and plastic behaviour of classifier tailings and fly ash

Downloaded by [Delhi Technological University] at 03:33 04 November 2015

Downloaded by [Delhi Technological University] at 03:33 04 November 2015

mixtures. Results from cyclic triaxial testing were used to study the resilient and plastic response of fly ash, classifier tailings, and a mixture of the two materials. Gray *et al.* (1994) evaluated a cement-stabilised fly ash base. In their study, the performance of compacted, aggregate-free, cement-stabilised fly ash beneath a highway shoulder was established. A field evaluation of pavement sections containing cement-treated bases with and without fly ash was undertaken by Ksaibati and Conklin (1994). In the study, pavement performance models were developed on the basis of the physical attributes of the sections. Dawson *et al.* (1996) used various combinations of secondary aggregates and binders in pavement foundations. They proposed various methods and procedures for the standard assessment of secondary materials viz. fly ash mixed with gypsum and lime, fly ash mixed with cement kiln dust and granular blast furnace slag and some combination of china clay and coarse aggregate. Ksaibati and Bowen (2001) undertook a wide range of laboratory testing in order to evaluate the feasibility of incorporating bottom ash into a crushed based material. Singh and Kumar (2005) studied the utilisation of fibre-reinforced fly ash in road subbases. Singh and Ramaswamy (2005) investigated the utilisation potential of cement-stabilised fly ash and granulated blast furnace slag mixes in highway construction. Mishra and Karanam (2006) carried out geotechnical characterisation of fly ash composites for backfilling mine voids. Chand and Subbarao (2007) carried out experiments on strength and slake durability of lime-stabilised pond ash. They attempted to check strength and durability aspects of lime-stabilised pond ash to determine its suitability for base and subbase courses of pavements. Titi *et al.* (2009) studied the resilient characteristics of bottom ash. The main aim of their research was to evaluate the characteristics of coal combustion bottom ash for potential utilisation as pavement construction materials.

From the above literature review, it is seen that fly ash can be used as a direct replacement material for unbound layers (subbase or base) of a pavement, with or without admixtures. Very little or no work has been done on the behaviour of the pavement structures incorporating various thicknesses of such ash as candidate layers for a pavement.

Another challenge is to determine the appropriate thicknesses of different layers to get the optimum pavement thickness. This challenge is important as, otherwise, service life or cost of construction of the pavement section may be intolerable. The cost of construction may be less due to the reduction in thickness of a particular layer of pavement, but if the service life is less, then the assumed benefit may, in practice, turn out to be a deterioration.

6. Aim and scope of work

The aim of this work is to determine ways of using coal pond ash as a subbase material in road construction that deliver adequate structural performance and that are economic. To achieve this general aim, an experimental study was carried out to understand the behaviour of pond ash mixed with admixtures, namely fibre and lime. The purpose of mixing these additives with pond ash is to improve the strength, deformability, volume stability (shrinking and swelling), permeability, erodibility, durability, etc. of the mix for their use in the pavement construction. The pond ash was characterised with respect to its physical and geotechnical behaviour. Proctor compaction and triaxial tests were carried out on pond ash alone and also after stabilisation of the pond ash by the addition of different percentages of the above admixtures within practical limits. The optimum percentage of the above admixtures was chosen based on these tests. Important geotechnical properties such as modulus of elasticity, cohesion and an angle of shearing resistance to be used in the numerical analysis were also evaluated from the test results.

Numerical studies on the performance of pavements constructed using these pond ashes, mixed with fibre and lime, were then carried out to evaluate the design life of pavements. A nominal pavement structure was designed considering Delhi silt as the subgrade soil. A stress–strain analysis was then performed, considering that the subbase layer is made up of pond ash stabilised with both admixtures, using the commercially available finite element software 'PLAXIS'. A parametric study was performed by varying the thickness of different layers with respect to a reference structure for each subbase material (pond ash + admixtures). Design charts were produced for different conditions including that of 'equal design life' based on the above parametric study. Finally, cost comparisons of the different pavement structures were carried out.

7. Materials used

7.1. Pond ash

The pond ash samples used in the present research work were obtained from the Badarpur plant site of the National Thermal Power Corporation located in the National Capital Region – Delhi. Pond ash is a pozzolanic material and can be stabilised with fibres and lime. The purpose of mixing these additives with pond ash is to improve the strength, deformability, volume stability (shrinking and swelling), permeability, erodibility, durability, etc. of the mix for its use in pavement construction. The chemical and geotechnical properties of the pond ash sample used in this study are given in Tables 1 and 2, respectively.

7.2. Fibre

A recent technique of soil or pond ash improvement is the mixing of randomly oriented fibres to the soil or pond ash (Chakraborty and Dasgupta 1996). The process is similar to the stabilisation using admixtures, i.e. discrete fibres are simply added and mixed with the pond ash. The compaction characteristics of fibre-reinforced pond ash do not differ significantly from unreinforced specimens (Kumar *et al.* 1996). One of the main advantages of randomly oriented fibres is the maintenance of strength isotropy and the absence of potential plane of weakness, which may develop parallel to oriented reinforcements. The physical and engineering properties of the polypropylene fibres used in this study are listed in Table 3.

Table 1. Chemical properties of Badarpur pond ash.

Constituents in percentage	Badarpur pond ash
SiO_2	49.5
Al_2O_3	25.01
MgO	1.21
Fe_2O_3	9.81
CaO	4.48
Loss on ignition	9.79
Others	0.08

Table 2. Geotechnical properties of Badarpur pond ash.

Properties	Badarpur Pond ash
Fine sand size, 0.475–0.075 mm, %	72
Silt size, 0.075–0.002 mm, %	22
Uniformity coefficient, C_u	4.8
Coefficient of curvature, C_c	1.05
Effective size D_{10}, mm	0.049
D_{30} size, mm	0.11
D_{60} size, mm	0.235
Specific gravity	2.1
LL and PL	Non-plastic
Maximum dry unit weight, kN/m^3	11.7
Optimum moisture content, %	32
Triaxial (CD) Test	
Cohesion intercept (c′), kPa	0
Angle of shearing resistance Φ′, °	28.9

Downloaded by [Delhi Technological University] at 03:33 04 November 2015

7.3. Lime

Calcium oxide (CaO) is a chemical compound, widely used to treat soils in the form of quicklime (CaO), hydrated lime (calcium hydroxide – $Ca(OH)_2$, or as a lime slurry. Quicklime is manufactured by high-temperature transformation of calcium carbonate (limestone – $CaCO_3$) into calcium oxide. Hydrated lime is created when quicklime chemically reacts with water. Hydrated lime reacts with silicates and aluminates in fly ash and clay particles and permanently transforms them into a strong cementitious matrix. The lime used in the present study was procured from the open market in the form of quicklime. This lime was then mixed with pond ash and water in the required proportions, by weight. Since the lime was procured from the open market, it is expected that its chemical composition will be similar to that given in Table 4.

The values of density, shear parameters and modulus of elasticity for different materials are given in Table 7.

8. Experimental investigations

Fibre was added to the pond ash at an increasing percentage of 0.2, 0.3, 0.4 and 0.5. Similarly, the lime was added with the pond ash at an increasing percentage of 2, 3, and 5. The details of the experimental programme are summarised in Table 5. The tests were performed conforming to the specifications given in Table 6.

9. Structural analysis

9.1. Pavement section

First, a typical pavement structure was designed with the selected subgrade material having a CBR equal to 9% and to carry a traffic load of 100 million standard axles (msa) as per IRC: 37-2001. This pavement structure is shown in Figure 1.

9.2. Modelling details

The following assumptions are made in the analysis:

- All layers have finite thickness including the bottom layer (subgrade).
- All layers are of finite extent in the lateral direction (even though infinite in extent in reality).
- Bituminous concrete (BC) and DBM exhibit linear elastic response.
- WBM, subbase and subgrade soils exhibit an elasto-plastic response and failure can be modelled using the Mohr–Coulomb constitutive relationship.

The pavement section was modelled as suggested by Huang (1993) to mechanistically solve the layered pavement response to traffic loading and to investigate the effect of subbase material on flexible pavement design. The pavement section considered for the finite element modelling is shown in Figure 2. A pressure of 575 kPa was applied at the surface distributed over a radius of 150 mm based on specifications of the Indian Road Congress. This uniform pressure is caused by a single wheel load of 40.8 kN. Dimensions of the axisymmetric finite element model employed were selected so that it was sufficiently large and, thus, the constraints imposed at the boundaries will have very little influence on the stress distribution in the system. Based on a small parametric study, this necessitated that the right boundary be placed 1100 mm from the outer edge of loaded area, which is more than seven times the radius of the applied load. The bottom extent of the subgrade was fixed at a subgrade depth of 500 mm, based on usual practice (IRC: 37-2001). Roller supports were provided along the axis of symmetry to achieve the condition that radial

Table 3. Physical and engineering properties of polypropylene fibres (supplier's data).

Properties	Value
Molecular formula	$(CH_2–CH_2)_n$
Young's modulus GN/m^2	7.1
Melting point, °C	89
Tensile strength, N/mm^2	125.28
Unit weight, kN/m^3	9.2
Diameter, mm	0.3
Aspect ratio	90

Table 4. Chemical composition of lime (supplier's data).

Minimum array (acidimetric)	95.00%
Maximum limits of impurities	
Chloride (Cl)	0.10%
Sulphate (SO_4)	0.50%
Iron (Fe)	0.10%
Lead (Pb)	0.02%
Loss on ignition	10%

Table 5. Experimental programme.

Source of pond ash	Details of experiments
Badarpur	Specific gravity Grain size distribution Atterberg limit tests Compaction tests:Light compaction (standard Proctor) test and heavy compaction (modified Proctor) test Consolidated drained triaxial tests under confining pressures of 100, 200 and 300 kPa

Table 6. Standard codes used to perform laboratory tests.

Laboratory tests	Standards/Procedures
Specific gravity	RILEM recommendations (1989)
Grain size analysis	IS: 2720 (Part 4) – 1985
Atterberg limit test	IS: 2720 (Part 5) – 1985
Standard Proctor compaction test	IS: 2720 (Part 7) – 1980
Modified Proctor compaction test	IS: 2720 (Part 8) – 1983
Consolidated drained triaxial shear test	IS: 2720 (Part 19) – 1981

Downloaded by [Delhi Technological University] at 03:33 04 November 2015

displacements are equal to zero. Also, the roller supports were provided along the right boundary which was placed sufficiently away from the centre of loading. At the bottom boundary, roller supports were provided for permitting free movement in the radial direction and a restraint to any movement in the vertical direction.

During the generation of the mesh, clusters were divided into triangular elements. The meshes are composed of 15-noded triangular elements which have a greater ability to model continuously varying stress–strain fields for less computational effort than would be needed using a far greater number of 6-noded triangular elements. Results were found to converge for the adopted mesh as shown in Figure 2.

The finite element analysis of the pavement system was carried out by considering values of resilient modulus, E, and Poisson's ratio, ν, given in Table 7. The pond ash collected from the Badarpur site, as well as the pond ash stabilised with admixtures, was considered as the subbase material in the present study. The adopted properties of these materials are summarised in Table 7.

The resilient modulus of the subgrade has been calculated as per IRC: 37-2001. In India, coarse sand or a mixture of river bed material and crushed stones are commonly used as a conventional subbase material (CSM) for pavement construction (Sinha, 2009). The properties of CSM are derived from the investigations of Lee *et al.* (2001) and Shodhganga (2006). Titi et al. (2009), Kumar and Singh (2008) and Ornebjerg *et al.* (2006) considered the value of resilient modulus of alternative subbase material, bottom ash and fly ash, similar to those being considered in this paper, obtaining values within the range 60–70 MPa. So, in the present study, the value of resilient modulus of pond ash was taken as 70 MPa. Similarly, Kumar and Singh (2008) considered the value of resilient modulus of fly ash mixed with fibre of 0.2 and 0.3% as 102.36 and 142.35 MPa. So in the present study, for simplicity, the values of pond ash mixed with fibre 0.2, 0.3, 0.4 and 0.5% are considered to be 100, 140, 160 and 170 MPa, respectively. Potentially the moduli of the mixes with higher moduli could be underestimated. In the case of pond ash mixed with lime, the resilient modulus is calculated by considering the initial tangent modulus of the triaxial stress–strain graph for 7-day-old material and subject to a confining stress of 100 kPa. The properties of WBM are considered on the basis of studies of Dawson *et al.* (1996) and Theyse (2002). Loulizi *et al.* (2006) tested hot-mix asphalt specimen from −15 °C to a maximum temperature of 40 °C to determine the resilient modulus of hot-mix asphalt. So, a small extrapolation was performed to determine the resilient modulus of hot-mix asphalt for a temperature of 45 °C (assuming

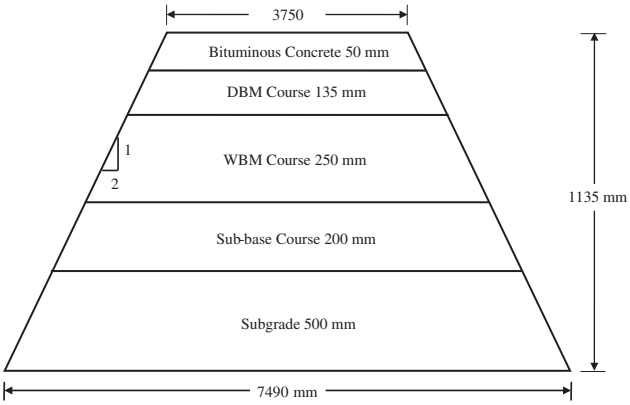


Figure 1. Pavement structure.

Downloaded by [Delhi Technological University] at 03:33 04 November 2015

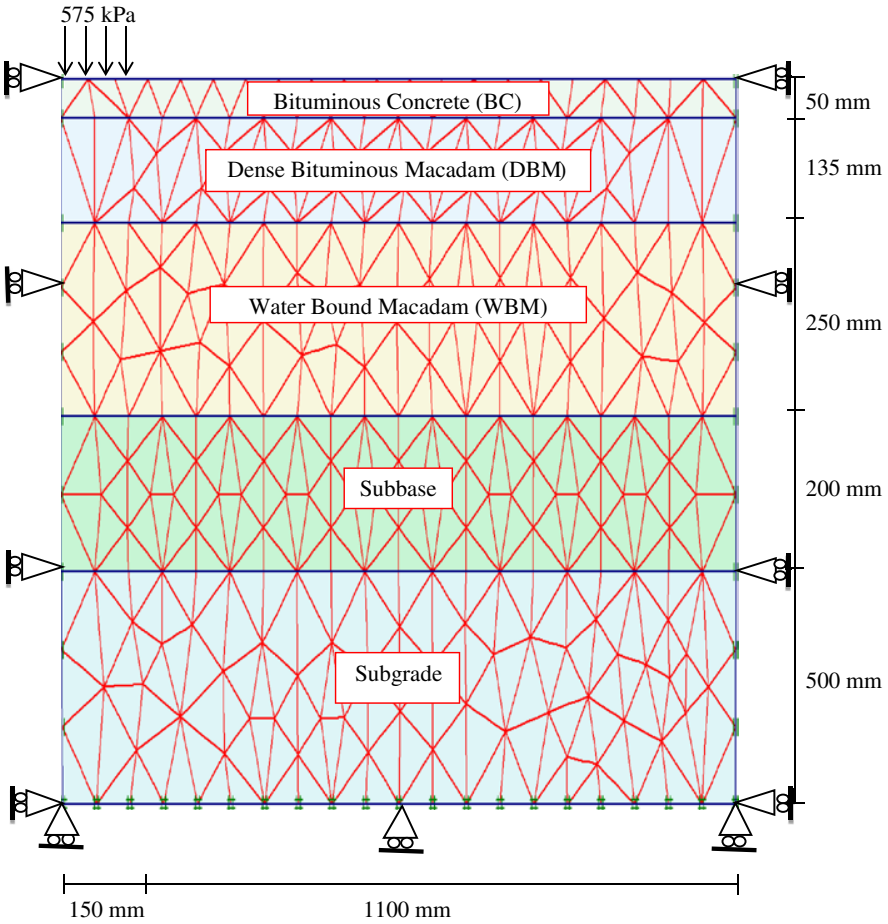


Figure 2. Finite element discretization of pavement section.

the maximum temperature during the summer period). The elastic modulus for bituminous concrete is considered as per IRC: 37-2001.

9.3. Parametric study

To develop design charts which help in decision-making and better utilisation of the technique of pond ash stabilisation by admixtures, a detailed parametric study was carried out by considering the nominal pavement as the reference structure and then varying the thickness of each layer within practical limits with respect to this nominal pavement, as given in Table 8. Other materials considered for subbase layer were as follows: Badarpur pond ash mixed with percentage of fibre and lime as mentioned in Table 7 and CSM. Given the expectation that stabilised ash might not perform so well as a CSM, greater thicknesses of this were considered than that of the CSM in the reference pavement. Also, since the ash-based material is expected to be economic

Table 7. Values of modulus of elasticity, Poisson's ratio and shear parameters for different pavement materials.

Layer	Constitutive model	Material	Maximum dry density (MDD) (kN/m^3)	Specific gravity *G*	Cohesion c′ (kPa)	Angle of repose s Φ′ (°)	Resilient modulus *E* (MPa)	Poisson's ratio (*v*)
BC	Elastic	Bitumen	21				700	0.35
DBM	Elastic	Bitumen Mix	18	2.3	–	–	1400	0.35
WBM	Elasto-plastic (Mohr–Coulomb)	Graded Aggregate	17.6	2.25	40	45	110	0.35
Subbase	Elasto-plastic (Mohr–Coulomb)	CSM[a]	20.4	2.67	14	37	140	0.35
		PA[b]	11.7	2.1	0	28.9	70	
		PA + Fibre						
		0.2%	11.8	2.11	18	30.3	100	
		0.3%	11.9	2.22	21.4	31.6	140	
		0.4%	12	2.25	24.8	33	160	
		0.5%	12	2.26	26.9	34	170	
		PA + Lime						
		2%	12.8	2.22	14	31.5	80	
		3%	13.5	2.25	20	32.2	110	
		5%	13.9	2.31	23.4	33.2	135	
Subgrade	Elasto-plastic (Mohr–Coulomb)	Delhi Silt	18	2.64	20	30	70	0.35

[a]Conventional subbase material.
[b]Pond ash.

Table 8. Variation in thickness considered in pavement study.

Layer	Reference pavement thickness (mm)	Variation in thickness (mm)
Bituminous concrete (BC)	50	None
Dense bituminous macadam (DBM)	135	110, 135, 160, 185
Base course (WBM)	250	150, 200, 250
Subbase course	200	200, 250, 300, 350, 400, 450, 500
Subgrade	300	None

Downloaded by [Delhi Technological University] at 03:33 04 November 2015

compared with the base and asphaltic layers, greater thicknesses of the ash layer might allow thinner layers of the higher pavement layers, introducing the possibility of overall cost savings.

9.4. Design life of pavement

Structural failures in a flexible pavement are of two main types, namely surface cracking and rutting.

9.4.1. Rutting

As per IRC: 37-2001, the occurrence of a rut depth of 20 mm is considered as the failure criterion. The design life or service life of a pavement is defined in terms of the cumulative number of standard axles that can be carried before strengthening of the pavement is necessary. The following equation is proposed in IRC: 37-2001 to calculate the design life on account of rutting failure alone:

$$N_R = 4.1656\ X\ 10^{-8}\left[1/\varepsilon_v\right]^{4.5337} \quad (1)$$

where N_R = Number of cumulative standard axles to produce rutting depth of 20 mm and

ε_v = Maximum vertical compressive strain at the top of subgrade in microns.

A service life ratio (SLR) as given below can be used to compare the effect of subbase material type on service life of a pavement:

$$\mathrm{SLR} = \mathrm{N}_1/\mathrm{N}_2 \quad (2)$$

and using Equation (1),

$$SLR = \left[\varepsilon_{v2}/\varepsilon_{v1}\right]^{4.5337} \quad (3)$$

where N_1, N_2 = Number of passes of a standard axle required to produce allowable rutting in a pavement with subbase material types 1 and 2, respectively, and

ε_{v1}, ε_{v2} = Vertical compressive strain at the top of subgrade layer with subbase material types 1 and 2, respectively

In the following analyses, subbase 1 is taken to be the one comprising CSM, 200-mm thick.

9.4.2. Fatigue

In a similar manner, a SLR can be computed for fatigue failure. The actual relationship will depend on the material that is subject to fatigue. For the purpose of this paper, the fatigue characteristics determined by IRC: 37-2001 for a DBM were adopted:

$$SLR = \left[\varepsilon_{t2}/\varepsilon_{t1}\right]^{3.89} \quad (4)$$

where ε_{t1}, ε_{t2} = Tensile strain at the bottom of the bound DBM course with subbase material types 1 and 2, respectively.

10. Test results and discussion

Figure 3(a–b) plots the maximum vertical compressive strain at the top of the subgrade vs. subbase thickness for the cases when the subbase layer is made up of Badarpur pond ash alone and mixed with fibre and lime, respectively, having the properties as given in Table 8, which vary with stabilisation rate. The magnitude of the maximum subgrade strain decreases with the increase in subbase thickness and with degree of stabilisation. The thicknesses of all layers except the subbase are maintained at their reference values (see Table 8). The magnitude of the vertical strain is simply and positively related to the rutting in the pavement.

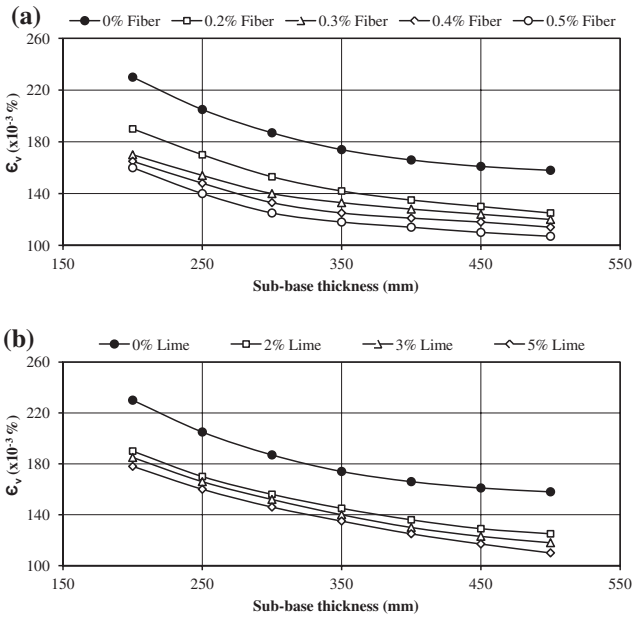


Figure 3. Vertical compressive strain-subbase thickness behaviour of pond ash mixed with (a) fibre and (b) lime.

The lesser the value of the maximum vertical compressive strain in the subgrade, the lesser is the rutting in the pavement and the longer is the life of the pavement.

It can be seen that, for fibre stabilisation, improvement continues until 0.3% fibre has been added but then, adding more fibre, causes little further benefit. In the case of lime, 2% addition achieves significant reductions in strain, whereas additional lime stabilisation achieves little further benefit.

Figure 4(a)–(c) shows the vertical compressive strain at the top of subgrade when the thickness of the subbase and of the bound courses (WBM and DBM) are varied. In each case, the subbase course is made up of pond ash stabilised with the preferred percentages of each admixture as mentioned above. For each arrangement, Figure 4(a–c) shows that the pond ash stabilised with 0.5% fibre gives the minimum strain (i.e. the shortest life). As expected, the maximum strain is obtained when the pond ash is used without any stabiliser.

Figure 5(a–b) shows the plots of the maximum tensile strain at the bottom of the DBM and subbase thickness behaviour for the cases when the subbase layer is made up of Badarpur pond ash mixed with fibre and lime, respectively, in the same percentages as mentioned above. The magnitude of the maximum tensile strain decreases with the increase in subbase thickness. For any particular type of bound material, the magnitude of the tensile strain is simply and positively related to the cracking in the pavement. The lesser the value of the tensile strain at the bottom of the DBM, the lesser is the cracking in the pavement and thus longer is the life of the pavement.

Figure 6 compares the minimum tensile strain at the bottom of the DBM with varying subbase thickness for the cases when the subbase layer is made up of pond ash stabilised with those percentages of each admixture that gave the probable optimal improvement in rutting behaviour (0.5% fibre and 2% lime) as well as for reference cases. As for the vertical subgrade strain, Figure 6 shows that the pond ash stabilised with 0.5% fibre gives the minimum tensile strain. Similarly, as for the case of vertical strain at the top of subgrade, the maximum tensile strain is obtained when the pond ash is used without any stabiliser.

The values of vertical compressive subgrade strain ε_v and tensile strain at the bottom of the bound, DBM, course, ε_t as picked from Figure 3(a–b) and Figure 5(a–b), for the structures including the range of selected subbase, are given in Table 9. The corresponding SLR for different pavement sections was evaluated using Equation (3). The maximum SLR following stabilisation of a 200-mm-thick subbase layer are 1.79 and 0.82 (considering vertical compressive strain), and 1.56 and 0.75 (considering tensile strain), respectively, for 0.5% fibres and 2% lime treatments, respectively. Thus, for the same thickness of ash subbase, treatment by fibres, but not by lime, yields a SLR that is higher than that for the conventional subbase. Vertical strains and tensile strains for pond ash alone and mixed with lime are much higher than that for CSM and so the SLRs are much lower than CSM. For all three alternatives given in Table 9, it is the tensile strain at the bottom of the asphaltic layers which is the limiting condition.

From Figure 7, which plots this SLR data, it is observed that the stiffness ratio (i.e. stiffness of ash compared to stiffness of CSM) increases monotonically with the increase in the SLR when the pond ash is mixed with various percentages of fibre and lime and used as subbase material.

The inverse of the above – the variation in the thickness of different layers of a pavement having a stabilised subbase layer needed to provide the same lifetime of the pavement as the conventional pavement is given in Table 10. As per IRC: 37-2001, the required thickness of the subbase layer for a traffic of 100 msa and for a CBR value of subgrade material of 9% is 200 mm when CSM is used as the subbase material. Thus, it needs to be increased to 315 mm when pond ash alone is used as the subbase material if the service life of the pavement is to remain unaffected (columns 2 and 3 of Table 10). This increased thickness for the same service life is termed as equivalent thickness.

Downloaded by [Delhi Technological University] at 03:33 04 November 2015

Downloaded by [Delhi Technological University] at 03:33 04 November 2015

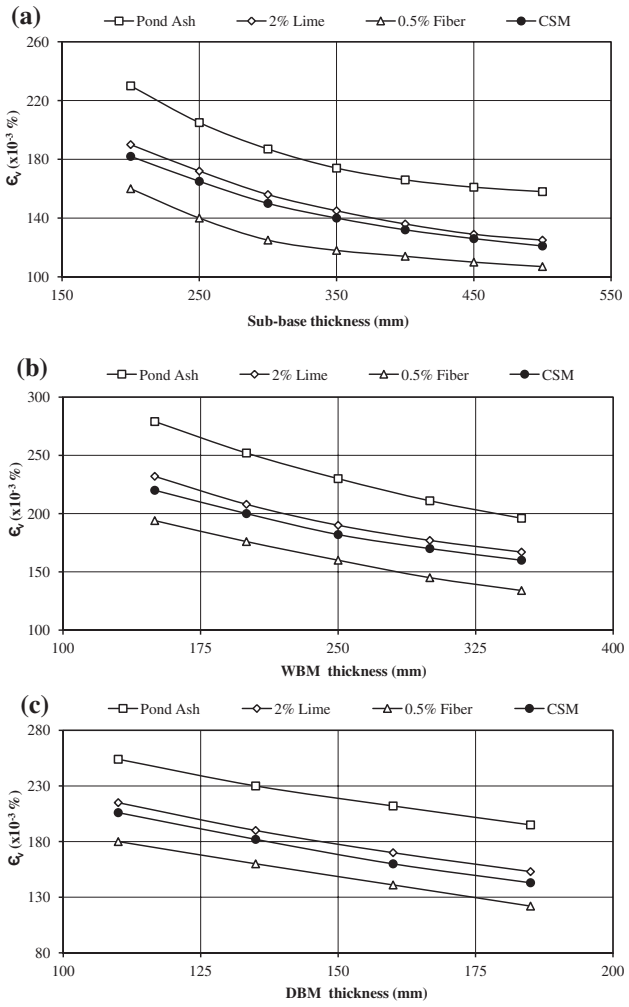


Figure 4. Comparison of variation of vertical compressive strain with (a) subbase, (b) WBM and (c) DBM thickness behaviour of pond ash and its mixes.

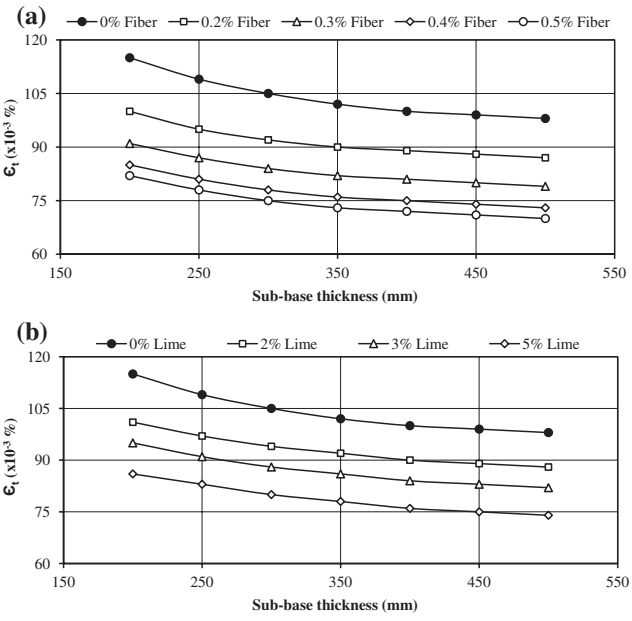


Figure 5. Tensile strain at the bottom of the DBM and subbase thickness behaviour of pond ash mixed with (a) fibre and (b) lime.

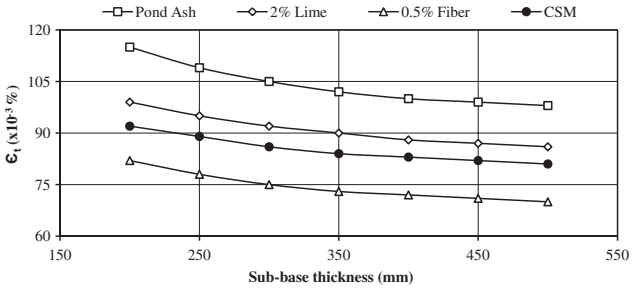


Figure 6. Comparison of variation of tensile strain at the bottom of the DBM as a function of the subbase thickness of pond ash and its mixes.

Table 9. SLR considering vertical compressive strains (VCS) at the top of subgrade and tensile strain (TS) at the bottom of the DBMfor different subbase materials (subbase thickness = 200 mm, WBM = 250 mm).

	Pond ash (PA)	PA + Fibre (0.5%)	PA + Lime (2.0%)	CSM
VCS ($\times 10^{-3}$%)	230	160	190	182
SLR (VCS)	0.35	1.79	0.82	1.00
TS ($\times 10^{-3}$%)	115	82	99	92
SLR (TS)	0.42	1.56	0.75	1.00

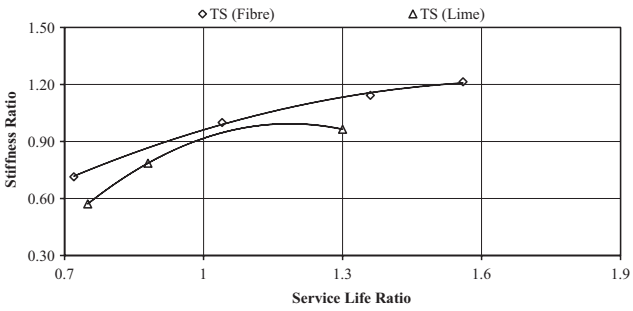


Figure 7. Variation of stiffness ratio (ash:CSM) with SLR of pond ash mixed with fibre and lime.

Table 10. Variation in equivalent thicknesses of different subbase materials for the same life of pavement.

	Subbase		WBM		DBM	
Material	Required thickness (mm)	Increase in thickness (%)	Required thickness (mm)	Increase in thickness (%)	Required thickness (mm)	Increase in thickness (%)
CSM as per IRC (2001)	200	0	250	0	135	0
Pond ash + Fibre (0.5%)	95	−52.5	150	−40.0	97	−28.2
Pond ash + Lime (2.0%)	300	50.0	352	40.8	169	25.2
Pond ash alone	580	190	463	85.2	210	55.6

The problem of a thick pavement section in such cases can be easily overcome by keeping the subbase thickness of 200 mm the same (as per design) but increasing the thickness (usually by a much smaller amount) of either the WBM layer or the DBM layer (as shown in the last 4 columns of Table 10). The decision of such replacement will naturally be guided by economy of construction.

Figure 8 depicts the equivalent thickness of subbase, WBM or DBM layers that will give the same SLR; in each case, the other layers retain their reference thickness. The procedure to pick equivalent thickness is illustrated in Figure 8(b), e.g. when the WBM thickness would be 240 mm over a CSM, its thickness can be reduced to 140 mm if an ash + 0.5% fibre is used as the subbase or must be increased to 445 mm if the ash is used unstabilised (see dashed lines on Figure 8(b)). The results are summarised in Table 10.

11. Economic assessment

In the present study, the pavement is designed for a single subgrade soil. The various layers are considered as shown in Figure 1. Based on assumption made by Central Road Research Institute (CRRI), Delhi (2009), on daily commercial traffic volume of a major part of Delhi, the design data for the cost analysis in the current study are assumed as follows:

Initial traffic in the year of completion of construction	= 100 msa
Design life	= 15 years
CBR value of subgrade (Table 7)	= 9%

Downloaded by [Delhi Technological University] at 03:33 04 November 2015

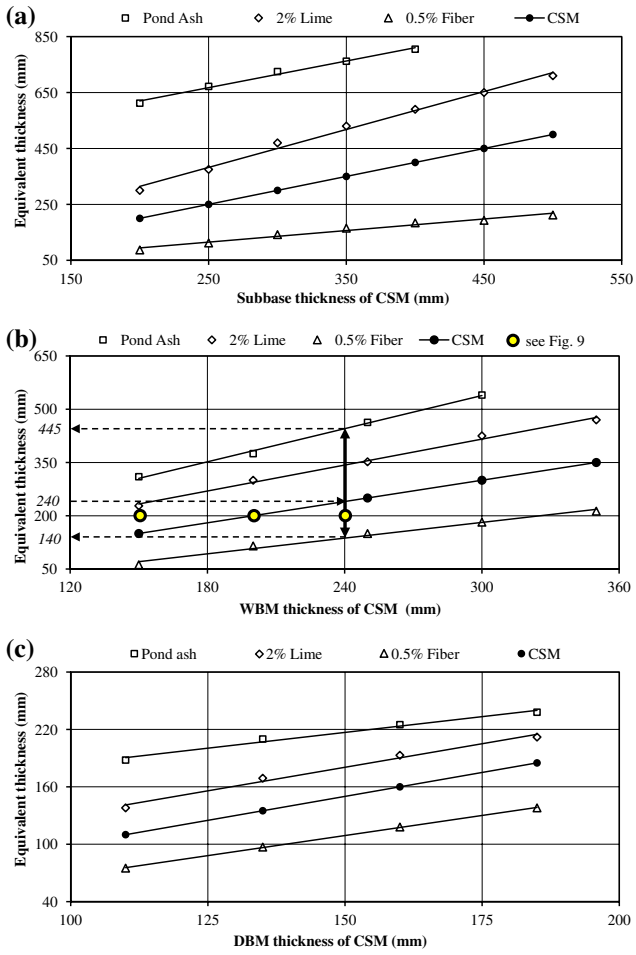


Figure 8. Variation of equivalent thickness of (a) subbase (b) WBM (c) DBM of different materials for same service life when pond ash mixture is used as subbase material.

The pavement was designed as per IRC 37:2001 and a pavement thickness of 635 mm was obtained as shown in Figure 1. Based on IRC 86:1983, the other details were assumed as given below:

Top width of embankment	= 3750 mm
Side slope	= 2H:1 V
Length of embankment	= 1000 m

For simplicity, the cost of the preparation of subgrade, CSM subbase, granular base, DBM and bituminous concrete is considered to be the same in all cases and were taken from Tirumala (2007). However, the cost of the preparation of different subbase layers varies, depending upon the thickness and the material of the subbase. The current schedule of rates for Delhi region is used for the cost analysis of subgrade, subbase, WBM, DBM and BC course.

The details of the cost analysis per $m^3$for subgrade are shown in Table 11.

The cost analysis of subbase constructed by pond ash, pond ash mixed with admixtures and CSM is shown in Table 12. The details of the cost are worked out assuming the plant output per day is 300 m^3. The calculations of admixtures are done as below:

Density of polypropylene fibre	= 920 kg/m^3
Density of lime	= 3350 kg/m^3
The amount of fibre required for the pond ash–fibre mix	= (300 × 0.5% × 920/1000) = 1.38 T
The amount of lime required for the pond ash–lime mix	= (300 × 2% × 3350/1000) = 20.1 T

The details of the cost analysis per $m^3$for base course WBM of Grade-3 are shown in Table 13 on a similar basis.

The cost analysis of DBM as per Ministry of Road Transport & Highways (MORT&H), Government of India, Grade-2 is shown in Table 14, using the same approach. The compositions of the adopted DBM materials are considered as per Sinha (2009):

Coarse aggregate (CA)	= 65%
Fine aggregate (FA)	= 35%
Bitumen content of mix	= 4.5% by wt.
Bulk density of mix	= 2352 kg/m^3
The unit wt. of CA	= 1545 kg/m^3
The unit wt. of FA	= 1650 kg/m^3

The details of the cost are worked out assuming the plant output per day = 147 MT (62.5 m^3)

Finally, the cost analysis of bituminous concrete (BC) is shown in Table 15. The adopted BC materials are as per MORT&H, with the following composition (Sinha, 2009):

Coarse aggregate (CA)	= 62%
Fine aggregate (FA)	= 35%
Filler (lime)	= 3%
Bitumen content of mix	= 5.5% by wt.

Downloaded by [Delhi Technological University] at 03:33 04 November 2015

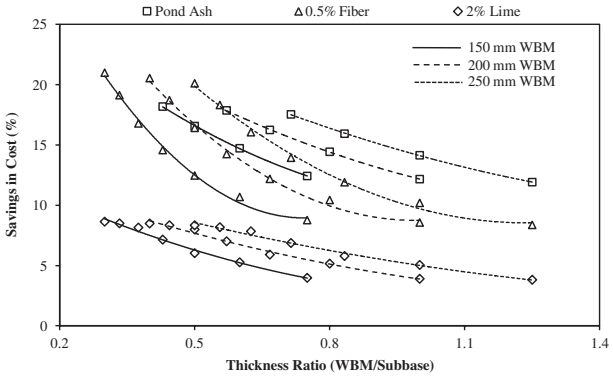


Figure 9. Comparison of percentage saving of cost and thickness ratio considering vertical strain at the top of subgrade.

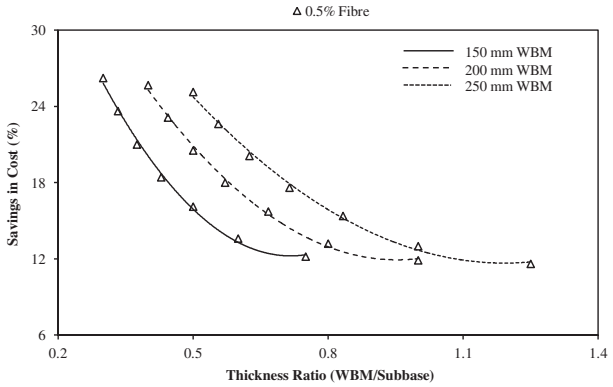


Figure 10. Comparison of percentage saving of cost and thickness ratio considering tensile strain at the bottom of DBM.

Bulk density of mix	= 2376 kg/m^3
The unit wt. of CA	= 1545 kg/m^3
The unit wt. of FA	= 1650 kg/m^3

The details of the cost are worked out assuming the plant output per day = 147 MT (61.9 m^3)

The cost analysis per m^{3}for subgrade, subbase, WBM, DBM and BC is summarised in Table 16. The construction cost of different layers including the subbase layers consisting of pond ash alone and the pond ash stabilised with two different admixtures for the same service life is given in Table 17 for a 1-km-long pavement (using the results summarised earlier in the 'subbase thickness' column of Table 10). Percentage savings in the total cost by direct replacement of CSM by pond ash alone and of ash mixes with admixtures are also shown in Table 17.

As mentioned earlier, for the same pavement life, an increased thickness of subbase made of ash-based material could be used to partially replace a thickness of WBM. A comparison of the savings in the cost of construction with respect to thickness ratio of WBM to subbase for various subbase materials considering maximum vertical compressive strain at the top of subgrade and maximum tensile strain at the bottom of DBM is shown in Figures 9 and 10, respectively. This is based on the thickness data presented in the subbase and WBM thickness columns of Table 10 and on similar computations for other thickness combinations.

Table 11. Cost analysis of subgrade course.

Taking Output: 100 m^3						
(a)	Labour component					
	Sl. No.	Item	Unit	Quantity	Rate (Rs.)	Amount (Rs.)
	1	Mate	Day	0.04	360.49	14.42
	2	Labour (unskilled)	Day	1.50	238.07	357.11
	Total					371.53
	Total per m^3					3.72
(b)	Machinery					
	Sl. No.	Item	Unit	Quantity	Rate (Rs.)	Amount (Rs.)
	1	Grader	Hr	2.00	1800.00	3600.00
	2	Dozer	Hr	0.50	1200.00	600.00
	3	Water tanker	Hr	5.00	350.00	1750.00
	4	Vibratory compactor	Hr	1.25	760.00	950.00
	5	Dumper	Hr	1.25	1400.00	1750.00
	6	Excavator	Hr	1.00	1700.00	1700.00
	7	Soil spreading unit	Hr	0.36	2250.00	810.00
	Total					11160.00
	Total per m^3					111.60

Downloaded by [Delhi Technological University] at 03:33 04 November 2015

Table 12. Cost analysis of subbase constructed by pond ash, pond ash mixed with admixtures and CSM.

Taking Output: 300 m^3						
(a)	Labour component					
	Sl. No.	Item	Unit	Quantity	Rate (Rs.)	Amount (Rs.)
	1	Mate	Day	0.48	360.49	173.04
	2	Labour (Skilled)	Day	2.00	292.45	584.90
	3	Labour (Unskilled)	Day	10.00	238.07	2380.70
	Total					3138.64
	Total per m^3					10.46
(b)	Machinery					
	Sl. No.	Item	Unit	Quantity	Rate (Rs.)	Amount (Rs.)
	1	Grader	Hr	6.00	1800.00	10800.00
	2	Water Tanker	Hr	5.00	350.00	1750.00
	3	Vibratory Compactor	Hr	10.00	760.00	7600.00
	4	Tractor with Rotavator	Hr	10.00	360.00	3600.00
	Total					23750.00
	Total per m^3					79.17
(c)	Material cost					
	Sl. No.	Item	Unit	Quantity	Rate (Rs.)	Amount (Rs.)
	1	Pond Ash (30% extra for loose state)	m^3	390.00	0.00	0.00
	2	Fibre (0.5%)	T	1.38	96000.00	132480.00
	3	Lime (2%)	T	20.1	7000.00	140700.00
	4	CSM*	m^3	384.00	591.10	226982.40
	Combinations		1 (Rs.)	1+2 (Rs.)	1+3 (Rs.)	4 (Rs.)
	Total		0.00	132480.00	140700.00	226982.40
	Total per m^3		0.00	441.60	469.00	756.61
(d)	CP & OC**		11.20	66.40	69.83	105.78
	Grand Total (a + b + c + d)		100.83	597.63	628.46	952.02

*Rate of CSM (75% of RBM @ Rs. 572.20 and 25% of 45–63 Stone Ballast @ Rs.647.80)
**Contractor's Profit and Overhead Charges @12.5% on (a) + (b) + (c).

Table 13. Cost analysis of base course WBM of Grade-3.

Taking Output: 360 m^3						
(a)	Labour component					
	Sl. No.	Item	Unit	Quantity	Rate (Rs.)	Amount (Rs.)
	1	Mate	Day	10.08	360.49	3633.74
	2	Labour(Skilled)	Day	2.00	292.45	584.90
	3	Labour(Unskilled)	Day	200.00	238.07	47614.00
	Total					51832.64
	Total per ^{m3}					143.98
(b)	Machinery					
	Sl. No.	Item	Unit	Quantity	Rate (Rs.)	Amount (Rs.)
	1	Vibratory Compactor	Hr	45.00	760.00	34200.00
	2	Water Tanker	Hr	24.00	350.00	8400.00
	Total					42600.00
	Total per m^3					118.33
(c)	Material cost					
	Sl. No.	Item	Unit	Quantity	Rate (Rs.)	Amount (Rs.)
	1	GSB Material*	m^3	522.00	659.64	344332.08
	Total					344332.08
	Total per m^3					956.48
(d)	Contractor's Profit and Overhead Charges @12.5% on (a) + (b) + (c)					152.35
	Grand Total (a + b + c + d)					1371.14

*Rate of GSB Material (80% of 22–53 Stone Ballast @ Rs. 647.80 and 20% of 10–12.5 Aggregate @ Rs.707.00).

From Figure 9, the saving in the total cost of construction is 11.49, 5.18 and 12.41% when 200-mm-thick subbase layer is made up of pond ash with no addition, 0.5% fibre and 2% lime, respectively, keeping the WBM thickness at 250 mm (thickness ratio = 1.25). The saving in the total cost of construction is 12.13, 5.54 and 12.69% when 200-mm subbase layer is made up of the same materials as mentioned above, keeping the WBM thickness as 200- mm (thickness ratio = 1.0); and savings of 12.39, 5.68 and 12.97% are achieved for a 150-mm WBM thickness and a 200-mm subbase layer (thickness ratio = 0.75).

The saving in the total cost of construction for the equivalent thicknesses of subbase layer made up of pond ash alone and with 2% lime, considering tensile strain at the bottom of DBM, could not be made. This is because, instead of a saving, the cost of construction of the pavement is increased due to the application of these materials (due to the cost of subbase preparation being greater than for the saving in subbase made up of CSM). Only 0.5% fibre treatment produces a cost saving when tensile strain at the bottom of the DBM layer is considered. Figure 10 shows the possible savings as a function of WBM and subbase thickness.

The sensitivity of the percentage saving of the cost of construction of 1-km pavement was checked based on a small parametric study considering maximum vertical compressive strain at the top of subgrade and maximum tensile strain at the bottom of DBM. In the study, the cost of WBM, DBM or BC course was (separately) increased by 10% from the basic price. The thickness

Downloaded by [Delhi Technological University] at 03:33 04 November 2015

Table 14. Cost analysis of DBM of Grade-2.

Taking Output: 62.5 m^3						
(a)	Labour component					
	Sl. No.	Item	Unit	Quantity	Rate (Rs.)	Amount(Rs.)
	1	Labour(Unskilled)	Day	16.50	238.07	3928.16
	Total					3928.16
	Total per m^3					62.85
(b)	Machinery					
	Sl. No.	Item	Unit	Quantity	Rate (Rs.)	Amount(Rs.)
	1	Plant	Day	1.00	10000.00	10000.00
	2	Tipper	Day	3.60	1600.00	5760.00
	3	Loader	Day	1.00	900.00	900.00
	4	Road Roller	Day	3.60	1000.00	3600.00
	Total					20260.00
	Total per m^3					324.16
(c)	Material cost					
	Sl. No.	Item	Unit	Quantity	Rate (Rs.)	Amount(Rs.)
	1	Bitumen	T	6.615	33000.00	218295.00
	2	Coarse Aggregate	m^3	58.90	647.80	38155.42
	3	Fine Aggregate	m^3	29.70	707.00	20997.90
	Total					277448.32
	Total per m^3					4439.17
(d)	Contractor's Profit and Overhead Charges @12.5% on (a)+(b)+(c)					603.27
	Grand Total (a + b + c + d)					5429.45

Table 15. Cost analysis of bituminous concrete (BC).

Taking Output: 61.9 m^3						
(a)	Labour component					
	Sl. No.	Item	Unit	Quantity	Rate (Rs.)	Amount (Rs.)
	1	Labour (Unskilled)	Day	16.50	238.07	3928.16
	Total					3928.16
	Total per m^3					62.85
(b)	Machinery					
	Sl. No.	Item	Unit	Quantity	Rate (Rs.)	Amount (Rs.)
	1	Plant	Day	1.00	10000.00	10000.00
	2	Tipper	Day	3.60	1600.00	5760.00
	3	Loader	Day	1.00	900.00	900.00
	4	Road Roller	Day	3.60	1000.00	3600.00
	Total					20260.00
	Total per m^3					324.16
(c)	Material cost					
	Sl. No.	Item	Unit	Quantity	Rate (Rs.)	Amount (Rs.)
	1	Bitumen	T	8.09	33000.00	266970.00
	2	Coarse Aggregate	m^3	55.78	647.80	36134.28
	3	Fine Aggregate	m^3	29.50	707.00	20856.50
	4	Lime	T	4.20	1800.00	7560.00
	Total					331520.00
	Total per m^3					5304.32
(d)	Contractor's profit and overhead charges @12.5% on (a) + (b) + (c)					711.42
	Grand Total (a + b + c + d)					6402.75

Table 16. Thickness and cost of construction of various layers.

		Subbase course						
Pavement component	Sub-grade	CSM	Pond ash	Pond ash +Fibre (0.5%)	Pond ash +Lime (2%)	WBM course	DBM course	Bituminous concrete
Thickness (mm)	500			200		250	135	50
Cost per m^3 (Rs.)	111.6	952.02	100.83	597.63	628.46	1371.14	5429.45	6402.75

ratio was varied by keeping WBM thickness (=250 mm) constant but increasing the subbase thickness from 200 mm to 500 mm, as mentioned in Table 7.

For these 10% increases in material costs, the parametric study revealed that the saving in the cost of construction reduced by 1.7–2.2% (pond ash alone), 3.1–4.0% (ash + 5% fibre) and 1.3–1.6% (ash + 2% lime); the range being a consequence of the particular material that was 10% more expensive. These figures are based on the change in pavement performance as predicted by the change in vertical compressive strain. The predicted cost saving reduced a little less (by only 1.4–3.9% for the ash + 5% fibre) when the change in tensile strain at the bottom of the DBM was considered. Thus, rutting is expected to be the controlling factor in determining sensitivity to material prices.

12. Design recommendations

From Figure 9, for the thickness ratio of 0.3 (thickness of WBM = 150 mm and subbase = 500 mm) considering vertical strain at the top of subgrade, the percentage saving of the

Downloaded by [Delhi Technological University] at 03:33 04 November 2015

Table 17. Percentage saving in the cost for 1-km-long pavement section with stabilised subbase layer for the same service life.

Sl. No.	Pavement component		Top width (m)	Bottom width (m)	Height* (m)	Volume (m^3)	Rate per m^3 (Rs.)	Total Rate (Rs.)	Total Cost (Rs.) (1+2+3+4+5)	Saving in cost (%)
1	Bituminous Course		3.75	3.95	0.05	192.5	6402.75	1232529	–	–
2	DBM Course		3.95	4.49	0.135	569.7	5429.45	3093158		
3	WBM Course		4.49	5.49	0.250	1247.5	1371.14	1710497		
4	Subbase Course		5.49							
(a)	CSM			6.29	0.200	1178	952.02	1121480		–
(b)	Pond Ash			6.75	0.315	1928	100.83	194380		
(c)	Pond Ash + Fibre (0.5%)			6.07	0.145	838	597.63	500874		
(d)	Pond Ash + Lime (2%)			6.378	0.222	1317	628.46	827901		
5	Subgrade	(a)	6.29	8.29	0.5	3645	111.60	406782	7564446	–
		(b)	6.75	8.75		3875		432450	6663014	11.92
		(c)	6.07	8.07		3535		394506	6931564	8.37
		(d)	6.378	8.378		3689		411692.4	7275777	3.82

*Equivalent height of same SLR.

Downloaded by [Delhi Technological University] at 03:33 04 November 2015

cost of construction of 1-km pavement is maximum (=21.00%) when pond ash mixed with 0.5% fibre is used as subbase material. Similarly, for the thickness ratio of 1.25 (thickness of WBM = 250 mm and subbase = 200 mm), the percentage saving of the cost of construction of 1-km pavement is minimum (=3.82%) when pond ash mixed with 2% lime is used as subbase material. As per IRC: 37-2001, considering a traffic load of 100 msa and CBR of 9% subgrade, the recommended thicknesses of WBM and subbase are 250 mm and 200, respectively, (Figure 1), i.e. thickness ratio = 1.25. For this recommended thickness ratio, the percentage savings of the cost of construction of pavement are minimum than the rest when subbase layer is made up of pond ash alone and mixed with admixtures. However, if we consider the above-recommended thicknesses of WBM and subbase as per IRC: 37-2001, the SLR of the pavement will be reduced by 18% (SLR = 0.82) taking SLR = 1.00 for CSM.

Similarly, from Figure 10, for the thickness ratio of 0.3 (thickness of WBM = 150 mm and subbase = 500 mm) considering tensile strain at the top of WBM, the percentage saving of the cost of construction of 1-km pavement is maximum (=26.23%) when pond ash mixed with 0.5% fibre is used as subbase material. Similarly, for the thickness ratio of 1.25 (thickness of WBM = 250 mm and subbase = 200 mm), the percentage saving of the cost of construction of 1-km pavement is minimum (=11.89%) when same material is used as subbase material.

The main purpose/aim of the present study is to maximise the utilisation of pond ash as subbase material alone or with admixture to replace the CSM, without affecting the service life of the pavement. Again while selecting the subbase material, the cost of construction of the pavement is also to be considered. So keeping both the points in mind and considering Figures 9 and 10, the thickness ratio of 0.3 (thickness of WBM = 150 mm and subbase = 500 mm) when pond ash mixed with 0.5% fibre is used as subbase material is recommended for the construction of pavement keeping other course of pavement section constant.

13. Conclusions

In the present study, induced vertical strain and tensile strain at the top of subgrade and at the top of WBM, respectively, are used to compare the quality and cost of different pavements when the subbase layer is made up of Badarpur pond ash alone and Badarpur pond ash stabilised with different admixtures. A commercially available finite element-based software 'PLAXIS' is used to evaluate the vertical and tensile strain at the top of subgrade and at the top of WBM, respectively, and as well as the distribution of strain inside different layers of pavement. The pavement section was modelled as an axisymmetric problem and standard boundary conditions were used. The extent of the boundaries of the section was then fixed by a small parametric study.

A nominal pavement structure used for the parametric study was first designed as per IRC: 37-2001 considering a traffic load of 100 msa and CBR of 9% corresponding to Delhi silt subgrade at Jamia Millia Islamia. The thickness of subbase layer, WBM layer and DBM layer was then varied with respect to this nominal pavement and the response of the pavement was evaluated.

Designed life and service life of a pavement is defined as the cumulative number of standard axles that can be carried before strengthening of pavement is necessary based on rutting failure criterion. A standard equation is available that uses maximum subgrade vertical strain to evaluate the design life and thus, the quality of the pavement. A SLR is defined as a function of induced subgrade strain in a given pavement vis-à-vis in a conventional pavement structure. Thus, the SLR indicates the lifetime of other pavements vis-à-vis conventional pavement structure.

An equivalent thickness is defined as the modified thickness of a particular layer of a new pavement required that has one of the layers made up of new material such that the lifetime of the new pavement remains the same as that of the conventional pavement. Based on the above parametric study, the equivalent thickness of subbase, WBM and DBM layers are calculated when the subbase layer is made up of Badarpur pond ash mixed with no additive, 0.5% fibre and 2% lime. This was followed by the cost analysis of 1-km-long pavement structure with a top width of 3.75 m based on the schedule of rates for Delhi region. Based on this study, the following conclusions are drawn.

(1) The vertical compressive strain was found to be maximum for pond ash.
(2) i) With the increase in the percentage of fibre (up to 0.5%), the stiffness of pavement increases and the maximum strain decreases.
ii) With the increase in the percentage of lime (up to 5%), the stiffness of pavement increases and the maximum strain decreases. But from simplicity of mixing

point of view, the percentage of lime used was 2% in the test.

(3) For the same SLR, the thickness of subbase layer made up of CSM (=200 mm) varies from 0.145 to 0.315 m. The maximum thickness is obtained from pond ash and minimum from fibre. The corresponding saving in the total cost is 3.82%–11.92%. The maximum cost saving is in pond ash and minimum is in lime.

(4) Keeping the subbase layer made of different admixtures constant (=200 mm), the same service life can be obtained by varying the thickness of WBM. Based on this, the thickness of WBM varies from 0.181 to 0.460 m for 200-mm-thick subbase layer of different admixtures. The maximum WBM thickness was obtained where pond ash used as subbase material and minimum thickness was obtained where fibre-reinforced pond ash used as subbase material. The saving in the total cost of construction is 11.49, 5.18 and 12.41% when 200-mm-thick subbase layer is made up of pond ash with no addition, 0.5% fibre and 2% lime, respectively, considering WBM thickness as 250 mm (thickness ratio = 1.25). Again, the saving in the total cost of construction is 12.13%, 5.54% and 12.69 and 12.39, 5.68 and 12.97% when 200-mm subbase layer is made up of same materials as mentioned above, considering WBM thickness as 200 mm (thickness ratio = 1.0) and 150 mm (thickness ratio = 0.75), respectively.

(5) Keeping the subbase layer made of different admixtures constant (=200 mm), the same service life can be obtained by varying the thickness of DBM. Based on this, the thickness of DBM varies from 0.108 to 0.200 m for 200-mm-thick subbase layer of different admixtures. The maximum DBM thickness was obtained where pond ash was used as subbase material and minimum thickness was obtained where pond ash mixed with 0.5% fibre used as subbase material.

(7) Comparing subbase and WBM, the variation in subbase thickness gives the maximum saving for same SLR.

(8) Based on a parametric study, it is seen that the percentage saving of the cost of construction of the pavement is between 1.3 and 4% for a 10% increase in WBM, DBM or BC costs.

Downloaded by [Delhi Technological University] at 03:33 04 November 2015

Acknowledgements

The first author wishes to thank M/s PDP Steels Limited, Assam, for funding and Delhi Technological University for allowing a short sabbatical visit to the University of Nottingham where most of the research reported here was performed. Both authors thank the Nottingham Transportation Engineering Centre at the University of Nottingham for providing the facilities to host this visit.

Disclosure statement

No potential conflict of interest was reported by the authors.

References

Atkinson, V.M., Chaddock, B.C., and Dawson, A.R., 1999. *Enabling the use of secondary aggregates and binders in pavement foundations*. Crowthorne: Transport Research Laboratory, TRL Report 408.

Bauer, G.E. and Fatani, M.N., 1991. Strength characteristics of sand reinforced with rigid and flexible elements, *Proceedings of ix Asian Regional Conference on soil mechanics and foundation engineering*, Bangkok, 1, 471–474.

Blodgett, S., 2004. *Environmental impacts of aggregate and stone mining-New Mexico case study*. New Mexico, NM: Center for Science in Public Participation.

Bullen, F. and Dawson, A.R., 1991. Furnace bottom ash: its engineering properties and its use as a sub-base material. *ICE Proceedings*. 90, 993–1009.

Central Road Research Institute, 2009. *Pavement engineering and materials – pavement evaluation*. Annual Report 2009–10, 51–76.

Chakraborty, T.K. and Dasgupta, S.P., 1996. Randomly reinforced fly ash foundation material, *Indian Geotechnical Conference*, Madras, India, 1, 231–235.

Chakroborty, P. and Das, A., 2003. Principles of transportation engineering. New Delhi: Prentice Hall of India.

Chand, S.K. and Subbarao, C., 2007. Strength and slake durability of lime stabilized pond ash. *Journal of Materials in Civil Engineering*. ASCE, 19 (7), 601–608.

Chu, T.Y., *et al.*, 1995. Soil stabilization with lime-fly ash mixtures: preliminary studies with silty and clayey soils. *Highway Research Board Bulletin*, 108, 102–112.

Consoli, N.C., Prietto, P.D.M., and Ulbrich, L.A., 1998, Influence of fiber and cement addition on behavior of sandy soil. *Journal of Geotechnical and Geoenvironmental Engineering*. ASCE, 124 (12), 1211–1214.

Dawson, A.R., *et al.*, 1996. Enabling the use of secondary aggregates and binders in pavement foundations, *Results of Phase 2 Study. Link II Project*. UK: University of Nottingham.

DiGioia, A.M. and Nuzzo, W. L., 1972. Fly ash as structural fill. *Journal of Power Division*, ASCE, 98 (1), 77–92.

Fawconnier, C.J. and Korsten, R.W.O., 1982. *Ash fill in pillar design-Increased Underground Extraction of Coal*. The SAIMM Monograph Series, 4, 277–361.

Galvin, J.M. and Wagner, H., 1982. Use of ash to improve strata control in bord and pillar working. *In: Proceedings symposium on strata mechanics*. University of Newcastle-upon-Tyne, 264–270.

Gopalan, M.K. and Haque, M.N., 1986. Strength development of clinically cured plain fly ash concretes, In *Proceedings of Australian Road Research Board*, vol. 13, Pt. 5, 27–33.

Gray, D.H. and Maher, M.H., 1989. Admixture stabilization of sand with discrete randomly distributed fibers. *Proceedings of XII international conference on soil mechanics and foundation engineering, Rio de Janeiro, Brazil*, vol. 2, 1363–1366.

Gray, D.H., Tons, E., and Thiruvengadam, T.R., 1994. Performance evaluation of a cement-stabilized fly ash base. *Transportation Research Record*, 1440, 51–59.

Gulhati, S.K. and Datta, M., 1999. *Geotechnical engineering*. New Delhi: Tata McGraw-Hill.

Hoover, J., *et al.*, 1982. *Performance of randomly oriented fiber-reinforced roadway soils: A laboratory and field investigation*. Iowa DOT Project HR-211, Iowa State University, Department of Civil Engineering, Ames, Iowa.

Huang, Y.H., 1993. *Pavement analysis and design*. Englewood Cliffs: Prentice-Hall.

IRC:37, 2001. *Guidelines for the design of flexible pavement*. New Delhi: Indian Roads Congress.

IRC:86, 1983. *Geometric design standards for urban roads in plains*. New Delhi: Indian Roads Congress.

Joshi, R.C., Natt, G.S., and Wright, P.J., 1981. Soil improvement by lime-fly ash slurry injection, *In:* Proceedings of 10th International Conference on Soil Mechanics & Foundation Engineering, Stockholm, vol. 3, 707–712.

Kaniraj, S.R. and Havanagi, V.G., 2001. Behavior of cement-stabilized fiber-reinforced fly ash-soil mixtures. *Journal of Geotechnical and Geoenvironmental Engineering*, ASCE, 127 (7), 574–584.

Ksaibati, K. and Bowen, M.M., 2001. Utilization of bottom ash in pavement bases, *In*: T.T. Eighmy, ed. *Proceedings of Beneficial Use of Recycled Materials in Transportation Applications*, Edi. , Nov. 13–15, Arlington, Virginia, 875–884.

Ksaibati, K. and Conklin, T.L., 1994. Field performance evaluation of cement-treated bases with and without fly ash. *Transportation Research Record*, 1440, 16–21.

Kumar, P. and Singh, S.P., 2008. Fiber-reinforced fly ash subbases in rural roads. *Journal of Transportation Engineering*. ASCE, 134, 171–180.

Kumar, R., Kanaujia, V.K., and Chandra, D., 1996. Engineering behaviour of fibre-reinforced pond ash and silty sand. *J. Geosynthetics Internationals 1996*, 6 (6), 509–518.

Lee, S.W. and Fishman, K.L., 1993. Resilient and plastic behavior of classifier tailings and fly ash mixtures. *Transportation Research Record*, 1418, 8–15.

Lee, K.W., *et al.*, 2001. *Structural analysis of New England subbase materials and structures*. The New England Transportation Consortium, Report of Project No. 94-1 (NETCR 26). Connecticut, CT.

Loulizi, A., *et al.*, 2006. Comparing resilient modulus and dynamic modulus of hot-mix asphalt as material properties for flexible pavement design, *Transportation Research Record*: Journal of the Transportation Research Board of the National Academies, Washington, DC, 161–170.

Maher, M.H. and Gray, D.H., 1990. Static response of sands reinforced with randomly distributed fibers. *Journal of Geotechnical Engineering, ASCE*, 116 (11), 1661–1667.

Maher, M.H. and Ho, Y.C., 1994. Mechanical-properties of kaolinite fiber soil composite. *Journal of Geotechnical Engineering, ASCE*, 120 (8), 1381–1393.

Maser, K.R., Wallhagen, R.E., and Dieckman, J., 1975. Development of fly ash cement mine sealing system, USBM, Open File Report 26-76, NTIS –PB-250611.

Michalowski, R.L. and Zhao, A., 1996. Failure of fiber-reinforced granular soils. *Journal of Geotechnical Engineering*, ASCE, 122 (3), 226–234

Mishra, M.K. and Karanam, U.M., 2006. Geotechnical characterization of fly ash composites for backfilling mine voids. *Geotechnical and Geological Engineering*, 24 (6), 1749–1765.

MORT&H, 2011. Report of the working group on central roads sector, 12th Five Year Plan (2012–17), Ministry of Road Transport & Highways, Government of India.

Nataraj, M.S. and McManis, K.L., 1997. Strength and deformation properties of soils reinforced with fibrillated fibers. *Geosynthetics International*, 4 (1), 65–79.

Ornebjerg, H., *et al.*, 2006. Management of bottom ash from WTE plants - an overview of management options and treatment methods. *Report of Working Group on Thermal Treatment of Waste*. Kongens Lyngby: International Solid Waste Association.

Palariski, J., 1993. The use of fly ash tailings, rock and binding agents as consolidated backfill for coal mines. *In*: H.W. Gelen, ed. *Proceedings of Mine fill*. Johannesburg: SAIMM, 403–408.

Raymon, S., 1961. Pulverized fuel ash as embankment material. *ICE Proceedings*, 19, 515–536.

Santoni, R.L. and Webster, S.L., 2001. Airfields and roads construction using fiber stabilization of sands. *Journal of Transportation Engineering*, ASCE, 127 (2), 96–104.

Sarkar, R., Abbas, S.M., and Shahu, J.T., 2012. A comparative study of geotechnical behaviour of lime stabilized pond ashes from Delhi region. *International Journal of GEOMATE*, 3 (1), 273–279.

Setty, K.R.N.S. and Rao, S.V.G., 1987. Characteristics of fibre reinforced lateritic soils, *Indian geotechnical conference*. Banglore, India, 1, 329–333.

Sherwood, P., 1995. *Alternative materials in road construction*. London: Thomas Telford Publishing.

Shewbridge, S.E. and Sitar, N., 1989. Deformation characteristics of reinforced sand in direct shear. *Journal of Geotechnical Engineering*, ASCE, 115 (8), 1134–1147.

Shodhganga. 2006. Engineering properties of subgrade soils, moorum and aggregate. Available from: http://shodhganga.inflibnet.ac.in/bitstream/10603/8702/12/12_chapter%204.pdf

Singh, S.P. and Kumar, P., 2005. Utilization of fibre reinforced flyash in road sub-bases, *Fly Ash Utilization Programme (FAUP)*. TIFAC, DST, New Delhi, VIII 17.1–17.8.

Singh, S.P. and Ramaswamy, S.V., 2005. Utilization potential of cement stabilized flyash-gbfs mixes in highway construction, *Fly Ash Utilization Programme (FAUP)*. TIFAC, DST, New Delhi, VIII, 4.36–14.11.

Sinha, A.K., 2009. *Study on subbase materials for rural roads*. Thesis (PhD). Dept. of Civil Engineering, IIT-Roorkee.

Subbarao, C., *et al*., 2001. Fly ash and stabilized fly ash as construction materials, Proceedings of International Conference on Advances in Civil Engineering, 1085–1092.

Theyse, H.L., 2002, *Stiffness, strength, and performance of unbound aggregate material: application of South African HVS and laboratory results to California flexible pavements*. University of California, Report – California Partnered Pavement Research Program.

Tirumala, K.G., 2007. *Geotechnical characteristics of pond ash mixed with randomly oriented Fibres*. MTech thesis. Depatment of Civil Engineering, IIT-Delhi.

Titi, H.H., Coenen, A.R., and Elias, M.B., 2009. Resilient characteristics of bottom ash. *In*: E. Tutumluer and I.L. Al-Qadi, eds. *Bearing Capacity of Roads, Railways and Airfields*, London: Taylor & Francis Group, 117–124. ISBN 978-0415-87199-0.

Downloaded by [Delhi Technological University] at 03:33 04 November 2015

Hindawi Publishing Corporation
Journal of Thermodynamics
Volume 2015, Article ID 756452, 8 pages
http://dx.doi.org/10.1155/2015/756452

Research Article

Effect of Condenser Fouling on Performance of Vapor Compression Refrigeration System

Naveen Solanki,[1] Akhilesh Arora,[2] and S. C. Kaushik[3]

[1]*Department of Mechanical and Automation Engineering, Maharaja Agrasen Institute of Technology, Sector 22, Rohini, Delhi 110086, India*
[2]*Department of Mechanical Engineering, Delhi Technological University, Delhi 110042, India*
[3]*Department of Energy Studies, IITD, Hauz Khas, New Delhi 110016, India*

Correspondence should be addressed to Akhilesh Arora; akhilesharora@dce.ac.in

Received 15 July 2015; Accepted 30 August 2015

Academic Editor: Shripad T. Revankar

Copyright © 2015 Naveen Solanki et al. This is an open access article distributed under the Creative Commons Attribution License, which permits unrestricted use, distribution, and reproduction in any medium, provided the original work is properly cited.

Effect of condenser fouling is evaluated on the performance of a vapour compression system with refrigerants HFO1234yf and HFO1234ze as an alternative to HFC134a. The condenser coolant temperature has been varied between 35 and 40°C to evaluate the effect of fouling at different condenser temperatures. A simulation model is developed in EES for computing the results. The results have been computed by varying condenser conductance. The same has been validated with literature available before calculating the results. It is observed that the condenser fouling has larger effect on compressor power (W_{cp}%) as it increases up to 9.12 for R1234yf and 7.41 for R1234ze, whereas for R134a its value increases up to 7.38. The cooling capacity (Q_{evap}%) decreases up to 13.25 for R1234yf and 8.62 for R1234ze, whereas for R134a its value decreases up to 8.76. The maximum percentage of decrease in value of COP is up to 19.29 for R1234yf and 14.47 for R1234ze, whereas for R134a its value decreases up to 14.49. The second-law efficiency is also observed to decrease with decrease in the condenser conductance. The performance of HFO1234ze is found to be better under fouled conditions in comparison to R134a and R1234yf.

1. Introduction

The most commonly used refrigerants in recent past were R11, R12, and R22 which because of their high ODP have been either phased out or under consideration for the same. After the revelation of the harmful effects of CFC and HCFC refrigerants on the ozone layer, search to find alternative working fluids gained more interest in the recent few years. The HFC134a was found to be a suitable candidate for replacing R12 and is being successfully used to date in small equipment like domestic refrigerators and water coolers and in mobile air-conditioning. HFC134a has very high GWP which is a matter of environmental concern. Calm [1] reviewed the progression of refrigerants from early uses to the present and addressed future direction by identifying pending policy and regulation that may impact the next generation of refrigerants significantly. Presently the fourth-generation refrigerants are in progress and these have low GWP such as HFO1234yf and HFO1234ze.

Karber et al. [2] examined refrigerants HFO1234yf and HFO1234ze as drop-in replacements for R134a in domestic refrigerators. Their results showed that HFO1234yf consumes 2.7% and 1.3% higher energy than HFC134a in baseline refrigerator and refrigerator based on advanced technology respectively; whereas HFO1234ze showed 16% and 5.4% lower energy consumption than HFC134a.

Ansari et al. [3] carried out the exergy analysis of HFO1234yf and HFO1234ze as a replacement to HFC134a. Their results indicate that HFO1234yf and HFO1234ze can be good replacement for HFC134a.

McLinden et al. [4] measured the thermodynamic properties of HFO1234ze and compared the experimental data with calculated data to establish the accuracy of EOS.

Reasor et al. [5] identified that refrigerant R1234yf has a low GWP of 4 in comparison to 1430 for R134a and has similar thermodynamic properties to those of HFC134a which make R1234yf a worthy choice for future automotive refrigerants.

A computer simulation was also conducted for feasibility of using R1234yf as a replacement for R134a and R410A.

Jarall [6] calculated and compared the theoretical cycle data and heat transfer of HFO1234yf with HFC134a in a refrigeration plant using a hermetic rotary compressor of 550 W nominal output power. The experimental results showed that HFO1234yf gives less refrigerating capacity, COP, and compressor efficiency by 3.4–13.7%, 0.35–11.88%, and 0–6.3% in comparison to HFC134a. Yamada et al. [7] examined that HFO1234yf is a potential working fluid of organic rankine cycle for low to medium temperature. HFO1234yf was found to offer almost similar thermal efficiency as that of HFC134a for all organic rankine cycle models. Thus HFO1234yf can be replaced by HFC134a.

Lee and Jung [8] examined the performance of HFO1234yf and HFC134a in a mobile air-conditioning bench tester under summer and winter conditioning. The results showed that the COP, capacity, and compressor discharge temperature for HFO1234yf are 2.7%, 4.0%, and 6.5°C lower than those of HFC134a and the amount of charge required for HFO1234yf reduced up to 10%.

According to this literature survey HFOs are future refrigerant for use in vapour compression systems. However the performance evaluation of these alternate refrigerants is necessary before these are commercially used in the system. The commercial usage demands the performance evaluation not only under ideal conditions but also under actual working conditions. The performance under actual conditions also depends on the fouling of heat exchangers (condensers) during operation of system. The material deposits on the surfaces of the heat exchanger tubes (fouling) add more thermal resistance to heat transfer which significantly affects the heat exchanger performance thereby affecting the system performance. A few notable studies on the effect of fouling on a vapor compression system have been reported in the next paragraph.

Qureshi and Zubair [9] discussed the effect of fouling on the performance of VCRS on the basis of first and second law and calculated the results for a particular set of data assuming condenser coolant temperature of 40°C and inlet air temperature to evaporator as 0°C and isentropic efficiency of compressor is assumed as 65%. Their results substantiate that R134a performs better among R134a, R410A, and R407C and similarly R717 performs better among R717, R404, and R290. The results of Qureshi and Zubair [9] are of limited use because the analysis has been performed for a condenser coolant temperature equal to 40°C. The condenser temperature in a real system depends on ambient conditions which keep on varying throughout the day.

Qureshi and Zubair [10] examined that energy can be saved by incorporating a mechanical subcooling to existing refrigeration and air-conditioning system under fouled condition. The results have been presented for HFC134a, R410A, R407C, R717, R404, and R290.

Qureshi and Zubair [11] examined experimentally the effect of condenser fouling on performance characteristics of a simple vapour compression system using HCFC22. The effect of condenser fouling was examined by blocking a part of air flow passage in condenser and its effect was studied on condenser pressure, superheat temperature at compressor exit, compressor power consumption, and COP. Their results indicate a logarithmic behavioral change in above-mentioned parameters. In above-mentioned studies on fouling, the analysis has been performed for refrigerants which have high GWP, that is, R134a, R407C, R410A, and R404A, besides low GWP refrigerants HC290 and R717. The high GWP refrigerants are to be replaced by low GWP refrigerants such as HFO1234yf and HFO1234ze.

Presently the system performance is being computed using two approaches, namely, (i) on the basis of first law of thermodynamics and (ii) on the basis of combined first and second law of thermodynamics. The analysis of systems based on combined first and second laws of thermodynamics is a better approach. Many researchers are focusing on the analysis of thermal systems based on this approach. The analysis based on second approach is also known as exergy analysis. The concept of exergy analysis as compared to energy analysis is more useful as it helps to quantify the irreversibility occurring in the system components. The effect of variation in condenser conductance's and condenser coolant inlet temperatures has been examined on the performance of the system. The parameters computed are percentage of change in COP, cooling capacity, compressor work, and effectiveness. The second-law efficiency is also computed. The following paragraph highlights how the fouling may occur in actual conditions.

Refrigerant R134a is commonly used refrigerant in VCRS, especially in mobile air-conditioning (Lee and Jung [8]) system such as cars; however its GWP is 1430. HFO1234yf and HFO1234ze have very low GWP value of 4 and are used as alternatives to R134a in mobile air-conditioning system. In the present study, the focus area is mobile air-conditioning and the effect of condenser fouling on system performance. The condenser fouling in mobile air-conditioning system is a very common phenomenon over a period of time which results in drop of performance. The fouling may happen due to accumulation of dust and dirt and scale formation (i.e., fluid impurities, corrosion, chemical reactions, encrustation, slagging, and sludge formation) on condenser tubes of air-conditioning system. The scale deposition offers an additional resistance to heat flow between the fluids and when resistance becomes double the condenser conductance drops to 50% in actual situations. Such situation of drop in conductance may occur due to nonservicing of the mobile air-conditioning system over a long period of usage of vehicle.

2. System and Model Descriptions

A simple vapour compression refrigeration cycle consists of the following equipment: (i) compressor, (ii) condenser, (iii) expansion valve, and (iv) evaporator, as shown in Figure 1.

Figure 2 shows a simple vapour compression refrigeration cycle on T-S diagram for different compression processes. The cycle works between temperatures T_1 and T_2 representing the condenser and evaporator temperatures, respectively:

(i) Process 4-5s: isentropic compression of the vapor from state 4 to state 5s. However, the compression

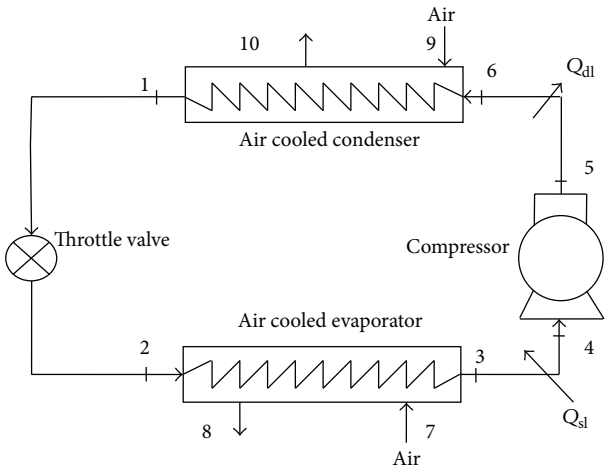


Figure 1: Schematic diagram of a simple VCRS.

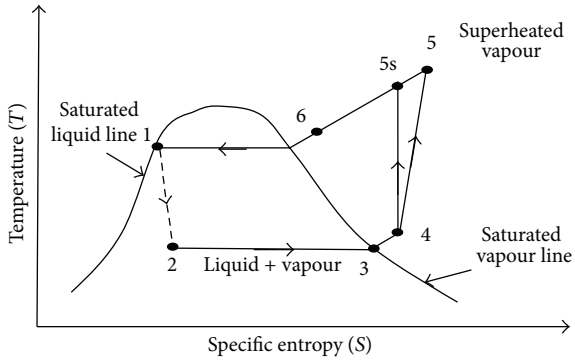


Figure 2: Temperature-entropy diagram of VCRC.

is never isentropic and hence in actual compression process (4-5) the exit state from the compressor is 5.

(ii) Process 5-6: heat rejection at constant pressure to the surroundings from the discharge line.

(iii) Process 6-1: heat rejection in condenser at constant pressure.

(iv) Process 1-2: an irreversible adiabatic expansion of vapor through the expansion valve or throttling device. The pressure and temperature of the liquid are reduced. The process is accompanied by partial evaporation of some liquid. The process is shown by dotted line because it is irreversible.

(v) Process 2-3: heat absorption in evaporator at constant pressure. In the final state 3 the refrigerant is in the dry saturated state at the exit from the evaporator.

(vi) Process 3-4: the temperature at the exit is lower than the ambient temperature; hence heat is transferred from surroundings to the refrigerant in the suction line at constant pressure.

Considering the steady-state cyclic operation and applying the first law of thermodynamics to the system as shown in Figure 2, (1) can be obtained. Consider

$$\dot{Q}_{\text{cond}} + \dot{Q}_{\text{loss,cond}} - \left(\dot{Q}_{\text{evap}} + \dot{Q}_{\text{loss,evap}}\right) - \dot{W}_{\text{cp}} = 0. \quad (1)$$

The heat transfer rate in the evaporator is given by

$$\dot{Q}_{\text{evap}} = \dot{m}_{\text{ref}}\left(h_3 - h_2\right). \quad (2)$$

In terms of effectiveness (ϵ), minimum heat capacity ($C_{\min}$) and temperature difference $\dot{Q}_{\text{evap}}$ can be written as

$$\dot{Q}_{\text{evap}} = \left(\epsilon C_{\min}\right)_{\text{evap}}\left(T_7 - T_2\right), \quad (3)$$

where T_2 is the temperature of refrigerant entering to evaporator and T_7 is the outside air temperature entering to evaporator.

Similarly, the heat transfer rate in the condenser is given by

$$\dot{Q}_{\text{cond}} = \dot{m}_{\text{ref}}\left(h_6 - h_1\right) = \left(\epsilon C_{\min}\right)_{\text{cond}}\left(T_1 - T_9\right), \quad (4)$$

where T_1 is the temperature of saturated liquid refrigerant leaving the condenser and T_9 is the outside air temperature entering the condenser for cooling the refrigerant in the condenser.

The power required by the compressor is presented in terms of isentropic efficiency of the compressor, given by

$$\dot{W}_{\text{cp}} = \dot{m}_{\text{ref}}\left(h_5 - h_4\right) = \frac{\dot{m}_{\text{ref}}\left(h_{5\text{s}} - h_4\right)}{\eta_{\text{cp,isn}}}, \quad (5)$$

where point 5 shows the actual state of refrigerant vapour at the exit from compressor.

Work input to the compressor can also be expressed using steady flow energy equation as follows:

$$\dot{Q}_{\text{cp}} - \dot{W}_{\text{cp}} = \dot{m}_{\text{ref}}\left(h_5 - h_4\right), \quad (6)$$

where $\dot{Q}_{\text{cp}}$ is the heat transfer from the compressor to the surroundings.

The heat leaking into the suction line is represented by

$$\dot{Q}_{\text{sl}} = \dot{m}_{\text{ref}}\left(h_4 - h_3\right). \quad (7)$$

The heat leakage from the discharge line to surroundings can be expressed as

$$\dot{Q}_{\text{dL}} = \dot{m}_{\text{ref}}\left(h_6 - h_5\right). \quad (8)$$

The COP is the ratio of refrigerating effect to compressor power; that is,

$$\text{COP} = \frac{Q_{\text{evap}}}{W_{\text{cp}}}. \quad (9)$$

The first-law efficiency alone is not a realistic measure of performance of engineering device. To overcome this deficiency, we define second-law efficiency (η_{II}) of a refrigeration system

Table 1: Model, specification and equations of components considered in the analysis (Qureshi and Zubair [9], Stoecker and Jones [13]).

Component	Model and specification	Equation	Remarks
Compressor	H62SP-22E (1750 rpm)	$W_{cp} = \frac{m_{ref}(h_{5s} - h_4)}{\eta_{cp,isn}}$	Hermetic reciprocating
Condenser	Model number 36	$Q_{cond} = F * (T_1 - T_{in,cond})$	$F = (\epsilon C_{min})_{cond} = 9.39$ kW/K F = capacity per unit temperature difference (kW/K)
Evaporator	CH660B	$Q_{evap} = G * (T_{in,evap} - T_2)$	$G = (\epsilon C_{min})_{evap} = 6\left[1 + 0.046\left(T_{in,evap} - T_2\right)\right]$ G = proportionality factor (kW/K)

Table 2: Comparison of performance data from Stoecker and Jones [13] and current model for refrigerant R22.

$T_{in,evap}$ (°C)	Q^*_{cond} (kW)	$Q_{cond,mod}$ (kW)	Error (%)	W^*_{cp} (kW)	$W_{cp,mod}$ (kW)	Error (%)	T^*_1 (°C)	$T_{1,mod}$ (°C)	Error (%)	COP* (kW)	COP $_{mod}$ (kW)	Error (%)
0	82.16	**82.40**	**0.29**	24.92	**25.19**	**1.07**	48.75	**48.77**	**0.04**	2.30	**2.27**	**−1.32**
15	122.0	**122.93**	**0.57**	31.45	**32.37**	**2.84**	52.99	**53.09**	**0.18**	2.88	**2.80**	**−2.77**

*From the performance data of stoecker and jones [13].

which is the ratio of the actual coefficient of performance (COP) to the maximum possible coefficient of performance (COP_{rev}) under the same operating conditions:

$$\eta_{II} = \frac{COP}{COP_{rev}} = \frac{\eta_I}{\eta_{th,rev}}, \tag{10}$$

where

$$COP_{rev} = \frac{T_7}{T_9 - T_7}. \tag{11}$$

The effectiveness of a heat exchanger is defined using

$$\epsilon = \frac{\text{Actual heat transfer}}{\text{maximum possible heat transfer}}. \tag{12}$$

The effectiveness of evaporator and condenser is given by

$$\epsilon_{evap} = \frac{T_7 - T_8}{T_7 - T_2}, \qquad \epsilon_{cond} = \frac{T_{10} - T_9}{T_6 - T_9}. \tag{13}$$

Incropera et al. [12] derived the expression for relation between effectiveness, heat capacity, and overall conductance (UA) which is expressed as

$$UA = C_{min} * \ln\left(\frac{1}{1 - \epsilon}\right). \tag{14}$$

The fouling on air side of a heat exchanger is the reason for reduction of UA. The percentage reduction in conductance is represented using

$$UA\% = \left(1 - \frac{UA}{UA_{cl}}\right) * 100. \tag{15}$$

In this study, a programme is developed using Engineering Equation Solver (EES) for the simulation of system performance using set of (1) to (15) in which percentage of decrease in the conductance value due to fouling has been varied from 0% to 50% in condenser. The flow chart showing the simulation procedure of the EES program, developed for computation of results, is given in Figure 3. The properties (of refrigerants R134a, R1234yf, and R1234ze) such as enthalpy, entropy, pressures, and temperatures are given in the form of inbuilt functions in EES and are called in the EES program for calculation of parameters, namely, cooling effect, compressor work, and heat rejected in condenser. The clean conditions refer to no fouling; that is, percentage of reduction in conductance is 0%. Heat leakages in the suction line and discharge line and pressure drops in the heat exchangers are considered negligible in all the calculations and hence not taken into account.

2.1. Model Validation. This section presents the model validation of the EES program used for the evaluation of vapour compression system. The data used for the validation purpose have been obtained from Stoecker and Jones [13]. The details of equations with model are given in Table 1.

The comparison of performance data from Stoecker and Jones [13] and current model for refrigerant R22 (refer to Table 2) depicts that all relevant quantities (Q_{cond}, W_{cp}, and COP along with the temperature of refrigerant at condenser outlet (T_1) and temperature of air entering the evaporator (T_7)) can be prognosticated by the property based model correctly and the maximum error was found to be 2.84.

(i) Table 3 gives the comparison of data from Qureshi and Zubair [9] with current model for refrigerant R134a. It is observed that error (%) in COP is less than 1%.

3. Results and Discussion

The thermodynamic model given above is used to evaluate the performance of vapor compression system. The performance is evaluated with three refrigerants (R134a, R1234yf, and R1234ze).

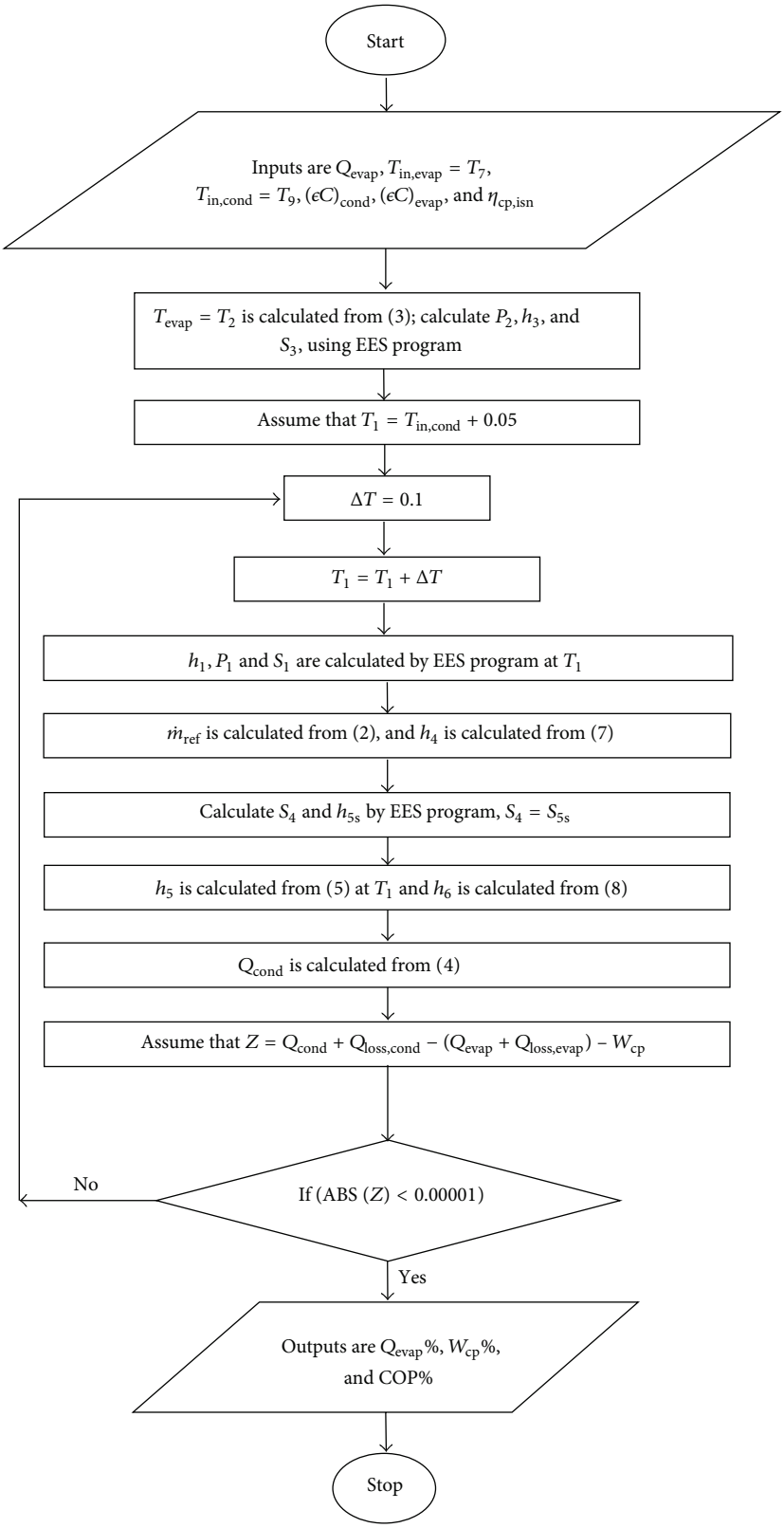


Figure 3: A flow chart for thermodynamic model of simple VCRS.

Table 3: Comparison of present model with work of Qureshi and Zubair [9] for condenser fouling of refrigerant R134a (Te = 0°C).

Reduction in UA_{cond} (%)	Change in Q_{evap} (%)		Change in W_{cp} (%)		Change in COP (%)		Error (%) in COP with reference to Qureshi and Zubair [9]
	Qureshi and Zubair [9]	Current model	Qureshi and Zubair [9]	Current model	Qureshi and Zubair [9]	Current model	
0	0	0	0	0	0	0	0
10	−0.901	−0.907	0.731	0.714	−1.620	−1.609	−0.67
20	−2.065	−2.070	1.665	1.650	−3.669	−3.659	−0.27
30	−3.611	−3.611	2.880	2.873	−6.309	−6.303	−0.09
40	−5.725	−5.748	4.479	4.447	−9.782	−9.761	−0.21
50	−8.761	−8.767	6.710	6.690	−14.499	−14.49	−0.06

Table 4: Values of inputs at design point.

Parameters	Values
Evaporator coolant inlet temperature ($T_{in,evap} = T_7$ in K)	273
Condenser coolant inlet temperature ($T_{in,cond} = T_9$ in K)	308–313
Rate of heat absorbed by evaporator (Q_{evap} in kW)	100
Product of condenser effectiveness and capacitance rate of external fluid $[(\epsilon C_{min})_{cond}$, kW/K]	9.39
Product of evaporator effectiveness and capacitance rate of external fluid $[(\epsilon C_{min})_{evap}$, kW/K]	8.2
Isentropic efficiency of compressor ($\eta_{cp,isn}$)	0.65
Effectiveness (ϵ)	0.80
Refrigerants	R134a, R1234yf, R1234ze

3.1. Input Conditions. The value given in Table 4 has been referred to from Qureshi and Zubair [9] and Khan and Zubair [14] for computation of results in current work.

3.2. Effect of Condenser Fouling on Compressor Power, Cooling Capacity, and COP. Figures 4, 5, and 6 represent the effect of condenser fouling with variation on condenser coolant temperature for the refrigerants R134a, R1234yf, and R1234ze, respectively. It is observed that with increase in condenser fouling COP decreases because cooling capacity decreases and compressor work goes on increasing.

Tables 5 and 6 show the comparison of result of percentage of change in compressor power, COP, and cooling capacity with condenser fouling at condenser inlet temperature values of 40°C and 35°C for the above mentioned refrigerants.

From Tables 5 and 6, it is observed that the refrigerant R1234yf shows maximum increase in value of change in compressor power (%) at $T_{in,cond}$ = 35°C and maximum decrease in values of change in COP (%) and change in cooling capacity (%) at $T_{in,cond}$ = 40°C.

3.3. Effect of Condenser Fouling on Second-Law Efficiency. The comparisons of the results of second-law efficiency at condenser inlet temperature of 40°C, 37.5°C, and 35°C

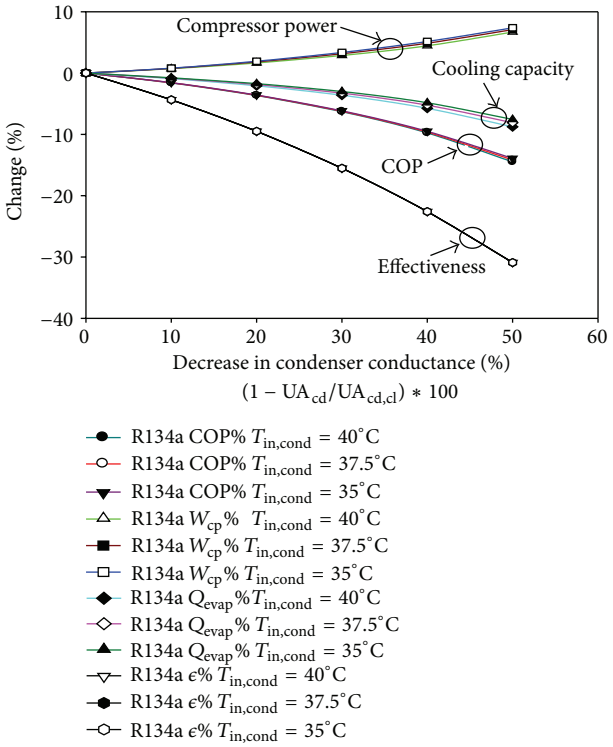


Figure 4: Percentage of change in cooling capacity, compressor power, COP, and effectiveness with decrease in condenser conductance for R134a.

for unfouled condition and 50% reduction in condenser conductance due to fouling are shown in Table 7.

From the values given in Table 7, it is clear that the second-law efficiency decreases both under fouled conditions of condenser and for increase in condenser coolant inlet temperature. Among the three refrigerants considered, R1234ze has the highest second-law efficiency whereas R1234yf has the lowest value.

The above results have been calculated for the rated working conditions only. However, under part load conditions cooling capacity (Q_{evap}) decreases; hence the load on the condenser reduces. Therefore, with fouling and reduced load on condenser, the reduction in COP and second-law

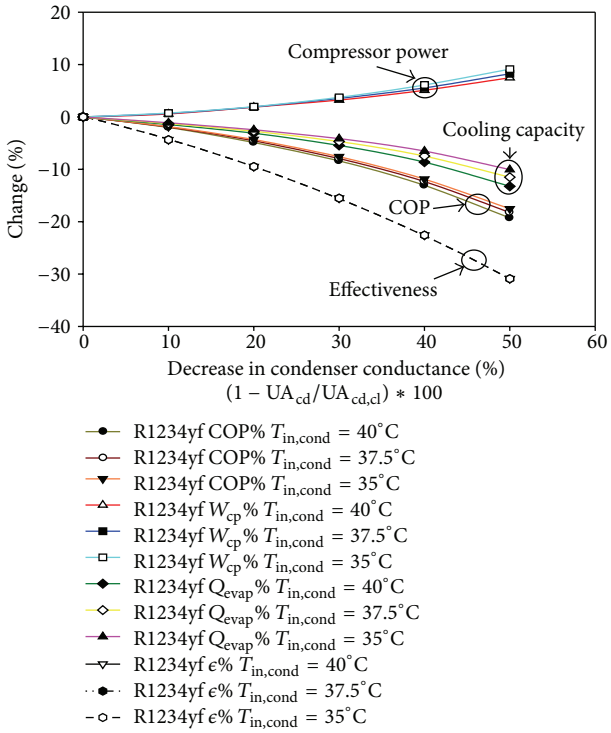


Figure 5: Percentage of change in cooling capacity, compressor power, COP, and effectiveness with decrease in condenser conductance for R1234yf.

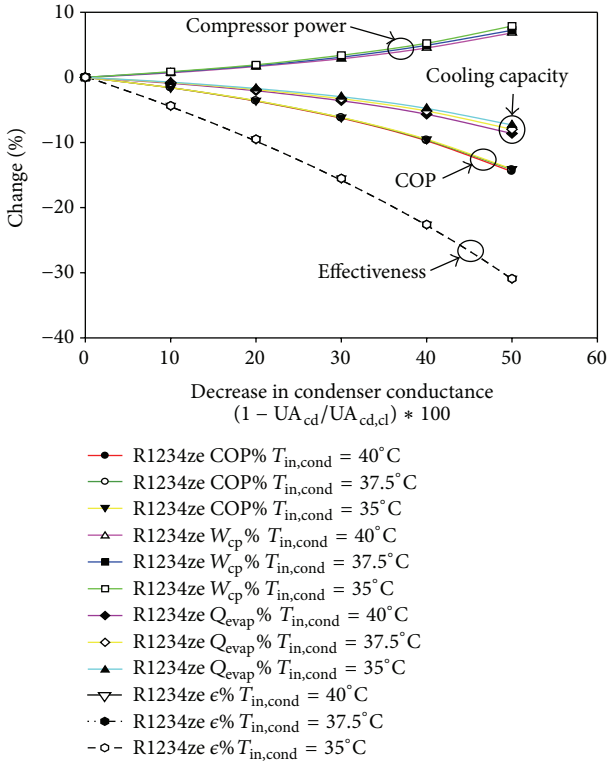


Figure 6: Percentage of change in cooling capacity, compressor power, COP, and effectiveness with decrease in condenser conductance for R1234ze.

Table 5: Comparison of results for R1234yf and R1234ze with R134a at $T_{in,cond}$ = 40°C.

Refrigerant	Change in UA_{cond} (%)	Change in W_{cp} (%)	Change in COP (%)	Change in Q_{evap} (%)
R1234yf	10	0.57	−2.01	−1.46
	50	7.48	−19.29	−13.25
R1234ze	10	0.70	−1.59	−0.91
	50	6.83	−14.47	−8.63
R134a	10	0.71	−1.61	−0.91
	50	6.69	−14.49	−8.77

Table 6: Comparison of results for R1234yf and R1234ze with R134a at $T_{in,cond}$ = 35°C.

Refrigerant	Change in UA_{cond} (%)	Change in W_{cp} (%)	Change in COP (%)	Change in Q_{evap} (%)
R1234yf	10	0.74	−1.85	−1.12
	50	9.12	−17.55	−10.06
R1234ze	10	0.87	−1.59	−0.73
	50	7.41	−13.88	−7.50
R134a	10	0.79	−1.56	−0.77
	50	7.38	−13.91	−7.56

Table 7: Comparison of second-law efficiency (condenser under fouled condition) for refrigerants R1234yf and R1234ze with R134a.

Refrigerant	Change in UA_{cond} (%)	η_{II} (%) $T_{in,cond}$ = 40°C	η_{II} (%) $T_{in,cond}$ = 37.5°C	η_{II} (%) $T_{in,cond}$ = 35°C
R1234ze	0	24.52	24.83	25.01
	50	20.97	21.31	21.49
R1234yf	0	19.60	20.53	21.23
	50	15.82	16.78	17.50
R134a	0	24.37	24.69	24.88
	50	20.84	21.19	21.41

efficiency will be less in comparison to the case when the system is operating under full-load conditions. This happens because the increase in condenser temperature will not be as much as when the condenser was operating under full-load conditions.

4. Conclusions

On the basis of results obtained from thermodynamic model, the following conclusions are drawn.

In the present work, effect of condenser fouling on the performance of a simple vapour compression cycle has been evaluated by varying condenser conductance, that is, increasing the condenser fouling from 0 to 50%, and also by varying condenser coolant inlet temperature ($T_{in,cond}$) from 35°C to 40°C for the refrigerants R134a, R1234yf, and R1234ze. It is observed that, under above-mentioned conditions, the maximum percentage increase of compressor power, the

maximum percentage decrease of cooling capacity, and the maximum percentage decrease in value of COP occur for R1234yf when condenser conductance is assumed to reduce by 50% followed by R134a and R1234ze. The changes in the above-mentioned parameters are found to be severest for R1234yf.

Further, it is also observed that changes in these parameters are nearly the same for R134a and R1234ze. Thus, on the basis of results obtained, it is evident that R1234ze is a better alternative for R134a.

Nomenclature

CFCs:	Chlorofluorocarbons
COP:	Actual coefficient of performance
COP_{rev}:	Maximum possible coefficient of performance
EOS:	Equation of state
GWP:	Global warming potential
HCFCs:	Hydrochlorofluorocarbons
HFO:	Hydrofluoroolefin
LGWP:	Low global warming potential
ODP:	Ozone depletion potential
VCRC:	Vapour compression refrigeration cycle
VCRS:	Vapour compression refrigeration system
mod:	Model
Q_{cond} and Q_{evap}:	Rate of heat transfer from the condenser and evaporator (kW)
$Q_{loss,cond}$ and $Q_{loss,evap}$:	Heat loss in condenser and evaporator (kW)
W_{cp}:	Power requirement of compressor (kW)
ϵ, ϵ_{evap}, and ϵ_{cond}:	Heat exchanger effectiveness and effectiveness of evaporator and condenser
C_{min}:	Minimum value of the thermal capacitance rate (kW/K)
m_{ref}:	Refrigerant mass flow rate (kg/s)
Q_{cp}:	Rate of heat transfer from the compressor to the surroundings (kW)
η_I, η_{II}:	First-law efficiency and second-law efficiency (%)
$\eta_{th,rev}$:	Maximum thermal efficiency (%)
$\eta_{cp,isn}$:	Isentropic efficiency of compressor (%)
UA:	Overall conductance (kW/K)
T_1 to T_{10}:	Temperature at state points (K)
h_1, h_2, h_3, h_4, h_5, and h_6:	The enthalpies of refrigerant at condenser exit, evaporator inlet, evaporator outlet, compressor inlet, compressor outlet, and condenser inlet (KJ/kg)
$T_{in,evap}$:	Evaporator coolant inlet temperature (K)
$T_{in,cond}$:	Condenser coolant inlet temperature (K).

Conflict of Interests

The authors declare that there is no conflict of interests regarding the publication of this paper.

References

[1] J. M. Calm, "The next generation of refrigerants—historical review, considerations, and outlook," *International Journal of Refrigeration*, vol. 31, no. 7, pp. 1123–1133, 2008.

[2] K. M. Karber, O. Abdelaziz, and E. A. Vineyard, "Experimental performance of R-1234yf and R1234ze as drop in replacements for R134a in domestic refrigerator," in *Proceedings of the International Refrigeration and Air Conditioning Conference*, Paper no. 1228, Purdue University, West Lafayette, Ind, USA, 2012.

[3] N. A. Ansari, B. Yadav, and J. Kumar, "Theoretical exergy analysis of HFO1234yf and HFO1234ze as an alternative replacement of HFC134a in simple vapour compression refrigeration system," *International Journal of Scientific and Engineering Research*, vol. 4, no. 8, pp. 2229–5518, 2013.

[4] M. O. McLinden, T. Monika, and E. W. Lemmon, "Thermodynamic properties of *trans*-1,3,3,3-tetrafluoropropene [R1234ze(E)]: measurements of density and vapor pressure and a comprehensive equation of state," in *Proceedings of the International Refrigeration and Air Conditioning Conference*, Paper no. 2189, Purdue, Ind, USA, 2010.

[5] P. Reasor, V. Aute, and R. Radermacher, "Refrigerant R1234yf performance comparison investigation," in *Proceedings of the International Refrigeration and Air Conditioning Conference at Purdue*, Paper No. 1085, West Lafayette, Ind, USA, July 2010.

[6] S. Jarall, "Study of refrigeration system with HFO-1234yf as a working fluid: etude sur un système frigorifique utilisant le HFO-1234yf comme fluide actif," *International Journal of Refrigeration*, vol. 35, no. 6, pp. 1668–1677, 2012.

[7] N. Yamada, M. N. A. Mohamad, and T. T. Kien, "Study on thermal efficiency of low- to medium-temperature organic Rankine cycles using HFO-1234yf," *Renewable Energy*, vol. 41, pp. 368–375, 2012.

[8] Y. Lee and D. Jung, "A brief performance comparison of R1234yf and R134a in a bench tester for automobile applications," *Applied Thermal Engineering*, vol. 35, no. 1, pp. 240–242, 2012.

[9] B. A. Qureshi and S. M. Zubair, "Performance degradation of a vapor compression refrigeration system under fouled conditions," *International Journal of Refrigeration*, vol. 34, no. 4, pp. 1016–1027, 2011.

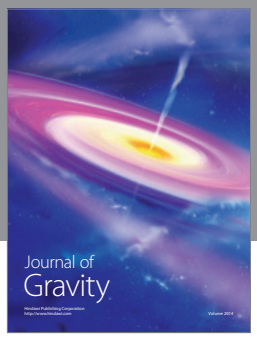
[10] B. A. Qureshi and S. M. Zubair, "The impact of fouling on performance of a vapor compression refrigeration system with integrated mechanical sub-cooling system," *Applied Energy*, vol. 92, pp. 750–762, 2012.

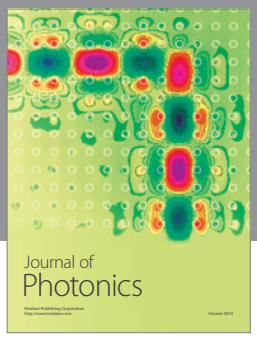
[11] B. A. Qureshi and S. M. Zubair, "The impact of fouling on the condenser of a vapor compression refrigeration system: an experimental observation," *International Journal of Refrigeration*, vol. 38, no. 1, pp. 260–266, 2014.

[12] F. P. Incropera, D. P. DeWitt, T. Bergman, and A. Lavine, *Fundamentals of Heat and Mass Transfer*, John Wiley & Sons, 6th edition, 2006.

[13] W. F. Stoecker and J. W. Jones, *Refrigeration and Air Conditioning*, McGraw-Hill, New York, NY, USA, 1982.

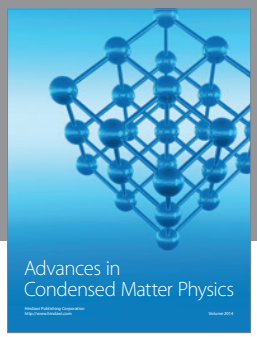
[14] J.-U. Khan and S. M. Zubair, "Design and performance evaluation of reciprocating refrigeration systems," *International Journal of Refrigeration*, vol. 22, no. 3, pp. 235–243, 1999.

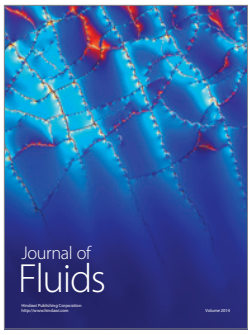


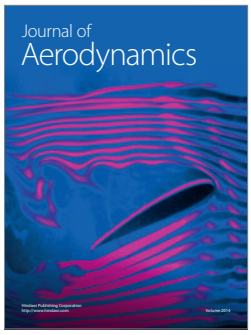






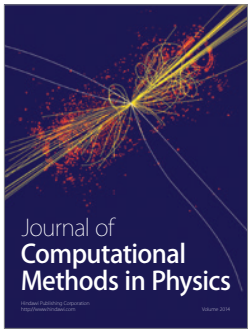


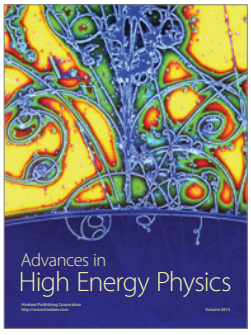




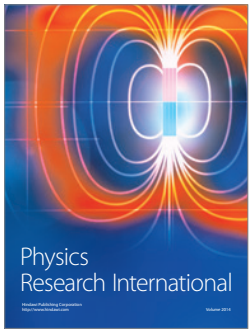


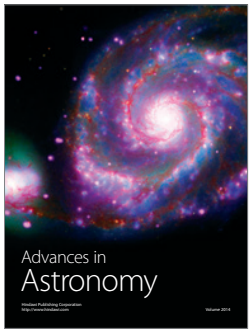










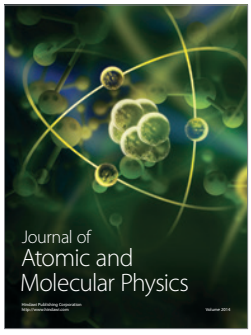












Hindawi

Submit your manuscripts at
http://www.hindawi.com

Journal of Material Science and Mechanical Engineering (JMSME)
Print ISSN: 2393-9095; Online ISSN: 2393-9109; Volume 2, Number 7; April-June, 2015 pp. 64-69
© Krishi Sanskriti Publications
http://www.krishisanskriti.org/jmsme.html

Energy and Exergy Analyses of a new Solar Assisted Cogeneration Cycle for Simultaneous Production of Power and Double Effect Cooling

Surendra Kumar Agrawal[1], Rajesh Kumar[2]

[1]*Department of Mechanical Engineering, Madhav Institute of Technology & Science Gwalior-474005, M.P., India*
surendra_srcem@yahoo.com
[2]*Department of Mechanical Engineering, Delhi Technological University, Bawana Road, Delhi-110042, India*
dr.rajeshmits@gmail.com
** Corresponding author*

Abstract: **In this paper, a solar operated combined power and ejector-absorption refrigeration cycle is proposed and thermodynamically analyzed for simultaneous production of cooling at two different evaporators at different temperatures along with power. The thermodynamic analysis is carried out from view point of energy and exergy. The effect of key thermodynamic parameters like; hot oil outlet temperature, refrigerant turbine inlet pressure and ejector evaporator temperature on energy and exergy efficiency along with exergy destructions in various components of the proposed cycle is observed. It is observed that out of 100% solar heat energy supplied to the system around 7.68% is produced as refrigeration output in ERC and ARC cycle, 5.49% is produced as power output in RC cycle and 102.19% is lost to the environment. The irreversibility in central receiver 52.5%, heliostat field 25%, condenser of ERC 3.98%, HRVG 3.79% and ejector 3.72% is observed. The exergy efficiency of around 6% is obtained which is much lower than energy efficiency 13% of solar assisted cogeneration cycle for simultaneous production of power and double effect cooling. With the increase in hot oil outlet temperature from central receiver (160^{o}C-180^{o}C), the energy efficiency decreases (15.22% -11.74%) significantly and exergy efficiency increases (5.06%-7.37%) marginally. With increase is turbine inlet pressure from 0.9 MPa to 1.7 MPa., the energy efficiency increases significantly (13.17% to 36.86%) while exergy efficiency decreases marginally (6.22% to 4.4%).**

Keywords: ejector, absorption, energy, exergy, double effect cooling, power.

1. INTRODUCTION

In order to meet out the increasing demand of power and cooling simultaneously, the combined power and refrigerating cycle have been explored. Xu et al. [1] proposed a combined power and refrigeration cycle and some further researches on the cycle were carried out by Hasan et al. [2]; Yidal et al. [3]; Sadrameli and Goswami [4]). Zhang and Lior [5] proposed a new combined refrigeration and power system. They investigated the effects of the key thermodynamic parameters on both energy and exergy efficiencies. Wang et al. [6] also proposed a combined power and refrigeration system which combined Rankine cycle and absorption refrigeration cycle. These systems are relatively complicated, resulting in a higher capital investment. Although much research has been carried out on the combined power and refrigeration cycle, most of them have combined the Rankine cycle or Kalina cycle with the absorption refrigeration cycle, and a very little attention has been paid to the combination of Rankine cycle and ejector refrigeration cycle. The ejector refrigeration cycle has the possibility of using a wide range of refrigerants with the system.

Recently, in refrigeration industry the use of efficient dual-evaporator refrigeration systems has been paid a lot of attention. These systems sound even more interesting when they are a combination of different kinds of conventional refrigeration systems for simultaneously production of power and producing cooling effects at two different temperatures in the cycle by using low grade heat source. In this context, a new solar powered ejector-absorption refrigeration cycle is proposed and analyzed in this paper. This cycle will produce power and cooling effect at two evaporators at different temperatures in the cycle by using the single source of solar heat.

2. SYSTEM DESCRIPTION

The proposed cogeneration cycle consists of Rankine cycle (RC), ejector refrigeration cycle (ERC) and absorption refrigeration cycle (ARC) by using only single source of solar

heat for simultaneous production of power and double effect cooling as shown in Figure1. Solar energy falls on the heliostat field and reflected on the aperture area of central receiver which is located at the top of the tower. The concentrated rays which falls on to the central receiver results in higher temperature of the central receiver, is used to heat the oil (Duratherm600). The oil flows through the pipes which transfer the thermal energy from central receiver to the HRVG (1-2) and generator (2-12). Superheated refrigerant vapour of R141b (4) is expanded in a turbine to generate power. The turbine exhaust (5) passes through converging diverging supersonic nozzle of ejector. The very high velocity refrigerant vapour at the exit of the nozzle creates a very high vacuum at the inlet of the mixing chamber and extract secondary vapour (11) from the evaporator of ERC into the mixing chamber and this causes cooling effect at evaporator-1(E1) of ERC. The primary vapour (5) and secondary vapour (11) are mixed in the mixing chamber. The mixed stream (6) is condensed in the condenser-1(C1). The saturated liquid (7) is divided in to two parts (8, 9), one part (9) is passed through throttling valve-1 (TV1) where pressure is reduced to evaporator (E-1) pressure (10) and feed to evaporator-1 (E1), and second part (8) is pumped by pump-1(P1) to the HRVG of RC cycle. The stream (2) coming out from HRVG passes through the generator of ARC and finally enters to the central receiver (12). The superheated pure water vapour (13) coming from generator is condensed in condenser-2 (C2). Saturated liquid (14) at condenser pressure passes through throttle valve-2 (TV2) to generate saturated liquid (15) at reduced pressure i.e. pressure in the evaporator-2(E2). Saturated vapour (16) after receiving heat from evaporator-2 (E2) enters into the absorber. Solution (20) which is a mixture of LiBr-H_2O passes through heat exchanger and cooled to (21) and then passes through throttle valve-3 (TV3) to reduce its pressure i.e. absorber pressure. Absorption temperature is maintained at 35^0C at evaporator-2(E2) pressure. Two streams (16, 22) mixed at absorber and form a new mixture (17), which passes through pump-2 (P2) and solution heat exchanger (SHX) and then finally enters to the generator (19).

For the analysis, the specifications of the combined RC, ERC and ARC are given in Table 1.

TABLE 1: Main parameters considered for the analysis

Environment Temperature (^{0}C)	15
Environment pressure (MPa)	0.10135
Turbine inlet pressure range (MPa)	0.9 - 1.7
Hot oil outlet temperature from central receiver (^{0}C)	160 – 180
Hot oil inlet temperature to central receiver (^{0}C)	85
Generator temperature (^{0}C)	80
Solar radiation received per unit area (Wm^{-2})	850
Apparent Sun temperature (K)	4500
Heliostat aperture area (m^2)	3000
Turbine back pressure range (MPa)	0.22-0.3
Turbine isentropic efficiency (%)	85
Ejector evaporator temperature range (K)	264 – 272
Evaporator temperature of ARC (^{0}C)	5
Condenser-2 temperature (^{0}C)	35
Absorber temperature (^{0}C)	35
Hot oil mass flow rate (kg s^{-1})	8.0
Pump isentropic efficiency (%)	70
HRVG efficiency (%)	100
Pinch point temperature difference (^{0}C)	10.0
Nozzle efficiency (%)	90
Mixing chamber efficiency (%)	85
Diffuser efficiency (%)	85
Energy efficiency of heliostat field (%)	75
Energy efficiency of central receiver (%)	90
Exergy efficiency of heliostat field (%)	75
Exergy efficiency of central receiver (%)	30
Effectiveness of SHX (%)	100

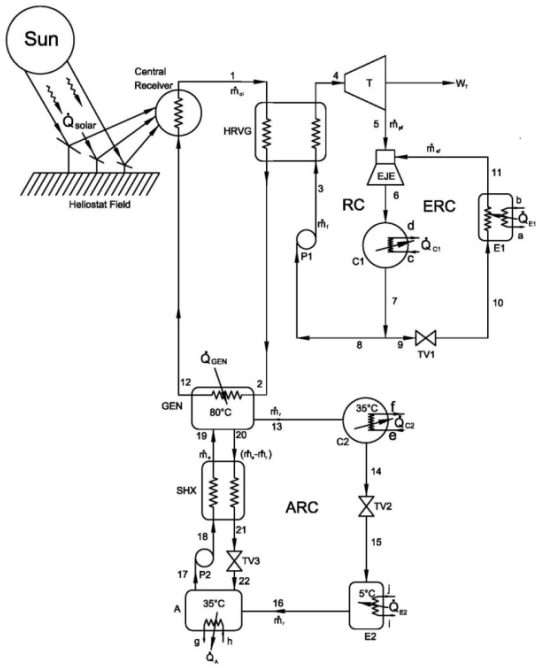


Fig. 1. Schematic diagram of solar assisted cogeneration cycle for simultaneous production of power and double effect cooling

3. THERMODYNAMIC ANALYSIS

A method of exergy analysis which combines basic principles of conservation of mass and conservation of energy along with the second law of thermodynamics is applied for the analysis of thermodynamic cycles of power and refrigeration. This methodology is expected to provide a complete thermodynamic view of the given refrigeration system with a view to provide a guidance for performance improvement.

Exergy analysis, calculates the system performance based on exergy, which is defined as the maximum possible reversible work obtainable in bringing the state of the system to equilibrium with that of the environment, which may be defined mathematically as:

$$\dot{E} = \dot{m}[(h - h_0) - T_0(s - s_0)] \quad (1)$$

The entropy generation over a control volume is given by Bejan [7]

$$\dot{S}_{gen} = \frac{dS}{dt} - \sum_{i=o}^{n} \frac{\dot{Q}_i}{T_i} - \sum_{in} \dot{m}s + \sum_{out} \dot{m}s \geq 0 \quad (2)$$

According to Gouy-Stodola theorem, the exergy destruction and entropy generation are related as

$$\dot{E}_D = T_0 \dot{S}_{gen} \quad (3)$$

3.1. Energy Efficiency (η_{energy})

Energy efficiency is defined as the ratio of the desired effect ($\dot{Q}_{E1}$, $\dot{Q}_{E2}$, $\dot{W}_T$) to the thermal energy of solar heat input ($\dot{Q}_{solar}$).
The energy efficiency of the proposed cycle for simultaneous production of power and double effect cooling is given by

$$\eta_{energy} = \frac{\dot{Q}_{E1} + \dot{Q}_{E2} + \dot{W}_T}{\dot{Q}_{Solar}} \quad (4)$$

where, $\dot{Q}_{E1}$ and $\dot{Q}_{E2}$ are the refrigeration output of ERC and ARC and $\dot{W}_T$ is the turbine work output.

3.2. Exergy Efficiency (η_{exergy})

The exergy efficiency of simultaneous production of power and double effect cooling cycle may be reported as

$$\eta_{exergy} = \frac{\Delta \dot{E}_{E1} + \Delta \dot{E}_{E2} + \dot{W}_T}{\dot{E}_{Solar}} \quad (5)$$

Where, $\dot{E}_{Solar}$ is incoming exergy associated with solar radiation falling on heliostat, $\Delta\dot{E}_{E1}$, $\Delta\dot{E}_{E2}$ and $\dot{W}_T$ are the change in exergy at ejector evaporator of ERC, evaporator of ARC and power output from turbine of RC respectively.

$$\Delta\dot{E}_{E1} = \dot{m}_{sf}[(h_{10} - h_{11}) - T_0(s_{10} - s_{11})] \quad (6)$$

$$\Delta\dot{E}_{E2} = \dot{m}_r[(h_{15} - h_{16}) - T_0(s_{15} - s_{16})] \quad (7)$$

$$\dot{E}_{Solar} = \dot{Q}_{Solar}\left(1 - \frac{T_0}{T_S}\right) \quad (8)$$

where, T_s = Apparent Sun temperature (K)=4500K

4. RESULTS AND DISCUSSION

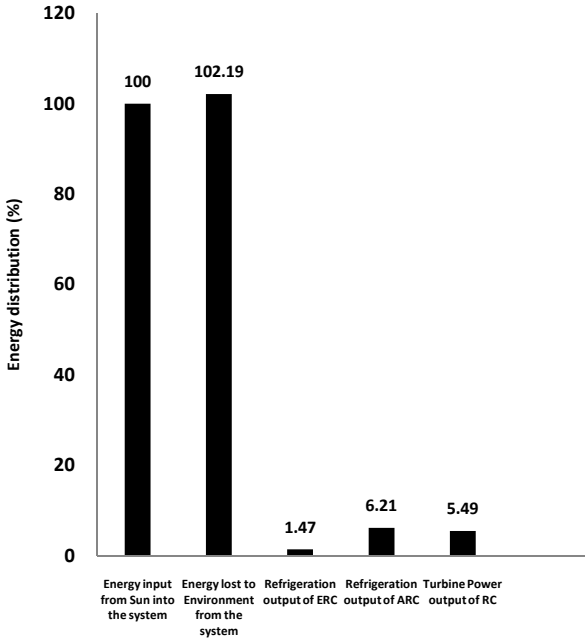


Fig. 2 Percentage (%) of Suns energy distribution in the cycle for simultaneous production of power and double effect cooling

In this paper, parametric analysis is carried out to find out the effect of variation of hot oil (Duratherm600 oil) outlet temperature fro central receiver, turbine inlet pressure and ejector evaporator temperature on energy and exergy efficiency of the solar assisted cogeneration cycle for

simultaneous production of power and double effect cooling. The thermodynamic properties of refrigerant R141b used in the ERC cycle were calculated by NIST Standard Reference Database 23 [8] and thermodynamic properties; enthalpy and entropy of LiBr- H_2O mixture for the operation of ARC are taken from chua et al. [9].

Figure 2 shows that out of 100% solar heat energy supplied to the system, around 7.68% is available as useful refrigeration output in ERC and ARC, 5.49% as turbine power output in RC cycle and the rest of the energy which includes the heat rejected at the condenser and absorber of ARC and heat rejected at the condenser of ERC is lost to the environment.

Figure 3 indicates that out of 100% exergy associated with solar heat, around 0.35% is produced as exergy output of refrigeration (exergy associated with cooling produced in ERC and ARC cycle), around 5.87% is produced as exergy output (exergy associated with turbine power output) of RC cycle for production of power. The rest of the exergy is destroyed due to irreversibilities in various components of the cogeneration cycle. In this context, it is indicated that majority of the irreversibility occurred in central receiver (52.5%), Heliostat field (25%), condenser of ERC (3.98%), HRVG (3.79%) and ejector (3.72%). The component like central receiver, heliostat field, condenser of ERC, HRVG and ejector where maximum exergy destroyed needs special attention from second law point of view. A reduction in the irreversibility in these components will improve the overall performance of the cycle.

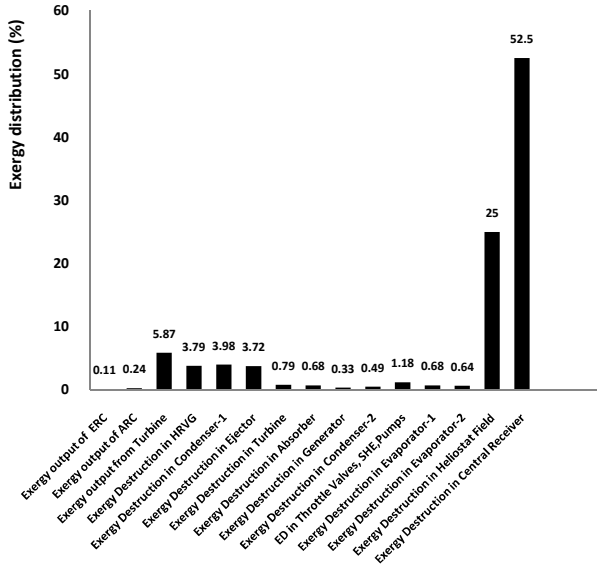


Fig. 3. Percentage (%) of Suns exergy distribution in refrigeration, power output and exergy destructions in the cycle

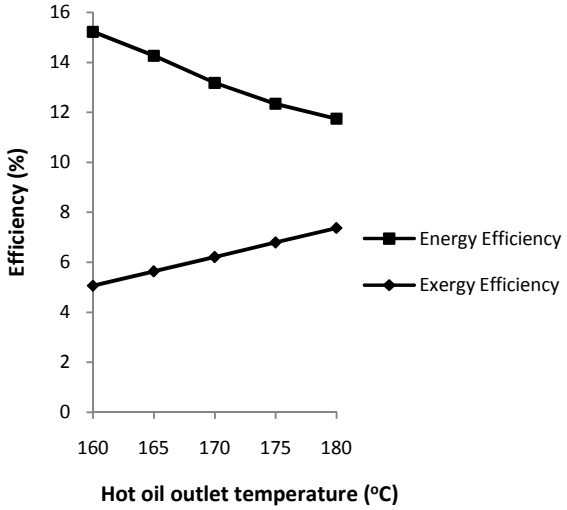


Fig. 4. Effect of hot oil outlet temperature on energy and exergy efficiency

Figure 4 indicates the effect of variation of hot oil outlet temperature on energy and exergy efficiency of proposed cogeneration cycle. It is found that refrigeration output of ERC and power output of RC increases while refrigeration output of ARC and total energy output decreases with the increase in hot oil outlet temperature. Since the rate of decrease of refrigeration output of ARC is greater than the rate of increase of refrigeration output of ERC and power output of RC cycle, the total energy output decreases with increase in hot oil outlet temperature. It is observed that exergy output of ERC and RC cycle increases while exergy output of ARC decreases with increase in hot oil outlet temperature. The total exergy output increases due to the fact that the rate of increase of exergy output of ERC and RC cycle is higher than rate of decrease in exergy output of ARC. Hence, the energy efficiency decreases while exergy efficiency of the cycle increases with increase in hot oil outlet temperature.

Figure 5 shows the variation of energy and exergy efficiency with increase in turbine inlet pressure of proposed cogeneration cycle for simultaneous production of power and double effect cooling. It is clearly observed that the energy efficiency increases significantly with increase in turbine inlet pressure of combined cycle. This is due to the fact that increase in turbine inlet pressure causes a significant increase in refrigeration output of ARC and reduction in refrigeration output of ERC and power output from turbine of RC cycle. Since the rate of increase in the refrigeration output of ARC is much greater than the rate of decrease is refrigeration output of ERC and power output from turbine of RC cycle, therefore, the overall energy efficiency of proposed cogeneration cycle increases with increase in turbine inlet pressure. The exergy efficiency of the proposed cycle shows the trend of decreasing

with increase in turbine inlet pressure. This is only because of increase in turbine inlet pressure the total exergy output of proposed cogeneration cycle for power and double effect cooling decreases.

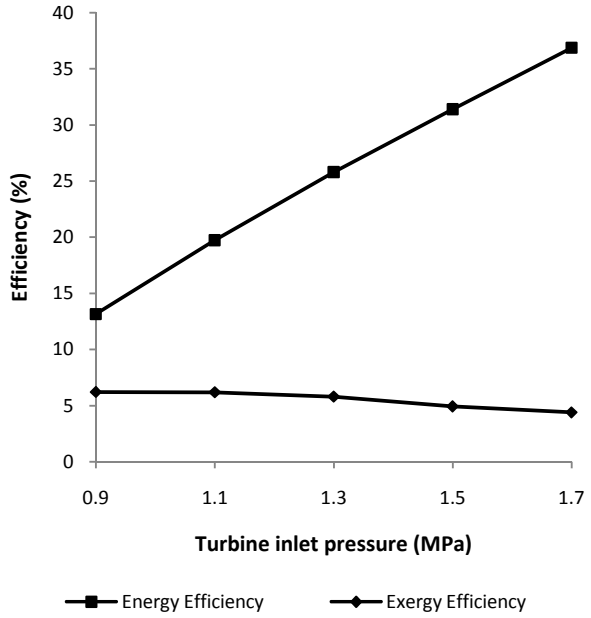


Fig. 5. Effect of turbine inlet pressure on energy and exergy efficiency

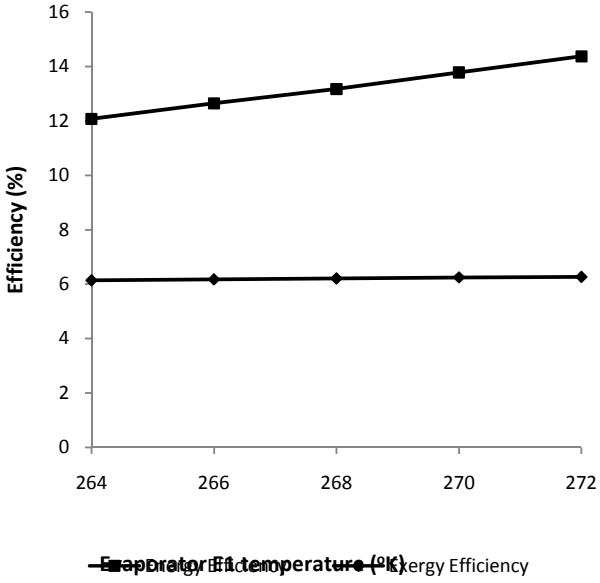


Fig. 6. Effect of evaporator E1 temperature on energy and exergy efficiency

Figure 6 shows the effect of variation of ejector evaporator (E1) temperature on energy and exergy efficiency of proposed cogeneration cycle. It is observed that an increase in the ejector evaporator temperature the energy efficiency increases significantly and exergy efficiency increases marginally.

5. CONCLUSION

A combined energy and exergy analysis of a new solar assisted cogeneration cycle for simultaneous production of power and double effect cooling is presented. The effect of various operating parameters was observed on energy and exergy efficiency of the proposed cycle. The main conclusions from present study can be summarized as follows:

- out of 100% solar heat energy supplied to the system around 7.68% is produced as refrigeration output in ERC and ARC cycle, 5.49% is produced as power output in RC cycle and 102.19% is lost to the environment.
- out of 100% solar exergy input to the system, around 0.35% is available as exergetic refrigeration output in ERC and ARC cycle, 5.87% is available as exergetic power output from turbine of RC and remaining is lost due to irreversibilities in the components and via thermal lost to the environment.
- the irreversibility in central receiver 52.5%, heliostat field 25%, condenser of ERC 3.98%, HRVG 3.79% and ejector 3.72% is observed.
- the exergy efficiency of around 6.218% is obtained which is much lower than energy efficiency 13.17% of solar assisted cogeneration cycle for simultaneous production of power and double effect cooling.
- with the increase in hot oil outlet temperature from central receiver (160^{o}C-180^{o}C), the energy efficiency decreases (15.22% -11.74%) significantly and exergy efficiency increases (5.06%-7.37%) marginally.
- with increase is turbine inlet pressure from 0.9 MPa to 1.7 MPa., the energy efficiency increases (13.17% to 36.86%) while exergy efficiency decreases (6.22% to 4.4%).
- with increase in ejector evaporator temperature from 264K to 272K, the increase in energy efficiency from 12.07% to 14.37% and increase in exergy efficiency from 6.14% to 6.22% is observed.

Presented cogeneration cycle is expected to meet out the demand of simultaneous production of power and double effect cooling by using only single source of solar heat in an effective and sustainable manner.

REFERENCES

[1] Xu, F., Goswami, D.Y. and Bhagwat, S.S., "A combined power/cooling cycle", *Energy*, 25, 2000, pp. 233-246.

[2] Hasan, A.A., Goswami, G.Y. and Vijayaraghavan, S., "First and second law analysis of a new power and refrigeration thermodynamic cycle using a solar heat source", *Solar Energy,* 73, 2002, pp. 385-393.

[3] Yidal, A., Best, R., Rivero, R. and Cervantes, J., "Analysis of a combined power and refrigeration cycle by the exergy method", Energy, 31, 2006, pp. 3401-3414.

[4] Sadrameli, S.M. and Goswami, D.Y., "Optimum operating conditions for a combined power and cooling thermodynamic cycle", *Applied Energy*, 84, 2007, pp. 254-265.

[5] Zhang, N. and Lior, N., "Development of a novel combined absorption cycle for power generation and refrigeration", ASME *Journal of Energy Resources Technology*, 129, 2007, pp. 254-265.

[6] Wang, J.F., Dai, Y.P. and Lin, G., "Parametric analysis and optimization for a combined power and refrigeration cycle", *Applied Energy*, 85, 2008, pp. 1071-1085.

[7] Bejan, A., "Fundamentals of exergy analysis, entropy generation minimization and the generation of flow architecture", *International Journal of Energy Research,* 26, 2002, pp. 545-565.

[8] NIST Standard Reference Database 23, NIST Thermodynamic and Transport Properties of Refrigerants and Refrigerants Mixtures', *REFPROP*, Version 6.01., 1998, USA.

[9] Chua, H.T., Toh, H.K., Malek, A., Ng, K.C. and Srinivasan, K., "Improved thermodynamic property fields of LiBr-H_2O solutions", *International Journal of Refrigeration,* 23, 2000, pp.412-429.

Research Article – JTEN – 2015 – 23

Journal of Thermal Engineering
Yildiz Technical University Press, Istanbul, Turkey
Vol. 2, No. 1, pp.541-549, January, 2016.

http://eds.yildiz.edu.tr/journal-of-thermal-engineering/Articles
Manuscript Received March 17, 2015; Accepted April 27, 2015

This paper was recommended for publication in revised form by Regional Editor Hafiz Muhammad Ali

ENERGY AND EXERGY ANALYSIS OF A DOUBLE EFFECT PARALLEL FLOW LIBR/H_2O ABSORPTION REFRIGERATION SYSTEM

Akhilesh Arora
Department of Mechanical Engineering, Delhi Technological University
Delhi, Delhi, India

***Manoj Dixit**
Centre for Energy Studies, Indian Institute of Technology Delhi
New Delhi, Delhi, India

S.C. Kaushik
Centre for Energy Studies, Indian Institute of Technology Delhi
New Delhi, Delhi, India

Keywords: Parallel flow, Absorption system, Exergy, Exergetic efficiency, Solution distribution ratio.
* *Corresponding author:* Phone: 91-9540660289
E-mail address: mandix@ces.iitd.ac.in

ABSTRACT

In the present communication the analysis of a parallel flow double effect absorption refrigeration system is performed to compute the optimum solution distribution ratio (optimum distribution of strong solution masses between low and high pressure generators) from the viewpoint of maximum COP and maximum exergetic efficiency. A computational model is developed for the parametric investigation of a double effect parallel flow LiBr/H_2O absorption refrigeration system. The effect of generator, absorber and evaporator temperatures on optimum solution distribution ratio is also studied. The results show that the maximum COP and maximum exergetic efficiency is achieved corresponding to same value of optimum solution distribution ratio.

INTRODUCTION

Most absorption cooling systems adopt the double-effect cycle to increase the cooling performance of the system when the heat source available is at high temperature with water lithium bromide. However, when using series flow double effect system the range of operation comes close to the crystallization line of the LiBr solution and the absorption ability becomes weak. The parallel-flow type of double-effect cycle has been proposed to eliminate these difficulties compared with the series-flow type. Compared to the series-flow type, the range of operating conditions of the parallel-flow type is far away from the crystallization line of the LiBr solution, but the control and regulation of the flow rate of solutions are complicated. Many studies are available in literature [1-12] on the first law performance evaluation of both series and parallel flow double effect absorption refrigeration systems. Most of these studies examined the effect of operating parameters like temperatures, solution circulation ratio, and effectiveness of heat exchangers on the system performance. The maximum cop of parallel flow double effect system depends on the optimum distribution of solution, leaving the absorber, between high and low temperature generators. In some of these studies [5, 7, 9] the effect of solution distribution ratio on the cop and cooling capacity has been discussed but the analysis does not include the effect of variation in parameters on optimum value of solution distribution ratio. Lee and Sherif [13], Izquierdo et al. [14] and lee and Sherif [15] are among the earliest researchers who presented the performance analysis of absorption systems based on second law of thermodynamics. Gebreslassie et al. [16] carried out the exergy analysis, considering only unavoidable exergy destruction, for single, double, triple and half effect water-lithium bromide absorption cooling cycles. Izquierdo et al. [17] designed experimental prototype of 7 kW of cooling power. A new type of flat-sheet adiabatic absorber was used to operate at outdoor temperatures of about 45 °c without any sign of crystallization. Exergoeconomic analyses is carried out by Farshi et al. [18] for three types of double effect LiBr-water absorption cooling systems to assess the influence of

various operating parameters on investment cost. Li et al. [19] did the performance analysis of solar air cooled double effect LiBr/H_2O absorption refrigeration system.

It is to be noted that in all the studies mentioned above the optimum solution distribution ratio is not computed corresponding to maximum exergetic efficiency. It is important to determine optimum solution distribution ratio corresponding to maximum exergetic efficiency because minimum irreversibility occurs in a thermal system corresponding to maximum exergetic efficiency.

Keeping this viewpoint, in the present communication the analysis of a parallel flow double effect absorption refrigeration system is performed to compute the optimum solution distribution ratio from the viewpoint of maximum cop and maximum exergetic efficiency. The effect of operating parameters such as generator, absorber and evaporator temperatures is also presented on optimum solution distribution ratio.

MODELLING OF LiBr / H_2O DOUBLE EFFECT PARALLEL FLOW ABSORPTION SYSTEM

Description of the system

Fig. 1 shows schematic diagram of a LiBr/H_2O parallel-flow, double-effect refrigeration system. It includes the most important components of the double-effect cycle: absorber (a), evaporator (e), HP generator (hpg), LP generator (lpg), condenser (c), HT heat exchanger (she_2), LT heat exchanger (she_1) and a solution pump (p). The strong (in absorbent) solution produced in the absorber is separated at the outlet of the LT heat exchanger and is distributed separately to the HP and LP generators. This is the main feature of the parallel-flow double effect absorption refrigeration system. The ratio of solution entering the HP generator to the solution leaving the solution pump is known as solution distribution ratio. The solution in the high-pressure generator is heated externally from solar energy or waste heat or any other heat source. The refrigerant vapour (steam) produced in the HP generator is used as a heat source for the low-pressure generator. The weak (in refrigerant) solution from the HP generator passes through the HT heat exchanger and mixes with the weak solution coming from LP generator through the solution throttle valve (stv_2) at the inlet of the LT heat exchanger. The solution then enters the absorber and is diluted by absorbing the refrigerant vapour coming from evaporator. The refrigerant vapour produced by the LP generator is condensed in the condenser, and flows to the evaporator. The refrigerant generated in LP and HP generators mix before entering the evaporator. In evaporator, liquid refrigerant extracts heat from the space to be cooled and evaporates, thereby producing cooling effect.

Mathematical Modelling

The thermodynamic analysis of the system involves the application of principles of mass conservation, species conservation, energy balance and exergy balance to individual components of the system. Mass and species conservation for each component can be written in general form as follows:

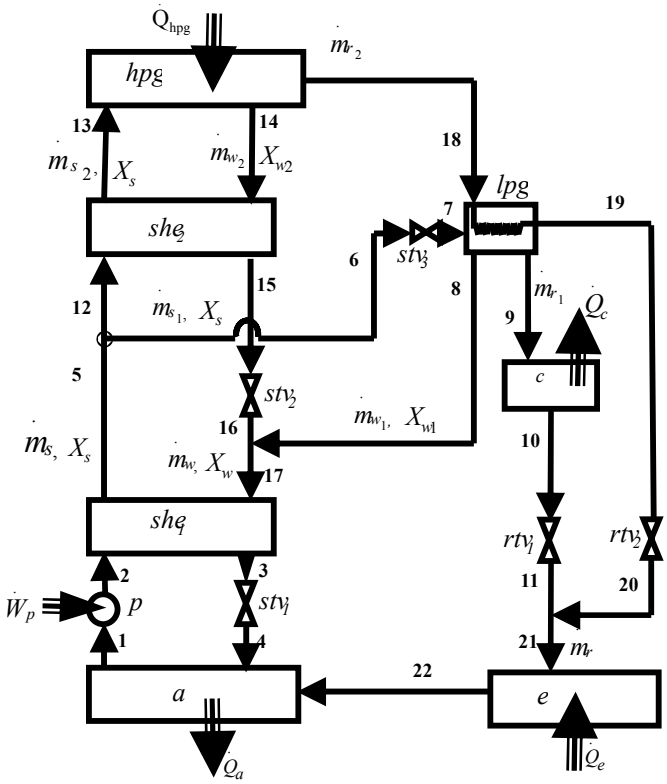


Fig. 1. Schematic diagram of a Parallel Flow Double Effect Absorption Refrigeration System

$$\Sigma \dot{m}_i = \Sigma \dot{m}_e \quad (1)$$

$$\Sigma \dot{m}_i \, X_i = \Sigma \dot{m}_e \, X_e \quad (2)$$

The energy balance of the system is specified by equation (3).

$$\Sigma \dot{Q} - \Sigma \dot{W} = \Sigma \dot{m}_e h_e - \Sigma \dot{m}_i h_i \quad (3)$$

Properties at various state points are calculated using the equations (4) to (10).

LiBr/H_2O solution: $f_1 (h, X, T) = 0$ (4)

f_2 (s, X, T) = 0 (5)
f_3 (P, T, X) = 0 (6)

Refrigerant (water): f_4 (h, P, T) = 0 (7)
f_5 (s, P, T) = 0 (8)
f_6 (h, T_{sat}) = 0 (9)
f_7 (s, T_{sat}) = 0 (10)

Exergy is the property of a system relative to a reference state, which gives the maximum power that can be extracted from the system when it is brought in to thermodynamic equilibrium with the reference state [20]. Exergy balance for a control volume undergoing steady state process is expressed as [13].

$$\dot{E}D_i = \sum\left(\dot{m}e\right)_{in} - \sum\left(\dot{m}e\right)_{out} + \left[\sum\left(\dot{Q}\left(1-\frac{T_0}{T}\right)\right)_{in} - \sum\left(\dot{Q}\left(1-\frac{T_0}{T}\right)\right)_{out}\right] \pm \sum\dot{W} \quad (11)$$

where $\dot{E}D_i$ represents the rate of exergy destruction or the irreversibility occurring in the process. The first two terms on the right hand side represent exergy of streams entering and leaving the control volume. The third and fourth terms are the exergy associated with heat transfer $\dot{Q}$ from the source maintained at constant temperature T and is equal to work obtained by Carnot engine operating between T and T_0, and is therefore equal to maximum reversible work that can be obtained from heat energy $\dot{Q}$. The last term is the mechanical work transfer to or from the control volume.

Second law performance of the system can be measured in terms of exergetic efficiency [21]. It is defined as the useful exergy or available energy gained from a system to that supplied to the system. For the double effect system under consideration, it is the ratio of the exergy of the cooling effect produced by the evaporator to the exergy of the heat supplied at the HP generator plus pump work supplied.

$$\eta_{ex} = \frac{E\dot{Q}_e}{E\dot{Q}_{hpg} + \dot{W}_p} = 1 - \frac{\dot{E}D_t}{E\dot{Q}_{hpg} + \dot{W}_p} \quad (12)$$

The above modeling procedure forms the basis for the equations given in the subsequent paragraph.

Mass, material and energy balance of parallel flow double effect absorption refrigeration system

The mass and material balance at high temperature generator, second effect generator and condenser are given by:

HP Generator

$$\dot{m}_{s_2} = \dot{m}_{r_2} + \dot{m}_{w_2} \quad (13)$$

$$\dot{m}_{s_2} X_s = \dot{m}_{w_2} X_{w_2} \quad (14)$$

LP generator

$$\dot{m}_{s_1} = \dot{m}_{r_1} + \dot{m}_{w_1} \quad (15)$$

$$\dot{m}_{s_1} X_s = \dot{m}_{w_1} X_{w_1} \quad (16)$$

Splitter (state points 5-6-12)

$$\dot{m}_s = \dot{m}_{s_1} + \dot{m}_{s_2} \quad (17)$$

Mixer (state points 8-16-17)

$$\dot{m}_w = \dot{m}_{w_1} + \dot{m}_{w_2} \quad (18)$$

$$\dot{m}_w X_w = \dot{m}_{w_1} X_{w_1} + \dot{m}_{w_2} X_{w_2} \quad (19)$$

Mixer (state points 11-20-21)

$$\dot{m}_r = \dot{m}_{r_1} + \dot{m}_{r_2} \quad (20)$$

Solution circulation ratio is specified by equation (21).

$$SCR = \frac{\dot{m}_s}{\dot{m}_r} = \frac{X_w}{X_w - X_s} \quad (21)$$

Solution distribution ratio (R) is specified by equation (22).

$$R = \frac{\dot{m}_{s_2}}{\dot{m}_s} \quad (22)$$

The energy balance in each component of a parallel flow double effect system is given by the following equations:

$$\dot{Q}_a = \dot{m}_r h_{22} + \dot{m}_w h_4 - \dot{m}_s h_1 \quad (23)$$

$$\dot{Q}_{hpg} = \dot{m}_{r_2} h_{18} + \dot{m}_{w_2} h_{14} - \dot{m}_{s_2} h_{13} \quad (24)$$

$$\dot{Q}_{lpg} = \dot{m}_{r_2}(h_{18} - h_{19}) = \dot{m}_{r_1} h_9 + \dot{m}_{w_1} h_8 - \dot{m}_{s_1} h_7 \quad (25)$$

$$\dot{Q}_c = \dot{m}_{r_1}(h_9 - h_{10}) \quad (26)$$

$$\dot{Q}_e = \dot{m}_r(h_{22} - h_{21}) \quad (27)$$

$$\dot{Q}_{she_1} = \dot{m}_s(h_5 - h_2) = \dot{m}_w(h_{17} - h_3) \quad (28)$$

$$\dot{Q}_{she_2} = \dot{m}_{s_2}(h_{13} - h_{12}) = \dot{m}_{w_2}(h_{14} - h_{15}) \quad (29)$$

$$\dot{W}_p = \dot{m}_s(h_2 - h_1) \quad (30)$$

$$\dot{E}_{in} = \dot{Q}_{hpg} + \dot{Q}_e + \dot{W}_p \quad (31)$$

$$\dot{E}_{out} = \dot{Q}_a + \dot{Q}_c \quad (32)$$

$$COP = \frac{\dot{Q}_e}{\dot{Q}_{hpg} + \dot{W}_p} \quad (33)$$

Exergy destruction in each component of a parallel flow double effect absorption refrigeration system is furnished below.

$$\dot{E}D_a = \dot{m}_r(h_{22} - T_o s_{22}) + \dot{m}_w(h_4 - T_o s_4) - \dot{m}_s(h_1 - T_o s_1) - \dot{Q}_a\left(1 - \frac{T_o}{T_a}\right) \quad (34)$$

$$\dot{E}D_{hpg} = \dot{m}_{s_2}(h_{13} - T_o s_{13}) - \dot{m}_{w_2}(h_{14} - T_o s_{14}) - \dot{m}_{r_2}(h_{18} - T_o s_{18}) + \dot{Q}_{hpg}\left((1 - \frac{T_o}{T_{hpg}}\right) \quad (35)$$

$$\dot{E}D_{lpg} = \dot{m}_{s_1}(h_7 - T_o s_7) - \dot{m}_{w_1}(h_8 - T_o s_8) + \dot{m}_{r_2}(h_{18} - T_o s_{18}) - \dot{m}_{r_2}(h_{19} - T_o s_{19}) - \dot{m}_{r_1}(h_9 - T_o s_9) \quad (36)$$

$$\dot{E}D_c = \dot{m}_{r_1}\left((h_9 - h_{10}) - T_o(s_9 - s_{10})\right) - \dot{Q}_c\left(1 - \frac{T_0}{T_c}\right) \quad (37)$$

$$\dot{E}D_e = \dot{m}_r((h_{21} - h_{22}) - T_o(s_{21} - s_{22})) + \dot{Q}_e\left(1 - \frac{T_0}{T_r}\right) \quad (38)$$

$$\dot{E}D_{she_1} = \dot{m}_s((h_2 - h_5) - T_o(s_2 - s_5)) + \dot{m}_w((h_{17} - h_3) - T_o(s_{17} - s_3)) \quad (39)$$

$$\dot{E}D_{she_2} = \dot{m}_{s_2}((h_{12} - h_{13}) - T_o(s_{12} - s_{13})) + \dot{m}_{w_2}((h_{14} - h_{15}) - T_o(s_{14} - s_{15})) \quad (40)$$

$$\dot{E}D_{rtv_1} = \dot{m}_{r_1} T_o(s_{10} - s_{11}) \quad (41)$$

$$\dot{E}D_{rtv_2} = \dot{m}_{r_2} T_o(s_{19} - s_{20}) \quad (42)$$

$$\dot{E}D_{stv_1} = \dot{m}_w T_o(s_3 - s_4) \quad (43)$$

$$\dot{E}D_{stv_2} = \dot{m}_{w_2} T_o(s_{15} - s_{16}) \quad (44)$$

$$\dot{E}D_{stv_3} = \dot{m}_{s_1} T_o(s_6 - s_7) \quad (45)$$

$$\dot{E}D_{mixer_{8\text{–}16\text{–}17}} = \dot{m}_{w_1}((h_8 - T_0 s_8) + \dot{m}_{w_2}((h_{16} - T_0 s_{16}) - \dot{m}_w((h_{17} - T_0 s_{17}) \quad (46)$$

$$\dot{E}D_{mixer_{11\text{–}20\text{–}21}} = \dot{m}_{r_1}((h_{11} - T_0 s_{11}) + \dot{m}_{r_2}((h_{20} - T_0 s_{20}) - \dot{m}_r((h_{21} - T_0 s_{21}) \quad (47)$$

$$\dot{E}D_t = \dot{E}D_a + \dot{E}D_{hpg} + \dot{E}D_{lpg} + \dot{E}D_c + \dot{E}D_e + \dot{E}D_{she_1} + \dot{E}D_{she_2} + \dot{E}D_{rtv_1} + \dot{E}D_{rtv_2} + \dot{E}D_{stv_1} + \dot{E}D_{stv_2} + \dot{E}D_{stv_3} + \dot{E}D_{mixer_{8\text{–}16\text{–}17}} + \dot{E}D_{mixer_{11\text{–}20\text{–}21}} \quad (48)$$

Equation (12) can now be rewritten in the form as shown in equation (49).

$$\eta_{e_x} = \frac{\dot{Q}_e\left|\left(1 - \frac{T_0}{T_r}\right)\right|}{\dot{Q}_{hpg}\left(1 - \frac{T_0}{T_{hpg}}\right) + \dot{W}_p} \quad (49)$$

RESULTS AND DISCUSSION

The present work is based on the following assumptions:-

1. Pressure and heat losses through the system components are negligible.
2. Solution leaving the absorber and the generator are assumed to be saturated in equilibrium conditions at their respective temperatures and concentrations.
3. Refrigerant leaving the condenser and vapour leaving the evaporator are assumed to be saturated at their respective saturation temperatures.
4. Refrigerant vapour leaving the HP generator is considered to be superheated vapour at the generator temperature.
5. Non equilibrium states at the inlet to the HP generator, and the absorber and states at outlet to the solution pump and the solution heat exchanger are taken to be at their actual conditions.
6. Pumping process is assumed to be reversible adiabatic.
7. Throttling of the refrigerant is assumed to be isenthalpic and non-isentropic while solution throttling is considered to be isothermal, isenthalpic and non-isentropic.

8. The temperature in high temperature heat source, medium temperature heat sink and low temperature heat source are assumed to be constant while the fluid temperature varies in non-isothermal components due to different inlet/outlet solution concentrations.
9. The reference enthalpy (h_o) and entropy (s_o) used for calculating exergy of the working fluid are the values for water at an environment temperature (T_o) of 25°C.

A computer program has been developed using Engineering Equation Solver (EES) software [22] for carrying out the energy and exergy analysis of the single effect and double effect absorption refrigeration systems. The properties of LiBr/H_2O solution used for the analysis purpose have been obtained from correlations developed by Pátek and Klomfar [23]. Subroutines for calculating the properties of LiBr-H_2O solution were linked to the library file of the EES. Following parameters are assumed for parametric computations:-

1. High pressure generator temperature (T_{hpg}) = 120 °C – 170 °C
2. Evaporator temperature (T_e) = 7.2 °C
3. Condenser and absorber temperatures are assumed to be equal. ($T_c = T_a$) = 29.4 °C /37.8 °C
4. Effectiveness of solution heat exchanger(s), (ε) = 0.7
5. Temperature of the space to be cooled (T_r) = 17.2 °C
6. Cooling capacity of the system ($\dot{Q}_e$) = 100 kW

The results computed from the present work are compared with the results given in Riffat and Shankland (1993) and are detailed in Table 1. The difference in values of heat transfers in various components is less than 3%. The difference in value of COP is less than 0.6%.

Table 1. Comparison of present results with the results of Riffat and Shankland [6]

Parameter	Results reported by Riffat and Shankland [6]	Computed results	Difference in reported and Computed values
Heat supplied in HP generator, ($\dot{Q}_{hpg}$), kW	71.2	70.81	-0.55 %
Cooling effect ($\dot{Q}_e$), kW	100	100	---
Heat rejected by the absorber ($\dot{Q}_a$), kW	119.99	121.5	1.26%
Heat rejected by the condenser ($\dot{Q}_c$), kW	51.20	49.32	-3.67%
Pump work ($\dot{W}_p$), kW	0.0	0.0083	----
COP	**1.404**	**1.41**	**0.43%**

Fig. 2 illustrates the effect of variation in solution distribution ratio and HP generator temperature on the COP ($T_c = T_a$ = 29.4 °C). The COP increases with reduction in HP generator temperature. The reason being that for same solution distribution ratio, the increase in HP generator temperature cause an increase in exergy destruction in HP generator, absorber, condenser, LP generator and total exergy destruction. The maximum value of COP varies between 1.39 and 1.42. The global maximum of COP is observed at 135°C HP generator temperature. Further with increase in solution distribution ratio, it is observed that total exergy destruction first decreases up to the optimum and then again starts increasing.

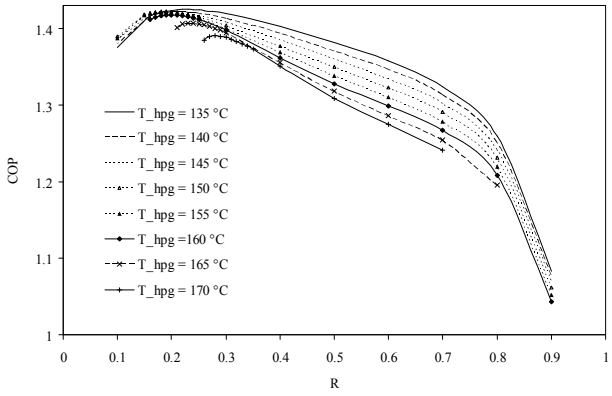


Fig. 2. Effect of solution distribution ratio (R) and high pressure generator temperature on COP (Te=7.2 °C, Ta= Tc=29.4 °C).

The optimum value of solution distribution ratio for maximum COP varies between 0.19 and 0.28 depending upon the HP generator temperature, indicating best results are achieved when most of the solution is distributed to the LP generator and simultaneously minimum total exergy destruction is observed corresponding to these values. Secondly, it is observed that with increase in HP generator temperatures (i.e. between 135 °C to 155 °C) the optimum solution distribution ratio decreases from 0.23 to 0.19 and for temperatures between 155 °C and 170 °C, it increases to 0.28. Moreover lower values of R_{opt} show that circulation losses are also less when lesser amount of solution is entering the HP generator. The nature of the curve obtained in

the present analysis is similar to the curve obtained by Gommed and Grossman [5] in their analysis.

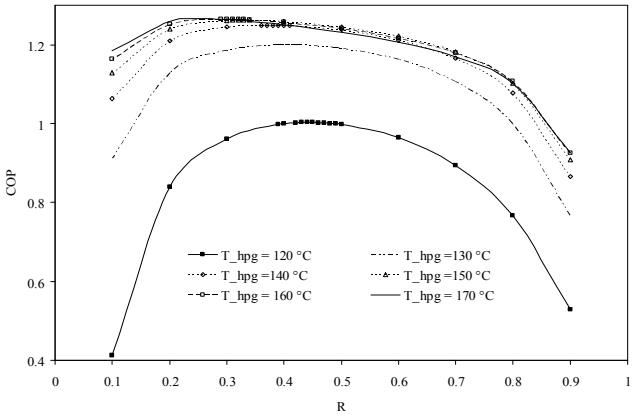


Fig. 3. Effect of solution distribution ratio (R) and high pressure generator temperature on COP (Te=7.2 °C, Ta= Tc=37.8 °C)

Fig. 3 presents the effect of increasing the absorber and condenser temperatures on the COP and optimum solution distribution ratio. It is observed that with increase in the absorber and condenser temperatures (from 29.4 to 37.8 °C), the COP and its maximum value drops for the range of generator temperatures considered. It happens because of increase in solution circulation ratio, with increase in absorber and condenser temperatures, and it causes increase in circulation losses and hence reduction in COP. Further the optimum solution distribution ratio is achieved at higher values of solution distribution ratio than before. It indicates that more solution is required to be pumped to HP generator at higher absorber and condenser temperatures to achieve maximum value of the COP. However increasing the HP generator temperature causes the optimum distribution ratio to shift toward lower values of solution distribution ratio.

Fig. 4 depicts the effect of solution distribution ratio and HP generator temperature on exergetic efficiency. It is observed that increase in the HP generator temperature brings down the exergetic efficiency. The same reasons can be attributed for such a behaviour as already explained for the trend of COP curve. Secondly, with increase in solution distribution ratio, there is increase in exergetic efficiency up to optimum value of solution distribution ratio and beyond which there is drop in exergetic efficiency. The optimum value of solution distribution ratio lies between 0.23 - 0.19 for the HP generator temperatures between 135 °C and 155 °C, and for temperatures above 155 °C and up to 170 °C, it increases to 0.28.

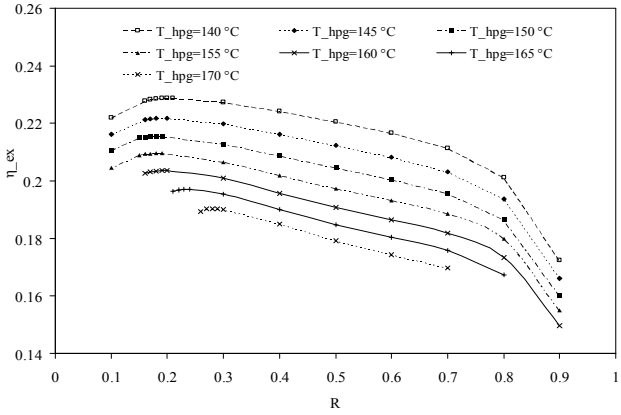


Fig. 4. Effect of solution distribution ratio (R) and high pressure generator temperature on exergetic efficiency (Te=7.2 °C, Ta= Tc=29.4 °C)

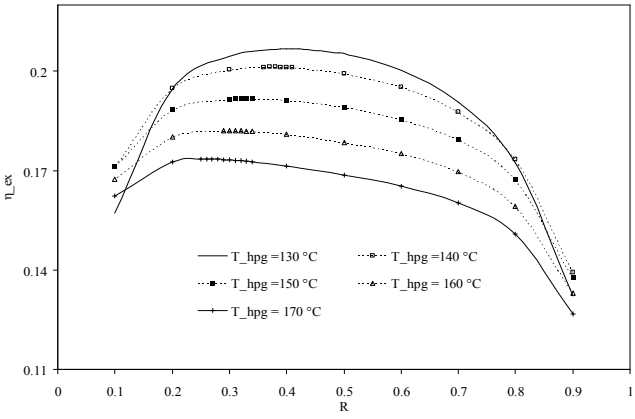


Fig. 5. Effect of solution distribution ratio (R) and high pressure generator temperature on exergetic efficiency (Te=7.2 °C, Ta= Tc=37.8 °C).

The effects of increase in absorber and condenser temperatures on exergetic efficiency and optimum solution distribution ratio are represented in Fig. 5. The increase in the absorber and condenser temperatures is responsible for reduction of exergetic efficiency. It happens because of overall increase in solution circulation ratio with increase in absorber and condenser temperatures which causes increase in circulation losses and irreversibility in various components of the system increase and hence reduction in exergetic efficiency. The higher values of the exegetic efficiency are achieved at lower values of HP generator temperature for solution distribution ratio varying between 0.2 and 0.77. The optimum value of solution distribution ratio increases as compared to the case when absorber and condenser temperatures are lower.

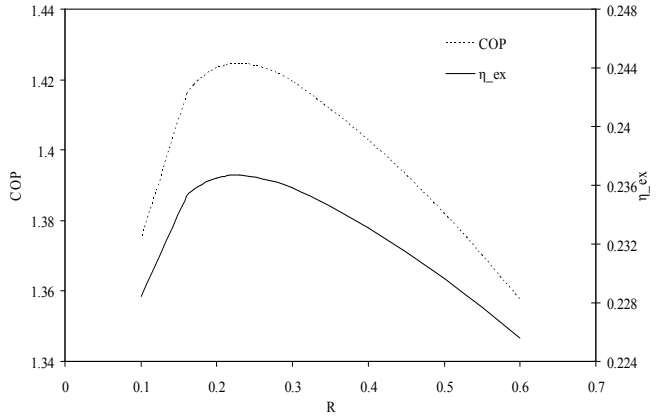


Fig. 6. Variation of COP and exergetic efficiency with solution distribution ratio (R) (T_{hpg}= 135 °C, Te = 7.2 °C, Ta = Tc = 29.4 °C)

Fig. 6 depicts the variation of the COP and exergetic efficiency with solution distribution ratio. It is observed that the maximum value of the COP and exergetic efficiency occur for same solution distribution ratio. This happens because minimum irreversibility occurs at optimum solution distribution ratio. The similar results were also obtained for different values of generator temperature at other absorber and condenser temperatures.

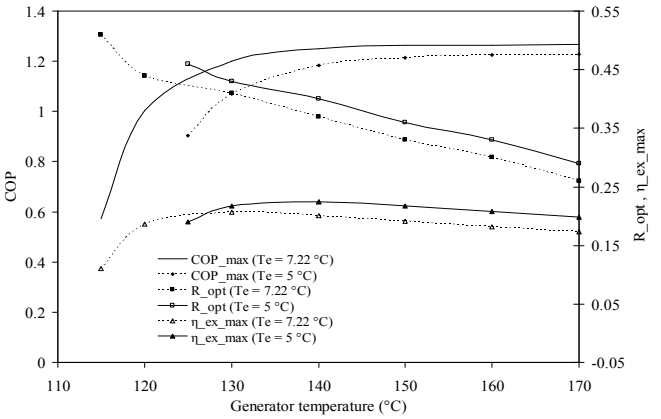


Fig. 7. Variation of maximum COP and exergetic efficiency and R_{opt} with T_{hpg} for varying evaporator temperatures

Fig. 7 shows the effect of variation in the evaporator temperature on the optimum solution distribution ratio, maximum COP and maximum exergetic efficiency at condenser and absorber temperature of 37.8 °C. The overall system irreversibility increases with reduction in evaporator temperature and hence maximum value of the COP and the exergetic efficiency reduce.

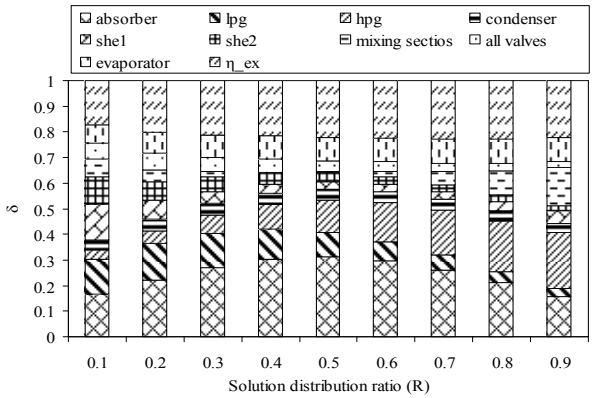


Fig. 8. Exergy destruction in different components at various solution distribution ratios (R)

Fig. 8 represents the variation of exergy destruction in different components with solution distribution ratio at high pressure generator temperature of 140 °C and condenser and absorber temperature of 29.4 °C. It is observed that total exergy destruction is lowest at optimum solution distribution ratio and it increases on either side of the optimum solution distribution ratio on either side. The absorber is the component in which percentage exergy destruction is maximum followed by HP generator, mixing sections, LP generator and evaporator.

CONCLUSIONS

In the present analysis, we have performed the energy and exergy analysis of a parallel flow double effect LiBr/H_2O absorption refrigeration system. The conclusions drawn from this analysis are specified point wise below.

1. The COP and exergetic efficiency increases with reduction in HP generator temperature. Thus global maximum of COP is observed at 135°C HP generator temperature. The maximum value of COP varies between 1.39 and 1.42. The optimum value of solution distribution ratio for maximum COP varies between 0.19 and 0.28 depending upon the HP generator temperature. The optimum value of solution distribution corresponds to minimum exergy destruction.

2. Increasing the absorber and condenser temperatures cause the COP, exergetic efficiency and their maximum values to drop. The optimum solution distribution ratio is achieved at higher values of solution distribution ratio.

3. The maximum values of the COP and exergetic efficiency occur for same solution distribution ratio.

4. The total exergy destruction is lowest at optimum solution distribution ratio and it increases on either side of the optimum solution distribution ratio. The absorber is the component in

which percentage exergy destruction is maximum followed by HP generator, mixing sections, LP generator and evaporator.

NOMENCLATURE

COP	Coefficient of performance
e, E	Specific exergy ($kJkg^{-1}$), Exergy (kJ)
$\dot{E}$	Rate of energy (kW)
$\dot{E}D$	Rate of exergy destruction (kW)
f	Function
h	Specific enthalpy ($kJ\ kg^{-1}$)
HP	High pressure
HT	High temperature
LP	Low pressure
LT	Low temperature
$\dot{m}$	Mass flow rate ($kg\ s^{-1}$)
P	Pressure (kPa)
$\dot{Q}$	Heat transfer rate (kW)
s	Specific entropy ($kJ\ kg^{-1}\ K^{-1}$)
SCR	Solution circulation ratio
R	Solution distribution ratio
T	Temperature (K)
$\dot{W}$	Work transfer rate (kW)
X	LiBr mass fraction
Subscripts	
0	Represents dead state
1, 2, 3…	Represent state points in fig. 1 and 2
a	Absorber
aev	All expansion valves
C	Condenser
e	Evaporator, exit
hpg	High pressure generator
i	Inlet, any component
in	input
lpg	Low pressure generator
max	Maximum
opt	Optimum
out	Out
p	Pump
r	Refrigerant, space to be cooled
rtv	Refrigerant throttle valve
s	Strong
she	Solution heat exchanger
stv	Solution throttle valve
t	Total
w	Weak
Greek letter	
δ	Efficiency defect
ε	Effectiveness of solution heat exchanger(s)
η	Efficiency

ACKNOWLEDGMENTS

The support of Ministry of New and Renewable Energy (MNRE), Government of India is duly acknowledged.

REFERENCES

[1] Vliet G.C., Lawson, M.B., Lithgow, R.A., 1982. Water-Lithium Bromide double effect absorption cooling system analysis. ASHRAE Transactions HO-82-5(2), 811-823.

[2] Fallek M., 1985. Parallel flow Chiller- heater. ASHRAE Transactions HI-85-41(5), 2095-2102.

[3] Kaushik S. C. and Chandra S., 1985. Computer modeling and parametric study of a double effect generation absorption refrigeration cycle. Energy Conversion Management 25(1), 9-14.

[4] Iyer, P. S. A, Murthy S. S. and Murthy M. V. K., 1988. Correlations for evaluation of the performance characteristics of vapour absorption refrigeration cycles. Solar & Wind Technology 5 (2), 191-197.

[5] Gommed K. and Grossman, G., 1990. Performance analysis of staged absorption heat pumps: water-lithium bromide systems. ASHRAE Transactions 30(6), 1590-1598.

[6] Riffat, S. B. and Shankland, N., 1993. Integration of absorption and vapour-compression systems. Applied Energy 46(4), 303-316.

[7] Oh M. D., Kim S. C., Kim Y. L. and Kim Y. I., 1994. Cycle analysis of an air-cooled $LiBr/H_2O$ absorption heat pump of parallel-flow type. International Journal of Refrigeration 17(8), 556- 565.

[8] Xu G. P., Dai Y. Q., Tou K. W. and Tso C. P.,1996. Theoretical analysis and optimization of a double-effect series-flow-type absorption chiller. Applied Thermal Engineering 16(12), 975-987.

[9] Xu G. P. and Dai Y.Q., 1997. Theoretical analysis and optimization of a double-effect parallel flow type absorption chiller. Applied Thermal Engineering 17(2), 157-170.

[10] Arun M.B., Maiya M.P., Murthy S. S, 2000. Equilibrium low pressure generator temperatures for double effect series flow absorption refrigeration systems. Applied Thermal Engineering 20, 227-242.

[11] Elsafty A and Al-Daini A.J., 2000. Theoretical Investigation of a water-lithium bromide vapour absorption cooler, Renewables: The Energy for the 21st Century World Renewable Energy Congress VI, Brighton, UK, 2202-2205.

[12] Arun M.B., Maiya M.P., Murthy S. S, 2001. Performance comparison of double effect parallel flow and series flow water lithium bromide absorption systems. Applied Thermal Engineering 21, 1273-1279.

[13] Lee, S.F., Sherif, S.A., 1999. Second law analysis of multi effect Lithium Bromide/Water absorption chillers. ASHRAE Transactions Ch-99-23(3), 1256- 1266.
[14] Izquierdo M., Vega M. D, Lecuona A., Rodríguez P., 2000. Entropy generated and exergy destroyed in lithium bromide thermal compressors driven by the exhaust gases of an engine. International Journal of Energy Research 24(13), 1123 – 1140.
[15] Lee, S.F., Sherif, S.A., 2001. Second law analysis of various double effect Lithium Bromide/Water absorption chillers. ASHRAE Transactions AT-01-9(5), 664-673.
[16] Gebreslassie B.H., Medrano M., Boer D., 2010. Exergy analysis of multi-effect water LiBr/absorption systems: From half to triple effect. Renewable Energy 35, 1773–1782.
[17] Izquierdo M., Marcos J.D., Palacios M.E., González-Gil A., 2012. Experimental evaluation of a low-power direct air-cooled double-effect LiBr-H2O absorption prototype. Energy 37, 737-748.
[18] Farshi L.G., Mahmoudi S.M.S., Rosen M.A., Yari M., Amidpour M., 2013. Exergoeconomic analysis of double effect absorption refrigeration systems. Energy Conversion and Management 65, 13–25.
[19] Li Z., Ye X., Liu J., 2014. Performance analysis of solar air cooled double effect LiBr/H_2O absorption cooling system in subtropical city. Energy Conversion and Management 85, 302-312.
[20] Arcaklıoğlu E., Cavuşoğlu A. and Erişen A, 2005. An algorithmic approach towards finding better refrigerant substitutes of CFCs in terms of the second law of thermodynamics. Energy Conversion and Management 46, 1595-1611.
[21] Bejan, A., Tsatsaronis, G., Moran, M., 1996. Thermal Design and Optimization. John Wiley and Sons Inc., USA, 143–156.
[22] Klein S.A., Alvarado F., 2005. Engineering Equation Solver, Version 7.441, F-Chart software, Middleton, WI.
[23] Pátek J., Klomfar J., 2006. A computationally effective formulation of the thermodynamic properties of LiBr/H2O solutions from 273 to 500 K over full composition range. International Journal of Refrigeration 29, 566-578.

Journal of Basic and Applied Engineering Research
Print ISSN: 2350-0077; Online ISSN: 2350-0255; Volume 2, Number 13; April-June, 2015 pp. 1159-1162
© Krishi Sanskriti Publications
http://www.krishisanskriti.org/jbaer.html

Evaluation of Protocols to Support IP Mobility in Aeronautical Communications

Kapil Sharma

Delhi Technological University
E-mail: kapil@ieee.org

Abstract— *The aviation trade is presently at the opening of a modernization phase about its communication systems. This involves a transition to IP-based networks for Air Traffic Manage and Airline Operational Communications. Due to the heterogeneous nature of the communication environment, support for mobility among dissimilar access technologies and access networks becomes required. We initial introduce the aeronautical communications environment and their domain specific requirements. The major part of this article is a survey of dissimilar protocols that can be used to solve the IP mobility difficulty in the aeronautical environment. These protocols are assessed with regard to the introduced requirements.*

Keywords: *Aeronautical Access Technologies, Mobility, IPv6, Mobile IP.*

1. INTRODUCTION

The communication infrastructure currently used for civil aeronautical communications is based on an analogue voice system that can neither cope with the expected improve in air traffic nor support the envisaged paradigm shift towards data or packet oriented communications. The digitalization effort is supposed to free-up the at this time congested analogue voice based system and to improves, operational efficiency. The Internet Protocol IPv6 has been select as the basis for the Aeronautical Telecommunications Network (ATN/IP) as:

- It is a widely used industry standard in telecommunications
- It is actively maintained and extended by the accountable standardization organization, the Internet Engineering Task Force (IETF).
- It provides sufficient address space for a world-wide deployment in each national state and aircraft.

2. THE AERONAUTICAL ENVIRONMENT

Before you begin to format your paper, first write and save the content as a separate text file. Keep your text and graphic files separate until after the text has been formatted and styled. Do not use hard tabs, and limit use of hard returns to only one return at the end of a paragraph. Do not add any kind of Units

3. AERONAUTICAL ACCESS TECHNOLOGIES

The future ATN will employ dissimilar access technologies for carrying IP-based traffic that makes this network ("greatly" heterogeneous. At airports standard IEEE 802.11 [1] (WiFi) equipment is already in use for providing wireless connectivity for AAC communications when the aircraft is standing at the gate.. This technology will provide some Mbit/sec per radio cell for ATS and AOC traffic. Standard WiMAX can be used to provide connectivity for AAC and APC. Most of the ATS traffic more continental areas, as well as AOC traffic, will be carried by the L-Band Digital Aeronautical Communications System L-DACS, a technology that is at present¬ in development.

4. MOBILITY REQUIREMENTS

In this section, we specify inherent, primary and secondary needs that have to be fulfilled by a mobility protocol used in the aeronautical environment. The word "aircraft" refers to a total mobile network, consisting of an airborne router and at least one network prefix. Some end-system (MNNs) are connected to this airborne router. The inherent requirements that must be completely fulfilled by all candidates are as follows.

a. Session continuity: This property provides a stable IP address for use to higher layer protocols, even in case of handovers.
b. Mobile Network support: Mobility should not only be provided for a single mobile host, but for a complete onboard network. More specifically, instead of providing a constant IP address (as the case for the previous requirement) one or some constant network prefixes should be provided. "Session continuity" is automatically fulfilled by all mobility protocols investigated later.

The requirements that should all be fulfilled by the candidate protocols are as follows:

Multihoming: The aircraft should be capable of routing data simultaneously over different interfaces/ paths from the

aircraft to the ground. This requirement covers both load-balancing and fault-tolerance. The latter addresses the main issue of reliability/availability

Security 1 (masquerading): An attacker must not be able to claim the constant addresses/prefixes of an aircraft, e.g. by means of man-in-the-middle attacks.

Security 2 (DoS): The mobility protocol itself should not introduce any new denial of service vulnerabilities.

End-to-end delay: The delay among the communication peers should be kept minimal.

Scalability: The impact of the mobility protocol on the universal routing infrastructure should be kept to a minimum, meaning that frequent route announcements/ withdrawals for each individual aircraft should be avoided.

Applicability to AAC/APC: Specifies whether the solution is also applicable to non-safety related services. This indicates whether the protocol stack on the last systems has to be modified in order to support mobility.

Secondary requirements are desirable and their fulfilment is a bonus:

1. Efficiency 1: The overhead incurred by the mobility protocol itself should be limited. The number of roundtrip times (RTTs) needed for mobility-related signalling should therefore be kept minimal.
2. Efficiency 2: The overhead imposed upon each individual packet with payload from the MNNs or CNs should be limited. The number of additional protocol headers, needed to support mobility, should therefore be kept minimal.
3. Convergence time: Convergence time is also influenced by the number of exchanged signalling messages as described by Efficiency 1, this need is restricted to the time it takes to propagate the new mobility state throughout the (routing) system.

Support for ground-initiated communications: End systems on the ground should be capable of sending packets to an aircraft they have not yet communicated with. This means that a routing path to the current location of an aircraft has to be available for these nodes. It is preferable to have a single protocol (family) as a solution for all domains, ATS/AOC/AAC/APC.

5. MOBILITY OPTIONS

The Protocols for providing IP mobility are also discussed in [2], [3], with a focus on the aeronautical environment in [4]. Our investigation is different from the previous ones by (a) having introduced numerous needs and (b) by assessing the protocols based on those requirements. While the work performed in [4] also specifies certain requirements, many of them are high level. We investigate the protocols and perform our analysis with a higher degree of detail. Also, the second addresses an main optimization problem that is not covered at all by [4]. We therefore focussed on protocols between the network and transport layer for our investigation. We identify dissimilar protocols that can be categorized as follows:

- Routing protocol based approach (network layer), with the example of the Border Gateway Protocol.
- Tunnelling based approaches (network layer), with the examples of the IPsec and Mobile IP protocol families.
- A transport protocol approach, with the example of the Stream Control Transmission Protocol.
- Locater-identifier split (between network and transport layer), with the example of the Host Identity Protocol.

6. BORDER GATEWAY PROTOCOL (BGPV4)

The Border Gateway Protocol Version 4 (BGPv4) [5] is the inter-domain routing protocol mostly used in the Internet. BGP is used between autonomous systems for exchanging information on routing paths to specific destination prefixes. Routing information is distributed to neigh boring routers that fill in their routing tables and forward the routing information to other selected routers. BGP has already been used in the past for providing (IPv4) Internet Connectivity to the APC domain via GEO satellites.

7. BORDER GATEWAY PROTOCOL (BGPV4)

IPSec [6] is a well known protocol providing confidentiality, data integrity and data source authentication. These services are provided by maintaining a joint state among the two communication peers, also called Security Association (SA). Establishing such a SA manually would not be scalable, hence the Internet Key Exchange (IKEv2) protocol [7] provides the means to create and manage them dynamically. IKE mutually authenticates the two peers, based on either pre-shared secrets, certificates or the Extensible Authentication Protocol (EAP) [8]. In case of a VPN-like approach where an IP-in-IP tunnel is established, if one of the two IPSec peers moves to a different network and configures a new IP address, the established SAs would not be usable anymore.

8. NETWORK MOBILITY (NEMO)

Text The Network Mobility (NEMO) protocol [9] is an extension to Mobile IPv6 (MIPv6) [10]. NEMO extends the concept of a mobile node to that of a Mobile Router (MR) with one or some mobile network prefixes. As soon as the MR attaches to a foreign network it registers the new CoA with its Home Agent (HA) in the home network and creates a bi-directional tunnel for forwarding traffic between the nodes of the mobile network and the communication peers on the ground via the HA.

9. NETWORK MOBILITY (NEMO)

SCTP is a connection-oriented transport layer protocol comparable to TCP, but with additional features such as

multihoming. The original SCTP specification allows specifying several IP addresses during connection setup time only. This limitation has been removed with [11] where newly configured IP addresses can be dynamically added to or deleted from an SCTP association by one of the two communication peers. This is particularly useful for a mobile node where IP addresses appear and disappear due to handovers between different access networks. The original SCTP specification allows specifying some IP addresses during connection setup time only. This limitation has been removed with [11] where newly configured IP addresses can be dynamically added to or deleted from an SCTP association by one of the two communication peers.

10. HOST IDENTITY PROTOCOL (HIP)

Another, more radical, approach for supporting mobility is the locator-identifier split, where a new shim layer between the network and the transport layer is introduced. This layer also introduces a new namespace on top of the IP address space. In HIP, Host Identity Tags (HITs - the identifiers) are mapped to the available IP addresses (locators) with the help of IPSec. The HITs are generated from the public key and therefore cryptographically bound to it. Only the owner of the corresponding private key can make use of the related HIT in the HIP protocol exchanges. If the HIP-enabled mobile node attempts to communicate with a HIP correspondent node, it initiates a message exchange to establish a common session based on the HITs of the two nodes and the IP addresses they want to use for message exchange

11. HOST IDENTITY PROTOCOL (HIP)

WINMO which stands for Wide-Area IP Network Mobility was introduced in 2008 to address the routing update overhead problem of Connexion. Like Connexion, WINMO also assigns each mobile network a stable prefix. However, through two new approaches, WINMO can reduce the BGP updates overhead for mobile networks by orders of magnitude lower than those of Connexion. Thus, packets destined to mobile networks are forwarded to DBR after they enter the border of an AS, and DBR will tunnel them to the current locations of mobile networks.

12. HOST IDENTITY PROTOCOL (HIP)

The discussion of all the various protocols shows that there is no optimal solution that is capable of fulfilling all requirements”out of the box”. In the following, we give idea a how the requirements are graded and discuss how they are fulfilled by each protocol.

13. GRADING OF MOBILITY REQUIREMENTS

The grading of the property Multihoming is either completely fulfilled/Optional (C.F/O.), Basically Fullfield/Fair fullfield with limitations (B.F/F.) or not Unsupported/Poor not fulfilled (U/P.). The latter is applied if load-balancing is not supported.

Security 1 is either completely fulfilled (C.F/O.), or not fulfilled (U/P.).

Security 2 has the additional grading levels (B.F/F.) and (U/P.) that point to those vulnerabilities exist but the probability for an attacker to exploit them is very small, given that sure precautions are taken.

The end-to-end delay can be either optimal (C.F/O) or suboptimal (U/P).

Scalability always refers to the entries in the BGP routing tables, except for HIP that only creates entries in the DNS (U/P.) indicates linear scalability with number of mobile nodes and (B.F/F.) Indicates linear scalability with number of aggregated prefixes. Finally Limitation/Average (L/A.) for HIP is scalability with number of mobile nodes, but graded better because it only impacts the DNS. More precisely, the DNS entry of a mobile node is only stored at a single DNS server.

Applicability to AAC/APC is either possible (C.F/O.) or not possible (U/P.).

Convergence time is either limited to the time it takes to signal the new location to a single node (C.F/O.), influenced by DNS lookup and forwarding of the initial packet by a rendezvous server (B.F/F.) or depending on the convergence time of the global routing tables (L/P.) for an inter network of limited size, such as the ATN.

The gradins of the individual protocols for Efficiency 1 and Efficiency 2 are relative to each other.

Ground-initiated communications is either fully supported (C.F/O.), supported with a dependency on the DNS (B.F/F.) or not supported at all (U/P.). Table 1 shows a brief comparison of six mobility protocol of Aeronautical Environment.

Table 1: Comparisons many type of protocol under the Aeronautical Environment

Protocol	BGP	IPSec	NEMO
Session Continuity	(C.F/O)	(C.F/O)	(C.F/O)
Mobile Network Support	(C.F/O)	(C.F/O)	(C.F/O)
Multihoming	(L/A)	(U/P)	(C.F/O)
Security 1	(C.F/O)	(C.F/O)	(C.F/O
Security 2	(B.F/F)/(L/A)	(C.F/O)	(C.F/O)
End-to-end delay	(C.F/O)	(U/P)	(U/P)
Scalability	(U/P)	(B.F/F)	(B.F/F)
Applicability to AAC/APC	(C.F/O)	(C.F/O)	(C.F/O)
Convergence time	(L/A)	(C.F/O)	(C.F/O)
Efficiency 1	(U/P)	(B.F/F)	(B.F/F)
Efficiency 2	(B.F/F)	(U/P).(U/P)	(U/P)
Ground -initiated comms	(C.F/O)	(C.F/O)	(C.F/O)

Protocol	SCTP	HIP	WINMO
Session Continuity	(C.F/O)	(C.F/O)	(C.F/O)
Mobile Network Support	(U/P)	(C.F/O)	(C.F/O)

Multihoming	(U/P)	(L/A)	(B.F/F)
Security 1	(U/P)	(C.F/O)	(C.F/O)
Security 2	(L/A)	(L/A)	(B.F/F)
End-to-end delay	(C.F/O)	(C.F/O)	(C.F/O)
Scalability	(C.F/O)	(L/A)(for	(B.F/F)
Applicability to AAC/APC	(U/P)	DNS)	(C.F/O)
		(U/P)	
Convergence time	(C.F/O)	(B.F/F)	(B.F/F)
Efficiency 1	(B.F/F)	(L/A)	(L/A)
Efficiency 2	(B.F/F)	(L/A)	(B.F/F)
Ground -initiated comms	(U/P)	(B.F/F)	(L/A)

14. CONCLUSION

In this paper, we use an aeronautical access technology that provides some Mbit/sec per radio cell for ATS and AOC traffic and Standard WiMAX can be used to provide connectivity for AAC and APC. we have described the various protocols and its mobility requirements We also enhanced a protocol WINMO and give the details of it and its requirements. This identifies it as the most promising approach among all the studied RO protocols. An advantage of the MR-to-HA approach though is the applicability to the AAC and APC domains where passenger owned devices have to be supported and data is routed over the public Internet. As mobility signalling is only performed between mobile router and home agent, both MNNs and CNs remain unaffected. In fact, the mobility protocol is completely transparent to these end-systems and they do not require any mobility extensions.

REFERENCES

[1] "IEEE Standard for Local and metropolitan area network. Wirless LAN Medium Access Cantrol (MAC) and Physical Layer (PHY) Specifications," IEEE Std 802.11-2007, pp. C1–1184, 2007.

[2] D. Le, X. Fu, and D. Hogrefe, "A review of mobility support paradigms for the Internet," IEEE Commun. Surveys and Tutorials, vol. 8, no. 1-4, pp. 38–51, 2006.

[3] E. Perera, V. Sivaraman, and A. Seneviratne, "Survey on network mobility support," SIGMOBILE Mob. Comput. Commun. Rev., vol. 8, no. 2, pp. 7-19, 2004.

[4] ICAO Aeronautical Communications Panel, WG I, "Analysis of Candidate Mobility Solutions," 13th meeting of the working group N-SWGI, Montreal, Canada.

[5] Y. Rekhter, T. Li, and S. Hares, "A Border Gateway Protocol 4 (BGP-4)," RFC 4271, Jan. 2006.

[6] S. Kent and K. Seo, "Security Architecture for the Internet Protocol," RFC 4301, Dec. 2005.

[7] C. Kaufman, "Internet Key Exchange (IKEv2) Protocol," RFC 4306, Dec. 2005.

[8] B. Aboba, L. Blunk, J. Vollbrecht, J. Carlson, and H. Levkowetz, "Extensible Authentication Protocol (EAP)," RFC 3748, Jun. 2004.

[9] V. Devarapalli, R. Wakikawa, A. Petrescu, and P. Thubert, "Network Mobility (NEMO) Basic Support Protocol," RFC 3963, Jan. 2005.

[10] D. Johnson, C. Perkins, and J. Arkko, "Mobility Support in IPv6," RFC 3775, Jun. 2004

[11] R. Stewart, Q. Xie, M. Tuexen, S. Maruyama, and M. Kozuka, "Stream Control Transmission Protocol (SCTP) Dynamic Address Reconfiguration, RFC 5061, Sep. 2007.

Journal of Material Science and Mechanical Engineering (JMSME)
Print ISSN : 2339-9095; Online ISSN : 2393-9109; Volume 2, Number 6; April – June, 2015 pp 29 – 31
Krishi Sanskriti Publications
http://www.krishisanskriti.org/jmsme.html

Exergetic analysis of Solar Operated Power and Cooling Cycle

Rajesh Kumar*

Department of Mechanical Engineering, Delhi Technological University
(Government of NCT of Delhi), Bawana Road, Delhi-110042, India
E-mail: dr.rajeshmits@gmail.com

Abstract—*A combined cycle is proposed for the production of power and cooling. Exergetic analysis has been done to observe the effect of turbine inlet temperature on the performance of the combined cycle. The variation of turbine inlet temperature on the performance of the cycle has significant effects on the net power output, cooling, energy efficiency and exergetic efficiency. It is also observed that the maximum percentage exergy destruction occurs in the heat recovery vapor generator followed in the ejector, and turbine components of the cycle.*

Keywords: *Exergy destruction, extraction ratio, ejector, energy efficiency, exergetic efficiency, entrainment ratio.*

1. INTRODUCTION

Many researchers have studied the ejector refrigeration cycle because it has many advantages like less movable parts, less maintenance and possibility to use wide variety of refrigerants. The COP of the ejector refrigeration cycle is relatively low (Yapici, R., 2007; Li et al., 2005; Pianthong et al., 2007; Sankarlal and Mani, 2007).

Recently, an energy and exergy analyses of combined power and ejector refrigeration cycles was reported by (Wang et al., 2008; Yapici and Yetisen, 2007; Dai et al., 2009; Wang et al., 2009; Gupta et al., 2014) which shows that the maximum irreversibility/exergy loss occurs in heat addition process followed by the ejector and turbine.

2. SYSTEM DESCRIPTION

Fig. 1 shows the simplified combined Rankine and ejector cooling cycle. The proposed system consists of Rankine cycle (RC), ejector cooling cycle (ECC), with only solar heat source. The oil transfers the thermal energy from central receiver to the refrigerant passing through the HRVG. Superheated refrigerant vapor (4) is expanded in a turbine to generate work. The working fluid at low pressure and temperature from the throttle valve is vaporized in the evaporator (12-13) to produce cooling effect.

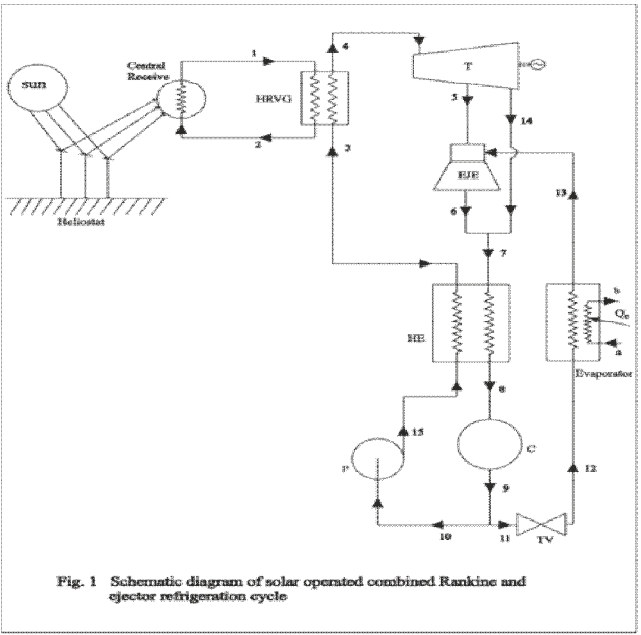


Fig. 1 Schematic diagram of solar operated combined Rankine and ejector refrigeration cycle

For the analysis, the specifications of the combined Rankine and ejector refrigeration cycle are given inTable 1.

Table 1: Main parameters considered for the analysis

Atmospheric Temperature (K)	298
Atmospheric pressure (MPa)	0.10135
Turbine inlet pressure (MPa)	0.650
Turbine inlet Temperature (K)	393-453
Extraction ratio	0.3
Extraction pressure ratio	2.5
Turbine isentropic efficiency (%)	85
Pump isentropic efficiency (%)	80
Condenser temperature (K)	293
Evaporator temperature (K)	268
Solar radiation received per unit area (kWm-2)	0.85
Apparent Sun temperature (K)	4500
Heliostat aperture area (m2)	3000
Oil temperature inlet to CR (oC)	373
Oil temperature inlet to HRVG (oC)	433

HRVG efficiency (%)	100
Pinch point temperature difference (oC)	10.0
Nozzle efficiency (%)	90
Mixing chamber efficiency (%)	85
Diffuser efficiency (%)	85
First law efficiency of heliostat field (%)	75
First law efficiency of central receiver (%)	90
Second law efficiency of heliostat field (%)	75
Second law efficiency of central receiver (%)	30

3. THERMODYNAMIC ANALYSIS

A thermodynamic analysis considering both the energy and the exergy provides an opportunity to evaluate the theoretical performance of the proposed cycle. Exergy analysis determines the system performance based on exergy, which is defined as the maximum possible reversible work obtainable in bringing the state of the system to equilibrium with that of the environment. Mathematically,

$$\dot{E} = \dot{m}[(h - h_0) - T_0(s - s_0)] \quad (1)$$

Entropy generation over a control volume is given by

$$\dot{S}_{gen} = \frac{dS}{dt} - \sum_{i=0}^{n} \frac{\dot{Q}_i}{T_i} - \sum_{in} \dot{m}s + \sum_{out} \dot{m}s \geq 0 \quad (2)$$

According to Gouy-Stodola theorem, the exergy destruction and entropy generation are related as

$$\dot{E}_D = T_0 \dot{S}_{gen} \quad (3)$$

3.1 First law efficiency (η_I)

The first law efficiency of the combined cycle is given by

$$\eta_I = \frac{\dot{W}_{net} + \dot{Q}_E}{\dot{Q}_{Solar}} \quad (4)$$

$$\dot{Q}_{Solar} = AI \quad (5)$$

$$\dot{W}_T = \dot{m}_f(h_4 - h_5) + \dot{m}_f(1 - E_r)(h_5 - h_{14}) \quad (6)$$

$$\dot{W}_p = \dot{m}_f(h_{15} - h_{10}) \quad (7)$$

$$\dot{W}_{net} = \dot{W}_T - \dot{W}_p \quad (8)$$

$$\dot{Q}_E = \dot{m}_f E_r \mu(h_{13} - h_{12}) = \dot{m}_w(h_a - h_b) \quad (9)$$

3.2 Second law Efficiency (η_{II})

The second law efficiency of combined cycle may be reported as

$$\eta_{II} = \frac{\dot{W}_{net} + \dot{E}_E}{\dot{E}_{Solar}} \quad (10)$$

$$\dot{E}_E = \dot{m}_{sf}[(h_{12} - h_{13}) - T_0(s_{12} - s_{13})] \quad (11)$$

$$\dot{E}_{Solar} = \dot{Q}_{Solar}\left(1 - \frac{T_0}{T_{Solar}}\right) \quad (12)$$

4. RESULTS AND DISCUSSION

An exergetic analysis has been carried out to find out to the variation of turbine inlet temperature on the performance of the combined power and cooling cycle. Exergy balance approach is applied to find out the exergy destruction in each component of the system. The exergy destruction in each component has been determined with the variation of turbine inlet temperature is shown in table 2.

Table 2: The exergy destruction in each component with the variation of turbine inlet temperature

Turbine inlet temperature	Exergy destruction (%)						
	Condenser	Ejector	Generator	Heat exchanger	Pump	Turbine	Throttle Valve
120	22.16	22.82	25.98	0.82	2.30	20.16	0.44
130	21.07	22.07	28.69	1.20	2.19	19.23	0.43
140	20.11	21.46	30.92	1.67	2.08	18.41	0.41
150	19.25	20.96	32.72	2.21	1.99	17.67	0.40
160	18.49	20.54	34.18	2.81	1.91	17.00	0.39
170	17.81	20.21	35.37	3.46	1.84	16.39	0.38
180	17.18	19.94	36.31	4.15	1.77	15.84	0.37

Fig. 2 shows the effect of variation of turbine inlet temperature on the energy and exergetic efficiency of the proposed cycle. As the turbine inlet temperature increases the energy and exergetic efficiencies increases.

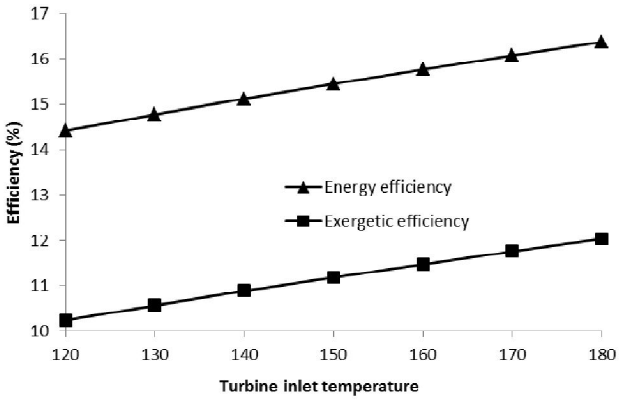


Fig. 2 Effect of turbine inlet temperature on energy and exergetic efficiency

Fig. 3: Shows the effect of variation of turbine inlet temperature on the net power output and cooling of the proposed cycle. As the turbine inlet temperature increases the net power output and cooling increases.

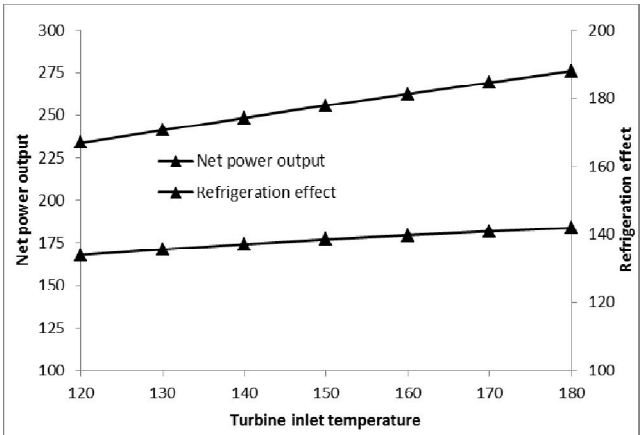


Fig. 3 Effect of turbine inlet temperature on net power output and refrigeration effect

5. CONCLUSION

A solar operated combined Rankine and ejector cooling cycle is proposed for the production of power and cooling output. Exergetic analysis has been done to identify the effects of variation of turbine inlet temperature on the performance of the proposed cycle. The conclusions of the present analysis can be summarized as follows:

- As the turbine inlet temperature increases the energy and exergetic efficiencies increases.
- As the turbine inlet temperature increases the net power output and cooling effect increases.
- The percentage of exergy loss is biggest in the heat recovery vapour generator followed in the ejector, and turbine components of the cycle.

Results obtained in the present study may be utilized by the engineers and scientists for a suitable thermodynamic design of solar operated combined Rankine and ejector cooling cycle.

REFERENCES

[1] Yapici, R., 2007, "Experimental investigation of performance of vapor ejector refrigeration system using refrigerant R123," Energy Conversion of Management, 49, pp. 953– 961.

[2] Li, D., Groll, E.A., 2005, "Transcritical CO2 Refrigeration Cycle with Ejector-Expansion Device," International Journal of Refrigeration, 28, pp. 766–773.

[3] Pianthong, K., Seehanam, W., Behnia, M., Sriveerakul, T., Aphornratana, S., 2007, "Investigation and Improvement of Ejector Refrigeration System Using Computational Fluid Dynamics Technique," Energy Conversion of Management, 48, pp. 2556–2564.

[4] Sankarlal, T., Mani, A., 2007, "Experimental Investigation on Ejector Refrigeration System with Ammonia," Renewable Energy, 32, pp. 1403–1413.

[5] Wang, J.F., Dai, Y.P., Gao, L.,2008,"Parametric analysis and optimization for a combined power and refrigeration cycle", Applied Energy, 85, pp. 1071-1085.

[6] Yapici, R., Yetisen, 2007, "Experimental Study on Ejector Refrigeration System Powered by Low Grade Heat," Energy Conversion of Management, 48, pp. 1560–1568.

[7] Dai, Y., Wang, J., Gao, L., 2009, "Exergy analysis, parametric analysis and optimization for a novel combined power and ejector refrigeration cycle", Applied Thermal Engineering, 29, pp.1983-1990.

[8] Wang, J., Dai, Y., Sun, Z., 2009, "A Theoretical Study on A Novel Combined Power and Ejector Refrigeration Cycle", International Journal of Refrigeration, 32, pp. 1186-1194.

[9] Gupta, D.K., Kumar, R., Kumar, N., 2014, "First and Second Law Analysis of Solar Operated Combined Rankine and Ejector Refrigeration Cycle" Applied Solar Energy, 50(2), pp. 113–121.

ResearchGate

See discussions, stats, and author profiles for this publication at: http://www.researchgate.net/publication/281581675

Is CSR a win-win situation? A study of Listed Companies of India

ARTICLE *in* GLOBAL BUSINESS AND MANAGEMENT RESEARCH: AN INTERNATIONAL JOURNAL · SEPTEMBER 2015

READS
17

2 AUTHORS, INCLUDING:



Seema Singh
Delhi Technological University
11 PUBLICATIONS **0** CITATIONS

SEE PROFILE

Available from: Seema Singh
Retrieved on: 11 October 2015

International Research Journal of Business and Management – IRJBM ISSN 2322- 083X

Is CSR a win-win situation? A study of Listed Companies of India

Seema Singh
Associate Professor in Economics

Anngad Singh
VII Semester Student, Electronics and Communication Engineering

Yatin Arora
VII Semester Student, Environmental Engineering
Delhi Technological University, Delhi, India

Abstract

As included in the Company Act 2013 of India, the Corporate Social Responsibility (CSR) is much in discussion among academia as well as business to understand the consequence of CSR activities from the point of view of the profit-making entities. There has been a constant debate whether the new CSR legislation is a mere obligation imposed on the companies or does it offer a new avenue to the companies to build goodwill and, in turn, improve their sustainability. In this background, the primary purpose of the paper is to understand the nature, scope and area of CSR activities by 52 Indian firms listed on BSE (Bombay Stock Exchange) and NSE (National Stock Exchange). An attempt has also been made to discuss the trends in CSR activities by companies segregated by the sectors of the operation, and their impact in terms of Brand Trust Rankings. This is a topic of high importance, since the sample companies are among the top ranking companies of the country, and have a huge potential to impact a large number of stakeholders. Most of the data collected are secondary, and have been obtained through Annual Reports and Business Responsibility Reports published by the companies in their websites.

Key words: Corporate Social responsibility, Corporate Sector, Sustainability, Branding

1. Introduction

The Corporate Social Responsibility (CSR) is an obligation of the organisation to act for the benefit of the society. The philosophy behind the concept of CSR rests on the ideology of give and take. Companies take resources in the form of raw materials, human resources etc. from the society. By performing the task of CSR activities, the companies give something back to the society. Vogel (2005) discussed Corporate Social Responsibility (CSR) as a practice that improves the workplace and benefits society in ways that go above and beyond what companies are legally required to do" (Vogel, 2005). Though India has a very long and healthy tradition of corporate philanthropy, the recent upsurge in the discussion on CSR can traced back to the globalisation of the Indian economy which completely changed the macroeconomic environment of India. So far reserved sectors for the public undertakings were opened up for private sector and foreign sector. Public Private Partnership (PPP) mode became most preferred practice. However, poverty and inequality also increased. During post-globalisation period, income inequality has increased. The gap between earning of lowest 10 per cent and highest 10 percent population has grown from six times to twelve times. Planners and policy makers in India are quite concerned about the situation. The eleventh five year plan (2007-12) and again, the twelfth five year plan (2012-17) have been designed to achieve inclusive growth (Singh, 2013). And CSR was thought of as a tool for private participation in poverty alleviation and inclusive growth. The Government of India has brought CSR under company's law. This has attracted attention of business and academia alike and brought CSR on the forefront of discussion. On the basis of study of fifty two listed companies in India, this paper tries to discuss CSR performed by them and its impact

© Global Wisdom Research Publications – All Rights Reserved.

on profit and branding of the companies. Second section reviews the literature. Companies under study have been discussed in the third section. Fourth section concludes the discussion.

2. Review of Literature

Milton Friedman (1970) was one of the pioneer to discuss the social responsibility of corporate sector and suggested to conduct business in accordance with the shareholder's desires which generally will be to make as much money as possible while conforming to the basic rule of the society as embodied in law and in ethical customs (Friedman, 1970). Since then different aspects of CSR have been discussed by authors. They can be grouped as below:

Sl. No.	Area	Authors
1.	Impact of CSR on the financial bottom line	Margolis & Walsh, 2003; Orlitzky, Schmidt &Rynes, 2003
2.	Impact of CSR on the firm's competitiveness	Kong et.al., 2002; Burke & Logsdon, 1996; Porter & Kramer, 2002 & 2006; and Weber, 2008
3.	The Corporate Social Performance perspectives	Hocevar&Bhambri, 1989; Sethi, 1979; Ullmann; 1985; Wartick& Cochran, 1985; Wood, 1991

However, no fixed definition and scope have been accepted by all. Though it has been discussed in multifarious and diverse perspectives, approaches and frameworks, however, most of these literatures converge into some widely accepted aspects that underpin the directions for the future of CSR which has been discussed below:

i. Most of the firms address the basic triple bottom line of social, environmental or economic aspects.
ii. Every firm has a moral and an *ethical responsibility* towards its internal and external stakeholders.
iii. A healthy and sustainable societal environment is a prerequisite for success of the organisation.

In support of CSR (Caroll, 1974; Davis, 1973; Epstein and Roy, 2001) following are some of the arguments which are given:

i. It enhances Public image (Kumar et.al., 2014);
ii. It upholds Stockholders' interest.
iii. It increases viability of business through cost reduction, resource management, employees' motivation and risk management but;
iv. Firms are responsible towards social and cultural norms; and
v. It helps firm in getting larger market share and long-term survival;

With the numerous and diverse approaches and understanding of CSR, the issue of what and how the firm or organisation can strategically manage CSR is still elusive and the fundamentals and principles of CSR are still widely debated in business communities (Shawyun, 2011).

Though India has long history of community work done by corporate sector but now, Government of India has made it a rule under Companies Act. India's new Companies Act 2013 introduced a provision for Corporate Social Responsibility, which rests upon the ideology that companies need to give back to the society in some way as they also take from the society in the form of raw materials, human resources. Ministry of Corporate Affairs had notified Section 135 and Schedule VII of the Companies Act as well as the provisions of the Companies (Corporate Social Responsibility Policy) Rules, 2014 (CRS Rules) which came into effect from 1 April, 2014. Every company, private limited or public limited, national or foreign which either has a net worth of Rs 500 crore or a turnover of Rs 1,000 crore or net profit of Rs 5 crore, needs to spend at least 2% of its average net profit for the immediately preceding three financial years on corporate social responsibility activities (Bahl, 2014). Some of the Indian studies may be grouped as below:

© Global Wisdom Research Publications – All Rights Reserved.

Sl. No.	Area	Authors
1.	Effective implementation of CSR	Sawant' 2014; Vijay 2014; Vitthal et. al. 2013
2.	Effect of CSR on consumer	Sarvankumar et. al. 2014;

These studies have not been able to discuss on which sector companies are performing CSR and whether it has any impact on 'Branding' of the company which is a very important indicator in present globalised environment.

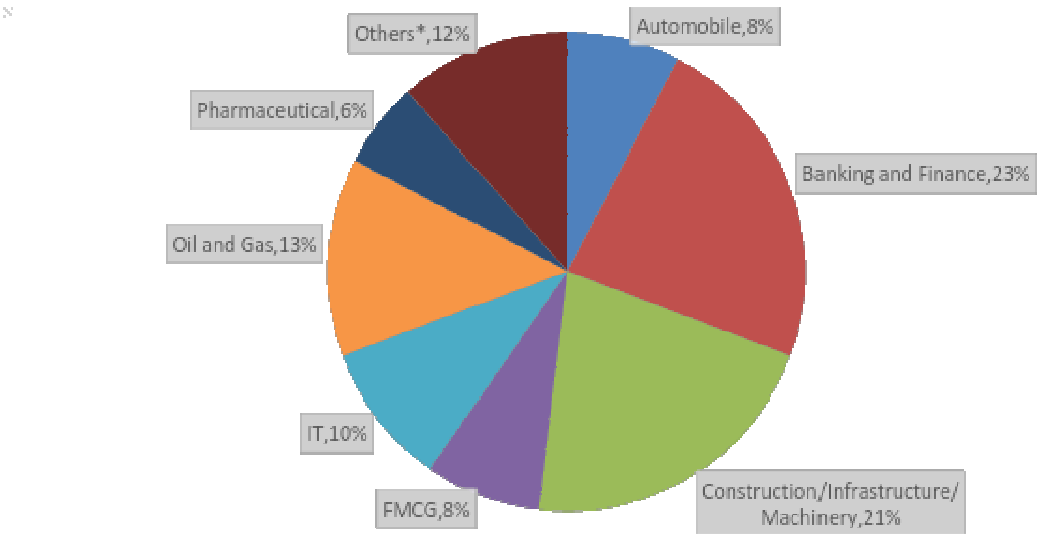
3. Objectives

In this background, there are following objectives of the paper.

1. To analyse the efforts made by top Listed Indian companies across various sectors, towards Corporate Social Responsibility for the fiscal year 2013-2014.
2. To study the nature of CSR activities by the companies of various sectors, with respect to their focus areas.
3. To analyse the positive impacts, if any, of CSR activities on the branding of the companies.

4. Data and Methodology

The study was started with 100 top listed companies at BSE (Bombay Stock Exchange) and NSE (National Stock Exchange). However, all the required information was available for only fifty two companies across the Automobiles, Construction, Infrastructure, Heavy Machinery, Banking, Finance, Pharmaceutical, Oil and Gas, FMCG, Information Technology, Entertainment, Telecom and Textiles sectors. The data include private as well as public sector companies. For the purpose of analysis, Construction, Infrastructure and Heavy Machinery industries were clubbed together. As small number of companies in Entertainment, Telecom and Textiles sectors, they were clubbed as 'others'. All data used in the analysis were for the fiscal year 2013-14. Data were collected through secondary sources, mainly from Annual Reports, Sustainability Reports and Business Responsibility Reports which were available on the website. The sector wise distribution of the companies have been shown in the pie chart-1. Largest share is of Banking and finance. They are almost one-fourth of the whole.



© Global Wisdom Research Publications – All Rights Reserved.

- Others include Entertainment, Telecom and Textiles industries

Pie Chart 1: Sector-wise Distribution of Companies Reviewed

The data considered for analysis are as below:

1. Profit After Tax (PAT) for the year 2013-14
2. CSR expenditure reported in the year 2013-14
3. CSR expenditure as a percentage of Profit After Tax
4. Focus areas of the CSR expenditure
5. Brand Trust Rankings for the year 2014-15, based on The Brand Trust Reportby Trust Advisory

The methodology of analysis used in the study can be summarized as follows-

- Data for Sectors of the companies and the Areas of their CSR activities were tabulated and studied.
- Data for CSR Expenditure as a percentage of Profit after Taxwere tabulated and studied.
- Data for CSR Expenditure as a percentage of Profit after Taxwere plotted against Brand Trust Rankings and studied.
- Data for CSR expenditure as a percentage of Profit after Tax were tabulated sector-wise for the sample companies.
- The data for Profit after Tax, CSR Expenditure, CSR Expenditure as a percentage of Profit after Tax and Brand Trust Rankings were studied.

5. Data Analysis

A back of the envelop analysis will tell that a lot of money is going to be spent on CSR by companies in India. So, it is significant to discuss areas of CSR expenditure with respect to sectors of companies to which they belong.

5.1. Relationship between Areas of CSR activities and Sectors to which the Companies belong:

All companies eligible for CSR are required to provide the list of activities in which the reported expenditure has been incurred. Activities were classified into five on the basis of areas on which the companies allocated their CSR expenditure. They are listed as below:

- Education
- Health
- Rural Development
- Disaster Relief
- Environment

Table 1: Sector Wise distribution of the companies contributing to an activity, as a percentage of the total companies in that sector

Sector of the Company	Companies contributing to an activity as a percentage of the total companies in a sector					Number of Companies
	Education	Health	Rural Development	Disaster Relief	Environment	
Automobile	75%	25%	25%	0%	0%	4
Banking and Finance	66.67%	41.67%	58.33%	9%	50%	12

© Global Wisdom Research Publications – All Rights Reserved.

Construction/ Infrastructure/ Machinery	90.91%	90.91%	27.27%	1.1%	54.5%	11
FMCG	75%	75%	50%	0%	25%	4
IT	80%	60%	60%	1.25%	80%	5
Oil and Gas	100%	100%	42.86%	3%	71.42%	7
Pharmaceutical	100%	100%	33.33%	0%	66.67%	3
Others*	100%	33.33%	33.33%	2%	66.67%	6
Total	**84.61%**	**65.38%**	**42.31%**	**25%**	**53.85%**	**52**

*includes Entertainment, Telecom and Textiles industries
Source: Annual Reports, Sustainability Reports and Business Responsibility Reports of Listed Companies for the financial year 2013-14

Based on the study, Education and Health emerged as the major activities where the companies are spending their CSR resources. Almost 85% of the sample companies contributed to the promotion of education related initiatives in some way or other. One such example is the Reliance Dhirubhai Ambani Protsaham Scheme initiated by Reliance India Ltd. to support the education of meritorious students from financially weaker sections in the East Godavari District.
Some companies contributed to livelihood generation initiatives and provided employment to the beneficiaries in their own company after the completion of training.

In order to tackle the natural disasters that hit the country lately, companies also diverted their CSR resources for disaster relief. For example, NALCO contributed Rs. 10 Crore to Chief Minister's relief fund to assist the rehabilitation work following the cyclone Phailin in Odisha. 25% of the companies under review contributed to disaster relief as a part of their CSR initiatives. RIL actively participated in preparatory help for cyclone Lehar relief operations. Arrangements were made to accommodate the evacuated public from Bhairavapalem and Theerdalamundi villages at Community Hall and PHC facilities at Gadimoga constructed by RIL. The foundation is also promoting soil and water conservation measures through its work in the rural transformation space. 24 million cubic meters of water harvesting facility has been created so far and the intervention has helped to conserve 1,19,000 tonnes of soil.

Kotak Mahindra supports underprivileged child cancer patients by funds raised through donation of old newspapers and magazines to Dhanwantari Medical Trust (DMT). Funds generated from the sale of old newspapers are utilised by the trust to help and support cancer-affected children for medicines and nutritional food required along with the treatment.

It was also observed that Banking and Finance sector showed maximum diversity in the range of CSR activities, with a high percentage of companies contributing to each activity.

5.2. Sector-wise analysis of CSR expenditure as a percentage of Profit After Tax

According to the Section 135 of the Companies Act, every qualifying company requires spending of at least 2% of its average net profit for the immediately preceding 3 financial years on CSR activities. Further, the qualifying company will be required to constitute a committee (CSR Committee) of the Board of Directors (Board) consisting of 3 or more directors (Bahl, 2014).

© Global Wisdom Research Publications – All Rights Reserved.

For the purpose of analysis, the CSR expenditure as a percentage of Profit after Tax of the same year has been discussed. CSR expenditure as a percentage of Profit After Tax is an important parameter to judge how sensitive a company is in allocating a share of its profits for societal causes. Since the 52 companies in the sample are market leaders and among the largest companies of the nation, the impact of their actions affects a wide variety and a large number of stakeholders. Therefore, to analyse the inclination of a company towards Corporate Social Responsibility, the CSR expenditure as a percentage of Profit After Tax has tabulated for each sector and studied in depth.

Table 2: Sector-wise analysis of CSR expenditure as a percentage of Profit After Tax

	CSR expenditure as a percentage of Profit After Tax (PAT)					
	0-0.5%	**0.5-1%**	**1-1.5%**	**1.5-2%**	**>=2%**	**Total**
Automobile	3	1	0	0	0	**4**
Banking and Finance	4	3	2	2	1	**12**
Construction/Infrastructure/Machinery	1	0	2	2	6	**11**
FMCG	0	1	2	0	1	**4**
IT	2	1	1	1	0	**5**
Oil and Gas	2	1	2	0	2	**7**
Pharmaceutical	1	2	0	0	0	**3**
Others*	3	3	0	0	0	**6**
Total	**16**	**12**	**9**	**5**	**10**	**52**

*includes Entertainment, Telecom and Textiles industries
Sources: Annual Reports, Sustainability Reports and Business Responsibility Reports of Listed Companies for the financial year 2013-14.

Through the analysis of Table 2, it is clear that some sectors show high levels of proactivity to contribute towards societal causes and very well exceed the required 2% threshold of their Profit after Tax to CSR causes. The Construction, Infrastructure and Heavy Machinery sectors had more than half the sample companies contributing more than 2% of their Profit After Taxto CSR. None of the companies in the sample that belonged to Automobile or Pharmaceutical sectors contributed more than 1% of their Profit After Tax. Looking at the overall picture, maximum number of companies fell in the category that contributed only 0-0.5% of their Profit After Tax. 54% of the companies reviewed spent less than 1% of their profits to CSR, while only 19% companies exceeded the required threshold of 2%, of which 11.4% belong to the Construction, Infrastructure and Heavy Machinery sectors alone. One can conclude that since the reforms are new, companies will take some time to align themselves with them in a proper manner.

Since we see a notable difference between sector-wise contribution to CSR, it is worthwhile to research further to analyse the impact of CSR contributions to the branding of individual companies as well as for the overall sectors.

5.3. Relationship between CSR Expenditure and Brand Trust Rankings

The CSR Bill states that "each company must spend at least two per cent of the average net profits of the company made during the three immediately preceding financial years". However, for the purpose of analysis, the CSR expenditure as a percentage of Profit-after-Tax for the current year has been used,

© Global Wisdom Research Publications – All Rights Reserved.

since the data are reported in the aforementioned format in the Business Responsibility Reports published by the companies.

The Brand Trust Rankings were used as an indicator of the strength of goodwill and trust of a brand among its customers. The rankings were obtained from a research conducted by Trust Research Advisory, which is "a Brand Intelligence and Data Insights Company dedicated to understand and analyze stakeholder behavior through two globally acclaimed, proprietary matrices of Brand Trust and Brand Attractiveness." The company ranked 1200 brands in the year 2014-15, based on its research as they pertain to the status of the brands for the years 2014-15. It is assumed that brand-building is a gradual process and the showcasing of efforts by a company takes at least a few months.

It was hypothesised that the companies spending more on CSR activities were expected to have better *Brand Trust Rankings*. The data on CSR expenditures as a percentage of Profit after Tax for the 52 listed companies were plotted against the Brand Trust Scores. Brand Trust Scores were calculated by subtracting the Brand Trust Ranking obtained by a company in the 2014-15 research conducted by Trust Research Advisory, from the total number of companies ranked, which is 1200. Hence a company ranked 422 on the list obtained a Brand Trust Score of 1200-422=778. A company that was not ranked got a score of 0. The data of Brand Trust Rankings published in the year 2015 were used, since they pertain to the status of the brands for the years 2014-15 (Brand Trust Ranking, 2015).

The American Marketing Association defines a brand as a name, term, sign, symbol, or design, or combination of them, which is intended to identify the goods and services of one seller or group of sellers and to differentiate them from those of competitors (Schneider, 2003). It is believed that companies with better existing brand images would continue to contribute more towards CSR in order to maintain their branding in the market. However, the Pearson Correlation Coefficient for these rankings turned out to be -0.23, which implies a weak negative correlation between Brand Trust Scores and the CSR expenditure as a percentage of Profit after Tax.

The underlying reason seems to stem from the fact that certain companies, which do not do very well on the branding front, perform CSR more widely and hence they are an anomaly to our hypothesis. These companies, which are mostly from Construction, Infrastructure and Heavy Machinery sectors, performed CSR well in excess of 2% of their Profit After Tax, but their brand rankings were lower than many companies which did CSR less than 1% of their Profit After Tax.

It is also possible that companies which already have a strong branding in the market, do not feel the need to enforce it using means such as CSR, or do not wish to redirect appreciably higher proportion of their resources back to the society. On the other hand, companies which are in the process of growing their brand image find CSR as a better means of building trust and goodwill in the market. Another more likely reason could be due to the very nature of the industry in which a company operates. The companies which have a more direct interaction with the end consumer tend to have better Brand Trust Rankings over those companies which operate on a Business-to-Business model.

NALCO did a CSR expenditure worth 4.51% of the Profit After Tax in 2013-14 but was not even featured in the top 1200 brands for Brand Trust Rankings for 2014-15. However, Colgate-Palmolive, which spent 2% of its profits on CSR was ranked high in the Brand Trust Rankings.

This established the need for a more sector-specific analysis between CSR expenditure and Brand Trust Rankings. This analysis has been elucidated in depth in the next section.

© Global Wisdom Research Publications – All Rights Reserved.

5.4. Sector-specific Relationship between CSR expenditure and Brand Trust Ranking

The average CSR expenditure as a percentage of Profit After Tax was computed for each sector separately.

It was obtained by dividing the total CSR expenditure by all companies in a sector by the total Profit After Tax made by all companies of that sector. Similarly, Average Brand Trust Rankings were obtained by taking the mean of the Brand Trust Rankings for all companies in a particular sector. We tabulate the data to test our hypothesis whether the nature of industry is a bigger contributing factor to Brand Trust Ranking than the CSR expenditure as a percentage of Profit After Tax

Table 3: Sector-Specific Analysis of CSR Expenditure and Brand Trust Rankings

Sector	Average CSR expenditure as a Percentage of Profit After Tax	Average Brand Trust Rank
Automobile	0.31	86.5
Banking and Finance	1.33	547.6
Construction/Infrastructure/Machinery	2.49	588.2
FMCG	1.25	44.5
IT	0.48	535.2
Oil and Gas	1.9	573.2
Pharmaceutical	0.42	742.7
Others*	0.53	304.5

*includes Entertainment, Telecom and Textiles industries
Sources: Annual Reports, Sustainability Reports and Business Responsibility Reports of Listed Companies for the financial year 2013-14. *The Brand Trust Rankings* from the 2014-15 research conducted by Trust Research Advisory.

Through the analysis, one can observe that CSR expenditure is not necessarily related to better branding. Our second hypothesis, that companies with less consumer interaction fare lower on Brand Trust Rankings in spite of higher CSR expenditures, is validated through the data in the Table 5. Automobile sector contributed only 0.31% of its Profit after Tax to CSR activities, and still had an average ranking in the top 100. Similarly, companies in the FMCG sector also contributed a little over 1% of their profits to CSR, but enjoyed superior brand image among consumers. The IT and Pharmaceutical sectors contributed paltry percentages of their profits towards CSR and were not ranked too high on the Brand Trust Rankings either. On the other hand, even though the companies of Construction, Infrastructure and Heavy Machinery sectors spent heavily on their CSR initiatives, they did not seem to feature high enough in the Brand Trust Rankings. This analysis shows that the sectors whose efforts towards the society are not being adequately showcased, can attempt to highlight them in a more effective manner and subsequently, make their businesses more sustainable and profitable. Even though CSR is a noble effort undertaken by the company to pay the society back, if a sector is doing more in that field compared to its competitors, it should be utilized to build better trust among the consumers to ensure more growth of the profit making entity.

Hence this analysis clearly shows that industries that are more CSR oriented, but do not enjoy comparatively better Brand Trust Rankings, should utilize their efforts to gain an edge over competitors by ensuring that their efforts get sufficient attention of their consumers. Construction, Infrastructure and Heavy machinery sectors are the best examples that fall under this category.

© Global Wisdom Research Publications – All Rights Reserved.

6. Conclusions

On the basis of companies under consideration, it can be said that most companies performed CSR on the Education, Health and Environment, with more than half of the companies working on Education and Health from each of the sectors.

Sector-wise analysis of CSR expenditure as a percentage of Profit After Tax data was used to categorize the companies according to the CSR contributions they made, which helped identify the sectors which performed better on CSR expenditure. Construction, Infrastructure and Heavy Machinery sectors came out as the top contributors followed by Oil and Gas, and Banking and Finance sectors. The sectors such as Automobiles, Pharmaceuticals and IT had the lowest percentage CSR expenditures. Most of the companies reviewed lagged in terms of meeting their CSR goals set as 2% by government directive, but since the reforms are new it can be expected that they can slowly catch up.

Relationship between CSR Expenditure and Brand Trust Scores has been studied and the Pearson Correlation Coefficient has been found to be weakly negative. This was contrary to the belief that the companies with better branding would perform better on CSR expenditure so that they can maintain their brand status in the market. The anomalies to this assumption were a few sectors which contributed towards CSR highly even though their Brand Trust Scores were low. Even though, sectors such as FMCG and Automobiles were relatively weaker contributors to CSR, they had superior Brand Trust Rankings. Hence, this study shows that sectors such as Construction, Infrastructure and Heavy Machinery have a lot of scope to utilize their additional efforts towards CSR for building trust and goodwill in the market.

As per the current analysis, it can be safely concluded that CSR does not emerge as the best means of investment for companies to compete in terms of goodwill in the market. Any expenditure made by a profit making entity needs to contribute towards its own sustainability as much as possible. Hence, it is suggested that companies make efforts to showcase their CSR contributions in a better manner to build a stronger trust for their business in the market. Moreover, it is expected that the sectors which are lagging in terms of their contribution towards the society, will be sensitized and use their potential to uplift the society.

7. Scope for Future Research

The current research is limited to 52 companies but can be extended further to obtain better results. Again, the current research focuses on the list of CSR activities performed by the company, but due to lack of detailed data published by the companies, it does not list the individual expenditures according to areas of CSR activities. The future research would focus on collecting data and quantifying the expenditure made towards each activity. This would provide a comprehensive analysis regarding the fronts receiving CSR aid from these companies.

Further, as the CSR legislation takes roots and more companies begin to contribute as per the directives within a few years, the data could provide better conclusions about the mutual impact of CSR on the society as well as the businesses.

© Global Wisdom Research Publications – All Rights Reserved.

References

1. Bahl, Ekta (2014), An overview of CSR Rules under Companies Act, 2013, retrieved http://www.business-standard.com/article/companies/an-overview-of-csr-rules-under-companies-act-2013-114031000385_1.html on 12/5/2015
2. Brand Trust Ranking, (2015), *The Brand Trust Rankings* from the 2014-15 research conducted by Trust Research Advisory, retrieved *http://www.trustadvisory.info/allindia_2015.htm*on 20/7/2015 .
3. Burke, L. & Logsdon, J.M. (1996). How corporate social responsibility pays off. *Long Range Planning*, 29(4), 495-502.
4. Carroll, A.B. (1974). Corporate Social Responsibility: Its Managerial Impact and Implications. *Journal of Business Research*, 2(1), 75-88.
5. Davis, K. (1973, June). The Case for and against Business Assumption of Social Responsibilities. *Academy of Management Journal*, pp. 312-317.
6. Epstein, M.J. & Roy, M.J. (2001). Sustainability in action: Identifying and measuring the key performance drivers. *Long Range Planning*, 34(5), 585-604.
7. Friedman, M. (1970, September 13). The Social Responsibility is to increase its profits, *New York Times Magazine*, pp. 32-34, 122-126.
8. Hocevar, S. P., &Bhambri, A. (1989). Corporate social performance: A model of assessment criteria. In J. E. Post (Ed.), *Research in corporate social performance and policy*, 11, 1-20. Greenwich, CT: JAI Press.
9. Kong, N., Salzmann, O., Steger, U. &lonescu-Somers, A. (2002). Moving business/industry towards sustainable consumption: The role of NGOs. *European Management Journal*, 20(2), 109-127.
10. Limbore, NileshVitthal and Chandgude, AjitAshokrao (2013), A review of the current scenario of Corporate Social Responsibility in IT business sector with the special reference to Infosys, Golden Research Thoughts, Vol 2, Issue 9, ISSN No : 2231-5063
11. Margolis, J.D., & Walsh, J.P. (2003). Misery loves Companies: Rethinking Social Initiatives by Business. *Administrative Science Quarterly*, 48(2), 268-305.
12. Orlitzky, M., Schmidt, F.L., &Rynes, S.L. (2003, March). Corporate social and financial performance: A meta-analysis. *Organization Studies*, 24(3), 403-441. Preston, L. E. (Ed.). (1978). *Research in corporate social performance and policy* (Vol. 1). Greenwich, CT: JAI Press.
13. Porter, M.E. & Kramer, M.R. (2006, December). Strategy and Society: The link between competitive advantage and corporate social responsibility. Harvard Business Review, 84(12), 4-17.
14. Porter, M.E., & Kramer, M.R. (2002). The Competitive Advantage of Corporate Philanthropy. *Harvard Business Review*, 80(12), 56-69.
15. S., SaravanakumarSakthi and K., Aiswariya (2014), Impact of CSR Initiatives on Consumer Behaviour, International Research Journal of Business and Management, Volume VII, ISSN: 2322 – 083X
16. Sawant D., Pravin (2014), Corporate Social Responsibility of Select Pharma Companies in India: An Exploratory Study, Global Journal of Commerce & Management Perspective, Vol.3(4): 205-219 , ISSN: 2319 – 7285
17. Schneider, L. (2003). What is branding and how is it important to your marketing strategy? Retrieved on 12.5.2015 from http://marketing.about.com/cs/brandmktg/a/whatisbranding.html
18. Shawyun, Teay (2011), "From Corporate Social Responsibility (CSR) to University Social Responsibility (USR)", 2nd Asia–Europe Education Workshop, Innsbruck, Australia during 5-7 June. pp. 14-17.

© Global Wisdom Research Publications – All Rights Reserved.

19. Singh Seema (2013), "Social Responsibility of Engineering Institutions for Inclusive Growth", Universities News*, 2013,* 51(03), pp. 01-04-12.
20. Sethi, S. P. (1979). A conceptual framework for environmental analysis of social issues and evaluation of business response patterns. *Academy of Management Review*, 4(1), 63-74.
21. Ullman, A. (1985). Data in search of a theory: A critical examination of the relationships among social performance, social disclosure, and economic performance. *Academy of Management Review*, 10, 540-577.
22. Vijay P. and N., Divya (2014), Impact of Corporate Social Responsibility Initiatives of Indian Banking Sector, International Research Journal of Business and Management, Volume VII, ISSN: 2322 – 083X
23. Vogel, D (2005), The Market for Virtue: The Potential and Limits of Corporate Social Responsibility, Washington DC, Brooking Institute.
24. Wartick, S. L. & Cochran, P. L. (1985). The evolution of the corporate social performance model. *Academy of Management Review,* 10, 758-769.
25. Weber, M. (2008). The business case for corporate social responsibility: A company-level measurement for CSR. *European Management Journal,* 26, 247-261.
26. Wood, D.J. (1991). Corporate Social Performance Revisited. *Academy of Management Review,* 16(4), 691-718

© Global Wisdom Research Publications – All Rights Reserved.

ResearchGate

See discussions, stats, and author profiles for this publication at: http://www.researchgate.net/publication/282603447

Literature review of multi-aspect research works carried out on the concept and implementation of GSCM

RESEARCH · OCTOBER 2015

DOI: 10.13140/RG.2.1.2996.8085

READS

12

3 AUTHORS, INCLUDING:



Sheetal Soda

National Institute of Technology Jalandhar

3 PUBLICATIONS **0** CITATIONS

SEE PROFILE

All in-text references underlined in blue are linked to publications on ResearchGate, letting you access and read them immediately.

Available from: Sheetal Soda
Retrieved on: 03 November 2015

Literature review of multi-aspect research works carried out on the concept and implementation of GSCM

Sheetal Soda*, Anish Sachdeva and Rajiv Kumar Garg

Department of Industrial and Production Engineering,
National Institute of Technology,
Jalandhar, India
Email: sheetugrey@gmail.com
Email: asachdeva@nitj.ac.in
Email: gargrk@nitj.ac.in
*Corresponding author

Abstract: Recent research advances in green supply chain management (GSCM) have thrown exciting opportunities for new dimensions of the subject to evolve. Individual findings, when pooled together, raise possibilities of further research yielding altogether new management practices with potential affirmative ramifications for environment and industry. This paper strives to scrutinise a sizable quantum of literature on GSCM to identify techniques for critically analysing various aspects of GSCM implementation and their prospective categorisation, implications and complications. Substantial literature on GSCM is prominently identified with application of techniques like AHP/ANP, ISM, TOPSIS, DEMATEL etc. to evaluate performance of the GSCM measures adopted, selection of suppliers, undertaking barrier analysis, mechanism formulation/implementation, inter-relationships between factors and generic/standard exploration of the intricacies of GSCM. Categorising the literature, on the basis of these six categories and their further investigation to assess prospects and deficiencies, extend an opportunity to the furtherance of our knowledge on GSCM practices.

Keywords: multi-criteria decision-making techniques; MCDM techniques; literature review; green supply chain management; GSCM; performance evaluation; barrier analysis, mechanism formulation.

Reference to this paper should be made as follows: Soda, S., Sachdeva, A. and Garg, R.K. (xxxx) 'Literature review of multi-aspect research works carried out on the concept and implementation of GSCM', *Int. J. Industrial and Systems Engineering*, Vol. X, No. Y, pp.xxx–xxx.

Biographical notes: Sheetal Soda is a Research Scholar with Department of Industrial and Production Engineering, Dr. B.R. Ambedkar National Institute of Technology, Jalandhar (India). She obtained her BTech in Mechanical and Automation Engineering from Guru Gobind Singh Indraprashtha University New Delhi (India) and ME in Production Engineering from Delhi Technical University (formerly Delhi College of Engineering), Delhi (India). She has to her credit, experience of more than seven years of industrial and teaching domains. She is life time member of Indian Society for Technical Education (ISTE).

Copyright © 20XX Inderscience Enterprises Ltd.

Anish Sachdeva is working as an Associate Professor in the Department of Industrial and Production Engineering at National Institute of Technology, Jalandhar, and Punjab, India. He obtained his Bachelor in Industrial Engineering from National Institute of Technology (erstwhile Regional Engineering College), Jalandhar, India. Subsequently, he obtained his Masters in Industrial Engineering from Punjab Technical University, Jalandhar and PhD from Mechanical and Industrial Engineering Department at Indian Institute of Technology (IIT), Roorkee, India. He has more than 16 years of experience in teaching and industry. His areas of interest are reliability and maintenance engineering, supply chain management, modelling and simulation.

Rajiv Kumar Garg is Professor in Industrial and Production Engineering Department at Dr. B.R. Ambedkar National Institute of Technology Jalandhar, India. He holds a BSc Engg (hons.) in Mechanical Engineering from Regional Engineering College Kurukshetra, and ME (hons.) in Industrial Engineering and a PhD from Thapar Institute of Engineering and Technology Patiala (India). He has over 26 years of industry and teaching experience. He has guided 37 MTech and 11 PhD candidates for pursuing their PhD degree. He has over 129 publications in international and national journals to his credit. He is a reviewer of eight international journals and also Chief Editor of *International Journal of Machining and Machinability of Materials* (*IJMMM*). He has been designated as a member of International and National Advisory Committees of various international and national conferences organised by various international and national organisations/institutions.

1 Introduction

Recent times have witnessed an increased consideration for environmental concerns on the part of industrial and manufacturing units, thereby giving a push to green technologies and other environment-friendly measures, to curtail the polluting effect inherent in the processes involved. This has led to the development of the discipline of green supply chain management (GSCM), which aims at developing such methodologies and process, concerning industrial production and distribution that have minimal or no hazardous impact on the environment, along with financial incentives for the adopting concern. According to Zhu and Sarkis (2004), GSCM encompasses a set of environmental management (EM) practices which are useful for logistics management and are designed to incorporate environmental considerations into the forward and reverse logistics (RL). Examples of GSCM practices include reducing packaging and waste, assessing suppliers based on environmental performance, developing more eco-friendly products, and reducing carbon emissions associated with the transport of goods (Walker et al., 2008).

GSCM has sparked of immense interest in industry and academic domain, with huge prospects of growth and development in coming times. Extensive research has been carried on the various aspects of the subject, which has led to emergence of a substantial quantum of literature on GSCM (Sarkis et al., 2011). Analysis of the researches carried out provide scholars with an opportunity to identify hidden and indirect facets of the subject, and find new leads that could unravel the potential of GSCM in elevating itself to be one of the most relevant tools on the part of industry to align their operations with an environmental-friendly approach and maximise their gains in the process. Advancement

of knowledge in the field of GSCM can be ensured by examining the studies already undertaken and building further knowledge-base, on the basis of the former (Srivastava, 2007).

Adoption of GSCM practices are adopted voluntarily, for the sake of only environmental is rare. In general, the adoption of GSCM measures is not necessarily a voluntary decision on the part of the manufacturer, rather it may be a result of various push and pull factors, as well as inputs by other stake holders in the supply chain. For example, the physical infrastructure associated with any enterprise also contributes to environmental degradation, which can be countered substantially by reusing and recycling of components in the construction supply chain. Besides that, the role of environment-centric innovations by the manufacturer plays a significant role in augmenting GSCM in an enterprise (Zhu et al., 2012). Activities influenced by GSCM have a tendency to affect the efficiencies of the entire supply chain (Pishdar et al., 2014). Thereby, companies are waking up to the benefits of GSCM, thereby making optimal use of their resources and securing competitive advantages (Farzianpour et al., 2014). GSCM affects major determinants of profitability such as quality, customer satisfaction and efficiency (Olugu et al., 2011). Interestingly, the consumers are also indirectly contributing to the espousal of GSCM measures, by raising their demands and showing their preference for eco-friendly products (Chang et al., 2013).

Companies are recognising that EM is a key strategic issue with the potential for a lasting impact on organisational performance. For example, more than 40,000 companies have implemented ISO14001, the EM system standard (Zhu and Sarkis, 2006). Greening the supply chain is increasingly a concern for many business enterprises and a challenge for logistics management in 21st century. Of particular concern is how to raise organisational environmental awareness and incorporate EM practices into the logistics activities (Zhu et al., 2008a, 2008b, 2008c).

Hitherto, adoption of environmental friendly measures was limited as a responsibility to individual departments of the manufacturing units; and not across the board of the organisation. For example, environmental excellence in product development, process design, operations, logistics, marketing, regulatory compliance and waste management are responsibilities of the respective departments only, and there was a conspicuous absence of an integrated approach in making the concern's undertaking green on a holistic basis. But slowly and steadily, the business units and manufacturing concerns across the world are waking to the economic gains that are associated with deployment of green practices.

The quality revolution of the 1980s and the supply chain management revolution of 1990s, has opened new vistas for industrial establishments to adopt eco-friendly practices that save money and augment brand image of the products before the customers. This coupled with strict government regulations apropos conservation of environment have pushed industrial units to join the GSCM bandwagon. Though even today, GSCM has not penetrated into the industrial establishments, the way it should have been; nevertheless the recent years have witnessed phenomenal rise in the popularity and espousal of the concept in a practical way across the globe (Diabata and Govindan, 2011).

2 Research methodology

Recent work on GSCM has led to emergence of extensive literature about its various aspects and facets. Comprehensive reviews on seminal work on GSCM such as green design (Zhang et al., 1997), production planning and control for remanufacturing (Bras and McIntosh, 1999; Daniel and Guide, 2000), issues in green manufacturing and product recovery (Daniel et al., 1996; Gungor and Gupta, 1999), RL (Carter and Ellram, 1998; Fleischmann et al., 1997) and logistics network design (Fleischmann et al., 2000; 2001; Jayaraman et al., 2003) have been published, and added to the repository of research work carried out on the subject. Though, there is plethora of literature on GSCM, yet it can be said with certainty that a substantially large part of the research work revolves around the theoretical aspects of the GSCM nature and falls short on extending practical models and methodologies that can be ascribed to the concept. This paper makes an attempt at presenting an across-the-board view of the available literature on various facets of GSCM, so that further addition can be made to the existing pool of knowledge compiled on the subject.

The objective of this paper is to gather a comprehensive understanding of the extent of evolution of GSCM, and the scope of its practical implementation by identifying major research works carried on the subject, which is identified with environmental thinking and its integration with existing models of supply-chain management. The study promises, to a considerable extent, the identification of gaps, issues and opportunities for further study and research on the subject. A literature review seems to be a valid approach, as it is a necessary step in structuring a research field and forms an integral part of any research conducted (Smith et al., 2002). This helps to identify the conceptual content of the field (Meredith, 1993) and guides towards theory development.

In this paper, in-depth study of the research papers is presented, to ensure that not only the essence of various studies undertaken is fully understood; but also the finer details enshrined in the literature are effectively captured. This has helped in correlating the commonalities as well as the disparities amongst the available literature on the subject. Efforts were made to see how the concept of GSCM, manifests itself in different form in diverse settings, yet aspiring to chase common goals. The existing literature studied on the subject can be grouped into various sets in accordance with main aspect of GSCM studied, therein. Resultantly, six major categories have been identified, i.e.,

1 identification of performance evaluation of the measures adopted

2 selection of suppliers

3 undertaking barrier analysis

4 mechanism formulation/implementation

5 inter-relationships between factors

6 generic/standard exploration.

Categorising the literature, on the basis of these six, and their further investigation to assess the prospects and deficiencies, extend an opportunity to the furtherance of our knowledge on GSCM practices. The tools/techniques deployed in various studies were also reviewed and their classification was also undertaken. The selection of methodology of choosing and subsequent analysis of the papers required careful consideration, so that

a comprehensive view of the work done on diverse aspects of GSCM may be ensured. This entailed that the papers should be chosen from different regional, organisational and industrial domains.

It is worth noting that the particular tool/technique used depends on a host of factors, such as the nature of the problem, the nature and availability of data, familiarity with the technique, compatibility between the analysis and solution tools/techniques envisaged, previous related works and the wish to use new emergent tools/techniques in operations research/decision science (OR/DS).

2.1 Research techniques deployed by researchers in studying/analysing various aspects of GSCM

The decision to adopt GSCM strategies that could lead to optimum gains for the manufacturer in terms of trade-off between the benefits and cost involved is of considerable significance. Making such a decision, however, is never an easy task as there are many factors concerned with the decision-making process. This is a typical multi-criteria decision-making (MCDM) problem. MCDM problems often feature themselves as research tasks, and are addressed by deploying an array of techniques to find an optimal solution to them. Green manufacturing and remanufacturing have used mathematical models, tools and techniques to a much larger extent. GSCM seems a promising area for trying out new operations research techniques and for using traditional techniques for overall GSCM Design. The problem is complex and challenging, as a very large number of parameters, decision variables and constraints are involved along with a large number of estimation requirements such as those of expected demands and returns and cost criteria associated with each decision. Perhaps, a combination of various tools and techniques (both traditional and new) may be combined for the purpose of formulation, approximation, analysis and solution of such complex problems.

Different approaches/techniques have been proposed by researchers to such problems, the most prominent being the 'analytic hierarchy process' (AHP) (Saaty, 1980) and 'technique for order preference by similarity to ideal solution' (TOPSIS) (Hwang and Yoon, 1981). AHP is the most widely used technique for multiple criteria analyses. TOPSIS is also widely used to solve many complicated decision-making problems because of its effectiveness in solving MCDM problems and computational simplicity (Wang and Chan, 2013). Other techniques that relate with MCDM problems involve fuzzy logic, DEMATEL method, analytic hierarchy processes, network analysis [analytic network process (ANP)], interpretive structural modelling (ISM) and grey relational analysis (GRA). Since the problems relating with application of GSCM techniques in real world situation are characterised by a multitude of factors, the assessment of the quantum and intensity of their respective effects acquires the proposition of MCDM problems, and hence call for the deployment of various techniques as mentioned above.

All the deployed techniques are associated with empirical studies carried on the part of the researchers, and are identified with logical results, reached therein. All the techniques are bracketed under the broad heading of MCDM techniques, and aim at factoring in various elements that form a part of a complex system, and are difficult to ascertain from their correlation point of view. This is pertinent to mention that many researchers have employed more than one technique in their research work, but the fact

that the objectives so chased were similar. Speaking in general, all the techniques corresponded to MCDM framework.

3 Literature review of GSCM

As the preliminary exercise of the research undertaken, an extensive and in-depth study of the existing research works in the field of GSCM was carried out to study the nature of work and deductions precipitated on the subject so far. Environmental sustainability has moved from the fringes of supply chain management research to an area of significant research activity (Pagell and Shevchenko, 2014). It needs to be stated that as a research subject, GSCM has caught the fancy of scholars in an extensive way, only recently. Nevertheless, a tremendous progress has been achieved in understanding the intricacies of GSCM, which has the potential of unleashing further research work that can have far reaching ramifications in the shape of new or more effective practical applications.

The literature apropos the research work undertaken on GSCM, which has been studied as part of this project, address diverse issues of the subject viz. Factors affecting the implementation and output of GSCM measures, prospective changes that can be introduced in the existing supply chain, the factors that act as de-motivators for producers/manufacturers to adopt GSCM practices and generic studies carried out on the management tool in focus. On the basis of same, the literature of research works has been categorised as addressing the following broad aspects.

3.1 Performance evaluation

There are a number of factors that play simultaneous respective roles, whenever a GSCM measure is put into practice. The factors however differ in their contribution towards achieving the desired objectives for which the management tool has been deployed. Conversely, there are also some factors that play detrimental roles in realising the objectives sought by GSCM measures. Such factors have also been studied and assessed by the researchers, so that they can be countered effectively. In nutshell, many of the research papers deal with the 'performance evaluation' of various factors that are identified with set up in which GSCM is introduced; or are part of the GSCM mechanism enforced.

Fuzzy alpha cut analysis has been deployed for the purpose of performance evaluation and supplier selection in manufacturing industry by Arunkumar et al. (2011). The Suppliers have been evaluated by undertaking usability evaluation of the AHP-based model of the problem, by making use of triangular fuzzy number to express their subjective preferences. Diabata and Govindan (2011) highlighted the 11 types of drivers, an ISM model was developed and the interaction between these drivers were analysed for the firm under study using the ISM model and MICMAC analysis by classifying the drivers into four sectors as autonomous, dependent, linkage, and driver/independent. Lin et al. (2011) in their study explored the criteria that influence the performance of the automobile manufacturing industry and evaluated its performance to find key factors in improving the manufacturers' green performance using the fuzzy set theory and decision making trial and evaluation laboratory (DEMATEL). The results provided directions to automobile manufacturers in determining the key criteria and seeking the best guidance for improving environmental image and competitive advantage. Wang and Zhang (2005)

introduced a performance assessment index system, thereby establishing a performance assessment model of GSCM using fuzzy assessment method with the help of case study. The assessment model of green supply chain performance was established according to the characteristics of green supply chain performance assessment. Muralidhar et al. (2012) presented a new decision making approach for group multi-criteria evaluation for GSCM strategies, which clubbed green procurement, manufacturing, green service to customer and EM process with order allocation for dynamic supply chains to cope market variations by using fuzzy-AHP method fuzzy TOPSIS method. Both these models gave highest rank to green manufacturing, followed by green purchasing. Muralidhar et al. (2013) proposed new strategies for evaluating the GSCM for according priority to environmental factors, in cement manufacturing life cycle analysis, thereby reducing the carbon foot prints. Then GRA was combined with TOPSIS methodology to obtain priority for measurement indicators. It was strongly recommended that if fly ash is used as primary raw material in cement manufacturing system, it will significantly reduce carbon foot prints and load on the environment. Lin (2013) deployed fuzzy set theory and DEMATEL method to form a structural model to find out the cause and effect relationships among criteria by dividing set of complex factors. The proposed method successfully extended the DEMATEL method by applying both linguistic variables and a fuzzy aggregation method; hence it can effectively avoid vague and imprecise judgments. Najjar and Alsyouf (2003) assessed the most popular maintenance approaches, i.e., strategies, policies or philosophies, using a fuzzy multiple criteria decision making (MCDM) evaluation methodology. By using the suggested fuzzy evaluation methodology they were able to identify and select, in advance, the most informative (efficient) maintenance approach that was the most cost-effective and suited the technical system in its operating context. Kenneth et al. (2012) worked to theorise and empirically assess a comprehensive GSCM practices and performance model using a structural equation modelling (SEM) methodology. The model incorporated green supply chain practices that link manufacturers with supply chain partners (both suppliers and customers) to support environmental sustainability throughout the supply chain. The results of this investigation supported the proposition that GSCM practices are both environmentally necessary and good business. Hu and Hsu (2006) developed and validated a set of critical factors of GSCM practices that could be used by managers in implementing and adopting their own GSCM practices by using statistical tests. Zhu and Sarkis (2006) compared drivers and practices of GSCM in a developing country (China), focusing on three typical sectors, the automobile industry, the thermal power plants and the electronic/electrical industry with the help of ANOVA technique. They sought to determine where the differences occur and which industries are further along. This study indicated that Chinese companies in different industries have differing drivers and practices. They tend to confirm that globalisation and China's entry into the world trade organisation have helped promote GSCM practices in manufacturing enterprises. Eltayeb et al. (2011) tried to assess the actual environmental, economic and intangible outcomes resulting from the adoption of green supply chain initiatives, using factor analysis with the help of a structured questionnaire. Through designing environmentally friendly products and taking back products and packaging, business organisations can generate benefits to the environment, in the form of reduced waste and better resource utilisation, in addition to economic benefits and cost reductions to the organisations. Zhu et al. (2012) developed and empirically tested a theoretical model on different types of institutional pressures

motivating manufacturing enterprises to pursue GSCM practices and commensurate performance outcomes. The statistic results showed that institutional pressures have driven the manufacturer adoption of internal GSCM practices which in turn related to their external GSCM practices adoption. The statistic results also suggested that GSCM practices do not directly affect economic performance, but can improve it indirectly. Francesco and Fabio (2010) assessed the determinants and motivations for the implementation of GSCM by using statistical tools. Drawing upon a database of over 4,000 manufacturing facilities in seven OECD countries this paper assessed the determinants and motivations for the implementation of GSCM.

While ascertaining the performance evaluation, researchers have tried various innovative methods in treating the underlying performance drivers. Some have focused their studies in identifying the most potent factors affecting GSCM, some have bracketed various factors into groups and then subjected them to analysis; some tried to observe the interactions between them; some put forward models on the basis of some case study conducted. A study has been carried our setting forth the cause and effect relationship between the various criteria that affect performance. Attempts have also been made to propose strategies capable of evaluating GSCM measures. The subject of motivations and determinants on part of the manufacturer to go for GSCM has also been studied by a substantial number of researchers. Majority of researchers have deployed a multitude of techniques used for analysing MCDM problems like ISM, MICMAC, DEMATEL, fuzzy logic, ANOVA, factor analysis, SEM methodology and hybrid models like fuzzy-AHP method and fuzzy TOPSIS method, GRA and TOPSIS.

With the evolution of GSCM studies in the last two decades, tremendous headway has been made in understanding the measures that help in making industrial operations and activities ‘green’. But have we been able to identify all such measures? Have we been able to extract the maximum from the measures that have already been identified? Have we tried to prune the undesirable components (such as cost, operational complexities, etc.) associated with such measures? It is in this context that the relevance of performance evaluation of GSCM measures and models assumes significance from research point of view.

3.2 Supplier selection

Supplier selection is an important criterion in GSCM practices. In a green supply chain, firms need to have extensive supplier selection and performance evaluation processes (Kainuma and Tawara, 2006) since the supplier plays an important role in GSCM implementation. Supplier selection is a process of selecting key suppliers based on a pre-established set of criteria; it plays an important role in deciding the right members in supply chain management, especially in GSCM because the environmental performance and sustainability of a company depends on these members (Tseng and Chiu 2013). Suitability of a supplier may be attributed to a number of criteria such as adoption of green practices at its end, cutting down of transportation/logistics cost at the end of manufacturer owing to locational attributes associated with the supplier, smart/tech-oriented endeavours on the part of the supplier that lead to slashing of environmentally hazardous procedures in the existing supply chain.

Table 1 Performance evaluation

S. no.	*Year*	*Title/author*	*Findings*	*Tool/technique used*
1	2011	'An analysis of the drivers affecting the implementation of green supply chain management', Diabata and Govindan	Develop a model of the drivers affecting the implementation of GSCM.	ISM
2	2011	'GSCM performance in automobile manufacturing industry under uncertainty', Lin et al.	Explores the criteria that influence the performance of the automobile manufacturing industry.	Fuzzy DEMATEL
3	2005	'Study on the performance assessment of green supply chain', Wang and Zhang	Performance assessment model of GSC is established using the fuzzy assessment method.	Fuzzy
4	2012	'Evaluation of green supply chain management strategies using fuzzy AHP and TOPSIS', Muralidhar et al.	Presents a new decision making approach for group multi-criteria evaluation for GSCM strategies.	Fuzzy AHP and TOPSIS
5	2013	'The influence of GRA and TOPSIS for assortment of GSCM strategies in cement industry', Muralidhar et al.	Proposed new strategies for evaluating the GSCM for enhancing the priority to environmental factors in cement manufacturing.	GRA and TOPSIS
6	2011	'GSCM performance in automobile manufacturing industry under uncertainty', Lin et al.	Explores the criteria that influence the performance of the automobile manufacturing industry.	Fuzzy DEMATEL
7	2011	'Using fuzzy DEMATEL to evaluate the GSCM practices', Lin	Examine the influential factors and to form a structural model to find out the cause and effect relationships among criteria.	Fuzzy DEMATEL

Note: Summary of the previous studies of GSCM according to mathematical tools/technique used.

Table 1 Performance evaluation (continued)

S. no.	*Year*	*Title/author*	*Findings*	*Tool/technique used*
8	2003	'Selecting the most efficient maintenance approach using fuzzy multiple criteria decision making', Najjar and Alsyouf	Assess the maintenance approaches, i.e., strategies, policies, or philosophies, using a fuzzy multiple criteria decision making (MCDM) evaluation methodology.	Fuzzy
9	2012	'Green supply chain management practices: impact on performance', Kenneth et al.	Theorise and empirically assess a comprehensive GSCM practices and performance model.	SEM
10	2006	'Empirical study in the critical factors of (GSCM) practice in Taiwanese electrical and electronics industries', Allen and Chia	Develop and validate a set of critical factors of green supply chain management (GSCM) practices that could be used by managers in implementing and adopting their own GSCM practices.	SEM
11	2006	An inter-sectoral comparison of GSCM in China: drivers and practices (Zhu and Sarkis)	Compares drivers and practices of GSCM in one developing country, China, focusing on three typical sectors, the automobile industry, the thermal power plants and the electronic/electrical industry.	ANOVA
12	2011	'Green supply chain initiatives among certified companies in Malaysia and environmental sustainability: investigating the outcomes', Tarig et al.	Assess the actual environmental, economic and intangible outcomes resulting from the adoption of green supply chain initiatives.	FA
13	2012	'Institutional-based antecedents and performance outcomes of internal and external GSCM practices', Zhu et al.	Develops and empirically tests a theoretical model on the different types of institutional pressures motivating manufacturing enterprises to pursue GSCM practices and commensurate performance out comes.	SEM
14	2010	'Shadows and lights of GSCM: determinants and effects of these practices based on a multi-national study', Francesco and Fabio	Assesses the determinants and motivations for the implementation of GSCM.	SEM
15	2011	'Multi-criteria supplier evaluation and selection using fuzzy AHP', Arunkumar et al.	Fuzzy alpha cut analysis has been deployed for the purpose of performance evaluation and supplier selection in manufacturing industry.	Fuzzy AHP

Note: Summary of the previous studies of GSCM according to mathematical tools/technique used.

Table 2 Supplier selection

S. no.	*Year*	*Title/author*	*Findings*	*Tool/technique used*
1	2011	'Evaluation the drivers of GSCM practices in uncertainty', Wu et al.	Find influential factors in selecting GSCM criteria and evaluated the supplier performance.	Fuzzy DEMATEL
2	2012	'Using FAHP to determine the criteria for partner's selection within a green supply chain – the case of hand tool industry in Taiwan', Lee et al.	FAHP approach is proposed to select the most important criteria for green supplier selection in the Taiwanese hand tool industry.	Fuzzy AHP
3	2012	'A novel hybrid MCDM approach based on fuzzy DEMATEL, fuzzy ANP and fuzzy TOPSIS to evaluate green suppliers', Buyukozkan and Cifci	Propose an evaluation framework for green suppliers.	Fuzzy DEMATEL, fuzzy ANP and fuzzy TOPSIS
4	2008	'A fuzzy goal programming approach for GSC optimization under activity-based costing and performance evaluation with a value-chain structure', Tsai and Hung	Integrates activity-based costing (ABC) and performance evaluation in a value-chain structure for optimal GSC supplier selection and flow allocation.	Fuzzy goal programming
5	2012	'Sustainable supplier selection: a ranking model based on fuzzy inference system', Amindoust et al.	A new ranking method on the basis of fuzzy inference system (FIS) is proposed for supplier selection problem.	Fuzzy
6	2010	'A multi-criteria decision making approach for location planning for urban distribution centers under uncertainty', Awasthi et al.	Presented a fuzzy multi criteria approach for evaluating environmental performance of suppliers.	Fuzzy TOPSIS
7	2008	'A decision support system for supplier selection based on a strategy-aligned fuzzy SMART approach', Chou and Chang	Assess different suppliers that make use of SCM strategy	SCM strategy
8	2007	'Global supplier development considering risk factors using fuzzy extended AHP-based approach', Chan and Kumar	Developed an efficient system for supplier selection at global basis.	SCM strategy

Note: Summary of the previous studies of GSCM according to mathematical tools/technique used.

Table 2 Supplier selection (continued)

S. no.	*Year*	*Title/author*	*Findings*	*Tool/technique used*
9	2009	'Selection of optimal supplier in supply chain management strategy with analytic network process and choquet integral', Tseng et al.	Selection of appropriate supplier using ANP.	ANP
10	2006	'A fuzzy approach for supplier evaluation and selection in supply chain management', Chen et al.	Grade appropriate suppliers based on a number of factors.	TOPSIS
11	2006	'Employing dynamic fuzzy membership functions to assess environmental performance in the supplier selection process', Humphreys et al.	Enable inclusion of environmental criteria in supplier selection.	Fuzzy
12	2007	'Environmental principles applicable to green supplier evaluation by using multi-objective decision analysis', Lu et al.	Proposed an MCDM process for performance evaluation of suppliers.	AHP
13	2007	'Supplier selection with multiple criteria in volume discount environments', Xia and Wu	Determine the number of suppliers to employ and the order quantity allocated to these suppliers in the case of multiple sourcing and multiple products.	AHP
14	2007	'An integrated model for supplier selection decisions in configuration changes', Wang and Che	Showed the integration of different criteria that allows the supplier selection of a specific commercial product to be explored and modelled.	Fuzzy
15	2008	'Analysis and selection of green suppliers using interpretative structural modeling and analytic hierarchy process', Kannan et al.	Applied an integrated model which analysed and selected green suppliers.	ISM and AHP
16	2006	'The impact of supply chain management practices on competitive advantage and organizational performance', Li et al.	Presented another way of supplier selection using grey-based approach.	Fuzzy
17	2009	'Contractor selection with multi criteria decision support tools', Baykasoglu et al.	Deployed techniques for understanding of relative performance, advantages and disadvantages of various contractors of construction projects.	AHP and ANP

Note: Summary of the previous studies of GSCM according to mathematical tools/technique used.

Baykasoglu et al. (2009) deployed MCDM techniques like AHP and ANP for understanding of relative performance, advantages and disadvantages of various contractors of construction projects while analysing them on the front of green operations. Wu et al. (2011) used fuzzy DEMATEL method to find influential factors out of 15 evaluation factors in selecting GSCM criteria. This study was designed to compare the importance of each criterion to represent the degree of significance. The DEMATEL method evaluated supplier performance to find key factor criteria to improve performance and provided a novel approach of decision-making information in GSCM implementation. Lee et al. (2012) proposed integrating fuzzy logic and analytical hierarchy process (AHP) approach to select the most important criteria for green supplier selection in the context of Taiwanese hand tool industry. A list of criteria, along with their priority levels, is presented. According the finding results, pollution control; green image, environment-related certificates, environmental purchasing managing systems, employment practices and purchase price are the most important criteria for Taiwan hand tool companies to select green suppliers. Buyukozkan and Cifci (2012) proposed an evaluation framework for green suppliers. The identified components were integrated into a novel hybrid fuzzy MCDM model by combining the fuzzy DEMATEL model, the analytical network process (ANP) and technique for order performance by similarity to ideal solution (TOPSIS) in a fuzzy context. The proposed model was implemented in Ford Otosan, one of the pioneering companies about environmental subjects in Turkey. The combined fuzzy ANP and fuzzy DEMATEL approaches used in this study offered a more precise and accurate analysis by integrating interdependent relationships within and among a set of criteria. Tsai and Hung (2008) propose a fuzzy goal programming (FGP) approach that integrates activity-based costing (ABC) and performance evaluation in a value-chain structure for optimal GSC supplier selection and flow allocation. The paper provides a new approach to assess and control a complex GSC based on value-chain activities, and obtain a more precise solution. The establishment of this GSC model not only helps decision-makers to monitor GSC comprehensive performance but also can facilitate further improvement and development of GSC management. Amindoust et al. (2012) applied fuzzy logic to handle the subjectivity of decision makers' assessments and a new ranking method on the basis of fuzzy inference system (FIS) was proposed for supplier selection problem. In the evaluation process, decision makers' opinions on the importance of deciding the criteria and sub-criteria, in addition to their preference of the suppliers' performance with respect to sub-criteria were considered in linguistic terms. Awasthi et al. (2010) presented a fuzzy multicriteria approach for evaluating environmental performance of suppliers by using fuzzy TOPSIS. Chou and Chang (2008) proposed a system to evaluate alternative suppliers that utilises SCM strategy to identify supplier qualified criteria and the resulting model allowed decision-maker to incorporate the supply risks of individual supplier into final decision making. Chan and Kumar (2007) identified some of the important and critical criteria including risk factors for the development of an efficient system for global supplier selection. Tseng et al. (2009b) studied the selection of appropriate suppliers using ANP and choquet integral, given a specific SCM strategy considering a set of requirements and evaluation criteria. Chen et al. (2006) used TOPSIS to rank suitable suppliers based on quantitative and qualitative factors such as quality, price, and flexibility and delivery performance. Recent studies in multi-criteria supplier selection problems such as one by Humphreys et al. (2006), proposed a hierarchical fuzzy system with scalable fuzzy membership functions

to facilitate incorporation of environmental criteria in the selection process. Lu et al. (2007) constructed an MCDM process for GSCM to help managers in measuring and evaluating performance of suppliers using fuzzy AHP. Xia and Wu (2007) developed an integrated approach of AHP improved by rough sets theory and multi-objective mixed integer programming to simultaneously determine the number of suppliers to employ and the order quantity allocated to these suppliers in the case of multiple sourcing and multiple products with multiple criteria and supplier capacity constraints. Furthermore, Wang and Che (2007) presented a model using fuzzy performance indicators, and showed the integration of different criteria that allows the supplier selection of a specific commercial product to be explored and modelled. Li et al. (2007) presented another way of supplier selection using grey-based approach, but the computation process seem to be insufficient, showing unreasonable approach for the fuzzy number. Kannan et al. (2008) applied an integrated model which analysed and selected green suppliers based on their environmental performance using the ISM and AHP.

A variety of techniques have been deployed for researchers to select the best of the suppliers, with an aim to make the supply chain greener. Some researchers have used fuzzy DEMATEL, while others fuzzy TOPSIS to evaluate performance evaluation of suppliers. Yet others have blended fuzzy logic and AHP for the same. A group of researchers have been tried deploying a hybrid technique featuring DEMATEL, ANP and TOPSIS using fuzzy as a base element. A FGP method which considers ABC while focusing on performance evaluation has also been tried. A ranking method based on FIS has also been proposed, as has been one in which ISM and AHP have been used simultaneously. Some researchers have undertaken. There is another group of researchers who have preferred to work on lesser technical method and adopted a more generalised approach in evaluating the suppliers. A hierarchical fuzzy system with scalable functions forms the basis of another research work. Apart from these, various models have been thrown by various research works which are characterised by integration of various criteria.

GSCM is a supply chain-oriented concept, and hence the importance of suppliers in the implementation and augmentation of the same cannot be discounted. Prudent selection of suppliers, with due consideration of green operations, multiply the effectiveness of the supply chain in achieving the objective of environmental conservation. If each link, in the supply chain associates itself with environment-conscious inputs, it snowballs into a massive green endeavour and manifests itself in the shape of an effective GSCM-based initiative, on a holistic basis. Therefore, the selection of supplier is of utmost importance, when embarking upon an operation that is intended to be ‘green’ in its nature and effects.

3.3 Functional barriers

GSCM measures are yet to reach the level of their desired adoption by industries/manufacturers throughout the world, most notably being in third world and developing countries. The reason is that there are many factors associated with implementation of GSCM, which demotivate many industries/manufacturers to incorporate the same in their scheme of things. Mostly cost escalation or inconvenience in implementation is cited as major barriers in the espousing GSCM practices. Various researches are carried out to figure out the factors that retard the growth of GSCM

propagation in industrial sectors, and methods have been suggested to counter them effectively.

The barriers in implementation of GSCM in a particular business establishment are inter-related, as they cast their influence on each other. They are classified as driving barriers if they support other barriers; and dependent barriers if they are influenced by other barriers. Singh et al. (2014) find the relationship between the barriers by ISM. Mathiyazhagan et al. (2012) deployed ISM qualitative analysis to understand the mutual influences amongst the 26 barriers by survey to identify which barrier was acting as the most influencing one and the result was helpful for industries to make easier the adoption of green concept in their supply chain by removing the dominant barrier. It indicated that different Indian auto component manufacturing industries have differing barriers for the implementation of GSCM. Luthra et al. (2011) put forward a structural model of 11 barriers to implement GSCM in Indian automobile industry using ISM and prioritise them. The structured model developed will help to understand interdependence of the barriers. Dashore and Sohani (2013) presented a hierarchical sustainable framework for evaluating the barriers to the implementation of the GSCM in an organisation, driving and dependence power analysis (DDPA) was used to classify and identify critical barriers. Balasubramanian (2012) presented a hierarchical sustainability framework for evaluating the barriers to the adoption of GSCM in the United Arab Emirates (UAE) construction sector by using ISM and DDPA Technique. Wooi and Zailani (2010) investigated the barriers that hinder the SMEs in Malaysia from implementing green supply chain and found that resources barrier is the key barrier that impedes the adoption of GSCM initiative and the technical barrier is expected to be the key barrier for the SMEs in the manufacturing sectors in Malaysia. A questionnaire-based survey was conducted to rank these enablers and they found contextual relationships among the enablers and developed a hierarchy-based model for the enablers by using ISM (Mudgal et al., 2009).

Researchers have been carried out by deploying various modelling techniques to rank the barriers in the way of implementing GSCM, or to gauge their effect in a particular scenario. Generally, ISM and DDPA has been used for the purpose. Some models have also been formulated to study the interdependence of barriers on each other.

GSCM has been an exciting concept theoretically, and gets more exciting when it is put into practice. It is a matter of concern, that so far the concept has not taken a practical shape with relation to its potential. There are number of barriers that impede the practical espousal of GSCM across the spectrum of industries. The first step in quashing these barriers understands them fully and then develops strategies to counter them effectively. Hence, the identification and study of GSCM barriers is of paramount importance, and the same needs to be carried out in general, as well as specifically for diverse industrial sectors.

Table 3 Functional barriers

S. no.	*Year*	*Title/author*	*Findings*	*Tool/technique used*
1	2012	'An ISM approach for the barrier analysis in Implementing GSCM', Mathiyazhagan et al.	Interpretive structural modelling (ISM) qualitative analysis was used to understand the mutual influences amongst the 26 barriers by survey.	ISM
2	2011	'Barriers to implement GSCM in automobile industry using interpretive structural modeling technique – an Indian perspective', Luthra et al.	Identify the barriers to implement GSCM in Indian automobile industry and to prioritise them.	ISM
3	2013	'Green supply chain management: a hierarchical framework for barriers', Dashore and Sohani	Presented a hierarchical sustainable framework for evaluating the barriers to the implementation of the green supply chain management (GSCM) in an organisation.	ISM
4	2012	'A hierarchical framework of barriers to green supply chain management in the construction sector', Balasubramanian	Presented a hierarchical sustainability framework for evaluating the barriers to the adoption of green supply chain management (GSCM) in construction sector.	ISM
5	2010	'Green supply chain initiatives: investigation on the barriers in the context of SMEs in Malaysia', Wooi and Zailani	Investigated the barriers that hinder the SMEs in Malaysia from implementing green supply chain.	Hypothesis testing
6	2009	'Greening the supply chain practices: an Indian perspective of enablers relationship', Mudgal et al.	Rank the enablers and found contextual relationships among the enablers and developed a hierarchy-based model.	ISM
7	2014	'An interpretive structural modelling approach for analysing barriers in total productive maintenance implementation', Singh et al.	Developed the relationships among the identified TPM barriers.	ISM

Note: Summary of the previous studies of GSCM according to mathematical tools/technique used.

3.4 Mechanism formulation/implementation

Various researchers have devised an assortment of models and mechanism for implementing GSCM in industry-specific, location-based or generic settings. Others have deduced findings pertaining to implications and inferences of implementing green measures in a supply chain. Certain models were proposed keeping in view specific limitations faced by a particular type of industry, or one which is faced with a particular set of situational factors. Mechanism formulation or implementation of GSCM in specific settings, present an interesting reading for scholars and help them to assess the limits that are generally attributed to the growth and proliferation of the management practices.

Chen et al. (2012) used ANP model to solve complex GSCM strategy-selection problems and evaluated the most important activity in each business functions viz, design, purchasing, manufacturing, and marketing and service – and associated their related activities with 'greenness'. A detailed procedure solved complex GSCM strategy-selection problems and evaluated the most important activity in each business function with the help of taking a case study on leading Taiwanese Electronics Company to identify the proposed procedure's stability. Xiangru and Jingang (2008) designed an evaluation index system on GSCM and the evaluation model was structured by AHP-Fuzzy comprehensive evaluation. The evaluation index system and evaluation model not only gave the results of comprehensive evaluation green degree to enterprise GSCM, but could also be carried out single-factor evaluation. RL may translate into GSCM practices if suitable policies and strategies may be made by a business establishments by using a dynamic simulation model. In this context, Mutingi (2014) carried simulation and analysis of various key variables by using system dynamics (SD) principles, to understand their influences. Jiance and Liying (2012) determined seven factors that affected implementation of GSCM in Chinese enterprises and an index system including 32 indexes (nodes) about these factors had been set up. They ranked these factors and indexes by ANP and found that the key factor of GSCM is government and laws especially regional laws and regulations. Sarkis (2003) modelled a decision framework which was solved as an ANP for decision making within the green supply chain. The focus of the paper was on the components and elements of GSCM and how they served as a foundation for the decision framework. Wang and Chan (2013) proposed a fuzzy hierarchical TOPSIS approach along with AHP in order to achieve sustainable economic and environmental performance. It provided a novel approach to examine various challenges that firms might be faced with when implementing GSCM initiatives and it also enabled organisations to identify improvement areas required for adopting these green initiatives. Luthra et al. (2012) used the ISM methodology for finding relationships among the various interrelated factors vital for implementing GSCM relevant to Indian manufacturing, for which MICMAC Analysis has been carried out. The model suggested how these factors were interrelated. An organisation may be benefited in analysing which factors they have to improve upon to implement GSCM in Indian manufacturing industry. Tseng and Chiu (2013) presented quantitative evaluation measures in uncertainty using fuzzy set theory. They proposed a hybrid MCDM approach to deal with the alternatives problem in linguistic preferences and ranked alternative suppliers using a GRA. The study illustrated the case of a printed circuit board manufacturer in Taiwan that seeks to implement GSCM and selected a green supplier to meet its requirements. Lee et al. (2012) in their research, explored the effect of GSCM

efforts and other organisational factors on firm performance of small and medium enterprises (SMEs) by using SEM. They developed a research model relating GSCM practice and business performance through three organisational variables (employee satisfaction, operational efficiency, and relational efficiency) as moderators. Their result indicated that business performance would be improved when GSCM enhanced operational efficiency. Gavronski et al. (2011) provided a model for development of GSM capabilities. Using the resource-based view (RBV) of the firm as the theoretical background, they postulated that plant resources are positively related to green manufacturing capabilities, which in turn are positively related to GSM capabilities. The data from a survey of a sample of manufacturing plants indicated that a managerial philosophy that included external knowledge exchange directly supported both greener process management and environmental collaboration with suppliers. Chan et al. (2012) proposed and empirically tested a model delineating the relationship among environmental orientation, GSCM activities (green purchase, customer cooperation and investment recovery) and corporate performance. The findings explicated the importance for firms, in particular those operating in a highly competitive market condition, to nurture a pro-environmental corporate culture and improve their sensitivity to salient external stakeholders' environmental demands so as to pursue greener supply chain management.

Various mechanisms have been proposed by different research scholars, which on implementation will push GSCM practices to greater heights. Mechanism formulation is a complex activity which calls for careful deployment of MCDM techniques. Some have proposed an evaluation index system, while others have focused on the inter relationship between the inherent factors that propel GSCM practices, while others tend to delineating the relationship among the same. Some researchers have based their studies by making use of SEM by taking in consideration various variables that are integral to the concept of GSCM, while others have focused on the resources at the disposal of the firm.

Mechanism formulation with intent to promote GSCM practices is research in the real and practical sense of the word, as it throws open new and innovative methods by which GSCM can be put into practice. Model formulation should rather be considered as extension of the domain of the concept. It helps in bringing forth new ideas and notions by which GSCM can be practically accomplished; and at the same time provides an opportunity to other scholars to build upon the model so formulated. The study of new models of GSCM implementation help a researcher to get informed about the latest practice-based aspects of subject.

3.5 Inter-relationships between factors

The factors that identify themselves with the implementation of a GSCM measure are interrelated with each other, and the quantum of their effect invariably depends upon the extent and mode of interaction between them. The correlation amongst the factors is of utmost importance to understand the manifestation of a GSCM measure in real-world settings, and to further improve upon the efficacy of the same, under a given set of conditions. The relations are invariably represented in the shape of mathematical equations featuring the variables, which signify the underlying factors affecting the outcome a GSCM measure.

Table 4 Mechanism formulation/implementation

S. no.	*Year*	*Title/author*	*Findings*	*Tool/technique used*
1	2012	'A business strategy selection of green supply chain management via an analytic network process', Chen et al.	Proposes a network to clarify managerial levels and firm-related content and to solve complex GSCM strategy-selection problems.	ANP
2	2008	'Research of evaluation model on enterprise's green degree of GSCM', Xiangru and Zhang	Designed an evaluation index system on GSCM and the evaluation model.	Fuzzy AHP
3	2012	'Study on the determining and importance sequence of factors affecting GSCM', Jiance and Liying	Determined 7 factors that affected implementation of GSCM in Chinese enterprises and an index system.	ANP
4	2002	'A strategic decision framework for green supply chain management', Joseph Sarkis	Modelled a decision framework for decision making within the green supply chain.	AHP
5	2012	'A hierarchical fuzzy TOPSIS approach to assess improvement areas when implementing green supply chain initiatives', Wang and Chan	Proposed a fuzzy TOPSIS approach along with AHP in order to achieve sustainable economic and environmental performance.	Fuzzy TOPSIS
6	2012	'Implementation of the GSCM In manufacturing industry in India using interpretive structural modeling technique', Luthra et al.	Finds the relationships among various interrelated factors vital for implementing GSCM relevant to Indian manufacturing.	ISM
7	2013	'Evaluating firms green supply chain management in linguistic preferences', Tseng and Chiu	Presented quantitative evaluation measures in uncertainty using fuzzy set theory	Fuzzy
8	2012	'Green supply chain management and organizational performance', Lee et al.	Developed a research model relating GSCM practice and business performance.	SEM
9	2011	'A resource-based view of green supply management', Gavronski et al.	Provide a model for development of GSCM capabilities.	Hypothesis testing
10	2012	'Environmental orientation and corporate performance: the mediation mechanism of green supply chain management and moderating effect of competitive intensity', Chan et al.	Proposed and empirically tested a model delineating the relationship among environmental orientation, (GSCM) activities.	SEM
11	2014	'The impact of reverse logistics in green supply chain management: a system dynamics analysis', Mutingi	Carried simulation and analysis of various key variables by using system dynamics (SD) principles, for reverse logistics.	SD

Note: Summary of the previous studies of GSCM according to mathematical tools/technique used.

Zhu and Sarkis (2004) examined the relationships between GSCM practice and environmental and economic performance. Using moderated hierarchical regression analysis they evaluated the general relationships between specific GSCM practices and performance. They also investigated how two primary types of management operations philosophies, quality management and just-in-time (or lean manufacturing) principles, influence the relationship between GSCM practices and performance. Zhu et al. (2008) investigated the correlation of two major factors, organisational learning and management support, with the extent of adoption of GSCM practices in Chinese manufacturing firms, where their inbound and outbound logistics activities were potential polluters to the environment. The hypotheses were tested using standard hierarchical multiple regression models employing ordinary least square (OLS) estimation. Their findings showed significant positive relationships between organisational learning mechanisms, organisational support and the adoption of GSCM practices, after controlling for a number of other influences including regulations, marketing, supplier, cost pressures, industry levels of the relevant practice and organisational size. Giovanni and Vinzi (2012) used SEM for testing the research hypotheses on a large sample of Italian firms, and estimated the structural paths between constructs by means of both covariance – and component-based approaches. They investigated the relationships between EM and performance to verify whether the implementation of an effective internal environmental is a firm's precondition to subscribe to a green supply chain.

Relationships between various aspects of GSCM are studied in various research works, using moderated hierarchical regression analysis, OLS estimation, SEM, etc. Relationship between GSCM practices and performances, cost and environmental gains, between adoption of GSCM measures and management support/organisational learning, inputs and results, internal initiatives on the part of the organisation and its subscription to GSCM on a desirable scale, etc. have been studied. The deductions of the studies on the inter-relationships of factors have led to establish the factors that are more effective in reaching the desired results on environmental and economic front, when GSCM initiatives are undertaken; subject to the peculiarity of the conditions in which the latter are enforced.

Though researchers have been able to pin point majority of factors that are individually relevant from the view point of understanding and proliferating GSCM; the interrelationships between them still remains an unexplored area. Surprisingly, the inter-relations between factors hold a key to massive potential gains the scale of which is still unknown to us. They will surely be as good as individual, perhaps more profound in their effect. It is in this background that their study assumes much significance.

3.6 Generic/standard exploration

Many studies are comparatively more theoretical in nature, limited to assess and ascertain the fundamental aspects of the subject. Such research works tend to address objectives of general nature, in context of adoption and implementation of GSCM by a particular industry, geographical domain or a specific firm. Some researches falling under this category tend to re-ascertain the existing attributes of the management practice in particular settings.

Table 5 Inter-relationships between factors

S. no.	*Year*	*Title/author*	*Findings*	*Tool/technique used*
1	2004	'Relationships between operational practices and performance among early adopters of GSCM practices in Chinese manufacturing enterprises', Zhu and Sarkis	Examined the relationships between GSCM practice and environmental and economic performance.	Regression analysis
2	2008	'Firm level correlates of emergent GSCM practices in the Chinese context', Zhu et al.	Investigates the correlation of two major factors, organisational learning and management support, with the extent of adoption of green supply chain management.	Regression analysis
3	2012	'Covariance versus component-based estimations of performance in GSCM', Giovanni and Vincenzo	Used SEM for testing the research hypotheses and estimated the structural paths between constructs by means of both covariance - and component-based approaches.	SEM

Note: Summary of the previous studies of GSCM according to mathematical tools/technique used.

Table 6 Generic/standard exploration

S. no.	*Year*	*Title/author*	*Findings*	*Tool/technique used*
1	2012	'An empirical study of green supply chain management in Indian perspective', Toke et al.	Recognise and select appropriate strategy for implementing GSCM.	AHP
2	2012	'Green supply chain management: a case study from Indian electrical and electronics industry', Kumar et al.	Investigated the GSCM practices likely to be adopted by the manufacturing industry.	Mean score
3	2007	'An empirical study of the implementation of GSCM practices in the electrical and electronic industry and their relation to organizational performances', Chien and Shih	Investigated the GSCM practices likely to be adopted by the electrical and electronic industry in Taiwan.	SEM
4	2012	'Why do firms adopt/implement green practices? – An institutional theory perspective', Lin and Sheu	Examined how institutional theory influenced GSCM practices and supply chain performance.	SEM
5	2006	'Extending green practices across the supply chain – the impact of upstream and downstream integration', Vachon and Klassen	Conceptualise and empirically test GSCP, and consider both and separately upstream and downstream interactions in the supply chain.	Hypothesis testing
6	2012	'A planning optimization framework for construction and demolition waste management', Xanthopoulos et al.	Deployed optimised-frameworks of disassembly processes of an end-of-life building.	SEM

Note: Summary of the previous studies of GSCM according to mathematical tools/technique used.

Toke et al. (2012) strived to rank interactions and weightage of critical success factors of GSCM in Indian manufacturing sector. They recognised and selected appropriate strategy for implementing GSCM and AHP, which was applied for determining relative importance and selecting appropriate approach in GSCM practice. The purpose of this study was to establish the consistency and priority approaches for implementing GSCM in response to critical success factors. Kumar, et al. (2012) investigated the GSCM practices likely to be adopted by the manufacturing industry of electrical and electronics products in India by analysing the data using 'mean score'. Study also focused on the impact of environmental collaboration in the supply chain on manufacturing and environmental performance. Lin and Sheu (2012) in their study examined how institutional theory influenced GSCM practices and supply chain performance by examining whether firms submit to institutional pressures in their adoption of green practices in addition to seeking economic efficiency. Based on the data collected from the USA and Taiwan manufacturing plants in the electric and electronics industry using survey method, SEM was performed to examine theoretical relationships among various institutional variables, green supply chain practices, and manufacturing performance. The findings proved that pressures from institutional actors have a significantly positive impact on GSCM practices adoption, which in turns improve organisational performance. Construction activities are considered to cause much of eco-destruction, coupled with resource depletion and wastage. Xanthopoulos et al. (2012) deployed optimised-frameworks of disassembly processes of an end-of-life building, by taking in consideration 'bill of materials', as an input; recycling and reusage can be encouraged in the supply chain of construction business. Chien and Shih (2007) investigated the GSCM practices likely to be adopted by the electrical and electronic industry in Taiwan. The data was then analysed using statistical package for the social sciences, and SEM was used as a path analysis model to verify the hypothetical construction of the study. The results indicated that the original equipment manufacturing and original designing and manufacturing manufacturers in Taiwan's electrical and electronic industry have adopted green procurement and green manufacturing practices in response to the current wave of international green issues and had generated favourable environmental and financial performances for the respective companies. Vachon and Klassen (2006) brought forth green practices along two dimensions viz. environmental collaboration and monitoring. Validity and reliability of scales for new and existing constructs were assessed through factor analysis. Hierarchical linear regression was used to test the hypotheses for the antecedents of GSCP. Technological integration with primary suppliers and major customers was positively linked to environmental monitoring and collaboration. For logistical integration, a linkage was found only with environmental monitoring of suppliers. Finally, as the supply base was reduced, the extent of environmental collaboration with primary suppliers increased.

Diverse studies on the extent of GSCM adoption, their attributive factors, their fall outs and concerned issues have been undertaken in a number of research studies. Efforts have been made to rank interactions and weightage of critical success factors of GSCM implementation. Certain studies focus on environmental collaboration and the subsequent monitoring of the initiatives taken. Management practices most likely to be adopted in future, impact of institutional pressures on GSCM adoption; relationships among various institutional variables, green supply chain practices, and manufacturing performance. The suitability of the factors taken into consideration have been of extreme significance, as

well as the hypotheses deliberated upon. Techniques like AHP, SEM, 'mean score', factor analysis, hierarchical linear regression have been deployed by the researchers while undertaking their studies.

Generic/standard explorations consolidate the validity of the existing knowledge base of the subject, and help in testing the same in diverse and specific industrial/geographical settings. They form the base of further studies, and act as a launch pad for more complex explorations. A researcher, who intends to carry out a new study, cannot afford to overlook the generic/standard explorations, for they form the foundations on which more challenging undertakings are based.

4 Gaps in literature

The literature that has been reviewed, presents interesting observations that hold a promise of providing possibilities for new researches and adoption of a fresh perspective on the concept of GSCM by researchers, on many counts. Various gaps have also been identified that point to the missing links that could be bridged to attain more insights on how GSCM can be more effectively implemented to get the desired benefits on front of environment friendly and cost effective operations. For example, apropos the research works conducted on the barriers in the implementation of GSCM practices, the factors are considered individually, as well as their inter-linkages are also taken into consideration. Nevertheless, some of the interrelations between the barriers can be reduced to mathematical equations. Though it will require hefty inputs, yet the results will help in a tremendous way to consolidate our understanding about the barriers in implementing GSCM. Some barriers are location-specific or sector specific in nature, and there is an element of ambivalence regarding their applicability in a universal manner. Similarly, studies conducted on one specific firm, always carry an uncertainty that whether the results achieved, can be generalised in the context of the subject studies, i.e., GSCM whatever is applicable to a part, may not be applicable to the whole. In fact, what is applicable for one firm, may not apply to a similar firm operating in a different geographical/industrial set up. In context of model formulation, researchers have worked upon creating models that are more effective to implement GSCM practically. But they themselves states that all the underlying factors have not been considered for the sake of convenience and computation. This points that though there is a scope for further improvisation of the deductions, the same was not carried out because of complexities involved in working them out. This is a gap, which has been purposely introduced; and it is hoped that with better management/computational tools one day the researchers will be able to fine tune their findings by making their deductions more inclusive in nature. In some research papers, among other things, factors such as green image, environment-related certificates, environmental purchasing are cited. But in most of the developing countries, where the need of deploying GSCM practices is felt more intensely, the availability of certificates/management systems at the end of the supplier may not reflect the real picture at his end. The reason being, that many of the mentioned 'criteria', can be secured easily; but the spirit underlying the same may generally be missing. Furthermore, some models are tested on only one firm; which casts aspersion on the validity of the model across the horizon of firms from different sectors and with a diverse spatial distribution. Last but not the least, the deductions of the many studies carried out, hinges upon the beliefs and opinions of the respondents to whom the

questionnaires were sent or responses were invited. This introduces an element of subjectivity in the results deduced. The lack of quantifiable information as well as numerical data, affects the objectivity of the results.

Nevertheless, the findings deduced by various researchers has helped in bringing forth new ideas and notions by which GSCM can be practically accomplished; and at the same time provides an opportunity to other scholars to build upon the findings so achieved. The study of research literature of GSCM implementation will help aspiring researchers to get informed about various aspects of subject. Their findings will form the base of further studies, and will act as a launch pad for more complex explorations. A researcher, who intends to carry out a new study, cannot afford to overlook the existing research works done, for they form the foundations on which more challenging undertakings are based.

5 Conclusions

The study carried out on the diverse type of literature on GSCM, extended by various researchers of the subject have led to the conclusion that though the mentioned management tool has gained wide popularity and acceptance on the academic front, still a lot needs to be done on ground (industrial front) level. It has been observed that much of work done on literary front is of subjective interest, and confines itself to the domain of describing the facets of GSCM or aspires to evaluate the performance of various factors that are identified with the application of the same. This, in the most practical terms, can be referred as highlighting the basics of the management concept with respect to a particular industry, industrial set up or geographical domain. Limited research literature has been generated corresponding to identifying hitherto unexplored aspects of GSCM, having the potential for large scale transformation in the implementation and adoption of the scale, across spatial or sectoral horizons. Though on one hand, this presents a monotonous view of the work done so far on the subject; at the same time, it offers bright optimism that there is still a lot to be explored and new discoveries can be made with regard to green practices that of can have far reaching positive ramifications for environment and economic/industrial progress of mankind. Integration of findings hitherto reached by researchers, throw exciting opportunities in developing a holistic approach of understanding the concept of GSCM and meditating on what new can be determined apropos the subject. The analysis of literature resulting from various research works gives a clear picture of the gaps and unattended aspects of GSCM. Extensive research can be carried out on such attributes that have so far not been worked upon. Gradual addition to the knowledge base of subject matter will help the concept to evolve and find new dimensions, which at later stage will help in rapid extension GSCM, both qualitatively and in magnitude.

5.1 Limitations of the study

The findings of this study are substantially helpful in understanding the conceptual and practical aspects of GSCM implementation; nevertheless the study has been characterised by a number of limitations. The most prominent is the scope and applicability of the models studied. Most of the studies undertaken limit themselves to particular

settings – industrial, geographical, etc.; and the validity of the models on a universal scale is debatable. Furthermore, many elements that constitute the green supply chain have subjective traits, which are non-quantifiable. Such elements, are either not featured in the models altogether; or are not optimally represented therein. This study is also limited by the lack of practical testing of the models studied. The study is theoretical in nature and the validity of the models/theories extended by the literature reviewed needs to be tested in peculiar spatial and operational settings. Though a large number of studies were reviewed while undertaking this study, the possibility of existence of hitherto unknown variable, and their interplay with others in a given supply chain cannot be ruled out. Furthermore, the nature of operational domain varies from case to case. A model which is workable in a developed country, say Germany may not be as effective in an underdeveloped country, say Sudan. This limits the validity of the findings only to those particular settings, where the original study was carried out and not necessarily in conditions opposite to it. There are many models in the study, which are theoretically derived and may not have been tested in real time conditions in diverse operational settings. Thus, there are a number of limitations attached with this study; nevertheless care and caution have been taken to make the finding comprehensive and inclusive to maximum possible extent.

References

Amindoust, A., Ahmeda, A., Saghafinia, A. and Bahreininejada, A. (2012) 'Sustainable supplier selection: a ranking model based on fuzzy inference system', *Applied Soft Computing*, Vol. 12, No. 6, pp.1668–1677.

Arunkumar, N., Karunamoorthy, L. and Muthukumar, S. (2011) 'Multi-criteria supplier evaluation and selection using fuzzy AHP (alpha cut analysis): a case study', *Int. J. Industrial and Systems Engineering*, Vol. 8, No. 4, pp.449–471.

Balasubramanian, S. (2012) 'A hierarchical framework of barriers to green supply chain management in the construction sector', *Journal of Sustainable Development*, Vol. 5, No. 10, pp.15–27.

Baykasoglu, A., Ozbay, E., Gogus, T.T. and Oztay, A. (2009) 'Contractor selection with multicriteria decision support tools', *Int. J. Industrial and Systems Engineering*, Vol. 4, No. 2, p p.174–197.

Bras, B. and McIntosh M.W. (1999) 'Product, process, and organizational design for remanufacture – an overview of research', *Robotics and Computer-Integrated Manufacturing*, Vol. 15, No. 3, pp.167–178.

Buyukozkan, G. and Cifci, G. (2012) 'A novel hybrid MCDM approach based on fuzzy DEMATEL, fuzzy ANP and fuzzy TOPSIS to evaluate green suppliers', *Expert Systems with Applications*, Vol. 39, No. 3, pp.3000–3011.

Carter, C.R. and Ellram, L.M. (1998) 'Reverse logistics: a review of the literature and framework for future investigation', *Journal of Business Logistics*, Vol. 19, No. 1, pp.85–102.

Chan, F.T.S. and Kumar, N. (2007) 'Global supplier development considering risk factors usingfuzzy extended AHP-based approach', *The International Journal of Management Science*, Vol. 35, No. 4, pp.417–31.

Chan, R.Y.K., He, H., Chan, H.K. and Wang, W.Y.C. (2012) 'Environmental orientation and corporate performance: The mediation mechanism of green supply chain management and moderating effect of competitive intensity', *Industrial Marketing Management*, Vol. 41, No. 4, pp.621–630.

Chang, B.Y., Kenzhekhanuly, Y. and Park, B. (2013) 'A study on determinants of green supply chain management practice', *International Journal of Control and Automation*, Vol. 6, No. 3, pp.199–208.

Chen, C., Shih, H.S., Shyur, H.J. and Wu, K.S. (2012) 'A business strategy selection of green supply chain management via an analytic network process', *Computers and Mathematics with Applications*, Vol. 64, No. 8, pp.2544–2557.

Chen, C.T., Lin, C.T. and Huang, S.F. (2006) 'A fuzzy approach for supplier evaluation and selection in supply chain management', *International Journal of Production Economics*, Vol. 102, No. 2, pp.289–301.

Chien, M.K. and Shih, L.H. (2007)'An empirical study of the implementation of green supply chain management practices in the electrical and electronic industry and their relation to organizational performances', *International Journal of Environment Science & Technology*, Vol. 4, No. 3, pp.383–394.

Chou, S.Y. and Chang, Y.H. (2008) 'A decision support system for supplier selection based on a strategy-aligned fuzzy SMART approach', *Expert Systems with Applications*, Vol. 34, No. 4, pp.2241–2253.

Daniel, V. and Guide Jr., R. (1998) 'Scheduling with priority dispatching rules and drum-buffer rope in a recoverable manufacturing system', *International Journal of Production Economics*, Vol. 53, No. 1, pp.101–116.

Daniel, V. and Guide Jr., R. (2000). 'Production planning and control for remanufacturing: industry practice and research needs', *Journal of Operations Management*, Vol. 18, No. 4, pp.467–483.

Daniel, V., Guide Jr., R., Srivastava, R. and Michael S. (1996) 'Are production systems ready for the green revolution?', *Production and Inventory Management Journal*, Vol. 37, No. 4, pp.70–78.

Dashore, K. and Sohani, N. (2013) 'Green supply chain management: a hierarchical framework for barriers', *International Journal of Engineering Trends and Technology*, *Vol.* 4, No. 5, pp.2172–2182.

Diabata, A. and Govindan.K. (2011) 'An analysis of the drivers affecting the implementation of green supply chain management', *Resources, Conservation and Recycling.*, Vol. 55, No. 6, pp.659–667.

Eltayeb, T.K., Zailani, S. and Ramayah, T. (2011) 'Green supply chain initiatives among certified companies in Malaysia and environmental sustainability: investigating the outcomes', *Resources, Conservation and Recycling*, Vol. 55, No. 5, pp.495–506.

Farzianpour, F., Pishdar, M., Shakib, M.D., Hashemi, S. and Toloun, M.R. (2014) 'Consumers perceived risk and its effect on adoption of online banking services management' *American Journal of Agricultural and Biological Sciences*, Vol. 11. No. 1, pp.47–56.

Fleischmann, M., Beullens, P., Ruwaard, J.M.B. and Wassenhove, L.N.V. (2001) 'The impact of product recovery on logistics network design', *Production & Operations Management*, Vol. 10, No. 2, pp.156–173.

Fleischmann, M., Krikke, H.S., Dekker, R. and Flapper, P.S.D. (2000) 'A characterization of logistics networks for product recovery', *Omega*, Vol. 28, No. 6, pp.653–666.

Fleischmann, M., Ruwaard, J.M.B., Dekker, R., Laan. E.V., Nunen J.A.E.E. and Wassenhove, L.N.V. (1997) 'Quantitative models for reverse logistics: a review', *European Journal of Operational Research*, Vol. 103, No. 1, pp.1–17.

Francesco, T. and Fabio, I. (2010) 'Shadows and lights of GSCM (green supply chain management): determinants and effects of these practices based on a multi-national study', *Journal of Cleaner Production*, Vol. 18, Nos. 10–11, pp.953–962.

Gavronski, I., Klassen, D.R., Vachon, S. and Nascimento, L.F.M. (2011) 'A resource-based view of green supply management', *Transportation Research Part E*, Vol. 47, No. 6, pp.872–885.

Giovanni, P.D. and Vinzi, V.E. (2012) 'Covariance versus component-based estimations of performance in green supply chain management', *International Journal of Production Economics*, *Vol.* 135, No. 2, pp.907–916.

Gungor, A. and Gupta, S.M. (1999) 'Issues in environmentally conscious manufacturing and product recovery: a survey', *Computers & Industrial Engineering*, Vol. 36, No. 4, pp.811–853.

Hu, A.H. and Hsu, C.W. (2006) 'Empirical study in the critical factors of green supply chain management (GSCM) practice in the Taiwanese electrical and electronics industries', *IEEE International Conference on Management of Innovation and Technology*, Vol. 2, No. 1, pp.854–857.

Humphreys, P., McCloskey, A., McIvora, R., Maguire, L. and Glackina, C. (2006) 'Employing dynamic fuzzy membership functions to assess environmental performance in the supplier selection process', *International Journal of Production Research*, Vol. 44, No. 12, pp.2379–2419.

Jayaraman, V. (2003) 'The design of reverse distribution networks: models and solution procedures', *European Journal of Operational Research*, Vol. 150, No. 1, pp.128–149.

Jiance, Z. and Liying, Y. (2012) 'Study on the determining and importance sequence of factors affecting GSCM', *9th International Conference on Service Systems and Service Management* IEEE, China.

Kainuma, Y. and Tawara, N. (2006) 'A multiple attribute utility theory approach to lean and green supply chain management', *International Journal of Production Economics*, Vol. 101, No. 1, pp.99 –108.

Kannan, G., NoorulHaq, A., Sasikumar, P. and Arunachalam, S. (2008)'Analysis and selection of green suppliers using interpretative structural modeling and analytic hierarchy process', *International Journal of Management and Decision Making*, Vol. 9, No. 2, pp.163–82.

Kenneth, W. G., Pamela J. Z., Meacham, J. and Bhadauria, V.S. (2012) 'Green supply chain management practices: impact on performance', *Supply Chain Management: An International Journal, Vol.* 17, No. 3, pp.290–305.

Kumar, S., Chattopadhyaya, S. and Sharma, V. (2012)' Green supply chain management: a case study from Indian electrical and electronics industry', *International Journal of Soft Computing and Engineering*, Vol. 1, No. 6, pp.275–281.

Lee, S.M., Kim, S.T. and Choi, D. (2012) 'Green supply chain management and organizational performance', *Industrial Management & Data Systems*, Vol. 112, No. 8, pp.1148–1180.

Lee, T.R., Le, T.P.H., Genovese, A. and Koh, S.C. (2012) 'Using FAHP to determine the criteria for partner's selection within a green supply chain The case of hand tool industry in Taiwan', *Journal of Manufacturing Technology Management*, Vol. 23, No. 1, pp.25–55.

Li, S., Nathan, B.R., RaguNathan, T.S. and SubbaRao, S. (2006) 'The impact of supply chain management practices on competitive advantage and organizational performance', *Omega*, Vol. 34, No. 2, pp.107–124.

Lin, R.J. (2013) 'Using fuzzy DEMATEL to evaluate the green supply chain management practices', *Journal of Cleaner Production*, Vol. 40, Special Volume: Sustainable Consumption and Production for Asia: Sustainability Through Green Design and Practice, pp.32–39.

Lin, R.J. and Sheu, C. (2012) 'Why do firms adopt/implement green practices? – an institutional theory perspective', *Procedia – Social and Behavioral Sciences*, Vol. 57, No. 9, pp.533–540.

Lin, R.J., Chen, R.H. and Nguyen, T.H. (2011) 'Green supply chain management performance in automobile manufacturing industry under uncertainty', *Procedia – Social and Behavioral Sciences*, Vol. 25, No. 1, pp.233–245.

Lu, Y.Y., Wu, C.H. and Kuo, T.C. (2007) 'Environmental principles applicable to green supplier evaluation by using multi-objective decision analysis', *International Journal of Production Research*, Vol. 45, Nos. 18–19, pp.4317–4331.

Luthra, S., Garg, D., Kumar, S. and Haleem A. (2012) 'implementation of the green supply chain management in manufacturing industry in india using interpretive structural modeling technique', *BPR Technologia : A Journal of Science, Technology & Management*, Vol. 1, No. 1, pp.1–17, ISSN: 2278–8387.

Luthra, S., Kumar, V., Kumar, S. and Haleem, A. (2011) 'Barriers to implement green supply chain management in automobile industry using interpretive structural modeling technique – an Indian perspective', *Journal of Industrial Engineering and Management*, Vol. 4, No. 2, pp.231–257.

Mathiyazhagan, K., Govindan, K., Noorulhaq, A. and Geng, Y. (2013) 'An ISM approach for the barrier analysis in implementing green supply chain management', *Journal of Cleaner Production, Vol.* 47, No. 1, pp.283–297.

Meredith, J. (1993) 'Theory building through conceptual methods', *International Journal of Operations & Production Management*, Vol. 13, No. 5, pp.3–11.

Mudgal, R.K., Shankar, R., Talib, P. and Raj, T. (2009) 'Greening the supply chain practices: an Indian perspective of enablers relationship', *International Journal of Advanced Operations Management*, Vol. 1, Nos. 2–3, pp.151–176.

Muralidhar, P., Ravindranath, K. and Srihari, V. (2012) 'Evaluation of green supply chain management strategies using fuzzy AHP and TOPSIS', *IOSR Journal of Engineering*, Vol. 2, No. 4, pp.824–830.

Muralidhar, P., Ravindranath, K. and Srihari, V. (2013) 'The influence of GRA and TOPSIS for assortment of GSCM strategies in cement industry', *International Journal of Supply Chain Management*, Vol. 2, No. 1, pp.49–54.

Mutingi, M. (2014) 'The impact of reverse logistics in green supply chain management: a system dynamics analysis' *International Journal of Industrial and Systems Engineering, Vol.* 17, No. 2, pp.186–201.

Najjar, B.A. and Alsyouf, I. (2003) 'Selecting the most efficient maintenance approach using fuzzy multiple criteria decision making', *International Journal of Production Economics*, Vol. 84, No. 1, pp.85–100.

Olugu, E.U., Wong, K. Y. and Shaharun, A. M. (2011) 'Development of key performance measures for the automobile green supply chain' *Resources, Conservation and Recycling*., Vol. 55, No. 1, pp.567–579.

Pagell, M. and Schevchenko, A. (2014) 'Why research in sustainable supply chain management should have no future', *Journal of Supply Chain Management*, Vol. 50, No. 1, pp.1–32.

Pishdar, M., Toloun, M.R.S.H., Zamani, S. and Farzianpour, F. (2014) 'Development of factors effective in the success of green supply chain management', *American Journal of Agricultural and Biological Sciences*, Vol. 9, No. 1, pp.33–43.

Sarkis, J. (2003) 'A strategic decision framework for green supply chain management', *Journal of Cleaner Production*, Vol. 11, No. 4, pp.397–409.

Sarkis, J., Zhu, Q. and Lai, K.H. (2011) 'An organizational theoretic review of green supply chain management literature', *International Journal of Production Economics*, Vol. 130, No. 1, pp.1–15.

Singh, M., Sachdeva, A. and Bhardwaj, A. (2014) 'An interpretive structural modelling approach for analysing barriers in total productive maintenance implementation', *International Journal of Industrial and Systems Engineering, Vol.* 16, No. 4, pp.433–450.

Smith, M.E., Richard. T. and Paul, J. (2002) *Management Research – An Introduction*, Sage Publications, London.

Srivastava, S. (2007) 'Green supply-chain management: a state-of the-art literature review', *International Journal of Management Reviews*, Vol. 9, No. 1, pp.53–80.

Toke, L.K., Gupta, R.C. and Dandekar, M. (2012) 'An empirical study of green supply chain management in Indian perspective', *International Journal of Applied Science & Engineering Research*, Vol. 1, No. 2, pp.372– 383.

Tsai, W.H. and Hung, S.J. (2008) 'A fuzzy goal programming approach for green supply chain optimization under activity-based costing and performance evaluation with a value-chain structure', *International Journal of Production Research*, Vol. 47, No. 18, pp.4991–5017.

Tseng, M.L. and Chiu, A.S.F. (2013) 'Evaluating firms green supply chain management in linguistic preferences', *Journal of Cleaner Production*, Vol. 40, Special Volume: Sustainable Consumption and Production for Asia: Sustainability Through Green Design and Practice, pp.22–31.

Tseng, M.L. and Lin, R.J. (2013)'Determine the driving criteria in firm's GSCM practices with dependence and uncertainty', *Journal of Cleaner Production*, Vol. 40, No. 1, pp.22–31.

Tseng, M.L., Chiang, J.H. and Lan, L.W. (2009b) 'Selection of optimal supplier in supply chain management strategy with analytic network process and choquet integral', *Computers & Industrial Engineering*, Vol. 57, No. 1, pp.330–340.

Vachon, S. and Klassen, R.D. (2006) 'Extending green practices across the supply chain: the impact of upstream and downstream integration', *International Journal of Operations &Production Management*, Vol. 25, No. 9, pp.898–916.

Walker, H., Sisto, L.D. and Mcbain, D. (2008) 'Drivers and barriers to environmental supply chain management practices: lessons from the public and private sectors', *Journal of Purchasing and Supply Management, Vol.* 14, No. 1, pp.69–85.

Wang, H.S. and Che, Z.H. (2007) 'An integrated model for supplier selection decisions in configuration changes', *Expert Systems with Applications*, Vol. 32, No. 4, pp.1132–1140.

Wang, S.Z. and Zhang, H.C. (2005) 'Study on the performance assessment of green supply chain', *IEEE International Conference on Systems, Man and Cybernetics,* , Vol. 1, pp.942–947.

Wang, X. and Chan, H.K. (2013) 'A hierarchical fuzzy TOPSIS approach to assess improvement areas when implementing green supply chain initiatives', *International Journal of Production Research*, Vol. 51, No. 10, pp.3117–3130.

Wooi, G.C. and Zailani, S. (2010) 'Green supply chain initiatives: investigation on the barriers in the context of SMEs in Malaysia', *International Business Management*, Vol. 4, No. 1, pp.20–27.

Wu, K.J., Liao, C.J., Tan, K.H., Chiu, S.F. and Tseng, M.L. (2012) 'Exploring decisive factors effecting green supply chain practices under uncertainty', *Proceedings of the Asia Pacific Industrial Engineering & Management Systems Conference*, pp.89–102.

Wu, K.J., Tseng, M.L. and Vy, T. (2011)'Evaluation the drivers of green supply chain management practices in uncertainty', *Procedia – Social and Behavioral Sciences, Vol.* 25, pp.384 – 397.

Xanthopoulos, A., Aidonis, D., Vlachos, D. and Lakovou, E. (2012) 'A planning optimisation framework for construction and demolition waste management', *International Journal of Industrial and Systems Engineering*, Vol. 10, No. 3, pp.257–276.

Xia, W. and Wu, Z. (2007) 'Supplier selection with multiple criteria in volume discount environments', *Omega*, Vol. 35, No. 5, pp.494–504.

Xiangru, M. and Jingang, Z. (2008) 'Research of evaluation model on enterprise's green degree of GSCM', *International Seminar on Business and Information Management.*

Zhang, H.C., Kuo, T.C., Huang, S.H. and Lu, H. (1997) 'Environmentally conscious design and manufacturing: a state-of-the-art survey', *Journal of Manufacturing Systems*, Vol. 16, No. 5, pp.352–371.

Zhu, Q. and Sarkis, J. (2004) 'Relationships between operational practices and performance among early adopters of green supply chain management practices in Chinese manufacturing enterprises', *Journal of Operations Management*, Vol. 22, No. 3, pp.265–289.

Zhu, Q. and Sarkis, J. (2006) 'An inter-sectoral comparison of green supply chain management in China: drivers and practices', *Journal of Cleaner Production*, Vol. 14, No. 5, pp.472–86.

Zhu, Q. and Sarkis, J. (2007) 'The moderating effects of institutional pressures on emergent green supply chain practices and performance' *International Journal of Production Research*, Vol. 45, No. 18, pp.4333–4355.

Zhu, Q., Sarkis, J. and Lai, K.H. (2008a) 'Green supply chain management implications for closing the loop', *Transportation Research Part E: Logistics and Transportation Review*, Vol. 44, No. 1, pp.1–18.

Zhu, Q., Sarkis, J. and Lai, K.H. (2008c) 'Confirmation of a measurement model for green supply chain management practices implementation', *International Journal of Production Economics*, Vol. 111, No. 2, pp.261–73.

Zhu, Q., Sarkis, J. and Lai, K.H. (2012) 'Green supply chain management innovation diffusion and its relationship to organizational improvement: an ecological modernization perspective', *Journal of Engineering and Technology Management*, Vol. 29, No. 1, pp.168–185.

Zhu, Q., Sarkis, J. and Lai, K.H. (2013) 'Institutional-based antecedents and performance outcomes of internal and external green supply chain management practices', *Journal of Purchasing and Supply Management*, Vol. 19, No. 2, pp.106–117, http://dx.doi.org/10.1016/j.pursup.2012.12.001.

Zhu, Q., Sarkis, J., Cordeiro, J.J. and Lai, K.H. (2008a) 'Firm-level correlates of emergent green supply chain management practices in the Chinese context', *Omega*, Vol. 36, No. 4, pp.577–591.

Zhu, Q., Sarkis, J., Cordeiro, J.J. and Lai, K.H. (2008b) 'Firm-level correlates of emergent green supply chain management practices in the Chinese context', *Omega*, Vol. 36, No. 1, pp.577–91.

ResearchGate

See discussions, stats, and author profiles for this publication at: http://www.researchgate.net/publication/280609065

Modeling and Analysis of Current and Weld Speed on Weld Hardness of Steel–Cu Weldments by RSM Approach

ARTICLE · MAY 2015

READS

7

6 AUTHORS, INCLUDING:



Ramakant Rana

Maharaja Agarsain Institute of Technology

9 PUBLICATIONS **3** CITATIONS

SEE PROFILE

Available from: Ramakant Rana
Retrieved on: 03 October 2015

OPEN ACCESS

International
Journal
Of Modern Engineering Research (IJMER)

Modeling and Analysis of Current and Weld Speed on Weld Hardness of Steel-Cu Weldments by RSM Approach

Ramakant Rana[1], Surabhi Lata[1], Alok Shankaran[2], Vinay Sharma[2], Amit Saraswat[2], Roop Lal[3]

[1]*Assistant Professor, Mechanical and Automation Engineering, Maharaja Agrasen Institute of Technology, Delhi, India*
[2,]*Student, Mechanical and Automation Engineering, Maharaja Agrasen Institute of Technology, Delhi, India*
[3]*Assistant Professor, Mechanical Engineering, Delhi Technological University, Delhi, India*

ABSTRACT: *In this paper, Response Surface Methodology (RSM) is used to investigate the effect of two controllable input variables viz. Current and Welding Speed for Weld Hardness of joined surfaces of Steel and Copper. To study the proposed model for Weld Hardness, a Central Composite Design (CCD) is used to estimate the model coefficients of the two factors, which are alleged to influence the Weld Hardness of the weld. Experiments were conducted on Steel and Copper. The response is modelled using RSM on experimental data. The significant coefficients are obtained by performing Analysis of Variance (ANOVA) at 5% level of significance.*

Keywords: *RSM, Welding, Dissimilar Metals, Weld Hardness, Modelling*

I. INTRODUCTION AND LITERATURE REVIEW

Industries have an increasing demand of dissimilar metal joints for various applications, viz. reduction in weight, concern regarding environment, high performance, cost saving and energy saving [Dong et al. (2012), Uzun et al. (2005)]. The transportation industry widely uses aluminium alloys for the purpose of reduction in weight [Chen et al. (2013), Zhang et al. (2007)]. [Korenyuk (1975)] tried to weld Aluminium to Titanium, this combination was not accomplished successfully by conventional arc welding processes. [Gorin (1964), Lv et al. (2012)] welded Titanium to nickel, an attempt to weld Ti and Ni using TIG was not successful. However, they used copper alloy as an insert which, led to a joint without harmful intermetallic compounds. [Mikhailov et al. (1965)] successfully welded Titanium to Copper, their produced joints were with the highest tensile strength and ductility with Ti-30Cb and Ti-3Al-6.5Mo-11Cr. [O'Brien (2011)] welded Copper alloys to Nickel, and found that, the Copper and nickel are mutually soluble in each other. [Shao et al. (2015)] welded Aluminium and Galvanized Steel. Their thermodynamic calculations predicted that the Fe_2Al_5 intermetallic compound layer was formed first in the steel side, when temperature gradually reduced. The joining of steel and copper has become an essential research and application focus [Chen (2015)]. It is nevertheless difficult to join them together due to the differences in physical characteristics such as the melting temperature, the poor metallurgical compatibility and thermal expansion, of these two metals. In this paper, gas metal arc welding (GMAW) method was used to join steel and copper.

II. EXPERIMENTAL SET-UP

A number of experiments were conducted to study the effects of various parameters on joining Steel and Copper with GMAW. These studies were undertaken to investigate the effects of Current, and Welding Speed for Weld Hardness. The selected workpiece material for the research work was steel (composition shown in Table 1) and 100 % Copper. Steel was selected due to its emergent range of applications in the field of manufacturing tools in mould industries. Workpiece materials used were steel square plates of dimensions 100×80 mm and of thickness 6 mm. the welding process is shown in Figure 2 (a) & (b). The test conditions are depicted in Table II.

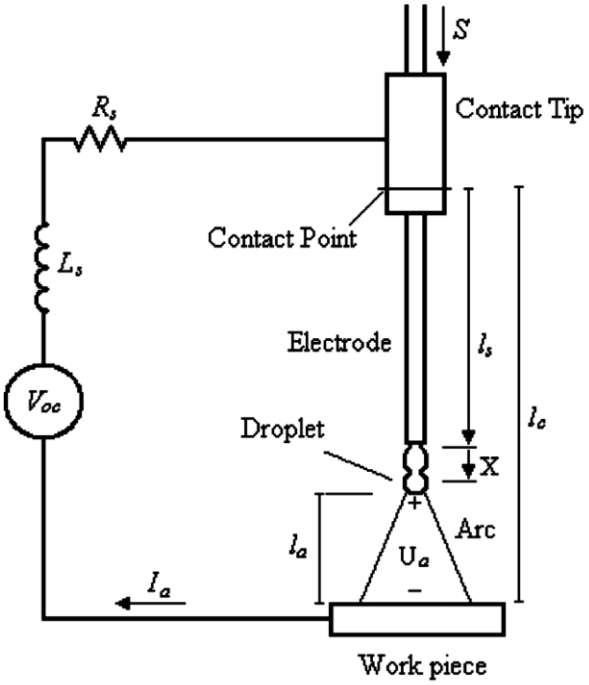


Figure 1: Model of GMAW Process [Shao et al. (2015)]

Table I: Composition of Steel Welded with copper

Carbon	Silicon	Manganese	Phosphorus	Sulphur	Chromium	Molybdenum	Nickel	Copper	Titanium	Cobalt	Vanadium
.352	.178	.61	.035	.037	.243	.033	.080	.089	.007	.003	.003



(a) (b)

Figure 2: Welded Process being conducted

III. RESPONSE SURFACE METHODOLOGY

The collection of statistical and mathematical techniques named Response Surface Methodology (RSM) is useful for modelling and analysis of the problems in several input variables influences the responses. RSM objective is to find the correlation between the variables investigated and the response [Montgomery (2001), Rana et al. (2014)]. Design of Experiments (DOE) was used to estimate an unknown function for which only a few values were computed. Least square error fitting was used to model the generated relations of the response surface. A Central Composite Design (CCD) gives a comparatively accurate prediction of all response variable

averages related to quantities measured during experimentation, hence it was used [Mason et al. (2003)]. Central Composite Design (CCD) offers the advantage that certain level adjustments are acceptable and can be applied in the two-step chronological RSM. In these methods, there is a possibility that the experiments will stop with few runs and decide that the prediction model is satisfactory.

Table Ii: Different Variables Used In The Experiment And Their Level

Variable	CODE	LEVELS	
		1	2
Current (A)	A	200	240
Welding Speed (mm/s)	B	1.11	1.44

The Current, and Welding Speed were the variables selected for this investigation. The different levels taken for this study are shown in Table II. Three replications of Weld Hardness were taken, and the average value of Weld Hardness used in the design matrix, is shown in Table III.

Table III: Planning Matrix Of The Experiments With The Optimal Model Data.

Current(A)	Welding speed(mm/s)	Hardness
240	1.11	162
240	1.44	227
200	1.44	160.67
200	1.11	167

The experimental values were analyzed and then a mathematical model was developed which, illustrated the relationship between the process response and the variables. The model in equation 1 explains the behaviour of the system.

$$y = \beta_0 + \beta_1 x_1 + \beta_2 x_2 + \in \quad \ldots 1$$

Where y = Hardness, x_1 = Current (A), x_2 = Welding speed (mm/s) and β_1, β_2= Partial Regressors.

IV. RESULT AND DISCUSSION

Based on the experimental data gathered, statistical regression analysis enabled to study the correlation of process parameters with the Weld Hardness. In this study, a polynomial regression was modelled for two variables under consideration. For simplicity, a quadratic model of Weld Hardness was proposed.

The coefficients of regression model was estimated from the experimental results. The effects of these variables and the interaction between them were included in this analyses and the developed model is expressed as interaction equation:

Hardness = -103 + 0.767 Current (A) + 89 Welding speed (mm/s) …2

Table IV: Anova Table For Weld Hardness

Term	**Coef SE**	**Coef**	**T-Value**	**P-Value**
Constant	-103	240	-0.43	0.743
Current (A)	0.767	0.892	0.86	0.548
Welding Speed (mm/s)	89	108	0.82	0.562

The unknown coefficients were determined from the experimental data as presented in Table IV. The standard errors on estimation of the coefficients were tabulated in the column 'SE coef'.

It was important to check the adequateness of the model, because under-specified or an incorrect model could have lead us to misleading conclusion. The model adequateness checking included the test for significance of the model coefficients, lack of fit and regression model, which were carried out subsequently using ANOVA on the curtailed model (Table. V).

Table V: Analysis Of Variance Table For The Fitted Models:

Source	**DOF**	**Adj. SS**	**Adj. MS**	**F-Value**	**P-Value**
Regression	2	1800.9	900.4	0.71	0.643
Current(A)	1	940.3	940.3	0.74	0.548
Welding speed(mm/s)	1	860.5	860.5	0.68	0.562
Error	1	1272.0	1272.0	*	*
Total	3	3072.9	*	*	*

Welding Speed and Current improves the weld Hardness with the increase in their values as that is depicted in the figure 3. Even from figure 4 also it is clear that that optimum value of Weld Hardness can be achieved with both the Welding Speed and Current. The surface plot of the Weld Hardness vs Welding Speed (mm/s) and Current (A) is plotted in figure 5.

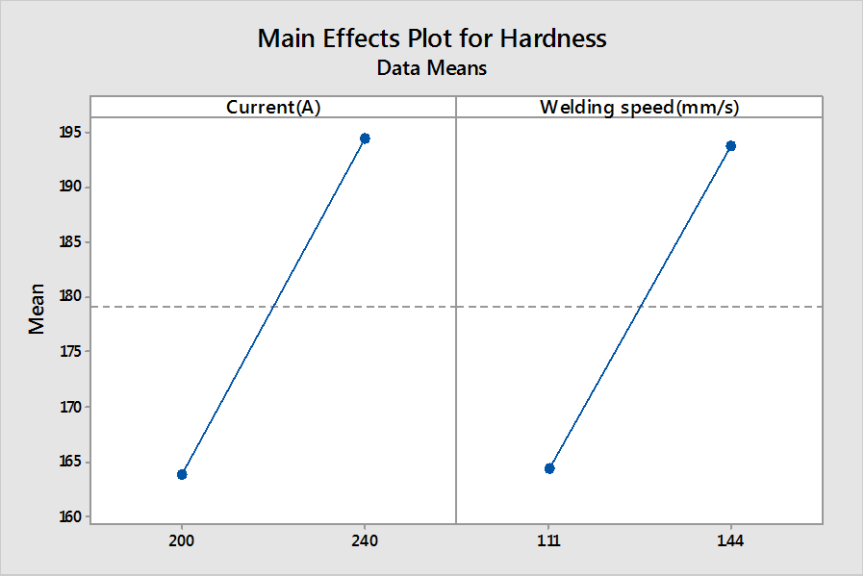


Figure 3: Effect of Current and Welding Speed on Weld Hardness

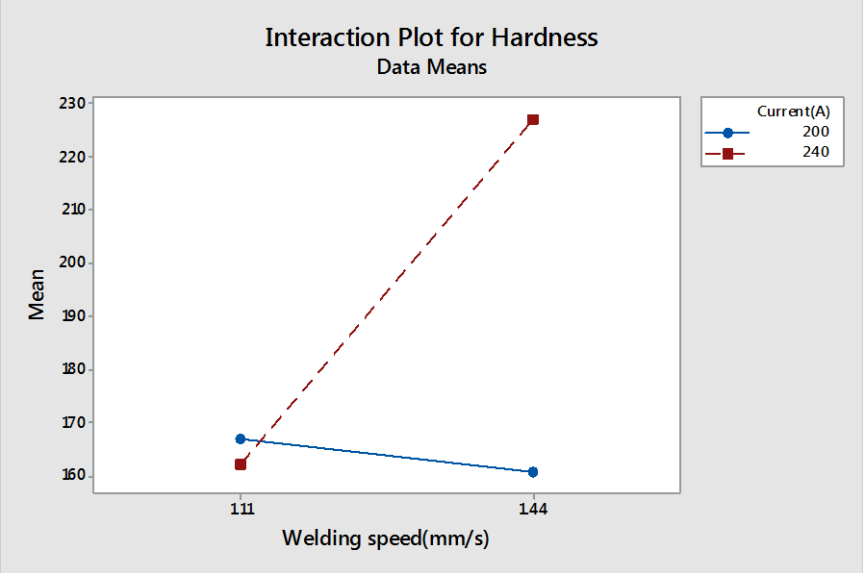


Figure 4: interaction plot of Current vs Welding Speed

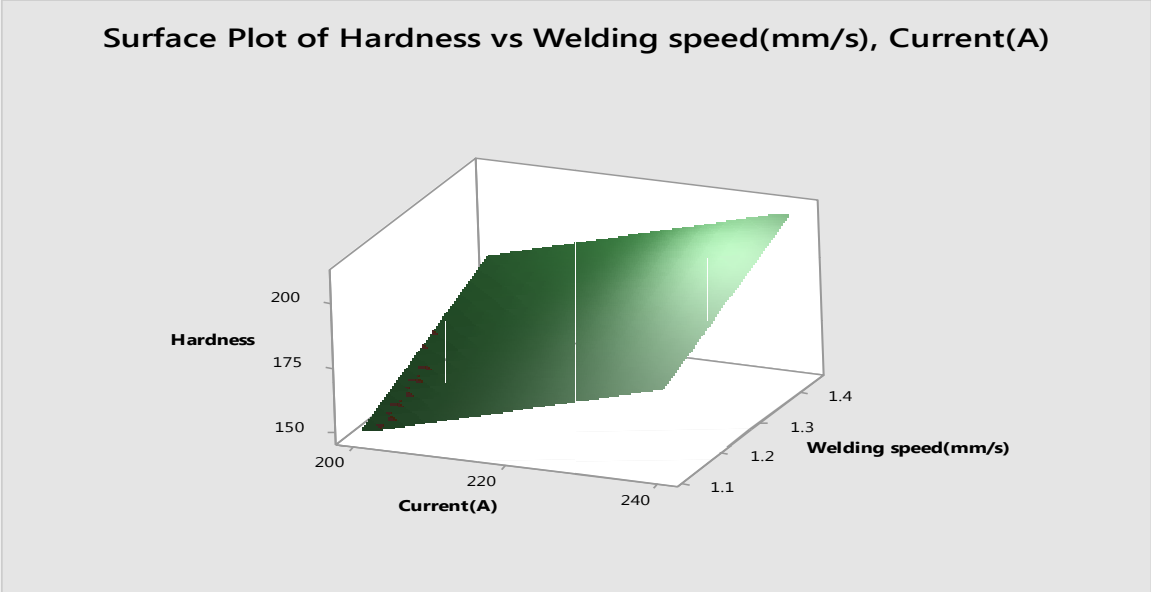


Figure 5: Surface plot of the Weld Hardness vs Welding Speed (mm/s) and Current (A)

V. CONCLUSION

In the present study, the process parameters with significant influence on Weld Hardness was determined by using RSM. A response model of these parameters were developed and found that Current, Welding Speed, and interaction term of Current with Welding Speed significantly affect the Weld Hardness. Weld Hardness is directly proportional to the linear effect of Current and Welding Speed. The higher value of Weld Hardness is achieved with I = 211 A, and Welding Speed = 1.18 mm/s within the experimental domain. The research findings of the present study is based on RSM models, and can be used effectively in joining of Steel with Copper, in order to obtain best possible strength of weld. This research can also help researches and industries for developing a reliable and robust knowledge base along with early prediction of Weld Hardness without experimenting with joining of materials.

REFERENCES

[1]. Chen Shuhai, Huang Jihua, Xia Jun, Zhao Xingke, Lin Sanbao, "Influence of processing parameters on the characteristics of stainlesssteel/copper laser welding", Journal of Materials Processing Technology, Vol. 222, 2015, pp. 43–51
[2]. Chen Y, Weyland M, Hutchinson CR. The effect of interrupted aging on the yield strength and uniform elongation of precipitation-hardened Al alloys. Acta Mater 2013;61:5877–94.
[3]. Cook, LA, & Stavish, MF. (1956). Welding aluminium to copper using the inert gas metal arc process. Welding Journal, 35(5), 348–355.
[4]. Dong HG, Liao CQ, Chen GQ, Dong C. Butt jointing of aluminum to steel by arc brazing process. Mater Manuf Process 2012, 27:1392–6.
[5]. Gorin, LG. (1964). Welding titanium alloys to nickel-base alloys. Welding Products, 11(12), 46–53.
[6]. Korenyuk, YM. (1975). Interaction of liquid aluminium and solid titanium in fusion welding [J]. Welding Production, 22(6), 3–5.
[7]. Lezovskaya, AV, & Rabkin, DM. (1966). Fusion welding aluminum to copper. Automatic Welding, 19(7), 65–66.
[8]. Lv, SX, Jing, XJ, Huang, YX, Xu, YQ, Zheng, CQ, & Yang, SQ. (2012). Investigation on TIG arc welding–brazing of Ti/Al dissimilar alloys with Al based fillers. Science and Technology of Welding and Joining, 17(7), 519–524.
[9]. Mason R. L., Gunst , R. F., Texas D. and Hess J. L., "Statistical Design and Analysis of Experiments With Applications to Engineering and Science", 2nd Edition, A John Wiley & sons publication, 2003.
[10]. Mikhailov, AS, Slonimaky, EV, Senic, AM, & Sukhorukov, AP. (1965). Welding titanium to copper and its alloys. Weld Product, 12(8), 1–6.
[11]. Minitab14, Minitab User Manual Release 14 MINITAB Inc, State College, PA, USA,, 2003.
[12]. Montgomery D. C., "Design and analysis of experiments," John wiley and Sons Inc., 2001.
[13]. Murray, JL. (1982). The magnesium-aluminum phase diagram. Bulletin Alloy Diagrams, 3, 60–74.
[14]. O'Brien, A. (2011). Welding handbook, volume 4 - material and application. Part 1, 9th edn. Doral: American Welding Society (AWS).
[15]. Rana Ramakant, Rajput Kunal, Saini Rohit, Lal Roop, "Opimization of Tool Wear: A Review", International Journal of Modern Engineering Research, Nov, 2014, vol. 4, Issue 11.
[16]. Shao L., Shi Y., Huang J.K., Wua S.J., "Effect of joining parameters on microstructure of dissimilar metal joints between aluminum and galvanized steel", Materials and Design, Vol. 66,2015, pp. 453–458.
[17]. Uzun H, Donne CD, Argagnotto A, Ghidini T, Gambaro C. Friction stir welding of dissimilar Al of 6013-T4 to X5CrNi18-10 stainless steel. Mater Des 2005, 26:41–6.
[18]. Zhang HT, Feng JC, He P, Hackl H. Interfacial microstructure and mechanical properties of aluminum–zinc-coated steel joints made by a modified metal inert gas welding–brazing process. Mater Charact, 2007, 58, pp. 588–92.

ResearchGate

See discussions, stats, and author profiles for this publication at:
http://www.researchgate.net/publication/281715015

Modelling of critical factors for responsiveness in supply chain

ARTICLE · JANUARY 2015

READS
14

1 AUTHOR:



Rajesh Kumar Singh
Delhi Technological University

31 PUBLICATIONS **266** CITATIONS

SEE PROFILE

Available from: Rajesh Kumar Singh
Retrieved on: 04 November 2015

Emerald Insight

Journal of Manufacturing Technology Management

Modelling of critical factors for responsiveness in supply chain
Rajesh Kumar Singh

Article information:

To cite this document:
Rajesh Kumar Singh , (2015),"Modelling of critical factors for responsiveness in supply chain", Journal of Manufacturing Technology Management, Vol. 26 Iss 6 pp. 868 - 888
Permanent link to this document:
http://dx.doi.org/10.1108/JMTM-04-2014-0042

Downloaded on: 12 September 2015, At: 09:24 (PT)
References: this document contains references to 91 other documents.
To copy this document: permissions@emeraldinsight.com
The fulltext of this document has been downloaded 115 times since 2015*

Users who downloaded this article also downloaded:

Sufian Qrunfleh, Monideepa Tarafdar, (2013),"Lean and agile supply chain strategies and supply chain responsiveness: the role of strategic supplier partnership and postponement", Supply Chain Management: An International Journal, Vol. 18 Iss 6 pp. 571-582 http://dx.doi.org/10.1108/SCM-01-2013-0015

Stefan Schaltegger, Roger Burritt, (2014),"Measuring and managing sustainability performance of supply chains: Review and sustainability supply chain management framework", Supply Chain Management: An International Journal, Vol. 19 Iss 3 pp. 232-241 http://dx.doi.org/10.1108/SCM-02-2014-0061

SHEETAL Soda, Anish Sachdeva, Rajeev Kumar Garg, (2015),"GSCM: practices, trends and prospects in Indian context", Journal of Manufacturing Technology Management, Vol. 26 Iss 6 pp. 889-910 http://dx.doi.org/10.1108/JMTM-03-2014-0027

Access to this document was granted through an Emerald subscription provided by emerald-srm:544911 []

For Authors

If you would like to write for this, or any other Emerald publication, then please use our Emerald for Authors service information about how to choose which publication to write for and submission guidelines are available for all. Please visit www.emeraldinsight.com/authors for more information.

About Emerald www.emeraldinsight.com

Emerald is a global publisher linking research and practice to the benefit of society. The company manages a portfolio of more than 290 journals and over 2,350 books and book series volumes, as well as providing an extensive range of online products and additional customer resources and services.

Emerald is both COUNTER 4 and TRANSFER compliant. The organization is a partner of the Committee on Publication Ethics (COPE) and also works with Portico and the LOCKSS initiative for digital archive preservation.

Downloaded by Delhi Technological University At 09:24 12 September 2015 (PT)

*Related content and download information correct at time of download.

Downloaded by Delhi Technological University At 09:24 12 September 2015 (PT)

The current issue and full text archive of this journal is available on Emerald Insight at:
www.emeraldinsight.com/1741-038X.htm

Modelling of critical factors for responsiveness in supply chain

Rajesh Kumar Singh
Mechanical Engineering Department,
Delhi Technological University, Delhi, India

Received 9 April 2014
Revised 16 March 2015
Accepted 22 April 2015

Downloaded by Delhi Technological University At 09:24 12 September 2015 (PT)

Abstract

Purpose – In globalized economy, product life cycle is reducing continuously, customers demands are changing fast, and lead time for response is decreasing. In such scenario, ability of firms to quickly respond to changes in their external environment is a primary determinant of firm's performance. This can be only possible when whole of the supply chain (SC) is responsive. For this, firms have to manage internal operations effectively to enable SC, responsive for market requirements. The purpose of this paper is to identify different factors for responsive SC.

Design/methodology/approach – Based on literature review, total 17 critical factors for the responsive SC have been identified. Some of these factors are process oriented and some are result oriented. To develop structural relationship among these factors from strategic perspective, interpretive structural modeling (ISM) approach has been applied.

Findings – It is observed that top management commitment, strategy development, resource development, use of technology, risk and reward sharing are major drivers for responsive SC. By managing these enablers, organizations can also benefit in terms of inventory management, lead time reduction and agility.

Research limitations/implications – ISM has got some limitations. Major limitation is that the relationships developed are subjective and there are chances of biasing. Therefore findings need to be validated with case studies and empirical findings.

Practical implications – Top management should strive for effective use of resources and technology to improve SC capabilities to meet market changes.

Originality/value – This study develops structural relationships between different factors and it will help organizations in taking initiatives for improving responsiveness.

Keywords Responsiveness, Trust, Value chain, Supply chain management

Paper type Research paper

1. Introduction

In globalized market, organizations are facing tough challenges due to rapid technological changes, shorter product life-cycles and dynamic market requirements. Gunasekaran (2005) has observed that presently manufacturing and logistics operations are increasingly driven by customer needs rather than forecasts. According to van Hoek and Chapman (2006), the growing unpredictability of supply chains (SC) and increased product proliferation has made time-to-market very critical to avoid obsolete inventories. Organizational responsiveness is a central issue in determining business success (Webb and Pettigrew, 1999). In particular, the ability of firms to quickly respond to changes in their external environment is a primary determinant of firm performance (Liao *et al.*, 2003, Charan, 2012). Organizational responsiveness enables companies to quickly detect market changes, reconfigure their processes to meet new market requirements, share

This research paper is part of research project sponsored by Department of Science and Technology, Govt of India. Author is grateful to the sponsoring organization for the support. Author would like to thank Editors of the journal and three unanimous referees for their rigorous review and valuable comments to improve quality and content of the paper.

Journal of Manufacturing Technology Management
Vol. 26 No. 6, 2015
pp. 868-888
© Emerald Group Publishing Limited
1741-038X
DOI 10.1108/JMTM-04-2014-0042

Downloaded by Delhi Technological University At 09:24 12 September 2015 (PT)

information across organizational borders, take maximum advantage of information processing systems and adopt new product and process technologies ahead of their competition. Thus, it is critical to understand the organizational conditions that contribute to the ability of firms to quickly and effectively respond to environmental change. Responsiveness is a critical factor in allowing organizations to develop a competitive advantage (Yu, 2001).

According to Malhotra and Mackelprang (2012), as businesses compete in increasingly complex and rapidly changing environments, managers are continually seeking to make their global SC more responsive. The responsiveness in SC system is defined by the speed with which the system can adjust its output within the available range of four external flexibility types: product, mix, volume and delivery, in response to an external stimulus, e.g. a customer order (Donk and Vaart, 2007). According to Holweg (2005), responsiveness is the ability to react purposefully and within an appropriate time-scale to customer demand or changes in the marketplace, to bring about or maintain competitive advantage. Under such circumstances, organizations need to take a more co-ordinated approach to supply chain management (SCM) and understand where they can remove the non-value adding activities in their total SC. Presently, customers demand greater responsiveness to meet a dynamic set of requirements. New competitive environment exposes local organizations to competition from organizations around the globe. In this new scenario, responsiveness may be one of the most important capabilities needed for firms to achieve competitive advantage (Storey *et al.*, 2005; Reichhart and Holweg, 2007). According to Holweg and Pil (2004), in a market environment of increasing levels of product variety and customization, the ability to respond to customer orders in a timely fashion can provide a critical competitive advantage. Across industry sectors, such as fashion, personal computers, consumer electronics, construction and automobiles, firms are contemplating strategies to increase their responsiveness to customer needs by offering high product variety with short lead-times.

SCM describes the discipline of optimizing the delivery of goods, services and information from supplier to customer in an effective manner (Charan, 2012). Formal definitions of SCM can be marketing oriented or have an operations management orientation (Christopher, 2000) but SCM is concerned with the effectiveness of dealing with final customer demand by the parties engaged in the provision of the product as a whole (Cooper *et al.*, 1997). Actions taken by one member of the chain can influence the responsiveness, efficiency and profitability of the complete SC. Therefore, firms are increasingly thinking in terms of competing SC rather than as a single firm against other individual firms (Govindan *et al.*, 2010). Here, firms have to set internal conditions to enable external SCM in an integrated way. As a matter of fact, integration has been recognized as one of the key dimensions of SCM by many authors (Lee and Ng, 1997; Stock *et al.*, 1998). "Integration" has been defined as the collaborative working between SC partners in a defined field (Christopher, 2000). Thus, the ultimate aim of integration is making the SC more competitive as a whole rather than improving profit of individual organizations.

SC performance depends on the overall performance of the whole value chain and not on individual member's performance. Therefore the main concern of SCM is how to coordinate the independent players to ensure responsiveness for market demands. Coordination among members ensures decreased costs through reduced inventory and shorter order cycle times (Hult *et al.*, 2002), improved quality through better design for manufacturability and faster delivery (Handfield, 1994) and enhanced innovation through more diverse intellectual inputs in the design process (Tan, 2002) and responsiveness in SC. The responsiveness of a SC describes how quickly it responds to

Downloaded by Delhi Technological University At 09:24 12 September 2015 (PT)

customer requirements. A responsive SC ensures reduction in lead time, service reliability, quick response and flexibility. Most of the SCs are not able to sustain global competition because of a lack of responsiveness to meet dynamic market requirements (Singh and Sharma, 2015). Developing strategies for responsive SC is a challenge across all sectors. It requires depth analysis of interaction among major factors responsible for responsiveness. Therefore main objectives of this study are:

- to identify critical success factors of responsiveness in the SC; and
- to establish the structural relationship among these factors of responsiveness.

This paper is organized as follows: Section 2 discusses the literature review for the identification of critical factors of responsiveness. Section 3 is followed by the discussion of the interpretive structural modeling (ISM) methodology and its application. Section 4 presents results and discussion and finally concluding remarks.

2. Literature review

To sustain competitiveness, SCs have to be responsive to meet challenges of shortening product life cycle, decreasing lead time for delivery and manufacturing and increasing variety of products (Singh and Sharma, 2015). Kim *et al.* (2006) have observed that a firm's ability to remain responsive comes not only from the firm itself but also from its SC partners. Singh and Sharma (2015) have observed that SCs should manage their resources, process and performance issues in a cohesive manner. Collaborative efforts and strategic foresights put together by the firm and its SC partners are more likely to enhance SC responsiveness (Moller, 2006). Collaboration among SC partners at various information systems levels is important as it integrates the individual systems of SC partners to provide the infrastructure necessary for effective strategic collaborations and inter-firm information exchange (Kim *et al.*, 2006). Many Indian firms such as Maruti Udyog Ltd, Tata Motors, Mahindra and Mahindra have gotten a competitive advantage due to strong collaboration and partnership between different SC partners at different levels. This is also making their operations more effective and responsive. Kim and Lee (2010) have observed that responsiveness have significant positive relationship with SC performance. Ganesen and Saumen, 2005 have observed that it is important to have top management support for cross-functional training, integration of departments within the organization and vendor development of a responsive SC.

Different SC strategies are appropriate for distinct environmental uncertainties. The success of the SC depends on the effectiveness of resource utilization (Sun *et al.*, 2009). Different resources like money, time, technology, manpower, material are used by the SC (Shin *et al.*, 2000). Kumar *et al.* (2014) have observed that SC strategy should focus on reduction of lead time and product cost simultaneously. Qi *et al.* (2011) have emphasized on the relationship between the firm's SC strategy and firm's business strategy. It is also observed that this synchronization enhances the firm's responsiveness and performance in the marketplace (Qi *et al.*, 2011; Mitra and Bhardwaj, 2010). A key objective of SC strategy should be to enhance the focal firm's SC responsiveness with respect to its customers (Melnyk *et al.*, 2010). Firms benefit greatly if they consider the resources of their SC, such as postponement and strategic supplier partnership in conjunction with their SC strategy and that such a matching yields improved SC responsiveness and firm performance (Qrunfleh and Tarafdar, 2013). Khan *et al.* (2012) have observed that by aligning product design with SC, responsiveness improves and it leads to competitive advantage of focal company.

Downloaded by Delhi Technological University At 09:24 12 September 2015 (PT)

Gunasekaran *et al.* (2008) and Yusuf *et al.* (2004) suggest that agility is needed to enhance the ability of the SC to respond faster to changes in customers' demand and thus improve the responsiveness of the SC. Lee argues that an agile SC strategy allows the SC to respond quickly to short-term changes in customer demand, and consequently enables the focal firm to handle the uncertainty in the market. The strategic development of suppliers and partnerships enable firms to proactively consider all the productivity and quality problems along a value chain (Gunasekaran and Ngai, 2005). This kind of suppliers' partnership requires a high degree of coordination between the organization and its suppliers. It emphasizes a direct association with suppliers, encouraging mutual planning and problem solving efforts, continuous improvement programs, and selection of a few suppliers (Gunasekaran *et al.*, 2001). Collaborative product design can also improve responsiveness and time-to-market. Process and product design modularity has been suggested as an approach for firms to reduce their supply chain risks (SCRs) and to achieve a high degree of flexibility (Kleindorfer and Saad, 2005). Flexibility can be achieved by making SC agile, i.e. adapting quickly and effectively to rapidly changing customer needs (Lin *et al.*, 2006).

It is observed that designed product characteristics should change over time in order to follow: market changes over the product life cycle (Doha *et al.*, 2013) and loss of unique character due to changes in competitors' product values, as can be seen in the example of once new innovative products (Talay *et al.*, 2014). Michiya *et al.* (2015), proposes that firms that want to maintain high competence over time should make efforts to strengthen the four overall SC strategy initiatives, i.e. shortening lead time, enhancing JIT control, improving quality (especially, quality conformance) and stabilizing demand. The strategic approach seems to outperform the reactive approach in terms of developing suppliers to offer their best possible services to companies.

Coordination among SC members also depends upon mutual trust among SC partners. Trust is a favorable attitude that exists when one SC member has confidence in another SC member (Anderson and Narus, 1990). Trust between buyers and suppliers help in improving coordination and thereby responsiveness of the SC (Tejpal *et al.*, 2013). Trust is required for flow of information in the SC. Information sharing between the SC members facilitates responsive SC (Stanley *et al.*, 2009). Information sharing may be of sharing of the inventory data, demand data and product quality data. The traditional communication between the manufacturer and the retailer is made through periodic ordering in large batches. This ordering behavior distorts original demand information because demand variance becomes larger (Ozer, 2003). SC organization's internal integration competence provides complementary information processing capabilities required to yield expected responsiveness from greater SC visibility (Williams *et al.*, 2013). A lack of visibility in a SC causes, consequences such as mistaken decision making, the bullwhip effect, excessive inventories, jeopardizing the profit margin of the whole SC (Prajogo and Olhager, 2012). Researchers generally agree that, for shared information to provide visibility of a high quality, it must be accurate, timely, complete and in a useful format (Barratt and Oke, 2007). Greater visibility into supply and demand conditions enable faster and better decision making for responsive production systems (de Treville *et al.*, 2004).

Risk and reward sharing influence individual SC member behavior and his interaction with other SC members. It also helps in maintaining mutual trust among SC members. Conflicts of interest are likely to occur when existing risk and reward sharing mechanism increases individuals benefit in spite of the benefit of all the SC members (Cachon and Lariviere, 2005). Recently, a study by Aon Risk Solutions reports that, on average, the percentage of global companies reporting a loss of income due to a SCRs have increased

Downloaded by Delhi Technological University At 09:24 12 September 2015 (PT)

from 28 percent in 2011 to 42 percent in 2013 (Saenz and Revilla, 2014). SCRs management is not just about responding to natural disasters. There are many other risks associated with doing business on a daily basis such as daily fluctuations in demand and supply and rapid growth (Sodhi *et al.*, 2008). In order to properly assess SCRs and respond to disruptions, visibility across the SC is required (Hendricks and Singhal, 2012). SC visibility is the capability of sharing on-time and accurate data on customer demand, amount and location of inventory, cost of transportation and other logistics entire SC (Hendricks and Singhal, 2005). Researchers assert that dimensions throughout an SCRs should be regarded as a corporate-level concern with strategic importance (Narasimhan and Talluri, 2009). Risk sharing mechanism pertains to the situation in which a firm aligns the incentives and obligations among SC members regarding how they share the duties to mitigate SCRs and face the consequences of SCRs in their SC (Juttner, 2005). Specifically, this joint practice involves using contracts with terms such as buy-back agreement or revenue sharing to coordinate the relevant SCRM activities (Faisal *et al.*, 2006). Zsidisin and Smith (2005) have observed that firms can manage supply risks through early supplier involvement. Gang *et al.* (2015) have observed that both risk information sharing and risk sharing mechanism improve financial performance, and the effectiveness of the former is strengthened by relationship length and supplier trust, while that of the latter is strengthened by shared SCRM understanding.

Crook and Combs (2007) have observed that both strong and weak members benefit from SCM. Whereas strong members reap most of the direct benefits, weak members can often gain by building switching costs with strong members, leveraging SCM outside the focal chain and increasing survival chances. According to them SCM helps chain members create a rising tide that lifts all boats. According to Mehrjerdi (2009a), collaborative decision making by SC members results in the accurate forecasting of demand, trust between the SC members and flow of timely information. Use of IT technology such as internet, intranet, software application packages and discussion support system can be applied to facilitate the information flow within the SC members (Stanley *et al.*, 2009). According to Hult *et al.* (2007), the firm integrates information systems with its major SC partners to improve data sharing. A collaborative information system makes SC to be more responsive to opportunities and threats arising from global competitors (Kim *et al.*, 2006). According to Gunasekaran and Ngai (2004), implementation of IT in SCM requires a project management approach with the right team for the planning and implementation of IT projects. Bayraktar *et al.* (2010) and Singh (2013) have also stressed the need for the use of information systems to improve the performance of SC.

Top management support is essential in order to provide moral support as well as the financial and technical support for the implementation of IT tools in SC. A co-ordinated SC allows SC members to develop collective capabilities. In turn, this collective capability offers new understanding about the market opportunity (Mehrjerdi, 2009a) and flexibility in SC (Singh and Sharma, 2014). For a lean SC, accurate forecasting of data is required (Michelino *et al.*, 2008). Accurate forecasting of data results in inventory reduction, agility in SC and finally a responsive SC. An integrated inventory management system at every node of the SC minimizes the inventory at SC nodes and makes it responsive (Pawlak and Malyszek, 2008). Coordinating the inventory systems in a SC can be challenging because the companies constituting the SC are often independent from each other and sometimes even compete against each other. As such, the participants in the SC can be reluctant to freely share private cost information, and to let a third party dictate their inventory policies.

Typical SCM goals include production schedule streamlining, inventory reduction, pinpointing of bottlenecks, general improvement of order response time and efforts for

Downloaded by Delhi Technological University At 09:24 12 September 2015 (PT)

SC lead time compression. The "supply chain lead time" is the time spent by the SC to process the raw materials to obtain the final products and deliver them to the customer. It includes supplier lead time, manufacturing lead time, distribution lead time and logistics lead time for transport of raw materials and semi-finished/finished goods. During the last decade, lead time compression has received increasing attention by researchers, because of its potential to generate competitive advantage in the SC, in terms of reduction of inventory levels and costs, and better service level delivered to customers. Furthermore, lead time compression can significantly reduce the bullwhip effect throughout the SC (Disney and Towill, 2003). It also helps in making SC agile. Agility in SC increases the responsiveness of the SC (Mehrjerdi, 2009b, Li *et al.*, 2008). Conflicts in the vision and goals of SC members may result in the individuals profit maximization in place of profit maximization of the whole SC (Arshinder *et al.*, 2006). Long-term orientation is expected to have three specific outcomes, i.e. increased relational behavior, decrease conflicts and increased satisfaction. Availability of point of sales data is important for a responsive SC (Michelino *et al.*, 2008). Responsive SC ensures delivery in time, quick response and accurate forecasting of data (Mehrjerdi, 2009b). Based on the literature, total 17 critical factors influencing responsiveness of SC have been identified. These factors are further summarized in the Table I.

3. Research methodology

Developing relationship model among selected critical factors from literature is very important to put research findings in usable form for organizations and researchers. To develop a structural model among these critical factors for responsiveness and to determine the relationship between dependent and drivers, ISM methodology has been used. ISM is an interactive learning process. The method is interpretive in that the group's judgment decides whether and how items are related; it is structural relationships among elements of a system (Sage, 1977). However, the direct and indirect relationships between the factors describe the situation far more accurate than the individual factor taken in isolation. Therefore, ISM develops insights into collective understandings of these relationships. However, for developing relationships between two variables, experience of experts/respondents is very crucial. For the developing relationship between different factors, a team of five experts was formed. Three experts were from industry and two were from academia. It may be noted here that this team was constituted only to develop the relationship between factors. Reliability test of these factors was done separately as a part of a research project (unpublished work) and Cronbach's α value for all these factors was found 0.83, i.e. more than the minimum requirement of 0.5 (Nunnally, 1978).

3.1 ISM

For developing structural relationship among variables, ISM is widely used technique. Jharkharia and Shankar (2005) applied ISM for understanding the barriers in IT – enablement of SC. Singh *et al.* (2007a, b) have used ISM methodology for implementation of AMTs and for improving SMEs competitiveness, respectively. The application of ISM typically forces managers to reassess perceived priorities and improve their understanding of the linkages among key concerns. The various steps involved in the ISM technique are:

(1) Identification of elements, which are relevant to the problem or issues, this could be done by literature review or any group problem solving technique.

Downloaded by Delhi Technological University At 09:24 12 September 2015 (PT)

S.N.	Critical factors	References
1	Top management commitment	Ganesen and Saumen, 2005, Arshinder *et al.* (2008), Singh and Sharma (2015)
2	Strategy development	Ganesen and Saumen, 2005, Melnyk *et al.* (2010), Sun *et al.* (2009), Mitra and Bhardwaj (2010), Qi *et al.* (2011), Khan *et al.* (2012), Doha *et al.* (2013), Talay *et al.* (2014), Kumar *et al.* (2014), Singh and Sharma (2015), Michiya *et al.* (2015)
3	Resource development	Shin *et al.* (2000), Singh (2013), Singh and Sharma (2015)
4	Trust development between SC members	Anderson and Narus (1990), Sahay (2003), Tejpal *et al.* (2013)
5	Information sharing between SC members	Ramdas and Spekman (2000), Ozer (2003), Stanley *et al.* (2009), Barratt and Oke (2007), Hendricks and Singhal (2012), de Treville *et al.* (2004)
6	Risk and reward sharing by SC members	Cachon and Lariviere, 2005, Lee (2000), Zsidisin and Smith (2005), Juttner (2005), Faisal *et al.* (2006), Sodhi *et al.* (2008), Saenz and Revilla (2014), Narasimhan and Talluri (2009), Gang *et al.* (2015)
7	Collaborative decision making and planning by supply chain members	Tsay (1999), Cachon and Fisher (2000), Disny and Towill (2003), Kim and Lee (2010), Mehrjerdi (2009a)
8	Use of IT technology	Lee *et al.* (1997), Hult *et al.* (2007), Kim *et al.* (2006), Stanley *et al.* (2009)
9	Co-ordinated supply chain	Mehrjerdi (2009b), Singh (2013), Kumar *et al.* (2014)
10	Accurate forecasting of data by SC Members	Michelino *et al.* (2008), Hendricks and Singhal (2005), Pawlak and Malyszek (2008)
11	Integrated inventory management by SC members	Sahay (2003), Hendricks and Singhal (2005), Pawlak and Malyszek (2008)
12	Lead time reduction	Forza and Vinelli (2000), Disney and Towill (2003), Gunasekaran *et al.* (2001)
13	Agility in supply chain	Li *et al.* (2008), Gunasekaran *et al.* (2008), Mehrjerdi (2009b), Lin *et al.* (2006), Qrunfleh and Tarafdar (2013)
14	Agreed vision and goals of the SC members	Togar *et al.* (2002), Arshinder *et al.* (2006), Kumar *et al.* (2014)
15	Long-term relationship between supply chain members	Olorunniwo and Hartfield (2001), Tejpal *et al.* (2013)
16	Availability of point of sales data	Michelino *et al.* (2008), Pawlak and Malyszek (2008), Prajogo and Olhager (2012)
17	Responsiveness in supply chain	Yu (2001), Storey *et al.* (2005); Reichhart and Holweg (2007), Mehrjerdi (2009b), Kim and Lee (2010), Malhotra and Mackelprang (2012),Singh (2013), Williams *et al.* (2013)

Table I.
Factors for responsive supply chain

(2) Establishing a contextual relationship between elements with respect to which pairs of elements will be examined.

(3) Developing a structural self-interaction matrix (SSIM) of elements, which indicates the pair-wise relationship between elements of the system?

(4) Developing a reachability matrix from the SSIM, and checking the matrix for transitivity. Transitivity of the contextual relation is a basic assumption in ISM which states that if element A is related to B and B is related to C, then A will be necessarily related to C.

(5) Partitioning of a reachability matrix into different levels.

(6) Based on the relationships given above in the reachability matrix draw a directed graph (digraph), and remove transitive links.

(7) Convert the resultant digraph into an ISM, by replacing element nodes with statements.

(8) Review the ISM model to check for conceptual inconsistency, and make the necessary modifications.

Above described steps, which lead to the development of ISM model, are discussed below.

3.1.1 SSIM. For analyzing the criteria a contextual relationship of "leads to" is chosen here. For developing contextual relationships among different factors/variables, expert opinion based on management technique such as brainstorming was considered. Final decision was taken based on majority decision of five experts. For expressing the relationship between different factors for responsiveness in SC, four symbols have been used to denote the direction of the relationship between the parameters i and j (here $i < j$):

- V: parameter i will lead to parameter j;
- A: parameter j will lead to parameter i;
- X: parameter i and j will lead to each other; and
- O: parameters i and j are unrelated.

The following statements explain the use of symbols V, A, X and O in SSIM:

- variable 1 leads to 5 (V);
- variable 4 and 5 lead to each other (X); and
- Variables 14 and 16 are unrelated (O).

Based on contextual relationships the SSIM is developed in Table II.

3.1.2 Reachability matrix. The SSIM has been converted into a binary matrix, called the initial reachability matrix by substituting V, A, X and O by 1 and 0 as per the case. The substitution of 1s and 0s are as per the following rules:

(1) if the (i, j) entry in the SSIM is V, the (i, j) entry in the reachability matrix becomes 1 and the (j, i) entry becomes 0;

(2) if the (i, j) entry in the SSIM is A, the (i, j) entry in the reachability matrix becomes 0 and the (j, i) entry becomes 1;

(3) if the (i, j) entry in the SSIM is X, the (i, j) entry in the reachability matrix becomes 1 and the (j, i) entry also becomes 1; and

(4) if the (i, j) entry in the SSIM is O, the (i, j) entry in the reachability matrix becomes 0 and the (j, i) entry also becomes 0.

Following above rules, the initial reachability matrix for the critical success factors is shown in Table III.

3.1.3 Final reachability matrix. After incorporating the transitivity as described in Step (4) of the ISM methodology, the final reachability matrix is shown in Table IV. There is only one transitivity that exists between trust development between SC members (4) and use of IT technology (8). So in row 8 and column 4, zero is replaced by one in the final reachability matrix (Table IV). In Table IV, the driving power and

Downloaded by Delhi Technological University At 09:24 12 September 2015 (PT)

Downloaded by Delhi Technological University At 09:24 12 September 2015 (PT)

Sr. No.	Critical factors	1	2	3	4	5	6	7	8	9	10	11	12	13	14	15	16	17
1	Top management commitment		V	V	V	V	V	V	V	V	V	V	V	V	V	V	V	V
2	Strategy development			O	V	V	V	V	V	V	V	V	V	V	V	V	V	V
3	Resource development				V	V	O	O	V	V	V	V	V	V	V	V	V	V
4	Trust development between SC members					X	A	A	O	V	V	V	V	V	V	V	V	V
5	Information sharing between SC members						A	A	A	V	V	V	V	V	V	V	V	V
6	Risk and reward sharing by SC members							X	O	V	V	V	V	V	V	V	V	V
7	Collaborative decision making by SC members								O	V	V	V	V	V	V	V	V	V
8	Use of IT technology									V	V	V	V	V	V	V	V	V
9	Co-ordinated supply chain										V	V	V	V	A	A	A	V
10	Accurate forecasting of data by SC members											V	V	V	A	A	A	V
11	Integrated inventory management												V	V	A	A	A	V
12	Lead time reduction													V	A	A	A	V
13	Agility in SC														A	A	A	V
14	Agreed vision and goals															X	O	V
15	Long-term relationship between SC members																O	V
16	Availability of point of sales data																	V
17	Responsiveness in SC																	

Table II.
Structural self-interaction matrix of factors for responsive supply chain

Sr. No.	Critical factors	1	2	3	4	5	6	7	8	9	10	11	12	13	14	15	16	17
1	Top management commitment	1	1	1	1	1	1	1	1	1	1	1	1	1	1	1	1	1
2	Strategy development	0	1	0	1	1	1	1	1	1	1	1	1	1	1	1	1	1
3	Resource development	0	0	1	1	1	0	0	1	1	1	1	1	1	1	1	1	1
4	Trust development between SC members	0	0	0	1	1	0	0	0	1	1	1	1	1	1	1	1	1
5	Information sharing between SC members	0	0	0	1	1	0	0	0	1	1	1	1	1	1	1	1	1
6	Risk and reward sharing by SC members	0	0	0	1	1	1	1	0	1	1	1	1	1	1	1	1	1
7	Collaborative decision making by SC members	0	0	0	1	1	1	1	0	1	1	1	1	1	1	1	1	1
8	Use of IT technology	0	0	0	0	1	0	0	1	1	1	1	1	1	1	1	1	1
9	Co-ordinated supply chain	0	0	0	0	0	0	0	0	1	1	1	1	1	0	0	0	1
10	Accurate forecasting of data by SC members	0	0	0	0	0	0	0	0	0	1	1	1	1	0	0	0	1
11	Integrated inventory management	0	0	0	0	0	0	0	0	0	0	1	1	1	0	0	0	1
12	Lead time reduction	0	0	0	0	0	0	0	0	0	0	0	1	1	0	0	0	1
13	Agility in SC	0	0	0	0	0	0	0	0	0	0	0	0	1	0	0	0	1
14	Agreed vision and goals	0	0	0	0	0	0	0	0	1	1	1	1	1	1	1	0	1
15	Long-term relationship between SC members	0	0	0	0	0	0	0	0	1	1	1	1	1	1	1	0	1
16	Availability of point of Sales data	0	0	0	0	0	0	0	0	1	1	1	1	1	0	0	1	1
17	Responsiveness in SC	0	0	0	0	0	0	0	0	0	0	0	0	0	0	0	0	1

Table III.
Initial reachability matrix of factors for responsive supply chain

Downloaded by Delhi Technological University At 09:24 12 September 2015 (PT)

Table IV. Final reachability matrix of factors for responsive supply chain

Sr. No.	Critical factors	1	2	3	4	5	6	7	8	9	10	11	12	13	14	15	16	17	DP
1	Top management commitment	1	1	1	1	1	1	1	1	1	1	1	1	1	1	1	1	1	17
2	Strategy development	0	1	0	1	1	1	1	1	1	1	1	1	1	1	1	1	1	15
3	Resource development	0	0	1	1	1	0	0	1	1	1	1	1	1	1	1	1	1	13
4	Trust development between SC members	0	0	0	1	1	0	0	0	1	1	1	1	1	1	1	1	1	11
5	Information sharing between members	0	0	0	1	1	0	0	0	1	1	1	1	1	1	1	1	1	11
6	Risk and reward sharing by SC members	0	0	0	1	1	1	1	0	1	1	1	1	1	1	1	1	1	13
7	Collaborative decision making by SC members	0	0	0	1	1	1	1	0	1	1	1	1	1	1	1	1	1	13
8	Use of IT technology	0	0	0	1	1	0	0	1	1	1	1	1	1	1	1	1	1	12
9	Co-ordinated supply chain	0	0	0	0	0	0	0	0	1	1	1	1	1	0	0	0	1	6
10	Accurate forecasting of data by SC members	0	0	0	0	0	0	0	0	0	1	1	1	1	0	0	0	1	5
11	Integrated inventory management	0	0	0	0	0	0	0	0	0	0	1	1	1	0	0	0	1	4
12	Lead time reduction	0	0	0	0	0	0	0	0	0	0	0	1	1	0	0	0	1	3
13	Agility in SC	0	0	0	0	0	0	0	0	0	0	0	0	1	0	0	0	1	2
14	Agreed vision and goals	0	0	0	0	0	0	0	0	1	1	1	1	1	1	1	0	1	8
15	Long-term relationship between SC members	0	0	0	0	0	0	0	0	1	1	1	1	1	1	1	0	1	8
16	Availability of point of sales data	0	0	0	0	0	0	0	0	1	1	1	1	1	0	0	1	1	7
17	Responsiveness in SC	0	0	0	0	0	0	0	0	0	0	0	0	0	0	0	0	1	1
Dependence		1	2	3	8	8	4	4	4	12	13	14	15	16	10	10	9	17	149

Note: DP, driving power

Downloaded by Delhi Technological University At 09:24 12 September 2015 (PT)

dependence of each variable is also shown. Driving power for each variable is the total number of variables (including itself), which it may help to achieve. On the other hand, dependence is the total number of variables (including itself), which may help in achieving it. These driving powers and dependencies will be later used in the classification of variables into the four groups, i.e. autonomous, dependent, linkage and drivers (independent).

3.1.4 Level partition. From the final reachability matrix, the reachability and antecedent set for each factor are found. The reachability set consists of the element itself and other elements to which it may help achieve, whereas the antecedent set consists of the element itself and the other elements which may help in achieving it. Then the intersection of these sets is derived for all elements. The element for which the reachability and intersection sets are same is the top-level element in the ISM hierarchy. The top-level element of the hierarchy would not help in achieving any other element above their own. Once the top-level element is identified, it is separated out from the other elements. Then by the same process, the next level of elements is found. These identified levels help in building the diagraph and final model. From Table V, it is seen that the performance improvement is found at level I. Thus, it would be positioned at the top of the ISM hierarchy. This iteration process is repeated till the levels of all factors are decided. Results of all iterations for deciding levels are shown in Table VI. The identified levels aids in building the final model of the ISM.

3.1.5 Classification of factors. In this section, the critical factors described earlier are classified into four clusters (Figure 1). The first cluster consists of the "autonomous factors" that have weak driving power and weak dependence. These factors are relatively disconnected from the system, with which they have only few links, which may not be strong. The "dependent factors" constitute the second cluster, which has weak driving power but strong dependence. Third cluster has the "linkage factors" that have strong driving power and strong dependence. These factors are unstable due to the fact that any change occurring to them will have an effect on others and also a feedback on themselves. Fourth cluster includes the

Table V.
Iteration 1

Sr. No.	Reachability set	Antecedent set	Intersection set	Level
1.	1,2,3,4,5,6,7,8,9,10,11,12,13,14,15,16,17	1	1	
2.	2,4,5,6,7,8,9,10,11,12,13,14,15,16,17	1,2	2	
3.	3,4,5,8,9,10,11,12,13,14,15,16,17	1,3	3	
4.	4,5,9,10,11,12,13,14,15,16,17	1,2,3,4,5,6,7,8	4,5	
5.	4,5,9,10,11,12,13,14,15,16,17	1,2,3,4,5,6,7,8	4,5	
6.	4,5,6,7,9,10,11,12,13,14,15,16,17	1,2,6,7	6,7	
7.	4,5,6,7,9,10,11,12,13,14,15,16,17	1,2,6,7	6,7	
8.	4,5,8,9,10,11,12,13,14,15,16,17	1,2,3,8	8	
9.	9,10,11,12,13,17	1,2,3,4,5,6,7,8,9,14,15,16	9	
10.	10,11,12,13,17	1,2,3,4,5,6,7,8,9,10,14,15,16	10	
11.	11,12,13,17	1,2,3,4,5,6,7,8,9,10,11,14,15,16	11	
12.	12,13,17	1,2,3,4,5,6,7,8,9,10,11,12,14,15,16	12	
13.	13,17	1,2,3,4,5,6,7,8,9,10,11,12,13,14,15,16	13	
14.	9,10,11,12,13,14,15,17	1,2,3,4,5,6,7,8,14,15	14,15	
15.	9,10,11,12,13,14,15,17	1,2,3,4,5,6,7,8,14,15	14,15	
16.	9,10,11,12,13,16,17	1,2,3,4,5,6,7,8,16	16	
17.	17	1,2,3,4,5,6,7,8,9,10,11,12,13,14,15,16,17	17	I

Critical factors	Reachability matrix	Antecedent set	Intersection set	Level
1	1	1	1	XI
2	2	1,2	2	X
3	3	1,3	3	X
4	4,5	1,2,3,4,5,6,7,8	4,5	VIII
5	4,5	1,2,3,4,5,6,7,8	4,5	VIII
6	6,7	1,2,6,7	6,7	IX
7	6,7	1,2,6,7	6,7	IX
8	8	1,2,3,8	8	IX
9	9	1,2,3,4,5,6,7,8,9,14,15,16	9	VI
10	10	1,2,3,4,5,6,7,8,9,10,14,15,16	10	V
11	11	1,2,3,4,5,6,7,8,9,10,11,14,15,16	11	IV
12	12	1,2,3,4,5,6,7,8,9,10,11,12,14,15,16	12	III
13	13	1,2,3,4,5,6,7,8,9,10,11,12,13,14,15,16	13	II
14	14,15	1,2,3,4,5,6,7,8,14,15	14,15	VII
15	14,15	1,2,3,4,5,6,7,8,14,15	14,15	VII
16	16	1,2,3,4,5,6,7,8,16	16	VII
17	17	1,2,3,4,5,6,7,8,9,10,11,12,13,14,15,16,17	17	I

Table VI.
Level partitions for critical factors based on multiple iterations

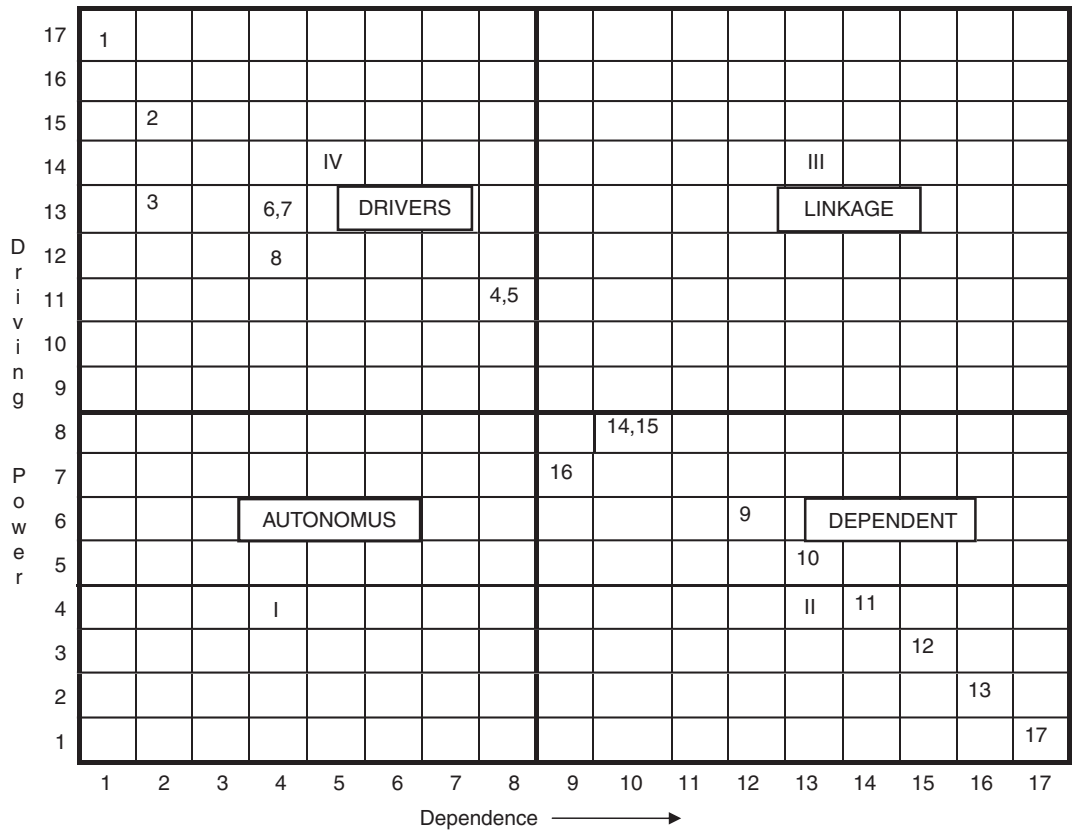


Figure 1.
Driving power and dominance diagram of the enablers

"independent factors" having strong driving power but weak dependence. The driving power and dependence of each of these factors are shown in Table IV. In this table, an entry of "1" added along the columns and rows indicates the dependence and driving power, respectively. Subsequently, the driver

Downloaded by Delhi Technological University At 09:24 12 September 2015 (PT)

Downloaded by Delhi Technological University At 09:24 12 September 2015 (PT)

power-dependence diagram is constructed as shown in Figure 2. For illustration, the factor 5 having a driving power of 11 and dependence of 8 is positioned in a place corresponding to driving power of 11 and dependency of 8 in the Figure 1. Similarly all other factors considered in this study are positioned on different quadrants depending on their driving power and dependency.

3.1.6 Formation of ISM. Digraph of the factors for responsive SC represents the relationship between the factors. From the final reachability matrix (Table IV), the structural model is generated by means of vertices or nodes and lines of the edges. If there is a relationship between the factors *i* and *j* this is shown by an arrow which points from *i* to *j*. This graph is called a directed graph or digraph as shown in Figure 2. After incorporating the transitivity as described in ISM methodology, the digraph is finally converted into ISM as shown in Figure 3.

4. Result and discussion

ISM model of the critical factors for responsive SC indicates the relationship between different critical factors and also gives the level of critical factors as

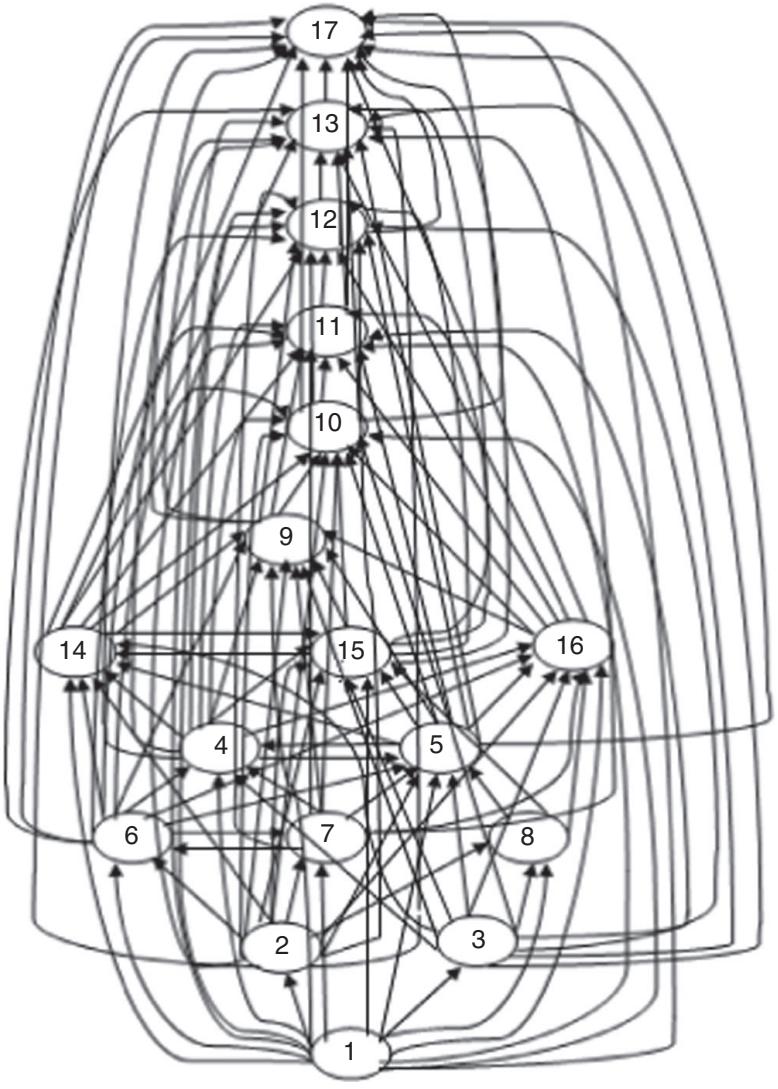


Figure 2.
Digraph of factors for responsive supply chain showing relationship between the factors

Downloaded by Delhi Technological University At 09:24 12 September 2015 (PT)

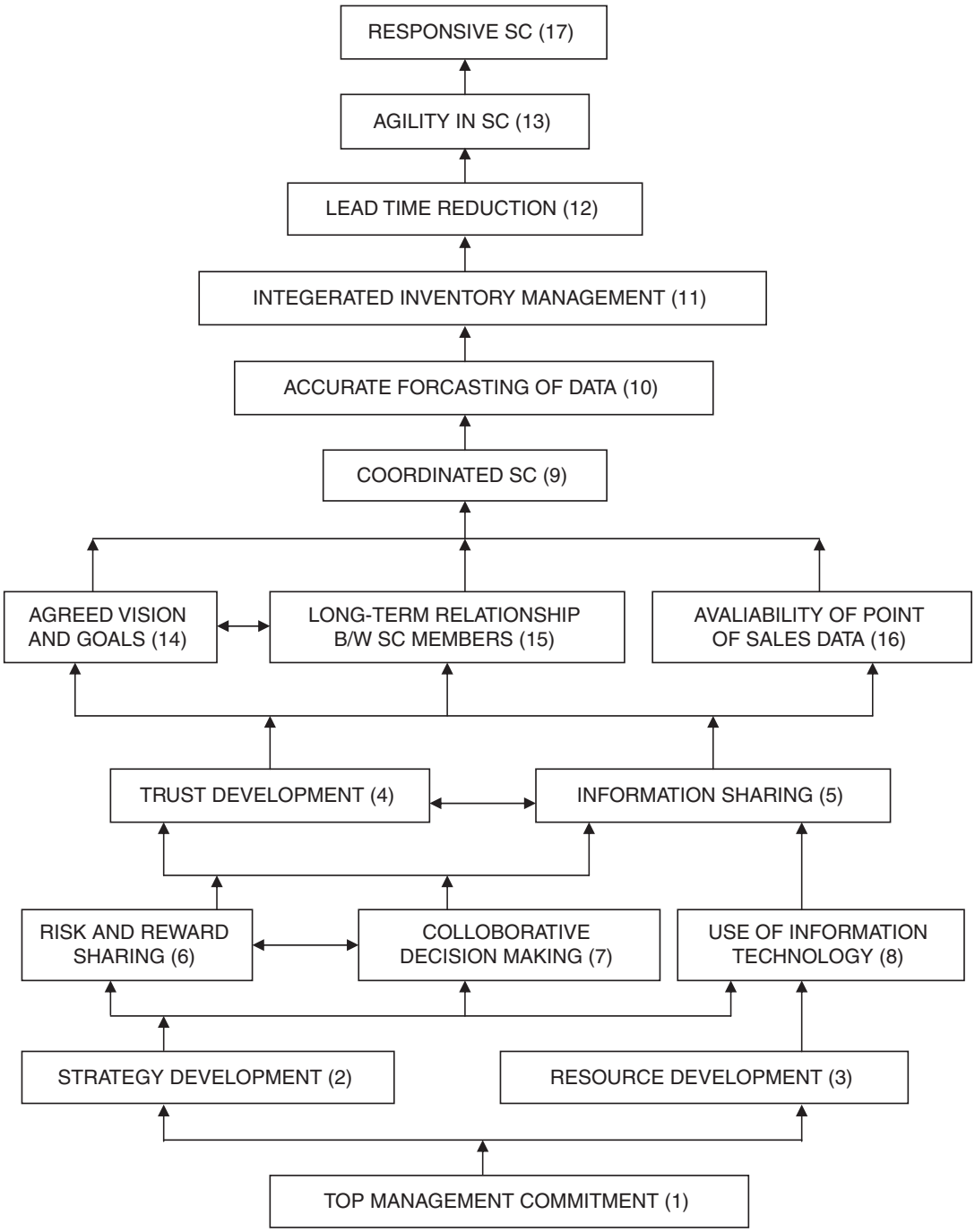


Figure 3.
ISM-based modal for critical factors of responsiveness in SC

determined in different iterations (Table VI). Driving power and dependence diagram of the critical factors for responsive SC divides the factors in four categories such as: autonomous, dependent, linkages and drivers due to which analysis of factors becomes easier:

- Autonomous variables generally appear as weak driver as well as weak dependent and are relatively disconnected from the system. These variables do not have much influence on the other variables of the system. Figure 1 shows that there is no autonomous factor for responsive SC.

Downloaded by Delhi Technological University At 09:24 12 September 2015 (PT)

- There is no linkage variable which has a strong driving power as well as strong dependence. Thus, it can be inferred that among all the 17 variables chosen in this study, no variable is unstable.
- The driver power-dependence diagram indicates that variables such as top management commitment, strategy development, resource development, trust development, information sharing, risk and rewards sharing, collaborative decision making and planning and use of IT technology are at the bottom of the model having strong driving power. These variables will help organizations to achieve a co-ordinated and responsive SC and are classified as independent variables or drivers.
- From the ISM model (Figure 3), it is observed that responsiveness is at the top. Agility in SC is at the second level. Reduction in lead time is at the third level. Integrated inventory management is at fourth level. Accurate forecasting of data is at fifth level. Co-ordinated SC is at sixth level. The remaining variables are at the lower levels. This finding implies that co-ordinated SC will help in reducing lead time, product cost and delivery time. It will also improve accurate forecasting of data and agility in the SC. Finally, all these factors will lead to a responsive SC.
- Top management commitment, strategy development and resource development are at the bottom level with highest driving power. It means top management commitment; strategy development and resource development are the major drivers for improving responsiveness of the SC.

5. Conclusion

These days competition is between integrated SC rather than individual organizations in isolation. To be more competitive and responsive for meeting dynamic market requirements, a SC should be well co-ordinated. This study has identified 17 factors from the literature for analyzing SC responsiveness. These factors are top management commitment, strategy development, resource development, trust development, information sharing between SC members, risk and reward sharing, collaborative decision making, use of IT technology, co-ordinated SC, accurate forecasting of data, integrated inventory management, lead time reduction, agility of SC, agreed vision and goals, long-term relationship between SC members, availability of point of sales data and responsiveness in SC. The ISM approach has been employed to develop the structural relationship among these factors. ISM approach helped in determining driving and dependence power for all these factors. It is observed that top management commitment, strategy development and resource development are major drivers for improving responsiveness in SC. These factors help in achieving integrated inventory management, lead time reduction, agility and responsiveness in SC through trust development, information sharing, collaborative decision making and accurate forecasting of data. Therefore major implication of this research is that for SC responsiveness, top management should be proactive in taking different initiatives to improve resource utilization and strategy implementation. For academicians, this research gives good scope for future research to analyze coordination and responsiveness issues of humanitarian SC in case of unplanned or accidental events, disasters such as earthquake and floods.

In this research, through ISM, a relationship model among different critical factors has been developed on the basis of experts' opinion. Structural equation modeling, also commonly known as linear structural relationship approach can be applied for testing

the validity of such hypothetical model as well as to analyze exact importance of these factors on responsiveness as future scope of study. Although present study has tried to involve major factors for responsiveness of SC but some researchers such as Kim (2000) has also talked about inter-firm power and channel climate for coordination in SC. Channel climate is based on collective perceptions about different attributes of responsive SC. Hunt and Nevin (1974) have also observed that powerful member in a SC can influence whole mechanism of coordination and bargaining power of different members in SC. It will change SC responsiveness perspective. Therefore in addition to these power-related factors, other uncontrollable factors related to accidents, floods and earthquakes and dynamic relationship among different factors with time can be also included in future research framework and effective resilient SC can be proposed. For generalizing these findings, some case studies should be carried out to validate the model under dynamic and uncontrollable conditions.

Downloaded by Delhi Technological University At 09:24 12 September 2015 (PT)

References

Anderson, J.C. and Narus, J.A. (1990), "A model of distributor firm and manufacturer firm working partnerships", *Journal of Marketing*, Vol. 54, pp. 42-58.

Arshinder, Kanda, A. and Desmukh, S.G. (2006), "Supply chain coordination issues: an SAP-LAP frame work", *Asia Pacific Journal of Marketing and Logistics*, Vol. 19 No. 3, pp. 240-264.

Arshinder, Kanda, A. and Desmukh, S.G. (2008), "Supply chain coordination: perspectives, empirical studies and research directions", *International Journal of Production Economics*, Vol. 115, pp 33-316.

Barratt, M. and Oke, A. (2007), "Antecedents of supply chain visibility in retail supply chains: a resource-based theory perspective", *Journal of Operations Management*, Vol. 25 No. 6, pp. 1217-1233.

Bayraktar, E., Gunasekaran, A., Lenny K., Tatoglu, M.D. and Zaim, S. (2010), "An efficiency comparison of supply chain management and information systems practices: a study of turkish and bulgarian small- and medium-sized enterprises in food products and beverages", *International Journal of Production Research*, Vol. 48 No. 2, pp 425-451.

Cachon, G.P. and Fisher, M. (2000), "Supply chain inventory management and value of shared information", *Management Science*, Vol. 46 No. 8, pp. 48-1032.

Cachon, G.P. and Lariviere, M.A. (2005), "Supply chain coordination with revenue sharing contracts: strengths and limitations", *Management Science*, Vol. 51 No. 1, pp. 30-44.

Charan, P. (2012), "Supply chain performance issues in an automobile company: a SAP-LAP analysis", *Measuring Business Excellence*, Vol. 16 No. 1, pp. 67-86.

Christopher, M. (2000), "The agile supply chain: competing in volatile markets", *Industrial Marketing Management*, Vol. 29, pp. 37-44.

Cooper, M.C., Lambert, D.M. and Pagh, J.D. (1997), "Supply chain management: more than a new name for logistics", *The International Journal of Logistics Management*, Vol. 8 No. 1, pp. 1-13.

Crook, T.R. and Combs, J.G. (2007), "Sources and consequences of bargaining power in supply chains", *Journal of Operations Management*, Vol. 25 No. 2, pp. 546-555.

de Treville, S., Shapiro, R.D. and Hameri, A.P. (2004), "From supply chain to demand chain: the role of lead time reduction in improving demand chain performance", *Journal of Operations Management*, Vol. 21 No. 6, pp. 613-627.

Disny, S.M. and Towill, D.R. (2003), "Vendor managed inventory and bullwhip effect reduction in a two level supply chain", *International Journal of Operations and Production Management*, Vol. 23 No. 6, pp. 625-651.

Downloaded by Delhi Technological University At 09:24 12 September 2015 (PT)

Doha, A., Das, A. and Pagell, M. (2013), "The influence of product life cycle on the efficacy of purchasing practices", *Int. J. Operations and Production Management*, Vol. 33 No. 4, pp. 470-498.

Donk, D.P.V. and Vaart, T.V.D. (2007), "Responsiveness through buyer-focused cells: exploring a new supply strategy", *International Journal of Operations & Production Management*, Vol. 27 No. 12, pp. 1362-1379.

Faisal, M.N., Banwet, D.K. and Shankar, R. (2006), "Supply chain risk mitigation: modeling the enablers", *Business Process Management Journal*, Vol. 12 No. 4, pp. 535-552.

Forza, C. and Vinelli, A. (2000), "Time compression in production and distribution within the textile-apparel chain", *Integrated Manufacturing Systems*, Vol. 11 No. 2, pp. 138-146.

Ganesen, K. and Saumen, B. (2005), "Corporate turnaround through effective supply chain management: the case of a leading jewellery manufacturer in India", *Supply Chain Management: An International Journal*, Vol. 10 No. 5, pp. 340-348.

Gang L., Huan F., Peter K.C., Lee, T.C.E. and Cheng (2015), "Joint supply chain risk management: an agency and collaboration perspective", *International Journal of Production Economics*, available at: http://dx.doi.org/10.1016/j.ijpe.2015.02.021, in press.

Govindan, K., Kanan, D. and Haq, A.N. (2010), "Analyzing supplier development criteria for an automobile industry", *Industrial Management & Data Systems*, Vol. 110 No. 1, pp. 43-62.

Gunasekaran, A. (2005), "The build-to-order supply chain (BOSC): a competitive strategy for the 21st century", *Journal of Operations Management*, Vol. 23 No. 5, pp. 419-422.

Gunasekaran, A. and Ngai, E.W.T. (2004), "Information systems in supply chain integration and management", *European Journal of Operations Research*, Vol. 159, pp. 269-295.

Gunasekaran, A. and Ngai, E.W.T. (2005), "Build-to-order supply chain management: a literature review and framework for development", *Journal of Operations Management*, Vol. 23, pp. 423-451.

Gunasekaran, A., Laib, K. and Cheng , T.C.E. (2008), "Responsive supply chain: a competitive strategy in a networked economy", *Omega*, Vol. 36, pp. 549-564.

Gunasekaran, A., Patel, C. and Tirtiroglu, E. (2001), "Performance measures and metrics in a supply chain environment", *International Journal of Operations & Production Management*, Vol. 21 Nos 1-2, pp. 71-87.

Handfield, R. (1994), "US global sourcing: patterns of development", *International Journal of Operations and Production Management*, Vol. 14 No. 6, pp. 40-51.

Hendricks, K.B. and Singhal, V.R. (2005), "An empirical analysis of the effect of supply chain disruptions on long-run stock price performance and equity risk of the firm", *Prod. Oper. Manag*, Vol. 14 No. 1, pp. 35-52.

Hendricks, K.B. and Singhal, V.R. (2012), "Supply chain disruptions and corporate performance, in Gurnani, H., Mehrotra, A. and Ray, S. (Eds), *Supply Chain Disruptions: Theory and Practice of Managing Risks*, Springer, London, pp. 1-19.

Holweg, M. (2005), "The three dimensions of responsiveness", *International Journal of Operations & Production Management*, Vol. 25 No. 7, pp. 603-622.

Holweg, M. and Pil, F.K. (2004), *The Second Century: Reconnecting Customers and Value Chain Through Build-to-Order*, The MIT Press, Cambridge, MA.

Hult, G.T.M., Ketchen, D. and Nichols, E. (2002), "An examination of cultural competitiveness and order fulfilment cycle time within supply chains", *Academy of Management Journal*, Vol. 45 No. 3 pp. 577-586.

Downloaded by Delhi Technological University At 09:24 12 September 2015 (PT)

Hult, G.T.M., Ketchen, D.J. and Arrfelt, M. (2007), "Strategic supply chain management: improving performance through a culture of competitiveness and knowledge development", *Strategic Management Journal*, Vol. 28 No. 10, pp. 1035-1052.

Hunt and Nevin (1974), "Power in a channel of distribution: sources and consequences", *Journal of Marketing Research*, Vol. 11 No. 2, pp. 186-193.

Jharkharia, S. and Shankar, R. (2005), "IT-enablement of supply chains: understanding the barriers", *The Journal of Enterprise Information Management*, Vol. 18 No. 1, pp. 285-309.

Juttner, U. (2005), "Supply chain risk management: understanding the business requirements from a practitioner perspective", *International Journal of Logistics Management*, Vol. 16 No. 1, pp. 120-141.

Khan, O., Christopher, M. and Creazza, A. (2012), "Aligning product design with the supply chain: a case study", *Supply Chain Management: An International Journal*, Vol. 17 No. 3, pp. 323-336.

Kim, D. and Lee, R. (2010), "Systems collaboration and strategic collaboration: their impacts on supply chain responsiveness and market performance", *Decision Sciences*, Vol. 41 No. 4, pp. 955-981.

Kim, D., Cavusgil, S.T. and Calantone, R.J. (2006), "Information system innovations and supply chain management: channel relationships and firm performance", *Journal of Academy of Marketing Science*, Vol. 34 No. 1, pp. 40-54.

Kim, K. (2000), "On inter firm power, channel climate, and solidarity in industrial distributor-supplier dyads", *Journal of Academy of Marketing Science*, Vol. 28 No. 3, pp. 388-405.

Kleindorfer, P.R. and Saad, G.H. (2005), "Managing disruption risks in supply chains", *Production and Operations Management*, Vol. 14 No. 1, pp. 53-68.

Kumar, R., Singh, R.K. and Shankar, R. (2014) "Strategy development by Indian SMEs for improving coordination in supply chain: an empirical study", *Competitiveness Review*, Vol. 24 No. 5, pp. 414-432.

Lee, H.L. (2000), "Creating value through supply chain integration", *Supply Chain Management Review*, Vol. 4 No. 4, pp. 30-36.

Lee, H.L. and Ng, S.M. (1997), "Introduction to the special issue on global supply chain management", *Production Operations Management*, Vol. 6 No. 3, pp. 191-192.

Lee, H.L., Padmanabhan, V. and Whang, S. (1997), "The bullwhip effect in supply chain", *Sloan Management Review*, Vol. 38 No. 3, pp. 93-102.

Li, X., Chung, C., Goldsby, T.J. and Holsapple, C.W. (2008), "A unified model of supply chain agility: the work-design perspective", *The International Journal of Logistics Management*, Vol. 19 No. 3, pp. 408-435.

Liao, J., Welsch, H. and Stoica, M. (2003), "Organizational absorptive capacity and responsiveness: an empirical investigation of growth-oriented SMEs", *Entrepreneurship Theory & Practice*, Vol. 28, pp. 63-85.

Lin, C., Chiu, H. and Chu, P. (2006), "Agility index in the supply chain", *International Journal of Production Economics*, Vol. 100 No. 2, pp. 285-299.

Malhotra, M.K. and Mackelprang, A.W. (2012), "Are internal manufacturing and external supply chain flexibilities complementary capabilities?", *Journal of Operations Management*, Vol. 30 No. 3, pp. 180-200.

Mehrjerdi, Y.Z. (2009a), "The collaborative supply chain", *Assembly Automation Journal*, Vol. 29 No. 2, pp. 127-136.

Mehrjerdi, Y.Z. (2009b), "Excellent supply chain management", *Assembly Automation Journal*, Vol. 29 No. 1, pp. 52-60.

Downloaded by Delhi Technological University At 09:24 12 September 2015 (PT)

Melnyk, S.A., Davis, E.W., Spekman, R.E. and Sandor, J. (2010), "Outcome-driven supply chains", *Sloan Management Review*, Vol. 51 No. 2, pp. 33-38.

Michelino, F., Bianco, F. and Caputo, M. (2008), "Internet and supply chain management: adoption modalities for Italian firms", *Management Research News*, Vol. 31 No. 5, pp. 359-374.

Michiya, M., Machuca, J.E., James Flynn, E.J. and Pérez, J.L. (2015), "Aligning product characteristics and the supply chain process – a normative perspective", *Int. J. Production Economics*, Vol. 161, pp. 228-241.

Mitra, A. and Bhardwaj, S. (2010), "Alignment of supply chain strategy with business strategy", *IUP Journal of Supply Chain Management*, Vol. 7 No. 3, pp. 49-65.

Moller, K. (2006), "Role of competences in creating customer value: a value creation logic approach", *Industrial Marketing Management*, Vol. 35 No. 8, pp. 913-924.

Narasimhan, R. and Talluri, S. (2009), "Perspectives on risk management in supply chains" *Journal of Operations Management*, Vol. 27 No. 2, pp. 114-118.

Nunnaly, J.C. (1978), *Psychometric Methods*, McGraw Hill, New York, NY.

Olorunniwo, P. and Hartfield, J. (2001), "The knowledge of coordination of supply chain integration", *Business Process Management Journal*, Vol. 8 No. 3, pp. 289-308.

Ozer, O. (2003), "Replenishment strategies for distribution system under advanced demand information", *Management Science*, Vol. 49 No. 3, pp. 255-272.

Pawlak, M. and Malyszek, E. (2008), "A local collaboration as the most successful coordination scenario in the supply chain", *Industrial Management & Data Systems Journal*, Vol. 108 No. 1, pp. 22-42.

Prajogo, D. and Olhager, J. (2012), "Supply chain integration and performance: the effects of long-term relationships, information technology and sharing, and logistics integration", *International Journal of Production Economics*, Vol. 135 No. 1, pp. 514-522.

Qi, Y., Zhao, X. and Sheu, C. (2011), "The impact of competitive strategy and supply chain strategy on business performance: the role of environmental uncertainty", *Decision Sciences*, Vol. 42 No. 2, pp. 371-389.

Qrunfleh, S. and Tarafdar, M. (2013), "Lean and agile supply chain strategies and supply chain responsiveness: the role of strategic supplier partnership and postponement", *Supply Chain Management: An International Journal*, Vol. 18 No. 6 pp. 571-582.

Ramdas, K. and Spekman, R.E. (2000), "Chain or shackles? Understanding what drives supply chain performance", *Interface*, Vol. 30 No. 4, pp. 3-21.

Reichhart, A. and Holweg, M. (2007), "Creating the customer-responsive supply chain: a reconciliation of concepts", *International Journal of Production Planning & Control*, Vol. 27 No. 11, pp. 72-1144.

Saenz, M.J. and Revilla, E. (2014), "Creating more resilient supply chains", *MIT Sloan Management Review*, Vol. 55 No. 4, pp. 22-24.

Sage, A.P. (1977), "Interpretive structural modeling: methodology for large-scale population density", *Small Business Economics*, Vol. 6, pp. 7-291.

Sahay, B.S. (2003), "Understanding trust in supply chain relationships", *Industrial Management and Data Systems*, Vol. 103 No. 8, pp. 553-563.

Shin, H., Collier, D.A. and Wilson, D.D. (2000), "Supply management orientation and supplier/buyer performance", *Journal of Operations Management*, Vol. 18 No. 3, pp. 33-317.

Singh, R.K. (2013), "Prioritizing the factors for coordinated supply chain using analytic hierarchy process (AHP)", *Measuring Business Excellence*, Vol. 17 No. 1 pp. 80-98.

Singh, R.K. and Sharma, M.K. (2014), "Prioritizing the alternatives for flexibility in supply chains", *Production Planning and Control*, Vol. 25 No. 2, pp. 176-192.

Singh, R.K. and Sharma, M.K. (2015), "Selecting competitive supply chain using fuzzy-AHP and extent analysis", *Journal of Industrial and Production Engineering*, Vol. 31 No. 8, pp. 524-538.

Singh, R.K., Garg, S.K. and Deshmukh, S.G. (2007a), "Interpretive structural modeling of factors for improving competitiveness of SMEs", *International Journal of Productivity and Quality Management*, Vol. 2 No. 4, pp. 40-423.

Singh, R.K., Garg, S.K., Deshmukh, S.G. and Kumar, M. (2007b), "Modelling of critical success factors for implementation of AMTs", *Journal of Modelling in Management*, Vol. 2 No. 3, pp. 232-250.

Sodhi, M., Son, B.G. and Tang, C.S. (2008), "What employers demand from applicant for MBA-level supply chain jobs and the coverage of supply chain topics in MBA courses", *Interfaces*, Vol. 38 No. 6, pp. 469-484.

Stanley, E.F., Wallin, C., Allred, C. and Gregory, M. (2009), "Supply chain information-sharing: benchmarking a proven path", *Benchmarking: An International Journal*, Vol. 16 No. 2, pp. 222-246.

Stock, G.N., Greis, N.P. and Kasarda, J.D. (1998), "Logistics, strategy and structure: a conceptual framework", *International Journal of Operations and Production Management*, Vol. 18 No. 1, pp. 37-52.

Storey, J., Emberson, C. and Reade, D. (2005), "The barriers to customer responsive supply chain management", *International Journal of Operations & Production Management*, Vol. 25 No. 3, pp. 60-242.

Sun, S.Y., Hsu, M.H. and Hwang, W.J. (2009), "The impact of alignment between supply chain strategy and environmental uncertainty on SCM performance", *Supply Chain Management: an International Journal*, Vol. 14 No. 3, pp. 201-212.

Talay, M.B., Calantone, R.J. and Voorhees, C.M. (2014), "Coevolutionary dynamics of automotive competition: product innovation, change, and marketplace survival", *J. Prod. Innov. Manag*, Vol. 31 No. 1, pp. 61-78.

Tan, K. (2002), "Supply chain management: practices, concerns, and performance issues", *Journal of Supply Chain Management*, Vol. 38 No. 1, pp. 42-53.

Tejpal, G., Garg, R.K. and Sachdeva, A. (2013), "Trust among supply chain partners: a review", *Measuring Business Excellence*, Vol. 17 No. 1, pp. 51-71.

Togar, M., Simatupang, A., Wright, C. and Sridharan, R. (2002), "The knowledge of coordination of supply chain integration", *Business Process Management Journal*, Vol. 8 No. 3, pp. 289-308.

Tsay, A. (1999), "The quantity flexibility contract and supplier customer incentives", *Management Science*, Vol. 45 No. 10, pp. 58-1339.

van Hoek, R.I. and Chapman, P. (2006), "'From tinkering around the edge to enhancing revenue growth: supply chain-new product development", *Supply Chain Management: An International Journal*, Vol. 11 No. 5, pp. 385-389.

Webb, D. and Pettigrew, A. (1999), "The temporal development of strategy: patterns in the UK insurance industry", *Organization Science*, Vol. 10 No. 5, pp. 22-601.

Williams, B.D., Roh, J., Tokar, T. and Swink, M. (2013), "Leveraging supply chain visibility for responsiveness: the moderating role of internal integration", *Journal of Operations Management*, Vol. 31, pp. 543-554.

Yu, T.F. (2001), "Toward a capabilities perspective of the small firm", *International Journal of Management Review*, Vol. 3 No. 3, pp. 185-197.

Downloaded by Delhi Technological University At 09:24 12 September 2015 (PT)

Yusuf, M.A., Gunasekaran, A., Adeleye, E.O. and Sivayoganathan, K. (2004), "Agile supply chain capabilities. Determinants of competitive objectives", *European Journal of Operations Research*, Vol. 159 No. 2, pp. 379-392.

Zsidisin, G.A. and Smith, M.E. (2005), "Managing supply risk with early supplier involvement: a case study and research propositions", *Journal of Supply Chain Management*, Vol. 41 No. 4, pp. 44-57.

Further reading

Van Hoek, R.I. and Chapman, P. (2007), "How to move supply chain beyond cleaning up after new product development", *Supply Chain Management: An International Journal*, Vol. 12 No. 4, pp. 44-239.

Corresponding author
Professor Rajesh Kumar Singh can be contacted at: rksdce@yahoo.com

Downloaded by Delhi Technological University At 09:24 12 September 2015 (PT)

For instructions on how to order reprints of this article, please visit our website:
www.emeraldgrouppublishing.com/licensing/reprints.htm
Or contact us for further details: **permissions@emeraldinsight.com**

ResearchGate

See discussions, stats, and author profiles for this publication at: http://www.researchgate.net/publication/280609167

Optimization of process parameters on Over-Cut in drilling of Al-B4C MMC

ARTICLE · JULY 2015

READS
11

7 AUTHORS, INCLUDING:



Ravinder Kumar
MAIT,Delhi-86
8 PUBLICATIONS **9** CITATIONS
SEE PROFILE



Ramakant Rana
Maharaja Agarsain Institute of Technology
9 PUBLICATIONS **3** CITATIONS
SEE PROFILE

Available from: Ramakant Rana
Retrieved on: 03 October 2015

OPEN ACCESS

International
Journal
Of Modern Engineering Research (IJMER)

Optimization of process parameters on Over-Cut in drilling of Al-B_4C MMC

Ravinder Kumar[1], Ramakant Rana[1], Surabhi Lata[1], Rahul kumar Sonkar[2], Abhinav Kumar[2], Shekhar Pawar[2], Roop Lal[3]

1Assistant Professor, Mechanical and Automation Engineering Department, Maharaja Agrasen Institute of Technology, Delhi, India

2 Student, Mechanical and Automation Engineering Department, Maharaja Agrasen Institute of Technology, Delhi, India

3Assistant Professor, Mechanical Engineering Department, Delhi Technological University, Delhi, India

ABSTRACT: *This paper presents an experimental investigation on Over-Cut in Drilling of aluminum hybrid metal matrix composite (Al-15%B_4C). The parameters used for drilling here was Depth of Cut, Spindle Speed, and Drill Diameter. Taguchi's L27 orthogonal array experimentation was used to optimize the parameters of Al-B_4C MMC. ANOVA method was used for finding significant parameter. Taguchi's technique was found using Minitab software. The experiments are conducted on vertical milling machine using High Speed Steel drills of 6 mm, 9 mm and 12 mm diameter under dry drilling conditions. A Taguchi analysis is carried out. The effect of drilling parameters on Over-Cut is studied and presented.*

Keywords: *Drilling, Metal Matrix Composites, Taguchi, Over-Cut*

I. INTRODUCTION

Amongst different classes of composites the Metal Matrix Composites (MMCs) have always been the forerunners. From being just a topic of scientific and intellectual interest, Metal Matrix Composites (MMCs) have been transformed into a material of broad commercial and technological significance, in past two decades. A unique balance of mechanical and physical properties is always offered by MMCs. In recent decades, Aluminium based MMCs have received quite high attention as engineering materials, as, majority of the Al based MMCs have possessed the advantages of wear resistance, high strength and hardness.

II. LITERATURE REVIEW

Suresh et al. (2012) [1] have used response surface methodology on AISI 4340 high strength low alloy steel to optimize surface roughness, machining force and tool wear. They concluded that, for minimizing the machining force, the combination of low feed rate, low depth of cut and low machining time with high cutting speed is beneficial. **Davim et al. (2001) [2]** found that when machining the PMMCs, the predominant wear mechanism is abrasive and the feed force increases with the flank wear of the drills. **Basavarajappa et al. (2007) [3]** have used response surface methodology on Al2219/15%SiCp to optimize effect of machining parameters on material, Surface finish and morphology. They concluded that with the increase in feed rate, Surface roughness increases and with the increase in cutting speed, Surface roughness decreases. **Palanikumar (2011) [4]** has used Taguchi's method on Glass fibre-reinforced polymer (GFRP) composite materials to optimize thrust force, work piece surface roughness. **Aouici et al. (2012) [5]** have used statistical analysis of variance (ANOVA) and response surface methodology (RSM) on AISI D3 cold work Steel to optimize surface roughness and cutting force. They concluded that cutting force is mostly affected by feed rate followed by depth of cut. **Ramesh et al. (2012) [6]** used Response surface methodology on titanium alloy to optimize the surface roughness. They concluded that the most influencing parameter was identified as the feed. **Suresh R et al. (2012) [7]** have used Taguchi technique on AISI 4340 steel to optimize Cutting force and thrust force. They concluded that for minimizing the machining force, the combination of low feed rate, low depth of cut with high cutting speed is beneficial. Machining force initially increases with increase in feed rate and depth of cut and decreases with increase in cutting speed.**Hessainia et al. (2013) [8]** have used Response surface methodology on 42CrMo4 hardened steel to optimize surface roughness. They concluded that the feed rate is the dominant factor affecting the surface roughness, whereas vibrations on both directions have a low effect on it. **Gopalakannan et al. (2013) [9]** have used Response surface methodology on Al–SiCnano-composites material

to optimize Surface roughness and feed rate. **Sahoo et al. (2013) [10]** have used Taguchi's L9 orthogonal array on Al/SiCp MMC to optimise Feed rate. They concluded that Cutting speed is found to be the most significant parameter for flank wear followed by feed. Depth of cut has the insignificant effect on flank wear. **Taskesen et al. (2013) [11]** have used Grey relational analysis on B4C reinforced Al-alloy to optimise thrust force, torque and surface roughness. They conclude that Flank wear of the cutting tool was found to be mostly dependent upon particle mass fraction, followed by feed rate, drill hardness and spindle speed, respectively. **Karabulut (2015) [12]** have used Taguchi method and neural network on AA7039/Al2O3 metal matrix composites material to optimise surface roughness and cutting force. ANOVA technique is also used. They concluded that the analysis results showed that material structure was the most effective factor on surface roughness and feed rate was the dominant factor affecting cutting force. ANOVA results show that the most effective control factor for surface roughness, with a percentage contribution of 85.24%, was the type of material. The feed rate and cutting speed affect the surface roughness by 7.12% and 5.05% respectively. The depth of cut has the least effect on surface roughness.**Suresh et al. (2012) [13]** have used response surface methodology on AISI 4340 high strength low alloy steel to optimize surface roughness, machining force and tool wear.They concluded that, for minimizing the machining force, the combination of low feed rate, low depth of cut and low machining time with high cutting speed is beneficial. **Gallab et al. (1998) [14]** have used Dry turning test on Al:SiC particulate metal-matrix composites to optimise Rake angles. They concluded that for the roughing operations, Polycrystalline tools with zero rake angle and large tool nose radii are recommended. The main tool wear mechanism is abrasion and micro-cutting of tool material grains, manifested as grooves on the tool face parallel to the chip flow direction.**Hayajneh et al. (2009) [15]** have used Artificial neural network modeling on aluminum / alumina / graphite hybrid composites to optimise Cutting speed ,Cutting feed ,volume fraction of the reinforced particles and thrust force. They concluded that ANN is an excellent analytical tool, if it is well trained, can be used for other machining processes. The models for the thrust force and cutting torque were identified by using the alumina (Al2O3) particles contents, graphite (Gr) particles contents, cutting feeds (F) and spindle speeds (N) as input data and thrust force and cutting torque as the output data.**Rajmohan et al. (2012) [16]** used Taguchi's method on hybrid mmc to optimise Surface finish, thrust force, tool wear, and burr height in the drilling of composites. They concluded that, the factors which affect the drilling process are feed rate and the type of drill. The tested parameters, the feed rate shows strongest correlation to the thrust force, surface roughness, tool wear and burr height (exit). **Rajmohan et al. (2013) [17]** used Microstructure and mechanical characterization on hybrid aluminium matrix composites to optimise strength and hardness. They concluded that the better strength and hardness are achieved with Al/10SiC−3mica composites. The increase in mass fraction of mica improves the wear loss of the composites. Mica reinforced composites exhibits less wear loss and higher density compared with the ceramic reinforced composites.**Taskesen et al. (2013) [18]** have used grey relational analysis on boron carbide reinforced metal matrix composites to optimise Feed rate and spindle speed. They concluded that the weight fraction of the B4C resulted in a considerable increase in the thrust force. Average surface roughness of drilled hole decreased with increasing particle content for carbide tools and increased for HSS tools. TiAlN coated carbide drills showed the best performance with regard to the surface roughness.**Davim (2003) [19]** have used Taguchi's method on MMC to optimise Correlation between cutting velocity, feed rate and cutting time. Feed rate is the cutting parameter which has greater influence on surface roughness and specific cutting pressure followed by cutting velocity and cutting time. To analyze interaction in the holes surface roughness, the interaction cutting velocity/feed is the most important. **Kumar et al. (2012) [20]** have used Optimization of drilling parameters on Al6061–SiC composites to optimise Hardness, Ultimate tensile strength and feed rate. They concluded that the experimental results showed that the density of the composites increase with increased SiC content. The wear resistance of the composites is higher than that of base alloy. Hardness of the composites was found to increase with increased filler content. The ultimate tensile strength properties of the composites are found to be higher than that of base matrix.**Barnes et al. (2000) [21]** have used Taguchi's method and ANOVA on Aluminum/SiC Metal Matrix Composite to optimiseDrill wear, Hole diameter and Surface roughness. They concluded that in the drilling performance, the application of through toolcoolant (even at low pressure) produced a significant improvement. In agreement with otherwork, the wear observed at some locations increased when usingconventional cooling relative to dry drilling.**Horvath et al. (2011) [22]** have used Response surface method (RSM) on Aluminum alloys to optimise Surface roughness, Feed rate Surface height and standard deviation. They concluded that the cutting speed and feed have the largest influence on surface roughness. Also the interactions of these factors also significantly affect surface roughness. The harder hyper-eutectic alloy has better finish turning and lower roughness values.**(Rana (2014) [27], Rana (2014)[28])**have alsoreviewed thepapers on Taguchi optimization which, shows that Taguchi can be applied to find whether the factors are significant or not on the optimized results.**(Rana (2015) [27], Lata (2015) [28])**haveapplied RSM on the welding techniques to improve the weld abilities.

III. EXPERIMENTAL SETUP

A number of experiments were conducted to study the effects of various parameters of drilling Al-B_4C MMC. These studies were undertaken to investigate the effects of D.O.C., Speed and Drill Diameter for drilling Al-B_4C MMC.

The selected workpiece material for the research work was Al 6061 (composition shown in Table 1) as the matrix and containing 15% wt. of B_4C particulate of 220 µm. Al-B_4C MMC was selected due to its emergent range of applications in the field of manufacturing. The Drilled pieces are shown in Figure 2 (a) & (b). The test conditions are depicted in Table II.

Table 1. Chemical composition of Al 6061

Element	Weight percentage
Cromium (Cr)	0.15
Copper (Cu)	0.40
Iron (Fe)	0.7
Magnesium (Mg)	0.80
Manganese (Mn)	0.15
Silicon (Si)	7.00
Titanium (Ti)	0.20
Zinc (Zn)	0.25
Aluminium (Al)	90.35



(a) (b)

Figure 2: Photographic View of Al-B_4C_p Drilled pieces

Table II: Different Variables Used In The Experiment And Their Level

Variable	CODE	LEVELS		
		1	2	3
D.O.C.	A	5	10	15
SPEED	B	660	1110	1320
DRILL DIA	C	6	9	12

IV. TAGUCHI OPTIMIZATION

One of the powerful and most important statistical technique is Design of Experiment (DOE), which is used to study the effect of multiple variables simultaneously. DOE involves a series of steps which must follow a certain sequence for the experiment to yield an improved understanding of process performance **(Taguchi (1990) [23])**.Analysis of the responses uses a signal to noise (S/N) ratio to determine the best process parameters. This method improves the design of machining processes. In the present work, experiments were performed by Taguchi method using orthogonal arrays **(Ross (1996) [24])**. This method yields the rank of various parameters with the level of significance of influence of a factor or the interaction of factors on a particular output response.

In present work Over-Cut (OC) is being measured by conducting total 27 numbers of experiments (shown in Table III). Digital Vernier Caliper was used for the measurement of Over-Cut. Over-Cut is the measure of cut produced exceeding the diameter of the tool. The hole created while drilling process is generally slightly larger than the original diameter of the Drill Diameter. Over-Cut is calculated as half the difference of the diameter of the hole produced to the tool diameter as shown in the equations below:

$$\text{Over-Cut} = \frac{D_i - D_o}{2} \quad \ldots (1)$$

Where D_i is the diameter of the hole and D_o is the outer diameter of the Drill.

Table III: Response parameters (Over-Cut) along with its S/N Ratio

DOC	SPEED	DRILL DIA	Over-Cut		S/N Ratio (db)
			R_1	R_2	
5	660	6	0.1	0.12	19.1364
5	1110	6	0.08	0.24	14.9485
5	1320	6	0.22	0.3	11.59894
10	660	6	0.13	0.58	7.528864
10	1110	6	0.13	0.23	14.57175
10	1320	6	0.18	0.38	10.53548
15	660	6	0.12	0.62	7.002748
15	1110	6	0.16	0.24	13.80907
15	1320	6	0.16	0.22	14.31798
5	660	9	0.08	0.09	21.39662
5	1110	9	0.09	0.12	19.48847
5	1320	9	0.22	0.9	3.673403
10	660	9	0.19	0.28	12.42225
10	1110	9	0.24	0.13	14.28874
10	1320	9	0.06	0.18	17.44727
15	660	9	0.07	0.02	25.76754
15	1110	9	0.05	0.18	17.58205
15	1320	9	0.02	0.15	19.41195
5	660	12	0.54	0.56	5.191311
5	1110	12	0.71	0.69	3.097153
5	1320	12	0.78	0.6	3.149752
10	660	12	0.66	0.54	4.393761
10	1110	12	0.88	0.75	1.749311
10	1320	12	0.63	0.49	4.968906
15	660	12	0.48	0.32	7.788467
15	1110	12	0.54	0.95	2.239893
15	1320	12	0.72	0.56	3.809067

V. RESULTS AND DISCUSSIONS

After the conduction of all the 27 experiments, the following results were obtained for Over-Cut. Results include the Response Table according to Taguchi method and Graphs for S/N ratio and Mean values along with Contour Plot, 3D Scatter Plots and Surface Plots. The S/N ratio and the mean values were calculated by putting the values of Over-Cut in Minitab software.

Table IV: Response Table for Signal to Noise Ratios (Smaller is better)

LEVEL	D.O.C.	SPEED	DRILL DIAMETER
1	11.519	8.732	12.491
2	14.101	9.242	7.439
3	3.743	11.389	9.433
DELTA	10.357	2.657	5.052
RANK	1	3	2

Table V: Response Table for Means

LEVEL	D.O.C.	SPEED	DRILL DIAMETER
1	0.2339	0.3578	0.3056
2	0.1706	0.3700	0.3722
3	0.6333	0.3100	0.3600
DELTA	0.4628	0.0600	0.0667
RANK	1	3	2

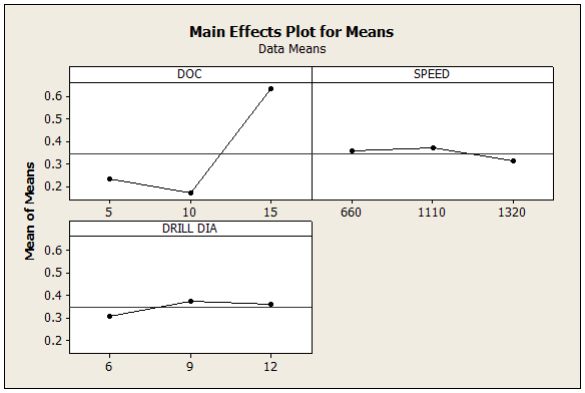


Figure 3: Effect of Mean on D.O.C., SPEED & Drill Diameter

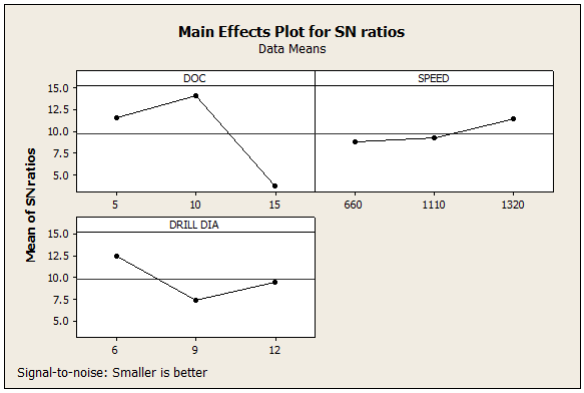
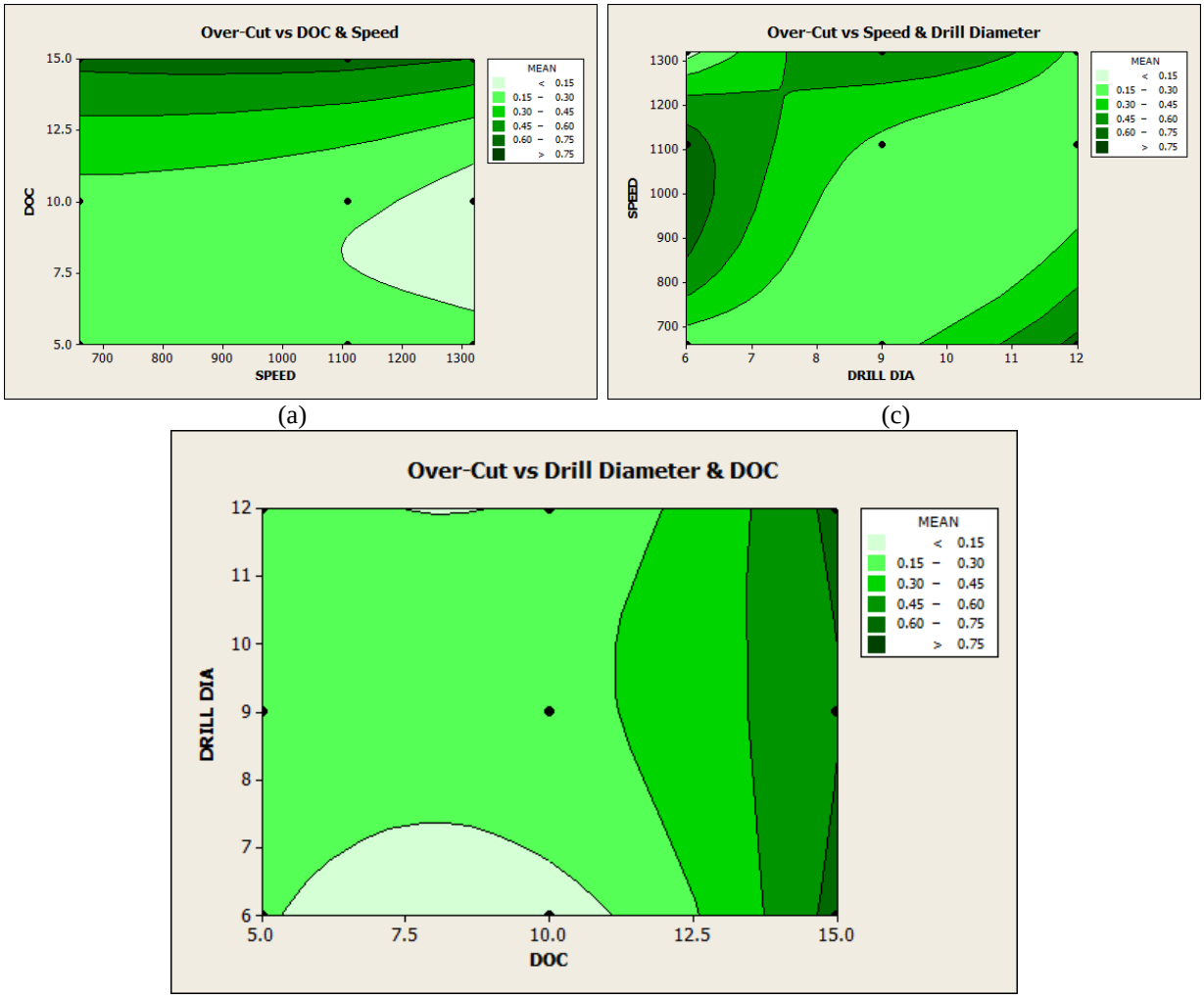


Figure 4: Effect of S/N Ratio on D.O.C., SPEED & Drill Diameter

Figure 3 & 4 depicts that, with the increase in the Depth of Cut Over-Cut decreases upto a level of 10 mm and then again starts increasing after 10mm, it also shows that with the increase in the speed of the drill there is a decrease in the Over-Cut but with a slight increase in between. The Figure 3& 4 also shows that drill diameter also affects the Over-Cut. All these ranges are also shown in the Figure 6,7,8, & 9.



(a) (c)

(b)

Figure 5: Contour Plots of Over Cut vs various Process Parameters

Figure 5 (a), (b) & (c) are the contour plot of Over-Cut vs Speed, D.O.C. and Drill Diameter respectively, and shows the range where one can achieve the minimum Over-Cut by selecting the shown range of parameters.

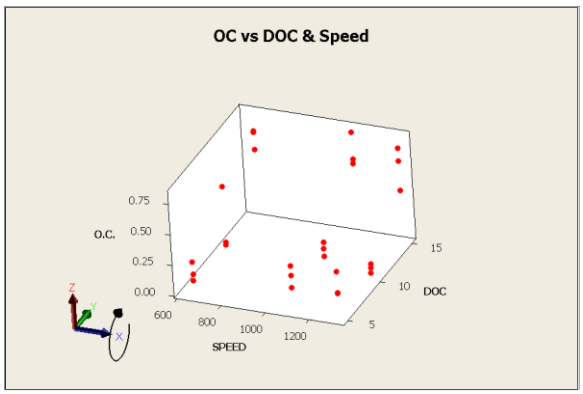


Figure 6:3D Scatter Plot of Over-Cut vs D.O.C. & Speed

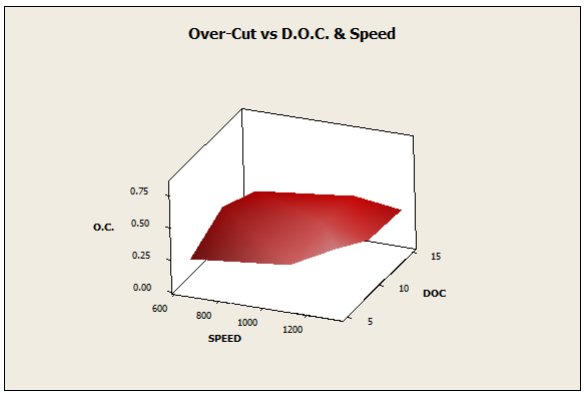


Figure 7: Surface Plot of Over-Cut vs D.O.C. & Speed

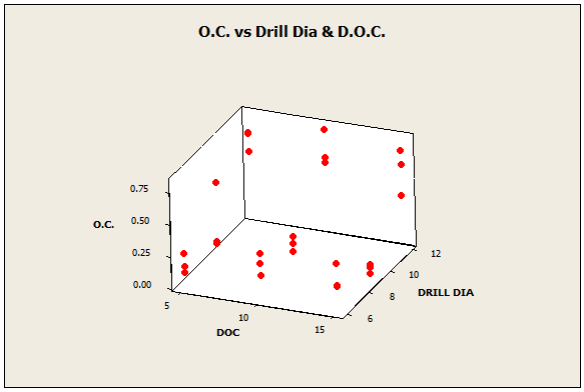


Figure 8:3D Scatter Plot of Over-Cut vs Drill Diameter & D.O.C.

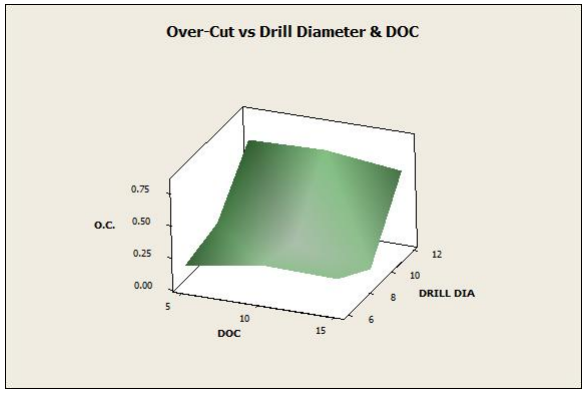


Figure 9: Surface Plot of Over-Cut vs Drill Diameter & D.O.C.

VI. CONCLUSION

The experiments were conducted on a vertical milling machine for the machining of Al/B_4Cp. The tool used for the drilling operation is a High Speed Steel. The response Over-Cut was studied. It was found that Speed, D.O.C. & Drill Diameter significantly affect the Over-Cut. Over-Cut is linearly proportional to the effect of Speed, D.O.C. & Drill Diameter. The lower value of Over-Cut is achieved with Speed = 1320 RPM, D.O.C. = 10 mm & Drill Diameter = 12 mm within the experimental domain. The research findings of the present study is based on Taguchi optimization, and can be used effectively in drilling of Al-B_4Cp, in order to obtain best drill hole.

REFRENCES

[1]. Suresh R., Basavarajappa S., Gaitonde V.N., Samuel G.L., "Machinability investigations on hardened AISI 4340 steel using coated carbide insert", International Journal of Refractory Metals and Hard Materials, vol. 33, 2012, pp. 75–86.

[2]. Davim J. Paulo, Antonio C.A. Conceicao., "Optimal drilling of particulate metal matrix composites based on experimental and numerical procedures", International Journal of Machine Tools & Manufacture, vol. 41, 2001,pp. 21–31.

[3]. Basavarajappa S., Chandramohan G., Prabu M., Mukund K., Ashwin M., "Drilling of hybrid metal matrix composites—Workpiece surface integrity", International Journal of Machine Tools & Manufacture, measurement, vol. 47, 2007,pp. 92–96.

[4]. Palanikumar K., "Experimental investigation and optimisation in drilling of GFRP composites",Measurement, vol. 44, 2011, pp. 2138–2148.

[5]. AouiciHamdi, Yallese Mohamed Athmane, ChaouiKamel, Mabrouki Tarek, Rigal Jean-François, "Analysis of surface roughness and cutting force components in hard turning with CBN tool: Prediction model and cutting conditions optimization",Measurement, vol. 45, 2012, pp. 344–353.

[6]. Ramesh S., Karunamoorthy L., Palanikumar K., "Measurement and analysis of surface roughness in turning of aerospace titanium alloy (gr5)",Measurement, vol. 45, 2012, pp. 1266–1276.

[7]. Suresh R., Basavarajappa S., Samuel G.L., "Some studies on hard turning of AISI 4340 steel using multilayer coated carbide tool",Measurement, vol. 45, 2012,pp. 1872–1884.

[8]. HessainiaZahia, Belbah Ahmed, Yallese Mohamed Athmane, Mabrouki Tarek, Rigal Jean-François, "On the prediction of surface roughness in the hard turning based on cutting parameters and tool vibrations",Measurement, vol. 46, 2013,pp. 1671–1681.

[9]. Gopalakannan S., Senthilvelan T., "Application of response surface method on machining of Al–SiCnano-composites",Measurement, vol. 46, 2013, pp. 2705–2715.

[10]. Sahoo Ashok Kumar, Pradhan Swastik., "Modeling and optimization of Al/SiCp MMC machining using Taguchi approach",Measurement, vol. 46, 2013,pp. 3064–3072.\

[11]. Taskesen A., Kutukde K., "Analysis and optimization of drilling parameters for tool wear and hole dimensional accuracy in B4C reinforced Al-alloy", Trans. Nonferrous Met. Soc. China, vol. 23,2013, pp. 2524−2536.

[12]. KarabulutSener., "Optimization of surface roughness and cutting force during AA7039/Al2O3 metal matrix composites milling using neural networks and Taguchi method",Measurement, vol. 66, 2015, pp. 139–149.

[13]. Suresh R., Basavarajappa S., Gaitonde V.N., Samuel G.L., "Machinability investigations on hardened AISI 4340 steel using coated carbide insert", International Journal of Refractory Metals and Hard Materials, vol. 33, 2012,pp. 75–86.

[14]. Gallab M. El, Sklad M., "Machining of Al:SiC particulate metal-matrix composites Part I: Tool performance", Journal of Materials Processing Technology, vol. 83, 1998,pp. 151–158.

[15]. Hayajneh Mohammed T., Hassan Adel Mahmood, Mayyas Ahmad Turki., "Artificial neural network modeling of the drilling process of self-lubricated aluminum/alumina/graphite hybrid composites synthesized by powder metallurgy technique", Journal of Alloys and Compounds, vol. 478, 2009,pp. 559–565.

[16]. Rajmohan T., Palanikumar K., Kathirvel M., "Optimization of machining parameters in drilling hybrid aluminium metal matrix composites",trans. Nonferrous Met. Soc. China,vol. 22, 2012, pp. 1286_1297.

[17]. Rajmohan T., Palanikumar K., Ranganathan S., "Evaluation of mechanical and wear properties of hybrid aluminium matrix composites", Trans. Nonferrous Met. Soc. China,vol. 23, 2013, pp. 2509−2517.

[18]. Taskesen Ahmet, KütükdeKenan.,"Experimental investigation and multi-objective analysis on drilling of boron carbide reinforced metal matrix composites using grey relational analysis",Measurement, vol. 47, 2013, pp. 321–330.

[19]. DavimJ.Paulo, "Study of drilling metal matrix composites based in the Taguchi's technique", Journal of Materials Processing Technology, vol. 132, 2003, pp. 250-254.

[20]. Kumar G.B. Veeresh, Rao C.S.P., Selvaraj N., "Studies on mechanical and dry sliding wear of Al6061–SiC composites",Composites: Part B, vol. 43, 2012, pp. 1185–1191.

[21]. Barnes S., Pashby I. R, and Hashim A. B., "Effect of Heat Treatment on the Drilling Performance of Aluminium/SiC MMC", Applied Composite Materials 6, pp.121–138, 1999.
[22]. HorváthRichárd, Drégelyi-Kiss Ágota., "Analysis of surface roughness of aluminum alloys fine turned: United phenomenological models and multi-performance Optimization",Measurement, vol. 65, 2015, pp. 181–192.
[23]. Taguchi G., introduction to quality engineering, Asian productivity organization, 1990.
[24]. Ross P. J., Taguchi Technique for Quality Engineering, McGraw Hill, New York, NY, USA, 2nd edition1996.
[25]. Rana Ramakant, LataSurabhi, ShankaranAlok, Sharma Vinay, Saraswat Amit, LalRoop, "Optimization of process parameters on Over-Cut in drilling of Al-B_4C MMC", International Journal of Modern Engineering Research, Vol. No.5, Issue 05, May 2015.
[26]. LataSurabhi, Rana Ramakant, ShankaranAlok, Sharma Vinay, Saraswat Amit, LalRoop, "Effect Of Welding Variables On Tensile Strength Of Cu-Steel Weldments Through Design Of Experiments And Regression Model", International Journal of Advance Research In Science And Engineering, Vol. No.4, Issue 04, April 2015.
[27]. Rana Ramakant, Mani Adarsh, Kochhar Anmol, WadhwaShrey, Daiya Sandeep Kumar, TaliyanSparsh, LalRoop, "An Overview On Process Parameters Improvement In Wire Electrical Discharge Machining", International Journal of Modern Engineering Research, April, 2014.
[28]. Rana Ramakant, Rajput Kunal, Saini Rohit, LalRoop, "Opimization of Tool Wear: A Review", International Journal of Modern Engineering Research, Nov, 2014, vol. 4, Issue 11.

ResearchGate

See discussions, stats, and author profiles for this publication at: http://www.researchgate.net/publication/275964475

Affinity of Smectite and Divalent Metal Ions (Mg2+, Ca2+, Cu2+) with L-leucine: An Experimental and Theoretical Approach Relevant to Astrobiology

ARTICLE *in* ORIGINS OF LIFE AND EVOLUTION OF BIOSPHERES · MAY 2015

Impact Factor: 1.11

READS

43

9 AUTHORS, INCLUDING:



Pramod Pandey

Kumaun University

7 PUBLICATIONS **8** CITATIONS

SEE PROFILE



Neetu Pandey

Kumaun University

7 PUBLICATIONS **3** CITATIONS

SEE PROFILE



Mohan Singh Mehata

Delhi Technological University

37 PUBLICATIONS **231** CITATIONS

SEE PROFILE

Available from: Pramod Pandey

Retrieved on: 01 October 2015

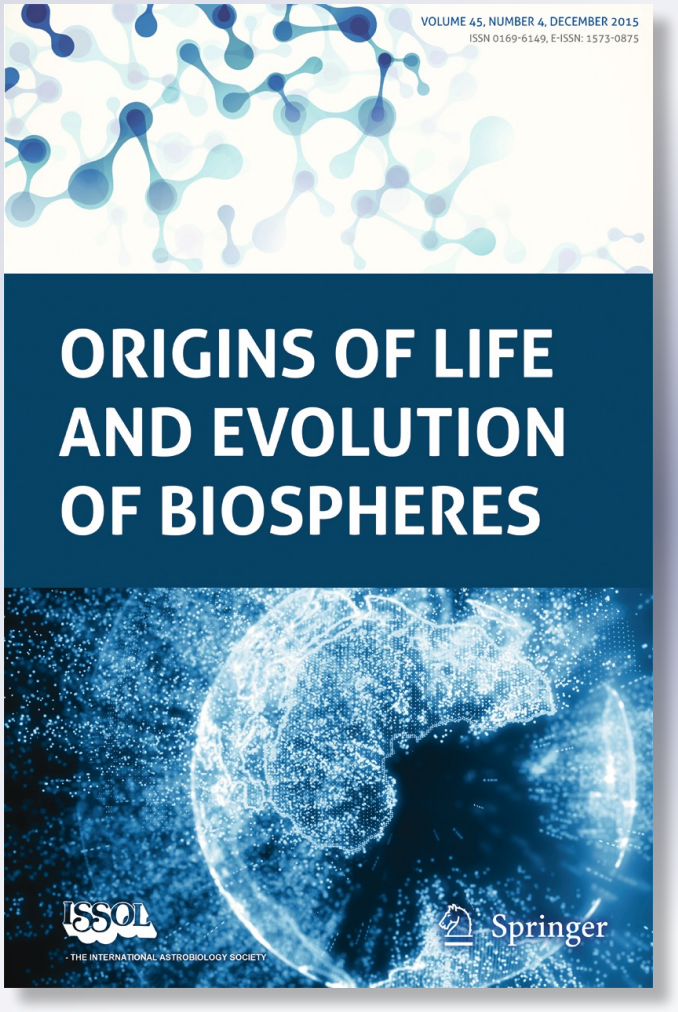
Affinity of Smectite and Divalent Metal Ions (Mg^{2+}, Ca^{2+}, Cu^{2+}) with L-leucine: An Experimental and Theoretical Approach Relevant to Astrobiology

Pramod Pandey, Chandra Kala Pant, Kavita Gururani, Priyanka Arora, Neetu Pandey, Preeti Bhatt, Yogesh Sharma, Jagmohan Singh Negi, et al.

Origins of Life and Evolution of Biospheres
The Journal of the International Astrobiology Society

ISSN 0169-6149
Volume 45
Number 4

Orig Life Evol Biosph (2015) 45:411-426
DOI 10.1007/s11084-015-9437-2



Springer

Your article is protected by copyright and all rights are held exclusively by Springer Science +Business Media Dordrecht. This e-offprint is for personal use only and shall not be self-archived in electronic repositories. If you wish to self-archive your article, please use the accepted manuscript version for posting on your own website. You may further deposit the accepted manuscript version in any repository, provided it is only made publicly available 12 months after official publication or later and provided acknowledgement is given to the original source of publication and a link is inserted to the published article on Springer's website. The link must be accompanied by the following text: "The final publication is available at link.springer.com".



Author's personal copy

Orig Life Evol Biosph (2015) 45:411–426
DOI 10.1007/s11084-015-9437-2

PREBIOTIC CHEMISTRY

Affinity of Smectite and Divalent Metal Ions (Mg^{2+}, Ca^{2+}, Cu^{2+}) with L-leucine: An Experimental and Theoretical Approach Relevant to Astrobiology

Pramod Pandey[1] · Chandra Kala Pant[1] · Kavita Gururani[1] · Priyanka Arora[2] · Neetu Pandey[2] · Preeti Bhatt[1] · Yogesh Sharma[1] · Jagmohan Singh Negi[3] · Mohan Singh Mehata[4]

Received: 3 December 2014 / Accepted: 17 March 2015 /
Published online: 8 May 2015
© Springer Science+Business Media Dordrecht 2015

Abstract Earth is the only known planet bestowed with life. Several attempts have been made to explore the pathways of the origin of life on planet Earth. The search for the chemistry which gave rise to life has given answers related to the formation of biomonomers, and their adsorption on solid surfaces has gained much attention for the catalysis and stabilization processes related to the abiotic chemical evolution of the complex molecules of life. In this communication, surface interactions of L-leucine (Leu) on smectite (SMT) group of clay (viz. bentonite and montmorillonite) and their divalent metal ion (Mg^{2+}, Ca^{2+} and Cu^{2+}) incorporated on SMT has been studied to find the optimal conditions of time, pH, and concentration at ambient temperature (298 K). The progress of adsorption was followed spectrophotometrically and further characterized by FTIR, SEM/EDS and XRD. Leu, a neutral/non polar amino acid, was found to have more affinity in its zwitterionic form towards Cu^{2+}- exchanged SMT and minimal affinity for Mg^{2+}- exchanged SMT. The vibrational frequency shifts of —NH_3^+ and —COO^- favor Van der Waal's forces

Electronic supplementary material The online version of this article (doi:10.1007/s11084-015-9437-2) contains supplementary material, which is available to authorized users.

✉ Pramod Pandey
pp.chem24@gmail.com

✉ Chandra Kala Pant
ckp.astrochem@gmail.com

[1] Chemical Laboratory, Department of Chemistry, DSB Campus, Kumaun University, Nainital 263002 Uttarakhand, India

[2] Photophysics Laboratory, Department of Physics, DSB Campus, Kumaun University, Nainital 263002 Uttarakhand, India

[3] Herbal Analytical Laboratory, Herbal Research and Development Institute, Mandal, Gopeshwar 246401 Uttarakhand, India

[4] Department of Applied Physics, Delhi Technological University, Bawana Road, New Delhi 110042, India

Author's personal copy

during the course of surface interaction. Quantum calculations using density functional theory (DFT) have been applied to investigate the absolute value of metal ion affinities of Leu (Leu—M^{2+} complex, M=Mg^{2+}, Ca^{2+}, Cu^{2+}) with the help of their physico-chemical parameters. The hydration effect on the relative stability and geometry of the individual species of Leu—$M^{2+}\times(H_2O)_n$, (n =2 and 4) has also been evaluated within the supermolecule approach. Evidence gathered from investigations of surface interactions, divalent metal ions affinities and hydration effects with biomolecules may be important for better understanding of chemical evolution, the stabilization of biomolecules on solid surfaces and biomolecular-metal interactions. These results may have implications for understanding the origin of life and the preservation of biomarkers.

Keywords Amino acids · Smectite · Metal ions Surface interaction · DFT Origin of life

Introduction

The origin of life is generally presumed to require a local concentration of life-forming biomolecules (e.g. amino acids, nucleic acid bases, phosphate and sugars etc.), which were either supplied abundantly or sufficiently stable to accumulate under primitive Earth conditions. Prebiotic syntheses of biomolecules from chemical precursors often suffer from low yields (Lucrezia et al. 2007; Orgel 2004; Lambert 2008; Shapiro 1999), thus the steady-state concentrations of amino acids (AAs) in the primitive oceans has been estimated to be on the order of 4 to 10^{-7} mM (Lahav and Chang 1976; Stribling and Miller 1987).The stability of these molecules under the conditions (viz. ultra-violet, thermal, electric discharge etc.) prevalent on Earth when life started ~4.4–3.5 Ga ago may also have been an impediment to their accumulation (Cleaves et al. 2012).

Bernal (1951) suggested a possible solution to these problems and postulated concentration of biomolecules on mineral surfaces like metal oxides. Metal oxides and silicates are widely distributed on the Earth's surface and also reported on another planet like Mars (Stephenson et al. 2013; Carr and Head 2010). Bentonite (BNT) and montmorillonite (MMT) clays, well known for their cation exchange capacities, had been widely investigated at different conditions of pH, temperature and concentrations to explore Bernal's ideas regarding their potential roles as concentrating surfaces and catalysts for polymerization (Zaia 2012; Lambert 2008 and references therein it). The sorption behavior of SMT surfaces is primarily governed by variables such as the interlayer conditions, presence of cations, water, etc. (Prabhakar et al. 2007).

Metal ions are known for their affinity to form peptide bonds in relevance to the prebiotic evolution of biomolecules (Rode et al. 1993; Pant et al 2009; Gururani et al. 2012a; Remko and Rode 2000). Metal ion-exchanged SMTs are good adsorbents for amino acids, nucleic acid bases, sugars etc., and also catalyst for biomolecule formation (Lambert 2008; Kalra et al. 2003; Gururani et al. 2012b). A detailed mechanism behind prebiotic mineral-organic interfacial processes and its potential implications for the origins of life have been reviewed by Cleaves et al. (2012).

Recently, the role of metal ions in chemical evolution has been bolstered with advances in computational chemistry (Remko and Rode 2000; Rode et al. 1993: Merz et al. 2014; Cleaves et al. 2012). The possible interaction of metal ions with biomolecules is often investigated with the help of high-pressure mass spectrometry along with guided ion beam mass spectrometry

Author's personal copy

(Kebarle and Hogg 1965; Rodgers and Armentrout 2000). However, quantum mechanical calculations give better insight into their possible complex formation mechanism, solvation and counter ions effects of the different complexes (Marino et al. 2001). Hydrated biomolecular complexes serve as simpler models for more complex protein–metal systems in an aqueous environment (Remko et al. 2011).

Among other prebiotically formed AAs, Leu has been reported from exogenous (Pizzarello 2009) as well as endogenous (Zaia 2012) sources. However, to the best of our knowledge, a systemic experimental study of the surface interactions of Leu on Ca^{2+}-, Mg^{2+}- and Cu^{2+}-exchanged SMTs (BNT and MMT), separately, has not been realized yet. In this communication, we investigate the adsorption behavior of different metal ion exchanged SMTs because such studies related to the biomolecular interaction on prebiotically available solid surface and their affinity towards silicates, are relevant to astrobiology (Lambert 2008; Cleaves et al. 2012). The stability of the adsorbate under different experimental conditions is also a major concern for astrobiological investigation as silicates are also known for their catalytic role in polymerization and decomposition of biomolecules (Zaia 2012; Marshall-Bowman et al. 2010; Ferris et al. 1996). Thus, the stability of Leu was also investigated under different sorption conditions.

Computational studies of metal-amino acid complexes (Leu—M^{2+}) were conducted using Gaussian 03 (Frisch et al. 2003) to understand the affinity of metal ions with biomolecules and the effect of hydration on Leu—$M^{2+} \times (H_2O)_n$, (n =2 and 4) complex formation, which has not been studied yet theoretically. The details of local interactions between metal ions and AAs are of prime importance in living systems (Marino et al. 2001).

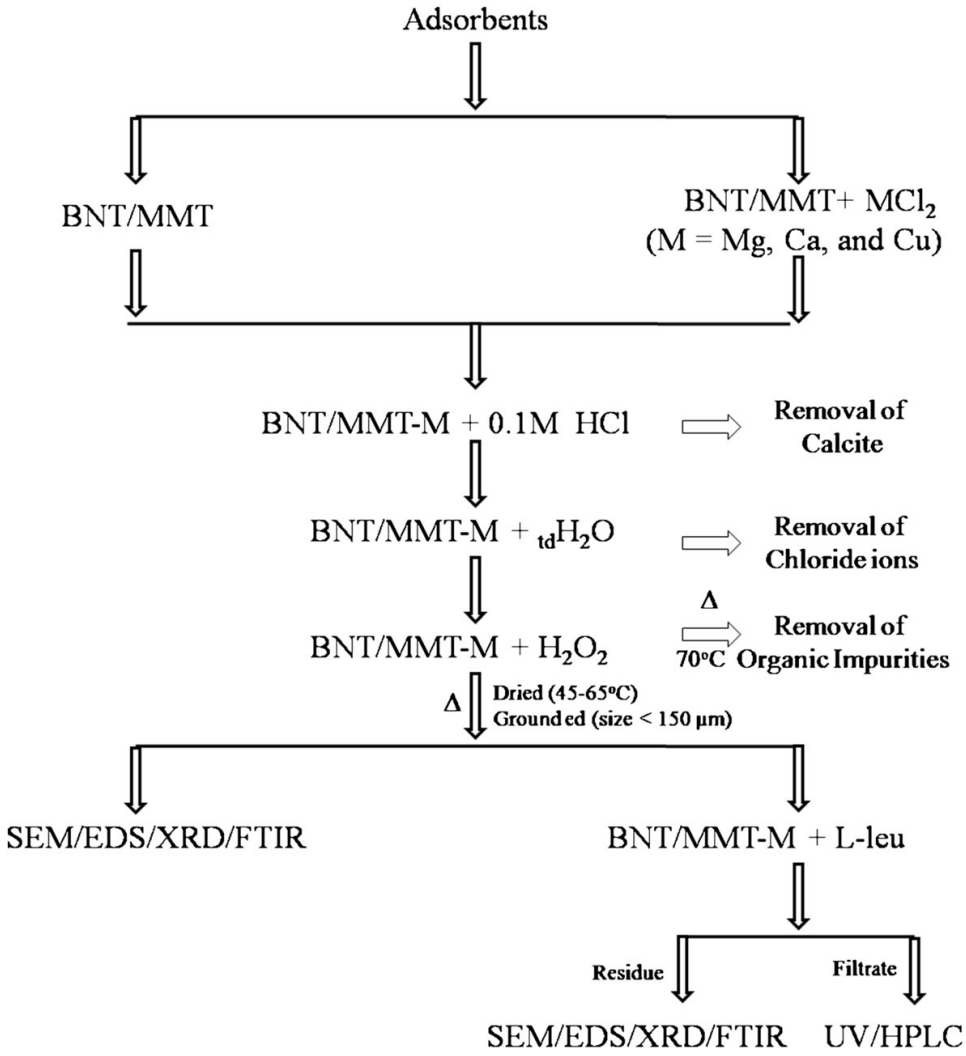
Experimental

All reagents were of analytical grade. BNT and MNT K10 clays were purchased from E. Merck, India and Sigma Aldrich, Germany respectively, while L-leucine (Leu), H_2O_2, $MgCl_2$, $CuCl_2$ were from Qualigens, India and $CaCl_2$ was obtained from CDH India. Triple distilled-deionized water (pH 6.8±0.1) was used throughout the study. All containers, measuring equipment and assemblies were of borosilicate glass. A JascoV-550, UV/VIS/NIR spectrophotometer was used for the absorbance measurements. The pH was recorded on Hanna pH meter (model pHep, accuracy: ±0.1 pH unit).

The sequential steps involved in the preparation/purification of adsorbents during analysis are shown in scheme I, and described by Prabhakar et al. 2007 and Kalra et al. 2003. Ca^{2+}, Cu^{2+} and Mg^{2+} exchanged BNT/MMT were prepared by the saturation method as mentioned earlier (Kalra et al. 2003). All the adsorbents (Scheme I) were ground, sieved using a 100 mesh size sieve (SETHI BSS 100) and then dried in vacuum desiccators. The color of the respective SMTs have been found to be 10R8/1 (white) and 7.5YR7/2 (light brown) on Munsell Notations, for MMT and BNT respectively.

The purity of adsorbents (BNT/MMT and their divalent cation-exchanged forms) were determined by scanning electron microscopy (SEM) and energy-dispersive X-ray spectrometry (EDS) using a Hitachi S-3700 N Instrument using an acceleration voltage 15.0 kV with a take-off angle 44.1°,and a ZEISS EHT 20 kV instrument. Purity was further checked by X-ray diffraction (relative intensity and inter-planar spacing) data, which were in good agreement with reported values (Caglar et al. 2009). X-ray powder diffraction analysis of adsorbent and adsorption adducts were performed on a Thermal X-TRA ARL diffractometer equipped with a

Author's personal copy



Scheme I Graphical representation of different steps involved in the preparation/purification of adsorbents and different analysis

'Peltier' detector, using Cu Kα radiation (wavelength=1.5406 Å) operated at 30 mA and 40 kV and graphite monochromator detection between range 0-40° 2θ angle. Vibrational studies were carried out using a PerkinElmer DX-II FT-IR spectrophotometer equipped with DTGS detector. The IR spectra were collected at 4 cm^{-1} resolution and 100 scan with frequency range from 400 to 4000 cm^{-1}.

The adsorption of Leu on different adsorbents in aqueous medium was studied as function of pH (4.0–9.2), time (1 min – 72 h) and concentration (1 mM to 10 mM) of adsorbate. Adsorption of Leu in varying concentration over different pH was studied in order to obtain saturation point by adding acetate-acetic acid (pH 4.0–6.0) or borax-boric acid (pH 6.6–9.2) buffer to the AA solution containing adsorbents, keeping in mind that the buffer solution should be a very poor ligand so that stable complex formation with the mineral could be avoided and this was confirmed by using different buffer concentration on Leu solution.

Buffer solution of Leu (5 ml) at different pH values was added to the adsorbents (50 mg) in separate conical flasks (10 ml) under air, stirred mechanically using magnetic stirrer and allowed to stand at room temperature (298 K) for different time intervals to determine the optimum conditions for adsorption. The solutions were then centrifuged at 2000 rpm for

Author's personal copy

25 min. The supernatant was decanted leaving the SMT as a residue. The supernatant in each experiment was used for quantitative estimation of AA content after adsorption and the SMT residue was separated, washed (3 times) and then, dried at ambient temperature under vacuum. Further, it was ground/ sieved and used for SEM/EDS, FTIR and XRD studies (Scheme I). The concentration of adsorbate before and after adsorption was determined using UV difference spectra (at 201 nm) in quartz cuvettes with a 1 cm path length using $_{td}H_2O$ as reference. Same amount of respective buffer had also been added into the $_{td}H_2O$ which was used as reference.

The amount of AA adsorbed under different conditions of pH, time and concentration was calculated from the difference between the initial AA concentration and the concentration after adsorption in each case. The initial concentration of AA and the quantity adsorbed were used to obtain the adsorption isotherms (Pandey et al. 2013). Percentage binding was calculated as follows-

$$\%\,binding = \frac{C_e - C_f}{C_e} \times 100 \tag{1}$$

Where, C_e is the initial concentration of adsorbate and C_f is the final concentration after adsorption. The theoretical limit of the concentration of adsorbate (Leu) available for adsorption is given (Fig. 1a).

Chromatographic techniques (Paper chromatography and HPLC) were used to measure the degradation products (if any) of Leu after adsorption studies as described in our previous work (Pandey et al. 2013).

Computational Study

Density functional theory (DFT) was used to investigate the interaction of Leu with metal cations (Ca^{2+}, Mg^{2+} and Cu^{2+}). Becke's three parameter exchange functional with a Lee, Yang and Parr type nonlocal correlation functional hybrid Hartee-Fock DFT method (B3LYP),was applied for metal ions and Leu with the all-electron 6-31G+(dp) internal basic set in Gaussian 03w (Becke 1993; Lee et al. 1988; Hohenberg and Kohn 1964). All the geometries were

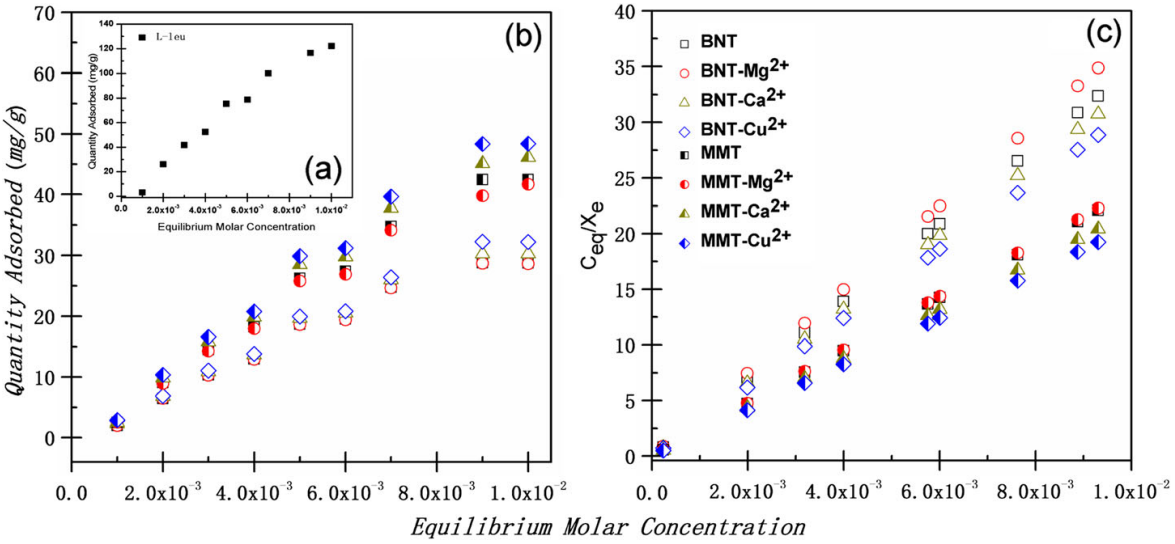


Fig. 1 Graph showing, (**a**) theoretical limit of availability of Leu for complete adsorption by 50 mg of adsorbents, (**b**) adsorption behaviour as a function of quantity adsorbed versus equilibrium molar concentration, and (**c**) Langmuir adsorption isotherm for different adsorbents for equilibrium time 8 h and pH 6.0

Author's personal copy

optimized and frequency calculations were used to cross-check the global minima of all the chemical species under study, where no imaginary frequencies were observed. Thermodynamic parameters are also obtained through frequency calculation. Open shell calculations using a spin-unrestricted formalism have been used for Leu—Cu^{2+}complex as Cu^{2+} is an open shell system with a $d^9(^2D)$ ground state (Remko et al. 2011). All the computational analysis were carried out with Intel(R) Core (TM) i5-3230 M CPU@2.60GHz PC on Windows-7 operating system. The formation of Leu—$M^{2+}\times(H_2O)_n$, (n=2 and 4) complexes can be described following, which has been used to compute the metal ion affinity as a negative enthalpy variation (ΔH) for the reaction-

$$\begin{array}{l} Leu + M^{2+} + (H_2O)_n \rightarrow Leu—M^{2+} \times (H_2O) \\ M = Mg^{2+},\ Ca^{2+} and\ Cu^{2+},\ n = 0,\ 2\ and\ 4. \end{array} \quad (2)$$

Results and Discussion

The adsorption of Leu on MMT/BNT and cation exchanged MMT/BNT, in aqueous medium was studied as a function of pH (4.0–9.2), temperature (298 K) and concentration (1 mM – 10 mM) of the adsorbate in order to find out the conditions of maximum adsorption. Moreover, the main aim is to study the role of divalent cation (Cu^{2+}, Mg^{2+} and Ca^{2+}) exchanged SMT as an adsorbent under prebiotic conditions.

The amount of adsorbate was determined from the standard concentration curve obtained from the optical density of the different Leu solutions monitored at their respective peak (λ_{max}) of absorption spectrum. Linear behaviour (r^2=0.97) was observed between the absorbance and concentration of Leu (Supplementary information S.1). Moreover, Leu adsorption was confirmed using EDS which showed the presence of C and N in addition to the elements present in the SMT.

The optimum conditions of surface interaction with respect to time and pH showed that the amount adsorbed depends on the contact time, and pH, where adsorption equilibrium is attained within 8 h (Supplementary information S.2). The optimum pH was found to be 6.0 which is also, isoelectric point of Leu (Supplementary information S.3).

The theoretical limit of the availability of total adsorbate (Leu) in 5 ml for 100 % adsorption by the 50 mg of SMT is shown in Fig. 1a. The adsorption isotherms (plot between equilibrium concentrations (C_{eq}) versus quantity adsorbed) are provided in Fig. 1b. The initial portion of the isotherm (From 1 to 6 mM of Leu) represents a linear relationship between the quantity adsorbed and C_{eq} of adsorbate, while at higher concentration (6 mM—10 mM), the isotherm saturates and adsorption becomes independent of Leu concentration. Langmuir type adsorption is observed (Fig. 1c) assuming the formation of a monolayer of adsorbate molecules on the surface of the adsorbent. The Langmuir parameters were determined form the equation below (Pandey et al. 2013).

$$\frac{C_{eq}}{X_e} = \frac{1}{K_L.X_m} + \frac{C_{eq}}{X_m} \quad (3)$$

Where C_{eq} is the equilibrium concentration of Leu.K_L is a constant which is a function of the adsorption energy *i.e.* the enthalpy of adsorption coefficient ($K_L=Ae^{-\Delta H/RT}$); X_e is amount of amino acid (mg) adsorbed per gram of SMT;X_m is the amount of Leu required for a definite weight of SMT for complete surface coverage.

Author's personal copy

The adsorption parameters (X_m and K_L) were calculated from the slope and intercept obtained from the graph of C_{eq}/X_e versus C_{eq} (Fig. 1c and Eq. 3). The goodness of linear fit of the Langmuir adsorption isotherm (Fig. 1c) was judged by the linear regression coefficients (r^2) which were ~0.99 (Table 1). Adsorption data were collected in triplicate and ~3.0–7.8 % error was observed in this study. Mean values are used to obtain isotherm (Fig. 1b, c).

Percentage binding of Leu on the two SMT is shown in Table 1, using eq. 1. Leu is ~24 % adsorbed on BNT while ~34 % is adsorbed for MMT, and same trend of the percentage adsorption with the divalent exchanged SMT has also been observed. Cu^{2+} exchanged SMT enhance the adsorbing ability of the both SMT (i.e. ~39 and ~26 % for MMT-Cu^{2+} and BNT-Cu^{2+} respectively) while in both the cases for Mg^{2+} exchanged SMT has apparently decreased (~24 and ~34 % respectively) the affinity of Leu for SMT(Table 1). SEM images of BNT-Cu^{2+} and its adduct with Leu are shown Fig. 2, clearly indicating the surface morphology of the BNT-Cu^{2+}, as Leu has finely covered its surface after adsorption (Fig. 2b).

Vibrational studies using FTIR were used to analyse the possible sites of interaction. FTIR spectra of Leu, MMT and Leu–MMT complex are provided in Fig. 3. The characteristic infrared spectral frequencies have been summarized in supplementary material (S.t.1).The bands at ~1035 $cm^{-1}$and ~3622 cm^{-1}corresponds to Si–O–Si stretching vibration and –OH stretching, respectively, while 3431 cm^{-1} and 1638 cm^{-1} are from the stretching and bending vibration of adsorbed water in MMT (Fig. 3b). In the case of Leu, no band corresponds to $-NH_2$ bending and absence of protonated –COOH (i.e. –OH stretching at ~3500 cm^{-1}, –C=O stretching at ~1700−1780 cm-1, –OH bending at ~1200–1300 cm-1), confirming amino group is protonated ($—NH_3^+$) while carboxylic group is deprotonated ($—COO^-$) (i.e. zwitter-ion) (Fig. 3a). Polymerization of Leu is not found in starting adsorbate as well as adsorption adduct as no peak correspond to amide (1640 cm^{-1} and 1550 cm-1) is found (Fig. 3a, c).

A band appears at 3073.17 cm^{-1} which is assigned to an leu-NH_3^+stretch (Fig. 3a) which changes to 3121.95 cm^{-1} after adsorption. Further, shift in the frequencies (i.e.$—COO^-$ symmetric stretching, $—COO^-$ anti-symmetric stretching) also suggest possible interaction via the COO^- moiety of Leu. A lower shift in the vibrational frequencies in adsorption adduct (Leu+MMT) also indicates, weak forces are applied in the course of surface interaction (Stevens and Anderson 1996).

Table 1 Percentage binding and Langmuir isotherm parameters of Leu on the surface of different adsorbents

Adsorbent	Binding (%)	Langmuir Parameters		
	Leu	X_m	K_L	r^2
BNT	24.72	28.83	62414.97	0.99
BNT-Mg^{2+}	24.62	28.75	62417.36	0.99
BNT-Ca^{2+}	25.98	30.36	62421.32	0.99
BNT-Cu^{2+}	26.39	32.32	62417.19	0.99
MMT	34.75	42.24	62422.88	0.99
MMT-Mg^{2+}	34.15	41.84	62413.69	1.00
MMT-Ca^{2+}	37.73	45.69	62421.28	0.99
MMT-Cu^{2+}	39.61	48.48	62410.89	0.99

Author's personal copy

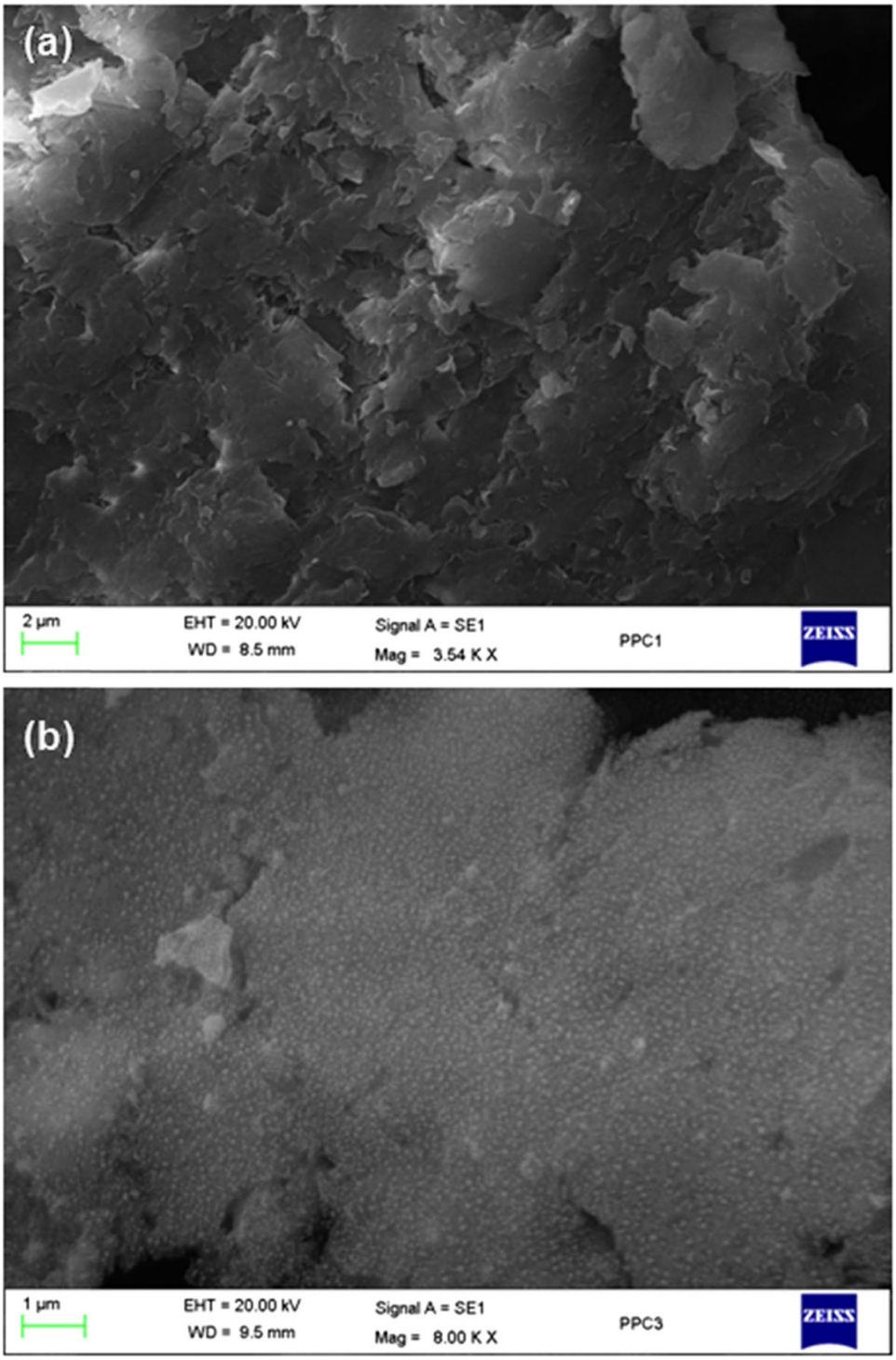


Fig. 2 SEM images of BNT-Cu^{2+} (**a**), and (**b**) adsorption adduct of Leu with BNT-Cu^{2+}

A proton sandwiched between two electronegative atoms (i.e. N of —$NH_3^+$and O of ─Si─O^- and ─Al─O^- of SMT) after adsorption require more energy to vibrate and thus, a shift in the hydrogen bond donor (—NH_3^+) as well as acceptor (—COO^-) sites of the zwitterion of AAs after adsorption on mineral surface found to be the crucial forces to stabilize AAs on SMT (Fig. 3 and S.t.1). The protonated amino group is an excellent hydrogen bond donor (Kollar et al. 2003; Fuchida et al. 2014; Marsh and Donohue 1967). The XRD of adsorption adducts have also, shown a shift in the basal spacing (001). The basal spacing of MMT is 15.56 Å which increases upto 17.18 Å after adsorption (Supplementary material S.4-

Author's personal copy

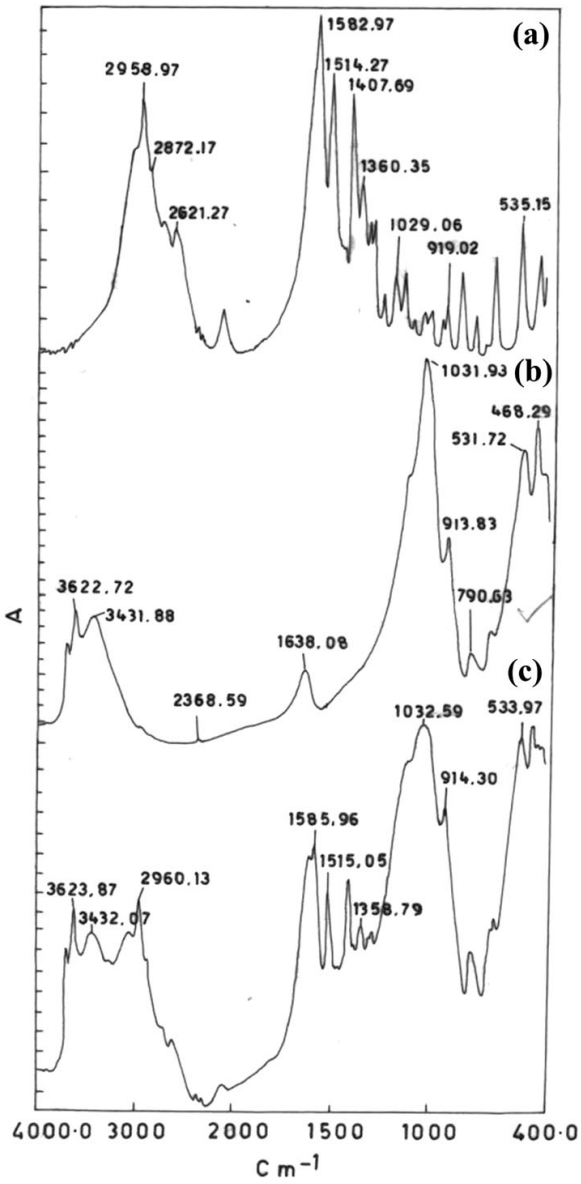


Fig. 3 IR spectra of (**a**) Leu, (**b**) MMT, and (**c**) adsorption adduct, Leu+MMT after adsorption at pH 6.0±0.1

S.6). The intercalation of AAs between the layers of SMT during the adsorption is more prominent than interaction on surfaces and edges of the SMT (Friebele et al. 1980) and an increment in the basal spacing (001) indicates towards the interlayer adsorption where AAs occupy the interlayer space of SMTs because AAs adsorbed on the surface may easily desorbs when SMTs are washed with $_{td}H_20$, prior to the FTIR and XRD analysis, due to the low activation energy of desorption (Lambert 2008). This interlayer acquisition of AAs in SMT may occur via cation exchange (Greenland et al. 1965) which has recently been shown by Fuchida et al. 2014.

Considering the SMT surface, previous reports have also shown surface interactions are largely dependant on interlayer cations, hydrogen bonding, physical forces and the clay's surface charge. (Ponnamperuma et al. 1982; Greenland et al. 1965) while net electric charge of the AAs, which depend on the pH in both the bulk solution and in the proximity of the clay layer or interlayer spaces, is another factor deciding adsorption (Prabhakar et al. 2007). Further, no decomposition or oligomerization of Leu was observed in our experiments.

Author's personal copy

Computational study

Complexation modes between M^{2+} and Leu with attractive interactions between electron rich (—COO^-) and electron deficient sites (M^{2+}) have been considered for zwitterionic amino acids as reported by Remko et al. (2011) and Marino et al.(2001).The respective atoms of zwitterionic Leu are numbered (not IUPAC) according to the scheme presented in Fig. 4a, and optimized geometric parameters of the Leu considered for theoretical studies along with hydrated or non-hydrated metal complexes Leu—$M^{2+}\times(H_2O)_n$,(where n=0, 2 or 4) are provided in supplementary material S.t.2-S.t.4. All of the output files can also be made available by contacting the corresponding author directly. For the hydrated system Leu—M^{2+}, metal ions are coordinated with two water molecules (Figs. 5a, c and e) using a supermolecule modelling of hydration while other two water molecules were placed near the polar part of the AA (Figs. 5 b, d and f), where the water molecules form intermolecular hydrogen bonds with the proton donor -NH_3^+ group (Remko et al. 2011).

The bond lengths, bond angles and dihedral angles of the computed Leu—M^{2+}complexesaregiven in Table 2, while calculated net charges on the metal, oxygen atoms, nitrogen atoms, dipole moment, total energies, relative energies including ZPE and thermodynamic parameters of nine different complexes of Leu—$M^{2+}\times(H_2O)_n$($M=Cu^{2+}$, Mg^{2+}, Ca^{2+} and n=0, 2 and 4) are summarized in Tables 3 and 4.

Preliminary computations of Leu suggest it forms stable complexes with divalent metal cations that may form in two different ways. First, binding of M^{2+} with the O3 of carboxylic acid group and the N5 of amine in neutral AA while, another, its interaction with both the oxygen (O3 and O4 ends) of the carboxylate ion of the zwitterionic form of the AA. The bicoordinated complexes of M^{2+}via simultaneous interactions of carbonyl oxygen and amine nitrogen is not possible as the lone pair of electron have already been associated with the proton (H^+) liberated from –COOH group in forming the zwitterion. The zwitterionic form of the AA may be stabilized by the presence of counter-ions and/or water molecules (Remko et al. 2011; Bush et al 2008). Further, harmonic vibrational frequencies of the optimized species have shown that all nine complexes are in their minimum energy state as no imaginary frequencies have been observed in their respective frequency calculations using the level of quantum theory as described in experimental section.

The selected geometrical changes for the Leu—M^{2+} complexes indicate that the O(4) ····M(9) bonds are always shorter (0.025 Å, 0.041 Å and 0.032 Å for Mg^{2+}, Ca^{2+} and Cu^{2+}

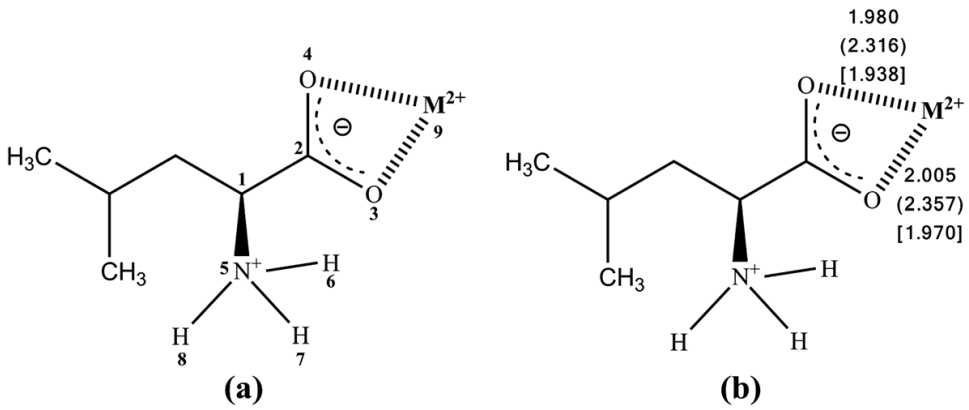


Fig. 4 Chemical structures of (**a**) Leu with numbering, and (**b**) B3LYP/631+G(d,p) optimized distances (Å) for different bicoordinated Leu—M^{2+} complexes with Mg^{2+}, Ca^{2+} and Cu^{2+} reported without enclosures, within parentheses, and with square brackets, respectively

Author's personal copy

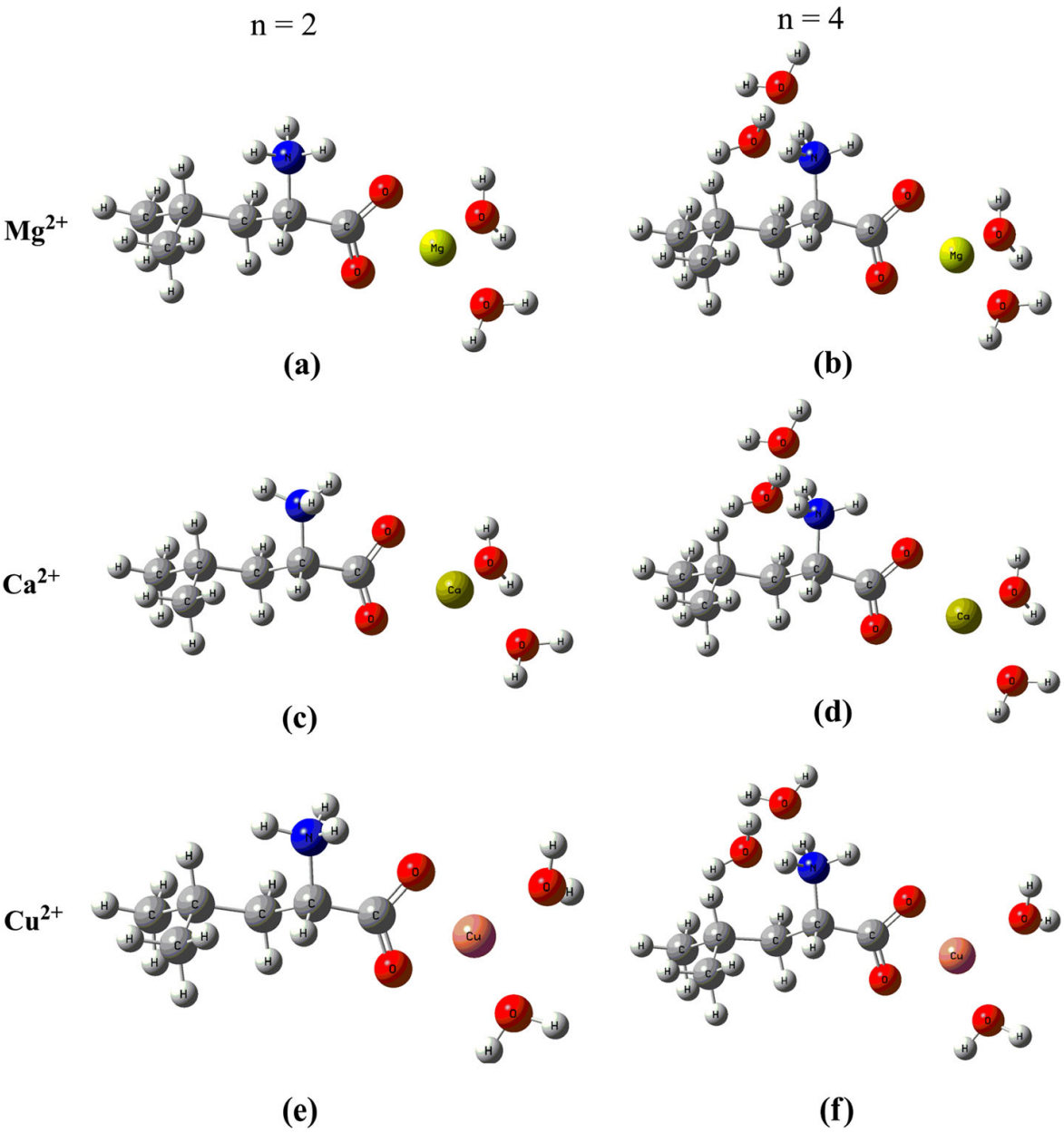


Fig. 5 Overall structure of the B3LYP/631+G(d,p) optimized complexes of Leu with Mg^{2+} (**a** and **b**), Ca^{2+} (**c** and **d**) and Cu^{2+} (**e** and **f**) in presence of water molecules (n=2 or 4)

respectively) than O(3)···M(9) bonds, indicating that these metal ions form stronger bonds with O(4) which are farther away from the ammonium group ($-NH_3^+$) of Leu. The equilibrium distance of O(4)···M(9) and O(3)···M(9) increases in the order: $Cu^{2+}<Mg^{2+}<Ca^{2+}$ (Fig. 4b). The M^{2+} in both the non-hydrated (Leu—M^{2+}) as well as hydrated (Leu—$M^{2+}\times(H_2O)_n$, n=2 or 4) lie in the same plane of carboxylate groups of Leu (Fig. 5).

Table 4 summarizes the different energies and thermodynamic parameters which reflect that the stability of Leu-M^{2+}can be substantially modified by the specific metal ion and hydration. Energy parameters were calculated using eq. 2 and all nine complexes studied were found to form exothermically (Table 4). Leu—$Cu^{2+}$was found to be the most stable complex while its hydration further increases its stability with a maximum enthalpy of -386.28 kcal/mol for Leu—$Cu^{2+}\times(H_2O)_4$, among all nine complexes studied(Table 4). Metal ion affinities as a negative enthalpy variation (ΔH) for Leu—M^{2+}complexes has found minimum with Ca^{2+}(Table 4). Gibbs energies, which measure the tendency to associate in real molecular

Author's personal copy

Table 2 B3LYP/6-31+G(d,p) optimized relevant bond lengths (Å), bond angles (deg) and dihedral angles (deg) for Leu—M^{2+} complex

Parameters	Leu−M^{2+} complex		
	Mg^{2+}	Ca^{2+}	Cu^{2+}
d[C(1)−C(2)]	1.51555	1.52482	1.50402
d[C(2)−O(3)]	1.28631	1.28202	1.28089
d[C(2)−O(4)]	1.27438	1.26606	1.28120
d[C(1)−N(5)]	1.52211	1.52463	1.52208
d[N(5)−H(6)]	1.02804	1.02950	1.02931
d[N(5)−H(7)]	1.02694	1.02558	1.02866
d[N(5)−H(8)]	1.02918	1.02819	1.03031
d[O(3)−H(6)]	2.51355	2.21961	2.69964
d[O(3)····M(9)]	2.00456	2.35692	1.97009
d[O(4) ····M(9)]	1.97993	2.31611	1.93847
Θ[C(1) –C(2)−O(3)]	121.11858	119.50021	124.50286
Θ[C(2) –C(1)−N(5)]	108.92713	108.00197	109.60729
Θ[O(3) –C(2)−O(4)]	119.02753	121.72136	113.79321
Θ[C(1) –O(4) ····M(9)]	120.48338	125.56861	122.20556
Θ[C(1) –O(3) ····M(9)]	118.24496	122.69798	119.25686
Θ[C(2) –O(3) ····M(9)]	86.16892	89.57749	89.09900
Θ[O(3)····M(9)····O(4)]	67.25545	56.87553	66.60602
ϕ[O(3)−C(2)−C(1)−N(5)]	−8.89928	−12.30457	−8.77769
ϕ[C(1)−C(2)−O(4)···· M(9)]	178.73075	178.25947	179.10865
ϕ[C(1)−C(2)−O(3)···· M(9)]	−178.71686	−178.25057	−179.06574

complexes, are found to be negative and have energies from -114.27 to -342.61 kcal/mol (Table 4). The energetic differentiation of all the complexes studied based on the type of different metal ions (Mg^{2+}, Ca^{2+} and Cu^{2+}) with Leu, a decreasing order of Gibbs energy is Leu—Cu^{2+}>Leu—Mg^{2+}>Leu—Ca^{2+}has been observed. The ΔG for the non-hydrated leu-M^{2+}complexes were calculated to be -173.09 k.cal/mol, -114.27 k.cal/mol and -251.34 k.cal/

Table 3 B3LYP/6-31+G(dp) calculated net charge of metal (q_{M+}), two oxygen ($q_{O(3)}$ and $q_{O(4)}$), nitrogen ($q_{N(5)}$) in |e|, dipole moments (μ in Debye) and amount of metal ion charge transfer (CT) for different Leu—M^{2+}×$(H_2O)_n$, (n=0, 2 and 4) systems calculated at 298.15 K and 1 atm. pressure

System	Species		q_{M+}	q_{Ons}	$q_{O(4)}$	$q_{N(5)}$	μ	CT/e
(Leu····M^{2+})×$(H_2O)_n$	M=Mg^{2+}	n=0	1.822	−0.834	−0.789	−0.818	15.25	0.178
		n=2	1.790	−0.834	−0.784	−0.818	12.92	0.210
		n=4	1.787	−0.840	−0.802	−0.855	13.11	0.213
	M=Ca^{2+}	n=0	1.924	−0.859	−0.808	−0.821	16.82	0.076
		n=2	1.907	−0.850	−0.793	−0.825	13.68	0.093
		n=4	1.902	−0.854	−0.813	−0.855	14.39	0.098
	M=Cu^{2+}	n=0	1.332	−0.624	−0.576	−0.821	6.60	0.668
		n=2	1.401	−0.714	−0.667	−0.818	7.17	0.599
		n=4	1.384	−0.712	−0.675	−0.854	7.58	0.616

Author's personal copy

Table 4 B3LYP/631+G(d,p) calculated absolute energy (E in au), energy change (ΔE in k.cal/mol), metal ion affinities (ΔH in k.cal/mol), Gibbs free energies (ΔG in k.cal/mol) and entropies (ΔS in cal/mol.K) for different Leu—M^{2+}×$(H_2O)_n$, (n=0, 2 and 4) systems calculated at 298.15 K and 1 atm pressure

Parameters	(Leu····M^{2+})×$(H_2O)_n$								
	M=Mg^{2+}			M=Ca^{2+}			M=Cu^{2+}		
	n=0	*n*=2	*n*=4	*n*=0	*n*=2	*n*=4	*n*=0	*n*=2	*n*=4
-E	641.25	794.28	947.20	1118.79	1271.78	1424.70	2081.39	2234.42	2387.34
-ΔE	182.73	284.14	321.72	123.74	199.61	234.69	260.10	356.99	394.52
-ΔH	181.11	278.72	313.24	122.27	194.60	226.61	259.23	349.62	386.28
-ΔG	173.09	252.94	271.25	114.27	170.81	187.68	251.34	323.48	342.61
-ΔS	26.89	86.46	140.86	26.83	79.81	130.57	26.47	87.66	146.45

mol for Mg^{2+}, Ca^{2+}, and Cu^{2+} complexes respectively. To analyze the affinity of hydration with the Leu—M^{2+} complexes, first two water molecules were coordinated to M^{2+} ions (Figs. 5a, c and e), which lowered the ΔG values for the complexes with Mg^{2+}, Ca^{2+}, and Cu^{2+} by-79.85 k.cal/mol, -56.54 k.cal/mol and -72.14 k.cal/mol respectively (Table 4). Addition of another two water molecules to give an Leu—M^{2+}×$(H_2O)_4$ complex further lowered the ΔG values by -18.31 k.cal/mol (Fig. 5b), -16.87 k.cal/mol (Fig. 5d) and -19.13 k.cal/mol (Fig. 5f) for Mg^{2+}, Ca^{2+}, and Cu^{2+} complexes respectively.

The net atomic charges on the different atoms of the complexes studied, have been investigated by the natural population analysis using the NBO program (Reed and Weinhold 1985; Reed et al. 1985; Glendening et al. NBO program, Version 3.1). The amounts of charge transfer (CT) for the M^{2+} along with dipole moments are summarized in Table 3. The stronger bond formation between O4····$M^{2+}$of different Leu—M^{2+}×$(H_2O)_n$ complexes can further be analyzed through the charges on O4 along with O4····M^{2+}distance (Å) in comparison to charge and bond distance (Å) of O3 and O3····M^{2+} respectively. The charge on O4 of different complexes is always in lower side than O3 which suggest the transfer of more of it charge towards M^{2+} from this end contrary to O3. The magnitude of CT contribution in Leu—$Ca^{2+}$is much lower (0.076 to 0.098*e*) for its non-hydrated as well as hydrated complexes while CT for all Leu—Cu^{2+} complexes are maximum from 0.559 to 0.668*e* (Table 3). The magnitudes of charge transfer on the metal ions studied are in good agreement with their metal ion affinities (Table 3 and 4). The interactions of glycine with 15 different metals at theoretical level, also showed the magnitude of CT correlates well with metal ion interaction energies (Hoyau et al. 2001).

Looking at the bigger picture, the experimentally studied adsorption processes of Leu on SMT and their Cu^{2+} and Ca^{2+} ion exchanged counterparts, essentially represents the enhanced affinity of biomolecules on metal-exchanged SMT, which have been suggested to have played a role during chemical evolution and the origin of life (Lambert 2008). The present study shows significant affinity of non-polar amino acid Leu with M^{2+} ion exchanged SMT surfaces, specially Cu^{2+} exchanged SMT, which might be helpful to give insight into the higher percentage of neutral and non-polar AAs in proteins of present day living systems as modern proteins comprise of total 74 % non polar amino acids (Zaia 2004). Metal exchanged minerals could possibly help to accumulate the non-polar amino acids via adsorption on their surfaces which may, facilitate their polymerization to get complex proteins. Further, this study may help

Author's personal copy

to understand the specific sites of attachments of amino acids, peptides or proteins onto different field of adsorption (peptide sequencing identification, nano technology, drug targeting/delivery and chemical evolution) (Roman et al. 2006) and the physico-chemical parameters (i.e. change in bond length, bond angles, electron density, charge and thermodynamic parameters) of M^{2+}—AAs complexes may also help in better understanding of the biochemistry of living systems and also serve as a simpler model for the AAs—M^{2+} interaction found in the more complex protein, enzyme-metal systems related to living systems such as Cu^{+} coordinated with peptides (viz. glycylglycine) has been reported to stabilize this peptide structure (Constantino et al. 2005).

Conclusion

The interaction of the Leu on BNT/MMT and its divalent metal ion (Mg^{2+}, Ca^{2+} and Cu^{2+}) exchanged forms was investigated with respect to the optimal conditions of pH, time and concentration at 298 K. Adsorption parameters such as percentage binding show that Leu is adsorbed more on the MMT than BNT. Further, Cu^{2+} exchanged BNT/MMT adsorbs Leu the most strongly, while Mg^{2+}exchanged SMTs showed the weakest sorption. Experimentally, interaction of biomolecules with metal exchanged clays and theoretically determined physico-chemical characteristics of different metal ion-biomolecular interactions, may shed light on the prebiotic formation of macromolecules and their significance in living systems such as affinity of Cu^{2+} for the biomolecular selectivity for the enhancement of peptide formation (Sakata et al. 2014; Constantino et al. 2005). A better surface interaction of AA in presence of Cu^{2+} incorporated minerals might possibly enhance the proximity effect of functional groups to form peptides. Moreover, it may be concluded that in prebiotic era of the earth adsorption processes involving metal ions might have played a key role for local concentration of biomolecules and thus facilitated further condensation and polymerization on their surfaces into more complex molecules essential for life.

Acknowledgment Authors are grateful to two anonymous reviewers for the major suggestion and corrections. The authors are also thankful to Head of the Chemistry Department and Prof. Sanjay Pant Photophysics Laboratory, Head of Physics Department, DSB Campus, Kumaun University, Nainital 263002, India for providing necessary research facilities. Prof. Sanjay Pant is specially acknowledged for providing computational facility of Gaussian 03w, along with other research facilities. Authors (PA and NP) acknowledge the UGC-RFMS (Sanction No:F, 5-53/2007 BSR), New Delhi, India for financial assistance.

References

Becke AD (1993) Density-functional thermochemistry. III. The role of exact exchange. J Chem Phys 98:5648

Bernal JD (1951) The Physical basis of life.ProcPhysSocLond A. 62:537-558

Bush MF, Oomens J, Saykally RJ, Williams ER (2008) Effects of alkaline earth metal ion complexation on amino acid zwitterion stability: results from infrared action spectroscopy. J Am Chem Soc 130:6463–6471

Caglar B, Afsin B, Tabak A, Eren E (2009) Characterization of the cation-exchanged bentonites by XRPD, ATR, DTA/TG analyses and BET measurement. Chem Eng J 149:242–248

Carr MH, Head (III) JW (2010) Geological history of mars. Earth Planet Sci Lett 294:185–203

Cleaves HJ(II), Scott AM, Hill FC, Leszczynski J, Sahai N, Hazen R (2012) Mineral–organic interfacial processes: potential roles in the origins of life. Chem Soc Rev 41:5502–5525

Author's personal copy

Constantino E, Rimola A, Santiago LR, Sodupe M (2005) Coordination properties of glycylglycine to Cu^{+}, Ni^{+} and Co^{+}: influence of metal cation electronic configuration. New J Chem 29:1585–1593

Ferris JP, Hill AR Jr, Liu R, Orgel LE (1996) Synthesis of long prebiotic oligomers on mineral surfaces. Nature 381:59–61

Friebele E, Shimoyama A, Ponnamperuma C (1980) Adsorption of protein and non-protein amino acids on a clay minerals: a possible role of selection in chemical evolution. J MolEvol 16:269–278

Frisch MJ, Trucks GW, Schlegel HB, Scuseria, Robb MA, Cheeseman JR, Montgomery JA, VrevenJrT, Kudin KN, Burant JC, Millam JM, Iyengar SS, Tomasi J, Barone V, Mennucci B, Cossi M, Scalmani G, Rega N, Petersson GA,Nakatsuji H, Hada M, Ehara M, Toyota K, Fukuda R, Hasegawa J, Ishida M, Nakajima T, Honda Y, Kitao O, Nakai H, Klene M, Li X, Knox JE, Hratchian HP, Cross JB, Adamo C, Jaramillo J, Gomperts R, Stratmann RE, Yazyev O, Austin AJ, Cammi R, Pomelli C,Ochterski JK, Ayala PY, Morokuma K, Voth GA, Salvador P, Dannenberg JJ, Zakrzewski VG, Dapprich S, Daniels AD, Strain MC, Farkas O, Malick DK, Rabuck AD, Raghavachari K, Foresman JB, Ortiz JV, Cui Q, Baboul AG, Clifford S, Cioslowski J, Stefanov BB, Liu G, Liashenko A, Piskorz P, Komaromi I, Martin RL, Fox DJ, Keith T, Al-Laham MA, Peng CY, Nanayakkara A, Challacombe M, Gill PMW, Johnson B, Chen W, Wong MW, Gonzalez C, Pople JA(2003) Gaussian 03, Revision A.1, Gaussian, Inc., Pittsburgh, PA

Fuchida S, Masuda H, Shinoda K (2014) Peptide formation mechanism on montmorillonite under thermal conditions. Orig Life EvolBiosph 44(1):13–28

Glendening ED, Reed AE, Carpenter JE, Weinhold F. The NBO program, Version 3.1

Greenland DJ, Laby RH, Quirk JP (1965) Adsorption of amino-acids and peptides by montmorillonite and illite. Part 1. Cation exchange and proton transfer. Trans Faraday Soc 61:2013–2023

Gururani K, Pant CK, Pandey N, Pandey P (2012a) Heat induced formation of peptides from reaction mixture of glycine-glutiamic acid and glycine-leucine in presence and absence of montmorillonite clay with or without metal ions under wetting drying cycles of primitive Earth. Int J Scie Techno Res 1(8):159–163

Gururani K, Pant CK, Pandey P, Pandey N (2012b) Heat induced synthesis of amino acids from reaction system comprised of acetylene, ammonia and water vapour in presence and absence of metal oxide (silica and alumina) under wetting-drying condition of primitive Earth. Asian J Res Chem 5(9):1150–1155

Hohenberg P, Kohn W (1964) Inhomogeneous electron Gas. Phys Rev 136:B864–B871

Hoyau S, Pelicier JP, Rogalewiez F, Hoppilliard Y, Ohanessian G (2001) Complexation of glycine by atomic metal cations in the gas phase. Eur J Mass Spectrom 7:303–311

Kalra S, Pant CK, Pathak HD, Mehata MS (2003) Studies on the adsorption of peptides of glycine/alanine on montmorillonite clay with or without co-ordinated divalent cations. Colloids and Surfaces A: Physicochem Eng Aspects 212:43–50

Kebarle P, Hogg AM (1965) Mass-spectrometric study of ions at near atmospheric pressures. I Ionic Polym Ethyl J Chem Phys 42(2):668–674

Kollar T, Palinko I, Konya Z, Kiricsi I (2003) Intercalating amino acid guests into montmorillonite host. J MolStruct 651:335–340

Lahav N, Chang S (1976) The possible role of solid surface area in condensation reactions during chemical evolution: reevaluation. J MolEvol 8:357–380

Lambert JF (2008) Adsorption and polymerization of amino acids on mineral surfaces: a review. Orig Life Evol Biosph 38:211–242

Lee C, Yang W, Parr RG (1988) Development of the colle-salvetti correlation-energy formula into a functional of the electron density. Phys Rev B 37:785

Lucrezia DD, Anella F, Chiarabelli C (2007) Question 5: on the chemical reality of the RNA world. Orig Life EvolBiosph 37:379–385

Marino T, Russo N, Toscano M (2001) Potential energy surfaces for the gas-phase interaction between α-alanine and alkali metal ions (Li+, Na+, K+): a density function study. Inorg Chem 40:6439–6443

Marsh RE, Donohue J (1967) Crystal structure studies of amino acids and peptides. AdvProtein Chem 22:235–256

Marshall-Bowman K, Ohara S, Sverjensky DA, Hazen RM, Cleaves HJ (2010) Catalytic peptide hydrolysis by mineral surface: implications for prebiotic chemistry. Geochim Cosmochim Acta 74:5852–5861

Merz KM, Aguiar EC, da Salvia JBP (2014) Adenine formation without HCN. J Phys Chem A 118(20):3637–3644

Orgel LE (2004) Prebiotic chemistry and the origin of the RNA world. Crit Rev Biochem Mol Biol 39:99–123

Pandey P, Pant CK, Gururani K, Arora P, Kumar S, Sharma Y, Pathak HD, Mehata MS (2013) Surface interaction of L-alanine on hematite: anastrobiological implication. Orig Life Evol Biosph 43:331–339

Pant CK, Lata H, Pathak HD, Mehata MS (2009) Heat-initiated prebiotic formation of peptides from glycine/aspartic acid and glycine/valine in aqueous environment and clay suspension. Int J Astrobiol 8(2):107–115

Pizzarello S (2009) The cosmochemical record of carbonaceous meteorites:an evolutionary story. J Mex Chem Soc 53(4):253–260

Author's personal copy

Ponnamperuma C, Shimoyama A, Friebele E (1982) Clay and origin of life. Orig Life Evol Biosph 12:9–40
Prabhakar A, Cuadros J, Sephton M, Dubbiam D, Coles BJ, Weiss D (2007) Adsorption of L-lysine on montmorillonite. Colloids Surf A Physicochem Eng Asp 307:142–149
Reed AE, Weinhold FA (1985) Natural localized molecular orbitals. J Chem Phys 83:1736–1740
Reed AE, Weinstock RB, Weinhold FA (1985) Natural population analysis. J Chem Phys 83:735–746
Remko M, Rode BM (2000) Bivalent cation binding effect on formation of the peptide bond. Chem Phys Lett 316:489–494
Remko M, Fitz D, Broer R, Rode BM (2011) Effect of metal ions (Ni^{2+}, Cu^{2+} and Zn^{2+}) and water coordination on the structure of L-phenylalanine, L-tyrosine, L-tryptophan and their zwitterionic forms. J Mol Model 17: 3117–3128
Rode BM, Bujdak J, Eder AH (1993) The role of inorganic substances in the chemical evolution of peptides on Earth. Trends Inorg Chem 3:45–62
Rodgers MT, Armentrout PB (2000) Noncovalent interactions of nucleic acid bases (uracil, thymine, and adenine) with alkali metal ions. Threshold collision-induced dissociation and theoretical studies. J Am Chem Soc 122(35):8548–8558
Roman T, Dino WA, Nakanishi H, Kasai H (2006) Glycine adsorption of Single-walled carbon nanotubes. Thin Solid Films 509:218–222
Sakata K, Yabuta H, Kondo T (2014) Effects of metal ions and p H on the formation and decomposition rates of di- and tri-peptides in aqueous solution. Geochem J 48(2):219–230
Shapiro R (1999) Prebiotic cytosine synthesis: a critical analysis and implications for the origin of life. Proc Natl Acad Sci U S A 96:4396–4401
Stephenson JD, Hallis LJ, Nagashima K, Freeland S (2013) Boron enrichment in martian clay. PLoS ONE 8(6): 1–4
Stevens JJ, Anderson SJ (1996) An FRIR study of water sorption on TMA- and TMPA-montmorillonites. Clay Clay Miner 44(1):142–150
Stribling R, Miller SL (1987) Energy yields for hydrogen cyanide and formaldehyde syntheses: the HCN and amino acid concentrations in the primitive ocean. Orig Life Evol Biosph 17:261–273
Zaia DAM (2004) A review of adsorption of amino acids on minerals: was it important for origin of life? Amino Acids 27:113–118
Zaia DAM (2012) Adsorption of amino acids and nucleic acid bases onto minerals: a few suggestions for prebiotic chemistry experiments. Int J of Astrobiol 11:1–6

ResearchGate

See discussions, stats, and author profiles for this publication at: http://www.researchgate.net/publication/276859948

An integrated framework of interpretive structural modeling and graph theory matrix approach to fix the agility index of an automobile manufacturing organization

ARTICLE · MARCH 2015

DOI: 10.1007/s13198-015-0350-x

READS

18

3 AUTHORS, INCLUDING:



Rajesh Kumar Singh

Delhi Technological University

30 PUBLICATIONS **256** CITATIONS

SEE PROFILE

Available from: Rajesh Kumar Singh

Retrieved on: 20 October 2015

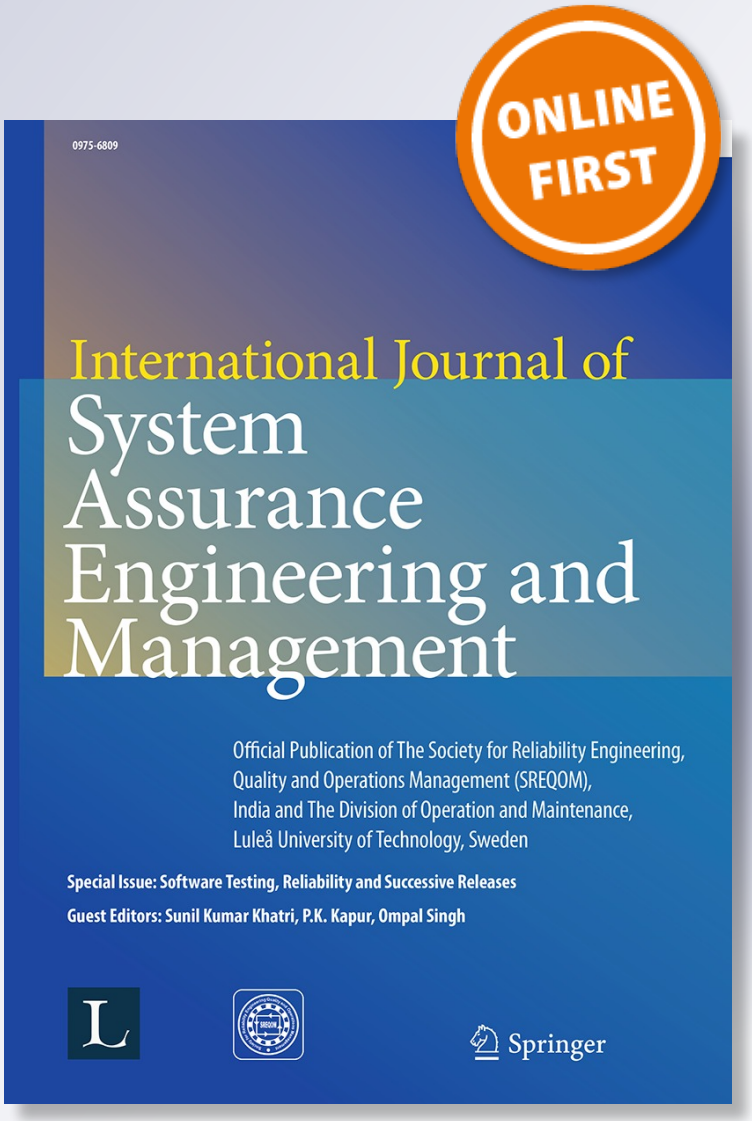
An integrated framework of interpretive structural modeling and graph theory matrix approach to fix the agility index of an automobile manufacturing organization

Pravin Kumar, Rajesh K. Singh & Rakesh Kumar

International Journal of System Assurance Engineering and Management

ISSN 0975-6809

Int J Syst Assur Eng Manag
DOI 10.1007/s13198-015-0350-x



Springer

Your article is protected by copyright and all rights are held exclusively by The Society for Reliability Engineering, Quality and Operations Management (SREQOM), India and The Division of Operation and Maintenance, Lulea University of Technology, Sweden. This e-offprint is for personal use only and shall not be self-archived in electronic repositories. If you wish to self-archive your article, please use the accepted manuscript version for posting on your own website. You may further deposit the accepted manuscript version in any repository, provided it is only made publicly available 12 months after official publication or later and provided acknowledgement is given to the original source of publication and a link is inserted to the published article on Springer's website. The link must be accompanied by the following text: "The final publication is available at link.springer.com".



Author's personal copy

Int J Syst Assur Eng Manag
DOI 10.1007/s13198-015-0350-x

ORIGINAL ARTICLE

An integrated framework of interpretive structural modeling and graph theory matrix approach to fix the agility index of an automobile manufacturing organization

Pravin Kumar[1] · **Rajesh K. Singh**[1] · **Rakesh Kumar**[1]

Received: 1 December 2014 / Revised: 4 March 2015
© The Society for Reliability Engineering, Quality and Operations Management (SREQOM), India and The Division of Operation and Maintenance, Lulea University of Technology, Sweden 2015

Abstract Free trade policies, globalization of the economy, and continuous changes in technology have increased competition among the manufacturers. Identification of customers' changing needs and its simultaneous fulfillment becomes more important for manufacturers as well as suppliers. The needs for flexible, rapid, cost effective and high quality product development have led to the concept of agile manufacturing. In this paper, some important variables of the agile manufacturing system that leads the agility of the systems have been analyzed and interrelationship has been developed using interpretive structural modeling. Finally, the weightage for the existing relations have been assigned by the executives of the case company. The agility index of the case company has been determined with the help of graph theory matrix approach. This paper may help the manufacturers identify its agility and compare with the agility of competitors' organizations.

Keywords Agility · Flexibility · Lean manufacturing · Interpretive structural modeling · Graph theory

✉ Pravin Kumar
pravin.dce@gmail.com

Rajesh K. Singh
rksdce@yahoo.com

Rakesh Kumar
rakeshtech1@gmail.com

[1] Department of Mechanical Engineering, Delhi Technological University, Bawana Road, Delhi 110042, India

1 Introduction

Agile manufacturing is a combination of flexible and responsive manufacturing systems. Flexible manufacturing shows the ability to change the entire systems, according to changes in customer requirements. Agility should not be confused with leanness. Lean manufacturing has focused on the elimination of waste and large inventories. Lean leads to high productivity and quality, but it does not necessarily imply being responsive. But, lean manufacturing reduces the cost of production by eliminating the waste. There is equal importance of cost and responsiveness for agile manufacturing systems (AMS). Yusuf et al. (1999) incorporated cost and quality into agile competitive bases.

Agility means using market knowledge and a virtual corporation to exploit profitable opportunities in a volatile marketplace (Naylor et al. 1999). AMS is intended to improve the competitiveness of manufacturers in continuously changing market conditions. There is requirement of complete integration of systems from supplier to customer to design, develop and manufacture the products rapidly and cost effectively. Agility becomes a tool to respond rapidly to continuous and unpredicted changes in the market driven by customer designed products and services (Cho et al. 1996). The concept of flexible and more responsive manufacturing led to the new concept of AMS (Gunasekaran and Yusuf 2002). The concept of agile manufacturing was first time launched in 1991 at Lehigh University.

Flexibility is a subset of agility. The concept of an agile enterprise came about as the result of a collaborative, cross-industry workshop in 1991. Agility was initially defined as "the ability of an organization to thrive in a continuously changing, unpredictable business environment" (Dove et al. 1991). Dove (1999) has since redefined the agility as "the

Published online: 15 March 2015

Author's personal copy

ability to manage and apply knowledge effectively", recognizing the importance of information in firm decision making. Agility has become more important in a rapidly changing business environment (Kumar et al. 2008).

The main drivers of AMS are: short product life cycle; tough competition due to globalization of business, region-wise customization of products and services, advancement in manufacturing technologies and equipments, global sourcing, advanced information technology, increasing customer awareness about products, improved global logistics, and inter-organizational relationships. Thus, for survival in global market an entire manufacturing system must be agile.

Gupta and Mittal (1996) stressed on both responsiveness as well as the leanness of the manufacturing system. They gave more priority to respond than cost effectiveness. De Vor and Mills (1995) defined AMS as "ability to thrive in a competitive environment of continuous and unanticipated change and to respond quickly to rapidly changing markets driven by customer-based valuing of products and services.

A number of research works concerning the agile manufacturing are available. However, very little effort made to present relationships among the variables and fix the agility index of an organization based on these relationships. Gunasekaran (1998) emphasized seven variables of AMS: virtual enterprise formation tools/metrics, physically distributed manufacturing architecture and teams, rapid partnership formation tools/metrics, concurrent engineering, integrated product/production/information system, rapid prototyping and e-commerce. He reviewed the literature works available in agile manufacturing and made a good effort to collect all the variables, but in the changing market scenario there is need to re-examine the variables with mutual interactions. This paper re-examines the variables of AMS in the present business scenario and shows the digraph relationship of variables with the mutual interaction to achieve the required agility.

Since, in interpretive structural modeling (ISM), the relations can be shown only in binary terms, i.e., 0 and 1, where 0 shows that there is no relation between the variables 'i' and 'j' and 1 shows the existence of the relationship between the variables 'i' and 'j'. But, ISM only shows the existence and nonexistence of relationships, not the weights of relationships. Therefore, to overcome this problem, graph theory matrix approach (GTMA) has been used to assign weights to show the weight of influence of one variable over another. In this paper, an integrated framework of ISM and GTMA has been used to fix the agility index of a company XYZ.

The remainder parts of the paper have been arranged as follows: Sect. 2 deals with the variables of AMS; Sect. 3 presents the ISM-GTMA model development and Sect. 4 presents background of the case study and result and discussion; Sect. 5 concludes the research.

2 Variables of agile manufacturing system

Total ten major variables of AMS have been incorporated to develop ISM-GTMA model; these variables are: (i) manufacturing flexibility; (ii) strategic production planning; (iii) concurrent engineering; (iv) automation in manufacturing; (v) integrated information system; (vi) cross-functional workforce; (vii) strategic partnership and supplier development; (viii) product design and development; (xi) product postponement and; (xiv) agile manufacturing. The brief discussions about these variables are given below:

2.1 Manufacturing flexibility

Manufacturing flexibility is the ability of an organization to change its manufacturing systems according to the requirements. Sethi and Sethi (1990) defined manufacturing flexibility in terms of the ability of reconfiguration of manufacturing resources to produce different products of acceptable quality level efficiently. Swafford et al. (2006) defined manufacturing flexibility as the ability of manufacturing system to adapt its capabilities to produce quality products, timely and cost effective manner to respond to changing product characteristics, material supply, and demand, or to employ technological process enhancements. Manufacturing flexibility continues to be a concern for companies as they strive to meet the changing demands of their customer (Krause et al. 2007). Avittathur and Swamidass (2007) divided the evolution of the manufacturing flexibility concept into four phases from concept development to supplier buyer integrations.

2.2 Strategic production planning

There are a number of uncertainties related to production activities such as fluctuation in demand, the introduction of new products or customization of existing products. To respond the demand uncertainties, a manufacturer should have multiple options such as outsourcing, subcontracting, overtime production, daily wages workers, expansion of plants, etc. To introduce new products into the market within short notice, there is requirement of generic machines and multi-skilled personals with advanced technologies and strong research and development. For customization of existing products the decoupling point in the manufacturing or assembly should be shifted to last stage. Gianesi (1998) identified the need for a formal mechanism aiming to integrate operational decisions both horizontally, between different functional areas, and vertically, within the manufacturing function. It outlined some of the desired characteristics of a potential method to fulfill

Author's personal copy

the aforementioned need and proposed that the integration should be done under the domain of the production planning process.

2.3 Concurrent engineering

Concurrent engineering also called simultaneous engineering was coined by the US in 1989. It means a way of work where the various engineering activities in the product development, process development and field support development are integrated and performed as much as possible in parallel rather than in sequential order. Medhat and Rook (1997) emphasized the need of multifunctional team and emerging techniques such as computer-aided design and computer-aided manufacturing (CAD/CAM), computer-aided engineering (CAE), computer-aided process planning (CAPM), design for manufacturing (DFM), design for assembly (DFA), and quality function deployment (QFD). Graham and Ragade (1994) highlighted the need of design improvement and concurrently to check the suitability for manufacturing.

Liu et al. (2010) presented a generic integration framework with a semantic feature model for knowledge representation and reasoning across domains in concurrent engineering. An implementation of the proposed semantic feature model was presented to demonstrate its advantage in knowledge representation by feature transformation across domains in concurrent engineering. Belay et al. (2011) observed the effect of quality management and concurrent engineering in business performance.

2.4 Automation in manufacturing

Automation is an integration of knowledge of various fields such as mechanical, electronics, computer and information technology to produce an item. It is very helpful to reduce production lead-time, improve quality, and lower the manufacturing cost. Some of the important technologies which have been frequently used are: flexible manufacturing system (FMS), group technology (GT), cellular manufacturing, computer aided quality control (CAQC), computer numerical control (CNC), direct numerical control (DNC), automated guided vehicle (AGV), automated storage and retrieval system (AS/RS), rapid prototyping (RP), etc.

Rapid prototyping is an important part of AMS. It is a combination of technology, which converts directly a design file into a prototype, which is used in analysis during the design development phase with the least time. It compresses the lead time of design and production. Rapid prototyping is able to produce a prototype in shorter lead-time with less material wastage. This valuable benefit of the technology makes it worth for agile manufacturing (Kumar and Kumar 2006). Prototyping is a process of analysis of product design before putting it into real use. Rapid prototyping has been used in the production of three-dimensional object by stereolithography. Wang et al. (2002) mentioned its utilization in their research work "conceptual approach for managing design recourses".

2.5 Integrated information system

Several research articles have been published on the use of information technology (IT) within an organization (Katayama and Bennett 1999; Powell and Dent-Micallef 1997; Palvia 1997). Information system flexibility can be defined as the ability of an organization's collective information system to adapt and support changing requirements of the business functions such as product development, sourcing, manufacturing and logistics, and other strategic goals. Sethi and King (1994) developed a concept called competitive advantage provided by and information technology application (CAPITA), which measures the firm's competitive benefits gained through the use of a single information technology application (Kumar et al. 2007a, b).

The market information system is a base for AMS. Agility means dancing to the tune of the market. Therefore, the strong market information system is required to know the changing customer needs and its behavior with competitor's strategies. It is also very helpful to forecast the demand and to customize the product according to customer requirements.

2.6 Cross-functional workforce

The need of frequent changing in roles and responsibilities shows the requirement of cross-functional workforce so that during new demand or in changing circumstances existing workforce can be employed in any work due to time constraints. Christian et al. (2001) termed it as people flexibility; and its components are employee skill flexibility, skills replaceability, and employee skills utilization.

2.7 Strategic partnership and supplier development

A manufacturing organization cannot be an expert of all the business activities such as supply chain, government policy, trade regulations and legislation and legal formalities, and competitor's action. Thus, strategic alliances have become a need for manufacturers in today's business environment. Rapid partnership with these service providers has become an influencing factor for agility (Gunasekaran 1998).

An organization may not be successful alone to respond rapidly to changing market. Therefore, the temporary

Author's personal copy

alliance based on core competencies can help to achieve improved flexibility and responsiveness of organizations (Gunasekaran and Yusuf 2002). Medhat and Rook (1997) highlighted three factors for a partnership: pre-qualifying partners, evaluation of product design and capability of potential partners, selecting the optimal number of partners for manufacturing of a particular product (Kumar et al. 2008).

Integrated-sourcing flexibility in supply chain management improves the organization's ability to deliver products and services in a timely and effective manner (Tan et al. 1996). Sourcing flexibility is the ability to change sourcing decisions such as the number of suppliers per part and delivery schedule. Sourcing flexibility facilitates a faster response when there is uncertainty; therefore, it has a positive impact on manufacturing flexibility (Gupta and Somers 1996). Sourcing flexibility may support the arms-length relationship with suppliers, but strategic partnership with flexibility is more beneficial to cover various uncertainties in the supply chain. Manufacturers always try to find the reliable suppliers and establish strategic relationships with them (Kumar et al. 2007a, b).

He et al. (2014) examined the relationship between supplier integration and customer integration when they influence new product performance. This study aimed to explore the complicated relationships among supplier integration, customer integration and new product performance via the mediating roles of manufacturing flexibility and service capability under the trust theory.

2.8 Product design and development

Product decision is based on market information, availability of resources, product mix and delayed product differentiation. In push-based system, production decision is based on long term forecasting while pull-based system is demand driven (Simchi-Levi et al. 2002). There should be strong information channel to know the changing market behavior.

Product mix is a set of similar or dissimilar products of various configurations and specifications provided by same manufacturer. This may help to satisfy the diversified demand of customers. Product mix is very helpful to design and produce new or customized product with short lead-time. Fernandes et al. (2012) worked on product mix strategy and manufacturing flexibility. They observed that the equipment flexibility is dependent on the technology flexibility factor, mix index and demand volatility.

Oke (2013) in his study, investigated the influence of the interaction of product mix flexibility and labor flexibility on product innovation based on a survey of UK manufacturing plants. He also investigated the role of climate for innovation both as an antecedent of product innovation and a moderator that moderates the influence of the interaction of mix flexibility and labor flexibility on product innovation.

2.9 Product postponement

He and Kusiak (1995) used product postponement strategy to achieve agility in manufacturing. Product postponement is delayed in time when a product gets its identity. Using high level of part commonality at early stages of the manufacturing process can delay the product differentiation. For example, in an apparel industry, traditionally, the manufacture of clothing starts with the dyeing of the yarn followed by the knitting of the garment. This process may result in out of stock of desired color and over inventory of unpopular color. In a market characterized by very short product life cycles, this mismatch of inventory and customer demand cannot be corrected using a traditional manufacturing approach. The typical result is the end of season markdown. Benetton uses the bleached yarn and delay dyeing until information on the preferred colors became available through electronic data interchange (EDI) to reduce the inventory size (Kumar et al. 2007a, b).

Ferreira et al. (2014) proposed a model approach to the postponement concept based on drivers, steps for implementation, and performance measures. This study used a qualitative approach and the theoretical-conceptual method focused on the literature review and the development of new theories on the adoption of the postponement strategy. Kampen and Donk (2014) studied how characteristics of the food processing industry affect the operational performance of implementing form postponement (FP) based on a case in a dairy company and a simulation model. They found that substantial operational performance improvements could be achieved when implementing FP diminishes the negative effects of some typical food processing industry characteristics. Saghiri and Hill (2014) examined the impact of the supplier relationship on postponement implementation in the buying firm. The links between three supplier relationship constructs and three postponement constructs were hypothesized and tested through structural modelling. It was observed that the buying firm's ability to delay the final product configuration (postponement in production operations) was not directly affected by those aspects of the supplier relationship investigated.

3 ISM-GTMA model development

ISM is an interactive learning process, which systematizes the different and directly related elements into a structured system (Warfield 1974; Sage 1977). It transforms a complex problem into visible, well-defined models serving the

Author's personal copy

purposes (Sage 1977). It helps in identifying the interrelationships among variables. It also helps to impose order and direction on the complexity of relationships among elements of a system. ISM develops a collective understanding of relationships among the variables. It is a modeling technique in which the specific relationships of the variables and the overall structure of the system under consideration are presented in a directed graph model.

Govindan et al. (2015) used ISM as a tool to identify interrelationships among lean, green and resilient practices and supply chain performance and to classify them according to their driving or dependence power. The same methodology ISM has been used by Kannan et al. (2014), for the making relationship among the drivers of end-of-life management of tires. Bouzon et al. (2015) used ISM as a tool to show the interactions of the barriers that impede reverse logistics development from a Brazilian perspective.

Muduli et al. (2013) used the graph theoretic matrix approach to quantify the adverse impact of the barriers on GSCM implementation in Indian mining industry. Malhotra et al. (2012) proposed a conceptual framework of various barriers associated with Remanufacturing systems (RMSs) along with their interdependencies. Using graph theory and matrix methods, the barriers of RMSs were presented in the form of a single numerical index.

ISM is primarily intended as a group learning process, but it can also be used individually. GTMA is used to assign a weight to the existing relationship between the variables and fix the agility index. The various steps involved in the ISM-GTMA integrated technique are:

(1) Identification of variables or factors that are relevant to the problem—this could be done by survey or any group problem-solving technique;
(2) Establishing a contextual relationship between the variables with respect to which pairs of elements would be examined;
(3) Developing a structural self-interaction matrix (SSIM) of elements, this indicates the pair-wise relationship between elements of the system;
(4) Developing a reachability matrix from the SSIM, and checking the matrix for transitivity—transitivity of the contextual relation is a basic assumption in ISM which states that if element A is related to B and B is related to C, then A is necessarily related to C;
(5) Assign weight of the influential relationship between the pairs and develop a matrix of order n × n.
(6) Solve the matrix and find the value of permanent of matrix with the help of Leveni's theorem.

3.1 Variables' permanent matrix

After preparation of agility matrix in step 5, the permanent of a matrix given by Eq. (1) is calculated, which is a multinomial function and is called permanent of A (permA). This permanent function is a standard matrix function and is used and defined in combinatorial mathematics. This is evaluated by standard procedures and is same as determinant of matrix but with all signs positive. The permanent for matrix in general form is written as (Darvish et al. 2009a, b):

$$
\begin{aligned}
permA = {} & \prod_{i=1}^{M} A_i + \sum_{i=1}^{M-1}\sum_{j=i+1}^{M}\cdots\sum_{m=t+1}^{M}\left(a_{ij}a_{ji}\right)A_kA_lA_mA_nA_o\ldots A_tA_M \\
& + \sum_{i=1}^{M-2}\sum_{j=i+1}^{M-1}\sum_{k=j+1}^{M}\cdots\sum_{M=t+1}^{M}\ldots\left(a_{ij}a_{jk}a_{ki}+a_{ik}a_{kj}a_{ji}\right)\left(A_lA_nA_o\ldots A_tA_m\right) \\
& + \left[\begin{array}{l}
\sum_{i=1}^{M-3}\sum_{j=i+1}^{M}\sum_{k=i+1}^{M-1}\sum_{l=i+2}^{M}\cdots\sum_{M=t+1}^{M}\left(a_{ij}a_{ji}\right)\left(a_{kl}a_{lk}\right)A_mA_nA_o\ldots A_tA_M+ \\
\sum_{i=1}^{M-3}\sum_{j=i+1}^{M-1}\sum_{k=i+1}^{M}\sum_{l=j+1}^{M}\cdots\sum_{M=t+1}^{M}\left(a_{ij}a_{jk}a_{kl}a_{li}+a_{il}a_{lk}a_{kj}a_{ji}\right)A_mA_nA_o\ldots A_tA_M
\end{array}\right] \\
& + \left[\begin{array}{l}
\sum_{i=1}^{M-2}\sum_{j=i+1}^{M-1}\sum_{k=j+1}^{M}\sum_{l=1}^{M-1}\sum_{m=l+1}^{M}\cdots\sum_{M=t+1}^{M}\left(a_{ij}a_{jk}a_{ki}+a_{ik}a_{kj}a_{ji}\right)\left(a_{lm}a_{ml}\right)A_nA_o\ldots A_tA_M+ \\
\sum_{i=1}^{M-4}\sum_{j=i+1}^{M-1}\sum_{k=i+1}^{M}\sum_{l=i+1}^{M}\sum_{m=j+1}^{M}\cdots\sum_{M=t+1}^{M}\left(a_{ij}a_{jk}a_{kl}a_{lm}a_{mi}+a_{im}a_{ml}a_{lk}a_{kj}a_{ji}\right)A_nA_o\ldots A_tA_M
\end{array}\right]
\end{aligned}
$$

Author's personal copy

$$+\left[\begin{array}{l}
\sum_{i=1}^{M-3}\sum_{j=i+1}^{M-1}\sum_{k=i+1}^{M}\sum_{l=j+1}^{M}\sum_{m=1}^{M}\sum_{n=m+1}^{M}\cdots\sum_{M=t+1}^{M}\left(a_{ij}a_{jk}a_{kl}a_{li}+a_{ik}a_{lk}a_{kj}a_{ji}\right)(a_{mn}a_{nm})A_o\ldots A_tA_M+\\
\sum_{i=1}^{M-5}\sum_{j=i+1}^{M-1}\sum_{k=i+1}^{M}\sum_{l=1}^{M-2}\sum_{m=l+1}^{M-1}\sum_{n=m+1}^{M}\cdots\sum_{M=t+1}^{M}\left(a_{ij}a_{jk}a_{ki}+a_{ik}a_{kj}a_{ji}\right)(a_{lm}a_{mn}a_{nl}+a_{\ln}a_{nm}a_{ml})A_o\ldots A_tA_M+\\
\sum_{i=1}^{M-5}\sum_{j=i+1}^{M}\sum_{k=i+1}^{M-3}\sum_{l=i+2}^{M}\sum_{m=k+1}^{M-1}\sum_{n=k+2}^{M}\cdots\sum_{M=t+1}^{M}\left(a_{ij}a_{ji}\right)(a_{kl}a_{lk})(a_{mn}a_{nm})A_o\ldots A_tA_M+\\
\sum_{i=1}^{M-5}\sum_{j=i+1}^{M-1}\sum_{k=i+1}^{M}\sum_{l=i+1}^{M}\sum_{m=l+1}^{M}\sum_{n=j+1}^{M}\cdots\sum_{M=t+1}^{M}\left(a_{ij}a_{jk}a_{kl}a_{lm}a_{mn}a_{ni}+a_{in}a_{nm}a_{ml}a_{lk}a_{kj}a_{ji}\right)A_o\ldots A_tA_M+\ldots
\end{array}\right] \quad (1)$$

The calculation of permanent of matrix is based on the Leibniz formula to calculate the determinant of a matrix as shown in Eq. (2). But, the value of all the elements of the matrix in calculation is considered as positive in the case of permanent of a matrix. The detail calculation of permanent of matrix is shown in Eq. (3).

$$\det A = sign(\sigma)\sum_{\sigma\in A_n}\prod_{i=1}^{n}a_{i,\sigma(i)} \quad (2)$$

$$permF = \sum_{\sigma\in A_n}\prod_{i=1}^{n}a_{i,\sigma(i)} \quad (3)$$

The permanent function defined above, i.e. Eq. (3) is the complete expression for Variables effect as it considers the presence of all attributes and their interdependencies. A close look at multinomial, i.e. Eq. (1) reveals the presence of variables' effect in a systematic manner. The expression contains terms arranged in n groupings.

The permA contains terms arranged in (M + 1) groups, and these groups represent the measures of variables and the relative importance loops.

- The first group represents the measures of M variables.
- The second group is absent as there is no self-loop in the digraph.
- The third group contains 2-variable relative importance loops and measures of (M-2) variables.
- Each term of the fourth group represents a set of a 3-variable relative importance loop, or its pair, and measures of (M-3) variables.
- The fifth group contains two sub-groups. The terms of the first sub-group is a set of two 2-variable relative importance loops and the measures of (M-4) variables. Each term of the second sub-group is a set of a 4-attribute relative importance loop, or its pair, and the measures of (M-4) variables.
- The sixth group contains two subgroups. The terms of the first sub-group are a set of a 3-variable relative importance loop, or its pair, and 2-variable importance loop and the measures of (M-5) criteria. Each term of the second sub-group is a set of a 5-variable relative importance loop, or its pair, and the measures of (M-5) criteria.

Similarly, other terms of the equation are defined. Thus, the permA fully characterizes the considered contractor selection, evaluation problem, as it contains all possible structural components of the variables and their relative importance. It may be mentioned that this equation is the determinant of an M × M matrix and considering all the terms as positive. To calculate the permanent function of a square matrix of M × M size, the computer program can be used for simplicity.

3.2 Example to calculate permanent of matrix

Let us consider a 3 × 3 matrix (as shown in Eq. 4), the determinant for this matrix can be calculated as the sign of the path and path shown in the Fig. 1a and Eq. (5). But, the calculation of permanent of matrix is slightly different from the determinant of the matrix. In the case of permanent of matrix all the sign will be positive and also, the path will be different as shown in Fig. 1b.

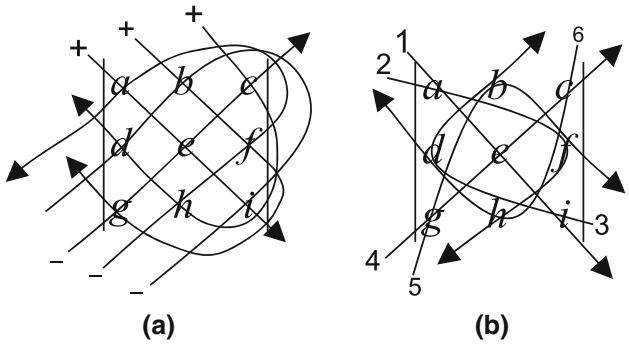


Fig. 1 Path to calculate determinant and permanent of 3 × 3 matrix

Author's personal copy

$$A = \begin{vmatrix} a & b & c \\ d & e & f \\ g & h & i \end{vmatrix} \tag{4}$$

$$\det A = aei + bfg + chd - gec - hfa - ibd \tag{5}$$

In permanent of a matrix, the number of terms is equal to $|\underline{n}$ for n × n matrix. In 3 × 3 matrix the number of terms will be $|\underline{3} = 6$ as shown in Eq. (6). The path of the elements will follow as shown in Fig. 1b.

$$permA = aei + afh + idb + ged + gbf + chd \tag{6}$$

But for 4 × 4 matrix or higher order square matrix the permanent of the matrix (as shown in Eq. 7) will be calculated as:

$$B = \begin{bmatrix} a & b & c & d \\ e & f & g & h \\ i & j & k & l \\ m & n & o & p \end{bmatrix}$$

$$\begin{aligned} permB = a \times perm \begin{bmatrix} f & g & h \\ j & k & l \\ n & o & p \end{bmatrix} + e \times perm \begin{bmatrix} b & c & d \\ j & k & l \\ n & o & p \end{bmatrix} \\ + i \times perm \begin{bmatrix} b & c & d \\ f & g & h \\ n & o & p \end{bmatrix} + m \\ \times perm \begin{bmatrix} b & c & d \\ f & g & h \\ j & k & l \end{bmatrix} \end{aligned} \tag{7}$$

There will be six terms for each 3 × 3 matrix, therefore, total terms in 4 × 4 matrix will be equal to $|\underline{4} = 24$.

4 Case illustration

XYZ Limited is India's largest automobile company, with consolidated revenues of USD 38.9 billion in 2013–2014. It is the leader in commercial vehicles, and among the top in passenger vehicles with winning products in the compact, midsize car and utility vehicle segments. It is also the world's fifth largest truck manufacturer and fourth largest bus manufacturer.

Established in 1945, the company's manufacturing base in India is spread across Jamshedpur (Jharkhand), Pune (Maharashtra), Lucknow (Uttar Pradesh), Pantnagar (Uttarakhand), Sanand (Gujarat) and Dharwad (Karnataka). It has set up an industrial joint venture with Fiat Group Automobiles at Ranjangaon (Maharashtra) to produce both Fiat and Tata cars and Fiat powertrains. The company's dealership, sales, services and spare parts network comprises over 6600 touch points, across the world.

XYZ, also listed in the New York Stock Exchange, has emerged as an international automobile company. Through subsidiaries and associate companies, XYZ has operations in the UK, South Korea, Thailand, South Africa and Indonesia. In 2004, it acquired the South Korea's second largest truck maker. Today two-thirds of heavy commercial vehicle exports out of South Korea are from XYZ. In 2006, XYZ formed a 51:49 joint venture with the Brazil-based company, a global leader in body-building for buses and coaches to manufacture fully-built buses and coaches for India—the plant is located in Dharwad.

XYZ is also expanding its international footprint, established through exports since 1961. The company's commercial and passenger vehicles are already being marketed in several countries in Europe, Africa, the Middle East, South East Asia, South Asia, South America, CIS and Russia. It has franchisee/joint venture assembly operations in Bangladesh, Ukraine, and Senegal.

4.1 Structural self-interaction matrix (SSIM)

For analyzing the variables a contextual relationship of "leads to" is used. To develop contextual relationships among variables, expert opinions based on various management techniques such as brainstorming, nominal group technique, idea generation, etc. were considered. For expressing the relationship between different variables to improve the agility of manufacturing system, four symbols have been used to denote the direction of relationship between the parameters i and j (here i < j) as shown in Table 1:

(1) V: variable i will lead to variable j;
(2) A: variable j will lead to variable i;
(3) X: variable i and j will lead to each other; and
(4) O: variable i and j have no relationship.

4.2 Reachability matrix

The SSIM has been converted into a binary matrix, called the initial reachability matrix by substituting V, A, X and O by 1 and 0 as per the case. The substitution of 1s and 0s are as per the following rules:

- If the (i, j) entry in the SSIM is V, then (i, j) entry in the reachability matrix becomes 1 and the (j, i) entry becomes 0.
- If the (i, j) entry in the SSIM is A, then (I, j) entry in the reachability matrix becomes 0 and the (j, i) entry becomes 1.
- If the (i, j) entry in the SSIM is X, then (I, j) entry in the reachability matrix becomes 1 and the (j, i) entry also becomes 1.

Author's personal copy

Table 1 Sructural self-interaction matrix

Enablers		10	9	8	7	6	5	4	3	2
1	Manufacturing flexibility	V	A	O	A	A	A	A	A	A
2	Strategic production planning	V	V	A	V	O	A	O	X	
3	Concurrent engineering	V	V	A	O	A	A	A		
4	Automation in manufacturing	V	O	O	O	O	A			
5	Integrated information systems	V	V	V	A	O				
6	Cross-functional workforce	V	O	O	O					
7	Strategic partnership and supplier development	V	O	X						
8	Product design and development	V	V							
9	Product postponement	V								
10	Agile manufacturing									

- If the (i, j) entry in the SSIM is O, then (i, j) entry in the reachability matrix becomes 0 and the (j, i) entry also becomes 0.

The initial reachability matrix for the variables is shown in Table 2.

4.3 Final reachability matrix

After incorporating the transitivity as described earlier in step (4) of the ISM methodology, the final reachability matrix with driving power and dependence for each variable is shown in Table 3. The digraph based on Table 3 can be developed as shown in Fig. 2.

4.4 Agility matrix

After finding the existence of relationships among the variables that are shown by 1, a weight to the relation has been assigned on a 5 point rating scale with the help of executives of the case company and these weights are inserted in the Table 3 for all the variables showing relationships as 1 to prepare an agility matrix. Since, the relation 1 only shows that variable '*i*' influences or leads to variable '*j*' but, does not show the weight of leading capacity. Suppose the relationship other than 0 is shown by a_{ij} and between the same variable as A_i then the agility matrix in the symbolic form can be shown as in Eq. (8).

$$A = \begin{array}{c} \begin{matrix} 1 & 2 & 3 & 4 & 5 & 6 & 7 & 8 & 9 & 10 \end{matrix} \\ \begin{bmatrix} A_1 & 0 & 0 & 0 & 0 & 0 & 0 & 0 & 0 & a_{110} \\ a_{21} & A_2 & a_{23} & 0 & a_{25} & 0 & a_{27} & 0 & a_{29} & a_{210} \\ a_{31} & a_{32} & A_3 & 0 & 0 & 0 & 0 & 0 & a_{39} & a_{310} \\ a_{41} & a_{42} & a_{43} & A_4 & 0 & 0 & 0 & 0 & a_{49} & a_{410} \\ a_{51} & a_{52} & a_{53} & a_{54} & A_5 & 0 & a_{57} & a_{58} & a_{59} & a_{510} \\ a_{61} & 0 & a_{63} & 0 & 0 & A_6 & 0 & 0 & 0 & a_{610} \\ a_{71} & a_{72} & a_{73} & a_{74} & a_{75} & 0 & A_7 & a_{78} & a_{79} & a_{710} \\ a_{81} & a_{82} & a_{83} & 0 & a_{85} & 0 & a_{87} & A_8 & a_{89} & a_{810} \\ a_{91} & 0 & 0 & 0 & 0 & 0 & 0 & 0 & A_9 & a_{910} \\ 0 & 0 & 0 & 0 & 0 & 0 & 0 & 0 & 0 & A_{10} \end{bmatrix} \end{array} \begin{matrix} 1 \\ 2 \\ 3 \\ 4 \\ 5 \\ 6 \\ 7 \\ 8 \\ 9 \\ 10 \end{matrix} \quad (8)$$

After inserting the assigned weights, we can get the weighted matrix as shown in Eq. (9).

Table 2 Initial reachability matrix

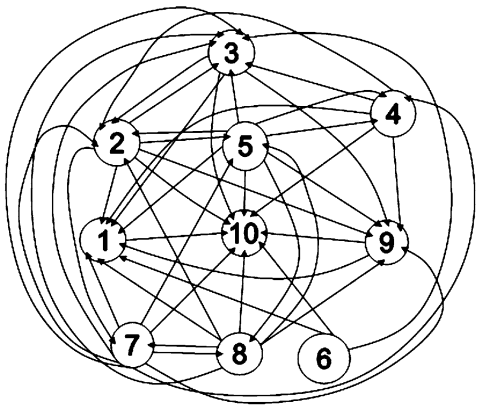
Enablers		1	2	3	4	5	6	7	8	9	10
1	Manufacturing flexibility	1	0	0	0	0	0	0	0	0	1
2	Strategic production planning	1	1	1	0	0	0	1	0	1	1
3	Concurrent engineering	1	1	1	0	0	0	0	0	1	1
4	Automation in manufacturing	1	0	1	1	0	0	0	0	0	1
5	Integrated information systems	1	1	1	1	1	0	0	1	1	1
6	Cross-functional workforce	1	0	1	0	0	1	0	0	0	1
7	Strategic partnership and supplier development	1	0	0	0	1	0	1	1	0	1
8	Product design and development	0	1	1	0	0	0	1	1	1	1
9	Product postponement	1	0	0	0	0	0	0	0	1	1
10	Agile manufacturing	0	0	0	0	0	0	0	0	0	1

Author's personal copy

Table 3 Final reachability matrix incorporating the transitivity

Enablers		1	2	3	4	5	6	7	8	9	10
1	Manufacturing flexibility	1	0	0	0	0	0	0	0	0	1
2	Strategic production planning	1	1	1	0	**1**	0	1	0	1	1
3	Concurrent engineering	1	1	1	0	0	0	0	0	1	1
4	Automation in manufacturing	1	**1**	1	1	0	0	0	0	**1**	1
5	Integrated information systems	1	1	1	1	1	0	**1**	1	1	1
6	Cross-functional workforce	1	0	1	0	0	1	0	0	0	1
7	Strategic partnership and supplier development	1	**1**	**1**	**1**	1	0	1	1	**1**	1
8	Product design and development	**1**	1	1	0	**1**	0	1	1	1	1
9	Product postponement	1	0	0	0	0	0	0	0	1	1
10	Agile manufacturing	0	0	0	0	0	0	0	0	0	1

Bold number indicates the reachability of one variable to the other by transitivity, i.e., indirect relationship



1-Manufacturing Flexibility, 2- Strategic Production Planning,
3- Concurrent Engineering, 4-Automation in Manufacturing,
5- Integrated Information Systems, 6- Cross-functional workforce,
7- Strategic Partnership & Supplier Development,
8- Product Design & Development, 9- Product Postponement,
10- Agile Manufacturing Systems

Fig. 2 Digraph for the relationships among the variables

$$A = \begin{array}{c} \begin{matrix} 1 & 2 & 3 & 4 & 5 & 6 & 7 & 8 & 9 & 10 \end{matrix} \\ \begin{bmatrix} 1 & 0 & 0 & 0 & 0 & 0 & 0 & 0 & 0 & 5 \\ 3.8 & 1 & 1.8 & 0 & 1.2 & 0 & 3.6 & 0 & 4.2 & 3.2 \\ 3.8 & 2.2 & 1 & 0 & 0 & 0 & 0 & 0 & 2.8 & 4.2 \\ 3.6 & 2.8 & 3.2 & 1 & 0 & 0 & 0 & 0 & 1.8 & 5 \\ 4.8 & 4.6 & 1.6 & 3.6 & 1 & 0 & 3.8 & 3.2 & 4.8 & 5 \\ 2.8 & 0 & 1.8 & 0 & 0 & 1 & 0 & 0 & 0 & 2.8 \\ 4.8 & 3.2 & 1.6 & 1 & 3.6 & 0 & 1 & 3.6 & 3.6 & 5 \\ 3.6 & 2.8 & 2.2 & 0 & 4.2 & 0 & 3.6 & 1 & 4.8 & 3.6 \\ 4.2 & 0 & 0 & 0 & 0 & 0 & 0 & 0 & 1 & 4.2 \\ 0 & 0 & 0 & 0 & 0 & 0 & 0 & 0 & 0 & 1 \end{bmatrix} \end{array} \begin{matrix} 1 \\ 2 \\ 3 \\ 4 \\ 5 \\ 6 \\ 7 \\ 8 \\ 9 \\ 10 \end{matrix} \quad (9)$$

Using Eq. (1), we can get permA = 6094.3

The agility index of the company XYZ is 6094.3. Similarly, the agility index of the competitor companies can be found and compared with the case company. Thus it may help to know about a company that how much it is agile compared to its competitors. This paper shows the model to calculate the agility index. There may be a number of other variables which may be incorporated in the analysis. Also, the weight of relations between the variables may be different in different companies or organizations. The comparison may help to improve these relationships.

5 Conclusions

This research paper is based on the extension of the model ISM. In ISM, we can draw a hierarchy of relationships, but in this integrated model of the ISM-GTMA, we can show a digraph of one-to-one relationship. Also, we can assign the weights to the relationship between the variables. Finally, we calculate the agility index of the company using GTMA.

This model may be used to find the maximum agility index by assigning the maximum weights to the existing relationships among the variables and this can be used as a benchmark to improve the agility of the organization. In the future scope of the work, a benchmark of the agility index of an industry will be fixed so that the individual organization may compare their agility index and also they can prepare a rank of the organizations based on the agility index.

This approach cannot only be used for the agility index; it can also be used for the other performance parameters of

Author's personal copy

the organization. It can be applied in quality management, supply chain performance measurement, the sustainability index of a supply chain, financial management, etc.

This paper may help the manager to evaluate the agility of a manufacturing systems. He/she can compare the agility of his/her manufacturing systems with the competitors manufacturing systems. Also, on the basis of interactions among the variables of agility, further the agility can be improved as per requirement of the market or customer. Finally, it will be helpful in improving the competitiveness in the market.

References

Avittathur B, Swamidass P (2007) Matching plant flexibility and supplier flexibility: lesson from small suppliers of U.S. manufacturing plants in India. J Oper Manag 25(3):717–735

Belay AM, Helo P, Takala J, Kasie FM (2011) Effects of quality management practices and concurrent engineering in business performance. Int J Bus Manag 6(3):45–62

Bouzon M, Govindan K, Rodriguez CMT (2015) Reverse logistics barriers: an analysis using interpretive structural modeling, enhancing synergies in a collaborative environment. Lect Notes Manag Ind Eng 3:95–103

Cho H, Jung MY, Kim M (1996) Enabling technologies of agile manufacturing and its related activities in Korea. Comput Ind Eng 30:323–334

Christian I, Ismail H, Mooney J, Snowden S, Toward M, Zhang D (2001) Agile manufacturing transitional strategies, manufacturing information systems. In: Proceedings of the fourth SME international conference, pp 1–9

Darvish M, Yasaei M, Saeedi A (2009) Application of the graph theory and matrix methods to contractor ranking. Int J Proj Manag 27:610–619

De Vor R, Mills J (1995) Agile manufacturing. American Society of mechanical engineers, manufacturing engineering division. MED 2(2):977

Dove R (1999) Knowledge management, response ability and the agile enterprise. J Knowl Manag 3(1):1–17

Dove R, Nagel R, Goldman S, Preiss K (1991) 21st century manufacturing enterprise strategy: an industry led view. Iacocca Institute, Lehigh University, Bethlehem

Fernandes R, Gouveia JB, Pinho C (2012) Product mix strategy and manufacturing flexibility. J Manuf Syst 31:301–311

Ferreira KA, Tomasb RN, Alcântara RLC (2014) A theoretical framework for postponement concept in a supply chain. Int J Logist. doi:10.1080/13675567.2014.945403

Gianesi IGN (1998) Implementing manufacturing strategy through strategic production planning. Int J Oper Prod Manag 18(3):286–299

Govindan K, Azevedo SG, Carvalho H, Cruz-Machado V (2015) Lean, green and resilient practices influence on supply chain performance: interpretive structural modeling approach. Int J Environ Sci Technol 12(1):15–34

Graham JH, Ragade RK (1994) Design support system for agile manufacturing. In: Proceedings of the IEEE international conference on systems, man and cybernetics, vol 1. pp 512–517

Gunasekaran A (1998) Agile manufacturing: enablers and an implementation framework. Int J Prod Res 36(5):1223–1247

Gunasekaran A, Yusuf YY (2002) Agile manufacturing: a taxonomy of strategic and technological imperatives. Int J Prod Res 40(6):1357–1385

Gupta UG, Mittal RO (1996) Quality, time, and innovation based performance measurement system for agile manufacturing. In: Proceedings—annual meeting of the decision sciences institute, vol 3. pp 1511–1513

Gupta YP, Somers TM (1996) Business strategy, manufacturing flexibility, and organizational performance relationships: a path analysis approach. Prod Oper Manag 5(3):204–233

He DW, Kusiak A (1995) The delayed product differentiation strategy in agile manufacturing. In: IERC proceedings 1995, 4th annual industrial engineering research conference. Norcross, pp 701–708

He Y, Lai KK, Sun H, Chen Y (2014) The impact of supplier integration on customer integration and new product performance: the mediating role of manufacturing flexibility under trust theory. Int J Prod Econ 147:260–270

Kampen TV, Donk DPV (2014) Coping with product variety in the food processing industry: the effect of form postponement. Int J Prod Res 52(2):353–367

Kannan D, Diabat A, Shankar KM (2014) Analyzing the drivers of end-of-life tire management using interpretive structural modeling (ISM). Int J Adv Manuf Technol 72(9–12):1603–1614

Katayama H, Bennett D (1999) Agility, adaptability and leanness: a comparison of concepts and a study of practice. Int J Prod Econ 60:43–51

Krause DR, Handfield RB, Typer BB (2007) The relationships between supplier development social capital accumulation and performance improvement. J Oper Manag 25(2):528–545

Kumar A, Kumar P (2006) Role of rapid prototyping in agile manufacturing. In: Proceedings of RDFTME-2006, pp 258–264

Kumar P, Shankar R, Yadav SS (2007) Flexibility in global supply chain: a review of perspectives. In: Proceedings of seventh global conference on flexible system management (GLOGIFT-07), pp 377–385

Kumar P, Shankar R, Yadav SS (2007b) Flexibility in global supply chain: modeling the enablers. J Model Manag 3(3):277–297

Kumar P, Shankar R, Yadav SS (2008) Modeling the enablers of agile manufacturing system. In: Proceedings of eighth global conference on flexible systems management (GLOGIFT-08), NJ, USA, pp 1–8

Liu Y-J, Lai K-L, Dai G, Yuen MM-F (2010) A semantic feature model in concurrent engineering. IEEE Trans Autom Sci Eng 7(3):659–665

Malhotra V, Raj T, Arora A (2012) Evaluation of barriers affecting reconfigurable manufacturing systems with graph theory and matrix approach. Mater Manuf Process 27(1):88–94

Medhat SS, Rook JL (1997) Concurrent engineering—processes and techniques for the agile manufacturing enterprise. IIE Conference Publication, vol 435. pp 9–14

Muduli K, Govindan K, Barve A, Geng Y (2013) Barriers to green supply chain management in Indian mining industries: a graph theoretic approach. J Clean Prod 47:335–344

Naylor JB, Naim MM, Berry D (1999) Leagility: integrating the lean and agile manufacturing paradigm in the total supply chain. Int J Prod Econ 62:107–118

Oke A (2013) Linking manufacturing flexibility to innovation performance in manufacturing plants. Int J Prod Econ 143:242–247

Palvia PC (1997) Developing a model of the global and strategic impact of information technology. Inf Manag 32(5):229–244

Powell TC, Dent-Micallef A (1997) Information technology as competitive advantage: the role of human, business and technology resources. Strateg Manag J 18(5):375–405

Author's personal copy

Sage AP (1977) Interpretive structural modeling: methodology for large-scale systems. McGraw-Hill, New York, pp 91–164

Saghiri S, Hill A (2014) Supplier relationship impacts on postponement strategies. Int J Prod Res 52(7):2134–2153

Sethi V, King WR (1994) Development of measures to assess the extent to which an information technology application provides competitive advantage. Manag Sci 40(12):1601–1627

Sethi AK, Sethi SP (1990) Flexibility in manufacturing: a survey. Int J Flex Manuf Syst 2(4):289–328

Simchi-Levi D, Kaminsky P, Simchi-Levi E (2002) Designing and managing the supply chain: concepts, strategies and case studies, 2nd edn. Irwin/McGraw-Hill, New York

Swafford PM, Ghosh S, Murthy N (2006) The antecedents of supply chain agility of a firm: scale development and model testing. J Oper Manag 24(2):170–188

Tan KC, Kannan VR, Handfield RB (1996) Supply chain management: supplier performance and firm performance. Int J Purch Mater Manag 34:2–9

Wang F, Mill JJ, Devarajan V (2002) A conceptual approach for managing design resources. Comput Ind 47:169–183

Warfield JN (1974) Developing interconnection matrices in structural modeling. IEEE Trans Syst Man Cybern 4(1):81–87

Yusuf YY, Sarhadi MS, Gunasekaran A (1999) Agile manufacturing: the drivers, concepts and attributes. Int J Prod Econ 62(1–2):23–32

Regression Analysis for the Adsorption Kinetics of Methylene Blue onto Activated Carbon

Abhinav Jain, Abhishek Pandey
Department of Environmental Engineering
Delhi Technological University

ABSTRACT

Adsorption is the preferential partitioning of substances from the gaseous or liquid phase onto the surface of a solid substrate and is an effective technique for removing harmful substances. Dyes are coloured compounds used in industries and pose certain hazards and environmental problems. Dyes can have acute and/or chronic effects on exposed organism. Due to their chemical structure, dyes possess a high potential to resist fading on exposure to light and water. Chemical kinetics explains how fast the rate of reaction occurs and also on the factors affecting the reaction rate, the higher the value of r^2 (regression coefficient) for a pseudo second-order kinetics (close to 1) suggests this model can be used to represent the kinetic uptake of methylene blue onto activated carbon .Kinetic experiments were carried out for the adsorption of methylene blue on activated carbon for different initial concentrations and were fitted to the pseudo first-order and pseudo second-order kinetics. Graphical representations of the pseudo first-order and pseudo second-order kinetics are carried out followed by three error analysis techniques: Least square test, Chi square test and standard deviation. The adsorption process was found to follow pseudo second-order kinetics, least error and high regression coefficient, and was found to be directly proportional to the initial concentration. Hence, determination of the order of the adsorption kinetics can be useful in estimating the time required to remove methylene blue and quantity of activated carbon that is required to remove different initial concentration of methylene blue.

1. ADSORPTION

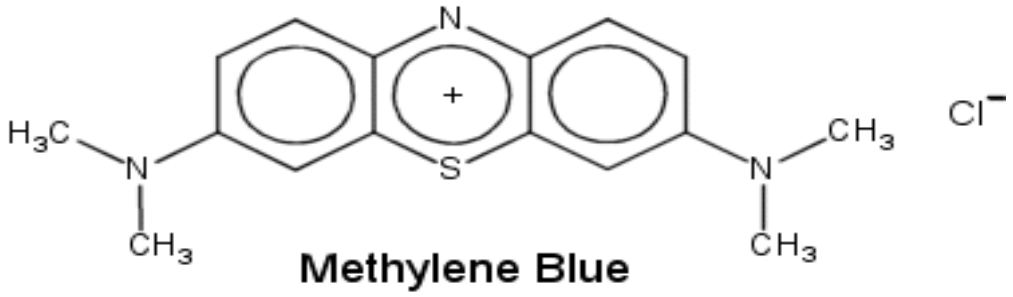
Assimilation of molecular species throughout the bulk of the solid or liquid is called as adsorption. It consists of two components: adsorbate, adsorbent. Adsorbing phase is the adsorbent, and the material concentrated or adsorbed at the surface of that phase is the adsorbate.

Types of adsorption:-

- Physisorption
- Chemisorption
- Exchange Adsorption

2. MATERIAL USED

The dye used in all the experiments was methylene blue. The structure of methylene blue is given by:



Methylene Blue

Amorphous solid consisting of micro-crystallites with a graphite lattice, activated carbon, is usually prepared in small pellets or a powder. Activated carbon can be manufactured from carbonaceous material, including coal, peat, wood, or nutshells. Activated carbon is used for adsorption of organic substances and non-polar adsorbates and it is also usually used for waste gas (and waste water) treatment. Since activated carbon is highly porous, cheap and non-polar, it is used is adsorption of dyes like Methylene Blue

3. REACTION RATES

- **Pseudo first order**

The adsorption of methylene blue following the first order kinetics can be represented as-

$$\frac{dq_t}{dt} = k_1(q_e - q_t)$$

Where qe- adsorption capacity at equilibrium
q_t - adsorption capacity at time t
k_1- rate constant of pseudo-first order sorption

Upon integration and applying boundary conditions, $q_t = 0$ to $q_t = q_t$ at $t = 0$to $t = t$;

$$\log(q_e - q_t) = \log q_e - \frac{k_1}{2.303}t$$

- **Pseudo second order**

The adsorption of methylene blue following the second order kinetics can be represented as-

$$\frac{dq_t}{dt} = k(q_e - q_t)^2$$

Upon integration and applying boundary conditions, $q_t = 0$ to $q_t = q_t$ at $t = 0$ to $t = t$;

$$\frac{t}{q_e} = \frac{1}{k_2 q_e^{\,2}} + \frac{1}{q_e} t$$

4. OBSERVATIONS

Co- Initial concentration of methylene Blue

Initially we had values of qt vs t(mins) for different Co values. The value of qe is taken as the last qt value (at t=120 mins). Then the values of Ln(qe-qt) and t/qt for different values of t are found out.

Following are the values obtained for adsorption of Methylene Blue on Activated carbon at different initial concentrations.[1]

Co=100			
t(mins)	**qt**	**ln(qe-qt)**	**t/qt**
2	198	2.484907	0.010101
5	200	2.302585	0.025
10	202	2.079442	0.049505
20	205	1.609438	0.097561
30	206	1.386294	0.145631
60	207	1.098612	0.289855
90	208	0.693147	0.432692
120	210	0	0.571429

Co=150			
t(mins)	**qt**	**ln(qe-qt)**	**t/qt**
2	220	2.995732	0.009091
5	225	2.70805	0.022222
10	230	2.302585	0.043478
20	236	1.386294	0.084746
30	237	1.098612	0.126582
60	238	0.693147	0.252101
90	239	0	0.376569
120	240	0	0.5

Co=150			
t(mins)	**qt**	**ln(qe-qt)**	**t/qt**
2	220	2.995732	0.009091
5	225	2.70805	0.022222
10	230	2.302585	0.043478
20	236	1.386294	0.084746
30	237	1.098612	0.126582
60	238	0.693147	0.252101
90	239	0	0.376569
120	240	0	0.5

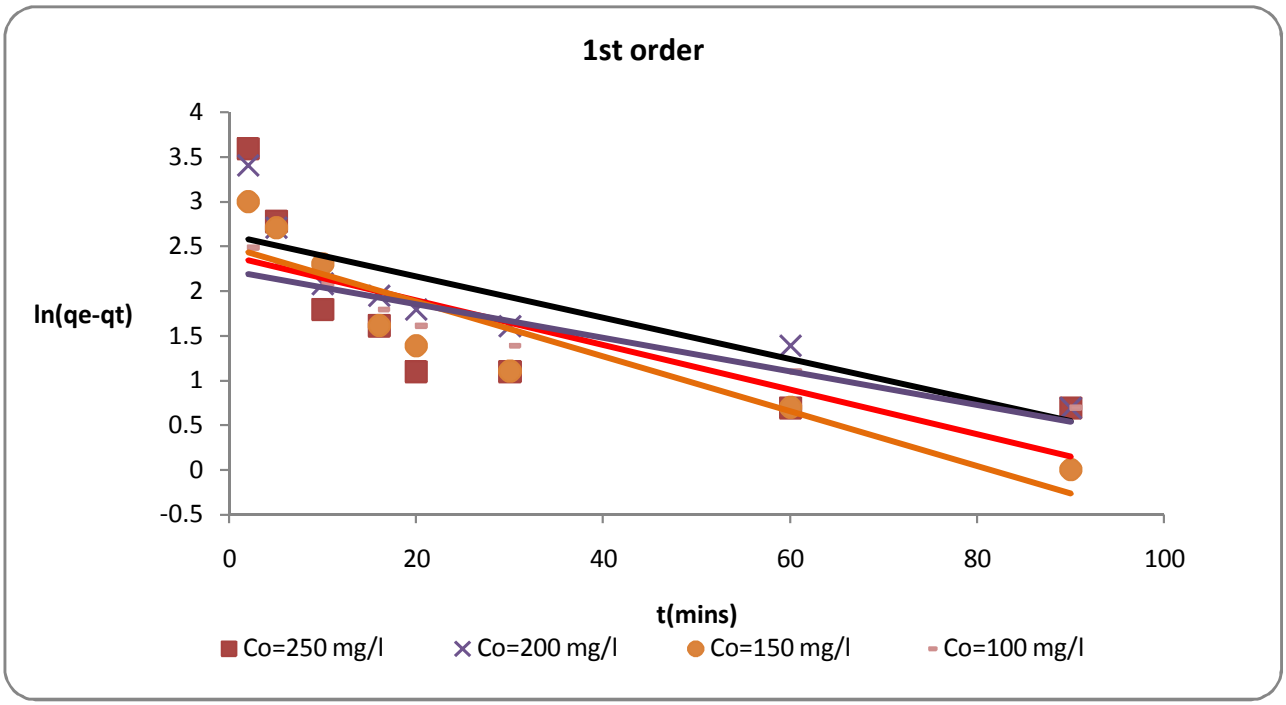
Co=250			
t(mins)	qt	ln(qe-qt)	t/qt
2	290	3.583519	0.006897
5	310	2.772589	0.016129
10	320	1.791759	0.03125
20	323	1.098612	0.06192
30	323	1.098612	0.092879
60	324	0.693147	0.185185
90	324	0.693147	0.277778
120	326	0	0.368098

5. GRAPHICAL REPRESENTATION

Using pseudo first and pseudo second order kinetics equations, line equations for different Co values are formed and plotted. The values of the regression coefficient at different values of t for both pseudo first and pseudo second order kinetics are calculated.

The combined graphs for pseudo first and pseudo second order kinetics are shown below:-

1st Order for all the concentrations



2nd Order for all the concentrations

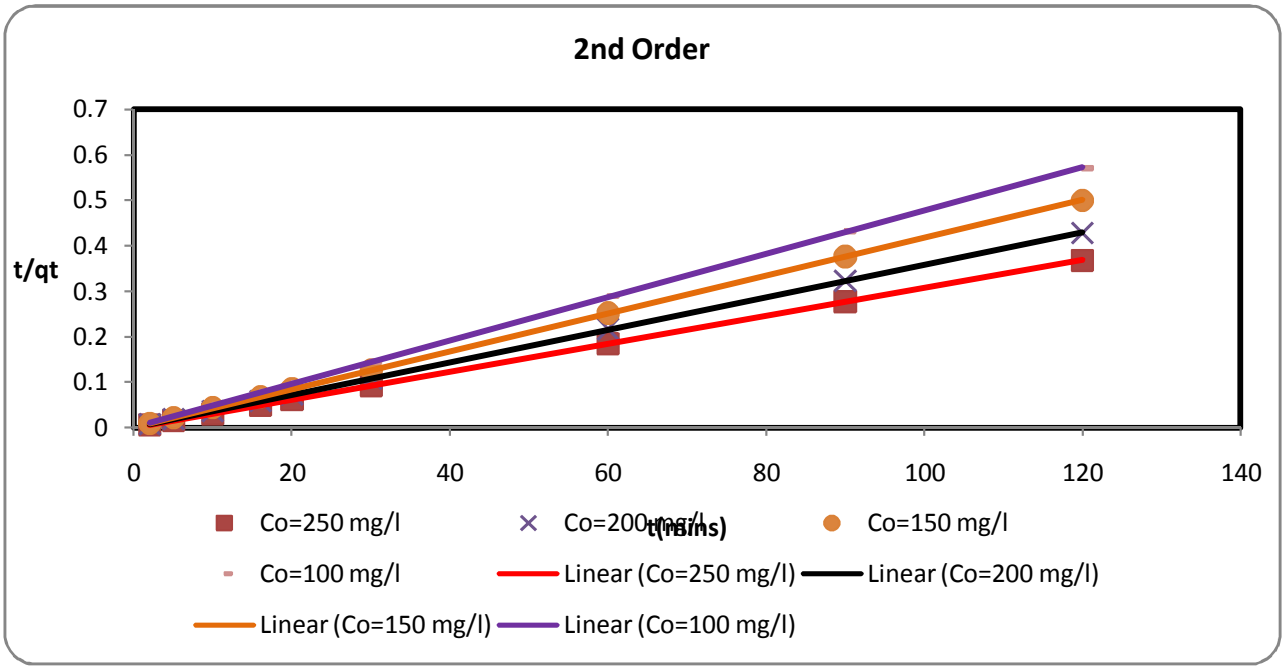


Table 1(Regression coefficient)

Initial Concentration (mg/l)	1st order	2nd order
100	0.8867	0.99999
150	0.8417	1
200	0.7475	1
250	0.5529	1

6. ERROR ANALYSIS

After forming the Line equations for pseudo first and pseudo second order kinetics, three different error analysis techniques: Least square test, Chi square test and standard deviation, were used to calculate the magnitude of error and to predict the order. Following table shows the error analysis details:-

Table 2(Error Analysis)

Initial Concentration (mg/l)	Least Square		Chi Square		Standard Deviation	
	1st order	2nd order	1st order	2nd order	1st order	2nd order
100	0.3	0.01	0.12	10^(-13)	1.499	0.13
150	2.39	0.0007	0.48	10^(-12)	3.67	0.01
200	1.213	0.009	1.196	0.000000009	6.2	0.2
250	3.69	0.0001	2.39	0.0007	9.1	0.04

7. CONCLUSION

- The adsorption of methylene blue onto activated carbon was found to be well represented by the pseudo first-order and pseudo second-order kinetics.[1]
- Chemical kinetics explain how fast the rate of reaction occurs and also on the factors affecting the reaction rate. , the very higher $\mathbf{r^2}$ values for a pseudo second-order kinetics suggests that this model can be used to represent the kinetic uptake of methylene blue onto activated carbon. Refer table 1
- The low $\mathbf{r^2}$ value of pseudo first-order kinetics obtained show that the method fails to well represent the kinetics of methylene blue onto activated carbon.
- The adsorption of methylene blue onto activated carbon was found to follow pseudo second-order kinetics
- Rate of adsorption is directly proportional to the initial concentration which can be depicted by the study at four different concentrations.

- Looking at table 2, we see that second-order kinetics shows very less errors as compared to first order kinetics and hence it can be concluded that adsorption of methylene blue onto activated carbon follows second order kinetics.

8. REFERENCES

[1] K. Vasanth Kumar: *Linear and non-linear regression analysis for the sorption kinetics of methylene blue onto activated carbon.* Journal of Hazardous Materials B137 (2006) 1538–1544

[2] Suhong Chen, Jian Zhang , Chenglu Zhang, Qinyan Yue, Yan Li, Chao Li: *Equilibrium and kinetic studies of methyl orange and methyl violet adsorption on activated carbon derived from Phragmites australis.* Desalination 252 (2010) 149–156.

[3] K.V. Kumar, S. Sivanesan, J. Hazard. Mater. B 123 (2005) 288–292

[4] http://www.sciencedirect.com/science/article/pii/S0263876212002730

Int J Adv Manuf Technol
DOI 10.1007/s00170-015-7920-6

ORIGINAL ARTICLE

Sliding wear behavior of aluminum alloy coating prepared by two-wire electric arc spray process

Dalip Kumar[1] · **Qasim Murtaza**[1,2] · **R. C. Singh**[1]

Received: 2 May 2012 / Accepted: 30 September 2015
© Springer-Verlag London 2015

Abstract Free standing aluminum alloy coating was successfully prepared by two-wire arc spray process which can in future replace sheet metal work in light industries. The wear behavior of the coating was determined using pin on disc machine under dry conditions at 20 ° C with three different pin materials, viz., brass, medium-carbon steel, and high-carbon steel. The wear rate was found to increase whereas the coefficient of friction of the coating was found to decrease with increased load and sliding conditions. The worn surfaces were examined with scanning electron microscopy (SEM), X-ray diffractometry (XRD), and energy-dispersive X-ray spectroscopy (EDS), and the microhardness to determine the wear mechanism of the coating.

Keywords Two-wire arc spray · Aluminum alloy · Sliding wear · Hardness

1 Introduction

In arc spraying method, an arc is formed between two wires. The molten ends of the wires are dispersed and accelerated by a gas stream (air or nitrogen gas). The arc can attain temperatures of up to 5000 °C with the particle velocities lying in the range 100–300 m/s [1]. A combination of high arc temperature and particle velocity gives arc sprayed coatings superior bond strengths and lower porosity levels when compared with flame sprayed coatings [2]. However, use of compressed air for atomization of droplets and propulsion gives rise to high coating oxide content. Wire arc spraying is an inexpensive thermal spray deposition process in which the materials to be deposited through wires are in the form of consumable arc electrodes. Low running costs, high deposition rates, and efficiency make it a good process for spraying large areas [3–5]. Recent equipments and process developments have improved the quality and expanded the potential application range for arc sprayed coatings. Typical general applications are thermal barriers, wear resistance, corrosion resistance, high dielectric strength, hard dense coatings, and decorative arts. Al alloy arc sprayed coatings also provide excellent resistance to atmospheric corrosion and are used on bridges and other infrastructure components [1–5].

Many researchers have studied the different types of wear behavior of Al alloy coating prepared by thermal spray technology such as Dwivedi et al. [6], who investigated the effects of copper additions, load, sliding time on wear, and friction coefficient of Al-18 %, Si-0.5 %, and Mg alloy, and it was found that addition of copper does not affect the oxidative wear resistance appreciably at low loads. However, alloy with higher percentage of copper (3–5 %) was found to have increased wear rate especially at higher loads. Copper-based alloys such as aluminum bronze have been widely used in the marine industry because of their excellent erosion–corrosion- and cavitation-resistant properties. Although aluminum bronzes are considered to be relatively erosion- and corrosion-resistant materials, wear will inevitably occur over time leading to the replacement of components [7]. Nickel–aluminum bronzes (NABs) are widely used for propulsion and seawater handling systems in naval platforms. Nickel–aluminum bronzes offer high strength and high corrosion resistance and are available in a number of different forms [8]. Sarikaya et al.

✉ Qasim Murtaza
qasimmurtaza@gmail.com; qasimmurtaza@dce.ac.in

[1] Delhi Technology University (formerly Delhi College of Engineering), Delhi, India

[2] Mechanical Engineering Department, Aligarh Muslim University, Aligarh, India

Published online: 12 October 2015

[9] found that the addition of B_4C particles to Al-Si increased the mechanical properties and thermal stability of the coating.

In the present study, free standing aluminum alloy coating was prepared and its wear behavior was studied. The coating of the composition Al 98.76 %, Mg 0.81 %, and Mn 0.41 % has not been reported yet. To study the wear behavior of thermal spray coating, any wear tester can be applied, but for thin coatings, pin on disc wear test is most commonly used [10]. Therefore, the wear behavior of Al alloy was investigated through pin on disc at different loading and sliding conditions. The X-ray diffractometry, scanning electron microscopy, and energy-dispersive X-ray spectroscopy of the wear track have been done to examine the worn surfaces. The Vickers microhardness test of the coating was also done to find the variation of the microhardness at the cross section of the wear track.

2 Experimental details

2.1 Materials

Commercially available Al alloy (Al 98.76 %, Mg 0.81 %, and Mn 0.41 %) was successfully prepared by two-wire arc spray coatings. The two-wire arc spray operation was performed by a Model 9000 TAFA, and its spray gun was mounted on ABB-400 robot arm so that the spray process could be controlled precisely.

2.2 Wear test

Pin on disc wear tester with data acquisition system was used to evaluate the wear behavior of aluminum alloys against the pin made of brass, medium-carbon steel, and high-carbon steel. The diameter for all pin materials used was 3 mm. The wear test was performed in dry conditions at 20 °C. Loads(29.4, 44.1, and 58.8 N) were applied on pin by dead weight through pulley and wire string arrangements, and the sliding speeds were 150, 200, and 250 rpm. The system had maximum loading capacity of 200 N. Disc was rotated by a D.C. motor, having speed range of 0–2000 rev min^{-1} to yield sliding speeds between 0 and 10 m/s. The radius of rotation of the disc was 25 mm and the rotation distance measured was found to be 74.4 m. Both the specimen and counter body were cleaned using ethanol to avoid the presence of humidity and other non-desirable films such as grease on the surface (Fig. 1).

The coefficient of friction of the Al alloy coating was calculated with help of frictional force recorded by the torque transducer. The wear rate was determined by means of mass loss by weighing the specimen before and after the wear test in terms of gram per 74.4-m sliding distance on an electronic balance of least count 0.1×10^{-5} g and represent in the form of specific wear rate of the specimens by the following relation:

$$\textit{Specific wear rate}\ (K) = \Delta m/W \times L$$

where Δm is the mass loss during test duration (g), W is the normal load (N), and L is the sliding distance (m). In this case, the unit of specific wear rate (K)=g/N.74.4 m.

2.3 Microhardness at the cross section of worn surfaces of the coating

The microhardness at the cross section of the worn surface was determined on Vickers microhardness tester. The microhardness of the coating was determined at a distance of 0.05 μm from the end of the surfaces at the interval of 1 μm. The cross section of the worn surface was first fixed in a Bakelite cylinder with the help of automatic mounting press (Simplimet 1000, Buehler) at a pressure of 60 psi. The heating time of the thermosetting plastic having sample piece was 12 min and cooling time was 3 min. After fixing the sample in Bakelite cylinder, it was polished with carbon paper of grit sizes 100, 200, and 600. The sample was then polished with aluminum powder paste on polishing machine up to mirror finishing of the sample (surface finish up to 1 μm). The load applied on the work piece was 5 g keeping in consideration that the aluminum is soft and the indenter very large. The

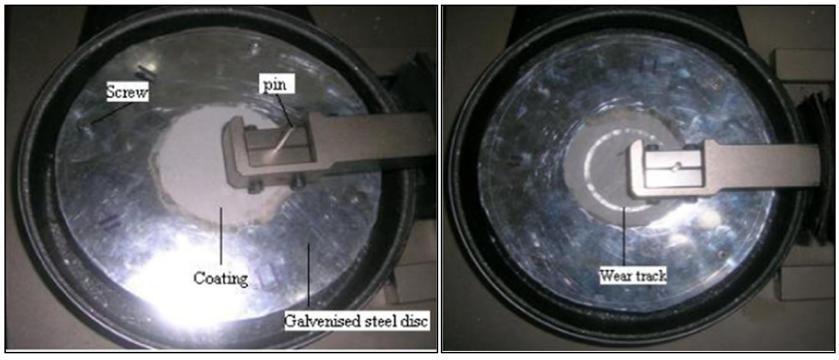


Fig. 1 Coating before and after the wear test

time of loading was 10 s. The resolution of the indenter was chosen to be ×400. Upon completion of indentation, the two diagonals were measured as D_1 and D_2, respectively. The microhardness of the coating was calculated with the help of these two diagonals.

3 Results and discussion

3.1 Coating characterization

It was observed from the microstructure of the coating's surface that the sprayed material did not form a continuous layer; instead, the coating material was deposited in the form of splats (Fig. 2). The porosity of the coating was found to be as low as1–2 %. The cross-sectional microstructure images revealed that the coating material deposited was very homogeneous and compact (Fig. 2b). On the inner side, the coating material was observed to be deposited in continuous layers probably because, in the two-wire electric spray coating, the wire material got melted completely, due to negligible porosity and blow holes. Some small particles of the unmelted wire were also observed on the cross section of the coating.

From the energy-dispersive X-ray spectroscopy (EDS) analysis, it was observed that the main constituents of the coating material were aluminum (98.76 %), magnesium (0.82 %), and manganese (0.43 %). But, some particles of copper and iron were also present as impurities. Owing to the fact that the major constituent of the coating material is aluminum, some oxidation of the coatings was observed in the form of a layer of aluminum oxide (Fig. 3a, b). The latter is thought to provide protection against corrosion [10].

3.2 Wear rate of thermal spray coating

3.2.1 Wear rate with brass pin

The wear rate of the coating in terms of mass loss per 74.4-m sliding distance was calculated. The two variables chosen for calculations were load (29.4, 44.1, and 58.8 N) and sliding speed (150, 200, and 250 rpm). By using these two variables and three levels, a set of ANOVA was designed. The ANOVA model gives the F-value and compares it with the standard table to decide whether the model variables are significant or not. In this case, the Model F-value is 518,420.92 which implies that the model is significant. There is only a 0.01 % chance that the "Model F-value" is larger that can be attributed to noise. This noise may be due to some hard particles in the coating. Calculated values of probability of the design model are greater than F-value, and less than 0.05 indicates that model terms are significant. In this case, load, sliding speed, and their interaction are significant model terms (Eq. 1). If the probability values are greater than 0.10, it indicates that the model terms are not significant. The errors in the model are given in Table 1.

Final equation in terms of coded factors:

$$\begin{aligned} \textit{Wear rate} = K = {} & +0.62 - 0.56{*}A \\ & + 0.14{*}A^2 - 0.069{*}B - 0.017{*}B^2 \\ & + 0.058{*}AB - 8.944\text{E}{-}003{*}A^2B \\ & + 0.011{*}AB^2 - 0.017{*}A^2B^2 \end{aligned} \quad (1)$$

where A is the load (N) and B is the sliding speed (rpm).

Figure 4 shows the variation of the wear rate of the coating at different loads as well as sliding speeds. The wear rate at low load and low sliding speed was found to be very low. The wear rate was observed to increase more with an increase in load as compared to increased sliding speed.

From the observations, it can be concluded that at lower sliding speed and lower load, the wear was caused by adhesion and very less abrasion. When either one of the two surfaces of triboelements in sliding or rolling contact has thin soft surface layer that can be partly transferred to the counter surface by adhesion, relative displacement takes place at the interface between the surfaces of coating and transfer layer with smaller shear strength of the soft material than that of the underlying element material [12]. This was further explained by Subramanian et al. [13] that, during wear test of aluminum alloy with a copper pin, a tribolayer of aluminum alloy forms on the copper pin. This tribolayer was formed at low load and

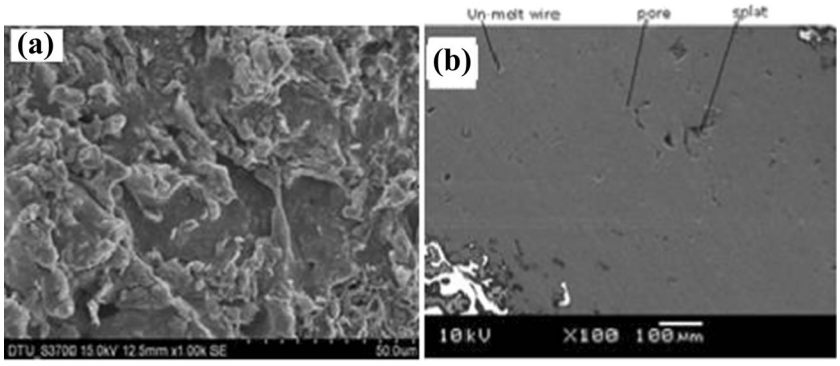


Fig. 2 **a** SEM micrograph of top view **b** and cross section of the Al alloy coating

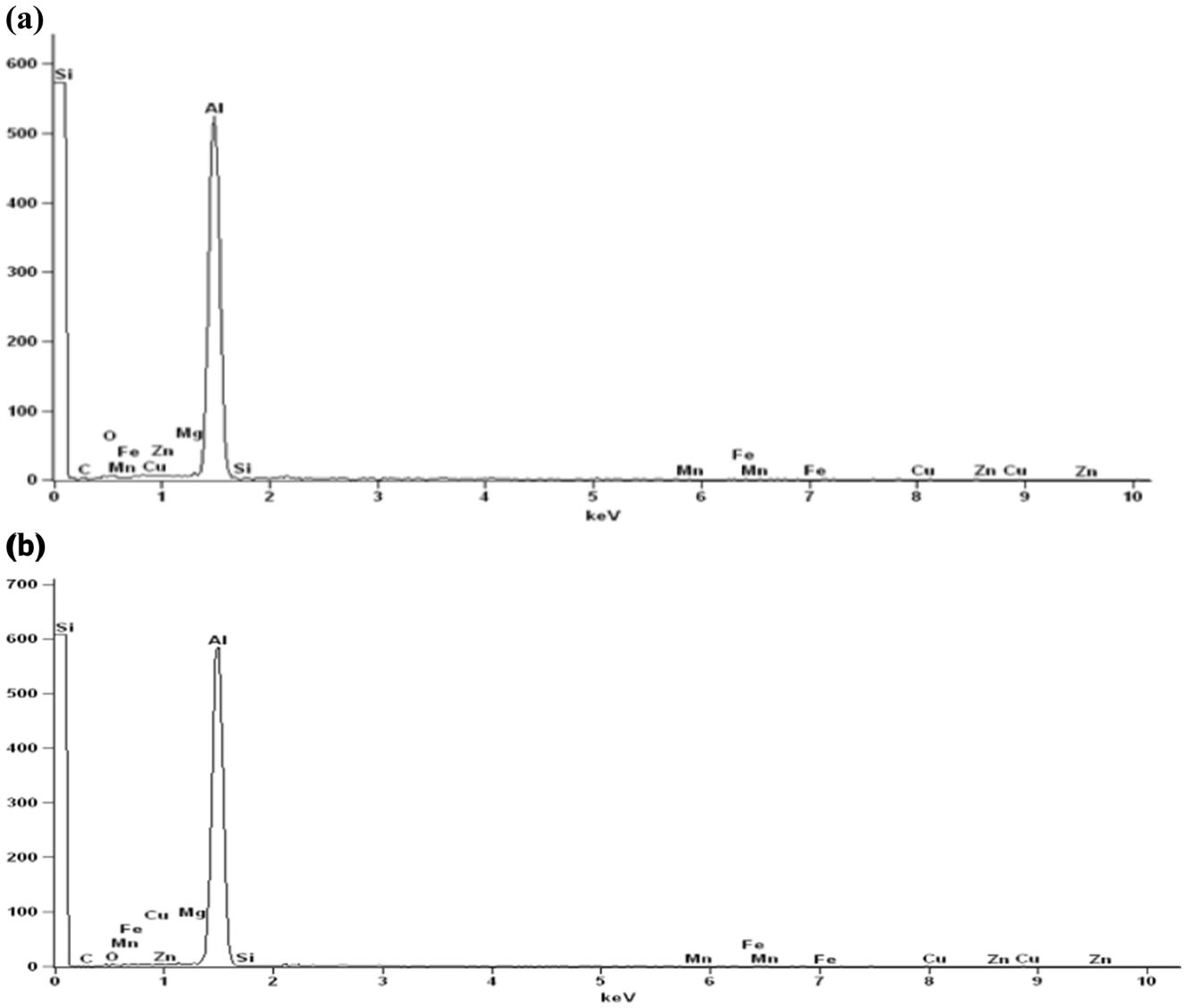


Fig. 3 **a** EDS analysis of coating surface before wear test. **b** EDS analysis of coating surface after wear test at 58.8-N load and 150 rpm speed with medium-carbon steel pin

Table 1 Design expert output for wear rate with brass pin

Term	Coefficient Estimate	df	Standard Error	95 % CI Low	95 % CI High
Intercept	0.62	1	2.194E-004	0.62	0.62
A	−0.56	1	3.043E-004	−0.57	−0.56
A^2	0.14	1	3.043E-004	0.14	0.14
B	−0.069	1	3.043E-004	−0.070	−0.068
B^2	−0.017	1	3.043E-004	−0.018	−0.016
A × B	0.058	1	4.128E-004	0.057	0.059
A^2 × B	−8.944E-003	1	4.128E-004	−0.010	−7.883E-003
A × B^2	0.011	1	4.128E-004	9.828E-003	0.012
A^2 × B^2	−0.017	1	4.513E-004	−0.018	−0.015

CI confidence interval

low sliding velocity. The wear rate of the coating was decreased by the tribolayer. The brass pin at low speed and high load showed high deformation and low wear rate because the microhardness of coating used was 58 Hv at 0.049-N load, which is very less as compared to hardness of the brass. Sannino et al. [14] found that the wear rate also depends on the sliding speed; it is low at low speed and increases with increasing speed. The similar behavior that the wear rate increases with increase in load has also been reported by Kato et al. [12].

3.2.2 Wear rate with medium-carbon steel pin

Wear rate of the coating with medium-carbon steel under similar loading and sliding conditions was calculated as described earlier. The Model F-value of 1144.41 implies that the model

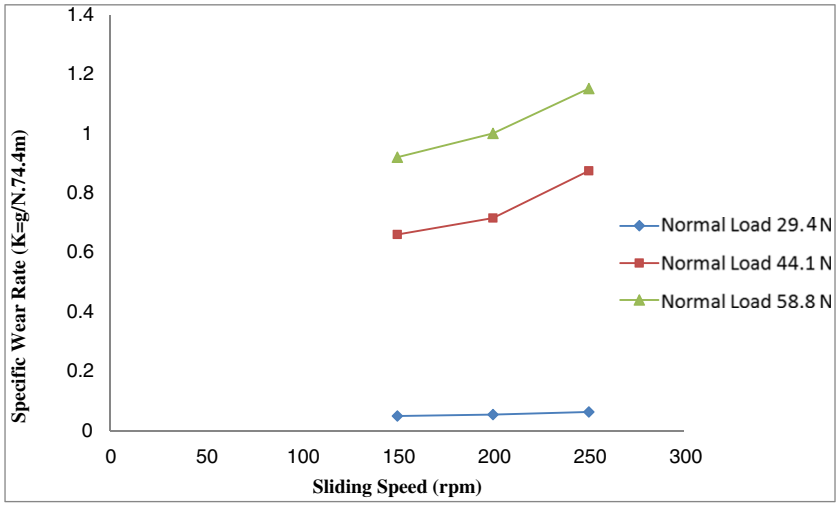


Fig. 4 Specific wear rate of the coating with brass pin at various loading and sliding conditions

is significant. In this case, load, sliding speed, and interaction effects are significant model terms (Eq. 2). The error and coefficient of estimate are given in Table 2.

Final equation in terms of significant coded factors:

$$\begin{aligned} \textit{Wear rate} = K = {} & +1.83 - 0.23*A \\ & + 0.031*A^2 - 0.23*B - 0.056*B^2 - 0.034*AB \\ & + 0.039*A^2B \\ & + 0.086*A\,B^2 - 0.061*A^2B^2 \end{aligned} \tag{2}$$

where A is the load (N) and B is the sliding speed (rpm).

Figure 5 shows the wear rate of the coating with medium-carbon steel pin at different loads and sliding speeds. The wear rate of the coating with medium-carbon steel pin was found to be higher than the wear rate of the coating with brass pin. The specific wear rate of the coating at 150 rpm speed and 29.4-N load was calculated as 1.34 g/N.74.4 m. Maa et al. [15] showed that the wear behavior of different materials is different with different counter materials. The wear rate of the coating increased slightly with increase in the sliding speed at low load. In case of medium-carbon steel pin, the material was found to erode faster; hence, the wear rate was greater [15, 16]. The wear rate of the coating with medium-carbon steel pin was higher as the steel pin is much harder compared to the aluminum alloy coating and also because the wear mechanism was mainly due to microcutting.

3.2.3 Wear rate with high-carbon steel pin

The wear of the coating was also analyzed with high-carbon steel pin under the same loading and sliding conditions. The ANOVA of these two variables was also designed to find the significance of the two variables and

Table 2 Design expert output for wear rate with medium-carbon steel pin

Term	Coefficient Estimate	df	Standard Error	95 % CI Low	95 % CI High
Intercept	1.83	1	3.103E-003	1.82	1.83
A	−0.23	1	4.303E-003	−0.24	−0.21
A^2	0.031	1	4.303E-003	0.020	0.042
B	−0.23	1	4.303E-003	−0.24	−0.21
B^2	−0.056	1	4.303E-003	−0.067	−0.044
A × B	−0.034	1	5.837E-003	−0.049	−0.019
A^2 × B	0.039	1	5.837E-003	0.024	0.054
A × B^2	0.086	1	5.837E-003	0.071	0.10
A^2 × B^2	−0.061	1	6.383E-003	−0.078	−0.045

CI confidence interval

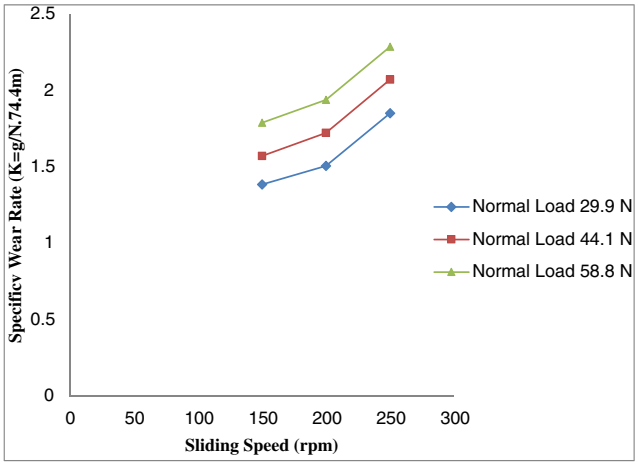


Fig. 5 Specific wear rate of the coating with medium-carbon steel pin coating at various sliding and loading conditions

Table 3 Design expert output for wear rate with high-carbon steel pin

Term	Coefficient Estimate	df	Standard Error	95 % CI Low	95 % CI High
Intercept	2.10	1	3.103E-003	2.09	2.11
A	−0.31	1	4.303E-003	−0.32	−0.30
A^2	−0.076	1	4.303E-003	−0.087	−0.064
B	−0.62	1	4.303E-003	−0.63	−0.61
B^2	0.12	1	4.303E-003	0.11	0.13
A × B	0.052	1	5.837E-003	0.037	0.067
A^2 × B	0.029	1	5.837E-003	0.014	0.044
A × B^2	−0.028	1	5.837E-003	−0.043	−0.013
A^2 × B^2	0.019	1	6.383E-003	2.481E-003	0.035

CI confidence interval

their interactions. The Model F-value of 4533.67 implies that the model is significant. The significant model terms are load, sliding speed, and their interaction effects (Eq. 3). The errors are given in Table 3.

Final equation in terms of significant coded factors:

$$\begin{aligned} \textit{Wear rate} = K = {} & +2.10-0.31{*}A-0.076{*}A^2-0.62{*}B \\ & + 0.12{*}B^2 + 0.052{*}AB \\ & + 0.029{*}A^2B-0.028{*}A\,B^2 \\ & + 0.019{*}A^2B^2 \end{aligned} \quad (3)$$

where A if the load (N) and B is the sliding speed (rpm).

It is clear from Fig. 6 that the wear rate of the coating with high-carbon steel was low at low load and low sliding speed [6], but when the sliding speed was increased, the wear rate was found to increase abruptly. At high speed, the worn debris were observed as microchips, but at lower speed, surface deformations were more. The wear rate was also found to be increased with the increase in load [12]. When observed at low speed, the wear rate was found to increase with load, although the increment was very less. However, at higher sliding speed, the value of wear rate increased abruptly with increased loading conditions. It was clear from the coating wear rate analysis that with high-carbon steel pin, the wear rate was greater when compared with the brass pin and the medium-carbon pin at higher sliding speeds [15, 16]. From the above mentioned observations, it can be concluded that at the lower loads, the coating wear was mainly due to adhesion and deformation while the other modes of wear could not be observed contrary to earlier reports [17].

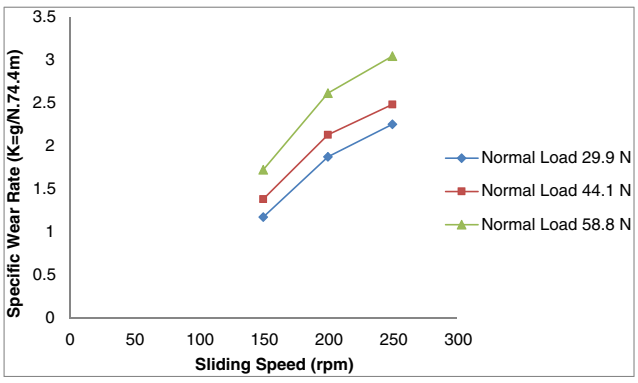


Fig. 6 Specific wear rate of the coating with high-carbon steel pin coating at various sliding and loading conditions

3.3 Coefficient of friction of the coating

3.3.1 Coefficient of friction of the coating with brass pin

The coefficient of friction of the coating at three loads (29.4, 44.1, and 58.8 N) and three sliding conditions (150, 200,and 250 rpm) was analyzed. A statistical ANOVA was designed based on two variables and three levels of each variable in Design-Expert 8.0.1 software. The standard error and degree of freedom are given in Table 4. The Model F-value of 3592.52 implies that the model is significant. In this case, the load, sliding speed, and interaction effects are significant model terms (Eq. 4).

Final equation in terms of significant coded factors:

$$\begin{aligned} \textit{Coefficient of friction} = {} & + 0.74 + 0.042{*}A + 3.333\text{E}{-}004{*}A^2 \\ & + 0.089{*}B{-}0.026{*}B^2{-}0.013{*}AB \\ & + 0.018{*}A^2B + 3.500\text{E}{-}003{*}AB^2 \\ & -6.333\text{E}{-}003{*}A^2B^2 \end{aligned} \quad (4)$$

where A is the load (N) and B is the sliding speed (rpm).

Figure 7 shows the variation of the coefficient of friction of the coating at different loading and sliding conditions with brass pin. The coefficient of friction of the coating decreased, when the sliding speed was increased.

Table 4 Design expert output for coefficient of friction with brass pin

Term	Coefficient Estimate	df	Standard Error	95 % CI Low	95 % CI High
Intercept	0.74	1	4.824E-004	0.74	0.75
A	0.042	1	6.690E-004	0.040	0.043
A^2	3.333E-004	1	6.690E-004	−1.386E-003	2.053E-003
B	0.089	1	6.690E-004	0.087	0.091
B^2	−0.026	1	6.690E-004	−0.028	−0.024
A × B	−0.013	1	9.074E-004	−0.015	−0.011
A^2 × B	0.018	1	9.074E-004	0.016	0.020
A × B^2	3.500E-003	1	9.074E-004	1.167E-003	5.833E-003
A^2 × B^2	−6.333E-003	1	9.923E-004	−8.884E-003	−3.783E-003

CI confidence interval

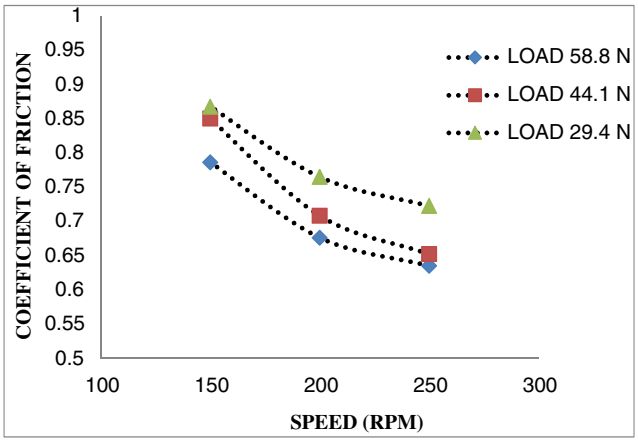


Fig. 7 Variation of coefficient of friction with brass pin at various loading and sliding conditions

Edrisy et al. [18] has earlier reported that at high sliding speed and load, the coefficient of friction was low. However, the variation in the coefficient of friction with variation in load was lower contrary to earlier reports by Xua et al. [19] that the coefficient of friction of aluminum alloy decreases with an increase in load. This might have occurred as the brass pin is a soft material and gets deformed easily during the wear test.

3.3.2 Coefficient of friction of the coating with medium-carbon steel

The coefficient of friction of coating with medium-carbon steel pin was analyzed under similar loading and sliding conditions, and a set of experiment was designed to do the ANOVA of the process variables (Table 5). The Model F-value of 3183.89 implies that the model is significant.

Table 5 Design expert output for coefficient of friction with medium-carbon steel pin

Term	Coefficient Estimate	df	Standard Error	95 % CI Low	95 % CI High
Intercept	0.75	1	3.230E-004	0.75	0.75
A	0.039	1	4.479E-004	0.038	0.040
A^2	8.167E-003	1	4.479E-004	7.015E-003	9.318E-003
B	0.036	1	4.479E-004	0.035	0.037
B^2	−1.500E-003	1	4.479E-004	−2.651E-003	−3.486E-004
A × B	0.029	1	6.076E-004	0.027	0.031
A^2 × B	−0.014	1	6.076E-004	−0.016	−0.012
A × B^2	−0.018	1	6.076E-004	−0.020	−0.016
A^2 × B^2	−2.500E-003	1	6.643E-004	−4.208E-003	−7.922E-004

CI confidence interval

Final equation in terms of significant coded factors:

$$\begin{aligned} \textit{Coefficient of friction} = {} & +0.75+0.039*A+8.167\text{E}{-}003*A^2 \\ & +0.036*B{-}1.500\text{E}{-}003*B^2+0.029*AB \\ & -0.014*A^2B{-}0.018*AB^2{-}2.500\text{E}{-}003*A^2B^2 \end{aligned} \quad (5)$$

where A is the load (N) and B is the sliding speed (rpm).

Figure 8 shows the variation of the coefficient of friction of the coating at different loading and sliding conditions with medium-carbon steel pin. The coefficient of friction in case of the medium-carbon steel pin was higher than in case of brass pin [15, 16]. The coefficient of friction was decreased with increased loading conditions. It was found to decrease probably because at increased load, the wear rate was more. Hence, direct rubbing was lesser and coefficient of friction was low. The wear rate also decreased with increase in sliding speed. The coefficient of friction was found to be low at high load and sliding speed [18–20]. Xua et al. [19] have earlier reported that the coefficient of friction of aluminum alloy decreases with an increase in load.

3.3.3 Coefficient of friction of the coating with high-carbon steel

The coefficient of friction of the coating was also analyzed with high-carbon steel pin at similar loading and sliding conditions, as described in the above cases. The ANOVA was designed for analyzing the coefficient of friction. The Model F-value of 1439.88 implies that the model is significant (Table 6). Load, sliding speed, and their interactions are the significant model terms (Eq. 6).

Final equation in terms of coded factors:

$$\begin{aligned} \textit{Coefficient of friction} = {} & +0.81+0.054*A+8.222\text{E}{-}003*A^2 \\ & +0.083*B{-}7.944\text{E}{-}003*B^2+0.013*AB \\ & -8.222\text{E}{-}003*A^2B{-}0.018*AB^2{-}7.222\text{E} \\ & -003*A^2B^2 \end{aligned} \quad (6)$$

where A is the load (N) and B is the sliding speed (rpm).

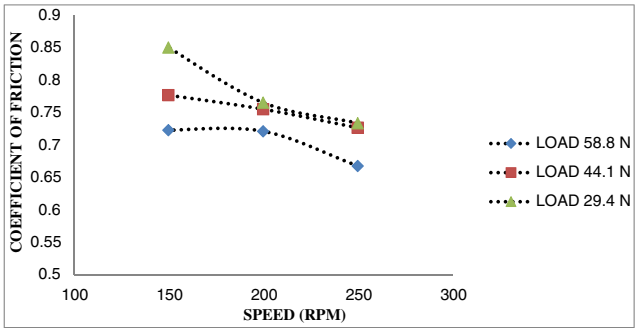


Fig. 8 Variation of coefficient of friction with medium-carbon steel pin at various loading and sliding conditions

Table 6 Design expert output for coefficient of friction with high-carbon steel pin

Term	Coefficient Estimate	df	Standard Error	95 % CI Low	95 % CI High
Intercept	0.81	1	8.062E-004	0.81	0.81
A	0.054	1	1.118E-003	0.051	0.057
A^2	8.222E-003	1	1.118E-003	5.348E-003	0.011
B	0.083	1	1.118E-003	0.080	0.086
B^2	−7.944E-003	1	1.118E-003	−0.011	−5.070E-003
A × B	0.013	1	1.517E-003	9.046E-003	0.017
A^2 × B	−8.222E-003	1	1.517E-003	−0.012	−4.324E-003
A × B^2	−0.018	1	1.517E-003	−0.022	−0.014
A^2 × B^2	−7.222E-003	1	1.658E-003	−0.011	−2.959E-003

CI confidence interval

Figure 9 shows the variation of the coefficient of friction of the coating at different loading and sliding conditions. It was observed that the coefficient of friction of the coating with high-carbon steel was more than coefficient of friction with brass and medium-carbon steel pin [15, 16]. The coefficient of the friction of the coating was decreased with increase in load [19, 20]. It was also observed that the coefficient of friction decreased with the increase in sliding speed [18–22]. The coating was found to have hardness of 58.8 Hv at 0.049-N load, which was very less as compared to hardness of the high-carbon steel pin. However, there was no deformation observed of the high-carbon steel pin during the wear test.

All the experimental values of specific wear rate and coefficient friction analysis of Al alloy coating with different pin materials, the predicted values from regression equations, and the percentage error in prediction are summarized in Tables 7 and 8. The regression equations predict the specific wear rate and the coefficient of friction within the range of 0.05 % error; therefore, these equations will be used to predict the wear behavior of Al alloy coating.

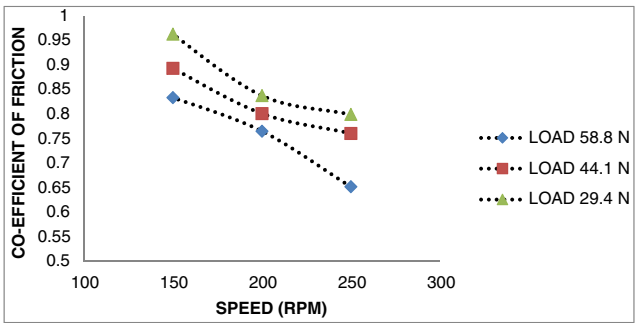


Fig. 9 Variation of coefficient of friction with high-carbon steel pin at various loading and sliding conditions

3.3.4 Microhardness of the worn surfaces with brass pin

Figure 10a shows the microhardness at the cross section of the wear track of the coating worn with brass pin at a load 58.8 N and 250 rpm sliding speed. The microhardness of the worn surface was higher near the wear track due to more deformation and work hardening of the track. The work hardening effects decreased away from the wear track. The various grades of aluminum, as well as alloy with manganese and magnesium as the major additions do not provide strengthening by heat treatment. Approximately, 95 % of all aluminum flat rolled products (sheet, plate, and foil) are made from these three alloy groups. Strength is developed by strain hardening usually by cold working during fabrication. In accordance with the dynamic theory, during deformation of aluminum and its alloys, the dislocation content increases when dislocation generation and multiplication occur faster than annihilation. Dislocation tangles, cells, and subgrain walls are formed, all of which decrease the mean free slip distance and give increased strength. During deformation, owing to high stacking fault energy of aluminum, a cellular substructure is formed within the grain which causes some strengthening. The work hardenability of the aluminum alloy was found to increase with increase in magnesium content [11]. When the pin was slid on the coating surface, strain hardening effects developed due to force exerted by the pin on the coating surfaces. At higher load, high work hardening was observed.

3.3.5 Microhardness of the worn surfaces with medium-carbon steel pin

Figure 10b shows the variation of microhardness at the cross section of the wear track at a load of 58.8-N load and 250 rpm speed with medium-carbon steel. It was observed that the microhardness at a distance of 0.05 μm was maximum and then decreased away from the cross section of wear track. The microhardness of the worn surfaces with medium-carbon steel pin was found to be lower than that of microhardness of the worn surfaces with brass pin. It was may be due to the reason that the coating deformed more and the microcutting was less with brass pin. It was observed by SEM results that the main wear mechanism of coating with medium-carbon steel pin was mainly due to microcutting, and lesser deformation of the wear track was observed. As the deformation was very less, strain hardening effects were found to be low. The deformation effects were uniform so that the variation in the microhardness was much lower.

Table 7 Specific wear rates of Al alloy coating with brass, carbon steel, and high-carbon steel pins

Normal load (N)	Sliding speed (rpm)	Specific wear rate of Al alloy coating with pins (g/N.74.4 m)								
		Brass pin			Carbon steel pin			High-carbon steel pin		
		Experimental	Predicated	Error (%)	Experimental	Predicated	Error (%)	Experimental	Predicated	Error (%)
29.4	150	0.041	0.0415	<0.5	1.334	1.331	<0.5	1.231	1.221	<0.5
	200	0.046	0.046	<0.5	1.632	1.622	<0.5	1.874	1.882	<0.5
	250	0.069	0.069	<0.5	1.833	1.831	<0.5	2.272	2.271	<0.5
44.1	150	0.679	0.678	<0.5	1.672	1.67	<0.5	1.432	1.432	<0.5
	200	0.722	0.722	<0.5	1.745	1.742	<0.5	2.161	2.163	<0.5
	250	0.866	0.867	<0.5	2.162	2.171	<0.5	2.472	2.482	<0.5
58.8	150	0.924	0.924	<0.5	1.792	1.792	<0.5	1.783	1.783	<0.5
	200	1.031	1.0305	<0.5	1.941	1.941	<0.5	2.614	2.613	<0.5
	250	1.17	1.171	<0.5	2.334	2.332	<0.5	3.061	3.061	<0.5

3.3.6 Microhardness of the worn surfaces with high-carbon steel pin

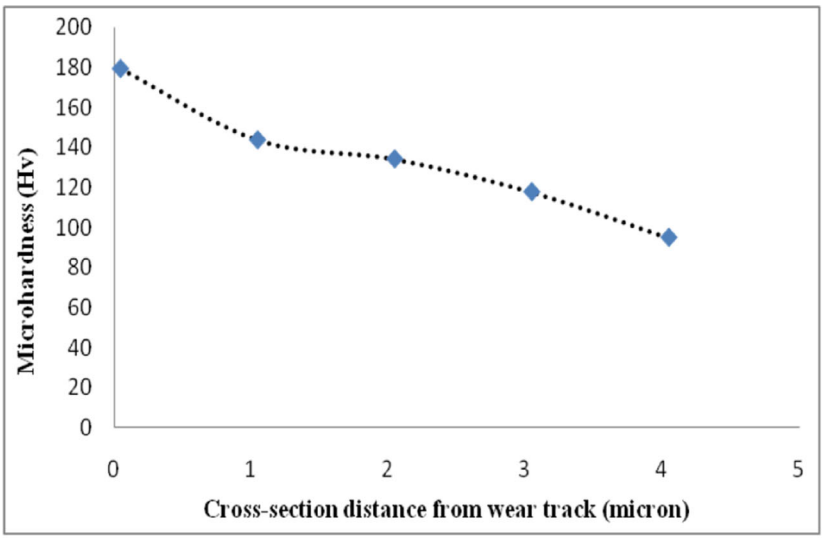
Figure 10c shows the microhardness of the cross section of worn surface with high-carbon steel pin at a load of 58.8 N and 250 rpm sliding speed. At a distance 0.05 μm from the wear track, the microhardness was found to be more on the worn surface of the coating formed by brass and medium-carbon steel at the same load and sliding speed. However, away from the cross section of the wear track, the microhardness decreased at a faster rate. The microhardness near the wear track was as high as 197.93 Hv, but at a distance of 4 μm, the hardness was only 69.85 Hv. It was possibly due to the reason that the wear mechanism in case of high-carbon steel pin is mainly due to microcutting and the deformation was only on the wear track, whereas the work hardening was only over the wear track, below which the work hardening effects were not present.

3.4 EDS analysis of worn surfaces

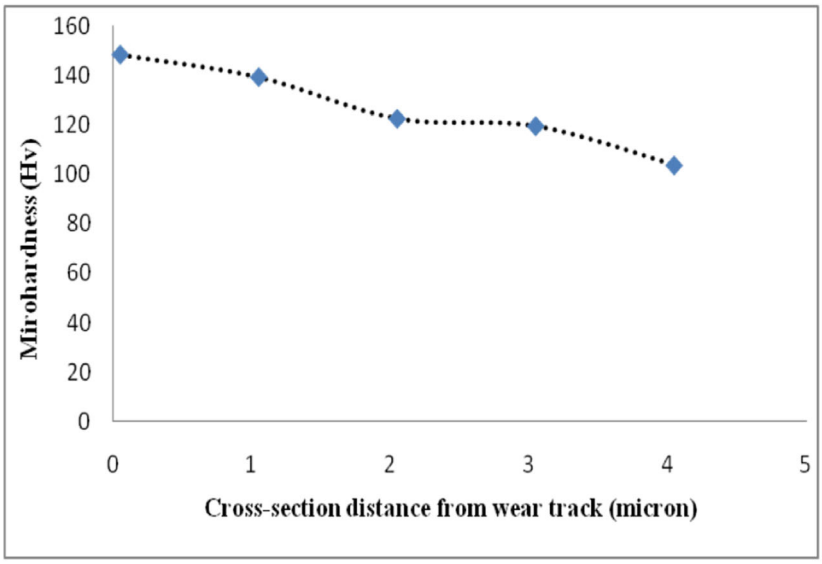
Figure 2b shows the EDS peaks of the coating, worn with medium-carbon steel pin load of 58.8 N and at a speed of 150 rpm. It was found that aluminum was the major component, but some amount of copper, magnesium, manganese, iron, and carbon were also found to be present. During the wear test, some pin material was also found diffused over the coating surface, so negligible a amount of iron and carbon was also transferred on the wear track. Some amount of copper, iron, and zinc was found as impurities (Table 9).

Table 8 Coefficient of friction of Al alloy coating with brass, carbon steel, and high-carbon steel pins

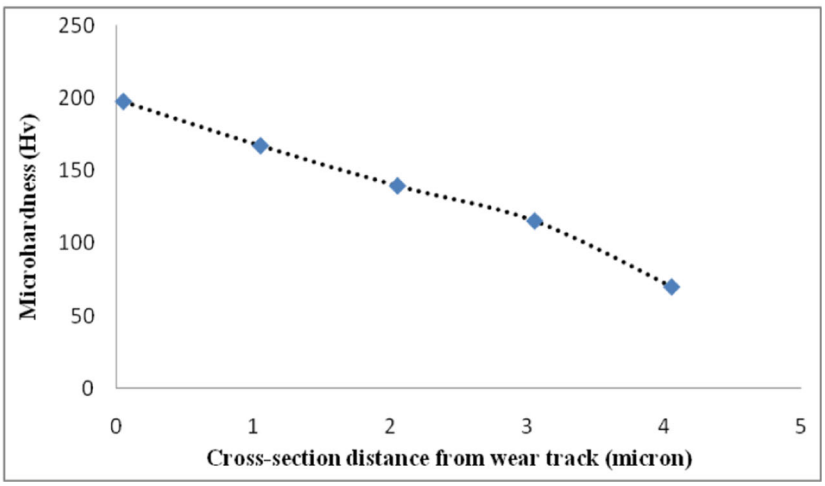
Normal load (N)	Sliding speed (rpm)	Coefficient of friction of Al alloy coating with pins (μ)								
		Brass pin			Carbon steel pin			High-carbon steel pin		
		Experimental	Predicated	Error (%)	Experimental	Predicated	Error (%)	Experimental	Predicated	Error (%)
29.4	150	0.863	0.861	<0.5	0.850	0.851	<0.5	0.963	0.960	<0.5
	200	0.764	0.763	<0.5	0.767	0.767	<0.5	0.838	0.838	<0.5
	250	0.732	0.732	<0.5	0.741	0.741	<0.5	0.794	0.794	<0.5
44.1	150	0.851	0.851	<0.5	0.778	0.778	<0.5	0.893	0.893	<0.5
	200	0.712	0.712	<0.5	0.752	0.752	<0.5	0.803	0.803	<0.5
	250	0.668	0.669	<0.5	0.739	0.738	<0.5	0.760	0.758	<0.5
58.8	150	0.786	0.786	<0.5	0.722	0.722	<0.5	0.823	0.826	<0.5
	200	0.679	0.679	<0.5	0.720	0.720	<0.5	0.768	0.765	<0.5
	250	0.641	0.641	<0.5	0.661	0.661	<0.5	0.652	0.652	<0.5



(a) Micro hardness of worn surfaces with brass pin.



(b) Micro hardness of worn surfaces with medium carbon steel pin



(c) Micro hardness of worn surfaces with high carbon steel pin

Fig. 10 Variation of microhardness of worn surfaces from cross section at 58.8-N load and 250 rpm speed with (**a**) brass pin, (**b**) medium-carbon steel pin, and (**c**) high-carbon steel pin

Table 9 Quantitative EDS analysis of wear track of thermal spray coating with medium-carbon steel pin at 150 rpm and 58.8-N loads

Element	Net counts	ZAF	Weight %	Weight % error	Atom %	Atom % error	Compound%
C K	4	11.332	0.77	±0.96	1.72	±2.15	0.77
O K	8	2.985	0.58	±0.51	0.97	±0.85	0.58
Mg K	0	0.997	0.00	–	0.00	±0.00	0.00
Al K	6215	1.027	96.60	±1.23	96.35	±1.22	96.60
Si K	0	2.182	0.00	–	0.00	±0.00	0.00
Si L	0	0.000	–	–	–	–	–
Mn K	7	1.185	0.64	±0.55	0.31	±0.27	0.64
Mn L	0	0.000	–	–	–	–	–
Fe K	8	1.162	0.83	±0.83	0.40	±0.40	0.83
Fe L	8	0.000	–	–	–	–	–
Cu K	3	1.215	0.59	±0.98	0.25	±0.42	0.59
Cu L	0	0.000	–	–	–	–	–
Zn K	0	1.218	0.00	–	0.00	±0.00	0.00
Zn L	0	0.000	–	–	–	–	–
Total			100.00		100.00		100.00

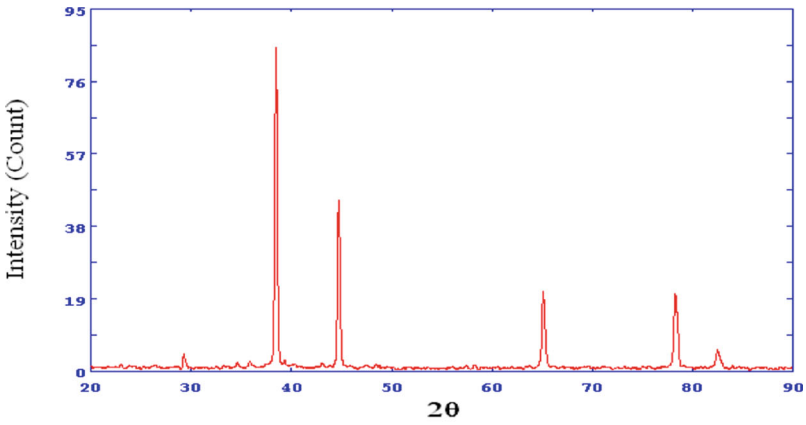
3.5 XRD analysis of worn surfaces

The XRD analysis of the worn surfaces was done with the help of X-ray diffractometry with CuKα radiation= 1.5418 Å. Conversion of the diffraction peaks to d-spacing allows identification of the material because each material has a set of unique d-spacing. Typically, this is achieved by comparison of d-spacing with standard reference patterns. As the wear of the coating occurs, the d-spacing of the crystal is expected to decrease. If the stress is non-uniform, different crystal or different parts of the same crystal may be deformed to differing degrees and the crystal line becomes broadened [21, 22]. Stress in the coating may be caused by application of external load. Internal stress may also result as a consequence of the deformation taking place inside the crystal.

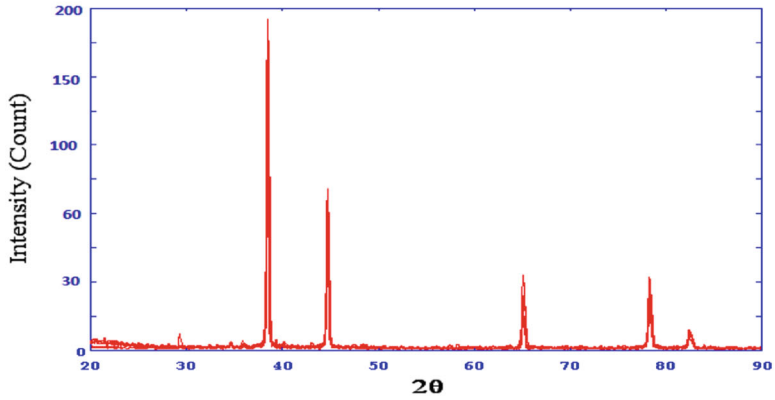
The value of d-spacing of coating at the wear track at a load of 29.4 N and 250 rpm sliding speed with brass pin was found to be 3.69634 Å (Fig. 11a). When the load was increased to 44.1 N, the value of d-spacing was found to be 2.34347 Å. It was observed that the value of d-spacing decreased with an increase in the load. The value of the "θ" was found to be increased with the increased load. Initially, the value of 2θ was found to be 38.380° at 250 rpm speed and 29.4-N load. When the load was increased to 44.1 N, the value of 2θ was found to be 38.4494°. It further increased to 38.5690 at 58.8-N load and the same sliding speed. The peaks of XRD were found to be shifted toward right-hand side with increased load. It was clear from these observations that the deformation of the wear track of the coating increased with the increased load. It was also observed that when the sliding speed was decreased, the value of d-spacing was found to be decreased possibly due to the reason that, at lower speed, the deformation of the crystals was more.

The value of d-spacing of the coating worn with medium-carbon steel at a load of 29.4-N load and 250 rpm speed was found to be 3.68879 Å (Fig. 11b). It was found to decrease to 3.67745 Å at a load of 58.8 N under similar sliding speed. The value of d-spacing of the worn surfaces of the coating with high-carbon steel at a load of 29.4 N and 250 rpm speed was found to be 3.69145 Å (Fig. 11c). It was found to decrease to 3.69028 Å at a load of 44.1-N load and 250 rpm sliding speed.

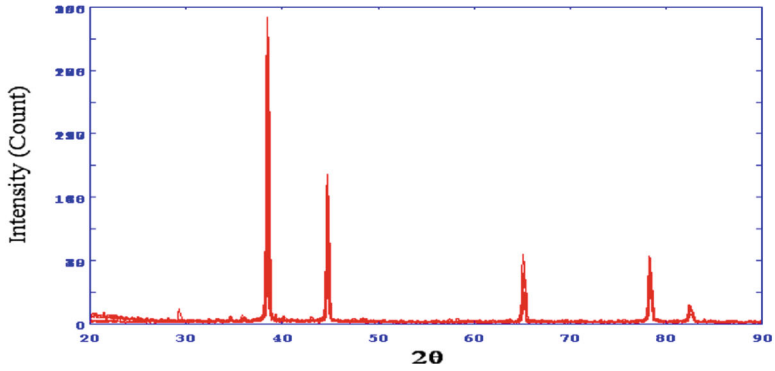
When the load was increased to 58.8 N, the value of d was found to decrease to 3.67745 Å. From these observations, it can be concluded that the value of d-spacing decreased with increased load. The decrease in the d-spacing at increased load was due to the reason that at high load, the coating crystals were deformed more and the intermolecular space between the two atoms was decreased. However, the value of d-spacing of the worn surfaces with brass pin was found to be more possibly because the brass pin was less hard as compared to medium-carbon and high-carbon steel pin, so the coating surface was more deformed with brass pin. Due to this deformation, the particles of the coating tend to come closer to each other which may decrease the value of d-spacing. However, in the wear track of the coating with medium-carbon and high-carbon steel, the deformation was very less and microcutting was more, so the value of d-spacing was found to be high.



(a) XRD peaks with brass pin at 250 rpm speed and 29.4 N loads



(b) XRD peaks with medium carbon steel pin at 29.4 N load and 250 rpm speed



(c) **XRD peaks with high carbon steel pin at 29.4 N load and 250 rpm speed.**

Fig. 11 XRD peaks worn surface aluminum alloy coating with **a** brass pin, **b** medium-carbon steel, and **c** high-carbon steel pin

3.6 Wear mechanism

3.6.1 Wear mechanism with brass pin

In order to study the wear mechanism, the worn surface was examined by scanning electron microscope. Figure 12a shows the worn surface of the thermal spray coating with brass pin, at 29.4-N load and 250 rpm speed. At that low load and high sliding speed, the wear mechanism was mainly due to microcutting and abrasion. When the load was increased to 44.1 N at the same sliding speed, some adhesion was also observed (Fig. 12b). However, when the load was increased to 58.8 N, the long worn debris was generated at high loads and sliding speed indicating the occurrence of severe metallic wear by physical metallic failure [6]. Very low deformation was observed while the microcuttings were more (Fig. 12c). At 200 rpm and the load of 29.4 N, the wear of the coating was very less, but higher than that at 250 rpm speed. It was possibly due to reason that at this speed, it rubbed against the coating material and the wear was only due to erosion of the coating (Fig. 12d). When the load was increased to 44.1 N, then the wear mechanism of the coating was also comprised of

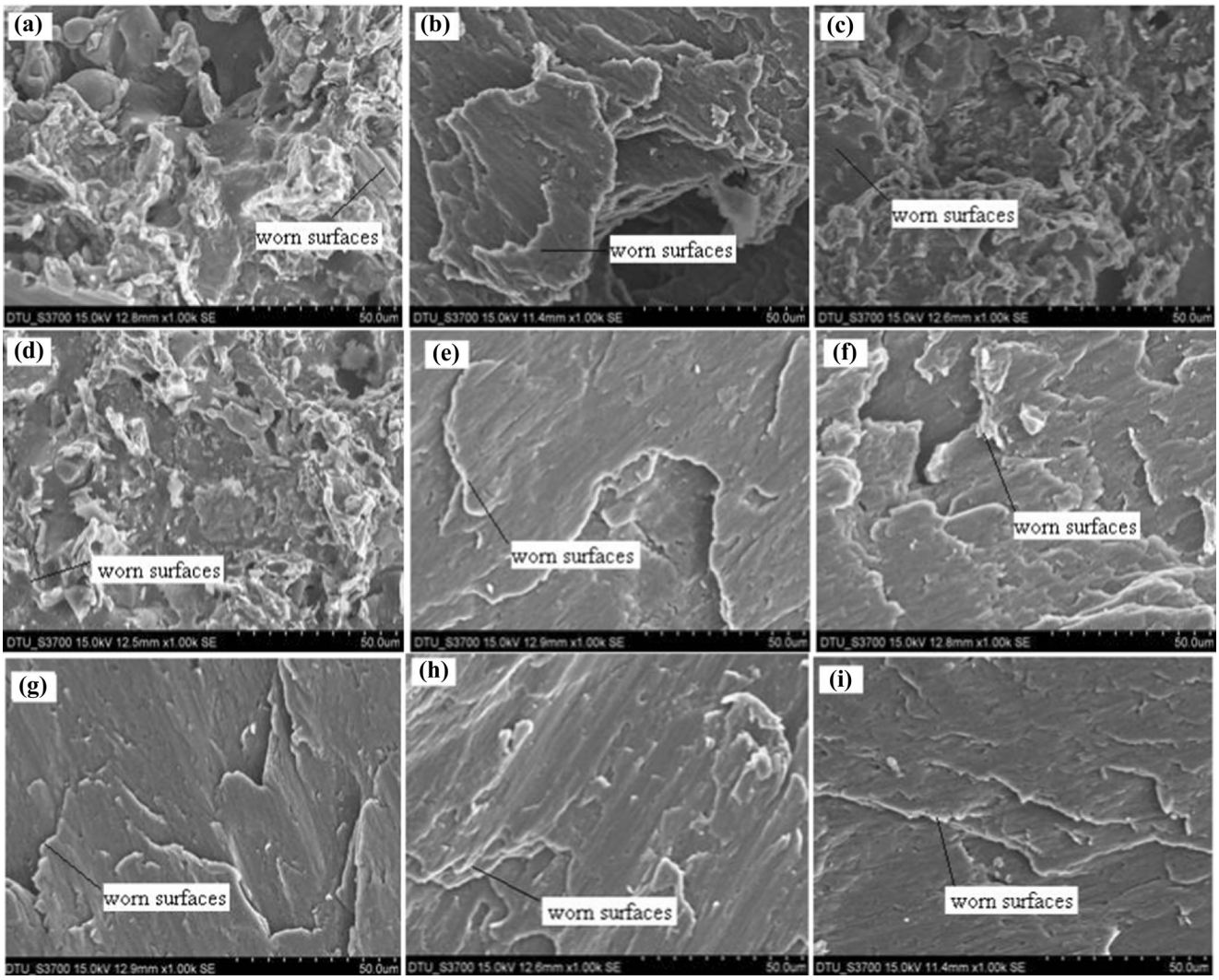


Fig. 12 Worn surface with brass pin **a** at 250 rpm speed and 29.4-N load, **b** at 250 rpm speed and 44.1-N load, **c** at 250 rpm speed and 58.8-N load, **d** at 200 rpm speed and 29.4-N load, **e** at 200 rpm speed and 44.1-N load, **f** at 200 rpm speed and 58.8-N load, **g** at 150 rpm speed and 29.4-N load, **h** at 150 rpm speed and 44.1-N load, and **i** at 150 rpm speed and 58.8-N load

adhesion wear with some microcutting (Fig. 12e). Wear mechanism at 58.8-N loads and 200 rpm was found to generate more adhesion, and the coating material gets more deformed and deposited over the coating surface (Fig. 12f).

Figure 12g shows the wear mechanism of the coating at 150 rpm speed and 29.4-N loads, it shows some deformation and microcutting of the coating. When the load was increased to 44.1 N, the deformation of the worn surfaces was more (Fig. 12h). When the load was further increased to 58.8 N at the same speed, the deformation of the coating on the wear track was increased (Fig. 12i).

3.6.2 Wear mechanism with medium-carbon steel

Figure 13a shows the worn surface of the coating with medium-carbon steel pin at load 29.4 N and 250 rpm sliding speed. It was observed that at this load and sliding speed, abrasion wear of the coating was more and the wear debris was in the form of microchips. These microchips were suddenly removed over the track due to high sliding speed. When the load was further increased to 44.1 N at same sliding speed, the surface deformation was more, with high microcutting of the coating as shown in Fig. 13b. The deformation of the coating was further increased with increase in load (Fig. 13c).

When the speed of the disc was decreased to 200 rpm, there was more deformation of the wear track on coating. When the load was 29.4 N and the sliding speed was 200 rpm, the deformation was less and microcutting was the main wear mechanism (Fig. 13d). When the load was increased to 44.1 N at the same sliding speed, the deformation of the coating was more (Fig. 13e). At 58.8-N loads, the coating got more deformed and microcutting was found to be very high. Also, the wear track was observed to be more smooth

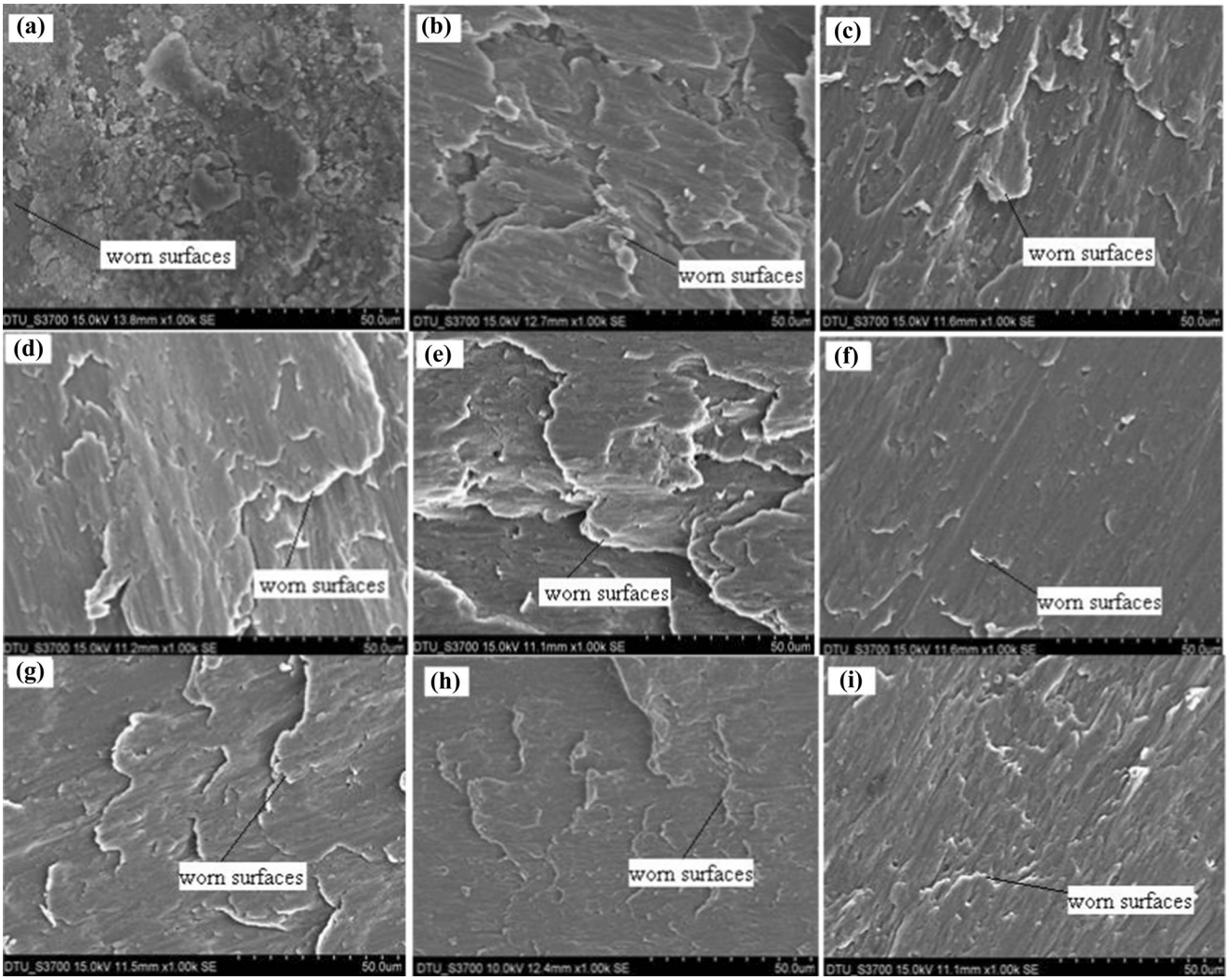


Fig. 13 Worn surfaces with medium-carbon steel **a** at 250 rpm speed and 29.4-N load, **b** at 250 rpm speed and 44.1-N load, **c** at 250 rpm speed and 58.8-N load, **d** at 200 rpm speed and 29.4-N load, **e** at 200 rpm speed and 44.1-N load, **f** at 200 rpm speed and 58.8-N load, **g** at 150 rpm speed and 29.4-N load, **h** at 150 rpm speed and 44.1-N load, and **i** at 150 rpm speed and 58.8-N load

(Fig. 13f). At slow speed, plastic deformation of the coating was more while its abrasion was lesser.

The wear mechanism at 150 rpm speed and a load of 29.4 N was also studied, and it was found that at this load, the deformation of the coating was more due to slow speed (Fig. 13g). When the load was increased to 44.1 N at the same sliding speed, the plastic deformation of the coating was found to be high (Fig. 13h). At a load of 58.8 N and the same sliding speed, the deformation of the coating was found to be increased as well as the microcutting of the coating was also found to be higher (Fig. 13i).

3.6.3 Wear mechanism with high-carbon steel

The high-carbon steel pin was harder as compared to brass pin and medium-carbon steel pin; hence, the deformation of the wear track was very less and the main wear mechanism was microcutting.

The wear mechanism at 250 rpm speed and 29.4 N was analyzed, and it was found that the deformations of the worn surfaces was less as compared to worn surfaces with brass and medium-carbon steel pin (Fig. 14a). When the load was increased to 44.1 N at the same sliding speed some deformation of the coating was observed, but the main wear mechanism was due to abrasion and microcutting (Fig. 14b). At the load of 58.8 N and the same sliding speed of 250 rpm, the deformation of the wear track was more but the deposition of the coating material over the coating was very less (Fig. 14c).

At 200 rpm speed and 29.4-N loads, the deformation was higher as compared to deformation in case of 250 rpm speed (Fig. 14d). When the load increased to 44.1 N at the same sliding speed, the deformation and microcutting were increased (Fig. 14e). At 58.8-N load and 200 rpm speed,

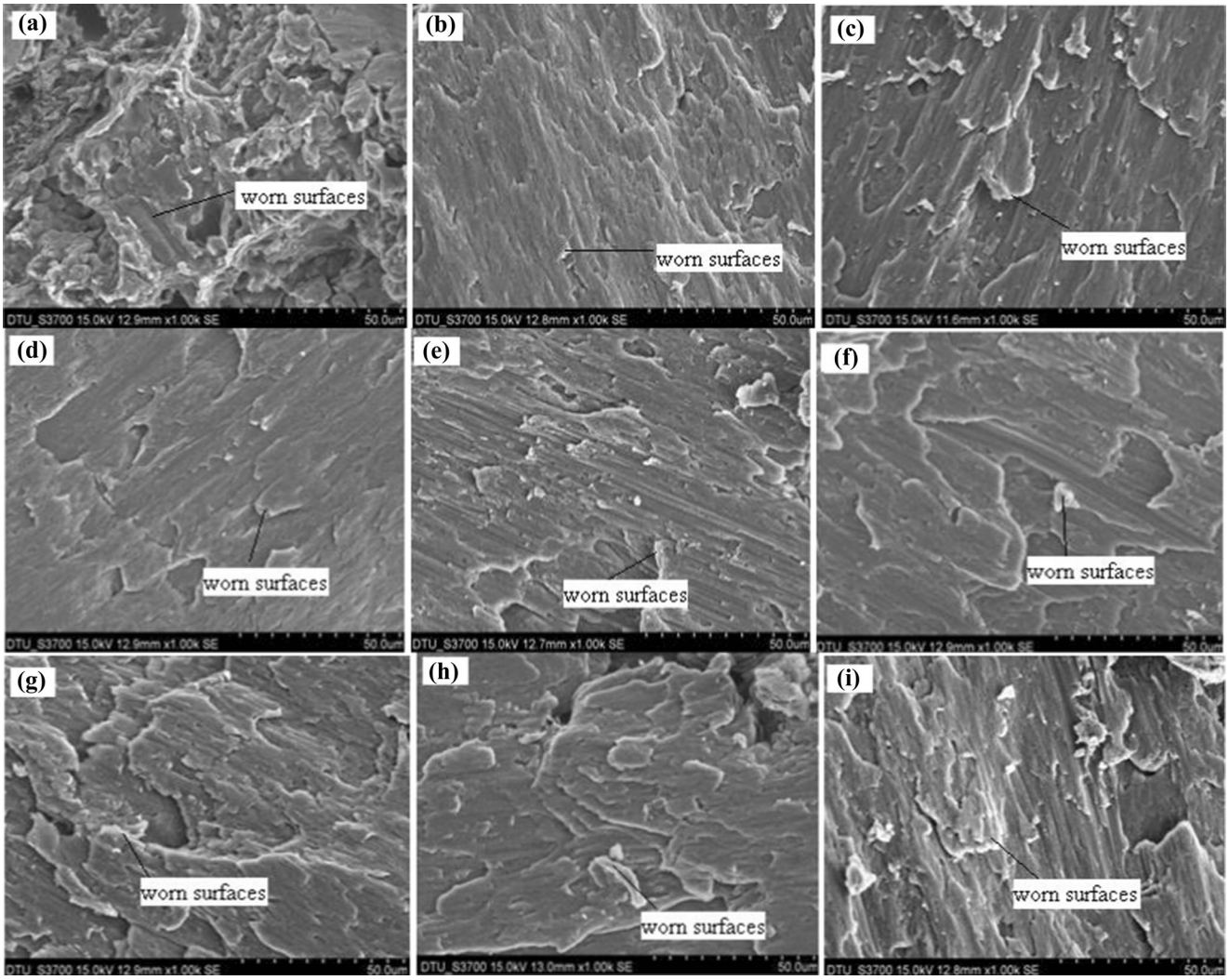


Fig. 14 Worn surfaces with high-carbon steel **a** at 250 rpm speed and 29.4-N load, **b** at 250 rpm speed and 44.1-N load, **c** at 250 rpm speed and 58.8-N load, **d** at 200 rpm speed and 29.4-N load, **e** at 200 rpm speed and 44.1-N load, **f** at 200 rpm speed and 58.8-N load, **g** at 150 rpm speed and 29.4-N load, **h** at 150 rpm speed and 44.1-N load, and **i** at 150 rpm speed and 58.8-N load

deformation was much higher and the microcutting and abrasion came into picture (Fig. 14f).

When the speed of the disc decreased, then the coating surface deformed more and microcutting was very less. At 150 rpm speed and 29.4-N loads, the deformation was less and microcutting was also less; the wear track was less deformed (Fig. 14g). At the same 150 rpm speed and load of 44.1 N, the deformation and the microcutting of the coating increased (Fig. 14h). When the load was increased to 58.8 N, the wear track surface got more deformed and the microcutting and worn debris were found to be more (Fig. 14i).

4 Conclusions

1. By the ANOVA analysis, all the variables (speed, load) on which the specific wear rate and coefficient of friction of the coating depends, and their interaction were found to be significant.
2. The wear rate of the coating was found to increase with increase in load and sliding speed whereas the coefficient of friction was found to decrease. The wear rate with brass pin at 29.4-N load and 150 rpm was found to be 0.0421 g/N.74.4 m; an increase up to 1.017 g/N.74.4 m at 58.8-N load and 250 rpm sliding speed was observed.
3. The microhardness at the cross section of the worn surfaces was found to be more near the wear track and decreased away from the wear track.
4. By the X-ray diffractometry, it was found that during the wear test, the intermolecular spacing between the molecules decreased with increasing load.
5. Adhesion, deformation, and microcutting of the coating were observed to be the main wear mechanisms by the scanning electron microscopy data.

References

1. Gedzevicius AV (2006) Valiulis, Analysis of wire arc spraying process variables on coatings properties. JMPT 175:206–211
2. Zixin Z, Xiubing L, Binshi X, Zeyu D (2002) Numerical simulation and measurement of droplet velocity during high velocity arc spraying. Trans China Weld Inst 1:5–8
3. Xu BS, Liang XB, Ma SN (1998) Study on a new designed gun for high velocity arc spraying. China Surf Eng 3:16–19
4. Herman H, Sampath S (1996) Thermal spray coatings, metallurgical and ceramic protective coatings., pp 261–289
5. Murtaza Q, Kelly P (2013) Optimization of two-wire arc thermal spray process for the production of free-standing tin alloy coating, AES technical reviews Int. Journal, Part C, International Journal of Advances and Trends in Engineering Materials and their Applications 1–1:21–27
6. Dwivedi DK, Arjun TS, Thakur P, Vaidya H, Singh K (2004) Sliding wear and friction behaviour of Al–18% Si–0.5% Mg alloy. J Mater Process Technol 152:323–328
7. Tan KS, Wood RJK, Stokes KR (2003) The slurry erosion behaviour of high velocity oxy-fuel (HVOF) sprayed aluminum bronze coatings. Wear 255:195–205
8. Tan KS, Wharton JA, Wood RJK (2005) Solid particle erosion–corrosion behaviour of a novel HVOF nickel aluminum bronze coating for marine applications—correlation between mass loss and electrochemical measurements. Wear 258:629–640
9. Sarikaya O, Anik S, Erdal C, Cem Okumus S, Aslanla S (2007) Wear behaviour of plasma-sprayed AlSi/B4C composite coatings. Mater Des 28:2177–2183
10. Kennedy DM, Hashmi MSJ (1998) Methods of wear testing for advanced surface coatings and bulk materials. Dublin City University, Glasnevin, Dublin 9, Ireland
11. I.J Polmear, Light alloys-Metallurgy of the light metals, Edward Arnold, ISBN 0-340-49175-2.
12. Kato K (2000) Wear in relation to friction—a review. Laboratory of Tribology, Wear 241:151–157
13. Subramanian. On mechanical mixing during dry sliding of aluminium-12.3 wt% silicon alloy against copper, Wear, 1993, 161, 53–60.
14. Sannino AP, Rack HJ (1995) Dry sliding wear of discontinuously reinforced aluminum composites review and discussion. Wear 189: 1–19
15. Maa W, Lua J, Wanga B (2009) Sliding friction and wear of Cu–graphite against 2024, AZ91D and Ti6Al4V at different speeds. Wear 266:1072–1081
16. Yamane M, Stolarskia TA, Tobeb S (2008) Influence of counter material on friction and wear performance of PTFE–metal binary coatings. Tribol Int 41:269–281
17. Subramanian C, Stratford KN, Wilks TP, Ward LP (1996) On the design of coating systems: metallurgical and other considerations. J Mater Process Technol 56:385–397
18. Edrisy A, Perry T, Chengb YT, Alpas AT (2001) Wear of thermal spray deposited low carbon steel coatings on aluminum alloys. Wear 251:1023–1033
19. BinshiXua ZZ, Maa S, Zhang W, Liu W (2004) Sliding wear behavior of Fe–Al and Fe–Al/WC coatings prepared by high velocity arc spraying. Wear 257:1089–1095
20. Gonzalez R, Cadenas M, Fernandez R, Cortizo JL, Rodriguez E (2007) Wear behavior of flame sprayed NiCrBSi coating remelted by flame or by laser. Wear 262:301–307
21. Anthony R. Vest, Solid state chemistry and its applications, Wiley Publication, 1984.
22. Fratila-Apachitei LE, Duszczyk J, Katgerman L (2003) Vickersmicrohardness of AlSi(Cu) anodic oxide layers formed in H_2SO_4 at low temperature. Surface & Coating Technology 17: 309–315

Journal of Material Science and Mechanical Engineering (JMSME)
Print ISSN : 2339-9095; Online ISSN : 2393-9109; Volume 2, Number 6; April – June, 2015 pp 41 – 44
Krishi Sanskriti Publications
http://www.krishisanskriti.org/jmsme.html

Solar Thermal Technologies for Power Generation in India

Rajesh Kumar*

Department of Mechanical Engineering, Delhi Technological University (Government of NCT of Delhi), Bawana Road, Delhi-110042, India
*E-mail: *dr.rajeshmits@gmail.com*

Abstract—*The development of solar thermal power generation has been implemented in various places of this country. Activities are proposed on research, design and development in the area of solar thermal energy with a view to lead deployment and commercialization of technologies for power generation. Research Development and Design activities developed on various components of solar thermal system viz. heliostats, tracking mechanism, tower structure, receiver and storage medium. Various projects are also aimed at to design and development of large area solar dish for application in decentralized solar thermal power generation in kW-range & design and development of Striling engines for power generation.*

1. INTRODUCTION

India is a endowed with a very vast solar energy potential. Most of the part of the country has good Sunshine about 200-250 days, which is available at 4-6.5 kWh/m^2/day of Direct Normal Irradiance (DNI) [1-4]. When incident solar radiation (i.e. DNI, GHI) is captured and transferred as heat, to perform various useful applications, is called solar thermal energy. It is easy for anyone to comprehend the role of heat from solar energy in our daily life and importance of availability of fuel in the future. Depending on the solar thermal technologies, the temperature output of the thermal energy can be achieved up to 3000 ^{0}C. This temperature opens up a vast area of applications like water /air heating, cooking, drying of agricultural & food products and water distillation. Solar architecture for designing of energy efficient building based on the concepts of solar energy is an important emerging application. The current total installed solar thermal power generation capacity in India is 0.5 GW and occupies forth position in the World [5].

2. DIFFERENT SOLAR THERMAL TECHNOLOGIES FOR POWER GENERATIONS

2.1 Parabolic Trough Collector (PTC)

2.2 Linear Fresnel Reflector (LFR)

2.3 Central Solar Tower

2.4 Solar Dish

2.1 Parabolic Trough Collector (PTC) Technology for Power Generation

Parabolic Trough Collector (PTC) basically focuses the sunlight at receiver (line focusing) to achieve higher temperature up to 400 ^{0}C. PTC focuses the direct radiation coming from the sun and need to be tracked [1-axis for E-W & 2-axis for both E-W and N-S] along with the sun. The solar energy received on the collector surface on the 2-axis tracking is greater [6-7] due to the lower incident angle. However the most of the PTC are 1-axis solar tracking, due to the lower cost and ease installation & maintenance. When the PTC orientation axis is N-S, the annual incident energy received on the collector surface is greater, which results in a higher annual collector efficiency and smaller auxiliary energy requirement [8].Depending on their tracking arrangement; these can be put in the category of high temperature applications. The receiver is normally an evacuated tube series which contains heat transfer fluid. Parabolic troughs using thermal oil are the most advanced among all concentrated solar power (CSP) technologies and considered to be the most economical and high temperature solar thermal technology available today. In these tubes heat transfer fluid is circulated, such as synthetic thermal oil. It is heated up to 400 ^{0}C by the concentrated sun's rays, and pumped through a series of heat exchangers to produce superheated steam.

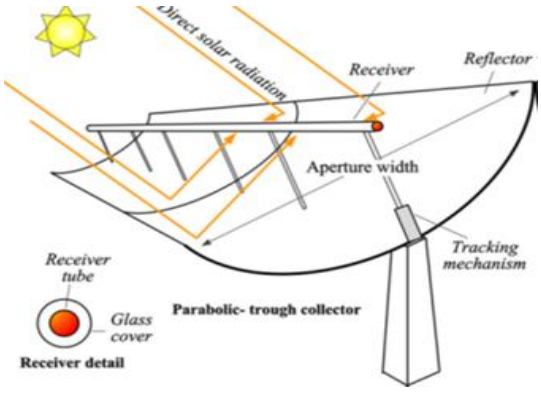


Fig. 2: Schematic of Parabolic Trough Collector

The steam is used to produce electrical energy in a conventional steam turbine power plant. PTC solar technology is the best proven and easy in operation, lowest-cost large scale solar power technology available in India. For other applications like cooling and process heat, some companies have undertaken specific efforts in the development of modular, small, lightweight and low cost PTC.

These developments have allowed a larger number of options of high temperature sources for power generation, fulfilling at the same time basic requirements on costs and maintenance & operation. A 50 MW Parabolic Trough Collectors (PTC) based Solar Thermal Power Plant has been commissioned in Rajasthan [9]. A grid-connected solar thermal power plant, with a capacity of 1 MWe at direct normal iradiance (DNI) radiation of 600 W/m^2, has been designed and commissioned at National Institute of Solar Energy (NISE, formerly solar energy centre), Gurgaon, New Delhi as a part of the project titled 'Development of a Megawatt-scale Solar Thermal Power Testing, Simulation and Research Facility'. The unique feature of the plant is the integration of two different solar fields (parabolic trough collectors and linear Fresnel reflectors) without fossil fuel backup. The plant intends to combine the advantages of synthetic oil based parabolic trough collector (PTC) field and direct steam generation of linear Fresnel reflector (LFR) field.



Fig. 3: MW Solar Thermal Power Plant at National Institute of Solar Energy

The hot oil from PTC field and saturated steam from LFR field are integrated to produce superheated steam at 350°C, 42 bar to run a turbine-generator to produce electricity. It has been designed for generating power for the period of 8 hours in a clear sunny day and having heating storage of the thermic oil for the period of 30 minutes [10]. The power generation of the plant achievedin the month of April and May is 220 MWh/month & 200MWh/monthrespectively as shown in fig.4.

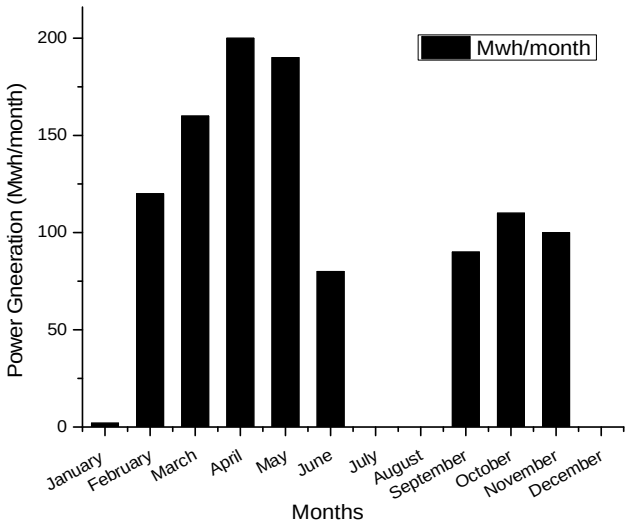


Fig. 4: Monthly Power Generation (MWh/month)

2.2 Linear Fresnel Reflector (LFR) Technology for Power Generation

A Linear Fresnel Reflector (LFR) is a 1-axis tracking technology that focuses sunlight reflected by long heliostats onto a linear receiver to convert solar energy to heat. The classical linear Fresnel system uses an array of mirror strips close to the ground to direct solar radiation to a single, linear, elevated, fixed receiver (Fig.5). The technology is seen as a low cost alternative to trough technology for the production of solar steam for power generation. The main advantages of the Linear Fresnel collector, compared to trough collectors, are seen to low cost [11].



Fig. 5: Linear Fresnel Reflector (LFR)

No need for flexible high pressure joints or thermal expansion bellows due to fixed absorber tube. There is no vacuum technology and no metal-to-glass sealing. The wind loads are substantially reduced on the reflector strips, so the reflector width for one absorber tube can be up to three times the width of parabolic troughs. Due to direct steam generation no heat

exchanger is necessary, although trough technology also is evolving to direct steam generation**.** Efficient use of land since the collectors can be placed close to one another.

2.3 Central Tower Technologie for Power Génération

A 2.75 MW of Solar tower power plant has been installed by ACME in Bikaner, Rajasthan. The turbine pressure and temperature are 60 bar at 440 ^{0}C [12]. World largest heliostatwith an area of 150 m^{2}has been installed at Gurgaon with an aim to set up 1 MW_{th} CSP Central Tower Pilot Facility in India [13].



Fig. 6: Central Tower Receiver implemented at NISE

The main objective of this power plant is to (i) development of optimized design of the heliostat field, volumetric air receiver and thermal storage, the three major components of a Concentrated Solar Power (CSP) Central Receiver plant and (ii) development of local sources for all the key components of the plant with a focus on lowering costs, which will make the technology competitive with other forms of energy.

2.4 Solar DishTechnology for Power Generation

Stirling engine for net 1.5 kWe electrical output has been designed at IIT Bombay. It was observed that the engine ran for 11 seconds with electrical heater furnace as the heat source. The maximum speed observed was about 1000 rpm during trial. The efficiency has been achieved in between 30 – 35%. Another solar Stirlingengine has been developed by ONGC with collaboration of INFINIA Company Ltd. USA installed at NISE for performance evaluation test under Indian climatic conditions. This system has 2-axis tracking, i.e. it tracks the sun according to the time of the day and also according to the time of the year. As a result, it always faces towards the sun and concentrates all the direct solar radiation falling on the aperture.

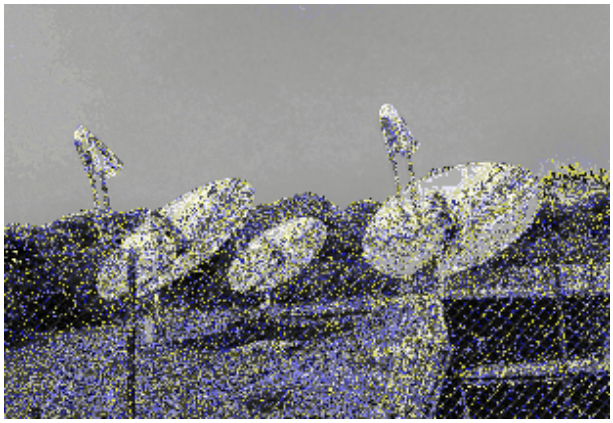


Fig. 7: Dish Concentrators with Stirling Engine

The stirling engine at the receiver point of the dish concentrator is a helium gas engine with ‘free piston’.

3. RESULTS AND DISCUSSIONS

Ministry has launched the Jawaharlal Nehru National Solar Mission to achieve 20,000 MW of solar power and its implementation in 3 phases (Phase-I has up to 2012-13, Phase-II is from 2013-2017 and Phase-III will be from 2017-2022) including grid connected solar power. In Phase-I, JNNSM planned a 500 MW grid connected concentrated solar thermal power, whereas 470 MW Concentrated solar power has been allotted for project in 2012-13.The DNI resources analysis results are reliable indication of the solar potential but the use of other DNI sources are slightly difference in results. This analysis is mainly focus on the CSP power plant. The availability of DNI in different states has been analyzed and it shows that, Gujarat and Rajasthan is having highest amount of DNI energy (19.2 and 18.3 MJ/m2/day) in a year as shown in fig. 8.

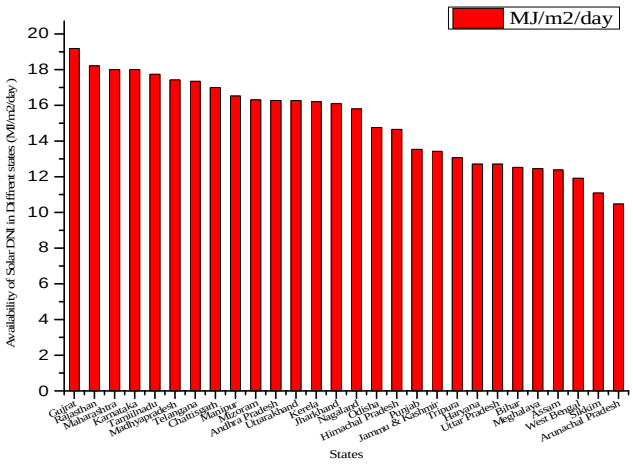


Fig. 8: Availability of yearly average of solar DNI (MJ/m2/day)

The different type of technologies has been used for solar thermal power generation as part of the JNNSM (Phase-II) as shown fig. 9.

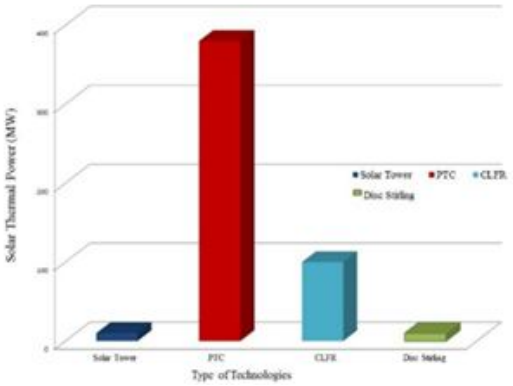


Fig. 9: Installation of Solar Thermal Technologies for Power generation in India

4. CONCLUSION

Taking a view of the trend of accelerated growth of Research & Development and applications of solar thermal technologies in India.Solar thermal power technologies are the most effective technologies to convert solar energy into thermal energy and are considered to be a developed and commercialized technology. However, there exist opportunities to further improve the system performance to increase its reliability and efficiency. The systems have been introduced in the market and are more commonly utilized in the tropical regions of developing countries. Our estimates indicate that, there is a substantial theoretical potential of CO_2 emissions reduction by the use of solar thermal technologies in India. The various benefits that grow by using these systems include saving of conventional fuels, reduction in peak load demand of electricity & emissions of carbon dioxide.

REFERENCES

[1] Marketassessment of solar water heating system.,(2011). Ministry of New and RenewableEnergy.

[2] Solar Radiation Energy over India. IndianMeteorologicalDepartment and Ministry of New and RenewableEnergy.,(2008). Govt. ofIndia.

[3] Policy Documents of Jawaharlal Nehru National Solar Mission, phase-II,(2012-13). Ministry of New and RenewableEnergy, India.

[4] Jawaharlal Nehru National Solar Mission phase-I.,(2011-12). Ministry of New and RenewableEnergy, India.

[5] Bakos GC.,(2006).Design and construction of a two-axis Sun tracking system for parabolictrough collector (PTC) efficiencyimprovement. Renewable Energy.31,2411–21.

[6] Mousazadeh H, KeyhaniA, JavadiA, MobliH, AbriniaK,SharifiA.,(2009). A review of principle and suntrackingmethods for maximizingsolarsystemsout-put. Renewable and SustainableEnergy Reviews.13,1800–1818.

[7] Kalogirou SA.,(2002). Parabolictrough collectors for industrialprocessheat in Cyprus. Energy.27, 813–30.

[8] Policy Documents of Jawaharlal Nehru National Solar Mission, phase-I.,(2012-13). Ministry of New and RenewableEnergy, India.

[9] Project Report on 50 kW solar thermal power plant.,(2002).Solar Energy Centre collaboration with The Energy and Research Institute. India.

[10] N.B.Desai, S.Bandyopadhyay, J.K.Nayak, R.Banerjee, S.B.Kedare.,(2014).Simulation of 1 MW Solar Thermal Power Plant. Energy Procedia.57,507-516.

[11] ECOSTAR.,(2005).EuropeanConcentrated Solar Thermal Roadmap Document, European Commission Document No. SES6- CT-2003-502578.

[12] eSolar Solar Thermal Projects, Bikaner. <http://www.esolar.com/projects/bikaner/>

[13] Development of modular central receiver CSP plant.,(2013-14). SunbornEnergyAnnual report. Ministry of New and RenewableEnergy, Govt. ofIndia.

AIP Advances

Stress induced enhanced polarization in multilayer BiFeO3/BaTiO3 structure with improved energy storage properties

Savita Sharma, Monika Tomar, Ashok Kumar, Nitin K. Puri, and Vinay Gupta

Citation: AIP Advances **5**, 107216 (2015); doi: 10.1063/1.4934578
View online: http://dx.doi.org/10.1063/1.4934578
View Table of Contents: http://scitation.aip.org/content/aip/journal/adva/5/10?ver=pdfcov
Published by the AIP Publishing

Articles you may be interested in

Electrostrictive and relaxor ferroelectric behavior in BiAlO3-modified BaTiO3 lead-free ceramics
J. Appl. Phys. **113**, 094102 (2013); 10.1063/1.4794022

Improved electrical properties of PbZrTiO3/BiFeO3 multilayers with ZnO buffer layer
J. Appl. Phys. **112**, 084101 (2012); 10.1063/1.4759123

Domain fragmentation during cyclic fatigue in 94%(Bi1/2Na1/2)TiO3-6%BaTiO3
J. Appl. Phys. **112**, 044101 (2012); 10.1063/1.4745900

Phase transitions and ferroelectric properties in BiScO 3 -Bi (Zn 1／2 Ti 1／2) O 3 -BaTiO 3 solid solutions
J. Appl. Phys. **102**, 044103 (2007); 10.1063/1.2769787

Crystallization and Properties of PbO -doped Ba 0.7 Sr 0.3 TiO 3 Films
J. Appl. Phys. **96**, 3417 (2004); 10.1063/1.1778220



All article content, except where otherwise noted, is licensed under a Creative Commons Attribution 3.0 Unported license. See: http://creativecommons.org/licenses/by/3.0/ Downloaded to IP: 14.139.251.107 On: Mon, 26 Oct 2015 04:38:16

AIP ADVANCES **5**, 107216 (2015)

Stress induced enhanced polarization in multilayer $BiFeO_3/BaTiO_3$ structure with improved energy storage properties

Savita Sharma,[1,3] Monika Tomar,[2] Ashok Kumar,[4] Nitin K. Puri,[3] and Vinay Gupta[1,a]

[1]*Department of Physics and Astrophysics, University of Delhi, Delhi, India*
[2]*Physics Department, Miranda House, University of Delhi, Delhi, India*
[3]*Department of Applied Physics, Delhi Technological University, Delhi, India*
[4]*CSIR-National Physical Laboratory, Dr. K.S .Krishnan Marg, Delhi, India*

(Received 28 August 2015; accepted 12 October 2015; published online 20 October 2015)

Present work reports the fabrication of a multilayer (5-layer) structure of $BiFeO_3$(BFO)/$BaTiO_3$(BTO) using spin-coating technique. The crystallographic structure, surface morphology and ferroelectric behavior of multilayer structure in metal-ferroelectric-metal capacitor have been studied. Le-Bail refinement of X-ray diffraction data revealed the formation of polycrystalline pure perovskite phase with induced stress. The values of remnant (P_r) and saturation polarization (P_s) for BFO/BTO multilayer structure are found to be 38.14 $\mu C/cm^2$ and 71.54 $\mu C/cm^2$ respectively, which are much higher than the corresponding values reported for bare BFO thin film. A large value of dielectric constant of 187 has been obtained for multilayer structure with a low leakage current density of 1.09×10^{-7} A/cm^2 at applied bias of 10 V. The BFO/BTO multilayer structure favors the enhanced energy storage capacity as compared to bare BFO thin film with improved values of energy-density and charge-discharge efficiency as 121 mJ/cm^3 and 59% respectively, suggesting futuristic energy storage applications. © *2015 Author(s). All article content, except where otherwise noted, is licensed under a Creative Commons Attribution 3.0 Unported License.* [http://dx.doi.org/10.1063/1.4934578]

INTRODUCTION

The atomic scale combination of dissimilar materials is expected to produce not only striking control but also ample scope of enhancement in new combinations of functional properties. In recent years, novel multilayers comprising of different ferroelectric/multiferroic materials have been intensively studied to find better system with superior electrical and ferroelectric properties having strong coupling and interaction among its layers.[1–4] The interfacial strain due to the lattice mismatch can lead to modulation of ferromagnetic anisotropy and improvement in electrical properties. Also, the ferroelectric switching affects the interface magnetization due to the change in collection of spin-polarized electrons at the ferromagnetic/ferroelectric (FM/FE) interface, as was discussed by many workers for $Fe/BaTiO_3$,[5] $Co_2MnSi/BaTiO_3$[6] and $Fe_3O_4/BaTiO_3$[7] hetrostructures. Reddy *et al*. reported improved ferroelectric as well as ferromagnetic properties for four-layered thin films over two-layered BLFCO-BFO thin films due to the interface coupling and interaction between the thin layers.[8] Pintilie *et al*. studied the capacitance of PZO–PZT (80/20) multilayers with enhanced polarization with increase in number of interfaces due to the presence of some interfacial polarization, trapped charges at the multilayer interfaces.[9] Lee *et al*. studied the enhancement of polarization by strain in superlattices of $BaTiO_3$, $SrTiO_3$ and $CaTiO_3$.[10] Wu *et al*. observed the high saturation polarization in a $(BaTiO_3)_8/(SrTiO_3)_3$ superlattice film.[11] Bao discussed that constructing multilayers or superlattices is an effective way to improve properties of ferroelectric/dielectric thin films.[12]

[a]Email: vgupta@physics.du.ac.in, drguptavinay@gmail.com

 © Author(s) 2015

All article content, except where otherwise noted, is licensed under a Creative Commons Attribution 3.0 Unported license. See: http://creativecommons.org/licenses/by/3.0/ Downloaded to IP: 14.139.251.107 On: Mon, 26 Oct 2015 04:38:16

Such systems can be effectively combined for the high density ferroelectric random access memory (FE-RAM) and energy storage devices.

Due to the marked improvement in integration of modern electric system, there are great needs for systems which can harness energy from natural sources i.e. implicit self-powered energy storage devices for "green" energy capable of producing both high power and high energy density which can replace batteries to power the microelectronic devices like health monitoring systems, wireless sensors, mobile communication systems etc.[13,14] Two important aspects of energy storage devices are high energy density i.e. capability of storing energy per unit volume or mass and high power density i.e. capability of discharging the stored energy quickly to the external load. Our area of interest focuses on these two aspects although it is difficult to obtain both at the same time.[13] Besides this, low dielectric loss and economic cost are the other important factors to pay attention to. The $BaTiO_3$, $PbTiO_3$ and $CaCuTiO_3$ with large dielectric permittivity are generally employed in energy storage applications, however, due to their low electrical breakdown strength, these ceramic materials exhibit poor energy storage properties.[15]

Among various multiferroic materials, BFO has captivated most of the researchers owing to the existence of two ferroic orders simultaneously at room temperature with a Curie temperature (T_C) of 1103 K and Neel temperature (T_N) of 643 K which enables it to be used for high temperature applications.[16–19] However, the device applications of BFO are mainly hindered due to the high leakage current resulting in poor ferroelectric properties.[16] These problems can also be overcome by combining two or more ferroelectric materials with multiferroic materials retaining the excellent room temperature ferromagnetism in BFO. The resultant structure may yield superior properties compared to the individual constituent materials enabling it to be used for device applications. Recent studies on BFO have confirmed the existence of large magnetization and ferroelectric polarization in strained thin films. Few workers reported improvement in the electric and magnetic properties, as well as a large magnetoelectric coupling in the hetrostructure of BFO such as $La_{0.7}Sr_{0.3}MnO_3$ (LSMO)/BFO, Fe_2O_4/BFO, CoFe/BFO, Co/BFO, Ni/BFO and $BiTiO_3$/BFO, due to the interface coupling interaction between the individual layers.[20–22] The BTO is a potential ferroelectric material which has been used widely from the last many decades in device applications.[23–25] On the contrary, BTO does not possess ferromagnetic properties. Hence, combining the two ferroic materials i.e. BTO and BFO might give rise to better multiferroic properties.[26–28] Some research groups have studied BFO/BTO multilayered structures, but their strain induced polarization and energy storage properties are scarcely reported.[29] Touplet *et al.* and Yang *et al.*[30,31] reported an improvement in the magnetic property of the BFO/BTO multilayered system due to the interfacial effects and the multiferroic coupling between them.

Film deposition process are also known to affect the properties of deposited thin films or layered structures. Sol-gel spin coating method is known to be the simplest and cost effective for the deposition of BTO and BFO thin films while maintaining appropriate stoichiometry. Hence, in the present work, an effort has been made to prepare a multilayered (five-layer) structure of BFO/BTO on Pt/Ti/SiO_2/Si substrate using sol-gel spin coating method with the improved electrical property.

EXPERIMENTAL

The multilayered structure of BFO/BTO is deposited on platinized silicon (Pt/Ti/SiO_2/Si) substrates using sol-gel spin coating technique. Prior to the deposition of BFO/BTO multilayer structure, the thin film of Pt (70 nm thickness) was deposited over the passivated Si (SiO_2/Si) substrate by E-beam evaporation technique. A buffer layer of Ti (20 nm) was deposited *in-situ* over SiO_2/Si substrate prior to Pt deposition to improve its adhesion. The precursors for the synthesis of BTO and BFO were barium acetate ($Ba(CH_3COO)_2$), bismuth nitrate (($Bi(NO_3)_3.5H_2O$), iron nitrate (($Fe(NO_3)_3.9H_2O$), titanium n-butoxide ($Ti(C_4H_9O)_4$). Acetic acid and 2-methoxyethanol were used as solvents and acetylacetone was used as the chelating agent. The BTO thin film was deposited on Pt coated Si substrate as a first layer by spin coating technique and was annealed at 800°C for one hour. It was followed by the deposition of BFO thin film as second layer with annealing at 550°C for two hours to get BFO/BTO structure. Similar process was repeated to get five layered structure namely BTO/BFO/BTO/BFO/BTO on Pt/Ti/SiO_2/Si substrate with total thickness

All article content, except where otherwise noted, is licensed under a Creative Commons Attribution 3.0 Unported license. See: http://creativecommons.org/licenses/by/3.0/ Downloaded to IP: 14.139.251.107 On: Mon, 26 Oct 2015 04:38:16

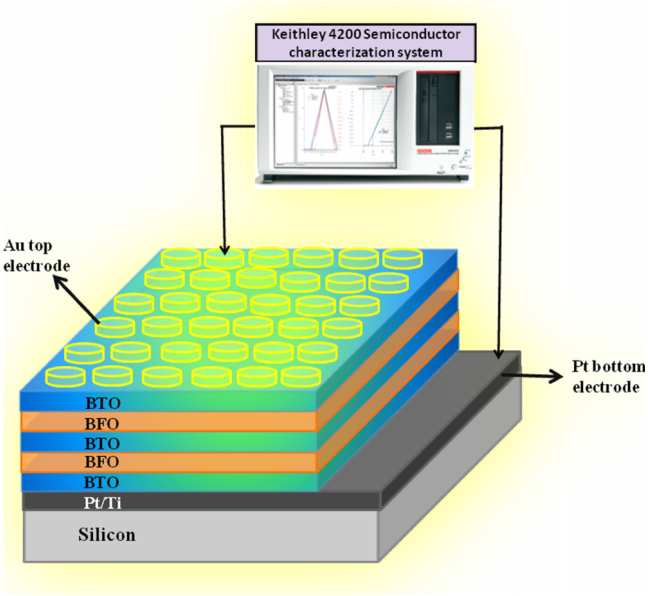


FIG. 1. Schematic of the MFM capacitor configuration of the BFO/BTO multilayer structure deposited on Pt/Ti/SiO_2/Si substrate with Au top electrodes.

of 350 nm, the average thickness of each layer being ~70 nm. For electrical measurements, circular top electrodes of Au metal (200 μm diameter, 40 nm thickness) were deposited on the BFO/BTO surface by thermal evaporation technique through a shadow mask. The schematic of prepared metal-ferroelectric-metal (MFM) capacitor configuration (Au/BTO/BFO/BTO/BFO/BTO/Pt/SiO_2/Si) is shown in figure 1.

X-ray diffraction (XRD) technique (Bruker D8) was used to study the crystalline structure of the BFO/BTO bilayer structure. The surface morphology of multilayer structure was studied using scanning electron microscopy (SEM) (FEI Quanta 200 F). A Radiant Technology precision ferroelectric workstation was used to measure the room temperature ferroelectric polarization-electric field (P-E) hysteresis loop of the prepared multilayer sample in MFM capacitor configuration at a frequency of 1 kHz and applied bias of 10 V. The current-voltage (I-V) and capacitance-voltage (C-V) characteristics of prepared sample were studied using a semiconductor characterization system (Keithley; 4200 SCS) at room temperature.

RESULTS AND DISCUSSION

Figure 2(a) shows the XRD pattern of the prepared multilayer (BFO/BTO) structure on Pt/Ti/SiO_2/Si substrate. The diffraction peaks corresponding to constituent BFO and BTO were obtained which confirm the growth of multilayer structure of BTO and BFO films of polycrystalline nature. However, no peak exhibiting the formation of any secondary phase in the prepared multilayer structure was obtained. The polycrystalline nature of deposited rhombohedral distorted structure of BFO and tetragonal structure of BTO is clearly evident from Fig. 2(b). Lattice parameters "a" and "c" and c/a distortion ratio for both BTO and BFO layers in BFO/BTO multilayer structure were determined using the Le-Bail intensity extraction method with the help of commercially available Bruker TOPAS 3 Software. The estimated values of lattice parameters (a, c), the volume of unit cell and the strain induced along 'c' axis for both BFO and BTO thin films in the multilayer structure are summarized in Table I. The corresponding reported values for bulk BFO and BTO are also included in Table I for comparison. The value of lattice parameters, a and c are estimated to be 4.256 Å and 4.079 Å, respectively, for BTO thin film and 5.518 Å and 13.561 Å, respectively, for BFO thin film. The obtained values of lattice parameters for BFO thin film are slightly lower than the corresponding bulk values for BFO but for BTO thin film, the values are greater than that of bulk

All article content, except where otherwise noted, is licensed under a Creative Commons Attribution 3.0 Unported license. See: http://creativecommons.org/licenses/by/3.0/ Downloaded to IP: 14.139.251.107 On: Mon, 26 Oct 2015 04:38:16

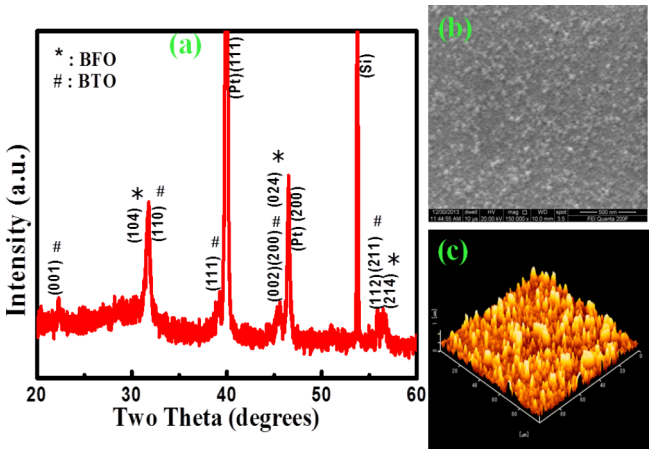


FIG. 2. (a) XRD pattern of BFO/BTO multilayer structure deposited on platinized silicon substrate, (b) SEM image of BFO/BTO multilayer structure (c) A 100 μm X 100 μm AFM image of the surface of BFO/BTO multilayer structure.

BTO [JCPDS card No. 01-072-0138 and 01-072-2035]. The results obtained indicate the presence of tensile stress and compressive stress in the BFO and BTO thin films in multilayer structure. The value of stress modulus (%) for BTO and BFO thin films is found to be about 1.1405% and 2.206%, respectively. The large value of stress modulus in BFO thin film is responsible for the increase in the lattice distortion which leads to an improvement in ferroelectric property of the multilayer structure. Fig. 2(b) shows the SEM micrograph of the surface of BFO/BTO multilayer structure. It can be clearly seen from Fig 2(b) that the prepared multilayer structure has a dense and smooth surface with uniformly distributed grains of ~40 nm size. The AFM image of the surface of prepared BFO/BTO multilayer structure is shown in Fig. 2(c). The homogeneous distribution of grains of ~40 nm size is seen on the surface of BFO thin film (Fig. 2(c)), which is in agreement with the SEM micrograph. The root mean square (RMS) value of the roughness (R_a) of the surface of multilayer structure lies between 10 and 15 nm (Fig. 2(c)).

Fig. 3 shows the semi-log plot of current versus voltage (I-V) for the multilayer structure of BFO/BTO and bare BFO thin film recorded with both polarities of the applied voltage at room temperature. Both the I-V curves exhibit good symmetry under both applied positive and negative bias in terms of the absence of any barrier at the electrode and the presence of ohmic contacts. However, a significant difference in the leakage current density for multilayer is observed in comparison to that of bare BFO film. Leakage current (1.09 x 10^{-7} A) of multilayer BFO/BTO structure was found to be two order less in comparison to that of bare BFO thin film (1.10 x 10^{-5} A) with an applied voltage of 10 V. The obtained results show significant reduction in the leakage current density with fabrication of artificial multilayer. The presence of ferroelectric BTO layer helps in reducing the leakage current by two orders of magnitude which is desirable for functional device applications. The reduced leakage current in multilayer structure is due to the blocking of ions migration by resistive ferroelectric BTO layers and the presence of trap centers of carriers formed

TABLE I. Lattice parameters "a" and "c", c/a distortion ratio and stress modulus along c-axis for the BTO and BFO thin films in BFO/BTO multilayer structure.

	BTO thin film				**BFO thin film**			
	Lattice parameter		**Stress**	**c/a distortion**	**Lattice parameter**		**Stress**	**c/a distortion**
	a (Å)	**c (Å)**	**Modulus (%)**	**ratio**	**a (Å)**	**c (Å)**	**Modulus (%)**	**ratio**
Bulk	3.999	4.033	—	1.0085	5.876	13.867	—	2.3599
Multilayer	4.256	4.079	1.1405	0.9584	5.518	13.561	2.206	2.4575

All article content, except where otherwise noted, is licensed under a Creative Commons Attribution 3.0 Unported license. See: http://creativecommons.org/licenses/by/3.0/ Downloaded to IP: 14.139.251.107 On: Mon, 26 Oct 2015 04:38:16

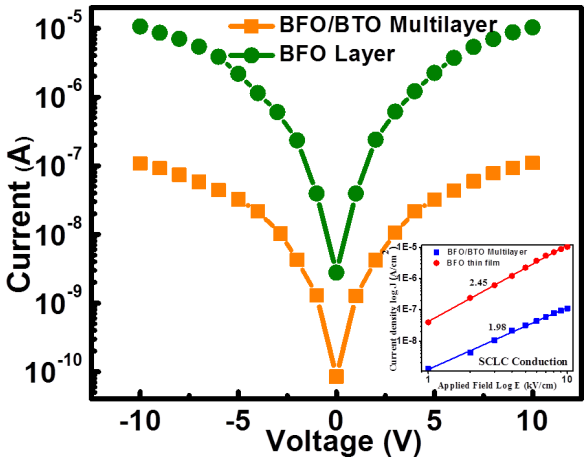


FIG. 3. I-V characteristics of BFO/BTO multilayer structure and bare BFO thin film. Inset shows the variation in leakage current density as a function of electric field fitted with SCLC mechanism.

at the interfaces between BFO and BTO films. Also, the surface roughness might result in the decrease of the leakage current. Jo *et al.* and Xu *et al.* reported the superior electrical and ferroelectric properties in the case of PZT/BFO and $BaSrTi_{1.1}O_3/BaSrTi_{1.05}O_3/BaSrTiO_3$ multilayer thin films, respectively.[32,33] It may be recalled that the bare BFO thin film has a high leakage current when grown on the Pt-coated Si substrate. Further, BFO/BTO multilayer system exhibits a stable insulating behaviour over the entire measured range of applied voltage. Inset of figure 4 represents the log–log plot of J–E which exhibits linear behaviour over the entire voltage range for pure BFO thin film as well as BFO/BTO multilayer structure. The slope of the straight line is found to be 2.45 and 1.98, respectively, confirming trap assisted SCLC behavior. Hence, it may be inferred that the leakage current in BFO and BFO/BTO multilayer thin films exhibits trap-controlled SCLC transport at applied electric fields.

Figure 4 shows the capacitance-voltage (C-V) characteristics for the BFO/BTO multilayer system in MFM capacitor configuration. Inset (a) of Fig. 5 shows the dielectric vs. voltage curve measured for BFO/BTO multilayer system while inset (b) shows the capacitance-voltage (C-V) characteristics of bare BFO thin film for the comparison. The observed characteristic butterfly loop (Fig. 5) confirms the good ferroelectric property of the prepared BFO/BTO multilayer structure.

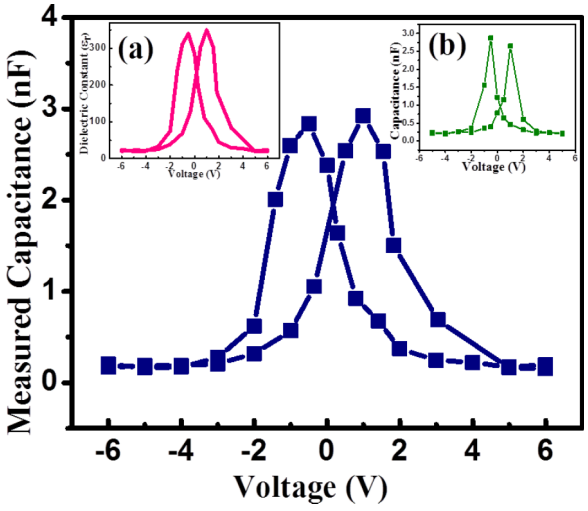


FIG. 4. C-V characteristics of BFO/BTO multilayer structure. Inset (a) shows the dielectric vs. voltage curve measured for BFO/BTO multilayer system while inset (b) shows the capacitance-voltage (C-V) characteristics of bare BFO thin film for the comparison.

All article content, except where otherwise noted, is licensed under a Creative Commons Attribution 3.0 Unported license. See: http://creativecommons.org/licenses/by/3.0/ Downloaded to IP: 14.139.251.107 On: Mon, 26 Oct 2015 04:38:16

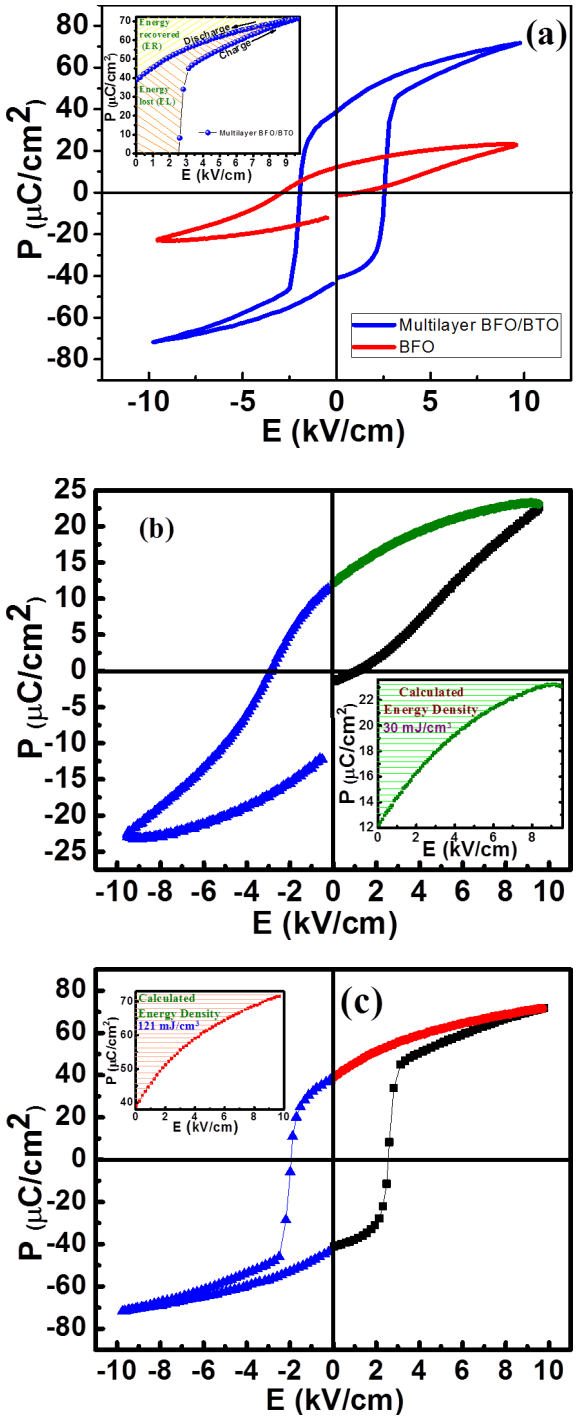


FIG. 5. (a) Room temperature ferroelectric (P-E) hysteresis curves of BFO/BTO multilayer structure and bare BFO thin film. Inset of (a) Yellow Shaded area of P–E loop illustrates the capacity to store (recoverable) energy and orange shaded area the energy loss. (b) and (c): Room temperature ferroelectric P-E hysteresis loop of the BFO thin film and BFO/BTO multilayer structure respectively, along with inset representing the stored energy density (shaded area shown) corresponding to PE loops.

The two peaks at applied bias of +1 V and -0.6 V in the C-V curve (Fig. 5) reveal the polarization reversal of the ferroelectric domains in the multilayer system. Further it can be seen from Fig 5 that the capacitance tends to a constant value C_o with increase in the magnitude of applied bias. The capacitance can be written as $C_o = \varepsilon_o.\varepsilon_r.S/d$, where ε_o is the permittivity of vaccum

All article content, except where otherwise noted, is licensed under a Creative Commons Attribution 3.0 Unported license. See: http://creativecommons.org/licenses/by/3.0/ Downloaded to IP: 14.139.251.107 On: Mon, 26 Oct 2015 04:38:16

TABLE II. Ferroelectric properties, Leakage current and Energy density of BFO/BTO multilayer structure and single layered BFO thin film.

	$P_r(\mu C/cm^2)$	$P_s(\mu C/cm^2)$	$2E_c$ (kV/cm)	Leakage current (A)	U_{ER} (mJ/cm^3)	U_{EL} (mJ/cm^3)	U_{ET} (mJ/cm^3)	η(%)
BFO	12.52	23.24	4.08	1.10×10^{-5}	30	105	135	22
Multilayer BFO/BTO	38.14	71.54	4.53	1.09×10^{-7}	121	84	205	59

(8.85×10^{-12} F/m); ε_r is the relative dielectric constant of BFO/BTO multilayer; S is the electrode area (3.14×10^{-8} m^2) and d is the thickness of the multilayer system (350 nm). Considering the value of C_o as 0.15 nF at ±6 V (Fig. 5), the estimated value of ε_r for BFO/BTO multilayer system is about 187, which is higher than the corresponding reported value of the dielectric constant for bare BTO or BFO thin film.[34,35] The obtained results clearly highlight the importance of combining BTO and BFO thin films. The combination of both layers enhances the coupling between the ferroelectric and ferromagnetic domains that lead to a net high polarization for the BFO/BTO multilayer structure.

Figure 5(a) shows the room temperature ferroelectric (P-E) hysteresis curves of BFO/BTO multilayer structure and bare BFO thin film at 1 KHz over an applied bias range from -10 V to +10 V. The yellow shaded area in the inset of fig. 5(a) illustrates the energy storage capacity (recoverable energy), whereas the orange shaded portion reflects the energy loss. It may be seen from Fig. 5(a) that the ferroelectric property of the multilayer structure is enhanced in comparison to the bare BFO thin film. The obtained values of remnant polarization (P_r), saturation polarization (P_s) and coercive field (E_c) for the multilayer structure along with that of bare BFO thin film are summarized in Table II. The BFO/BTO multilayer system exhibits the maximum saturation polarization (P_s) of about 71.54 $\mu C/cm^2$ and remnant polarization (P_r) of 38.14 $\mu C/cm^2$ (Fig. 5(a)). The enhanced ferroelectric property of the BFO/BTO multilayer structure may be related to the induced strain at the interface of two layers and large lattice distortion (c/a ratio).

Energy storage capacity of BFO/BTO multilayer system is estimated from the P-E hysteresis loop.[36] Fig. 5(b) and 5(c) shows the room temperature ferroelectric P-E hysteresis loop of BFO and BFO/BTO multilayer structure, respectively. The shaded area shown in the inset corresponds to the stored energy density (recoverable energy). The green shaded area in the inset of Fig. 5(b) represents the energy density recovered (ER) and the red shaded area inside the loop in the inset of Fig. 5(c) represents the energy loss (EL). The sum of ER and EL represents the total energy density (ET) stored in the material. The charge–discharge efficiency η can then be calculated by $\eta = (U_{ER}/U_{ET}) \times 100\%$.[15] All the calculated values of energy density and efficiency for BFO/BTO multilayer structure and bare BFO thin film have been tabulated in Table II. To minimize the size and weight of capacitors, thin films with high recoverable energy density (U_{ER}) and high charge-discharge efficiency (η) are required. The U_{ER} value for BFO thin film structure was found to be ~30 mJ/cm^3 with an energy loss of 105 mJ/cm^3, while for BFO/BTO multilayer structure, the enhanced U_{ER} value of 121 mJ/cm^3 was obtained with reduced energy loss of 84 mJ/cm^3 (Table II). The η value of BFO thin film was 22% while it is greatly enhanced in the case of BFO/BTO multilayer structure to 59% (Table II). This enhancement in U_{ER} and η values and the reduction in energy loss observed for BFO/BTO multilayer structure favors its potential usage in energy storage applications.

CONCLUSION

The BFO/BTO multilayer structure was fabricated on $Pt/Ti/SiO_2/Si$ substrate by sol-gel spin coating technique. X-ray diffraction studies reveal the formation of polycrystalline and pure phase of perovskite structure for both BTO and BFO. Electrical study of the multilayer structure indicates an enhancement in ferroelectric properties (P_s = 71.54 $\mu C/cm^2$ and P_r = 38.14 $\mu C/cm^2$) and reduction in leakage current by two orders (1.09×10^{-7} A) in comparison to that of bare BFO

All article content, except where otherwise noted, is licensed under a Creative Commons Attribution 3.0 Unported license. See: http://creativecommons.org/licenses/by/3.0/ Downloaded to IP: 14.139.251.107 On: Mon, 26 Oct 2015 04:38:16

film. The improved electrical properties of the multilayer system is related to the coupling between the ferroelectric and ferromagnetic domains of BTO and BFO, respectively, that lead to an enhancement in polarization in the multilayer structure. Low leakage current (0.1 μA) and improved energy density (121 mJ/cm^3) with high charge-discharge efficiency (59%) obtained for BFO/BTO multilayer structure suggests its futuristic energy storage applications.

ACKNOWLEDGEMENT

Authors are thankful to Department of Science and Technology (DST), University of Delhi and Delhi Technological University (DTU) for providing all the facilities to carry out the research work.

[1] R. Nechache, P. Gupta, C. Harnagea, and A. Pignolet, Appl. Phys. Lett. **91**, 222908 (2007).
[2] N. Ichikawa, M. Arai, Y. Imai, K. Hagiwara, H. Sakama, M. Azuma, Y. Shimakawa, M. Takano, Y. Kotaka, M. Yonetani, H. Fujisawa, M. Shimizu, K. Ishikawa, and Y. Cho, Appl. Phys. Exp. **1**, 101302 (2008).
[3] H. C. Ding, Y. W. Li, W. Zhu, Y. C. Gao, S. J. Gong, and C. G. Duan, J. Appl. Phys. **113**, 123703 (2013).
[4] M. Dawber, N. Stucki, C. Lichtensteiger, S. Gariglio, P. Ghosez, and J. M. Triscone, Adv. Mater. **19**, 4153–4159 (2007).
[5] S. Valencia, A. Crassous, L. Bocher, V. Garcia, X. Moya, R. O. Cherifi, C. Deranlot, K. Bouzehouane, S. Fusil, A. Zobelli, A. Gloter, N. D. Mathur, A. Gaupp, R. Abrudan, F. Radu, and A. Barthélémy, Nature Materials **10**, 753 DOI: 10.1038/nmat3098 (2011).
[6] L. Y. Chen, C. L. Chen, K. X. Jin, and X. J. Du, EPL **99**, 57008 DOI: 10.1209/0295-5075/99/57008 (2012).
[7] T. L. Qu, Y. G. Zhao, P. Yu, H. C. Zhao, S. Zhang, and L. F. Yang, Appl. Phys. Lett. **100**, 242410 DOI: 10.1063/1.4729408 (2012).
[8] V. A. Reddy, N. Dabra, K. K. Ashish, J. S. Hundal, N. P. Pathak, and R. Nath, Adv. Mater. Lett. **6**(8), 678–683 (2015).
[9] L. Pintilie, K. Boldyreva, M. Alexe, and D. Hesse, New Journal of Physics **10**, 013003 (2008).
[10] H. N. Lee, H. M. Christen, M. F. Chisholm, C. M. Rouleau, and D. H. Lowndes, Nature **433**, 27 (2005).
[11] P. Wu, X. Ma, Y. Li, V. Gopalan, and L. Q. Chen, Appl. Phys. Lett. **100**, 092905 (2012).
[12] D. Bao, Current opinion in solid state and material science **12**, 55–61 (2008).
[13] C. A. Paz de Araujo, J. D. Cuchiaro, L. D. Mcmillan, M. C. Scott, and J. F. Scott, Nature **374**, 627 (1994).
[14] S. A. Sherrill, P. Banerjee, G. W. Rubloff, and S. B. Lee, Phys. Chem. Chem. Phys. **13**, 20714 (2011).
[15] Z. Hu, B. Ma, S. Liu, M. Narayanan, and U. Balachandran, Ceram. Int. **40**, 557–562 (2014).
[16] J. F. Ihlefeld, N. J. Podraza, Z. K. Liu, R. C. Rai, X. Xu, T. Heeg, Y. B. Chen, J. Li, R. W. Collins, J. L. Musfeldt, X. Q. Pan, J. Schubert, R. Ramesh, and D. G. Schlom, Appl. Phys. Lett. **92**, 142908 (2008).
[17] S. Gupta, M. Tomar, and V. Gupta, J. Exp. Nanosci. **8**(3), 261 (2013).
[18] H.W. Chang, F.T. Yuan, Y.C. Yu, P.C. Chen, C.R. Wang, C.S. Tu, and S.U. Jen, J. Alloys Compd. **574**, 402 (2013).
[19] K. Jiang, J. J. Zhu, J. D. Wu, J. Sun, Z. G. Hu, and J. H. Chu, Appl. Mater. Interf. **3**, 4844 (2011).
[20] Q. Xu, Z. Wen, J. Gao, D. Wu, S. Tang, and M. Xu, Physica B **406**, 2025 DOI : 0.1016/j.physb.2011.03.011 (2011).
[21] H. Singh, A. Kumar, and K. L. Yadav, Mat. Sci. Eng. B **176**, 540 DOI: 10.1016/j.mseb.2011.01.010 (2011).
[22] V. A. Reddy, N. Dabra, J. S. Hundal, N. P. Pathak, and R. Nath, Science of Advanced Materials **6**, 1043 (2014).
[23] I. Kingon, J. P. Maria, and S. K. Streiffer, Nature **406**, 1032 (2000).
[24] K. J. Choi, M. Biegalski, Y. L. Li, A. Sharan, J. Schubert, R. Uecker, P. Rerche, Y. B. Chen, X. Q. Pan, V. Gopalan, L. Q. Chen, D. G. Schlom, and C. B. Eom, Science **306**, 1005 (2004).
[25] V. Vaithyanathan, J. Lettieri, W. Tian, A. Sharan, A. Vasudevarao, Y. L. Li, A. Kochhar, H. Ma, J. Levy, P. Zschack, J. C. Woicik, L. Q. Chen, V. Gopalan, and D. G. Schlom, J. Appl. Phys. **106**, 024108 (2009).
[26] S. Sharma, M. Tomar, A. Kumar, N. K. Puri, and V. Gupta, Physica B **448**, 125–127 (2014).
[27] S. Sharma, M. Tomar, A. Kumar, N. K. Puri, and V. Gupta, Adv. Sci. Lett. **20**, 1316–1320 (2014).
[28] M. Kumar, A. Srinivas, and S.V. Suryanarayana, J. Appl. Phys. **87**(2), 855 (2000).
[29] M. Lorenz, V. Lazenka, P. Schwinkendorf, F. Bern, M. Ziese, H. Modarresi, A. Volodin, M. J. V. Bael, K. Temst, A. Vantomme, and M. Grundmann, J. Phys. D: Appl. Phys **47**, 135303 (2014).
[30] H. Toupet, V. V. Shvartsman, F. Lemarrec, P. Borisov, W. Kleemann, and M. Karkut, Integ. Ferroelectrics **100**, 165–176 (2008).
[31] P. Yang, K. M. Kim, J. Y. Lee, J. Zhu, and H. Y. Lee, Integrated Ferroelectrics **113**, 26–30 (2009).
[32] Z. Xu, D. Yan, D. Xiao, P. Yu, and J. Zhu, Ceramics International **39**, 1639–1643 (2013).
[33] S. H. Jo, S. G. Lee, and S. H. Lee, Materials Research Bulletin **47**, 409–412 (2012).
[34] D. Huang, H. Deng, P. Yang, and Junhao Chu, Mater. Lett. **64**, 2233–2235 (2010).
[35] R. R. Das, Y. I. Yuzyuk, P. Bhattacharya, V. Gupta, and R. S. Katiyar, Phys. Rev. B **69**, 132302 (2004).
[36] H. Borkar, V. N. Singh, B. P. Singh, M. Tomar, V. Gupta, and A. Kumar, RSC Adv. **4**, 22840 (2014).

All article content, except where otherwise noted, is licensed under a Creative Commons Attribution 3.0 Unported license. See: http://creativecommons.org/licenses/by/3.0/ Downloaded to IP: 14.139.251.107 On: Mon, 26 Oct 2015 04:38:16

Journal of Material Science and Mechanical Engineering (JMSME)
Print ISSN: 2393-9095; Online ISSN: 2393-9109; Volume 1, Number 2; October-December, 2014 pp. 94-97
© Krishi Sanskriti Publications
http://www.krishisanskriti.org/jmsme.html

Study of Automobile Exhaust Emissions

Kshitij Aggarwal[1] and Mridul Garg[2]

[1,2]B.Tech (Delhi Technological University)
E-mail: [1]kshitijagg@hotmail.com, [2]mridulgarg11@gmail.com

Abstract: *On account of more stringent regulations being imposed on the automotive industry to mitigate exhaust emissions to curb the problem of pollution and global warming worldwide, extensive research is being conducted to study the effect of various combustion parameters on exhaust emission gases. This paper deals with a comprehensive study of the various factors that affect exhaust emissions. The effect of compression ratio, ignition timing, exhaust gas recovery (EGR) and engine load is studied on the major exhaust emission gases, namely NOx, CO, CO2 and Hydrocarbons (HC). Extensive studies have been carried out by reviewing the work of other scholars and analyzing their observations to come up with a general trend on how exhaust emissions are affected. It is observed that increase in compression ratio leads to an increase in amount of NOx and HC emissions whereas the amount of CO and CO2 emissions increase till the best compression ratio after which they gradually decrease. Advancing ignition timing has no effect on CO and CO2 emissions but leads to an increase in NOx levels and installing EGR leads to reduction in NOx and CO2 levels but an increase in CO levels on account of lower charge temperature and greater availability of O2. Also increasing the load leads to increased levels for almost all the exhaust emissions on account of higher combustion rates.*

1. EMISSIONS

NOx

Experiments carried out on a PCCI engine running on diesel demonstrated that under premixed combustion, NOx emissions were only mildly reduced when compression ratio was reduced from 18.4:1 to 16.0:1 within the SOI timing range of 5°BTDC to 3°ATDC. The reductions in NOx can be explained by the retardation in Injection Delay which leads to a reduction in the gas temperature at TDC of the compression stroke and more complete mixing of air and fuel mixture.

Fig. 1 shows the variation of NOx with the compression ratios for diesel and WCO blends [1] at best injection timing. In general NOx emission increases with the increase in load and also for higher compression ratios the NOx emission was increased because of increased operating temperature. NOx emissions for the biodiesel operation are higher than the neat diesel, since the biodiesel contained the inbuilt oxygen in their molecular structure.

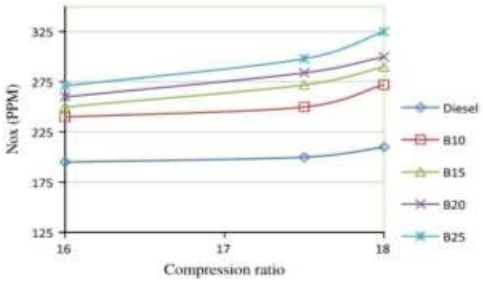


Fig. 1: Variation of NOx with the compression ratios for diesel and biodiesel blends at best injection timing (27°).

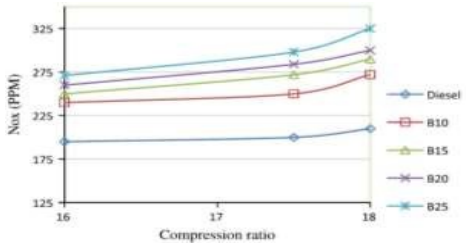


Fig. 2 shows the variation of NOx with the injection timings [2] at full load condition for best compression ratio for different diesel and biodiesel blends. For the retarded injection timings NOx emissions were found to be less whereas for advanced injection timings it increased.Fig. 2. Variation of NOx with injection timing for diesel and biodiesel blends best compression ratio (18°).

EGR effects on combustion and NOx formation Exhaust Gas Recirculation (EGR) is effective in reducing NOx formation since it lowers the peak flame temperature attained during the combustion process. Several effects may contribute to this result when the intake charge is diluted with exhaust gases. These effects are listed below hereafter:

- The dilution or oxygen displacement effect, i.e. the reduction in the oxygen mass fraction due to the displacement of some of the oxygen in the fresh intake air charge by inert gases, which causes a reduction in the local flame temperature because of the spatial broadening of the flame due to the reduction in the oxygen molar fraction.

- The thermal effect, due to the increase in the average specific heat capacity of the gases in the combustion zone, since re-circulated exhaust contains CO_2 and H_2O with higher specific heat than that of air.
- The chemical effect, i.e. the reduction in the combustion temperature due to endothermic chemical reactions, such as the dissociation of CO_2 and H_2O.

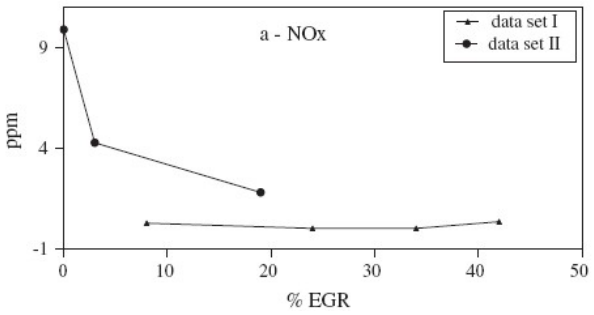


Fig. 3 The influence of EGR on emission characteristics of NOx.

The influence of EGR on exhaust emissions of n-heptane/natural gas fueled HCCI engines [3] and found the same results.

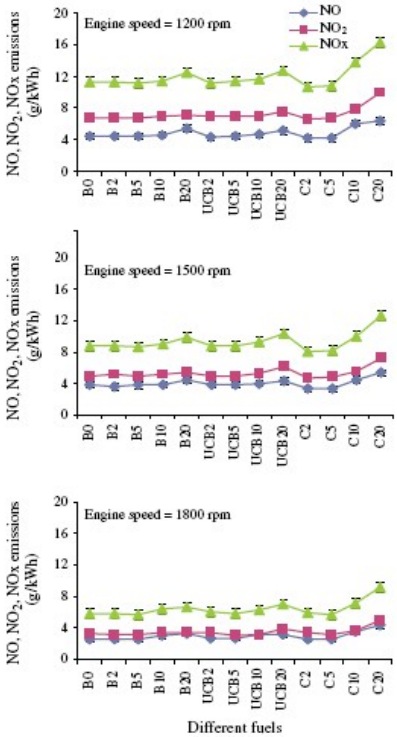


Fig. 4 NOx emissions at different engine speeds for various fuels: (a) with engine speed of 1200 rpm, (b) 1500 rpm, and (c) 1800 rpm.

CO

The results showed that the CO emissions increased drastically at lower loads and decreased slightly at higher loads for the blends compared to diesel fuel. The drastic increase in the CO percentage at low load for blend is due to decrease in the cylinder gas temperature and delayed combustion process. The lower temperature and delayedcombustion would have suppressed the oxidation process even though enough oxygen was available for combustion. Slight reduction in CO emissions is noticed for blends at high load and that would be due to inbuilt fuel oxygen and improved combustion process due to better mixing.

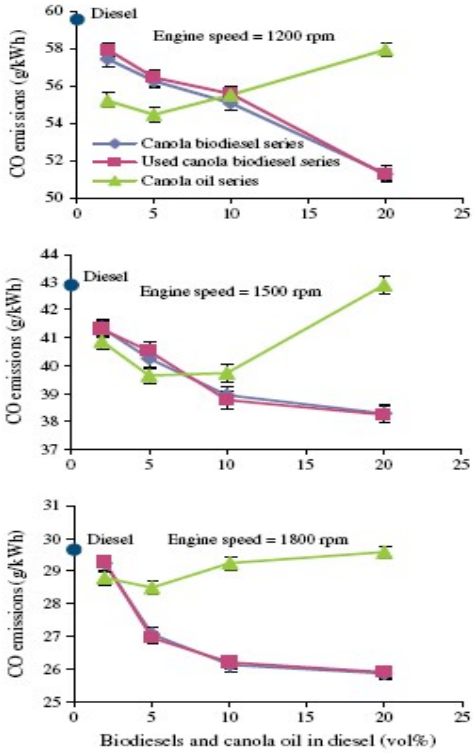


Fig. 5. CO emissions at different engine speeds for various fuels: (a) with engine speed of 1200 rpm, (b) 1500 rpm, and (c) 1800 rpm.

The CO emission remains unchanged with respect to injection timing for blends as well diesel fuel at both speeds. The advanced injection timing should have produced a higher cylinder temperature to increase in the chemical reaction speed of combustion region. Also, the advanced injection timing should have increased the oxidation process between carbon and oxygen molecules to reduce CO emissions as noticed. However the variation of CO emissions with respect to injection timing in this study is curious and may be air fuel ratio would have played a major role compared to the combustion temperature to keep CO emissions unchanged with respect to injection timing.

Fig. 6 shows the variation of carbon monoxide emission of the biodiesel blends (WCO methyl ester) and diesel [4] with v

arious compression ratios. The CO emission of the blend B40 is close to the standard diesel and it is found to be higher for compression ratio 21:1. The other blends B20, B60 and B80 have slightly lesser CO emission for compression ratio 21:1. The percentage of CO increases due to rising temperature in the combustion chamber, physical and chemical properties of the fuel, air–fuel ratio, shortage of oxygen at high speed, and lesser amount of time available for complete combustion. The effects of fuel viscosity on fuel spray quality would be expected to make some CO increase with vegetable oil fuels.

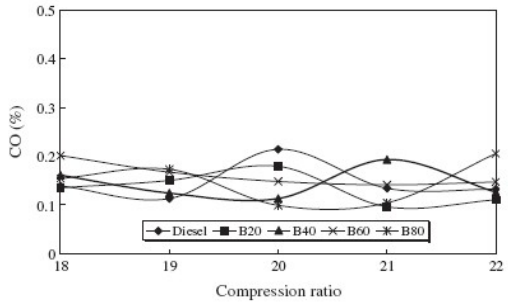


Fig. 6: Variation of carbon monoxide with compression ratio for different biodiesel blends.

CO emissions increase with increased amount of EGR [5] in an n-heptane/natural gas HCCI engine due to lower charge temperature and available O2, which leads to incomplete combustion and as a result high CO formation.

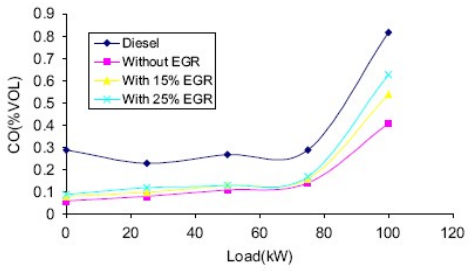


Fig. 7: The influence of EGR on emission characteristics of CO.

CO_2

The variation of carbon dioxide emission with different compression ratios are shown in Fig. 8. The WCO methyl ester biodiesel blend [6] emits higher percentage of CO_2 than diesel at lower compression ratios and vice versa. More amount of CO_2 is an indication of complete combustion of fuel in the combustion chamber. It also relates to the exhaust gas temperature. CO_2 emission of the blend B40 for compression ratio 21:1 is lesser due to incomplete combustion and inadequate supply of oxygen.

The variation of carbon dioxide with brake power [7] of the engine for different values of hydrogen enrichment without EGR, with 15% EGR and 25% EGR is shown in Fig. 9. The Fig. reveals that the formation of carbon dioxide is 14.7% by volume for neat diesel operation, while it is 12.3% by volume with EGR of 15% and 25%, without EGR it is 11.1% by volume. The reduction in carbon dioxide emission is due to the absence of carbon in hydrogen fuel.

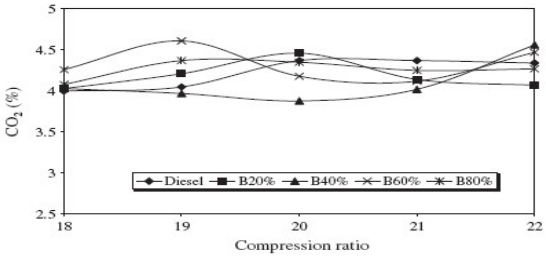


Fig. 8: Variation of CO_2 with compression ratio for different blends.

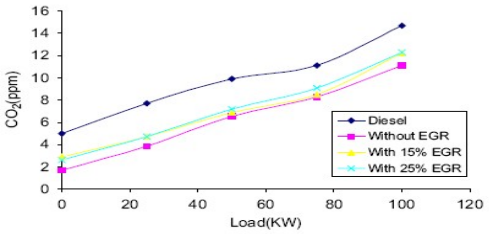


Fig. 9. Variation of $CO_2$with load.

HC

The variation of hydrocarbon emission with different compression ratios for different WCO biodiesel blends [8] is given in Fig. 10. It shows that the hydrocarbon emission of various blends is higher at higher compression ratios. The effects of fuel viscosity, on the fuel spray quality, are expected to produce some HC increase with vegetable oil fuels. It is show that the increase in compression ratio increases the HC emission for Blend B40. The other blends B20, B60 and B80 produce lesser hydrocarbon emissions at higher compression ratio than the standard diesel. Due to the longer ignition delay, the accumulation of fuel in the combustion chamber may cause the higher hydro carbon emission.

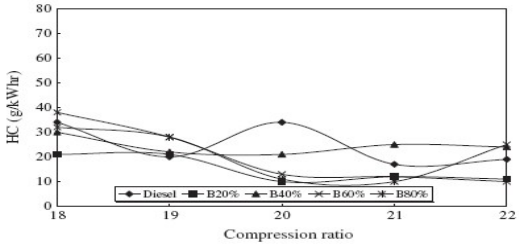


Fig. 10: Variation of HC emission with compression ratio for different blends.Fig. 11. HC emissions at different engine speeds for various fuels: (a) with engine speed of 1200 rpm, (b) 1500 rpm, and (c) 1800 rpm

Fig. 11 demonstrates HC emissions at different engine speeds [9] for canola oil biodiesel fuels. At 1200 rpm, diesel fuel produces 2.98 g/kW h of HC; it decreases gradually with biodiesel–diesel blends and becomes 22% lower for UCB20 and 20% lower for B20. No significant change is observed for canola oil–diesel series. At 1500 rpm, diesel fuel produces 2.5 g/kW h HC, and then decreases to 1.92 g/kW h for UCB20 (about 23% reduction) and to 1.97 g/kW h for B20, which is about 21% reduction. Again there is no significant change with canola oil–diesel series. At 1800 rpm, diesel fuel produces 1.88 g/kW h of HC; UCB20 and B20 show 23% and 21% reduction, respectively. At this speed, canola oil–diesel series shows approximately 6% increase than that of diesel.

2. ACKNOWLEDGEMENTS

We are really thankful to our Project Guide Dr. Bhupendra Singh Chauhan, Assistant Professor, Department of Mechanical & Automotive Engineering, Delhi Technological University, New Delhi, for his invaluable guidance and assistance, without which the accomplishment of the task would have never been possible. We hope to continue our upcoming projects in the following year on the same line.

We would like to express our sincere & heartfelt obligation towards all the personages who have helped us in this endeavor. Without their active guidance, help, cooperation & encouragement, we would not have made headway in the project.

Any omission in this brief acknowledgement does not mean lack of gratitude.

REFERENCES

[1] Shivakumar, P. Srinivasa Pai, B.R. Shrinivasa Rao, “Radial-Basis-Function-Network-Based Prediction of Performance and Emission Characteristics in a Bio Diesel Engine Run on WCO Ester“, *Advances in Artificial Intelligence*, Volume 2012 (2012), pp. 1-7.

[2] Mustafa Canakci, Ahmet Necati Ozseze, Erol Arcaklioglu, Ahmet Erdil, "Performance and exhaust emissions of a biodiesel engine”, *Applied Energy*, 2006.

[3] Morteza Fathi, R. Khoshbakhti Saray, M. David Checkel, “The influence of Exhaust Gas Recirculation (EGR) on combustion and emissions of n-heptane/natural gas fueled Homogeneous Charge Compression Ignition (HCCI) engines*”*, *Applied Energy*, Volume 88, December 2011.

[4] T. Korakianitis, A.M. Namasivayam, R.J. Crookes "Natural-gas fueled spark-ignition (SI) and compression-ignition (CI) engine performance and emissions", *Progress in Energy and Combustion Science*, 2009.

[5] Haiqiao Wei, Tianyu Zhu, Gequn Shu , Linlin Tan, Yuesen "Wang Gasoline engine exhaust gas recirculation – A review", *Applied Energy*, 2011,

[6] S. Imran, D.R. Emberson , D.S. Wena, A. Diez , R.J. Crookes , T. Korakianitis, "Performance and specific emissions contours of a diesel and RME fueled compression-ignition engine throughout its operating speed and power range", *Applied Energy*, 2012.

[7] Avinash Kumar Agarwal, “Biofuels (alcohols and biodiesel) applications as fuels for internal combustion engines”, *Progress in Energy and Combustion Science*, 2006.[8] K. Muralidharan, D. Vasudevan, "Performance, emission and combustion characteristics of a variable compression ratio engine using methyl esters of waste cooking oil and diesel blends", *Applied Energy*, 2010.

[8] Shivakumar, P. Srinivasa Pai , B.R. Shrinivasa Rao, "Artificial Neural Network based prediction of performance and emission characteristics of a variable compression ratio CI engine using WCO as a biodiesel at different injection timings", *Applied Energy*, 2010.

[9] Fig. 1-2. Shivakumar, P. Srinivasa Pai, B.R. Shrinivasa Rao, “Radial-Basis-Function-Network-Based Prediction of Performance and Emission Characteristics in a Bio Diesel Engine Run on WCO Ester“, *Advances in Artificial Intelligence*, Volume 2012 (2012), pp 1-7.

[10] Fig. 3. Morteza Fathi, R. Khoshbakhti Saray, M. David Checkel, “The influence of Exhaust Gas Recirculation (EGR) on combustion and emissions of n-heptane/natural gas fueled Homogeneous Charge Compression Ignition (HCCI) engines”, *Applied Energy*, Volume 88, December 2011.

[11] Fig. 4. S. Imran, D.R. Emberson, D.S. Wena, A. Diez, R.J. Crookes, T. Korakianitis, School of Engineering and Materials Science, Queen Mary University of London, Mile End Road, London E1 4NS, UK; Parks College of Engineering, Aviation and Technology, Saint Louis University, St. Louis, MO 63103, USA.

[12] Fig. 5-Murari Mohon Roy, Wilson Wang, Justin Bujold, Department of Mechanical Engineering, 955 Oliver Road, Lakehead University, Thunder Bay, Ontario, Canada P7B 5E1.

[13] Fig. 6-K. Muralidharan, D. Vasudevan, Department of Mechanical Engineering, PSNA College of Engineering & Technology, Dindigul 624 622, India.

[14] Fig. 7-Morteza Fathi, R. Khoshbakhti Saray, M. David Checkel, Iran Heavy Duty Diesel Engine Mfg. Co. (DESA), Tehran, Iran; Faculty of Mechanical Engineering, Sahand University of Technology, Tabriz, Iran; Mechanical Engineering Department, University of Alberta, Edmonton, AB, Canada T6G 2G8.

[15] Fig. 8-K. Muralidharan, D. Vasudevan, Department of Mechanical Engineering, PSNA College of Engineering & Technology, Dindigul 624 622, India.

[16] Fig. 9-N. Saravanan, G. Nagarajan, K.M. Kalaiselvan, C. Dhanasekaran, Internal Combustion Engineering Division, Department of Mechanical Engineering, College of Engineering, Guindy, Anna University, Chennai 600025, India.

[17] Fig. 10-K. Muralidharan, D. Vasudevan, Department of Mechanical Engineering, PSNA College of Engineering & Technology, Dindigul 624 622, India.

[18] Fig. 11-Murari Mohon Roy, Wilson Wang, Justin Bujold, Department of Mechanical Engineering, 955 Oliver Road, Lakehead University, Thunder Bay, Ontario, Canada P7B 5E1.

ResearchGate

See discussions, stats, and author profiles for this publication at: http://www.researchgate.net/publication/275969438

TCAD Analysis of Frequency Dependent Intrinsic and Extrinsic Parameters of GEWE-SiNW MOSFET

CONFERENCE PAPER · JUNE 2015

DOI: 10.13140/RG.2.1.3867.6322

READS

28

3 AUTHORS:



Neha Gupta

Delhi Technological University

10 PUBLICATIONS **5** CITATIONS

SEE PROFILE



Ajay Kumar

Delhi Technological University

16 PUBLICATIONS **3** CITATIONS

SEE PROFILE



Rishu Chaujar

Delhi Technological University

73 PUBLICATIONS **111** CITATIONS

SEE PROFILE

Available from: Neha Gupta

Retrieved on: 04 November 2015

TCAD Analysis of Frequency Dependent Intrinsic and Extrinsic Parameters of GEWE-SiNW MOSFET

Neha Gupta[1], Ajay Kumar[2] and Rishu Chaujar[3]

Microelectronics Research Lab, Department of Engineering Physics,
Delhi Technological University, Bawana Road, Delhi-110042, India
nehagupta_dtu@yahoo.com[1]
ajaydtu@gmail.com[2]
rishu.phy@dce.edu[3]

ABSTRACT

In this paper, extrinsic parameters of Gate Electrode Workfunction Engineered (GEWE) Silicon Nanowire MOSFET are analyzed in terms of parasitics capacitances, resistances and inductances using 3D-TCAD device quantum simulations. All simulations have been performed using ATLAS and DEVEDIT-3D device simulators. Simulation results reveal significant reduction in intrinsic and extrinsic parameters of GEWE-SiNW in comparison to its conventional SiNW MOSFET. Also, significant improvement in the intrinsic gate and drain transconductance of GEWE-SiNW in comparison its counterpart. Hence, provide its efficacy in high speed switching applications.

Keywords: Gate Electrode workfunction engineering, Quantum Model, Transconductance, Intrinsic and Extrinsic Parameters, Silicon Nanowire MOSFET.

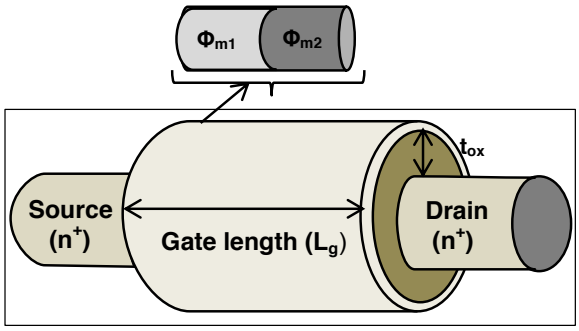
1. INTRODUCTION

Highly scaled CMOS device achieved cut-off frequencies in the range of 10-100 GHz making CMOS technology appropriate for HF and mobile applications [1-4]. However, with scaling down the device dimensions, the so-called Short Channel Effect arises such as mobility degradation, hot carrier effects, drain induced barrier lowering, parasitic capacitances etc. making the scaled devices inapt for high frequency applications [3]. From past few years, new novel device structures such as multi-gate, silicon-on-insulator and silicon nanowire MOSFET have been proposed as promising candidates to overcome the problem of scaling in bulk MOSFET [4-5].

Among them, cylindrical gate MOSFET [6-7] has emerged as a most promising candidate in recent years. Since, it allows excellent electrostatic control of the gate charges over the channel hence overcoming the scaling limitations caused due to the SCEs, thereby improving the device performance. Furthermore, silicon Nanowire MOSFET is receiving more scrutiny for its advantages of reduced short channel effects, high on-current and improved carrier efficiency [8-10], which are the predominant factors that limit how far a MOSFET can be scaled. Also it was proven that it has a merit of outstanding maximum oscillation frequency (f_{MAX}) [11].

In this paper, extrinsic parameters of Gate Electrode Workfunction Engineered (GEWE) Silicon Nanowire MOSFET are analyzed in terms of parasitics capacitances, resistances and inductances using 3D-TCAD device simulations. The extracted parameters have been compared with those of conventional SiNW MOSFET with identical device geometry.

2. DEVICE STRUCTURE AND METHODOLOGY



1 (a)

Fig.1 Simulated device structure of (a) SiNW MOSFET and (b) GEWE-SiNW MOSFET

Fig. 1(a-b) shows the simulated 3D device structure of SiNW and GEWE-SiNW MOSFET respectively. All simulations have been performed using ATLAS and DEVEDIT 3D device simulator. The Source/Drain region is highly doped with n-type impurity of 5×10^{19} cm^{-3}. While the silicon nanowire is doped with a p-type impurity of 1×10^{16} cm^{-3} and t_{ox} thick oxide layer of 1.5nm is embodied in it as shown in Fig.1 The device radius and channel length are 5nm and 30nm respectively. Length of region 1 (L1) and region 2 (L2) are 15nm each. In order to fairly analyze the device performances, both the devices are optimized to have the same threshold voltage, i.e., 0.4V. In this simulation all the junctions of the structure are assumed as abrupt and the biasing conditions are considered at room temperature (T=300K) and the doping profiles are uniform. Further, two numerical techniques Gummel and Newton have been considered to obtain the solutions [17]. To obtain the convergence in the inversion region, the DIRECT parameter is added for more

robust solution. In our simulation, we have adopted the Bohm Quantum mechanical model [2] since because the inversion charge layer thickness in the conducting silicon nanowire channel is comparable to the nanowire dimension.

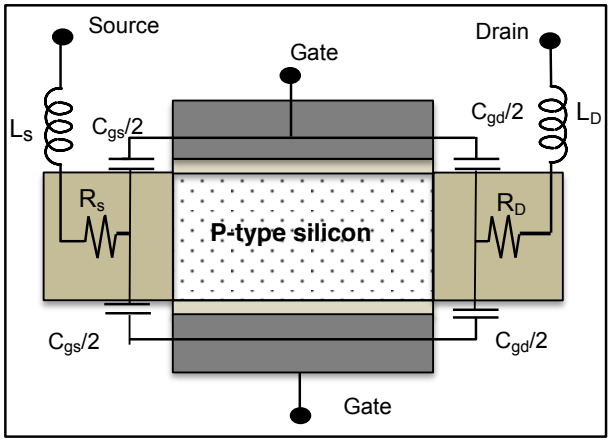


Fig.2 Schematic representation of Equivalent circuit of a SiNW MOSFET in an unbiased condition (V_{gs}=0V).

Fig. 2 shows the equivalent circuit of silicon nanowire MOSFET at zero gate bias. Cgde and Cgse are extrinsic gate-to-drain and gate-to-source capacitances, respectively. R_s and R_d are the source and drain resistances, respectively. L_s, L_d and L_g are source, drain and gate extrinsic inductances respectively. The values of R_d, R_s, L_d, L_s, C_{gs} and C_{gd} were extracted at zero gate bias, which is an OFF-state of the device.

3. RESULTS AND DISCUSSIONS

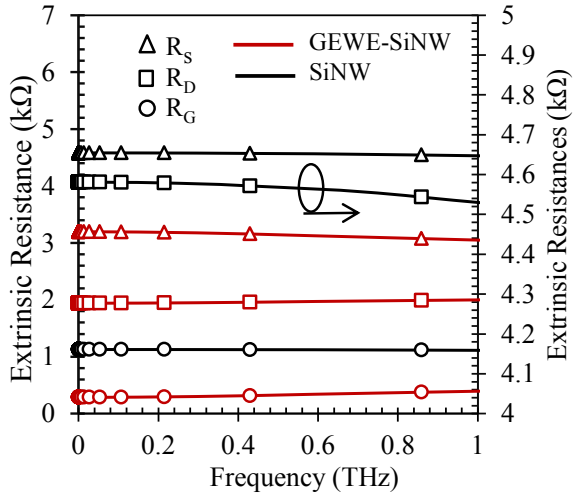


Fig. 3(a): Extrinsic Resistance as a function of frequency for Conventional SiNW and GEWE-SiNW MOSFET at V_{ds}=0V and V_{gs}=0V

Fig. 3(a-c) shows the extrinsic parameters of GEWE-SiNW MOSFET in comparison to conventional SiNW MOSFET. As is evident from Fig. 3(a), intrinsic source, drain and gate resistances are comparatively lower in comparison to SiNW MOSFET. Similarly, intrinsic capacitances and inductances reduce in our device compared to SiNW MOSFET.

These extrinsic parameters were determined by using the zero-biased and pinch-off cold FET methods, as described in [8-9], and the results were summarized in Table I. The detailed procedure for extracting these parameters was not explained here.

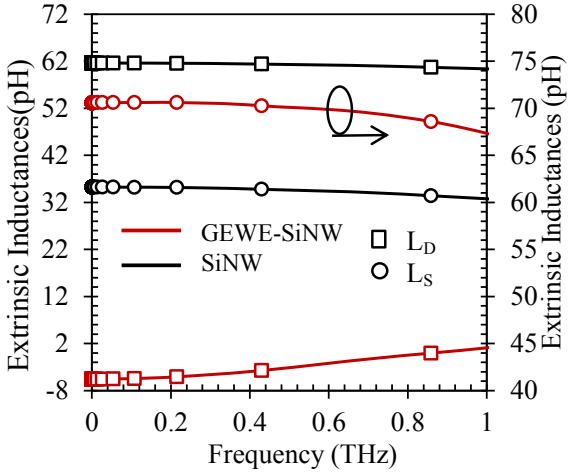


Fig. 3(b): Extrinsic Inductance as a function of frequency for Conventional SiNW and GEWE-SiNW MOSFET at V_{ds}=0V and V_{gs}=0V

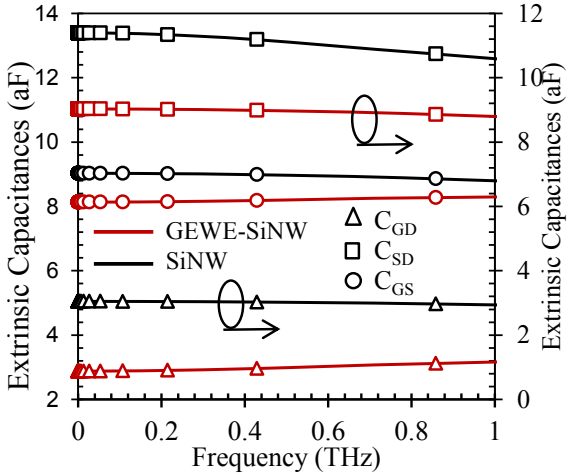


Fig. 3(c): Extrinsic Capacitance as a function of frequency for Conventional SiNW and GEWE-SiNW MOSFET at V_{ds}=0V and V_{gs}=0V

Direct extraction procedures for drawing out the intrinsic small-signal parameters were performed. Fig. 4(a-b) shows the bias dependence of the small-signal parameters for GEWE-SiNW MOSFET and SiNW MOSFET in terms of gate to source, gate to drain and source to drain capacitances. The parasitic capacitances of GEWE-SiNW MOSFET turned out to be smaller than that of SiNW MOSFET, as shown in

Fig. 4(a). With the incorporation of GEWE scheme onto Conventional SiNW MOSFET, the parasitic capacitances decreases further with increase in gate bias voltage. This is due to improved screening of channel region from drain bias variations. Hence, lower values of intrinsic parasitic capacitances mean lower intrinsic delay which is suitable for switching applications such as in logic gates. Similarly, in GEWE-SiNW MOSFET capacitance decreases with change in drain bias in comparison to conventional SiNW MOSFET as shown in Fig. 4(b).

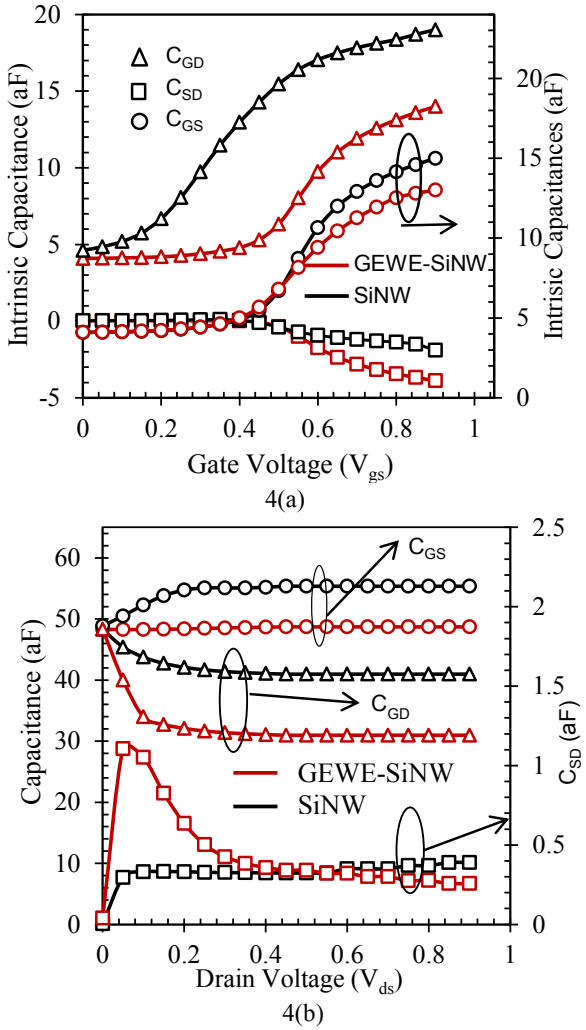


Fig.4: (a-b) Intrinsic Capacitance of Conventional SiNW and GEWE-SiNW MOSFET at different gate and drain voltages respectively.

Fig. 5(a-b) shows the intrinsic gate and drain transconductance of GEWE-SiNW and conventional SiNW MOSFET at gate and drain bias respectively. As is evident from Fig. 5(a), there is an appreciable increment in gate transconductance with increase in gate voltage in comparison to SiNW MOSFET. This is due to enhanced current driving capability of GEWE-SiNW MOSFET in contrast to conventional SiNW MOSFET [10], thus improves the gain of the device. Further, drain transconductance also increases with increase in drain voltage which also results in enhancement in current driving capability of our device as shown in Fig. 5(b).

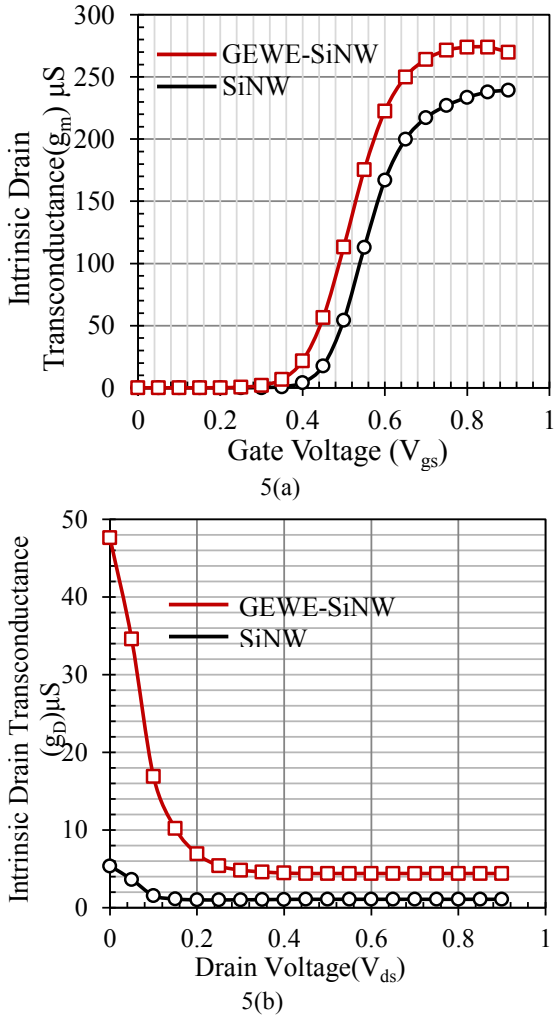


Fig.5: (a-b) Intrinsic gate and drain transconductance of Conventional SiNW and GEWE-SiNW MOSFET as a function bias voltage.

Table I: Extracted Parameters of GEWE-SiNW MOSFET

Parameter	Value Extracted
C_{sd}	9aF
C_{gs}	8.14aF
C_{gd}	0.21aF
R_s	3.0kΩ
R_d	1.98kΩ
R_g	0.37kΩ
L_d	53.22pH
L_s	0.02pH

CONCLUSION

In this work, both extrinsic and intrinsic parameters of GEWE-SiNW MOSFET are directly extracted and compared with conventional SiNW MOSFET with an aim to analyse the effect of these parameters at very high frequency. Simulation results evidence the effectiveness of gate electrode workfunction engineering on small signal parameters of GEWE-SiNW MOSFET by reducing both intrinsic and parasitic parameters of device which hinders the performance of a device at RF frequency.

ACKNOWLEDGMENT

The authors would like to thank the Microelectronics Research Lab, Department of Engineering Physics, Delhi Technological University (formerly DCE) and one of the authors (Neha Gupta) is grateful to the University Grant Commission (UGC) for providing the necessary financial assistance to carry out this research work.

REFERENCES

[1] L.E. Larson, " Silicon technology tradeoffs for radio-frequency/ mixed signal systems-on-a-chip", IEEE Trans. Electron Devices, Vol. 50(3), pp. 683-699, 2003

[2] P. H. Woerlee, M. J. Knitel, R. V. Langevelde, D. B. M. Klaassen, L. F. Tiemeijer, A. J. Scholten, and A. T. A. Zegers-van Duijnhoven, "RF–CMOS performance trends", IEEE Trans Electron Devices, Vol. 48(8), pp. 1776-1782, 2001.

[3] Q. B. Chen, "Compact Modeling of Multi-Gate MOSFETs for RF Designs", Presented at IEEE International Wireless Symposium, 2013.

[4] J. Yang, H. Jin, L. Feng, Z. Lining, L. Feilong, Xing Zhang and M. Chan, "A Compact Model of Silicon-Based Nanowire MOSFETs for Circuit Simulation and Design" IEEE Trans. Electron Devices, Vol. 55 (11), pp. 2898–2906, 2008.

[5] K. H. Yeo et al., IEDM Tech. Dig., pp. 1–4, 2006.

[6] ATLAS User's Manual, SILVACO Int., Santa Clara, CA, 2014.

[7] A. Chaudhry et al., Journal of Semiconductor Technology and Science, pp. 20-27, 2010.

[8] R. Tayrani et al., Proc. 23rd Eur. Microw. Conference, pp. 451–453, 1993.

[9] J. Lu et al., Solid State Electron, pp. 115–120, 2008.

[10] N. Gupta and R. Chaujar, "Implications of transport models on the analog performance of Gate Electrode Workfunction Engineered (GEWE) Silicon Nanowire MOSFET", Proc. IEEE 2nd ICDCS, pp. 1-5, 2014

Journal of Material Science and Mechanical Engineering (JMSME)
Print ISSN : 2339-9095; Online ISSN : 2393-9109; Volume 2, Number 6; April – June, 2015 pp 35 – 37
Krishi Sanskriti Publications
http://www.krishisanskriti.org/jmsme.html

Thermodynamic Analysis of Double-effect LiBr-H_2O Absorption Refrigeration System

Rajesh Kumar*

Department of Mechanical Engineering, Delhi Technological University (Government of NCT of Delhi), Bawana Road, Delhi-110042, India
*E-mail: *dr.rajeshmits@gmail.com*

Abstract—*Thermodynamic analysis of double-effect LiBr-H_2O refrigeration system being performed to observe the effect of temperature variation of various components on the coefficient of performance(COP), exergetic coefficient of performance(ECOP) and circulation ratio(f). The effect of most governing parameter such as generator temperature, evaporator temperature, absorber temperature and condenser temperature of the thermodynamic cycle have been studied*.

Keywords: *Energy, circulation ratio, double-effect,exergetic COP, ozone depletion, simulation*.

1. INTRODUCTION

The performance analysis and study of double-effect lithium bromide-water absorption system has been an area of research for distinct applications. Analysis of this system provides the detailed information about the effect of variation of pressure, temperature and concentration on the overall performance. For effective utilization of energy resources, absorption refrigeration cycle has been analysed to observe the change in performance of the system by varying some parameters. Arun et al. (2000) showed that suitable control systems can be incorporated when the necessary data are known to make the system operate at optimum conditions for maximum coefficient of performance (COP). In its operation, the strong solution of the absorbent-refrigerant is pumped from the absorber to the high pressure generator where it is heated at relatively higher temperature to separate the refrigerant vapour from the solution.

Huicochea et al. (2011) have performed the analysis of the trigeneration system at different ambient temperatures, generation temperatures and microturbine fuel mass flow rate. The results indicated that system shows an appreciable technology to use the energy from the microturbine exhaust gases for electric power, cooling and heating produced simultaneously. Jiang et al. (2002) have compared coefficient of performance and the cyclic characteristics between the three-pressure absorption–ejector hybrid refrigeration system (AEHRS) and small double-effect absorption refrigeration system. The thermo-economical models of the two systems in two cases of high-temperature heat resources: waste heat resources and natural gas fuel have been presented. Liu Y.L. and Wang R.Z. (2004) showed the Performance prediction of a solar/gas driving double effect LiBr–H_2O absorption system. In this system, the high-pressure generator is driven by conventional energy, natural gas, and solar energy together with water vapor generated in the high-pressure generator, which supplies energy to the low-pressure generator for a double effect absorption system. RabahGomri (2010) discussed that absorption heat transformer systems are good to use energy as heat source and delivering thermal energy to higher temperature than the temperature of the fluid. Study between single effect and double effect absorption heat transformer systems used for seawater desalination.

2. SYSTEM DESCRIPTION

Fig.1 shows the double-effect LiBr-H_2O absorption refrigeration cycle. It consists of an absorber (A) and generators having different pressure levels (HTG and LTG) which form the part of solution circuit. Condenser (C) and evaporator (E) are the parts of refrigeration circuit which produces cooling.

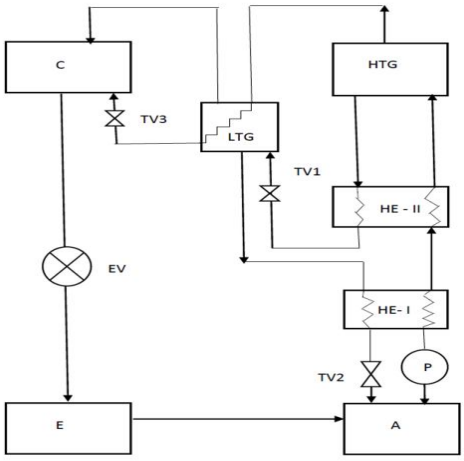


Fig. 1 Double-effect absorption cycle

Strong solution of refrigerant from heat exchangers (HE-I and HE-II) enters into the generator (HTG) and refrigerant water vapour being sent to the condenser. The remaining part of the solution subjected to LTG which further produces refrigerant vapour and the solution strong in LiBr reaches to the absorber. The absorber and evaporator are at low pressure levels while generators and condenser are at higher pressure level.

Table 1: Main parameters considered for the analysis

Environment Temperature (K)	298
Environment pressure (MPa)	0.10135
Absorber Temperature (K)	313
Heat exchanger effectiveness	0.82
Condenser temperature (K)	313
Evaporator temperature (K)	283
LTG temperature(K)	368
HTG temperature(K)	433

3. THERMODYNAMIC ANALYSIS

The thermodynamic behavior of the absorption refrigeration system and its components have been studied.

The coefficient of performance of the cycle is given as:

$$COP = Q_e/(Q_g+W_p) \quad (1)$$

The exergetic coefficient of performance is given as:

$$ECOP = Q_e\{1-(To/T_e)\}/[Q_g\{1-(T_o/T_g)+W_p] \quad (2)$$

The circulation ratio of EARS is given as:

$$f = m_a/m_e \quad (3)$$

Misra et al. (2005) showed that second law analysis calculates the system performance based on exergy, which is defined as the maximum theoretical, useful work obtainable in bringing the system to equilibrium with the environment. The total exergy of a system consists of two components: physical exergy and chemical exergy. In this analysis the temperatures in high temperature heat source, medium temperature heat sink and low temperature heat source are assumed to be constant while the fluid temperature varies in non-isothermal components due to different inlet/outlet solution concentrations.

The thermodynamic study of the absorption cycle is a necessity to observe the utilization of energy potential. The waste of energy potential leads to exergy crisis. The losses at throttling and expansion valves play a major role in the analysis. The utilization of energy observed with the study of exergy destruction. The second law of thermodynamics helps in calculating the performance of system based on exergy, which always decreases owing to irreversibility because of exergy destruction.

The refrigerant states leaving the condenser and evaporator are assumed to be saturated. Refrigerant vapour leaving the generator is considered to be superheated. Non-equilibrium states at the inlet to generator and absorber, and states at outlet to the solution pump and solution heat exchanger are taken to be at their actual conditions.

Solution leaving the absorber and the generator are assumed to be saturated in equilibrium conditions at their respective temperatures and concentrations. On the basis of this configuration, in this system it can be seen that energy potential can easily be determined with the help of thermodynamic equations.

4. RESULTS AND DISCUSSION

A thermodynamic analysis has been done to observe the effect of temperature variation of various components of double-effect absorption system.

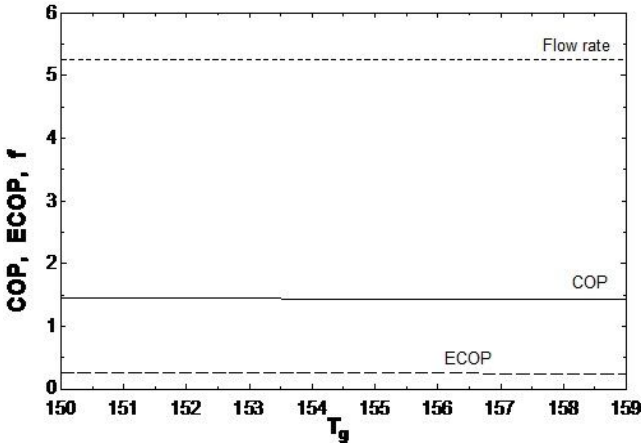


Fig. 2: Effect of generator temperature variation

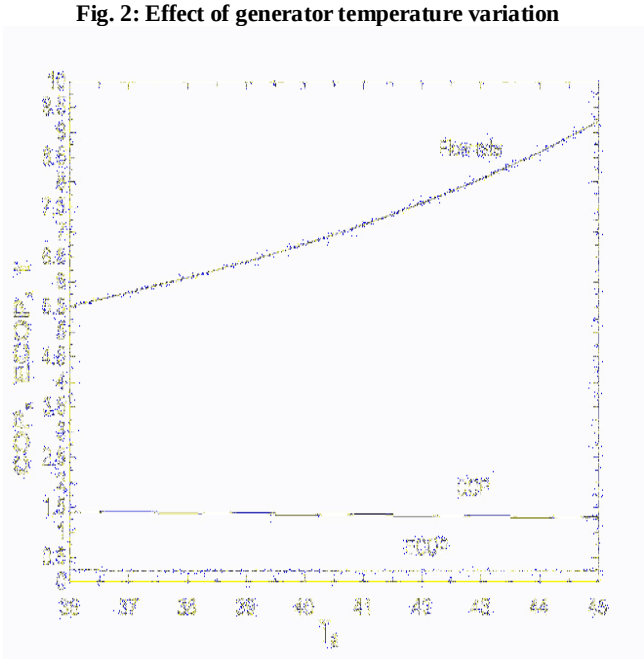


Fig. 3: Effect of absorber temperature variation

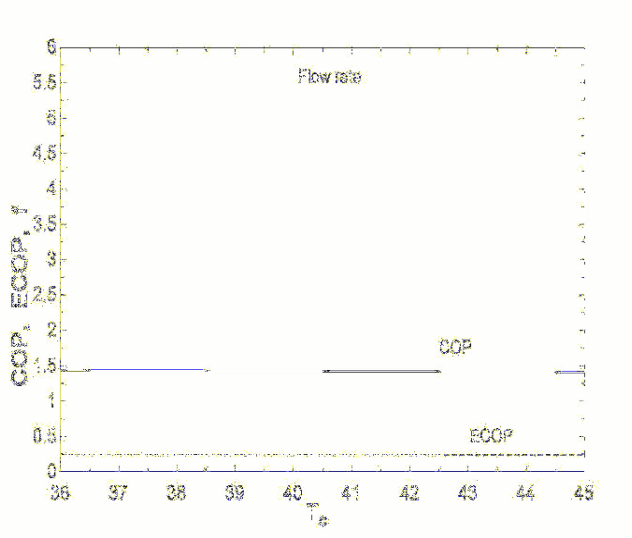


Fig. 4: Effect of condenser temperature variation

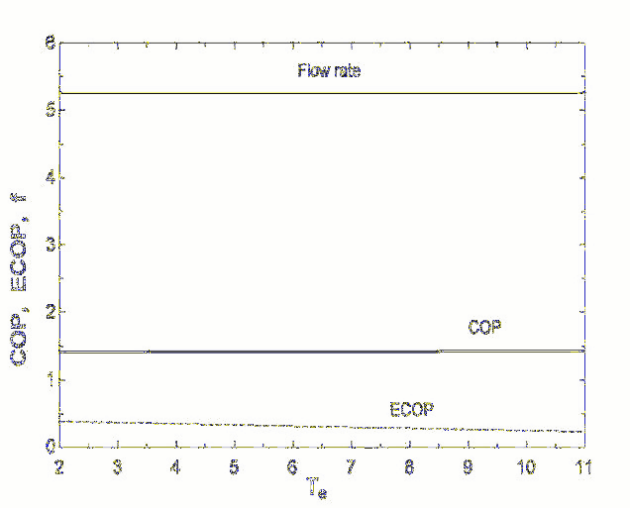


Fig. 5 : Effect of evaporator temperature variation

Fig. 2, 3, 4 and 5 shows the effect on circulation ratio with variation in generator, absorber, condenser and evaporator. The circulation ratio (f) remains same as the temperature increases in case of condenser, evaporator and generator. It varies non-linearly in case of absorber. The COP, however, increase in case of evaporator temperature but it decreases in other components like absorber, condenser and generator. The ECOP decreases with increase in the temperature of all four components. The results of this analysis also indicate that for the designing of the absorption refrigeration system has to be on the basis of thermal analysis. In the applications of residential and industrial, installation of the system is of great importance. The components of absorption refrigeration cycle like absorber, condenser, evaporator and generator play a significant role in the real world applications.

For small sacle applications the above study can be seen as a useful tool to consider the cooling load and other parameters. From this discussion we can easily find the essential and governing parameters of the cycle.

5. CONCLUSION

This study deals with the LiBr-H_2O operated absorption refrigeration system for cooling and air-conditioning with future possible working with ecofriendly refrigerants as working fluid. The effect of temperature variation has been observed on the performance with first law and second law of the proposed cycle.

From the above discussion, it can be concluded that

- As the temperature varies in absorber, the circulation ratio increases while COP nad ECOP decrease.
- As the temperature varies in evaporator, the circulation ratio and ECOP decrease while COP increases.
- As the temperature varies in condenser, the circulation ratio, COP and ECOP decease.
- As the temperature varies in the generator, the circulation ratio, COP nad ECOP decrease.

REFERENCES

[1] Arun M.B., Maiya M.P., Srinivasa Murthy S., "Equilibrium low pressure generator temperatures for double-effect series flow absorption refrigeration systems", *Applied Thermal Engineering* 20, 2000, pp. 227-242.

[2] HuicocheaArmando, Rivera Wilfrido, Gutiérrez-UruetaGeydy, Bruno Joan Carles, "Thermodynamic analysis of a trigeneration system consisting of a micro gas turbine and a double effect absorption chiller", Applied Thermal Engineering, 31,2011, pp. 3347-3353.

[3] Jiang Liben, GuZhaolin, Feng Xiao, LiYun,Thermo-economical analysis between new absorption–ejector hybrid refrigeration system andsmall double-effect absorption system", Applied Thermal Engineering, 22, 2002,pp.1027–1036.

[4] Liu Y.L., Wang R.Z., "Performance prediction of a solar/gas driving double effect LiBr–H2O absorption system" Renewable Energy, 29, 2004, pp. 1677–1695.

[5] GomriRabah,"Thermal seawater desalination: Possibilities of using single effect and double effect absorption heat transformer systems" Desalination, 253, 2010,pp.112–118.

[6] Misra R.D., Sahoo P.K., Gupta A.," Thermoeconomic evaluation and optimization of a double-effect H_2O/LiBrvapour-absorption refrigeration system", International Journal of Refrigeration, 28, 2005,pp.331–343.

Journal of Material Science and Mechanical Engineering (JMSME)
Print ISSN : 2339-9095; Online ISSN : 2393-9109; Volume 2, Number 6; April – June, 2015 pp 32 – 34
Krishi Sanskriti Publications
http://www.krishisanskriti.org/jmsme.html

Thermodynamic Analysis of Power and Ejector Cooling Cycle

Rajesh Kumar*

Department of Mechanical Engineering, Delhi Technological University (Government of NCT of Delhi), Bawana Road, Delhi-110042, India
*E-mail: *dr.rajeshmits@gmail.com*

Abstract: *In this study thermodynamic analysis of a combined power and ejector cooling cycle is carried out using R245fa as working fluid. The variation of turbine inlet pressure on the performance of the proposed cycle has significant effects on the specific work output, coefficient of performance (COP) and exergetic efficiency. Results show that the specific work output, coefficient of performance (COP) and exergetic efficiency increases with increasing of the turbine inlet pressure.*

Keywords: *Coefficient of performance, ejector, exergetic efficiency, specific work output.*

1. INTRODUCTION

Demand for renewable energy technologies and efficient use of conventional energy sources is increasing day by day due to the irreversible impact on the atmosphere of the use of fossil fuels (Pandiyarajan et al. 2011). Low-grade energy sources can be used for producing power and refrigeration. This can be obtained by combining a thermal power cycle with either absorption or ejector refrigeration cycle (Demirkaya et al. 2011). Habibzadeh et al. (2013) performed the thermodynamic study of a thermal system which combines an organic Rankine cycle and an ejector refrigeration cycle using classical and finite-size thermodynamics.

Recently, an energy and exergy analyses of combined power and ejector refrigeration cycles was reported by (Wang et al., 2008; Yapici and Yetisen, 2007; Dai et al., 2009; Wang et al., 2009; Gupta et al., 2014) which shows that the maximum irreversibility/exergy loss occurs in heat addition process followed by the ejector and turbine.

2. SYSTEM DESCRIPTION

Fig.1 shows the process diagram of combined power and cooling cycle. The proposed system consists of organic Rankine cycle (ORC), ejector refrigeration cycle (ERC), with only solar heat source. The oil transfers the thermal energy from PTC to the refrigerant passing through the HRVG. Superheated refrigerant vapor (4) is expanded in a turbine to generate work. The working fluid at low pressure and temperature from the throttle valve is vaporized in the evaporator (12-13) to produce cooling effect.

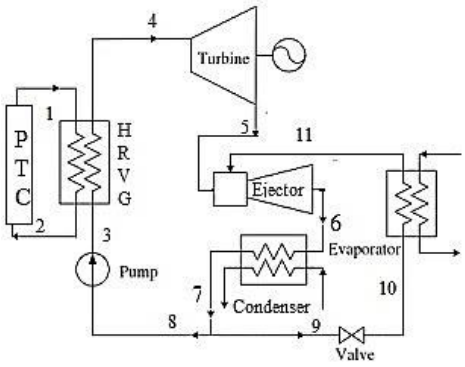


Fig. 1 Process diagram of combined power and cooling cycle

For the analysis, the specifications of the combined power and cooling cycle are given inTable 1.

Table 1: Main parameters considered for the analysis

Atmospheric Temperature (K)	298
Atmospheric pressure (bar)	1.01325
Turbine inlet pressure (bar)	5-7
Turbine inlet Temperature (K)	393
Turbine inlet pressure (MPa)	0.3
Turbine isentropic efficiency (%)	85
Pump isentropic efficiency (%)	70
Condenser temperature (K)	303
Evaporator temperature (K)	268
Oil temperature inlet to PTC (K)	363
Oil temperature inlet to HRVG (K)	433
HRVG efficiency (%)	100
Pinch point temperature difference (K)	10.0
Nozzle efficiency (%)	90
Mixing chamber efficiency (%)	85
Diffuser efficiency (%)	85

3. THERMODYNAMIC ANALYSIS

A thermodynamic analysis considering both the energy and the exergy provides an opportunity to evaluate the theoretical performance of the proposed cycle. Exergy analysis determines the system performance based on exergy, which is defined as the maximum possible reversible work obtainable in bringing the state of the system to equilibrium with that of the environment. Mathematically,

$$\dot{E} = \dot{m}[(h - h_0) - T_0(s - s_0)] \quad (1)$$

Entropy generation over a control volume is given by

$$\dot{S}_{gen} = \frac{dS}{dt} - \sum_{i=0}^{n} \frac{\dot{Q}_i}{T_i} - \sum_{in} \dot{m}s + \sum_{out} \dot{m}s \geq 0 \quad (2)$$

According to Gouy-Stodola theorem, the exergy destruction and entropy generation are related as

$$\dot{E}_D = T_0 \dot{S}_{gen} \quad (3)$$

3.1 Coefficient of performance (COP)

The first law efficiency of the combined cycle is given by

$$COP = \frac{\dot{W}_{net} + \dot{Q}_E}{\dot{Q}_{Solar}} \quad (4)$$

$$\dot{Q}_{Solar} = AI \quad (5)$$

$$\dot{W}_T = \dot{m}_f(h_4 - h_5) \quad (6)$$

$$\dot{W}_p = \dot{m}_f(h_3 - h_8) \quad (7)$$

$$\dot{W}_{net} = \dot{W}_T - \dot{W}_p \quad (8)$$

$$\dot{Q}_E = \dot{m}_f \mu(h_{11} - h_{10}) \quad (9)$$

3.2 Exergetic Efficiency (η_{II})

The exergetic efficiency of combined cycle may be reported as

$$\eta_{II} = \frac{\dot{W}_{net} + \dot{E}_E}{\dot{E}_{Solar}} \quad (10)$$

$$\dot{E}_E = \dot{m}_f \mu[(h_{10} - h_{11}) - T_0(s_{10} - s_{11})] \quad (11)$$

$$\dot{E}_{Solar} = \dot{Q}_{Solar}\left(1 - \frac{T_0}{T_{Solar}}\right) \quad (12)$$

4. RESULTS AND DISCUSSION

Thermodynamic analysis has been carried out to find out to the variation of turbine inlet pressure on the performance of the combined power and cooling cycle.

Fig. 2 shows the effect of variation of turbine inlet pressure on the exergetic efficiency of the proposed cycle. As the turbine inlet pressure increases the exergetic efficiency of the combined system increases.

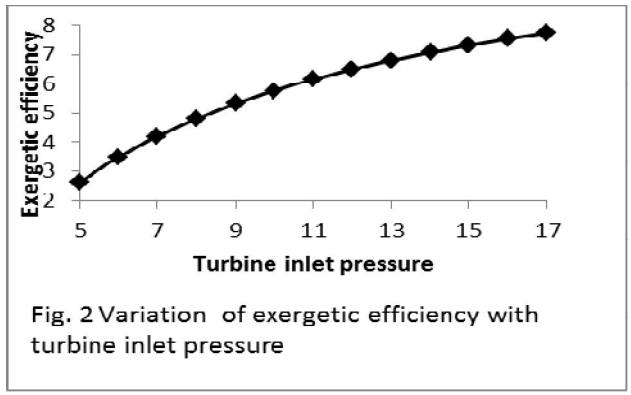


Fig. 2 Variation of exergetic efficiency with turbine inlet pressure

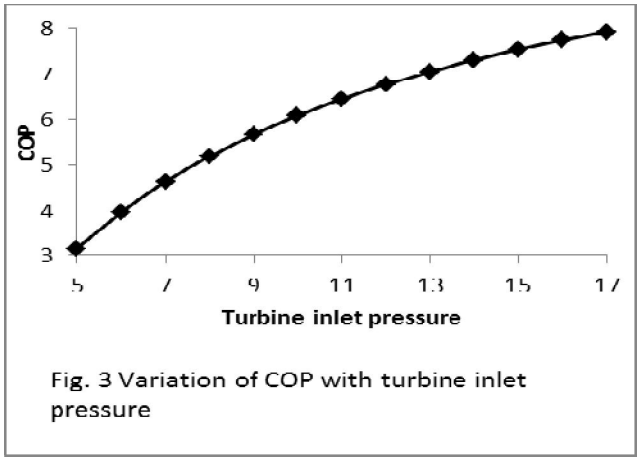


Fig. 3 Variation of COP with turbine inlet pressure

Fig. 3: shows the effect of variation of turbine inlet pressure on the coefficient of performance (COP) of the proposed cycle. As the turbine inlet pressure increases the COP of the combined system increases.

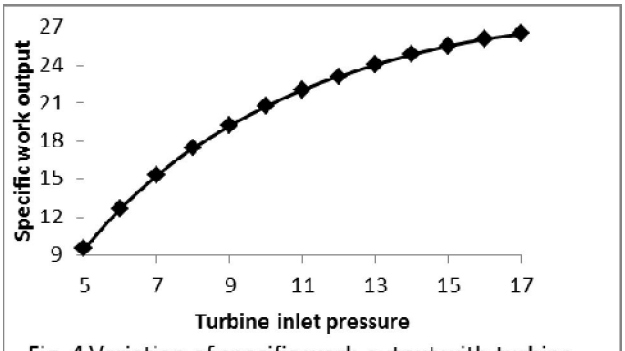


Fig. 4 Variation of specific work output with turbine inlet pressure

Fig. 4 shows the effect of variation of turbine inlet pressure on the specific work output (net work output per unit mass flow of working substance) of the proposed cycle. As the turbine inlet pressure increases the specific work output of the combined system increases.

5. CONCLUSION

A solar operated combined power and cooling cycle is proposed for the production of power and cooling simultaneously. Exergetic analysis has been done to identify the effects of variation of turbine inlet pressure on the performance of the proposed cycle. The conclusions of the present analysis can be summarized as follows:

- As the turbine inlet pressure increases the exergetic efficiency of the cycle increases.
- As the turbine inlet pressure increases the coefficient of performance of the cycle increases.
- As the turbine inlet pressure increases the specific work output of the cycle increases.

REFERENCES

[1] Pandiyarajan, V., Pandian, M.C., Malan, E., Velraj, R., 2011, " Experimental investigation on heat recovery from diesel engine exhaust using finned shell and tube heat exchanger and thermal storage system", Applied Energy, 88(1), pp. 77-87.

[2] Demirkaya, G., Padilla, R.V., Goswami, D.Y., Stefanakos, E., Rahman, M.M., (2011) "Analysis of a combined power and cooling cycle for low-grade heat sources", Int. J. Energy Res., 35, pp. 1145-1157..

[3] Habibzadeh, A., Rashidi M.M., Galanis N., (2013), "Analysis of a combined power and ejector-refrigeration cycle using low temperature heat", Energy Convs. Mgmt., 65, pp. 381-391.

[4] Wang, J.F., Dai, Y.P., Gao, L., 2008, "Parametric analysis and optimization for a combined power and refrigeration cycle", Applied Energy, 85, pp. 1071-1085.

[5] Yapici, R., Yetisen, 2007, "Experimental Study on Ejector Refrigeration System Powered by Low Grade Heat," Energy Conversion of Management, 48, pp. 1560–1568.

[6] Dai, Y., Wang, J., Gao, L., 2009, "Exergy analysis, parametric analysis and optimization for a novel combined power and ejector refrigeration cycle", Applied Thermal Engineering, 29, pp.1983-1990.

[7] Wang, J., Dai, Y., Sun, Z., 2009, "A Theoretical Study on A Novel Combined Power and Ejector Refrigeration Cycle", International Journal of Refrigeration, 32, pp. 1186-1194**.**

[8] Gupta, D.K., Kumar, R., Kumar, N., 2014, "First and Second Law Analysis of Solar Operated Combined Rankine and Ejector Refrigeration Cycle" Applied Solar Energy, 50(2), pp. 113–121.

ResearchGate

See discussions, stats, and author profiles for this publication at: http://www.researchgate.net/publication/282328094

Treatment of Heavy Metals Contaminated industrial waste water by functionalized polymers

ARTICLE *in* INTERNATIONAL JOURNAL OF ADVANCED RESEARCH · SEPTEMBER 2015

Impact Factor: 4.59

READS

9

3 AUTHORS, INCLUDING:



S. K. Singh

Delhi Technological University

76 PUBLICATIONS **84** CITATIONS

SEE PROFILE

Available from: S. K. Singh

Retrieved on: 15 October 2015

ISSN NO. 2320-5407

Journal homepage: http://www.journalijar.com

INTERNATIONAL JOURNAL OF ADVANCED RESEARCH

RESEARCH ARTICLE

Treatment of Heavy Metals Contaminated industrial waste water by functionalized polymers

Tarundeep Gill[1], S.K. Singh[2], P. Albino Kumar[3]

1. Research Scholar, Department of Environmental Engineering, Delhi Technological University, New Delhi – 42, India

2. Professor, Department of Environmental Engineering, Delhi Technological University, New Delhi - 42, India

3. Assistant Professor, Department of Civil Engineering, National Institute of Technology, Manipur, Imphal, India

Manuscript Info

Manuscript History:

Received: 15 July 2015
Final Accepted: 26 August 2015
Published Online: September 2015

Key words:

Aniline formaldehyde condensate; coordination bond; copper; hexavalent chromium; polynailine.

Corresponding Author

Tarundeep Gill

Abstract

Two amine base polymer aniline formaldehyde condensate (AFC) prepared and coated on silica gel and polyanilne synthesized on jute fiber (PANI-jute) were used as an adsorbent for removal of copper [Cu2+], and hexavalent chromium [Cr(VI)] from industrial wastewater. Series of batch adsorption experiments were conducted to investigate the effect of pH, mechanism of metal ions adsorption along with kinetics. With the increase in reaction pH, adsorption of cationic ions Cu2+ increased with maximum removal of 71% at pH 6through tridentate and bidentate coordination bond formed between nitrogen atom in AFC and positively charged Cu2+ by sharing electron. Both AFC and PANI achieved maximum removal of Cr(VI) at pH 3. Adsorption of both Cu(II) and Cr(VI) by AFC and PANI-jute were observed to obeyed Lagergren's pseudo second order kinetic model suggesting chemiosorption. However, the efficiency of the adsorbent reduce by 10-15% when employed for actual industrial waste water due to presence of other co-ions.

Copy Right, IJAR, 2015,. All rights reserved

1. INTRODUCTION

Heavy metals such as cadmium, nickel, copper, lead, zinc, mercury, arsenic, chromium etc. are generated largely from various industrial processes (Khezami et al, 2005; Singh et al 2015). Chromium exists in environment both as trivalent [Cr^{3+}] and hexavalent [Cr^{6+}] forms of which hexavalent form is five hundred times more toxic than the trivalent one. According to US Department of Health and Human Services, 1991, human toxicity of Cr(VI) includes skin irritation to lung cancer, as well as kidney, liver, and gastric damage**.** WHO (World Health Organization, 1993) and BIS (Bureau of Indian Standards, 1991) recommended guideline value for chromium (as total Chromium) in drinking water as 0.05 mg/L (desirable) with no relaxation on permissible limit. Industrial effluents are the major source of copper such as Electroplating, electricals (Aksu et al, 1991; Figueira et al, 2000). Adsorption is an effective and versatile method for removal of heavy metals when combined with appropriate desorption step solving the problem of sludge disposal (Bailey et al, 1999). During recent years, various low-cost and naturally available adsorbents like wool, saw dust, used tyres, seaweed, dead fungal biomass were used for removal of chromium (Dakiky et al, 2002; Tiwari et al 2014). The need for effective and economical adsorbents for removal of heavy metals from wastewater has directed attention to the development polyacrylonitrile fibers etc. due to their high affinity for metal ions, less equilibrium time, lower sludge generation and potential for metal (Neetu et al, 2014; Dhruv et al 2015). Aniline formaldehyde condensate (AFC) and polynailine (PANI) are functionalized polymer having amine ($-NH_2$) groups which can make coordination bond with cationic metals due to presence of lone pair of electrons in *sp3* hybridized amine nitrogen. Present study aims at investigating the feasibility of AFC and PANI for removal of toxic hexavalent chromium and copper from industrial waste water.

2. MATERIALS AND METHODS

Aniline formaldehyde condensate (AFC) was synthesized by reacting formaldehyde (HCHO) with aniline ($C_6H_5NH_2$) as per Liu and Freund, 1997 and the reaction scheme is shown in Fig. 1. Polyaniline was synthesized by oxidation of aniline in presence of 1,4-phenylenediamine, a chain terminator in acidic aqueous medium in presence of an oxidant, ammonium peroxydisulfate. The synthesis scheme of PANI is shown in Fig. 2.

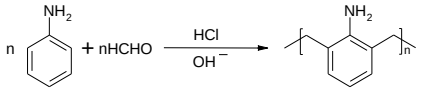


Fig 1. Synthesis scheme of Aniline formaldehyde condensate (AFC)

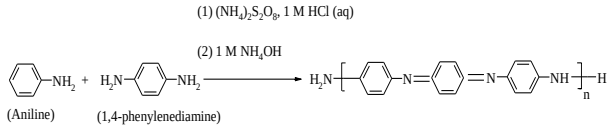


Fig 2. Synthesis scheme of short chain polyaniline

3. EXPERIMENTAL METHODOLOGY

All adsorption studies were carried out with 1000 mL of metal solution in two-liter beaker to prevent the spill off of the solution during mixing adsorbent. Predetermined quantities of adsorbent were added in the beaker and a paddle stirrer was also employed with speed adjusted at 1000 rpm. Solution pH ranges of 3 to 7 were well adjusted by 0.1 M NaOH and 0.1 N H_2SO_4. A blank solution experiment was run in each set and confirmed the inability of plastic reactor vessel to adsorb metal ions. The amount of metal ion adsorbed by adsorbent was calculated based on the difference of metal ion concentration in aqueous solution before and after adsorption according to the equation (1):

$$q_t = \frac{(C_0 - C_t)V}{m} \qquad \ldots\ldots\ldots\ldots\ldots [1]$$

where, q_t is the amount of metal ions adsorbed per unit weight of adsorbent (mg/g) at time t, C_0 and C_t are the concentrations of metal ions (mg/L) at initial time and at time t respectively, V is the initial volume of metal ions sample (L) and m is mass of adsorbent (g). When t is equal to the equilibrium contact time, $C_t = C_e$, $q_t = q_e$, then the amount of metal ions adsorbed at equilibrium, q_e was calculated using Eq. [1].

4. ANALYTICAL PROCEDURE

Concentration of Cr(VI) was measured by diphenyl carbazide colorimetric method at 540 nm wavelength using U.V. Spectrophotometer (Varian, model Cary 50) according to APHA. Concentration of Cu^{2+} were estimated using atomic absorption spectrophotometer using air-acetylene flame at wavelength of 218.2nm at slit width of 0.2 nm and working condition of lamp at 4 mA.

5. RESULTS AND DISCUSSION

5.1 Effect of pH

Solution pH is one of the most important factors during adsorption since it reflects the nature of the physico-chemical interaction of the species in solution and the adsorptive sites of adsorbent (Aksu et al, 2003; Alla et al 2012). Effect of reaction pH on Cu^{2+} and Cr(VI) by AFC coated silica gel and PANI-jute was studied varying solution pH form 1 to 11. Since Cu^{2+} precipitates above pH 6, experiments were conducted till pH 6. From Fig. 3, it

can be seen that Cu^{2+} uptake increased steadily with increase in pH. Negligible removal of Cu^{2+} ion was observed at solution pH 3 and at pH of 3.5 with less than uptake of 20%. With increase in pH, equilibrium Cu^{2+} uptakes increased to 30% at pH 5 to 55 at pH 5.4. When pH was further increased to 6, equilibrium Cu^{2+} uptakes increased to 71%. Copper ion (Cu^{2+}) exists in aqueous medium as square pyramidal form coordinated by water molecules. Nitrogen atom in amine can make coordinate bond with positively charged metal ions due to presence of lone pair of electrons in *sp3* hybridized amine nitrogen. In acidic medium amine exists as protonated ammonium ($-NH_3^+$) and affinity towards Cu^{2+} ion was negligible due to charge repulsion (Tiwari et. al). Hence very low removal of Cu^{2+} ion was achieved in acidic pH. With increase in solution pH, amine group was deprotonated ($-NH_2$ form) and it replaced one or more of water molecules from the coordination sphere of Cu^{2+}.

For adsorption of Cr(VI) by AFC and PANI-jute, the results are incorporated at Fig. 3. Optimum removal for both AFC and PANI-jute were observed at pH 3 with platue formation. At reaction pH of 1, Cr(VI) removal by AFC was 6% which increased significantly to 58% at reaction pH of 3. However Cr(VI) adsorption decreased drastically to 36% at pH 4 to insignificant removal of Cr(VI) at pH 7. Similarly for PANI-jute, Cr(VI) removal increase from 35 to 48% as pH increased from pH 1 to pH 3 and further drops in removal with further increased in pH. Similar pH trend with platue formation on removal of chromium were also observed by various adsorbents like wool, olive cake, sawdust, pine needles, almond, coal and cactus with optimum pH 2 as well as by modified PVP-coated silica gel at pH 5.5 (Garg et al , 2000). Within the studied pH range (2-6) used in the present work, the predominating form of Cr(VI) in solution is acid chromate ion ($HCrO_4^-$) **(**Benefield et al, 1982; Singh 2015). In acidic medium, amine group ($-NH_2$) of AFC and PANI-jute exists as protonated ammonium ($-NH_3^+$) form and electrostatic attraction between protonated ammonium ion and negatively charged $HCrO_4^-$ ion is expected for removal of Cr(VI) from solution. However reduction of Cr(VI) to Cr(III) at higher acidic pH decrease the binding of Cr(VI) to protonated amine as explained above With increase in pH, this electrostatic attraction is decrease due to deprotonation of amine group.

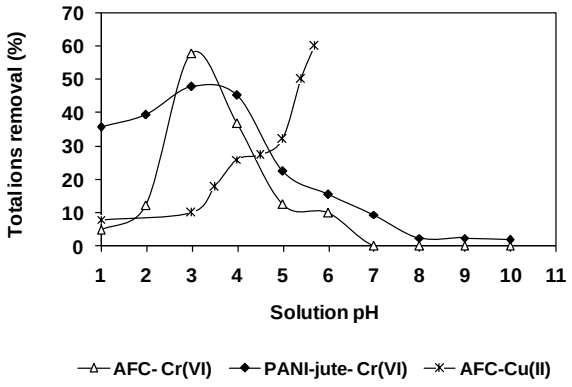


Fig. 3. Effect of pH on Cu(II) and Cr(VI) removal; initial Cr(VI) 50 mg/L

5.2 Adsorption Kinetics

Adsorption kinetics is one of the important parameters during the interaction of adsorbate and adsorbent since it reflects the requirement of volume of reactor. The adsorbent-Cu^{2+} ion interaction reached equilibrium within 120-150 min [Fig. 4]. The shape of the curve representing Cu^{2+} uptake versus time suggests that a two-step process involved. The first portion indicates rapid adsorption during initial 20-30 min after which equilibrium was achieved slowly in 120-150 min. Along with, to know the effect of time on Cr(VI) removal by AFC and PANI-jute, initial Cr(VI) of 50 mg/L were contacted separately with 4 g/L AFC dose and 2 g/L PANI-jute. Adsorption equilibrium for Cr(VI) were almost achieved within 90- 120 min of agitation time by AFC and 40- 120 min by PANI-jute. Such rapid adsorption suggests a readily available, large surface area and smaller diffusion path for both AFC and PANI-jute on chromium ions adsorption. As compared to 2 h equilibrium time of AFC and PANI-jute, seaweed biomass *Ecklonia* pre-treated with HNO_3 required 9 h for complete removal of Cr(VI) from initial concentration of 200 mg/L (Park et al, 2005).

The kinetics data of all the three adsorption of Cu(II) by AFC and Cr(VI) by AFC & PANI-jute were treated with Lagergren's linear pseudo first order kinetics model [Eq. 2 & Eq. 3 respectively].

$$log(q_e - q_t) = log\ q_e - \frac{k_1}{2.303}t \qquad \text{..... [2]}$$

$$\frac{t}{q_t} = \frac{1}{K_2 q_e^{\ 2}} + \frac{t}{q_e} \qquad \text{..... [3]}$$

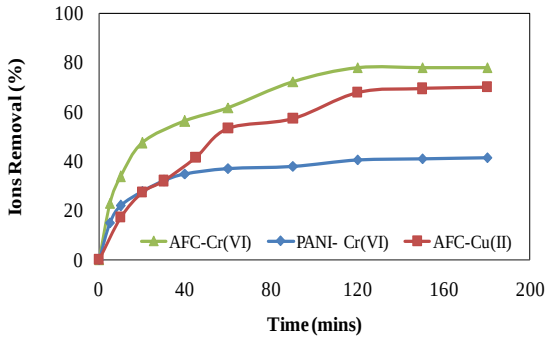


Fig. 4. Effect of time on Cu(II) & Cr(VI) removal: dose: 2 g/L PANI-jute, 8 g/L AFC

Second order kinetics showed better regression with R^2 value of above 0.99 as compared to lower value for first order model as shown in Table I. These suggest the adsorption kinetics obeying second order model indicating the chemical adsorption behavior. In order to confirm this hypothesis, error analyses were conducted through Chi square method. From Table 1, its clear that with error of less than unity for all adsorption of Cu(II) and Cr(VI) by both AFC and PANI-jute against high error of first order, chemical adsorption behavior of second order is thus confirmed.

In order to evaluate the actual performance of the adsorbents, industrial waste water was collected from electroplating unit from Okhla industrial area of Delhi. The concentration of the metal ions was diluted and make similar concentration of 50 mg/L to the synthetic samples. However on adsorption experiments, the uptake of all Cu(II), Cr(VI) were decreased by 15%. The reason was studied by assessing the sample and observed other co-ions Ni(II) and Zn(II) of similar concentrations. Along with Cu(II) and Cr(VI), both Ni(II) and Zn(II) were also absorded by the adsorbents by about 20- 30% thus occupying the active sites of Cu(II) and Cr(VI).

TABLE I: REGRESSION & ERROR ANALYSIS OF LAGERGREN'S FIRST AND SECOND ORDER KINETIC MODELS.

	1st Order		2nd Order	
	R^2	λ^2	R^2	λ^2
AFC-Cr(VI)	0.977	9.87	0.999	0.071
PANI-Cr(VI)	0.6	2725	0.999	0.046
AFC-Cu(II)	0.955	10.35	0.991	0.375

6. CONCLUSION

Two functionalized polymer with abundance of amine were prepared and employed as adsorbent for removal of Cu^{2+} and Cr(VI). With the increase in reaction pH, adsorption of Cu^{2+} increased with maximum removal of 71% at pH 6. At acidic pH, amine group in AFC gets protonated and repulsed the positively charged Cu^{2+} ions. With increase in solution pH, protonation on amine in AFC decreased and thus tridentate and bidentate coordination bond was formed between nitrogen atom in AFC and positively charged Cu^{2+} ions by sharing electron. Maximum removal of Cr(VI) by both AFC and PANI-jute were observed to be at pH 3 with maximum reduction to Cr(III) at acidic pH. Removal mechanism of Cr(VI) by AFC and PANI-jute were observed similar and can be explained as electrostatic attraction of negative chromate ions [HCO_4^-]and protonated amine (NH_3^+) sites of polymers along with reduction of Cr(VI) to Cr(III). On employment of adsorbents to actual industrial waste water, the efficiency reduced by almost 10-15%. The presence of other metal ions such a s Ni(II) and Zn(II) were the probable reasons.

REFERENCES

1. Aksu, Z., Kutsal, T., Gun, S., Haciosmanoglu, N., and Gholaminejad, M. (1991). "Investigation of biosorption of Cu(II), Ni(II) and Cr(VI) ions to activated sludge bacteria." Environ. Technol., 12, 915–21.
2. Alla M. Aenab and S.K. Singh (2012), "Evaluation of Drinking Water Pollution and Health Effects in Baghdad", Iraq Journal of Environment Protection, 2012 (3), 533-537.
3. Alla M. Aenab and S. K. Singh (2012), "Critical Assessment of Environmental Quality of Baghdad, Iraq ", Journal of Environmental Engineering, ASCE, 138 (5), 601-667.
4. APHA, WEF, AWWA, Standard Methods for the Examination of Water and Wastewater, 20th ed., APHA, Washington, D.C. USA, 1998.
5. D. Gang, S.K. Banerji, and T.E. Clevenger (2000), "Chromium (VI) removal by modified PVP-coated silica gel", Practice Periodical of Hazardous, Toxic, and Radioactive Waste Mgmt., 4, 105-110.
6. D. Park, Y.S. Yun, and J.M. Park (2005), "Studies on hexavalent chromium biosorption by chemically-treated biomass of Ecklonia sp", Chemosphere 60, 1356-1364.
7. D.P.Tiwari, S.K.Singh, Neetu Sharma (2014), "Sorption of Methylene Blue on Treated Agricultural Adsorbents: Equilibrium and Kinetic Studies", Journal of Applied water Science, 4 (1), 2014, 81-88
8. Dhruv Mehta, Siddharth Mazumdar, S.K. Singh (2015), Magnetic adsorbent for the treat ment of water/wastewater – A review. Water Process Engineering - Elsevier 7 (9), 244-265
9. Figueira, M. M., Volesky, B., Ciminelli, V. S. T., and Roddick, F. A. (2000). "Biosorption of metals in brown seaweed biomass." Water Res., 34,196–204.
10. G. Liu, and M.S. Freund (1997), "New approach for the controlled Cross-Linking of Polyaniline: Synthesis and Characterization", Macromolecules, 30, 5660-5665.
11. IS 10500:1991, Drinking water specifications, Bureau of Indian Standards, New Delhi, 1991.
12. L.D. Benefield, J.F. Judkins, and B.L. Weand (1982), Process chemistry for wastewater treatment. Prentice-Hall, Englewood Cliffs, NJ, 433-439
13. L.Khezami and R. Capart (2005), "Removal of chromium(VI) form aqueous solution by activated carbons: kinetic and equilibrium studies", J. Hazard. Mater. 123, 223-231
14. M. Dakiky, M. Khamis, A. Manassra and M. Mer'eb (2002), Selective adsorption of chromium (VI) in industrial wastewater using low-cost abundantly available adsorbents, Adv. Environ. Res. 6, 533-540
15. Neetu Sharma, D.P. Tiwari, S.K. Singh (2014), "The Efficiency Appraisal for Removal of Malachite Green by Potato Peel and Neem Bark: Isotherm and Kinetic Studies", International Journal of Chemical and Environmental Engineering, Vol.5, No. 2, 83-88
16. S.E. Bailey, T.J. Olin, R. M. Bricka and D.D. Adrian (1999), "A review of potentially low-cost sorbents for heavy metals", Water Res. 33, 2469-247
17. S.K.Singh, Lokesh Kumar (2015), Removal of Chloride from Groundwater by Bio adsorption, International Journal of Advance Research, 3(5), 140-154
18. Singh,S.K. and Kute, Sunil (1993),"Removal of colour from dye waste water by activated carbon", Jour. of IPHE,Vol.1993, No.3.
19. Singh S.K, Dhruv Katoria, Dhruv Mehta, Dhruv Sehgal (2015), "Fixed Bed Column Study and Adsorption Modelling on the Adsorption of Malachite Green dye from wastewater using Acid Activated Sawdust", IJAR, Vol.3, No. 7, 521-529

20. US Department of Health and Human Services, Toxicological Profile for Chromium. Public Health Service Agency for Toxic substances and Diseases Registry, Washington, DC, 1991.
21. WHO, Guidelines for drinking-water quality,(1993) World Health Organization, Geneva.
22. Z. Aksu, F. G¨onen,(2003), Biosorption of phenol by immobilized activated sludge in a continuous packed bed: prediction of breakthrough curves, Process Biochem. 39 (2003), 599–613

Two Layer Soil Modelling & Optimal Designing of Grounding System of High Voltage Gas Insulated Substation (GIS) & Air Insulted Substation (AIS) Using Matlab GUI



RAJESH KUMAR
Asst. Manager (Technical)
Delhi Transco Ltd.



KAMAL BANSAL
Professor
UPES, Dehradhun, India



DEVENDER K. SAINI
Assistant Professor
UPES, Dehradhun



IPS PAUL
Professor and Dean
HRIT, Ghaziabad

ABSTRACT

This paper presents an accurate method cum procedure for soil modeling & designing the grounding system of gas-insulated substation (GIS) and air insulted substation (AIS). A grounding system design of the gas- insulated substation (GIS) is a complicated task to provide an adequate grounding system and meet specific criteria with regards to personnel safety and integrity of equipment during a fault condition. Similarly design of air insulated system (AIS) also need special attention. MATLAB GUI has been used to find the two soil model and accurate designing of grounding system of high voltage GIS/AIS.

***Key Words**: Grounding, Resistivity and Soil Model, GPR, Touch and step Potential, Resistance*

1. INTRODUCTION

Grounding system is the heart of all electrical network/ systems. A well designed grounding system ensures Safety of equipments and personnel. It further helps in correct and timely operation of protection system connected with the system during abnormal conditions caused by earth faults, lightning surges / switching surges etc. The function of substation grounding system is to provide a grounding mat below ground surface in around the substation which will have uniformly zero potential with respect to ground and lowest earth resistance to ensure that[1,2,4,5]:

1. All non-current carrying parts connected to the grounding system shall be uniformly at zero potential with respect to ground.
2. The floor on which the operation and maintenance staff moves shall be at ground potential. Safe step-potential.
3. During any earth-fault in the substation, the potential of structures, tanks and other on-current carrying parts does not rise to unsafe value. (Safe touch-potential).



Fig. 1 : Air Insulated Substation and Grounding area with gravel surface

Earlier, the design criterion was to achieve lowest earth resistance, However, the modern design criterion for grounding system is to achieve low earth resistance and also to achieve safe' step-potential', 'touch potential' and

voltage gradient during an earth fault between conductor and any of the earthed bodies in the substation.

The word grounding is used in USA and the word grounding is used in England.

Designing of any substation depends upon the accurate calculation of soil resistivity and fault current which may flow through the substation during fault. Homogeneous soil is seldom found and designing based on the average value of soil resistivity measurement may results in over or under design of grounding system. In order to get the proper modeling of the soil, a algorithm has been used to get the soil model with the help of MATLAB GUI. This derived soil model is further used to design the grounding system of the high voltage substations.

2. STEP POTENTIAL AND TOUCH POTENTIAL

During an earth-fault in the substation the earth fault current flows from the fault-point to earth via the metallic path having certain total resistance R. This flow of fault current (I_f) flowing through resistance R causes a voltage drop V = $I_f R_0$. This voltage drop results in a voltage-gradient along the substation floor during the earth faults. This voltage gradient should be held in safe limits by proper design of station grounding system[5].

An operation maintenance person is subjected to 'step potential' and 'Touch Potential' during an earth-fault in the substation. The 'Step-Potential' is defined as the potential difference between two steps of a person standing on the substation floor during the flow of earth fault current. The 'Touch Potential' is defined as the potential difference between a step and the tip of the raised hand touching a substation structure during the flow of the earth fault current through the latter.

The Step Potential and touch Potential depend upon the following aspects:

1. Earth fault current I_f
2. Duration of earth fault
   (a) Whether short time (less than 3 sec.)
   (b) Whether sustained (more than 3 sec.)
3. Fault current flowing through body I_b
4. Values of body resistances in the path of I_b

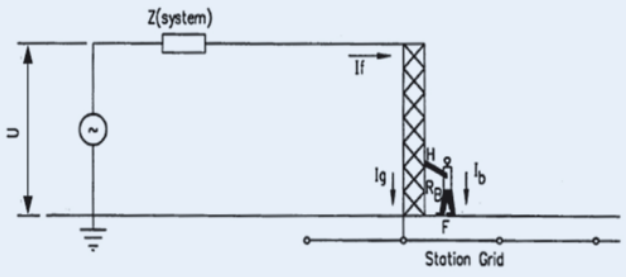


Fig. 2 : Touch Voltage in Substation[1]

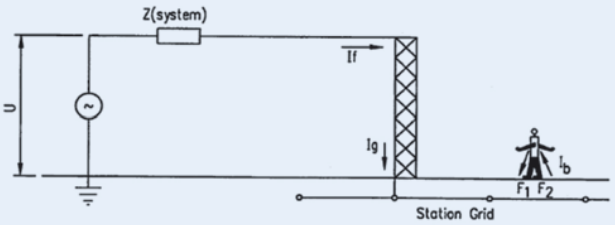


Fig. 3 : Step Voltage in Substation [1]

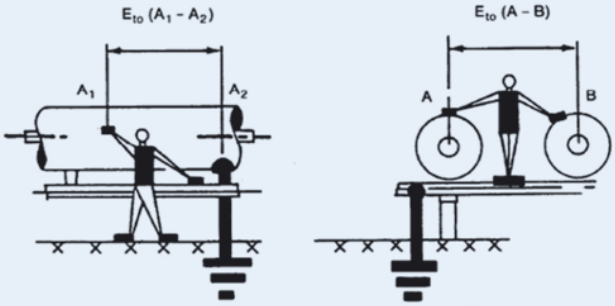


Fig 4 : Touch Voltage in Gas Insulated Substation[1]

3. SUBSTATION GROUNDING SYSTEM

A typical grounding system[3,4,5] for a substation comprises the following:

(a) An earth mat (grid) formed by copper on mild steel bars or bare cables placed in the ground at a depth of about 0.5 meter in a horizontal plane (Fig.5). The crossings are welded. The grid covers the entire substation area and sometimes a few meters beyond the fencing. The grounding rods are also run along the border of the fencing of the substation.

(b) Earth electrodes (1) driven vertically into the earth at several locations. These electrodes (spikers) are connected to the earth mat. Large number of earth-electrodes gives earth resistance.

(c) Grounding risers (3) are used for connection between the structures, equipment bodies and the grounding mat. These are usually clamped or welded or brazed (soldering is not permitted).

(d) Grounding strips between the transformer neutrals and the earth mat are usually in the form of bare copper or strips.

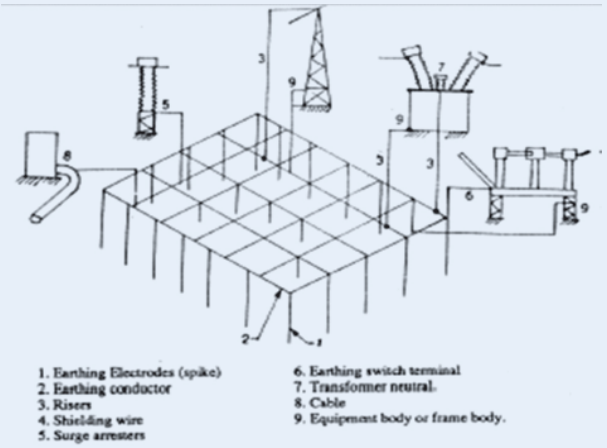


Fig 5 : Grounding System of Air Insulated Substation[5]

Example of power transformer grounding in substation is shown below.



Fig 6 : Grounding of Power Transformer in Substation

4. GROUNDING OF GIS SUBSTATIONS

GIS is acronym for as Insulated Substation and is also used for as Insulated Switchgear. The grounding system at a GIS is required to fulfill the conditions that have been described. Besides these another condition that can arise is that of very high frequency transients. These transients are caused by electrical breakdown in the insulating gas across the contacts of a switching device or in course of a fault. The transients can couple onto the grounding system and may have to be considered in its design. These transients may cause high magnitude, short duration earth potential rises and electromagnetic interference.[1,3]

GIS are subjected to the same magnitude of ground fault current and require the same low-impedance grounding as conventional substations. Typically, the GIS installation necessitates 10-25% of the land area required for conventional equipment. Because of this smaller area, it may be difficult to obtain adequate grounding solely by conventional methods. Particular attention should be given to the bonding of the metallic enclosures of the GIS assembly, as these enclosures carry induced currents of significant magnitude, which must be confined to specific paths. In this respect, grounding recommendations by the manufacturer of a given GIS usually need to be strictly followed.[1]



Fig. 7 : Grounding of Gas Insulated Substation

5. DIFFERENT SOIL MODELS

Uniform soil model is seldom found in the field. Grounding design engineers usually come across the following types of soil models.[12]

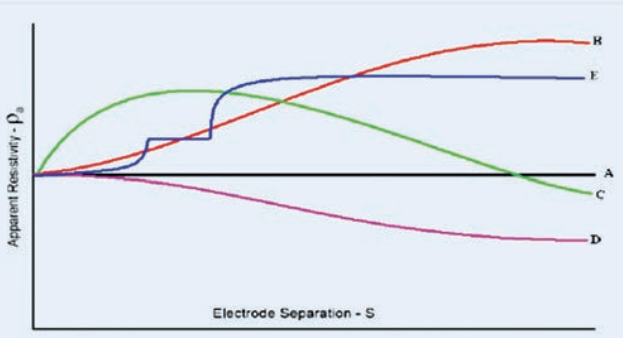


Fig 8 : Soil Resistivity Vs Electrode Separation Curve for Non- Uniform Soil

- Curve (A) represents homogenous resistivity
- Curve (B) represents a low resistance layer overlaying a higher resistivity layer
- Curve (C) represent a high resistivity layer between two low resistivity layer
- Curve (D) represents a high resistivity layer overlaying a lower resistivity layer
- Curve (E) represents a low resistivity layer over a high resistivity layer with vertical discontinuity.

Two Soil Model : Two layer soil model which has an upper layer of a finite depth H, and resistivity (rho1) over a lower layer of infinite depth and resistivity (rho2) is shown below:

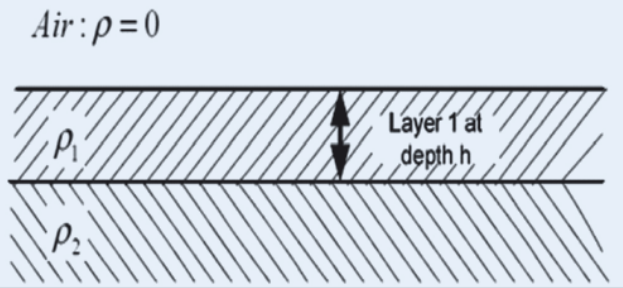
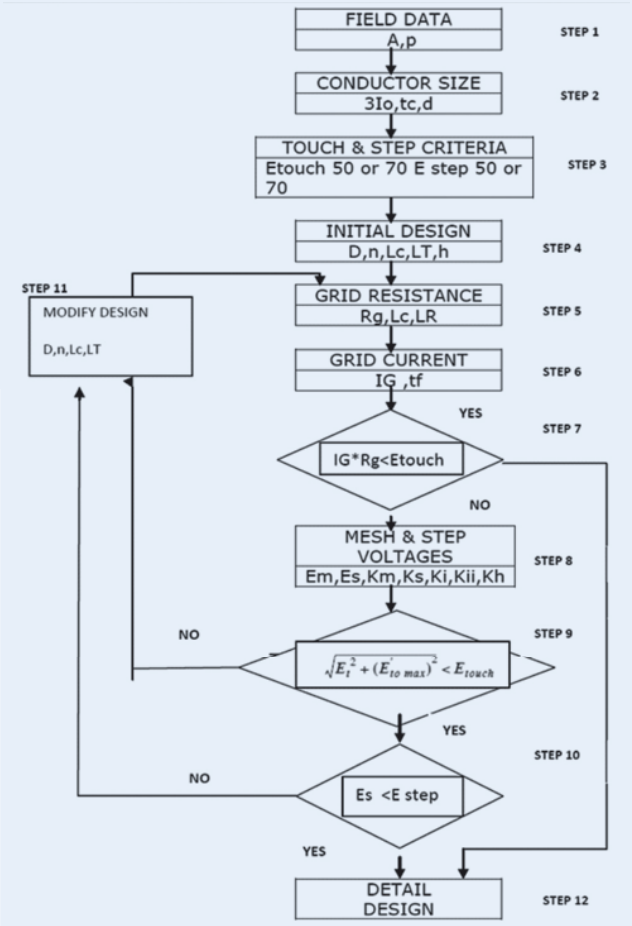


Fig. 9 : Two Layer Soil Model[11]

6. ALGORITHM FOR DESIGNING OF AIS/GIS SUBSTATION

The algorithm of the steps involved in the designing of the EHV substation is given below[1]:



7. EXAMPLE FOR DESIGNING OF GROUNDING SYSTEM

In order to understand the process involved in the designing of the substation , an example for grounding system design of 220/33 kV GIS substation is given below:

STEP 1 : First of all measure the earth resistivity of the substation soil at different locations and values are as follows :

Separtion (meter)	0.5	1	3	5	10	15
Apparent Resistivity (ohm-m)	58.96	35.54	8.60	7.11	6.91	6.23

2. Measure the total area of the substation, let us assume 80 x 80 metre.

The results obtained from the MATLAB software which has been developed for two layer soil model using the finite wenner resistivity expression and algorithm described[5,9] are as follows:

Description/ Model	RESISTIVITY (ohm-m)	
1. Single layer average	20.55	
2 Single layer average (max-min)	32.59	
3. Two layer soil	First layer = 68.33 & H1=0.8m	Second layer = 6.1 & H2 = infinity

STEP 2 : Input Parameters cum data for design:

INPUT DATA consist of the followings:

1. System / network data (system fault current, fault duration, and ambient temperature etc.)
2. Field data like average earth resistivity, surface layer type and resistivity and thickness of surface layer etc.
3. Grounding conductor type and constants.
4. Earth mat design parameters like duration of shock, weight of human working in the station, max grid current, no of electrodes required / to be buried and spacing of earth mat conductor (initial value) etc.

The input parameters, as discussed above, for this example is as follows:

Step	Description	Symbol	Value	Unit
1.	Symmetrical fault current in substation for conductor sizing	I_f	40000	A
2.	Duration of shock for determining allowable body current	t_s	1	s
3.	Surface Gravel layer resistivity	ρs	3000	Ωm
4.	Surface Gravel layer thickness	hs	0.15	m
5.	Soil resistivity	ρ	20.55	Ωm
6.	Depth of Burial of earth material	h	0.65	m
7.	Number of Rods in Switchyard	N_r	50	no
8.	Length of ground rod at each location	L_r	3	m
9.	Maximum length in X- Direction	L_x	80	m
10.	Maximum length in Y- Direction	L_y	80	m

Final Step Write down all the input parameters in the program and press the design button.

The screen shot of the MATLAB GUI program for designing of grounding system as per IEEE-80 is shown below:



SUMMARY OF RESULTS

S. No.	Description	Size/qty.	Unit
1	Size of Conductor Chosen for main mat	1256	Sq.mm
2	Equivalent Diameter of earth conductor (MS ROD)	40	mm
3	Depth of Buried Conductors	0.65	mts
4	Spacing between Conductors (D)	5	mts
5	E Step Tolerable (50kg)	1725.45	Volts
6	E Step Calculated	437.45	Volts
7	E Touch Tolerable(50kg)	518.35	Volts
8	E Touch Calculated	359.78	Volts
9	Resistance of Grounding System	0.120	Ohms
10	Ground Potential Rise (GPR)	4800	Volts

The Attainable touch as well as step voltage is well below the Tolerable limit. Hence the design is safe. In Case the attainable touch and step potential are above the tolerable limit then follow the steps shown in the algorithm above.

7. CONCLUSION

Grounding of all GIS equipments at a station is planned by the manufacturer of the equipments. Main problem about design of the earth grid electrode for a GIS is reduced area of land required for such a station. This makes it all the more important to calculate grid current correctly and give due attention to the measurement of soil resistivity and soil modeling for accurate designing of the grounding system of substation.

MATLAB software program helps to get the two soil model and further helps in optimal designing of grounding system of substation.

Acknowledgement

The first author would like to express his deepest gratitude to Mr Sonjiv Banerji & Mrs Anjuli Chandra for teaching me the essential knowledge (basic) of grounding. High appreciation is given to Mr. R K Malik and Mr. H.R. Seedhar for their constructive comments. The author is deeply indebted to Mr. Hitesh Kumar, Mr N B Soni for their fruitful discussion & kind assistance. Finally the author would like to thank Mrs Krishna Arora for her blessings and Mrs Poonam Arora & Master Divyanshu Arora for their unflinching support in this work.

REFERENCES

1. IEEE Std. 80-2000, IEEE Guide for Safety in AC Substation Grounding, New York, NY: IEEE
2. IEEE: 81: 1983, IEEE Guide for Measuring Earth Resistivity, Ground Impedance, and Earth Surface Potentials of a Ground System
3. Manual on," Grounding of A C Power Systems," Publication No 302, C.B.I.P. New Delhi,Oct. 2007
4. I.S.3043-1987,Indian Standard Code of Practice for Grounding.
5. Rao S , " EHV Substation Design ", Khanna Publishing House, Delhi, India

6. Hans R.Seedher, J.K.Arora, "Estimation of two layer soil Parameter using finite wenner Resistivity Expressive", IEEE Transaction on Power Delivery,Vol.7 No.3, July , 1992.
7. Gary Gilbert, "Soil modelling techniques", International Journal of Materials Science and Applications. Vol. 1, No. 1, pp. 8-13., 2012.
8. M. Nessereddine, J.Rizk, M. Nagrial, A Helleny, "Estimation of apparent soil resistivity for two - layer soil structure," International Journal of Energy And Environment, Volume 4, Issue 4, pp.573-580, 2013.
9. Adekitan I. Aderibigbe, Fakolujo A. Olaosebikan," Alogorithm for Determining the Parameters of a Two- Layer Soil Model", World Academy of Science, Engineering and Technology International Journal of Electrical, Computer, Electronics and Communication Engineering Vol:8, No:11, 2014
10. R.D.Southey, F.P. Dawalibi, "Improving the Reliability of Power systems with More accurate Grounding System Resistance Estimates", Safe Engineering Services & technologies ltd.
11. Hatim Ghazi Zaini,"Calculation Of Grounding Resistance And Earth Surface Potential For Two Layer Model Soil ",International Journal Of Electrical Engineering & Technology, Volume 3, Issue 3, 2012.
12. M. Nassereddine, J. Rizk, and G. Nasserddine," Soil Resistivity Data Computations; Single and Two - Layer Soil Resistivity Structure and Its Implication on Grounding Design," World Academy of Science, Engineering and Technology Vol:7 2013

BIOGRAPHICAL DETAILS OF THE AUTHORS

Rajesh Kumar was born in Delhi, India. He received the B.Tech. & Master of Engineering (ME) degrees in Electrical Engineering from Delhi College of Engineering, University of Delhi, India in 1999 and 2003, respectively. He is also certified Energy Manager and Auditor. He has worked in 400 kV and 220 kV Substation for more than 13 years in Delhi Transco Limited (DTL). He has also worked as Deputy Director (Transmission and Distribution) in Delhi Electricity Regulatory Commission (DERC) for 03 years and 06 months. Presently he is working in the OS department of Delhi Transco Limited (DTL). His research interests include high voltage technology, grounding system ,power electronics, computer application and power distribution automation

Dr. Kamal Bansal is a Professor in University of Petroleum and Energy Studies, Bidholi, Dehradhun, India. He obtained his B. Tech (Electrical Engineering) degree from Malaviya Regional Engineering College, Jaipur & M. Tech (Power System) from Regional Engineering College Kurukshetra and completed his PhD in "Analysis and Redesigning of watermills for sustainable development of Uttarakhand". He is a BEE Certified Energy Auditor and professional member of Energy Institute U.K.

Dr. Devender Kumar Saini is an Assistant Professor in University of Petroleum and Energy Studies, Bidholi, Dehradhun, India. He obtained his B.Tech (Electrical Engineering) degree from LIET, Alwar, University of Rajasthan, in 2006. He obtained M.Tech.(System and control) and PhD from IIT Roorkee in 2009 and 2012 respectively.

Dr. IPS Paul obtained B.E.(Mech) from MACT, Bhopal, P.G. Diploma in Energy Management-Italy, M.B.A. from Delhi University & PhD from IIT,Delhi. He started his career as Assistant Executive Engineer in PSEB, Patiala & worked there for 3 years & 6 months. He further joined NTPC, Badarpur as a Senior Engineer / Engineer & provided his services for 3 years. He further joined NPTI (PETS) New Delhi as Deputy Director/Director & worked there for 10 years. He further joined CPRI & worked as Joint Director/ Additional Director/ Additional Director Scientist-G for 16 years. Currently, he is working as Professor M. E., DEAN-R&D at BBDIT, HRIT. He has published 19 papers at National and International levels.

Cleaner Energy for a Cleaner World